



Vanessa Otero Matias

Mestre em Ciências da Conservação

Historically accurate reconstructions of Amadeo's chrome yellows: an integrated study of their manufacture and stability

Dissertação para obtenção do Grau de Doutor em
Conservação e Restauro
Especialização em Ciências da Conservação

Orientador: Professora Doutora Maria João Seixas de Melo, FCT NOVA

Co-orientador: Professora Doutora Márcia Vilarigues, FCT NOVA

Júri:

Presidente: Professor Doutor Paulo Manuel Assis Loureiro Limão Vieira, FCT NOVA

Arguentes: Professor Doutor João Pedro Botelho Veiga, FCT NOVA
Doutora Costanza Miliani, CNR-ISTM

Vogais: Professora Doutora Maria João Seixas de Melo, FCT NOVA
Professora Doutora Ana Maria Oliveira Carneiro, FCT NOVA
Professora Doutora Leslie Anne Carlyle, FCT NOVA
Doutor João Paulo Arriegas Estevão Correia Leal, IST-UL



Outubro 2018



Vanessa Otero Matias

Mestre em Ciências da Conservação

**Historically accurate reconstructions of
Amadeo's chrome yellows: an integrated study
of their manufacture and stability**

Dissertação para obtenção do Grau de Doutor em
Conservação e Restauro
Especialização em Ciências da Conservação

Orientador: Professora Doutora Maria João Seixas de Melo, FCT NOVA

Co-orientador: Professora Doutora Márcia Vilarigues, FCT NOVA

Júri:

Presidente: Professor Doutor Paulo Manuel Assis Loureiro Limão Vieira, FCT NOVA

Arguentes: Professor Doutor João Pedro Botelho Veiga, FCT NOVA
Doutora Costanza Miliani, CNR-ISTM

Vogais: Professora Doutora Maria João Seixas de Melo, FCT NOVA
Professora Doutora Ana Maria Oliveira Carneiro, FCT NOVA
Professora Doutora Leslie Anne Carlyle, FCT NOVA
Doutor João Paulo Arriegas Estevão Correia Leal, IST-UL

FCT FACULDADE DE
CIÊNCIAS E TECNOLOGIA
UNIVERSIDADE NOVA DE LISBOA

Outubro 2018

**Historically accurate reconstructions of Amadeo's chrome yellows:
an integrated study of their manufacture and stability**

Copyright © Vanessa Otero Matias, Faculdade de Ciências e Tecnologia, Universidade NOVA de Lisboa.

A Faculdade de Ciências e Tecnologia e a Universidade NOVA de Lisboa têm o direito, perpétuo e sem limites geográficos, de arquivar e publicar esta dissertação através de exemplares impressos reproduzidos em papel ou de forma digital, ou por qualquer outro meio conhecido ou que venha a ser inventado, e de a divulgar através de repositórios científicos e de admitir a sua cópia e distribuição com objectivos educacionais ou de investigação, não comerciais, desde que seja dado crédito ao autor e editor.

***'I hope to do it better in time.
I myself am very far from
satisfied with this but, well,
getting better must come through
doing it and through trying'.***

Vincent van Gogh

26 & 27 of November 1882

(Letter to Theo van Gogh)

Acknowledgements

I start by thanking the Portuguese Science Foundation (FCT-MCT) for funding my PhD studentship grant (SFRH/BD/74574/2010), the project “Crossing Borders: History, materials and techniques of Portuguese painters from 1850-1918” (PTDC/EAT-EAT/113612/2009) and the Associate Laboratory for Green Chemistry LAQV-REQUIMTE (UID/QUI/50006/2013).

I acknowledge the Calouste Gulbenkian Museum, in particular the director Isabel Carlos and curators Helena de Freitas and Ana Vasconcelos, for consenting the analysis of Amadeo de Souza-Cardoso’s paintings and materials. I am also grateful to Amadeo de Souza-Cardoso’s family for allowing access to his materials and paintings. I also thank Winsor & Newton, ColArt Ltd. for making the archive project possible and permitting my investigation. The European Synchrotron Radiation Facility (ESRF) is acknowledged for granting beamtime: experiments HG-28 (7-12 April 2014), HG-53 (12-18 March 2015) and HG-80 (13-19 June 2016).

Throughout this journey many things changed, limits surpassed, lessons learned, doors closed, windows opened. In fear of forgetting someone, I thank all those who helped me in one way or another during the PhD time, from those more institutional to those that allowed me to keep my relative sanity.

I am most grateful to my supervisor Maria João Melo, without whom my journey would not have been the same. In her own particular manner, she always pushes me to be a better researcher. It was very far from a bed of roses but in the end, she was the one who contributed the most to this work and for that I will always acknowledge her. I also express my deepest gratitude to Leslie Carlyle who was a co-supervisor without the official stamp and revised this thesis as if she was one. She always encouraged me to be detailed-oriented and helped me see the bigger picture. I am also thankful to my co-supervisor Márcia Vilarigues, who supported me in many ways, especially in critical moments, and showed me the advantages of diplomacy in academia. I would also like to thank my external committee: Costanza Miliari and João Paulo Leal for their final feedback.

This work counted on the technical support of Rui Rocha (SEM-EDS analysis at CEMUP, Porto) and Nuno Costa (XRD analysis at REQUIMTE, FCT NOVA), who always showed the highest patience with my overtime requests, for which I am very appreciative. Special thanks to Joana Pinto (CENIMAT, FCT NOVA), who help me with the diffraction analysis with great enthusiasm and interest, and Isabel Pombo Cardoso (DCR & LAQV-REQUIMTE NOVA), who supported me with the preparation of cross-sections and OM analysis. I also thank Marine Cotte, Emeline Pouyet and Wout De Nolf for their kind help during the synchrotron experiments at the ID 21, ESRF facility. A word of thanks to Sr. Zé Luís (VICARTE, FCT NOVA) for cutting more than two hundred small pieces of glass slides and quartz glass pieces. A special thank you to Paula Domingues and her team from Laborspirit for supplying the materials and answering to requests often for “yesterday”.

The support of some key administrative staff was also fundamental. I thank Maria Isabel Menezes Rodrigues and Maria do Carmo Rodrigues (REQUIMTE, FCT NOVA) for all their help. More recently, the support of Inês Rosa Santos and Beatriz Do Bem (REQUIMTE, FCT NOVA) was unquestionable and our short daily moments made all the difference.

I am profoundly grateful to Ana Maria (DCR, FCT NOVA) for her care, patience, competence and “mother’s” shoulder.

I am also thankful for the support of the professors and seniors of the Photochemistry and Supramolecular Chemistry Research Group (LAQV-REQUIMTE NOVA): A. Jorge Parola, João Carlos Lima, César Laia, Raquel Gavara, Luís Cabrita, Sandra Gago and Letícia Giestas. I specially thank Professor Fernando Pina for “being” and having the best chemistry library that saved me so many times and for giving me my favourite nickname. To João Avó, Noémi Jordão, Miguel Santos, Tiago Moreira and to my friend Ana Marta Diniz, I thank for all the help and shared laughs. My sincere thanks to the great seniors Nuno Basílio and Artur Moro for their inputs.

From the DCR, I acknowledge all colleagues who helped me at some point. A word of thanks to Professor Rita Macedo, Sara Babo, Ângela Ferraz, Catarina Miguel, Ana Isabel Pereira and Eva Mariasole Angelin. I am also thankful to Diogo Sanches, Cristina Montagner and Rita Castro for their support. I am grateful for the friendship and support of Joana Lia Ferreira and Andreia Ruivo. I thank Paula Nabais for her help and encouragement in the last phase of the PhD. I consider myself very blessed for having Tatiana Vitorino in my life, her smile lights up my life and her help is always invaluable.

I am deeply thankful to all students that helped me and motivated me to know better, so I may teach better. There are too many to mention individually but I would like to particularly thank those who became closer and with whom I hope to keep in touch.

A special thank you to Francisco Brites and Artur Neves for the friendship we are building and for all the great moments we have shared and hopefully will continue to share. To Artur Neves, also for all the heated, but also fruitful discussions we had in the past months.

Finally, I finish by thanking my friends and my sisters, Joana the human, for her support, and Luka the cat, my daily and most joyful company throughout the initial months of writing. To my other cat, it should be him thanking me for such an amazing name.

Enduring the chosen path was only possible due to the love and profound patience of my mother and Samuel. This thesis only saw the light because they fed me, they took care of me on the worst moments, and despite everything my mother always pushed me forward. There are not enough words, thoughts or thanks. To her, I will be eternally in debt.

Resumo

Esta tese de doutoramento foca-se no estudo dos pigmentos amarelos à base de cromato do século XIX, em particular, do pigmento amarelo de crómio (cromato de chumbo), que se encontra frequentemente nas obras do pintor moderno Português Amadeo de Souza-Cardoso (1887-1918) e de Vincent Van Gogh (1853-1890). É fundamental para compreender as suas técnicas, contextualizar as suas pinturas, determinar o seu estado de conservação e contribuir para a autenticação da sua obra, que os materiais utilizados pelos artistas sejam profundamente estudados. Neste sentido, esta tese produziu conhecimento novo através de uma abordagem multidisciplinar que combinou a investigação da tecnologia dos materiais para artistas e química da área das Ciências da Conservação.

Este é o primeiro trabalho doutoral a explorar o arquivo e a base de dados da Winsor & Newton (W&N) do século XIX, que oferece uma visão única sobre as práticas e escolhas da empresa. Este produtor de materiais para artistas tinha uma especial preocupação pela qualidade e durabilidade dos seus pigmentos amarelos à base de cromato. Uma avaliação completa dos seus 286 registos de produção sobre estes pigmentos permitiu determinar que a sua maioria (64%) corresponde a três diferentes tonalidades de amarelo de crómio: *Lemon/Pale* composta por cristais mistos de cromato e sulfato de chumbo $[PbCr_{1-x}S_xO_4]$ com $x \leq 0.4$; *Middle* composta por cromato de chumbo puro na forma monoclínica $[PbCrO_4]$; e *Deep* caracterizada pela presença de cromato de chumbo básico $[Pb_2CrO_5]$ juntamente com o cromato de chumbo. Foram ainda encontrados registos para a produção de cromato de bário, $BaCrO_4$ (25%), cromato de zinco e potássio, $4ZnCrO_4 \cdot K_2O \cdot 3H_2O$ (9%), e cromato de estrôncio, $SrCrO_4$ (2%). Apesar do elevado número de registos de produção, foi possível concluir que cada tipo de pigmento é caracterizado por apenas uma ou duas vias sintéticas principais. Também se concluiu que a W&N apenas utilizou aditivos nas formulações de amarelo de crómio, muito provavelmente para melhorar as propriedades dos pigmentos e não para diminuir os custos de produção. A identificação de um número reduzido de registos para a produção dos pigmentos mais sensíveis à luz, a tonalidade *Primrose* do amarelo de crómio (composta por cristais $PbCr_{1-x}S_xO_4$ ricos em enxofre) e o cromato de estrôncio, sugere que a W&N não produzia nem vendia estes pigmentos em larga escala, o que indica que durante o século XIX, a W&N estava de facto comprometida em vender pigmentos amarelos à base de cromato de alta qualidade e o mais duradouros possível.

A reprodução de pigmentos realizou-se seguindo-se as sínteses principais e os pigmentos obtidos foram caracterizados pelas seguintes técnicas analíticas complementares: Colorimetria, Espectroscopia de Reflectância por Fibra Óptica no UV-VIS (FORS), micro-Espectrometria por Fluorescência de Raios X Dispersiva de Energias (μ -EDXRF), Difracção de Raios X (XRD), Microscopia Eléctronica de Varrimento com microanálise por Raios X (SEM-EDS), e pelas micro-Espectroscopias de Raman (μ -Raman) e de Infravermelho com Transformada de Fourier (μ -FTIR). Estas análises permitiram estabelecer uma excelente correlação entre a composição química dos pigmentos reconstruídos e amostras de tubos de tinta do século XIX e de pinturas do Amadeo, o que valida o elevado rigor histórico destes pigmentos e atesta o seu uso como materiais de referência para estudos químicos adicionais.

A foto-estabilidade das formulações de amarelo de cromo foi estudada recorrendo-se a uma experiência de irradiação com uma lâmpada de Xenon ($\lambda_{\text{irr}} > 300 \text{ nm}$) de tintas preparadas com óleo e com poli(acetato de vinilo) (PVAc), em que o processo de degradação foi seguido com recurso às técnicas analíticas já referidas e estudado com técnicas baseadas em radiação de sincrotrão (SR) (μ -XRF, μ -FTIR and μ -XRD). Adicionalmente, utilizando-se a micro-Espectroscopia de Absorção de Raios X (μ -XANES) também foi desenvolvido um inovador Índice de Susceptibilidade à Luz (LSI) baseado na razão da intensidade do pico da descontinuidade K do Cr depois/antes da irradiação com uma lâmpada de Xenon, que diminui à medida que a quantidade dos produtos de degradação de Cr^{3+} aumenta. Este índice permitirá prever a estabilidade dos pigmentos de amarelo de cromo em obras de arte. Foram identificados três níveis de resistência à luz: 1) $\text{PbCr}_{1-x}\text{S}_x\text{O}_4$ com $0 \leq x \leq 0.4/0.5$, 2) $\text{PbCr}_{1-x}\text{S}_x\text{O}_4$ com $x \geq 0.4/0.5$, e 3) PbCrO_4 na presença de uma elevada quantidade dos aditivos giz (CaCO_3) e gesso ($\text{CaSO}_4 \cdot 2\text{H}_2\text{O}$). Este trabalho demonstra que as condições de produção, em particular o pH da produção dos $\text{PbCr}_{1-x}\text{S}_x\text{O}_4$ com $0.4 \leq x \leq 0.5$, também influenciam a foto-estabilidade destes pigmentos.

Este é o primeiro trabalho a formular mecanismos que explicam as principais causas de alteração de cor e identificam o papel crucial desempenhado pela formulação do pigmento e do ligante, inclusive dos seus aditivos. O uso das técnicas baseadas em radiação de sincrotrão permitiu aceder à distribuição espacial dos produtos e intermediários da degradação do amarelo de cromo à micro-escala, revelando que a redução do Cr^{6+} do amarelo de cromo a espécies de Cr^{3+} é provocada pela presença de ácido oxálico e/ou oxalatos. Este trabalho propõe que os oxalatos resultam da decomposição dos carbonatos (presentes como aditivos) em meio ácido ou via descarboxilação dos ácidos carboxílicos. Estes mecanismos de degradação são desencadeados pela fotodegradação do ligante e a taxa de degradação é profundamente dependente da formulação da tinta. Tendo em consideração os resultados obtidos, o papel do oxalato de cálcio como intermediário da degradação e/ou patina protectora da absorção da luz também é discutido. Pela primeira vez, foi possível identificar um composto de degradação de Cr^{3+} , um sulfato de cromo e potássio, $\text{CrK}(\text{SO}_4)_2 \cdot 12\text{H}_2\text{O}$, por espectroscopia de infravermelho.

Por fim, também foi possível determinar que não existem processos de degradação resultantes da redução de Cr^{6+} a ocorrer actualmente nas pinturas de Amadeo, contrariamente ao que a literatura reporta relativamente à degradação do amarelo de cromo nas obras de Van Gogh.

Palavras-chave: Amarelo de cromo, pigmentos amarelos à base de cromato, Amadeo de Souza-Cardoso, Winsor & Newton, manufatura do século XIX, reconstruções, foto-estabilidade, Índice de Susceptibilidade à Luz (LSI), micro-Espectroscopia de Infravermelho com Transformada de Fourier (μ -FTIR), Técnicas baseadas em radiação de sincrotrão (SR)

Abstract

The subject of this PhD is the study of 19th century yellow chromate pigments, in particular chrome yellow (lead chromate), which has been frequently found in the paintings by the Portuguese Modern painter Amadeo de Souza-Cardoso (1887-1918) and by Vincent Van Gogh (1853-1890). Detailed knowledge of the materials used by artists is fundamental for the understanding of their technique and to place their works in context as well as to determine the state of preservation and authenticity of their work. For this thesis new knowledge was gained through a multidisciplinary approach which combines art technological and conservation science research.

This is the first doctoral work that fully explores the Winsor & Newton (W&N) 19th Century Archive Database and provides a unique insight into the company's choices and workshop practices. W&N had a special concern for the quality and durability of their yellow chromate pigments. A complete evaluation of their 286 production records for yellow chromate pigments was undertaken. The majority of the production records (64%) pertain to different hues of lead chromate. W&N produced essentially three lead chromate pigment types: Lemon/Pale based on mixed crystals of lead chromate and lead sulfate [$\text{PbCr}_{1-x}\text{S}_x\text{O}_4$] where $x \leq 0.4$; Middle based on pure monoclinic lead chromate [PbCrO_4]; and Deep that contains the latter admixed with basic lead chromate [Pb_2CrO_5]. Production records for the manufacture of barium chromate, BaCrO_4 (25%), zinc potassium chromate, $4\text{ZnCrO}_4 \cdot \text{K}_2\text{O} \cdot 3\text{H}_2\text{O}$ (9%), and strontium chromate, SrCrO_4 (2%) were also found. Despite the high number of production records, each chromate pigment type is characterised by only one or two main synthetic pathways. W&N's addition of extenders in their lead chromate pigment formulations, indicates that they were mainly used to adjust pigment properties and not as a means to decrease costs. The reduced number of records found for the production of the light-sensitive Primrose type of lead chromate (a formulation composed of sulfur-rich $\text{PbCr}_{1-x}\text{S}_x\text{O}_4$), and strontium chromate, suggests W&N was not manufacturing or selling these pigment formulations on a large scale; more evidence that during the 19th century W&N was committed to primarily selling high quality durable chromate pigments.

Pigment reconstructions following the main methods of synthesis were produced for this research and characterised by complementary analytical techniques: Colourimetry, Fibre Optic Reflectance Spectroscopy (FORS), micro-Energy Dispersive X-Ray Fluorescence Spectrometry (μ -EDXRF), X-Ray Diffraction (XRD), Scanning Electron Microscopy with X-ray microanalysis (SEM-EDS), micro-Raman (μ -Raman) and micro-Fourier Transform Infrared (μ -FTIR) spectroscopies. A very good correlation was found between the chemical composition of the pigment reconstructions and historic paint samples from 19th century oil paint tubes and Amadeo's paintings. This validates their high degree of historical accuracy and attests their use as reference materials for further chemical studies.

The lead chromate pigment formulations were made into oil and poly(vinyl acetate) (PVAc) paints and irradiated with a Xenon lamp ($\lambda_{\text{irr}} > 300 \text{ nm}$) to assess their photostability. The degradation process was followed by the above mentioned techniques and was further studied by Synchrotron Radiation based techniques (μ -XRF, μ -FTIR and μ -XRD). By means of micro X-ray Absorption Near-Edge Structure (μ -XANES), an innovative Light Susceptibility Index (LSI) was developed based on the ratio of the Cr K pre-edge intensity after/before irradiation with a Xenon lamp, which decreases as the

quantity of Cr^{3+} degradation species increases. This index will enable the prediction of the stability of lead chromate pigments in works of art. Three degrees of lightfastness were identified: 1) $\text{PbCr}_{1-x}\text{S}_x\text{O}_4$ with $0 \leq x \leq 0.4/0.5$, 2) $\text{PbCr}_{1-x}\text{S}_x\text{O}_4$ with $x \geq 0.4/0.5$ and 3) PbCrO_4 admixed with a high quantity of the extenders chalk (CaCO_3) and gypsum ($\text{CaSO}_4 \cdot 2\text{H}_2\text{O}$). This work demonstrates that the manufacturing conditions, in particular the pH of the production of $\text{PbCr}_{1-x}\text{S}_x\text{O}_4$ with $0.4 \leq x \leq 0.5$, influences their photostability.

Most importantly, this is the first work to formulate integrated mechanisms that account for the main causes of colour alteration, and which identifies the crucial role played by the pigment and binder formulations, including their additives. The combined use of the Synchrotron Radiation based techniques allowed access at the micro-scale, to the spatial distribution of the degradation products and intermediaries. This led to the discovery that the reduction of Cr^{6+} from lead chromate to Cr^{3+} species is driven by the presence of oxalic acid and/or oxalate compounds. It is proposed that these compounds result from the decomposition of carbonate compounds (present as additives) in acidic media or via decarboxylation of carboxylic acids. These degradation pathways are triggered by the photodegradation of the binder and the degradation rate is deeply dependent on the paint formulation. The presence of calcium oxalate as a degradation intermediary and/or protective patina from light absorption is also discussed in relation to these findings. For the first time, it was possible to identify a Cr^{3+} degradation compound, a chromium potassium sulfate, $\text{CrK}(\text{SO}_4)_2 \cdot 12\text{H}_2\text{O}$, by infrared spectroscopy.

Finally, it was also possible to determine that no degradation resulting from the reduction of Cr^{6+} to Cr^{3+} is currently occurring in Amadeo's paintings which contrasts with literature reports on the degradation of lead chromate pigments in the work of Van Gogh.

Keywords: Chrome yellow, yellow chromate pigments, Amadeo de Souza-Cardoso, Winsor & Newton, 19th century manufacture, reconstructions, photostability, Light Susceptibility Index (LSI), μ -Fourier Transform Infrared Spectroscopy (μ -FTIR), Synchrotron Radiation (SR) based techniques

List of symbols and abbreviations

ν_{as}	Asymmetric stretching vibration
ν_s	Symmetric stretching vibration
δ	Bending vibration
λ	Wavelength
E^0	Standard Reduction Potentials
ΔE^*	Total colour variation
K_{sp}	Solubility Product Constant
ASC	<i>Amadeo de Souza-Cardoso</i>
ASTM	American Society for Testing and Materials
ATR-FTIR	Attenuated Total Reflection Fourier Transform Infrared Spectroscopy
BAFCG	<i>Biblioteca de Arte da Fundação Calouste Gulbenkian</i>
cat. n ^o	Catalogue number in <i>Catalogue Raisonné</i>
DCR	<i>Departamento de Conservação e Restauro</i> (Department of Conservation and Restoration)
DFT	Density Functional Theory
DSC	Differential Scanning Calorimetry
EDS	Energy Dispersive X-ray Spectroscopy
EELS	Energy Electron Loss Spectroscopy
ESRF	European Synchrotron Radiation Facility
EPR	Electron Paramagnetic Resonance spectroscopy.
FCG	<i>Fundação Calouste Gulbenkian</i> (Calouste Gulbenkian Foundation)
FCT	<i>Faculdade de Ciências e Tecnologia</i> (Faculty of Sciences and Technology)
FORS	Fibre Optic Reflectance Spectroscopy
HART	Historically Accurate Reconstruction Techniques
HPLC-DAD	High Performance Liquid Chromatography – Diode Array Detector
HRH	His Royal Highness
ICDD	International Centre for Diffraction Data
IFAC-CNR	<i>Istituto di Fisica Applicata “Nello Carrara” - Consiglio Nazionale delle Ricerche</i>
Inv.	Inventory number
IP	Inflection point
LSI	Light Susceptibility Index
LW	Lead white
μ -EDXRF	Micro-Energy Dispersive X-Ray Fluorescence Spectrometry

μ-FTIR	Micro-Fourier Transform Infrared Spectroscopy
μ-Raman	Micro-Raman Spectroscopy
μ-XRD	Micro-Diffraction
μ-XANES	Micro X-ray Absorption Near-Edge Structure
MUHNAC	<i>Museu Nacional de História Natural e da Ciência</i>
NOVA	<i>Universidade NOVA de Lisboa</i> (NOVA University of Lisbon)
NWO	Netherlands Organisation for Scientific Research
OM	Optical Microscope
PVAc	Poly(vinyl acetate)
RE	Researcher's Edition
REACH	Registration, Evaluation, Authorisation and Restriction of Chemicals
RH	Relative Humidity
SAXS	Small-Angle X-ray Scattering
sh	shoulder
SEM	Scanning Electron Microscopy
SR	Synchrotron Radiation
STEM	Scanning Transmission Electron Microscopy
TAG	Triacylglyceride
ToF-SIMS	Time-of-Flight Secondary Ion Mass Spectrometry
URC	Unique Recipe Code
W&N	Winsor & Newton
XRD	X-Ray Diffraction

Index of Contents

Acknowledgements	i
Resumo.....	iii
Abstract.....	v
List of symbols and abbreviations.....	vii
Index of Contents.....	ix
Index of Figures.....	xv
Index of Tables.....	xxvii
Chapter 1. General Introduction	1
1.1. Preamble.....	3
1.2. The 19 th century artists' colourmen.....	5
1.2.1. Brief context.....	5
1.2.2. The artists' colourman Winsor & Newton.....	8
1.3. Amadeo de Souza-Cardoso.....	11
1.3.1. The artist's biography.....	13
1.3.2. The artist's materials and techniques: an overview.....	17
Chapter 2. The Winsor & Newton 19th Century Archive Database	25
2.1. Introduction to the Archive Database.....	27
2.2. The content of the Database.....	30
2.2.1. Winsor & Newton's catalogues.....	30
2.2.2. Winsor & Newton's manuscript books.....	31
2.2.3. Winsor & Newton's yellow chromate and cochineal products.....	33
2.3. Advantages and limitations of the RE Archive Database.....	37
2.4. Conclusions.....	40
Chapter 3. Chrome yellow: the HART approach	41
3.1. Introduction.....	43
3.1.1. The pigment's history of manufacture and use.....	43
3.1.2. The pigment's colour and chemistry.....	46
3.2. The W&N 19 th century manufacture of lead chromate pigments.....	48
3.2.1. The main ingredients and their role in W&N's formulations.....	50
3.2.2. The W&N 19 th century manufacturing processes and experiments.....	51
3.2.2.1. Primrose Chrome.....	52
3.2.2.2. Lemon/Pale Chrome.....	53

3.2.2.3. Middle/Deep Chrome.....	54
3.2.2.4. Other experiments.....	55
3.3. The characterisation of W&N's lead chromate pigment reconstructions.....	55
3.3.1. Middle/Deep Chrome.....	57
3.3.2. Primrose and Lemon/Pale Chrome.....	59
3.4. Comparison with historic paint tubes	61
3.5. Chrome yellow in Amadeo's paintings	66
3.6. Other yellow chromate pigments.....	70
3.6.1. Introduction to barium, zinc and strontium chromate pigments.....	70
3.6.2. The W&N 19 th century manufacture of other yellow chromate pigments.....	73
3.6.2.1. The W&N 19 th century manufacturing processes and experiments for barium, zinc and strontium chromate pigments.....	74
3.6.2.1.1. Lemon Yellow (barium chromate).....	75
3.6.2.1.2. Citron Yellow (zinc potassium chromate).....	75
3.6.2.1.3. Strontian Yellow (strontium chromate).....	76
3.6.3. The characterisation of W&N's barium, zinc and strontium chromate pigment reconstructions.....	76
3.6.4. Comparison with historic oil paint tubes and Amadeo's paintings.....	80
3.7. Conclusions.....	82
Chapter 4. Chrome yellow: the photochemical study	85
4.1. Introduction.....	87
4.1.1. The degradation of chrome yellow.....	87
4.1.2. The oil paint system.....	90
4.1.3. An overview of the presence of metal oxalates in artworks.....	93
4.2. Photochemical study using lead chromate paint reconstructions.....	95
4.2.1. A multi-analytical approach.....	96
4.2.1.1. The development of a Light Susceptibility Index using μ -XANES.....	100
4.2.1.2. The lead chromate oil paint reconstructions.....	105
4.2.1.2.1. The Middle oil paint.....	105
4.2.1.2.2. The Lemon oil paint.....	111
4.2.1.3. The historic lead chromate oil paints.....	115
4.2.1.3.1. W&N's <i>Chrome Yellow</i> oil paint.....	115
4.2.1.3.2. W&N's <i>Chrome Deep</i> oil paint.....	118
4.2.1.3.2. Lefranc's <i>Jaune de Chrome</i> oil paint.....	120
4.3. Conclusions.....	122

Chapter 5. General conclusions & Future research	125
References	131
Appendices	155
Appendix I - Excerpts from <i>La science de la peinture</i> found in Amadeo's notebook	157
Appendix II - Winsor & Newton 19th Century Archive Database	161
II.1. A survey of selected database contents.....	161
Table II.1.1. W&N catalogues.....	161
Table II.1.2. W&N manuscript books.....	162
Table II.1.3. W&N database topics.....	163
Table II.1.4. W&N database sub-topics.....	166
Table II.1.5. W&N abbreviations, from original to modern terminology.....	173
Table II.1.6. Conversion of measures.....	174
II.2. Transcription of W&N's declaration on their pigments permanence.....	175
II.3. Transcription of selected W&N production records.....	187
II.3.1. Lead chromate pigments.....	187
II.3.2. Other yellow chromate pigments.....	200
Appendix III - Full description of all W&N 19th century manufacturing processes for lead chromate pigments	205
III.1. Primrose Chrome.....	205
III.2. Lemon/Pale Chrome.....	207
III.2.1. Lemon Chrome.....	209
III.2.2. Pale Chrome.....	212
III.3. Middle Chrome.....	216
III.4. Deep Chrome.....	220
Appendix IV - Full description of all W&N 19th century manufacturing processes for other yellow chromate pigments	225
IV.1. Lemon Yellow.....	225
IV.2. Citron Yellow.....	227
IV.3. Strontian Yellow.....	229
IV.4. Other experiments.....	231

Appendix V - Experimental section	233
V.1. Materials and suppliers.....	233
V.2. Experimental methods.....	233
V.2.1. Pigment synthesis methods.....	233
V.2.1.1. Lead chromate pigments.....	233
V.2.1.2. Other yellow chromate pigments.....	236
V.2.2. Micro-sampling.....	237
V.2.3. Calculation of the tinting strength of yellow chromate pigments.....	237
V.2.4. Irradiation experiment.....	237
V.2.4.1. Paint preparation.....	237
V.2.4.2. Accelerated ageing.....	238
V.2.5. Preparation of resin-embedded cross-sections.....	238
V.2.6. Preparation of embedding-free thin cross-sections.....	238
V.3. Equipment and data acquisition.....	239
Appendix VI - Spectral and SEM data of reference compounds	243
VI.1. X-ray Emission Lines.....	243
VI.2. SEM images.....	244
VI.3. μ -Raman spectra.....	245
VI.4. Infrared spectra.....	256
VI.5. μ -XANES spectra.....	267
Appendix VII - Characterisation of the synthesised lead nitrate and subacetate	273
Appendix VIII - Characterisation of references for $\text{PbCr}_{1-x}\text{S}_x\text{O}_4$	275
Appendix IX - pH measurements	287
IX.1. Lead chromate pigments.....	287
IX.2. Other yellow chromate pigments.....	291
Appendix X - Characterisation of lead chromate pigment reconstructions	293
X.1. Primrose Chrome.....	293
X.2. Lemon/Pale Chrome.....	298
X.3. Middle & Deep Chrome.....	305
Appendix XI - Additional characterisation of the historic lead chromate paint tubes	311
Appendix XII - μ-Raman characterisation of cross-sections from selected paintings by Amadeo	313

Appendix XIII - Characterisation of yellow and green micro samples from selected paintings by Amadeo	319
XIII.1. <i>Quadro G</i> (cat. n° P41).....	319
XIII.2. <i>Untitled (O Jockey)</i> , cat. n° P58).....	326
XIII.3. <i>Untitled</i> (cat. n° P75).....	334
XIII.4. <i>Mucha</i> (cat. n° P172).....	338
Appendix XIV - Characterisation of other yellow chromate pigment reconstructions	343
XIV.1. <i>Lemon Yellow</i> (barium chromate).....	343
XIV.2. <i>Citron Yellow</i> (zinc potassium chromate).....	344
XIV.3. <i>Strontian Yellow</i> (strontium chromate).....	345
Appendix XV - Additional characterisation of the historic W&N <i>Lemon Yellow</i> oil paint tube	347
Appendix XVI - Colourimetric values and $I_{Cr\ K\ pre-edge}$ before and after irradiation	349
Appendix XVII - FORS, μ-FTIR and Cr K-edge μ-XANES spectra of the PVAc paints before and after irradiation	353
Appendix XVIII - Additional characterisation of the PVAc paints before and after irradiation	359
Appendix XIX - Additional characterisation of the oil paints before and after irradiation	361
Appendix XX - Reduction reactions, standard reduction potentials (E^0) and dissociation constants (pKa at 25°C)	369

Index of Figures

Figure 1.1. On the left, detail from “ <i>Antoine-Laurent Lavoisier and His Wife</i> ” by Jacques-Louis David in 1788 © The Metropolitan Museum of Art (from Panopticon Lavoisier, 2018), and on the right, the 19 th century Chemical Laboratory of the <i>Escola Polytechnica</i> (Lisbon) built in 1857 (from MUHNAC, 2012).....	6
Figure 1.2. The development of the paint tube © Winsor & Newton (from Winsor & Newton, 2014)	7
Figure 1.3. Top: William Winsor (left) and Henry Charles Newton (right) and Bottom: W&N at 36, 37, 38 and 39 Rathbone Place, London, 1878 © Reckitt & Colman Leisure Ltd. (from Pavey & Staples, 1984).....	8
Figure 1.4. Top: W&N’s c.1835 catalogue and Bottom: the 1851 International Exhibition W&N’s colour palette, pigments from right to left (left) and their watercolour box (right) © Reckitt & Colman Leisure Ltd. (from Pavey & Staples, 1984).....	10
Figure 1.5. Amadeo de Souza-Cardoso, on the left, as a child (ASC 01/01 © BAFCG), on the centre, in c.1913 (ASC 03/39 © BAFCG), and on the right, Lucie de Souza-Cardoso, Amadeo’s wife, in 1915 (ASC 05/17 © BAFCG).....	13
Figure 1.6. <i>Los Borrachos</i> . Photograph by Eduardo Viana in 1908 (Paris). Domingos Rebelo, Amadeo de Souza-Cardoso, Emmerico Nunes, José Pedro Cruz and Manuel Bentes (behind) staging a Velázquez painting (ASC 03/01 © BAFCG).....	14
Figure 1.7. On the left, <i>La Tourmente</i> , 1912 (18 th drawing of the <i>XX Dessins</i> , Inv. 92DP1548 © FCG), and on the right, folio 136 of <i>La Légende de St Julien L’Hospitalier</i> , 1912 (Inv. DP1822 © FCG)...	16
Figure 1.8. Amadeo de Souza-Cardoso paintings, from left to right, top to bottom: untitled (<i>O Jockey</i>), c.1913, 61 x 50 cm, cat. n° P58 (Freitas, 2008: 209); untitled, c.1913, 34.4 x 28.2 cm, cat. n° P75 (Freitas, 2008: 229) and the X-radiograph (Melo <i>et al.</i> , 2009); <i>Janellas do pescador</i> , c.1915-1916, 27.4 x 34.8 cm, cat. n° P168 (Freitas, 2008: 318) and the X-radiograph (Vilarigues <i>et al.</i> , 2008: 98); untitled, c.1914, 18.7 x 12.8 cm, cat. n° P122 (Freitas, 2008: 269); <i>Ar livre nú</i> , c.1914, 18.8 x 13 cm, cat. n° P139 (Freitas, 2008: 286); <i>Mucha</i> , c.1915-1916, 27.3 x 21.4 cm, cat. n° P172 (Freitas, 2008: 322) © FCG & DCR FCT NOVA.....	18
Figure 1.9. Amadeo de Souza-Cardoso paintings, from left to right, top to bottom: untitled (<i>BRUT 300 TSF</i>), c.1917, 85.8 x 66.2 cm, cat. n° P196 (Freitas, 2008: 356); untitled (<i>Entrada</i>), c.1917, 93.5 x 75.5 cm, cat. n° P200 (Freitas, 2008: 364); untitled (<i>Coty</i>), c.1917, 94 x 76 cm, cat. n° P201 (Freitas, 2008: 367); untitled, c.1917, 93.5 x 93.5 cm, cat. n° P197 (Freitas, 2008: 358) © FCG (photos by Cristina Montagner).....	19
Figure 1.10. Molecular structures of carminic acid (left), alizarin (middle) and purpurin (right).....	23
Figure 1.11. Molecular structures of β -naphthol pigments (left) and eosin based lakes (right): fluorescein (R = H), eosin (R = Br) and erythrosin (R = I).....	23
Figure 2.1. Database window. Example: Damp Lake, URC: 08P042L01 © Winsor & Newton (ColArt Fine Art & Graphics Ltd.) (Winsor & Newton Archive, 2009; Clarke, 2012).....	28
Figure 2.2. Corresponding page image of the Damp Lake database record on Figure 2.1 © Winsor & Newton (ColArt Fine Art & Graphics Ltd.) (Winsor & Newton Archive, 2009).....	29
Figure 2.3. Distribution of pigment sub-topics relating to a colour in the W&N 19 th Century Archive Database.....	33
Figure 2.4. Distribution of the yellow (left) and red/purple lakes (right) in the pigment sub-topics from W&N’s RE database. For the yellows, 42% are yellow lakes, 23% are lead chromate pigments, and 11% consist of other yellow chromate pigments. The percentage of yellow ochres is 8%, 4% of cadmium yellows, 4% of Naples yellows and 8% of other yellow pigments. The red/purple lake includes 59% of cochineal lakes, 35% of madder lakes, 2% of lac lakes and 4% of other lake pigments.....	37

Figure 2.5. Page image of the Best Middle Chrome database record P1P192AL01, where two production records were identified; available on-line © 2009-2016 Hamilton Kerr Institute, University of Cambridge.....	39
Figure 3.1. Red crystals of crocoite © DCR FCT NOVA.....	44
Figure 3.2. Acid-base equilibrium established in the range $1 < \text{pH} < 11$ between chromate ion (CrO_4^{2-}) and dichromate ion ($\text{Cr}_2\text{O}_7^{2-}$) (Shriver & Atkins, 1999).....	46
Figure 3.3. Pourbaix diagram of the Cr-H ₂ O system at 25°C adapted from Pourbaix (1963).....	47
Figure 3.4. Monoclinic structure of lead chromate (PbCrO_4 , mineral form crocoite) (Quareni & Pieri, 1965).....	48
Figure 3.5. The final colour is modulated by pH during manufacture. On the left: the lemony mixed crystals of lead chromate and lead sulfate that precipitate at low pH; centre: the yellow pure lead chromate monoclinic phase (PbCrO_4) at neutral pH; on the right: an orange/red basic lead chromate (Pb_2CrO_5) formed in basic media.....	50
Figure 3.6. A) Normalized FORS spectra of the pigments representative of the main synthetic pathways and B) diffraction pattern of lead chromate, monoclinic and orthorhombic crystal structure.....	57
Figure 3.7. Infrared spectra of pigment reconstructions for Middle (M1a) and Deep (D2a); (●) CaCO_3 , (❖) PbCO_3 , (▲) BaSO_4 , (◆) $\text{CaSO}_4 \cdot 2\text{H}_2\text{O}$	58
Figure 3.8. SEM images of pigment reconstructions for A) Primrose (PR1a), B) Lemon (L1) and C) Middle (M2a).....	59
Figure 3.9. Infrared spectra of pigment reconstructions for Primrose (PR1a) and Lemon/Pale (L1 and L2a); (❖) PbCO_3 , (▲) BaSO_4	60
Figure 3.10. Variation of the $A_{\text{vas}}(\text{SO}_4^{2-})/A_{\text{vas}}(\text{CrO}_4^{2-})$ as a function of the SO_4^{2-} molar fraction. The ratio was calculated using the absorbance of $\nu_{\text{as}}(\text{SO}_4^{2-})$ at 1100 cm^{-1} normalized to the $\nu_{\text{as}}(\text{CrO}_4^{2-})$ at 853 cm^{-1} after baseline correction. (★) molar fraction of the Primrose pigment reconstruction (PR1a).....	61
Figure 3.11. Infrared (left) and Raman (right) spectra of the W&N <i>Chrome Yellow</i> and <i>Chrome Deep</i> oil paint tubes belonging to Columbano. In the inset, comparison with the matching pigment reconstructions, L2b and M1, for $1300\text{-}650 \text{ cm}^{-1}$. Also shown is the spectrum from Lefranc's <i>Jaune de Chrome foncé</i> oil paint tube. (▲) BaSO_4 , (❖) $\text{MgCO}_3 \cdot x\text{H}_2\text{O}$, (◇) zinc linoleate, (●) CaCO_3 , (⊖) lead azelate, (★) PbCrO_4 and (☆) $\text{PbCr}_{0.6}\text{S}_{0.4}\text{O}_4$	64
Figure 3.12. Infrared (left) and Raman (right) of the <i>Jaune de Chrome foncé - tempera farge</i> paint tube belonging to Amadeo. In the inset, comparison with the matching pigment reconstruction, L3b, for $1600\text{-}650 \text{ cm}^{-1}$. (★) $\text{PbCr}_{0.8}\text{S}_{0.2}\text{O}_4$, (❖) PbCO_3	65
Figure 3.13. SEM images of historic W&N A) <i>Chrome Yellow</i> and B) <i>Chrome Deep</i> oil paint tubes, C) L2a and D) M1a pigment reconstructions.....	65
Figure 3.14. Amadeo de Souza-Cardoso paintings: A) <i>Gemälde G / Quadro G</i> , c.1912, 51 x 29.5 cm, cat. n° P41 (Inv. 77P2; Freitas, 2008: 182); B) <i>Untitled (O Jockey)</i> , c.1913, 61 x 50 cm, cat. n° P58 (Inv. 77P5; Freitas, 2008: 209); C) <i>Untitled</i> , c.1913, 34.4 x 28.2 cm, cat. n° P75 (Inv. 92P209; Freitas, 2008: 229) and D) <i>Mucha</i> , c.1915-1916, 27.3 x 21.4 cm, cat. n° P172 (Inv. 86P21; Freitas, 2008: 322) © FCG.....	66
Figure 3.15. A) Cr K-edge μ -XANES spectra of lead chromate (PbCrO_4) and viridian ($\text{Cr}_2\text{O}_3 \cdot 2\text{H}_2\text{O}$). Complementary analysis of a green cross-section from Amadeo's painting <i>O Jockey</i> (c.1913, cat. n° P58) by B) visible light microscope image (50x), C) SEM image (1500x) and D) SR μ -XRF elemental maps at 5.993 keV of Cr and Pb and at 6.1 keV of Cr (map size: $170 \times 116 \mu\text{m}^2$, with $1 \times 1 \mu\text{m}^2$ pixel size).....	67

Figure 3.16. Infrared spectra (inset between 1000-750 cm ⁻¹) of μ-samples taken from Amadeo's paintings and matching pigment reconstructions: A) μ3 from <i>O Jockey</i> (c.1913, cat. n° P58) and L2a pigment reconstruction; B) μ3 from <i>Mucha</i> (c.1915-1916, cat. n° P172) and L2b pigment reconstruction; C) μ1 from <i>Mucha</i> and M1a pigment variation; D) μ1 from <i>Quadro G</i> (c.1912, cat. n° P41) and M2a pigment reconstruction. (☆) PbCr _{0.6} S _{0.4} O ₄ , (★) PbCrO ₄ , (■) 2PbCO ₃ .Pb(OH) ₂ , (⌘) lead soap, (▲) BaSO ₄ , (●) CaCO ₃ , (◆) Cr ₂ O ₃ .2H ₂ O and (✱) Fe ₄ [Fe(CN) ₆] ₃	69
Figure 3.17. SEM images of yellow colours from Amadeo's paintings A) <i>O Jockey</i> (c.1913, cat. n° P58) and B) <i>Quadro G</i> (c.1912, cat. n° P41).....	69
Figure 3.18. The final colour of Lemon Yellow (BaCrO ₄), Strontian Yellow (SrCrO ₄), Citron Yellow (4ZnCrO ₄ .K ₂ O.3H ₂ O), and pure chrome yellow (PbCrO ₄) manufactured following W&N 19 th century recipes.....	75
Figure 3.19. Normalized FORS spectra of all yellow chromate pigments representative of the main synthetic pathways shown in Table 3.2 and Table 3.9.....	77
Figure 3.20. Infrared (left) and Raman (right) spectra of pigment reconstructions for W&N's Lemon (LY1a), Citron (CY1a) and Strontian (SY1a) Yellows.....	79
Figure 3.21. A) Infrared spectra (inset between 1000 and 750 cm ⁻¹) and B) diffraction pattern of the W&N <i>Lemon Yellow</i> oil paint (private collection @ DCR FCT NOVA) compared with a LY1a pigment reconstruction; (▲) BaCrO ₄ , (●) MgCO ₃ .xH ₂ O.....	80
Figure 3.22. Infrared spectra (inset between 1000 and 800 cm ⁻¹) of A) Lefranc's <i>Jaune de Strontiane</i> oil paint tube, B) μ-sample 26 from Amadeo's painting <i>Entrada</i> (c.1917, cat. n° P200), compared with a SY1a pigment reconstruction; (☆) SrCrO ₄ , (■) 2PbCO ₃ .Pb(OH) ₂ , (▲) SrSO ₄ , (◆) CaSO ₄ .2H ₂ O, and (◇) zinc palmitate.....	81
Figure 4.1. Cr K-edge μ-XANES spectra of lead chromate (PbCrO ₄) and viridian (Cr ₂ O ₃ .2H ₂ O)...	88
Figure 4.2. The oil paint model adapted from Boon <i>et al.</i> (1997) and Burnstock & Van den Berg (2014). A) 'fresh oil' paint in the presence of metal ions (M), B) polyanionic network (after curing), and C) after hydrolysis of the ester bond (after maturation).....	92
Figure 4.3. Experimental sample set for the irradiation experiment carried out under a Xenon lamp, λ _{irr} > 300 nm. The codes of the reconstructed pigments presented refer to variations in the manufacturing processes as described in Chapter 3.2 (p. 48), see also Appendix III (p. 205). The pigments composed of PbCr _{1-x} S _x O ₄ with variable ratio of sulfate to chromate and pure PbCrO ₄ monoclinic phase are highlighted in yellow and orange, respectively.....	96
Figure 4.4. Normalized Cr K-edge μ-XANES spectra of the Middle, Lemon and the historic W&N <i>Chrome Yellow</i> oil paints and Middle (L3a*_2) PVAc paint before and after irradiation with a Xenon lamp (λ _{irr} > 300 nm).....	100
Figure 4.5. Normalized Cr K pre-edge intensity before and after irradiation of the oil paint samples: historic W&N oil paint tubes, <i>Chrome Deep</i> (☆) and <i>Chrome Yellow</i> (★); Lemon (○) and Middle (●) oil paint reconstructions; and lead chromate reference oil paint (■) (see Table 4.3).....	101
Figure 4.6. Normalized Cr K pre-edge intensity before and after irradiation of the PVAc paint samples (see Table 4.4).....	102
Figure 4.7. SEM images of the lead chromate pigment reconstructions composed of PbCr _{0.5} S _{0.5} O ₄ ; A) PR1b_2, B) PR1b_1 and C) L2b.....	104
Figure 4.8. A) Normalized FORS and B) infrared spectra of the Middle oil paint before and after irradiation with a Xenon lamp (λ _{irr} > 300 nm); (★) PbCrO ₄ , (●) CaCO ₃ , (◆) CaSO ₄ .2H ₂ O and (◇) CaC ₂ O ₄ . xH ₂ O.....	105
Figure 4.9. A) SEM image of a cross-section from the Middle oil paint after 7750h of irradiation and B) Raman spectra acquired at the interface of the gypsum aggregate outlined in the SEM image; (★) PbCrO ₄ , (●) CaCO ₃ , (◆) CaSO ₄ .2H ₂ O and (◇) CaSO ₄	106

Figure 4.10. Optical microscope image of an embedding-free thin cross-section of the Middle oil paint after 7750h of irradiation (analysed areas outlined in black). A) SR μ -FTIR chemical maps (size: $170 \times 160 \mu\text{m}^2$, with $10 \times 10 \mu\text{m}^2$ step size), ROI: acids ($1718\text{-}1700 \text{ cm}^{-1}$), esters ($1755\text{-}1720 \text{ cm}^{-1}$), calcium oxalate ($1340\text{-}1300 \text{ cm}^{-1}$), calcium carbonate ($1520\text{-}1350 \text{ cm}^{-1}$); B) SR μ -XRF maps around Cr K-edge at 5.993 and 6.1 keV (vertical map size: $92 \times 192 \mu\text{m}^2$ and diagonal map size: $152 \times 100 \mu\text{m}^2$, with $2 \times 2 \mu\text{m}^2$ step size) and around S K-edge at 2.473, 2.478 and 2.842 keV (size: $185 \times 220 \mu\text{m}^2$, with $5 \times 5 \mu\text{m}^2$ step size). The points labelled a) through to f) represent the location of μ -XANES spectra presented in Fig. 4.11. See also Figure XIX.4 (p. 362).....	107
Figure 4.11. A) Normalized Cr K-edge, B) & C) S K-edge μ -XANES spectra of the points in Figure 4.10...	107
Figure 4.12. SR infrared spectrum obtained on the surface of an embedding-free thin cross-section of the Middle oil paint after 7750h of irradiation and three reference compounds: chromium potassium sulfate $\text{CrK}(\text{SO}_4)_2 \cdot 12\text{H}_2\text{O}$, oxalic acid ($\text{C}_2\text{H}_2\text{O}_4$), calcium oxalate dihydrate ($\text{CaC}_2\text{O}_4 \cdot 2\text{H}_2\text{O}$, weddellite); (\blacklozenge) $\text{CaSO}_4 \cdot 2\text{H}_2\text{O}$, (\bullet) CaCO_3 and (\blackstar) PbCrO_4 . See also Figure XIX.5 (p. 363).....	108
Figure 4.13. Optical microscope image of an embedding-free thin cross-section of the Middle oil paint after 11000h of irradiation (analysed areas outlined in black). A) SR μ -FTIR chemical map (size: $190 \times 150 \mu\text{m}^2$, with $10 \times 10 \mu\text{m}^2$ step size), ROI: acids ($1718\text{-}1700 \text{ cm}^{-1}$) and calcium oxalate ($1340\text{-}1300 \text{ cm}^{-1}$); B) SR μ -XRD map (size: $173 \times 90 \mu\text{m}^2$, with $2 \times 2 \mu\text{m}^2$ step size), red = Rietveld scaling factor of calcite, green = intensity of the (200) Bragg peak of weddellite), and SR μ -XRF map around Cr K-edge at 5.993 and 6.1 keV (size: $150 \times 180 \mu\text{m}^2$, with $1 \times 1 \mu\text{m}^2$ step size); C) SR μ -XRF map around Ca K-edge at 4.0478 and 4.0536 keV (size: $72 \times 222 \mu\text{m}^2$, with $2 \times 2 \mu\text{m}^2$ step size). The points a), b) & c) represent the location of μ -XANES spectra presented in Fig. 4.14. See also Figures XIX.6 and XIX.7 (p. 364).....	109
Figure 4.14. a) Normalized Cr K-edge, b) & c) Ca K-edge μ -XANES spectra of the points in Figure 4.13, and the references compounds: chalk (CaCO_3), calcium oxalate monohydrate ($\text{CaC}_2\text{O}_4 \cdot \text{H}_2\text{O}$) gypsum ($\text{CaSO}_4 \cdot 2\text{H}_2\text{O}$) and calcium sulfate anhydrous (CaSO_4), see also Figure VI.5.7 (p. 271).....	109
Figure 4.15. A) Normalized FORS, B) SEM image of a cross-section ($t_{\text{irr}} = 7750\text{h}$), and C) infrared spectra of the Lemon oil paint before and after irradiation with a Xenon lamp ($\lambda_{\text{irr}} > 300 \text{ nm}$); (\blackstar) $\text{PbCr}_{0.6}\text{S}_{0.4}\text{O}_4$	112
Figure 4.16. A) SR μ -FTIR chemical maps (size: $130 \times 150 \mu\text{m}^2$, with $10 \times 10 \mu\text{m}^2$ step size), ROI: acids ($1718\text{-}1700 \text{ cm}^{-1}$), esters ($1755\text{-}1720 \text{ cm}^{-1}$), chromate ($920\text{-}800 \text{ cm}^{-1}$); B) SR μ -XRF map around Cr K-edge at 5.993 and 6.1 keV (map size: $26 \times 100 \mu\text{m}^2$, with $1.5 \times 1.5 \mu\text{m}^2$ pixel size); C) normalized Cr K-edge XANES spectrum at point a), and S K-edge μ -XANES spectrum acquired at the surface of a cross-section from the Lemon oil paint after 7750h of irradiation. See also Figure XIX.8 (p. 365).....	113
Figure 4.17. SR infrared spectrum obtained on the surface of an embedding-free thin cross-section of the Lemon oil paint after 11000h of irradiation and of the reference compound chromium potassium sulfate $\text{CrK}(\text{SO}_4)_2 \cdot 12\text{H}_2\text{O}$; (\blackstar) $\text{PbCr}_{0.6}\text{S}_{0.4}\text{O}_4$, (\blackplus) oxalic acid ($\text{C}_2\text{H}_2\text{O}_4$). See also Figure XIX.8 (p. 365).....	114
Figure 4.18. A) Normalized FORS and B) infrared spectra of the historic W&N <i>Chrome Yellow</i> oil paint before and after irradiation with a Xenon lamp ($\lambda_{\text{irr}} > 300 \text{ nm}$); (\blackstar) $\text{PbCr}_{0.6}\text{S}_{0.4}\text{O}_4$, (\blacktriangle) BaSO_4 , (\blacklozenge) $\text{MgCO}_3 \cdot x\text{H}_2\text{O}$, (\blackdiamond) zinc linoleate, (\blackodot) oxalate compound.....	116
Figure 4.19. A) SR μ -FTIR maps (size: $136 \times 72 \mu\text{m}^2$, with $8 \times 8 \mu\text{m}^2$ step size), ROI: acids ($1718\text{-}1700 \text{ cm}^{-1}$), esters ($1755\text{-}1720 \text{ cm}^{-1}$), oxalate compounds ($1620\text{-}1570 \text{ cm}^{-1}$), magnesium carbonate ($3480\text{-}3410 \text{ cm}^{-1}$); B) SR μ -XRF map around Cr K-edge at 5.993 and 6.1 keV (map size: $92 \times 46 \mu\text{m}^2$, with $2 \times 2 \mu\text{m}^2$ step size); C) Cr K-edge μ -XANES spectra acquired in point a) and S K-edge μ -XANES spectra acquired at the surface, of cross-sections from the W&N <i>Chrome Yellow</i> oil paint after 5250h (for μ -FTIR maps) and 8500h of irradiation. See also Figures XIX.10 and XIX.11 (p. 366).....	117

Figure 4.20. A) Normalized FORS and B) infrared spectra of the W&N <i>Chrome Deep</i> oil paint before and after irradiation with a Xenon lamp ($\lambda_{\text{irr}} > 300 \text{ nm}$); (★) PbCrO_4 , (●) CaCO_3 and (✧) $\text{MgCO}_3 \cdot x\text{H}_2\text{O}$...	118
Figure 4.21. A) SR μ -FTIR maps (size: $100 \times 100 \mu\text{m}^2$, with $10 \times 10 \mu\text{m}^2$ step size), ROI: acids ($1718\text{-}1700 \text{ cm}^{-1}$), esters ($1755\text{-}1720 \text{ cm}^{-1}$), calcium oxalate ($1615\text{-}1555 \text{ cm}^{-1}$), carbonate compounds ($1520\text{-}1350 \text{ cm}^{-1}$); B) SR μ -XRD maps (size: $49 \times 54 \mu\text{m}^2$, with $1.5 \times 1.5 \mu\text{m}^2$ step size) of cerussite (intensity of the (111) Bragg peak) and weddellite (Rietveld scaling factor); C) SR μ -XRF map around Cr K-edge at 5.993 and 6.1 keV (map size: $140 \times 200 \mu\text{m}^2$, with $1 \times 1 \mu\text{m}^2$ step size) and the Cr K-edge μ -XANES spectra acquired in point a), of cross-sections from the W&N <i>Chrome Deep</i> oil paint after 10000h of irradiation. See also Figures XIX.12 and XIX.13 (p. 367).....	119
Figure 4.22. A) Normalized FORS and B) infrared spectra of the historic <i>Lefranc Jaune de Chrome</i> oil paint a) fresh taken from the oil paint tube and b) exposed to ambient conditions for 6 years then exposed to irradiation with a Xenon lamp ($\lambda_{\text{irr}} > 300 \text{ nm}$); (★) PbCrO_4 , (⌘) lead azelate and (◎) oxalate compound.....	121
Figure 4.23. A) SR μ -XRF maps at 5.993 keV of Cr and Pb (map size: $171 \times 426 \mu\text{m}^2$, with $3 \times 3 \mu\text{m}^2$ step size) and the Cr K-edge μ -XANES spectra acquired in points a) and b) of a cross-section from the <i>Lefranc Jaune de Chrome</i> oil paint before irradiation (naturally aged for 6 years); B) SR μ -FTIR maps (size: $180 \times 110 \mu\text{m}^2$, with $10 \times 10 \mu\text{m}^2$ step size) of a embedding-free cross-section from the <i>Lefranc Jaune de Chrome</i> oil paint after 5250h of irradiation, ROI: acids ($1718\text{-}1700 \text{ cm}^{-1}$), esters ($1755\text{-}1720 \text{ cm}^{-1}$), oxalate compounds ($1615\text{-}1555 \text{ cm}^{-1}$), lead chromate ($920\text{-}800 \text{ cm}^{-1}$); see also Figures XIX.15 and XIX.16 (p. 368).....	122
Figure III.1.1. Number of production records and date range for each of the Primrose Chrome manufacturing processes.....	205
Figure III.2.1. Number of production records and date range for each of the Lemon (L) Chrome manufacturing processes.....	208
Figure III.2.2. Number of production records and date range for each of the Pale (P) Chrome manufacturing processes.....	208
Figure III.3.1. Number of production records and date range for each of the Middle Chrome manufacturing processes.....	216
Figure III.4.1. Number of production records and date range for each of the Deep Chrome manufacturing processes.....	220
Figure IV.1.1. Number of production records and date range for each of the Lemon Yellow manufacturing processes.....	225
Figure IV.2.1. Number of production records and date range for each of the Citron Yellow manufacturing processes.....	228
Figure IV.3.1. Number of production records and date range for each of the Strontian Yellow manufacturing processes.....	230
Figure VI.2.1. SEM image of lead chromate (lead chromate (PbCrO_4 , monoclinic crystal structure); lead chromate (PbCrO_4 , orthorhombic crystal structure); lead white obtained by the stack process ($2\text{PbCO}_3 \cdot \text{Pb}(\text{OH})_2$); barium sulfate (BaSO_4), calcium carbonate (CaCO_3) and calcium sulfate dihydrate ($\text{CaSO}_4 \cdot 2\text{H}_2\text{O}$).....	244
Figure VI.3.1. Raman spectra of lead chromate (PbCrO_4 , monoclinic crystal structure); lead chromate (PbCrO_4 , orthorhombic crystal structure); basic lead chromate (Pb_2CrO_5); lead sulfate (PbSO_4); barium sulfate (BaSO_4) and barium carbonate (BaCO_3).....	245
Figure VI.3.2. Raman spectra of lead carbonate (PbCO_3); lead white ($2\text{PbCO}_3 \cdot \text{Pb}(\text{OH})_2$); calcium carbonate (CaCO_3); magnesium carbonate ($\text{MgCO}_3 \cdot x\text{H}_2\text{O}$); sodium carbonate (Na_2CO_3) and potassium carbonate (K_2CO_3).....	246
Figure VI.3.3. Raman spectra of calcium sulfate anhydrous (CaSO_4); calcium sulfate hemihydrate ($\text{CaSO}_4 \cdot \frac{1}{2}\text{H}_2\text{O}$); calcium sulfate dihydrate ($\text{CaSO}_4 \cdot 2\text{H}_2\text{O}$); sodium sulfate (Na_2SO_4); zinc sulfate heptahydrate ($\text{ZnSO}_4 \cdot 7\text{H}_2\text{O}$) and magnesium sulfate heptahydrate ($\text{MgSO}_4 \cdot 7\text{H}_2\text{O}$)....	247

Figure VI.3.4. Raman spectra of lead nitrate ($\text{Pb}(\text{NO}_3)_2$); lead oxide (PbO); zinc nitrate ($\text{Zn}(\text{NO}_3)_2$); lead acetate trihydrate ($\text{Pb}(\text{CH}_3\text{CO}_2)_2 \cdot 3\text{H}_2\text{O}$); strontium nitrate ($\text{Sr}(\text{NO}_3)_2$) and lead subacetate ($\text{Pb}(\text{Ac})_2 \cdot 2\text{Pb}(\text{OH})_2$).....	248
Figure VI.3.5. Raman spectra of barium chloride (BaCl_2); strontium sulfate (SrSO_4); hematite ($\alpha\text{-Fe}_2\text{O}_3$); goethite ($\alpha\text{-FeOOH}$), maghemite ($\gamma\text{-Fe}_2\text{O}_3$) and manganese oxide (MnO_2).....	249
Figure VI.3.6. Raman spectra of zinc white (ZnO), vermilion (HgS); cadmium yellow (CdS); quartz (SiO_2); cobalt blue ($\text{CoO} \cdot \text{Al}_2\text{O}_3$) and cerulean blue ($\text{CoO} \cdot n\text{SnO}_2$).....	250
Figure VI.3.7. Raman spectra of ultramarine blue ($3\text{Na}_2\text{O} \cdot 3\text{Al}_2\text{O}_3 \cdot 6\text{SiO}_2 \cdot 2\text{Na}_2\text{S}$); cobalt yellow ($\text{K}_3\text{Co}(\text{NO}_2)_6 \cdot 3\text{H}_2\text{O}$); Prussian blue ($\text{Fe}_4[\text{Fe}(\text{CN})_6]_3$); emerald green ($\text{Cu}(\text{C}_2\text{H}_3\text{O}_2)_2 \cdot 3\text{Cu}(\text{AsO}_2)_2$); viridian ($\text{Cr}_2\text{O}_3 \cdot 2\text{H}_2\text{O}$); chromium (III) oxide (Cr_2O_3).....	251
Figure VI.3.8. Raman spectra of carbon black (C); potassium chromate (K_2CrO_4); potassium dichromate ($\text{K}_2\text{Cr}_2\text{O}_7$); sodium chromate ($\text{Na}_2\text{CrO}_4 \cdot x\text{H}_2\text{O}$); sodium dichromate ($\text{Na}_2\text{Cr}_2\text{O}_7 \cdot x\text{H}_2\text{O}$); chromium acetate hydroxide ($(\text{CH}_3\text{CO}_2)_7\text{Cr}_3(\text{OH})_2$).....	252
Figure VI.3.9. Raman spectra of chromium potassium sulfate dodecahydrate ($\text{CrK}(\text{SO}_4)_2 \cdot 12\text{H}_2\text{O}$); chromium acetylacetonate ($\text{Cr}(\text{C}_5\text{H}_7\text{O}_2)_3$); potassium chromium oxalate trihydrate ($\text{K}_3\text{Cr}(\text{C}_2\text{O}_4)_3 \cdot 3\text{H}_2\text{O}$); calcium oxalate monohydrate ($\text{CaC}_2\text{O}_4 \cdot \text{H}_2\text{O}$); zinc oxalate dihydrate ($\text{ZnC}_2\text{O}_4 \cdot 2\text{H}_2\text{O}$) and lead oxalate (PbC_2O_4).....	253
Figure VI.4.1. Infrared spectra of lead chromate (PbCrO_4 , monoclinic crystal structure); lead chromate (PbCrO_4 , orthorhombic crystal structure); basic lead chromate (Pb_2CrO_5); lead sulfate (PbSO_4); barium sulfate (BaSO_4) and lead carbonate (PbCO_3).....	256
Figure VI.4.2. Infrared spectra of lead white ($2\text{PbCO}_3 \cdot \text{Pb}(\text{OH})_2$); calcium carbonate (CaCO_3); magnesium carbonate ($\text{MgCO}_3 \cdot x\text{H}_2\text{O}$); calcium sulfate anhydrous (CaSO_4); calcium sulfate hemihydrate ($\text{CaSO}_4 \cdot \frac{1}{2}\text{H}_2\text{O}$) and calcium sulfate dihydrate ($\text{CaSO}_4 \cdot 2\text{H}_2\text{O}$).....	257
Figure VI.4.3. Infrared spectra of lead nitrate ($\text{Pb}(\text{NO}_3)_2$); lead acetate trihydrate ($\text{Pb}(\text{CH}_3\text{CO}_2)_2 \cdot 3\text{H}_2\text{O}$); zinc nitrate ($\text{Zn}(\text{NO}_3)_2$); lead subacetate ($\text{Pb}(\text{Ac})_2 \cdot 2\text{Pb}(\text{OH})_2$); strontium nitrate ($\text{Sr}(\text{NO}_3)_2$) and sodium carbonate (Na_2CO_3).....	258
Figure VI.4.4. Infrared spectra of potassium carbonate (K_2CO_3); ammonium carbonate ($(\text{NH}_4)_2\text{CO}_3$); sodium sulfate (Na_2SO_4); zinc sulfate heptahydrate ($\text{ZnSO}_4 \cdot 7\text{H}_2\text{O}$); magnesium sulfate heptahydrate ($\text{MgSO}_4 \cdot 7\text{H}_2\text{O}$) and kaolin ($\text{Al}_2\text{Si}_2\text{O}_5(\text{OH})_4$).....	259
Figure VI.4.5. Infrared spectra of cobalt yellow ($\text{K}_3\text{Co}(\text{NO}_2)_6 \cdot 3\text{H}_2\text{O}$); Prussian blue ($\text{Fe}_4[\text{Fe}(\text{CN})_6]_3$); ultramarine blue ($3\text{Na}_2\text{O} \cdot 3\text{Al}_2\text{O}_3 \cdot 6\text{SiO}_2 \cdot 2\text{Na}_2\text{S}$); emerald green ($\text{Cu}(\text{C}_2\text{H}_3\text{O}_2)_2 \cdot 3\text{Cu}(\text{AsO}_2)_2$), the only reference available is from an historic oil paint (\blacklozenge); viridian ($\text{Cr}_2\text{O}_3 \cdot 2\text{H}_2\text{O}$) and chromium (III) oxide (Cr_2O_3).....	260
Figure VI.4.6. Infrared spectra of and chromium (VI) oxide (CrO_3); potassium chromate (K_2CrO_4); potassium dichromate ($\text{K}_2\text{Cr}_2\text{O}_7$); sodium chromate ($\text{Na}_2\text{CrO}_4 \cdot x\text{H}_2\text{O}$); sodium dichromate ($\text{Na}_2\text{Cr}_2\text{O}_7 \cdot x\text{H}_2\text{O}$) and chromium acetylacetonate ($\text{Cr}(\text{C}_5\text{H}_7\text{O}_2)_3$).....	261
Figure VI.4.7. Infrared spectra of and chromium acetate hydroxide ($(\text{CH}_3\text{CO}_2)_7\text{Cr}_3(\text{OH})_2$); chromium sulfate ($\text{Cr}_2(\text{SO}_4)_3$); chromium potassium sulfate dodecahydrate ($\text{CrK}(\text{SO}_4)_2 \cdot 12\text{H}_2\text{O}$); lead palmitate; lead azelate and zinc linoleate.....	262
Figure VI.4.8. Infrared spectra of potassium chromium oxalate trihydrate ($\text{K}_3\text{Cr}(\text{C}_2\text{O}_4)_3 \cdot 3\text{H}_2\text{O}$); oxalic acid ($\text{C}_2\text{O}_4\text{H}_2$); calcium oxalate monohydrate ($\text{CaC}_2\text{O}_4 \cdot \text{H}_2\text{O}$); calcium oxalate dihydrate ($\text{CaC}_2\text{O}_4 \cdot 2\text{H}_2\text{O}$); zinc oxalate dihydrate ($\text{ZnC}_2\text{O}_4 \cdot 2\text{H}_2\text{O}$), lead oxalate (PbC_2O_4).....	263
Figure VI.4.9. Infrared spectra of linseed oil and poly(vinyl) acetate ($[\text{CH}_2\text{CH}(\text{O}_2\text{CCH}_3)]_n$).....	264
Figure VI.5.1. Cr K-edge μ -XANES spectra of Cr^{6+} reference compounds: lead chromate (PbCrO_4 , monoclinic crystal structure); lead chromate (PbCrO_4 , orthorhombic crystal structure); basic lead chromate (Pb_2CrO_5), potassium chromate (K_2CrO_4); sodium chromate ($\text{Na}_2\text{CrO}_4 \cdot x\text{H}_2\text{O}$) and chromium (VI) oxide (CrO_3).....	267
Figure VI.5.2. Cr K-edge μ -XANES spectra of Cr^{6+} reference compounds: potassium dichromate ($\text{K}_2\text{Cr}_2\text{O}_7$) and sodium dichromate ($\text{Na}_2\text{Cr}_2\text{O}_7 \cdot x\text{H}_2\text{O}$).....	268

Figure VI.5.3. Cr K-edge μ -XANES spectra of Cr ³⁺ reference compounds: chromium (III) oxide (Cr ₂ O ₃); viridian (Cr ₂ O ₃ ·2H ₂ O); chromium acetate hydroxide ((CH ₃ CO ₂) ₇ Cr ₃ (OH) ₂) and chromium acetylacetonate (Cr(C ₅ H ₇ O ₂) ₃).....	268
Figure VI.5.4. Cr K-edge μ -XANES spectra of Cr ³⁺ reference compounds: chromium sulfate (Cr ₂ (SO ₄) ₃); chromium potassium sulfate dodecahydrate (CrK(SO ₄) ₂ ·12H ₂ O) and potassium chromium oxalate trihydrate (K ₃ Cr(C ₂ O ₄) ₃ ·3H ₂ O).....	269
Figure VI.5.5. S K-edge μ -XANES spectra of chromium sulfate (Cr ₂ (SO ₄) ₃) and chromium potassium sulfate dodecahydrate (CrK(SO ₄) ₂ ·12H ₂ O).....	269
Figure VI.5.6. S K-edge μ -XANES spectra of calcium sulfate (CaSO ₄); calcium sulfate hemihydrate (CaSO ₄ ·½H ₂ O); calcium sulfate dihydrate (CaSO ₄ ·2H ₂ O); barium sulfate (BaSO ₄); lead sulfate (PbSO ₄) and lead sulfide (PbS).....	270
Figure VI.5.7. Ca K-edge μ -XANES spectra of calcium sulfate (CaSO ₄); calcium sulfate hemihydrate (CaSO ₄ ·½H ₂ O); calcium sulfate dihydrate (CaSO ₄ ·2H ₂ O); calcium carbonate (CaCO ₃) and calcium oxalate monohydrate (CaC ₂ O ₄ ·H ₂ O).....	271
Figure VII.1. Infrared spectra of A) lead nitrate (synthesised and reference) and B) lead subacetate ('correct' and 'wrong'). Diffraction patterns of the lead subacetate C) 'wrong' and reference, and D) 'correct'.....	273
Figure VIII.1. Variation of the $A_{\text{vas}}(\text{SO}_4^{2-})/A_{\text{vas}}(\text{CrO}_4^{2-})$ as a function of the SO ₄ ²⁻ molar fraction. The ratio was calculated using the absorbance of $\nu_{\text{as}}(\text{SO}_4^{2-})$ at 1100 cm ⁻¹ normalized to the $\nu_{\text{as}}(\text{CrO}_4^{2-})$ at 853 cm ⁻¹ after baseline correction.....	276
Figure VIII.2. Infrared (left) and Raman (right) spectra of CY1 (PbCrO ₄), CY2 and CY3 pigment references.....	277
Figure VIII.3. Infrared (left) and Raman (right) spectra of CY4, CY5 and CY6 pigment references	278
Figure VIII.4. Infrared (left) and Raman (right) spectra of CY7, CY8 and CY9 pigment references	279
Figure VIII.5. Infrared (left) and Raman (right) spectra of CY10 and CY11 (PbSO ₄) pigment references	280
Figure VIII.6. Diffraction pattern of CY1 (PbCrO ₄), CY2 and CY3 pigment references. The main diffraction peaks of lead chromate monoclinic crystal structure are marked in black dotted lines...	282
Figure VIII.7. Diffraction pattern of CY4, CY5 and CY6 pigment references. The main diffraction peaks of lead chromate monoclinic crystal structure are marked in black dotted lines.....	283
Figure VIII.8. Diffraction pattern of CY7, CY8 and CY9 pigment references. The main diffraction peaks of lead chromate monoclinic and lead sulfate orthorhombic crystal structure are marked in black and red dotted lines, respectively.....	284
Figure VIII.9. Diffraction pattern of CY10 and CY11 (PbSO ₄) pigment references. The main diffraction peaks of lead sulfate orthorhombic crystal structure are marked in red dotted lines.....	285
Figure X.1.1. PR1a pigment reconstruction: elements detected by μ -EDXRF, representative A) infrared, B) μ -Raman, C) FORS, D) Cr K-edge μ -XANES spectra, E) diffraction pattern and F) SEM image.....	293
Figure X.1.2. PR1b pigment reconstruction: elements detected by μ -EDXRF, A) infrared, B) μ -Raman, C) FORS spectra, D) diffraction pattern and E) SEM image.....	294
Figure X.1.3. PR1b* pigment reconstruction: elements detected by μ -EDXRF, A) infrared, B) μ -Raman, C) FORS, D) Cr K-edge μ -XANES spectra, E) diffraction pattern and F) SEM image.....	295
Figure X.1.4. PR1b_1 pigment reconstruction: elements detected by μ -EDXRF, A) infrared, B) μ -Raman, C) FORS, D) Cr K-edge μ -XANES spectra, E) diffraction pattern and F) SEM image...	296
Figure X.1.5. PR1b_2 pigment reconstruction: elements detected by μ -EDXRF, A) infrared, B) μ -Raman, C) FORS, D) Cr K-edge μ -XANES spectra, E) diffraction pattern and F) SEM image...	297
Figure X.2.1. L1 pigment reconstruction: elements detected by μ -EDXRF, representative A) infrared, B) μ -Raman, C) FORS spectra, D) diffraction pattern and E) SEM image; (\star) PbCr _{0.8} S _{0.2} O ₄ , (\diamond) PbCO ₃ and (\bullet) PbSO ₄	298

Figure X.2.2. L2a pigment reconstruction: elements detected by μ -EDXRF, representative A) infrared, B) μ -Raman, C) FORS, D) Cr K-edge μ -XANES spectra, D) diffraction pattern and E) SEM image; (\star) $\text{PbCr}_{0.6}\text{So}_{0.4}\text{O}_4$, (\blacktriangle) BaSO_4	299
Figure X.2.3. L2b pigment reconstruction: elements detected by μ -EDXRF, representative A) infrared, B) μ -Raman, C) FORS, D) Cr K-edge μ -XANES spectra, E) diffraction pattern and F) SEM image.....	300
Figure X.2.4. L3a pigment reconstruction: elements detected by μ -EDXRF, representative A) infrared, B) μ -Raman, C) FORS, D) Cr K-edge μ -XANES spectra, E) diffraction pattern and F) SEM image; (\star) $\text{PbCr}_{0.8}\text{So}_{0.2}\text{O}_4$, (\blacklozenge) PbCO_3 and (\blacklozenge) $\text{CaSO}_4 \cdot 2\text{H}_2\text{O}$	301
Figure X.2.5. L3b pigment reconstruction: elements detected by μ -EDXRF, representative A) infrared, B) μ -Raman, C) FORS, D) Cr K-edge μ -XANES spectra, E) diffraction pattern and F) SEM image; (\star) $\text{PbCr}_{0.8}\text{So}_{0.2}\text{O}_4$, (\blacklozenge) PbCO_3	302
Figure X.2.6. L3a*₁ pigment reconstruction: elements detected by μ -EDXRF, A) infrared, B) μ -Raman, C) FORS, D) Cr K-edge μ -XANES spectra, E) diffraction pattern and F) SEM image; (\star) PbCrO_4 , (\bullet) CaCO_3 and (\blacklozenge) $\text{CaSO}_4 \cdot 2\text{H}_2\text{O}$	303
Figure X.2.7. L3a*₂ pigment reconstruction: elements detected by μ -EDXRF, A) infrared, B) μ -Raman, C) FORS, D) Cr K-edge μ -XANES spectra, E) diffraction pattern and F) SEM image; (\star) PbCrO_4 , (\bullet) CaCO_3 and (\blacklozenge) $\text{CaSO}_4 \cdot 2\text{H}_2\text{O}$	304
Figure X.3.1. M1a pigment reconstruction: elements detected by μ -EDXRF, representative A) infrared, B) μ -Raman, C) FORS, D) Cr K-edge μ -XANES spectra, E) diffraction pattern and F) SEM image; (\star) PbCrO_4 , (\blacklozenge) PbCO_3 and (\bullet) CaCO_3	305
Figure X.3.2. M1b pigment reconstruction: elements detected by μ -EDXRF, A) infrared, B) μ -Raman, C) FORS spectra, and D) diffraction pattern; (\star) PbCrO_4 , (\blacklozenge) PbCO_3 and (\blackstar) Pb_2CrO_5 ..	306
Figure X.3.3. M2a pigment reconstruction: elements detected by μ -EDXRF, representative A) infrared, B) μ -Raman, C) FORS spectra, D) diffraction pattern and E) SEM image; (\star) PbCrO_4 , (\blacktriangle) BaSO_4 and (\blackstar) Pb_2CrO_5	307
Figure X.3.4. D1a pigment reconstruction: elements detected by μ -EDXRF, representative A) infrared, B) μ -Raman, C) FORS spectra, D) diffraction pattern and E) SEM image; (\star) PbCrO_4 , (\blacklozenge) $\text{CaSO}_4 \cdot 2\text{H}_2\text{O}$, (\blacktriangle) BaSO_4 and (\blacklozenge) PbCO_3	308
Figure X.3.5. D1b pigment reconstruction. elements detected by μ -EDXRF, representative A) infrared, B) μ -Raman, C) FORS spectra, D) diffraction pattern and E) SEM image; (\star) PbCrO_4 , (\blacktriangle) BaSO_4 and (\blackstar) Pb_2CrO_5	309
Figure X.3.6. D2a pigment reconstruction: elements detected by μ -EDXRF, representative A) infrared, B) μ -Raman, C) FORS spectra, D) diffraction pattern and E) SEM image; (\star) PbCrO_4 , (\blacklozenge) $\text{CaSO}_4 \cdot 2\text{H}_2\text{O}$, (\blacktriangle) BaSO_4 and (\blackstar) Pb_2CrO_5	310
Figure XI.1. μ -EDXRF spectra, FORS spectra (acquired in paints applied on filter paper) and diffraction patterns of the W&N <i>Chrome Yellow</i> (left) and <i>Chrome Deep</i> (right) oil paint tubes (see Table 3.5, p. 55); (\blacktriangle) BaSO_4 and (\bullet) CaCO_3 . μ -EDXRF and FORS spectra of the W&N <i>Chrome Deep</i> oil paint tube belonging to Columbano are similar to the one presented; no diffraction pattern was acquired due to the lack of quantity.....	311
Figure XI.2. Top: μ -EDXRF spectra of Lefranc's <i>Jaune de Chrome foncé</i> and <i>Jaune de Chrome foncé - tempera farge</i> (unidentified colourman) paint tubes (Melo <i>et al.</i> , 2009). Bottom: FORS and SEM image of the Lefranc's <i>Jaune de Chrome foncé</i> oil paint tube (bottom) (see Table 3.5, p. 55). No diffraction pattern was acquired due to the lack of quantity.....	312
Figure XIII.1.1. Amadeo de Sousa-Cardoso painting: <i>Gemälde G / Quadro G</i> , c.1912, 51 x 29.5 cm (Inv. 77P2, cat. n ^o P41, Freitas, 2008, p. 182) © FCG. Analysis areas: μ -EDXRF (\bullet), μ -sampling (\bullet) and cross-sections (\bullet).....	319
Figure XIII.1.2. Photomicrographs (7x to 25x) of Amadeo de Sousa-Cardoso painting: <i>Gemälde G / Quadro G</i> , c.1912 (Inv. 77P2, cat. n ^o P41).....	320

Figure XIII.2.1. Amadeo de Sousa-Cardoso painting: <i>Untitled, O Jockey</i> , c.1913, 61 x 50 cm (Inv. 77P5, cat. n° P58, Freitas, 2008, p. 209) © FCG. Analysis areas: μ -EDXRF (●), μ -sampling (●) and cross-sections (●).....	326
Figure XIII.2.2. Photomicrographs (10x) of Amadeo de Sousa-Cardoso painting: <i>Untitled, O Jockey</i> , c.1913 (Inv. 77P5, cat. n° P58).....	327
Figure XIII.3.1. Amadeo de Sousa-Cardoso painting: <i>Untitled</i> , c.1913, 34.4 x 28.2 cm (Inv. 92P209, cat. n° P75, Freitas, 2008, p. 229) © FCG. Analysis areas: μ -EDXRF (●), μ -sampling (●) and cross-sections (●).....	334
Figure XIII.3.2. Photomicrographs (7x to 10x) of Amadeo de Sousa-Cardoso painting: <i>Untitled</i> , c.1913 (Inv. 92P209, cat. n° P75).....	334
Figure XIII.4.1. Amadeo de Sousa-Cardoso painting: <i>Mucha</i> , c.1915-16, 27.3 x 21.4 cm (Inv. 86P21, cat. n° P172, Freitas, 2008, p. 322) © FCG. Analysis areas: μ -EDXRF (●), μ -sampling (●) and cross-sections (●).....	338
Figure XIII.4.2. Photomicrographs (7x to 32x) of Amadeo de Sousa-Cardoso painting: <i>Mucha</i> , c.1915-16 (Inv. 86P21, cat. n° P172), from Melo <i>et al.</i> , 2009.....	338
Figure XIV.1.1. Representative A) infrared, B) μ -Raman, C) FORS, D) μ -EDXRF spectra and E) diffraction pattern of LY1a pigment reconstruction.....	343
Figure XIV.2.1. Representative A) infrared, B) μ -Raman, C) FORS, D) μ -EDXRF spectra and E) diffraction pattern of CY1a pigment reconstruction.....	344
Figure XIV.3.1. Representative A) infrared, B) μ -Raman, C) FORS, D) μ -EDXRF spectra and E) diffraction pattern of SY1a pigment reconstruction.....	345
Figure XV.1. μ -EDXRF, Raman and FORS spectra of the W&N <i>Lemon Yellow</i> oil paint tube.....	347
Figure XVII.1. Normalized FORS, μ -FTIR spectra: (★) $\text{PbCr}_{1-x}\text{S}_x\text{O}_4$, (★) PbCrO_4 , (❖) PbCO_3 and (●) CaCO_3 , the remaining bands correspond to the PVAc binder; and normalized Cr K-edge XANES spectra of PR1b_2 and M1a PVAc paints before and after irradiation.....	353
Figure XVII.2. Normalized FORS, μ -FTIR spectra: (★) $\text{PbCr}_{1-x}\text{S}_x\text{O}_4$, (❖) PbCO_3 and (◆) $\text{CaSO}_4 \cdot 2\text{H}_2\text{O}$, the remaining bands correspond to the PVAc binder; and normalized Cr K-edge XANES spectra of L3a and L3b PVAc paints before and after irradiation.....	354
Figure XVII.3. Normalized FORS, μ -FTIR spectra: (★) $\text{PbCr}_{1-x}\text{S}_x\text{O}_4$, the remaining bands correspond to the PVAc binder; and normalized Cr K-edge XANES spectra of PR1b_1 and PR1a PVAc paints before and after irradiation.....	355
Figure XVII.4. Normalized FORS, μ -FTIR spectra: (★) $\text{PbCr}_{1-x}\text{S}_x\text{O}_4$, (▲) BaSO_4 , the remaining bands correspond to the PVAc binder; and normalized Cr K-edge XANES spectra of L2a and L2b PVAc paints before and after irradiation.....	356
Figure XVII.5. Normalized FORS, μ -FTIR spectra: (★) PbCrO_4 , (●) CaCO_3 , (◆) $\text{CaSO}_4 \cdot 2\text{H}_2\text{O}$, the remaining bands correspond to the PVAc binder; and normalized Cr K-edge XANES spectra of L3a*_2 PVAc paint before and after irradiation.....	357
Figure XVIII.1. SR μ -XRF elemental maps (left) obtained at Cr K-edge (5.993 and 6.1 keV) of an embedding-free thick cross-section of the PR1a PVAc paint after 5250h of irradiation time (map size: $26 \times 100 \mu\text{m}^2$, with $1.5 \times 1.5 \mu\text{m}^2$ pixel size), and the normalized Cr K-edge XANES spectrum (right) acquired at point a).....	359
Figure XVIII.2. SR μ -FTIR chemical maps (left) of an embedding-free thin cross-section of the PR1a PVAc paint after 5250h of irradiation time (map size: $80 \times 80 \mu\text{m}^2$, with $10 \times 10 \mu\text{m}^2$ pixel size), and the respective infrared map average spectrum (right); ROI: polyvinyl acetate ($1710\text{-}1770 \text{ cm}^{-1}$) and chromate ($800\text{-}920 \text{ cm}^{-1}$); (★) $\text{PbCr}_{1-x}\text{S}_x\text{O}_4$	359

Figure XVIII.3. Infrared spectra of the L3a*_2 PVAc paint before and after 5250h of irradiation time, obtained using the SR μ -FTIR; (★) PbCrO ₄ , (●) CaCO ₃ , (◆) CaSO ₄ .2H ₂ O, the remaining bands correspond to the PVAc binder. The ν (CH) and ν (C=O) regions are highlighted to show the differences resulting from the presence of degradation products.....	360
Figure XIX.1. FORS (left) and infrared (right) spectra of the lead chromate oil paint reference before and after irradiation with a Xenon lamp; (★) PbCrO ₄	361
Figure XIX.2. Normalized Cr K-edge μ -XANES spectra of the lead chromate reference and the W&N <i>Chrome Deep</i> oil paints before and after irradiation with a Xenon lamp ($\lambda_{irr} > 300$ nm).....	361
Figure XIX.3. SR μ -FTIR chemical maps (left) of an embedding-free thin cross-section of the Middle oil paint reconstruction, naturally aged for 2 and a half years (map size: 80 × 140 μm^2 , with 10 × 10 μm^2 pixel size), and the respective infrared map average spectrum (right); ROI: ester (1755-1720 cm^{-1}), acid (1718-1700 cm^{-1}) and CaCO ₃ (1550-1520 cm^{-1}); (★) PbCrO ₄ , (●) CaCO ₃ , (◆) CaSO ₄ .2H ₂ O.....	362
Figure XIX.4. A) Infrared map average spectrum for SR μ -FTIR maps shown in Figure 4.10 (p. 107); B) optical microscope image of an embedding-free thin cross-section of the Middle oil paint after 7750h of irradiation, where the black area highlighted corresponds to the SR μ -XRF maps at Cr 5.993 and 6.1 keV (left), and at 5.993 keV of Cr, S and Ca (right) (vertical map size: 92 × 192 μm^2 and diagonal map size: 152 × 100 μm^2 , with 2 × 2 μm^2 pixel size); (★) PbCrO ₄ , (●) CaCO ₃ , (◆) CaSO ₄ .2H ₂ O and (◇) CaC ₂ O ₄ . xH ₂ O.....	362
Figure XIX.5. SR infrared spectrum obtained on the surface of a embedding-free thin cross-section of the Middle oil paint CR7 after 7750h of irradiation and four reference compounds between 1800 and 850 cm^{-1} : chromium potassium sulfate CrK(SO ₄) ₂ .12H ₂ O, gypsum (CaSO ₄ .2H ₂ O), oxalic acid (C ₂ H ₂ O ₄), calcium oxalate dihydrate (CaC ₂ O ₄ .2H ₂ O, weddellite); (●) CaCO ₃ and (★) PbCrO ₄	363
Figure XIX.6. A) Infrared map average spectrum for SR μ -FTIR map and B) diffraction pattern obtained at the surface of the analysed cross-sections from the Middle oil paint after 11000h of irradiation, shown in Figure 4.13 (p. 109); (★) PbCrO ₄ , (●) CaCO ₃ , (◆) CaSO ₄ .2H ₂ O and (◇) CaC ₂ O ₄ . 2H ₂ O.....	364
Figure XIX.7. A) Optical microscope image of an embedding-free thin cross-section of the Middle oil paint after 11000h of irradiation, where the black area highlighted corresponds to the SR μ -XRF map around S K-edge at 2.473, 2.478 and 2.842 keV (size: 100 × 100 μm^2 , with 1 × 1 μm^2 step size); B) S K-edge μ -XANES spectra of the point in the map; and C) Ca K-edge μ -XANES spectra obtained at the lower part of the SR μ -XRF map around Ca K-edge shown in Figure 4.13 (p. 109).....	364
Figure XIX.8. A) Infrared map average spectrum for SR μ -FTIR maps ($t_{irr} = 7750$ h) shown in Figure 4.16 (p. 113) and B) SR infrared spectrum obtained on the surface of an embedding-free thin cross-section of the Lemon oil paint after 11000h of irradiation and of the reference compound oxalic acid C ₂ H ₂ O ₄ : (★) PbCr _{0.6} S _{0.4} O ₄	365
Figure XIX.9. Diffraction pattern obtained at the surface of a cross-section from the Lemon oil paint after 11000h of irradiation, which corresponds solely to monoclinic lead chromate (Figure 3.6, p. 57).....	365
Figure XIX.10. A) Infrared map average spectrum for SR μ -FTIR maps shown in Figure 4.19 (p. 117) and in B; B) SR μ -FTIR map (size: 136 × 72 μm^2 , with 8 × 8 μm^2 step size) of zinc linoleate (1560-1525 cm^{-1}) and oxalate compound (1620-1570 cm^{-1}); C) SR μ -XRF map at 5.993 keV of Cr and Ba (map size: 92 × 46 μm^2 , with 2 × 2 μm^2 step size), of cross-sections from the W&N <i>Chrome Yellow</i> oil paint after 5250h (for μ -FTIR maps) and 8500h of irradiation; (★) PbCr _{0.6} S _{0.4} O ₄ , (▲) BaSO ₄ , (❖) MgCO ₃ .xH ₂ O and (⊙) oxalate compound.....	366
Figure XIX.11. Diffraction pattern obtained at the surface of a cross-section from the W&N <i>Chrome Yellow</i> oil paint after 8500h of irradiation; (▲) BaSO ₄	366

Figure XIX.12. A) Infrared map average spectrum for SR μ -FTIR map shown in Figure 4.21 (p. 119); **B)** SR μ -XRF maps at Cr 5.993 and 6.1 keV (left), and at 5.993 keV of Cr and Ca (right) (map size: $140 \times 200 \mu\text{m}^2$, with $1 \times 1 \mu\text{m}^2$ step size) acquired on a cross-section of the W&N *Chrome Deep* oil paint after 10000h of irradiation; (★) PbCrO_4 , (●) CaCO_3 , (❖) $\text{MgCO}_3 \cdot x\text{H}_2\text{O}$ 367

Figure XIX.13. Diffraction patterns from the SR μ -XRD map shown in Figure 4.21 (p. 119) acquired on a cross-section of the W&N *Chrome Deep* oil paint after 10000h of irradiation, representative of the presence of **A)** calcium oxalate dihydrate and **B)** cerussite; (●) CaCO_3 , (◇) $\text{CaC}_2\text{O}_4 \cdot 2\text{H}_2\text{O}$ and (❖) PbCO_3 367

Figure XIX.14. A) SEM images of cross-sections from the *Lefranc Jaune de Chrome* oil paint **A)** before and **B)** after 5250h of irradiation with a Xenon lamp ($\lambda_{\text{irr}} > 300 \text{ nm}$)..... 368

Figure XIX.15. A) Infrared map average spectrum for SR μ -FTIR map shown in Figure 4.23 (p. 121); and **B)** diffraction pattern obtained at the surface of a cross-section from the *Lefranc Jaune de Chrome* oil paint after 8500h of irradiation; (★) PbCrO_4 368

Figure XIX.16. SR μ -FTIR maps (size: $180 \times 110 \mu\text{m}^2$, with $10 \times 10 \mu\text{m}^2$ step size) of a embedding-free cross-section from the *Lefranc Jaune de Chrome* oil paint after 5250h of irradiation, ROI: acids ($1718\text{-}1700 \text{ cm}^{-1}$), esters ($1755\text{-}1720 \text{ cm}^{-1}$), carboxylate compounds ($1555\text{-}1510 \text{ cm}^{-1}$), oxalate compounds ($1615\text{-}1555 \text{ cm}^{-1}$), lead chromate ($920\text{-}800 \text{ cm}^{-1}$)..... 368

Index of Tables

Table 1.1. Amadeo's main pigments: common names and chemical formulas (Melo <i>et al.</i> , 2009; Montagner, 2015).....	21
Table 1.2. Other pigments used in the paintings of c.1917 (Figure 1.9): common names and chemical formulas (Montagner, 2015).....	21
Table 2.1. Estimated dates of W&N's 19 th century catalogues (included by Mark Clarke in the database). For the dates highlighted in bold, these catalogues are complete. See also Table II.1.1. (p. 161).....	30
Table 2.2. General content of the 85 books (codes as in the database). Highlighted in bold is the book belonging to Henry Charles Newton, and bold+underlined to Arthur Henry Newton. See also Table II.1.2 (p. 162).....	32
Table 2.3. Availability of colours associated with yellow chromate and cochineal lake pigments in powder, watercolour and oil colour** throughout the 19 th century from W&N, adapted from Carlyle, 2001, Appendix 26, Table 6, p. 533-536.....	35
Table 3.1. Compositional classification of the three modern types of chrome yellow, adapted from Kühn & Curran, 1986: 193 (in accordance to ASTM D211 - 67(1977)).....	44
Table 3.2. W&N's chrome yellow key ingredients, main synthetic pathways and final pigment formulations...	49
Table 3.3. L*a*b* colour coordinates, inflection point (λ_{IP} , nm) of the reflectance (FORS) spectra and composition of pigments representative of the main synthetic pathways.....	56
Table 3.4. L*a*b* colour coordinates, inflection point (λ_{IP} , nm) of the reflectance (FORS) spectra and composition of pigments representative of other synthetic pathways.....	57
Table 3.5. Historic chrome yellow paint tubes: description, composition, L*a*b* colour coordinates and inflection point (λ_{IP} , nm) of the reflectance (FORS) spectra.....	62
Table 3.6. Correlation of W&N chrome yellow pigment formulations with pigments found in μ -samples from paintings by Amadeo, analysed by μ -FTIR. See also Appendix XIII, p. 319.....	68
Table 3.7. Chrome, barium, zinc and strontium yellow pigments: common and chemical names, chemical formula, Colour Index number (C.I.), refractive index, solubility product constants (K_{sp} at 25°C), crystal structure and space group (Chang, 1994; Liang <i>et al.</i> , 2005; Lide, 2006; Cameo, 2016).....	71
Table 3.8. Dates of the first appearance of colours associated with Lemon (barium chromate), Citron (zinc potassium chromate) and Strontian (strontium chromate) Yellow in powder and oil colour in the 19 th century from Reeves and Rowney. From Carlyle (2001, Appendix 26, Table 7, p. 540 & Table 8, p. 543).....	72
Table 3.9. W&N's Lemon, Citron and Strontian Yellow: key ingredients, main synthetic pathways and final pigment formula.....	74
Table 3.10. Reconstructions of W&N's Lemon (LY1a), Citron (CY1a) and Strontian (SY1a) Yellow pigments following their main synthetic pathways: final pH, L*a*b* colour coordinates, relative tinting strength (% TS) and inflection point (λ_{IP} , nm) of the reflectance spectra.....	77
Table 3.11. Reconstructions of W&N's Lemon (LY1a), Citron (CY1a) and Strontian (SY1a) Yellow pigments: pigment composition, ICDD diffraction cards, Raman and infrared characteristic bands (Alía <i>et al.</i> , 1999; Hummel, 2002; Stoilova <i>et al.</i> , 2005; Liang <i>et al.</i> , 2005; Correia <i>et al.</i> , 2007; Simonsen <i>et al.</i> , 2017; Nakamoto, 2009) (the main bands appear in bold)....	78
Table 4.1. Oil paints before and after irradiation with a Xenon lamp ($\lambda_{irr} > 300$ nm): pigment formulation, L*a*b* colour coordinates and ΔE^*	97
Table 4.2. PVAc paints before and after irradiation with a Xenon lamp ($\lambda_{irr} > 300$ nm): pigment formulation, L*a*b* colour coordinates and ΔE^*	99
Table 4.3. Historic W&N oil paint tubes and lead chromate oil paint reconstructions: total colour variation (ΔE^*) and Light Susceptibility Index (LSI).....	102

Table 4.4. PVAc paint set prepared with lead chromate pigment reconstructions: total colour variation (ΔE^*) and Light Susceptibility Index (LSI).....	103
Table II.1.1. Estimated dates and number of pages available for each of the 47 W&N's 19 th century catalogues (included by Mark Clarke in the database). For the dates highlighted in bold, these catalogues are complete. The letter T stands for Trade, R for Retail and F for French.....	161
Table II.1.2. Inferred manuscript (MS) date range (included by Mark Clarke in the database), pages and number of records for each of the 85 manuscript books.....	162
Table II.1.3. W&N database topics by alphabetical order.....	163
Table II.1.4. W&N database sub-topics by alphabetical order.....	166
Table II.1.5. W&N abbreviations, from original to modern terminology.....	173
Table II.1.6. Conversion of measures, adapted from Carlyle, 2001. <i>The Artist's Assistant</i> . Appendix 27 (pp. 545-546).....	174
Table III.1. Codes for the ingredients used by W&N.....	205
Table III.1.1. W&N Primrose Chrome (PR) manufacturing processes.....	205
Table III.1.2. PR1a production records: molar proportions between the chromate ion and the other ingredients used, their Unique Recipe Code (URC), name and date. The production record reproduced is highlighted.....	206
Table III.1.3. PR1b production record: molar proportions between the chromate ion and the other ingredients used, its URC, name and date.....	206
Table III.1.4. PR2 production record: molar proportions between the chromate ion and the other ingredients used, its URC, name and date.....	206
Table III.1.5. PR3 production record: molar proportions between the chromate ion and the other ingredients used, its URC, name and date.....	206
Table III.2.1. W&N Lemon (L) and Pale (P) Chrome manufacturing processes.....	207
Table III.2.1.1. L1 production records: molar proportions between the chromate ion and the other ingredients used, their URC, name and date. The production records reproduced are highlighted.	209
Table III.2.1.2. L2a production records: molar proportions between the chromate ion and the other ingredients used, their URC, name and date. The production record reproduced is highlighted.....	210
Table III.2.1.3. L2b production records: molar proportions between the chromate ion and the other ingredients used, their URC, name and date. The production record reproduced is highlighted.....	210
Table III.2.1.4. L3a production record: molar proportions between the chromate ion and the other ingredients used, its URC, name and date.....	210
Table III.2.1.5. L3b production record: molar proportions between the chromate ion and the other ingredients used, its URC, name and date.....	211
Table III.2.1.6. L4a production records: molar proportions between the chromate ion and the other ingredients used, their URC, name and date.....	211
Table III.2.1.7. L4b production records: molar proportions between the chromate ion and the other ingredients used, their URC, name and date.....	211
Table III.2.2.1. P1 production records: molar proportions between the chromate ion and the ingredients used, their URC, name and date.....	212
Table III.2.2.2. P2 production records: molar proportions between the chromate ion and the ingredients used, their URC, name and date.....	212
Table III.2.2.3. P3a production records: molar proportions between the chromate ion and the ingredients used, their URC, name and date.....	213

Table III.2.2.4. P3b production records: molar proportions between the chromate ion and the ingredients used, their URC, name and date.....	213
Table III.2.2.5. P4a production records: molar proportions between the chromate ion and the ingredients used, their URC, name and date.....	213
Table III.2.2.6. P4b production record: molar proportions between the chromate ion and the ingredients used, its URC, name and date.....	214
Table III.2.2.7. P5a production record: molar proportions between the chromate ion and the ingredients used, its URC, name and date.....	214
Table III.2.2.8. P5b production record: molar proportions between the chromate ion and the ingredients used, its URC, name and date.....	214
Table II.2.2.9. P6 production record: molar proportions between the chromate ion and the ingredients used, its URC, name and date.....	214
Table III.2.2.10. P7a production records: molar proportions between the chromate ion and the ingredients used, their URC, name and date.....	214
Table III.2.2.11. P7b production records: molar proportions between the chromate ion and the ingredients used, their URC, name and date.....	214
Table III.2.2.12. P8 production record: URC, name and date.....	215
Table III.2.2.13. P9 production records: molar proportions between the chromate ion and the ingredients used, their URC, name and date.....	215
Table III.2.2.14. P10 production record: molar proportions between the chromate ion and the ingredients used, its URC, name and date.....	215
Table III.2.2.15. P11 production record: molar proportions between the chromate ion and the ingredients used, its URC, name and date.....	215
Table III.3.1. W&N Middle Chrome (M) manufacturing processes.....	216
Table III.3.1.1. M1a production records: molar proportions between the chromate ion and the ingredients used, their URC, name and date. The production records reproduced are highlighted.	217
Table III.3.1.2. M1b production records: molar proportions between the chromate ion and the ingredients used, their URC, name and date.....	217
Table III.3.1.3. M2a production records: molar proportions between the chromate ion and the ingredients used, their URC, name and date. The production records reproduced are highlighted.	217
Table III.3.1.4. M2b production record: URC, name and date.....	218
Table III.3.1.5. M3a production records: molar proportions between the chromate ion and the ingredients used, their URC, name and date.....	218
Table III.3.1.6. M3b production record: molar proportions between the chromate ion and the ingredients used, its URC, name and date.....	218
Table III.3.1.7. M4 production record: molar proportions between the chromate ion and the ingredients used, its URC, name and date.....	218
Table III.3.1.8. M5a production record: URC, name and date.....	218
Table III.3.1.9. M5b production record: URC, name and date.....	218
Table III.3.1.10. M6 production records: molar proportions between the chromate ion and the ingredients used, their URC, name and date.....	219
Table III.3.1.11. M7a production record: molar proportions between the chromate ion and the ingredients used, its URC, name and date.....	219
Table III.3.1.12. M7b production records: molar proportions between the chromate ion and the ingredients used, their URC, name and date.....	219
Table III.3.1.13. M8 production records: molar proportions between the chromate ion and the ingredients used, their URC, name and date.....	219

Table III.4.1. W&N Deep (D) Chrome manufacturing processes.....	220
Table III.4.1.1. D1a production records: molar proportions between the chromate ion and the ingredients used, their URC, name and date. The production record reproduced is highlighted....	221
Table III.4.1.2. D1b production records: molar proportions between the chromate ion and the ingredients used, their URC, name and date. The production records reproduced is highlighted...	221
Table III.4.1.3. D2a production records: molar proportions between the chromate ion and the ingredients used, their URC, name and date. The production records reproduced is highlighted...	221
Table III.4.1.4. D2b production records: molar proportions between the chromate ion and the ingredients used, their URC, name and date.....	222
Table III.4.1.5. D3 production record: molar proportions between the chromate ion and the ingredients used, its URC, name and date.....	222
Table III.4.1.6. D4 production record: URC, name and date.....	222
Table III.4.1.7. D5a production record: URC, name and date.....	222
Table III.4.1.8. D5b production record: URC, name and date.....	222
Table III.4.1.9. D6a production record: URC, name and date.....	222
Table III.4.1.10. D6b production record: molar proportions between the chromate ion and the ingredients used, its URC, name and date.....	222
Table III.4.1.11. D7 production record: URC, name and date.....	223
Table III.4.1.12. D8 production record: molar proportions between the chromate ion and the ingredients used, its URC, name and date.....	223
Table III.4.1.13. D9 production record: molar proportions between the chromate ion and the ingredients used, its URC, name and date.....	223
Table III.4.1.14. D10a production record: molar proportions between the chromate ion and the ingredients used, its URC, name and date.....	223
Table III.4.1.15. D10b production record: URC, name and date.....	223
Table IV.1. Codes for the ingredients used by W&N	225
Table IV.1.1. W&N Lemon Yellow (LY) manufacturing processes.....	225
Table IV.1.2. LY1a production records: molar proportions between the chromate ion and barium chloride used, their URC, name and date. The production records reproduced are highlighted.....	226
Table IV.1.3. LY1b production records: molar proportions between the chromate ion and the ingredients used, their URC, name and date.....	227
Table IV.1.4. LY2a production records: URC, name and date.....	227
Table IV.1.5. LY2b production records: molar proportions between the chromate ion and the ingredients used, their URC, name and date.....	227
Table IV.1.6. LY3 production records: URC, name and date.....	227
Table IV.2.1. W&N Citron Yellow (CY) manufacturing processes.....	227
Table IV.2.2. CY1a production records: molar proportions between the chromate ion and the ingredients used, their URC, name and date. The production record reproduced is highlighted....	228
Table IV.2.3. CY1b production records: URC, name and date.....	229
Table IV.2.4. CY2 production record: URC, name and date.....	229
Table IV.2.5. CY3 production records: molar proportions between the chromate ion and the ingredients used, their URC, name and date.....	229
Table IV.3.1. W&N Strontian Yellow (SY) manufacturing processes.....	229
Table IV.3.2. SY1 production records: molar proportions between the chromate ion and the ingredients used, their URC, name and date. The production record reproduced is highlighted....	230

Table IV.3.3. SY2 production record: URC, name and date.....	230
Table IV.3.4. SY3 production record: molar proportions between the chromate ion and the strontium nitrate used, its URC, name and date.....	230
Table IV.4.1. Data on other experimental production records: order of ingredients (using the codes of tables III.1 and IV.1), URC, name and date.....	231
Table V.2.1.1.1. Summary of the conditions used for the synthesis of lead chromate references..	233
Table V.2.1.1.2. Summary of the conditions used for the lead chromate main synthetic pathways (Table 3.2, p. 49).....	234
Table V.2.1.1.3. Summary of the conditions used for other lead chromate synthetic pathways.....	235
Table V.2.1.2.1. Summary of the conditions used for the other yellow chromate main synthetic pathways	237
Table V.3.1. Regions of interest used for μ -FTIR mapping with PyMca software (see Appendix VI.4, p.256).	242
Table VI.1.1. Photon energies, in keV, of principal K-, L-, and M-shell emission lines, adapted from Kortright & Thompson, 2009. X-Ray Data Booklet, Table 1-2.....	243
Table VI.3.1. Main characteristic Raman bands of the reference compounds (see Figures VI.3.1 to VI.3.9) (Hummel, 2002; Mayo <i>et al.</i> , 2004; Nakamoto, 2009).....	254
Table VI.4.1. Main characteristic infrared bands of the reference compounds (see Figures VI.4.1 to VI.4.9) (Hummel, 2002; Mayo <i>et al.</i> , 2004; Nakamoto, 2009).....	265
Table VIII.1. Reference codes and quantities of the starting materials for the synthesis of $\text{PbCr}_{1-x}\text{S}_x\text{O}_4$ crystals with variable sulfate to chromate ratio.....	275
Table VIII.2. Semi-quantitative composition (determined by complementary analysis of XRD and μ -FTIR data), final pH and $L^*a^*b^*$ coordinates of the synthesised $\text{PbCr}_{1-x}\text{S}_x\text{O}_4$ crystals.....	276
Table VIII.3. Characteristic infrared and Raman bands of the synthesised references of $\text{PbCr}_{1-x}\text{S}_x\text{O}_4$ crystals (see Figures VIII.2 to VIII.5).....	281
Table IX.1.1. pH measurements throughout PR1a pigment syntheses. The pH of the solution is presented from top to bottom of the column, after each ingredient addition. pH range of the lead solution is shown in the end of the table. Final pH was obtained after the addition of all ingredients, before filtration.....	287
Table IX.1.2. pH measurements throughout PR1b pigment syntheses. The pH of the solution is presented from top to bottom of the column, after each ingredient addition. pH range of the lead solution is also shown in the end of the table. Final pH was obtained after the addition of all ingredients, before filtration.....	287
Table IX.1.3. pH measurements throughout L1 pigment syntheses. The pH of the solution is presented from top to bottom of the column, after each ingredient addition. pH range of the lead solution is also shown in the end of the table. Final pH was obtained after the addition of all ingredients, before filtration.....	287
Table IX.1.4. pH measurements throughout L2a pigment syntheses. The pH of the solution is presented from top to bottom of the column, after each ingredient addition. pH range of the lead solution is also shown in the end of the table. Final pH was obtained after the addition of all ingredients, before filtration.....	288
Table IX.1.5. pH measurements throughout L2b pigment syntheses. The pH of the solution is presented from top to bottom of the column, after each ingredient addition. pH range of the lead solution is also shown in the end of the table. Final pH was obtained after the addition of all ingredients, before filtration.....	288
Table IX.1.6. pH measurements throughout L3a pigment syntheses. The pH of the solution is presented from top to bottom of the column, after each ingredient addition. pH range of the lead solution is also shown in the end of the table. Final pH was obtained after the addition of all ingredients, before filtration.....	288

Table IX.1.7. pH measurements throughout L3b pigment synthesis. The pH of the solution is presented from top to bottom of the column, after each ingredient addition. pH range of the lead solution is also shown in the end of the table. Final pH was obtained after the addition of all ingredients, before filtration.....	289
Table IX.1.8. pH measurements throughout M1a pigment syntheses. The pH of the solution is presented from top to bottom of the column, after each ingredient addition. pH range of the lead solution is also shown in the end of the table. Final pH was obtained after the addition of all ingredients, before filtration.....	289
Table IX.1.9. pH measurements throughout M1b pigment synthesis. The pH of the solution is presented from top to bottom of the column, after each ingredient addition. pH range of the lead solution is also shown in the end of the table. Final pH was obtained after the addition of all ingredients, before filtration.....	289
Table IX.1.10. pH measurements throughout M2a pigment syntheses. The pH of the solution is presented from top to bottom of the column, after each ingredient addition. pH range of the lead solution is also shown in the end of the table. Final pH was obtained after the addition of all ingredients, before filtration.....	290
Table IX.1.11. pH measurements throughout D1a pigment synthesis. The pH of the solution is presented from top to bottom of the column, after each ingredient addition. pH range of the lead solution is also shown in the end of the table. Final pH was obtained after the addition of all ingredients, before filtration.....	290
Table IX.1.12. pH measurements throughout D1b pigment syntheses. The pH of the solution is presented from top to bottom of the column, after each ingredient addition. pH range of the lead solution is also shown in the end of the table. Final pH was obtained after the addition of all ingredients, before filtration.....	290
Table IX.1.13. pH measurements throughout D2a pigment syntheses. The pH of the solution is presented from top to bottom of the column, after each ingredient addition. pH range of the lead solution is also shown in the end of the table. Final pH was obtained after the addition of all ingredients, before filtration.....	291
Table IX.2.1. pH measurements throughout LY1a pigment syntheses. The pH of the solution is presented from top to bottom of the column, after each ingredient addition. pH range of the barium chloride is also shown in the end of the table. Final pH was obtained after the addition of all ingredients, before filtration.....	291
Table IX.2.2. pH measurements throughout CY1a pigment syntheses. The pH of the solution is presented from top to bottom of the column, after each ingredient addition. pH range of the zinc nitrate is also shown in the end of the table. Final pH was obtained after the addition of all ingredients, before filtration.....	291
Table IX.2.3. pH measurements throughout SY1a pigment syntheses. The pH of the solution is presented from top to bottom of the column, after each ingredient addition. pH range of strontium nitrate is also shown in the end of the table. Final pH was obtained after the addition of all ingredients, before filtration.....	292
Table XVI.1. Oil paints before and after irradiation with a Xenon lamp ($\lambda_{\text{irr}} > 300 \text{ nm}$): pigment composition, $L^*a^*b^*$ coordinates, ΔE^* , and intensity of the Cr K pre-edge peak at 5.993 keV.....	349
Table XVI.2. PVAc paints before and after irradiation with a Xenon lamp ($\lambda_{\text{irr}} > 300 \text{ nm}$): pigment composition, $L^*a^*b^*$ coordinates, ΔE^* , and intensity of the Cr K pre-edge peak at 5.993 keV.....	350
Table XX.1. Reduction reactions and standard reduction potentials (E° at 25°C) (Bard <i>et al.</i> , 1985; Lide, 2006).....	369
Table XX.2. Dissociation constants (pK_a at 25°C) (Cotton <i>et al.</i> , 1999; Lide, 2006).....	369

Chapter 1

General Introduction



Detail from painting *Entrada* by Amadeo de Souza-Cardoso, c.1917, Modern Collection / Calouste Gulbenkian Museum @ FCG

Chapter 1. General Introduction

1.1. Preamble

The study of the materials and techniques of Amadeo de Souza-Cardoso (1887-1918), one of the most important Portuguese Modern painters, was part of the interdisciplinary project, “Crossing Borders: history, materials and techniques of Portuguese painters from 1850-1918” (FCT, 2009). This study, as well as the research carried out for his *Catalogue Raisonné* (Vilarigues *et al.*, 2008; Melo *et al.*, 2009), demonstrates that Amadeo, although using traditional pigments too, showed a preference for pigments newly discovered in the 19th century. It is known that he used artists’ materials from leading artists’ colourmen established in the 19th century: Winsor & Newton (W&N), Lefranc & Co., and *Bourgeois* (Vilarigues *et al.*, 2008; Melo *et al.*, 2009). The modern pigment, chrome yellow, which is frequently found in Amadeo’s paintings (Vilarigues *et al.*, 2008; Melo *et al.*, 2009) is known to be unstable in the works of many of his international contemporaries (Monico *et al.*, 2011b & 2013a). Fortunately, in Amadeo’s paintings no deterioration in the form of darkening has been observed. This thesis seeks to expand knowledge on the 19th century manufacture and stability of chrome yellow pigments.

“Among the means essential to proficiency in Painting, none is more important than a just knowledge of Colours and Pigments - their qualities, powers, and effects”¹. Detailed knowledge of the materials used by artists is essential to reveal their techniques and to place their works in context as well as to establish the most adequate conservation and authentication procedures. The research design of this thesis is based on a four-part model consisting of: i) documentary research of sources of technical information contemporary to the artist; ii) preparation of references following historically accurate reconstruction techniques - HART² (Carlyle & Witlox, 2005; Carlyle *et al.*, 2008, Carlyle, 2012a); iii) characterisation with complementary analytical techniques of the paintings, artists’ materials contemporary to the artist and the historically accurate reference materials; and iv) a photodegradation study using samples from oil paint tubes contemporary to the artist and paints prepared with pigment reconstructions.

When studying historic artists’ materials, it is essential to have access to their methods of production since today’s materials do not represent the formulations used in the past. The Winsor & Newton 19th Century Archive Database provides unique and efficient access to their 19th century artists’ materials and their commercial preparation and application (Clarke & Carlyle 2005a & 2005b; Carlyle *et al.*, 2011; Otero *et al.*, 2012). Thorough investigation of the archive holdings enables new knowledge of W&N’s 19th century manufacturing processes and paint formulations, including pigments, additives and binders, allowing reconstructions with as much historical accuracy as

¹ George Field in “*Chromatography; or, A treatise on Colours and Pigments, and of their Powers in Painting*”, 1835, p. xix.

² The HART (Historically Accurate Reconstruction Techniques) project was part of ‘De Mayerne Programme’ on Molecular Studies in Conservation and Technical Studies in Art History, funded by the Netherlands Organisation for Scientific Research (NWO) from 2002 to 2006 (Carlyle, 2005).

possible. The accuracy³ of the reconstructions is validated by analytical comparison with samples from historic paintings and artists' materials, enabling to obtain historically accurate reference materials.

For a full characterisation of the pigment formulations, a multi-analytical approach is necessary. An overall characterisation is achieved by Energy Dispersive X-Ray Fluorescence Spectrometry (μ -EDXRF), that is used to obtain the elemental composition, Fibre Optic Reflectance Spectroscopy (FORS), and the fingerprinting techniques, micro-Raman (μ -Raman) and micro-Fourier Transform Infrared (μ -FTIR) spectroscopies, which provide characterisation at the molecular level, Scanning Electron Microscopy with X-ray microanalysis (SEM-EDS) that allows a morphological and elemental characterisation, and X-Ray Diffraction (XRD), which provides analysis of the crystal structure, also contribute with relevant data.

To the best of the author's knowledge, this work, for the first time, fully explores the Winsor & Newton 19th Century Archive Database and makes use of the analysis of its information to support the reproduction of their commercial recipes for artists' pigments, further validated by correlation with the chemical information of 19th century artists' materials and paintings. A general overview of the W&N Researcher's Edition (RE) database may be found in Chapter 2.

A complete evaluation of the W&N 19th century manufacturing processes of yellow lead chromates ($\text{PbCr}_{1-x}\text{S}_x\text{O}_4$, $0 \leq x \leq 0.8$) commonly known as chrome yellow pigments is detailed in Chapter 3. This chapter also describes the reconstruction of a selection of chrome yellow pigments based on the analysis of the archive production records and analytical comparison with chrome yellow formulations found in historic paint tubes and paintings by Amadeo de Souza-Cardoso. Polyester- oil and poly(vinyl acetate) paints were prepared with the reconstructed chrome yellow pigments, air-dried and then irradiated in a Xenon-light apparatus ($\lambda_{\text{irr}} > 300 \text{ nm}$). The degradation process was studied by the previously mentioned techniques and Synchrotron Radiation (SR) based techniques including μ -XRF, μ -XRD and μ -FTIR with higher spatial resolution and sensitivity at the micrometric level. Micro X-ray Absorption Near-Edge Structure (μ -XANES) was also employed to probe the chemical speciation (information on the oxidation state, coordination number and site symmetry) of the chromium, sulfur and calcium elements (Cr, S and Ca K-edge). Evidence that contributes to a prediction of the sensitivity of chrome yellow paints to photodegradation and the possible degradation mechanisms taking place is discussed in Chapter 4.

The study of the 19th century methods of production used by W&N for other yellow chromate pigments, namely barium (BaCrO_4), zinc ($4\text{ZnCrO}_4 \cdot \text{K}_2\text{O} \cdot 3\text{H}_2\text{O}$) and strontium (SrCrO_4) chromates, may also be found in Chapter 3 as well as a comparison between the reconstructions prepared and samples from historic paint tubes and Amadeo's paintings.

This pioneering work complements art technological and conservation science research. It demonstrates the importance of using historically accurate reference materials to conduct chemical studies, allowing a better understanding of the evolution of artists' paints over time. Furthermore, it

³ Herein, "the accuracy of a measurement is its closeness to the true value", which in this context is the historic artwork or material under study (Atkins & Jones, 1997; Vitorino *et al.*, 2015). It is important to note that the reconstructions prepared followed the original instructions, but no historically accurate reagents were used. Reagents of analytical grade were used in order to avoid contaminants, with the exception of the additives/extenders that were of natural origin. Future research may be done to identify the impact of using historically appropriate reagents, but this was outside the scope of this work.

offers a means to assess the original appearance and condition of paintings, as well as advancing knowledge towards their preservation.

1.2. The 19th century artists' colourmen

1.2.1. Brief context

For background information on 19th and early 20th century colourmen, surveys covering British artists' suppliers between 1650 and 1950 (Simon, 2018) and Parisian artists' suppliers between 1790 and 1960 (Labreuche, 2018) are available on-line. For information on British artist's materials between 1750 and 1900 as well as their suppliers, the work by Carlyle is still one of the best authoritative sources (Carlyle, 2001). It is also important to recognize the first substantial study of 19th century Parisian colourmen by Stéphanie Constantin focusing on the Barbizon painters' suppliers (Constantin, 2001) and the comprehensive study of the colourmen in Paris during the 19th century undertaken by Clotilde Roth-Meyer (Roth-Meyer, 2005). On American 19th century artists' materials suppliers the book by Alexander Katlan is a key reference (Katlan, 1987). The study of the Portuguese artists' suppliers between 1836 and 1914 has also been recently carried out by Ângela Ferraz (Ferraz, 2018).

By the beginning of the 19th century, chemistry was already an established scientific discipline (Levere, 2001), fuelling the material conditions for the 19th century art revolution (Harley, 1982; Bomford *et al.*, 1990; Ball, 2008). Winsor & Newton always acknowledge the importance of chemistry in their development as one of the leading artists' colourmen of the 19th century (further explained in Chapter 2). In fact, in their 1896 trade catalogue they stated that "from the outset Winsor & Newton recognized that the era of *Chemistry* had arrived, and that it behoved them to abandon all old ruled-of-thumb processes in favour of the more accurate and rigid methods of modern science" (p. xxv).

Carneiro notes that it is a general opinion among historians that the turning point in the history of modern chemistry was the work by Antoine Laurent Lavoisier⁴ (1743-1794) compiled in his '*Traité élémentaire de chimie: présenté dans un ordre nouveau et d'après les découvertes modernes; avec figures*', published in 1789. He developed new methods and instruments which allowed the qualitative and quantitatively study of all types of matter in dedicated chemistry laboratories, Figure 1.1 (Carneiro, 2006). Another groundbreaking work co-authored by Lavoisier was the establishment of a chemical universal language, the first version of the current chemical nomenclature. It was published in 1787, in the '*Méthode de Nomenclature Chimique*' together with Guyton de Morveau (1737-1816), Antoine Francois Fourcroy (1755-1809) and Claude Louis Berthollet (1748-1822) (Levere, 2001; Carneiro, 2006). This was a period of extraordinary findings and the majority of the elements of the periodic table were discovered between mid-18th and the 19th century⁵ (RSC Periodic Table, 2018).

⁴ Carneiro recounts that Antoine Laurent Lavoisier was born in a wealthy family, having studied law, botany, geology, astronomy and chemistry. Through a much disciplined way of living, he conciliated his work in public service with his investigation, supported by his fortune, which allowed him to buy expensive instruments. Lavoisier was decapitated by the Republic in 1794 due to his public work during the old Regime. He was married to Marie-Anne Pierrette Paulze (1758-1836), who interestingly was Jacques-Louis David (1748-1825) painter apprentice, see Figure 1.1. All the illustrations in Lavoisier works were of her authorship, including those in the '*Traité élémentaire de chimie*' (Carneiro, 2006, p. 6-7).

⁵ Sixty-seven of the current existing 118 elements were discovered between 1750 and 1900 (RSC Periodic Table, 2018).



Figure 1.1. On the left, detail from “*Antoine-Laurent Lavoisier and His Wife*” by Jacques-Louis David in 1788 © The Metropolitan Museum of Art (from Panopticon Lavoisier, 2018), and on the right, the 19th century Chemical Laboratory of the *Escola Polytechnica* (Lisbon) built in 1857 (from MUHNAC, 2012).

The experimentation inherent to the chemical revolution, especially around the newly discovered chemical elements resulted in new colourful inorganic pigments, opening new possibilities for 19th century painters (Harley, 1982; Bomford *et al.*, 1990; Ball, 2008). French scientists were at the forefront of this endeavor, such as Louis Nicolas Vauquelin (1763-1829), who discovered the element chromium in 1797 and later its potential to produce yellow to orange from lead chromate pigments (this will be more fully described in Chapter 3) and green from chromium (III) oxide (Vauquelin, 1809). Furthermore, with the expansion of the colour market, economic incentives were created to encourage the invention of new, faster and cheaper pigment production methods, preferably with improved properties. For example, in 1828, the *Société d'Encouragement pour l'Industrie Nationale* awarded J. B. Guimet with 6000 francs for his synthetic method to produce ultramarine blue (Eastaugh *et al.*, 2004: 375; Harley, 1982: 58). Some of these new pigments were reported to have gone directly from the chemical laboratory to the artists' Modern palette⁶ (Kühn & Curran, 1986), however, in general the commercial availability of the new colourants depended on the economic circumstances, more specifically on the accessibility of the raw materials (Eastaugh *et al.*, 2004; Harley, 1982). Sources of chromium, cadmium, cobalt, zinc, copper and arsenic became more available throughout the first half of the 19th century as the metallurgical industries grew in France and in Germany (Harley, 1982: 181).

Advances in organic chemistry, in particular the analysis and synthesis of complex dyestuff compounds only broke through in the second half of the 19th century, mostly developed by the impetus of the German scientists (Homburg, 1992). However, the first synthetic organic dye named mauveine⁷ had been discovered in 1856 by the young English chemist William Henry Perkin (1838-1907),

⁶ The artists' modern palette also sometimes referred to as the impressionist palette is further described in Chapter 1.3.2 (p. 17).

⁷ Mauveine is also known as aniline purple, Tyrian purple and mauve dye. It is an aniline based dye composed of a complex mixture of methyl derivatives of 7-amino-5-phenyl-3-(phenylamino)phenazin-5-ium (Sousa *et al.*, 2008).

displaying an intense purple colour (Garfield, 2000; Travis, 2006). For the first time, a natural organic dye was synthetically produced in 1868 by Carl Graebe (1841-1927) and Carl Lieberman (1842-1914); it was alizarin⁸, the main red chromophore of madder lake pigments (Hornix, 1992). The artificial dyestuffs industry rapidly became economically successful which diminished the commercial value of the natural dyestuff (Bomford *et al.*, 1990). Nevertheless, companies such as Lefranc & Co. and W&N continued to produce and sell natural red lake pigments (Carlyle, 2001: 506).

Industrialization also played a determinant role in the development of artists' materials and consequently of the colourmen. In 1896, W&N reported that "they had in 1844 progressed so rapidly as to be able to erect that perfectly appointed Chemical Manufactory which was to form the nucleus of the present large structure, known as the *North London Colour Works*⁹:- a fabric gradually built up in perfect adaptation to their particular requirements, and replete with every appliance for the manufacture and testing of colours that ingenuity can devise" (W&N's 1896 catalogue, p. xxv). The creation of better equipment, steam-powered machines and factories also enabled the invention of new artists' materials and tools as their manufacture was scaled-up (Pavey & Staples, 1984; Townsend, 2002). The invention of superior commercially manufactured paint containers is among one of the great achievements accomplished. Oil paints which had initially been sold in "bladders" were eventually replaced by the collapsible metal tube, Figure 1.2. In 1822, James Harris developed a paint metal syringe, and in 1840, William Winsor from W&N patented a glass syringe. Both failed to completely replace the bladders and only in 1841, John Goffe Rand (1801-1873), an American portrait painter living in London, invented the first collapsible metal tubes. In 1842, William Winsor bought its patent and upgraded it with a screw cap of his authorship (Harley, 1871; Pavey & Staples, 1984; Moya, 2002).



Figure 1.2. The development of the paint tube © Winsor & Newton (from Winsor & Newton, 2014).

⁸ The chemical name of alizarin is 1,2-dihydroxy anthraquinone (Melo, 2009).

⁹ The North London Colour Works site is further described below in Chapter 1.2.2.

As Carlyle notes there were complaints that as the colourmen became more involved in the production of commercial artists paints, artists lost first-hand knowledge of their materials and were less able to evaluate their quality or permanence (Carlyle, 2001, Chapter 15). Issues such as the adulteration of their materials and the lack of quality and durability were raised (Carlyle 1993 & 2001; Townsend *et al.*, 1995). On the other hand, during this period, there were also painters with privileged relationships with their colourmen, and for example Carlyle reports that Winsor & Newton supplied individual painters with custom made products (further detailed below; Woodcock, 1996; Carlyle, 2001; Constantin; 2001). Some artists' suppliers also acted as intermediaries between the artists and potential buyers, using their shops as exhibition spaces (Constantin, 2001). The particular role of the Winsor & Newton Company and their dedication to high quality durable materials will be described below and demonstrated in this dissertation.

1.2.2. The artists' colourman Winsor & Newton

The Winsor & Newton (W&N) company was founded in 1832 by William Winsor (1804-1865), a colour chemist and artist, and Henry Charles Newton (1805-1882), a professional artist (Killik, 1925; Pavey & Staples, 1984). It was established initially at 38 Rathbone Place, off Oxford St, a neighbourhood of already well-established artists' colourmen such as Rowney and Reeves, as well as artists' studios, Figure 1.3 (Killik, 1925; Pavey & Staples, 1984).

William Winsor was a friend of and an assistant to George Field (1777-1854), one of the most important colour chemists in the 19th century, whose work, *Chromatography; or A Treatise on Colours and Pigments, and of their Powers in Painting & c.*, first published in 1835, is a fundamental source of information on artists' pigments of this period. In fact, Field's work greatly influenced W&N pigments manufacture¹⁰, especially, of red lake pigments (Pavey & Staples, 1984; Gage, 2001; Carlyle, 2001).

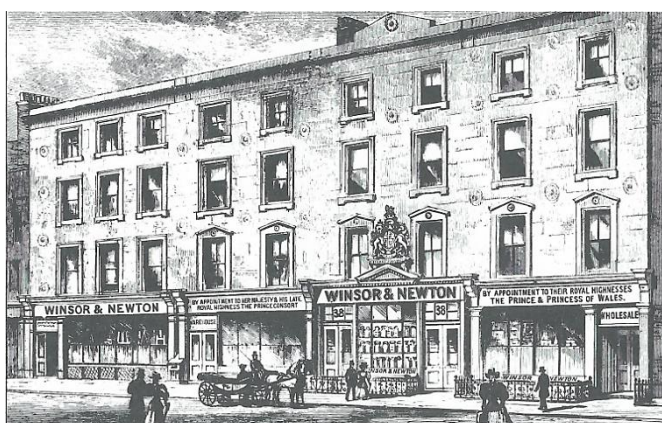
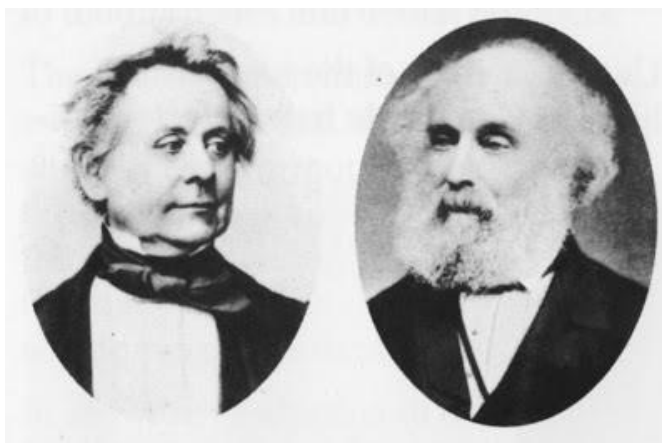


Figure 1.3. Top: William Winsor (left) and Henry Charles Newton (right) and **Bottom:** W&N at 36, 37, 38 and 39 Rathbone Place, London, 1878 © Reckitt & Colman Leisure Ltd. (from Pavey & Staples, 1984).

¹⁰ After Field's death, W&N acquired all his notebooks (Pavey & Staples, 1984).

W&N expresses a perfect match between science and art in the 19th century. Since the beginning, the company was committed to developing and improving the quality of artists' materials, a task they assumed as their responsibility as artists' colourmen. They rapidly became one of the leading colourmen worldwide, having supplied important painters as J. W. Turner¹¹ (1775-1851) and John Constable (1776-1837) (Harley, 1975; Fairbairn *et al.*, 1982)¹². Carlyle also notes that John Scott Taylor (W&N's superintendent of colour manufacture from 1890 to 1902 and Director from 1902 to 1939; Killik, 1925) advised the painter G. F. Watts (1817-1904) and supplied him with specially prepared oil paints and vehicles (Carlyle, 2001: 272). Their correspondence is part of the Watts collection held at the National Portrait Gallery Archive (Watts Collection, 2018).

W&N's first invention was the pigment Chinese white in 1834, a particularly opaque calcined zinc oxide, which was laboratory-tested by the famous British chemist, Michael Faraday (1791-1867). The year after, Henry Charles Newton made his most important contribution to the art world, the improvement of artists' watercolours, with his introduction of the moist watercolours based on the addition of glycerine and supplied in small pans, see Figure 1.4 from W&N c.1935 catalogue. The moist cakes were reported to be softer and more convenient to use than previously available watercolour cakes (Harley, 1975). As noted above, W&N also contributed to the development of modern tubes for oil paint and what is noteworthy is that although William Winsor had spent significant time and money on the improvement of his glass syringes for oil paint, he was quick to adopt the advantages of collapsible tubes, Figure 1.2 (Killik, 1925; Harley, 1975; Pavey & Staples, 1984).

In 1841, business was prospering and W&N extended their premises to Nos. 37, 38 and 39 at Rathbone Place. This was also the year W&N was recognized by Queen Victoria with a Royal Appointment, which was renewed ever since. Today, W&N remains by Appointment to HRH the Prince of Wales, (Killik, 1925; Harley, 1975; Winsor & Newton, 2018). In 1844, they expanded to a site in Kentish Town, building what became known as the "North London Colour Works". There, their man-made colourants were manufactured, and their earth and mineral pigments were carefully processed. All were ground in mills specially designed by Henry Charles Newton (Pavey & Staples, 1984).

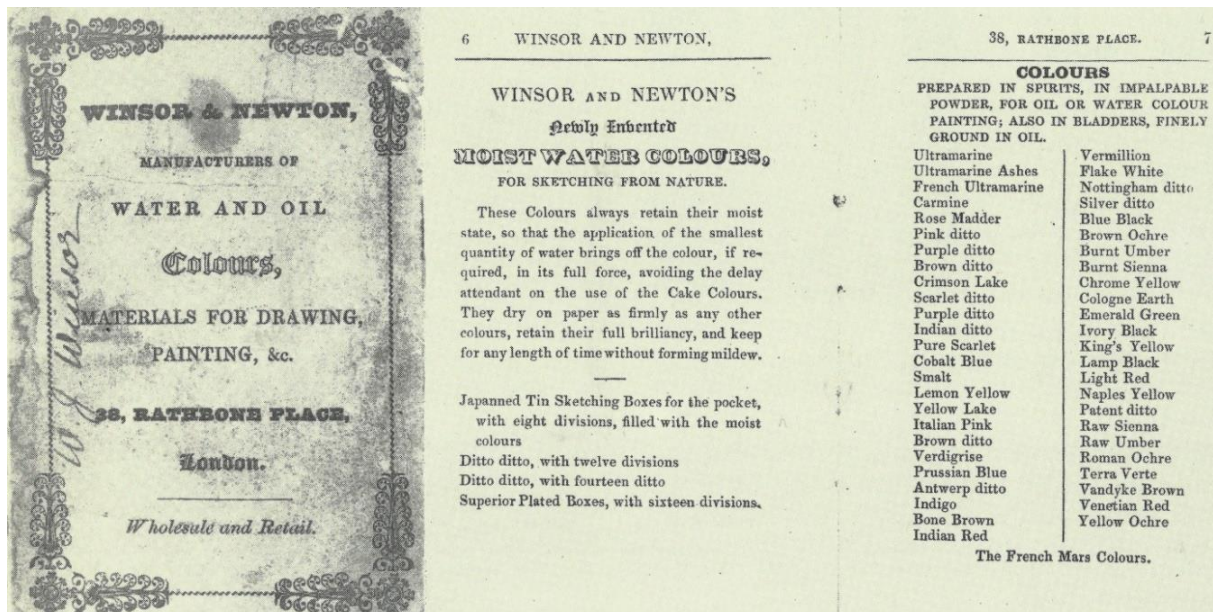
World recognition began with W&N being awarded the medallion for the chemistry of artists' colours, at the 1851 International Exhibition (see the remarkable colour palette and watercolour box specially made for the event in Figure 1.4). W&N was again awarded at the 1862 International Exhibition¹³ for the chemistry and display of artists' materials and at the 1893 Chicago World's Columbian Exposition for "a magnificent display of Artists' Colours and for their endeavour to substitute Permanent Colours for the more Fugitive Pigments used by artists", as cited in Pavey & Staples (1984: 33). Other international awards followed: gold medal at the International Exhibition

¹¹ There is a story cited in Killik (1925: 15) where William Winsor called Turner's attention to his use of fugitive colours and he replied: "*Your business Winsor is to make colour, mine is to use them*". Interestingly, W&N always made available fugitive colours together with the more durable modern and traditional pigments, claiming it was the painter's choice. This is further discussed below in Chapter 2 (Fairbairn *et al.*, 1982).

¹² In the W&N's 1849 catalogue, there were already fifty-nine painters cited for their testimonials on the quality of W&N moist colours (consulted in the W&N 19th Century Archive Database).

¹³ Charles Dickens, after seeing the W&N watercolour box at the 1862 International Exhibition wrote: "Has anyone ever seen anything like Winsor & Newton's cups of Chrome and Carnations and Crimson loud and fierce as a war-cry, and Pinks tender and loving as a young girl?", as cited in Pavey & Staples (1984: 32).

(Antwerp) in 1894, at the International Exhibition (Christchurch, New Zealand) in 1906 and at Paris and Wembley in 1924 (Killik, 1925; Pavey & Staples, 1984).



- | | |
|---------------------------|---------------------------------|
| 1 White Lead | 11 Rose Madder |
| 2 Naples Yellow and White | 12 Cobalt Violet |
| 3 Yellow ochre with White | 13 French Ultramarine |
| 4 Raw Sienna | 14 Cobalt Blue |
| 5 Burnt Umber | 15 Ivory Black |
| 6 Burnt Sienna | Second Row: |
| 7 Vermilion | 1 Lemon Yellow |
| 8 Light Red | 2 Green Oxide of Chromium |
| 9 Alizarin Crimson | 3 Cadmium Yellow |
| 10 Indian Red | 4 Mixtures of some of the above |



Figure 1.4. Top: W&N's c.1835 catalogue and **Bottom:** the 1851 International Exhibition W&N's colour palette, pigments from right to left (left) and their watercolour box (right) © Reckitt & Colman Leisure Ltd. (from Pavey & Staples, 1984).

William Winsor died in 1865 leaving his heritage to his son, William Henry Benyon Winsor (1852-1879) (Killik, 1925). After Benyon's death, Henry Charles Newton purchased Winsor's share and in 1882 he sold the business to the newly incorporated Winsor & Newton Limited¹⁴ with shareholders

¹⁴ The signatories to the Memorandum of Association were: Henry Charles Newton (founder); Arthur Henry Newton, an artists' colourman (founder's son); Arthur Anderson West, a civil engineer (son-in-law of Henry Charles Newton); Robert White Thrupp, an artists' colourman; William John Winsor (nephew of William Winsor, founder), a chemist (Pavey & Staples, 1984).

from both founding families. Henry Charles Newton died in 1882 only a few months later. Winsor descendants remained in the company until 1903 while the Newton's continued until the late 1970's (Killik, 1925; Harley, 1975).

By the end of the 19th century, W&N Ltd. was fully established not only in Europe but also overseas in the United States of America, Australia and India, maintaining the principles of quality which were laid down by the two founders. Consequently, it is not surprising that in 1892, W&N was the first artists' colourmen to publish a document on the composition and permanence of their colours¹⁵. At the time, however, they did not disclose their manufacturing processes (Killik, 1925; Winsor & Newton, 2014).

In the 20th century, due to changes in the painting materials market, prompted by the World Wars and the worldwide economic crisis, their trade was affected, and W&N Ltd. expanded their range of products for the amateur craft market, initiated in 1911, and student quality products, which were launched in 1933. To reduce costs, between 1938 and 1939 W&N Ltd. also centralised all activities at Wealdstone place (bought in 1898). Nevertheless, they continued to introduce new products such as their Designers Gouache in 1937, their first range of Artists' Acrylics in 1970 and alkyd colours in 1976. More recently, they introduced Artisan Water Mixable Oil Colour in 1998 (Harley, 1975; Winsor & Newton, 2014).

In 1976, W&N Ltd. was acquired by Reckitt & Colman Ltd., yet it preserved its identity. W&N's 150th anniversary was celebrated with an exhibition at the Tate Gallery: "Paint & Painting" and with the opening of their permanent Museum "The Artists' Colourmen Room" at Wealdstone¹⁶ (Fairbairn *et al.*, 1982; Pavey & Staples, 1984).

In 1990, W&N was bought by AB Wilh. Becker's business owned by the Swedish based Lindéngruppen Company. Currently, it belongs to its other independent subsidiary ColArt Ltd., headquartered in London, UK (Lindéngruppen, 2018). ColArt's portfolio includes Lefranc & Bourgeois, Reeves, Conté à Paris, Liquitex, Snazaroo and Letraset, with production facilities in the UK, France, China, India and Japan (Simon, 2018; ColArt, 2015).

1.3. Amadeo de Souza-Cardoso

For background on the artist and his context, the authoritative works by Alfaro (2007) and Freitas (2008a & 2008b) on the *Catalogue Raisonné* of Amadeo de Souza-Cardoso (the photobiography of Amadeo in Volume 1 and the painting of Amadeo in Volume 2), were used. The catalogue of the exhibition *Amadeo de Souza-Cardoso, Diálogo de vanguardas* (2006), curated by Helena de Freitas, was also consulted. Complementary information was extracted from works by other art historians, who also studied Amadeo, namely José Augusto França (1956, 1960, 1986, 1992 and 2009), Rui Mário Gonçalves (2006) and Joana Cunha Leal (2010).

¹⁵ The transcription of this document is available in Appendix II.2 (p. 175). See also Chapter 2.2.1 (p. 30).

¹⁶ Unfortunately, these facilities have been closed including the Museum.

Amadeo de Souza-Cardoso (1887-1918) is considered to be one of the most important Portuguese artists. During his lifetime, Amadeo's works diverged from the pictorial mainstream of Portuguese art and public taste and at the time of his death, he was mainly recognized at an international level and by his peers. In 1916, on the occasion of Amadeo's first exhibition in Lisbon, the Portuguese painter Almada Negreiros (1893-1970) described "Amadeo de Souza-Cardoso as the first Portuguese discovery in the 20th century Europe"¹⁷ (Alfaro, 2016).

Since the time of his death, Freitas (2008a) notes that Amadeo's critical reception has been uneven due to the discontinuity of exhibitions and the lack of a proper national museum of contemporary art. Between 1918 and 1956, Amadeo's work was almost unknown, his reputation only surviving due to the perseverance of other Portuguese artists. In 1956, the artist's first important anthological exhibition was organized by Jaime Isidoro¹⁸, in Porto (Freitas, 2008a). In the same year, the first monograph on Amadeo's work was written by the art critic and art historian José-Augusto França, who became one of his major promoters (França, 1956, 1960, 1986, 1992, 2009). Between 1958 and 1959, the Portuguese regime's propaganda office (SPN/SNI) organized retrospectives in Lisbon, Porto and Paris, mainly to promote Amadeo's works as propaganda (Freitas, 2008a).

It was only in 1983, when Calouste Gulbenkian Foundation opened the Modern Art Centre (CAM) with its contemporary art museum that new conditions were created to effectively and regularly promote and preserve Amadeo's work¹⁹, making it accessible to all. In 1987, the Modern Art Centre presented a retrospective marking the centenary of his birth and in 1991 a new internationalization process started with exhibitions worldwide²⁰ (Freitas, 2008a). In 2000, the renowned art Professor Robert J. Loescher calls Amadeo the "early Modernism's best kept secret" (as cited in Freitas, 2008: 443). The association between Amadeo and contemporary artists also began to be explored, resulting in two exhibitions: *Mondrian. Amadeo: da paisagem à abstracção* in 2001 (Serralves museum of contemporary art, Porto) and *Amadeo de Souza-Cardoso - Avant-garde Dialogues* in 2006 (Calouste Gulbenkian Foundation, Lisbon) (Freitas, 2006).

Finally, in 2007, coordinated by Helena de Freitas, a photobiography of Amadeo was released as the first volume of the *Catalogue Raisonné* with unpublished data (Freitas, 2007). In 2008, she coordinated the second volume of the *Catalogue Raisonné* which includes all his paintings (known at the time) together with critical texts (Freitas, 2008). This second volume also contains the first technical study of Amadeo's materials and techniques which was coordinated by Maria João Melo from the Department of Conservation and Restoration of the Faculty of Sciences and Technology of the NOVA University of Lisbon (DCR FCT NOVA) (Vilarigues *et al.*, 2008; Melo *et al.*, 2009). A promising tool to support authentication studies of paintings attributed to Amadeo was also developed

¹⁷ Almada Negreiros manifest is included in Amadeo's exhibition catalogue: *Exposição de Pintura: amadeo souza cardoso*. Lisbon: Liga Naval de Lisboa, 4 to 12 of December, 1916 (Alfaro, 2016: 248-249).

¹⁸ Jaime Isidoro (1924-2009) was a Portuguese painter and art dealer with a relevant role in the Portuguese artistic scene (Andrade, S. C., 2009).

¹⁹ The Calouste Gulbenkian Foundation has the largest collection of Amadeo's work (200, of which 63 are paintings) and part of his documental estate, donated by Amadeo's wife, Lucie de Souza-Cardoso, and friend, Paulo Ferreira (Freitas, 2008).

²⁰ *Amadeo de Souza-Cardoso, 1887-1918*. Brussels: Musée d'Art Moderne, 1991; *At the edge: a Portuguese futurist: Amadeo de Souza-Cardoso*. Washington: The Corcoran Gallery of Art, 1999; Chicago: The Arts Club of Chicago, 2000; *Amadeo de Souza-Cardoso (1887-1918): Ein pionier aus Portugal*. Hamburg: Ernst Barlach Haus, 2007.

within the outputs of the interdisciplinary project, “Crossing Borders: history, materials and techniques of Portuguese painters from 1850-1918” (Montagner *et al.*, 2015 & 2016).

The events detailed above demonstrate the substantial effort that has been made to disseminate Amadeo’s work nationally and internationally, not only with the objective of gaining recognition for him within the general public but also with the aim of achieving international recognition for his artistic genius. A significant step towards this was the major retrospective held at the Grand Palais (France), curated by Helena de Freitas and organized by the Calouste Gulbenkian Foundation and the Réunion des musées nationaux-Grand Palais, between 20 of April and 18 of July 2016 (Freitas, 2016). Furthermore, a recreation of Amadeo’s first exhibitions in Porto and Lisbon, entitled *Amadeo de Souza-Cardoso, Porto-Lisboa, 1916-2016*, curated by Raquel Henriques da Silva and Marta Soares, was also held at the Museu Soares do Reis (Porto) between 1 of November and 31 of December 2016, and at the Museu do Chiado (Lisbon) between 12 of January and 26 of February, 2017, respectively (Vasconcelos, 2016).

1.3.1. The artist’s biography

Amadeo de Souza-Cardoso, Figure 1.5, was born on the 14th of November of 1887 on his family’s farm in Manhufe, Amarante (Portugal). His father, José Emídio de Souza-Cardoso, was a wealthy wine producer in Northern Portugal. Amadeo was part of a large family with nine siblings (Alfaro, 2007; Freitas, 2008b).

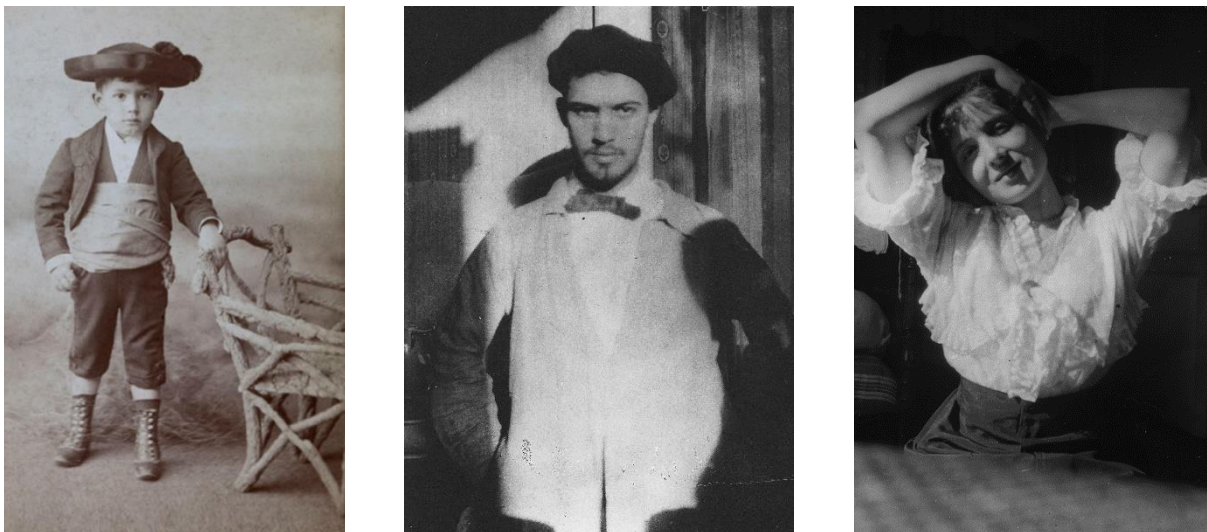


Figure 1.5. Amadeo de Souza-Cardoso, on the left, as a child (ASC 01/01 © BAFCG), on the centre, in c.1913 (ASC 03/39 © BAFCG), and on the right, Lucie de Souza-Cardoso, Amadeo’s wife, in 1915 (ASC 05/17 © BAFCG)²¹.

Amadeo started his studies in architecture at the Lisbon Academy of Fine Arts (1905). He was already demonstrating much interest and potential in the practice of drawing, sending caricatures to his sister Alice Cardoso and to one of his most supportive friends Manuel Laranjeira. In the following

²¹ For more information, please consult Amadeo de Souza-Cardoso’s estate (Biblioteca de arte (FCG), 2018).

year, Amadeo left for Paris to continue his studies with the financial support of his parents. He settled at Boulevard Montparnasse and attended some ateliers²² in preparation for his application to the *École des Beaux Arts*. However, he soon realized that the academic way was not his destiny and instead, let himself be inspired by the Parisian cultural and artistic scenes (Alfaro, 2007; Freitas, 2008b). At that time, he made acquaintances with the Portuguese artist community in Paris, namely with Francis Smith (1881-1961), Acácio Lino (1878-1956), Emmerico Nunes (1888-1968), Alberto Cardoso (1881-1942), Eduardo Viana (1881-1967), Manuel Bentes (1885-1961), Artur Alves Cardoso (1883-1930) and Domingos Rebelo (1891-1971), Figure 1.6 (Alfaro, 2007; França, 2009).

Amadeo continued to develop his drawings and caricatures. His first published caricature was a dinner menu in the Portuguese journal *O Primeiro de Janeiro*, in 1907. This was the year that he travelled to Brittany and Normandy, returning to Paris in time to see Cézanne's retrospective at the *Salon d' Automne* and the opening of the *Kahnweiler Gallery*. Freitas states that art historians agree this particular exhibition likely greatly influenced Amadeo's career as a painter (Freitas, 2008b).



Figure 1.6. *Los Borrachos*. Photograph by Eduardo Viana in 1908 (Paris). Domingos Rebelo, Amadeo de Souza-Cardoso, Emmerico Nunes, José Pedro Cruz and Manuel Bentes (behind) staging a Velázquez painting (ASC 03/01 © BAFCG).

Amadeo abandoned architecture in 1908 against his father will, who nevertheless continued to financially support his son. With his artistic path chosen²³, Amadeo moved to *Cité Falguière* in *Montparnasse*, an artists' neighbourhood where he was surrounded by academies such as the Russian Academy, art studios and *cafés*, which allowed him to expand his artistic horizons and relationships to other international artists. Amongst these was Amedeo Modigliani (1884-1920), with whom he was to have a close friendship. It was also in 1908 that Amadeo met his future wife, Lucie Meynardi Pecetto (1890-1987), Figure 1.5 (Alfaro, 2007).

²² e.g. Julien's Academy and Atelier of Godefroy and Freynet (Alfaro, 2007).

²³ In a letter to his mother, Emília Cândida Ferreira Cardoso, in 1908, Amadeo wrote "I am convinced that I am living a deeply artistic life - and I am happy" (Freitas, 2008b: 423).

In 1909, Amadeo started attending classes at the Vitti Academy by the Spanish painter Anglada-Camarasa (1871-1959). Freitas noted this academy was known to follow particular artistic techniques such as the use of free-flowing, thick brushstrokes and exuberant colours, both features easily identified in Amadeo's paintings (Freitas, 2006; Freitas, 2008; Vilarigues *et al.*, 2008). With a growing interest in painting, Amadeo also began to attend painting classes at the free academies in Paris. He moved again in *Montparnasse* to *Rue des Fleurus* and developed his relationship with the *Delta* group. Founded by doctor Paul Alexandre and his brother, this group was composed by Amedeo Modigliani, Constantin Brancusi (1876-1957), Maurice Drouard (1886-1915), Henri Doucet (1883-1915), Albert Gleizes (1881-1953) and Henri Le Fauconnier (1881-1946) (Alfaro, 2007; Leal, 2010).

Amadeo became fully integrated into the artistic environment of Paris, embracing inspirational cultural events happening at the time such as the *Le Figaro's* publication of the *Futurist Manifesto* by Marinetti (1876–1944), the performance of Serge Diaghilev's *Ballets Russes* at the Théâtre du Châtelet and the Brussels Universal Exhibition, where he was completely enchanted by the Flemish Primitives paintings (Freitas, 2008b).

Amadeo's choice of career won his father's acceptance in 1910, as he built him a studio at their Manhufe farm²⁴, for when he returned home. In 1911, Amadeo moved to *Rue Colonel Combes*, near the *Quai d'Orsay*, where he made a joint exhibition with Modigliani, which was visited by Picasso (1881-1973), Guillaume Apollinaire (1880-1918), Max Jacob (1876-1944) and Ortiz de Zárate (1887-1946). Next, he presented at the 27th *Salon des Indépendants*, described as the first major cubist exhibition. Here, he also had the opportunity to see a retrospective on Henri Rousseau (1844–1910), whose imaginative and decorative richness influenced Amadeo's most important drawings, namely the *XX Dessins* and the illustrated version of Gustave Flaubert's book: *La Légende de St Julien L'Hospitalier*²⁵, published in 1912, Figure 1.7. As Freitas reports, Amadeo's statement of his identity as a graphic artist was illustrated with these two extraordinary works. He seriously promoted his *XX Dessins* all around Europe and North America and his family was overjoyed with his illustration of *La Légende de St Julien L'Hospitalier* (Alfaro, 2007; Freitas, 2008b).

By 1911, Amadeo knew prominent figures of the Parisian art scene such as the couple Sonia (1885-1979) and Robert Delaunay (1885-1941), Alexander Archipenko (1887-1964), Blaise Cendrars (1887-1961), Marie Laurencin (1883-1956), Francis Picabia (1879-1953), Marck Chagall (1887-1985), Umberto Boccioni (1882-1916), Paul Klee (1879-1940), Franz Marc (1880-1916), August Macke (1887-1914) and Walter Pach (1883-1958) (Alfaro, 2007; Freitas, 2008b).

In the following years, Amadeo was distanced from the Portuguese artists group and strengthened his international artistic connections, exhibiting his works regularly and with noteworthy reviews. In 1912, he participated in the *Salon des Indépendants* and in the *Salon d'Automne*, and in 1913, he gained international recognition by participating in one of the most important art events of the 20th century, the *Armory shown*, held in New York, Chicago and Boston. This was possible thanks to the help of Walter Pach, and Amadeo was one of the most commercially successful artists of this exhibition. In the same year, he also exhibited at the *Erster Deutscher Herbstsalon* (1st Autumn Salon)

²⁴ The art studio was also financially supported by Amadeo's uncle, Francisco Cardoso, who always supported his artistic career (Alfaro, 2007).

²⁵ This book was studied in the framework of the PhD of Ana Margarida Silva at the DCR FCT NOVA (Silva, 2018).

in Berlin, and at the Applied Art School in Hamburg. This resulted from his friendship with the Delaunays, Otto Freundlich (1878–1943) and Wilhelm Niemeyer (1874-1960) (Alfaro, 2007; Freitas, 2018b).

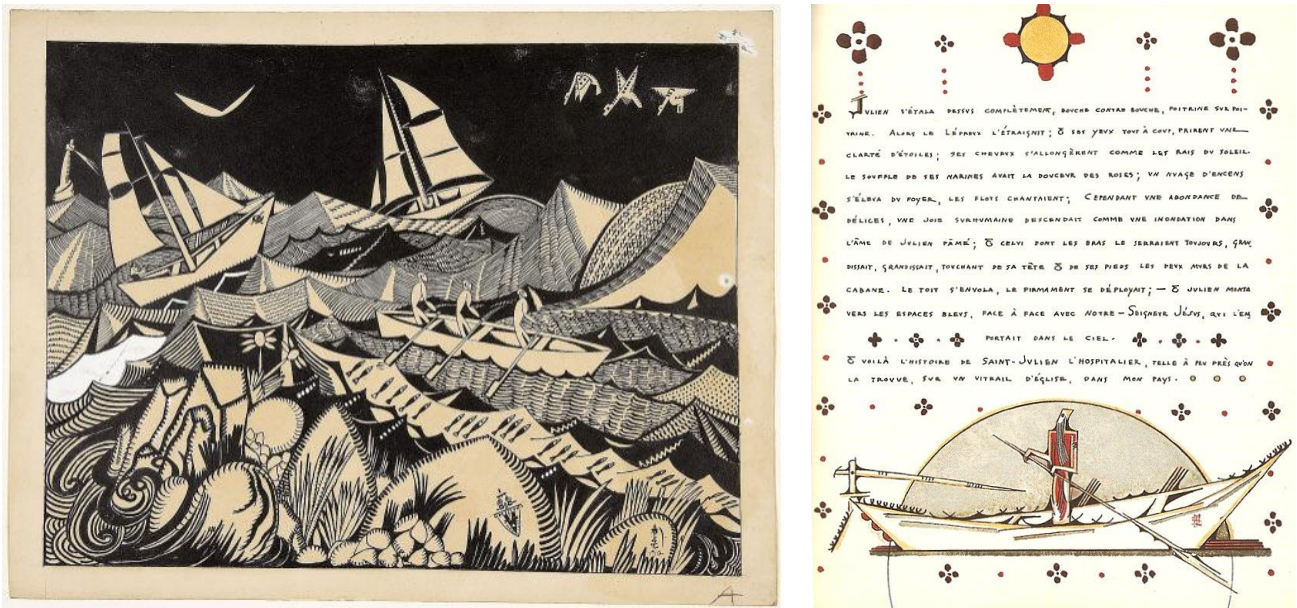


Figure 1.7. On the left, *La Tourmente*, 1912 (18th drawing of the *XX Dessins*, Inv. 92DP1548 © FCG), and on the right, folio 136 of *La Légende de St Julien L'Hospitalier*, 1912 (Inv. DP1822 © FCG).

Although associated with the Futurists and Cubists movements, his complex lines and use of colour completely veer away from them after 1913 and in a letter by Amadeo to his uncle Francisco he wrote: “I have progressed considerably. My way of feeling and understanding has nothing to do with the Futurists or Cubists and if anything, it confirms the opposite” (Alfaro, 2016: 181 & 358).

In 1914, Amadeo continued his strong stylistic, plastic and colouristic experimentation, relocating his studio to *Villa Louvat, Rue Boulard*. He had works in the “Modern Spirit” exhibition at the Milwaukee Art Society (USA), at the Salon of the Allied Artists’ Association (London) and at the German Modern and Decorative Art exhibition (Cologne). By the end of this year, Amadeo travelled with Lucie to Portugal, finally marrying her on the 16th of September, in Porto. With the beginning of the World War I, Amadeo was confined to Portugal for the rest of what would be his short life (Alfaro, 2007; Leal, 2010).

Amadeo lived with Lucie in his studio at Casa do Ribeiro (Manhufe), where he was fully dedicated to his work. According to Freitas, the period from 1915 to 1918 was the most personal, creative and expressive of his life. During this time, Amadeo kept in contact with the Delaunays who had moved to Vila do Conde (1915-1916) and with the Portuguese artists: Eduardo Viana, Almada Negreiros (1893-1970) and José Pacheco (1885-1934). Together with Baranoff-Rossiné (1888-1944), Guillaume Apollinaire and Blaise Cendrars, the *Corporation Nouvelle* was created, organizing itinerating exhibitions and planning the publication of artistic albums executed using the *pochoir* technique. The expectations were high and Amadeo worked tremendously hard but unfortunately, in the end, this was unsuccessful. No exhibitions occurred and the efforts of Walter Pach to help Amadeo exhibit in the USA were also unfruitful (Alfaro, 2007; Freitas, 2018b).

In 1916, Amadeo published the *12 Reproductions* album to promote his work and mounted his highly publicized but also criticized solo exhibitions in Porto and Lisbon called Abstractionism, where he displayed 114 works (Alfaro, 2007). As quoted in Alfaro, to the journal *O Dia*, Amadeo said: “I don’t follow any school. The schools have died. We, the new ones, only seek originality. Am I an impressionist, a cubist, a futurist, an abstractionist? I’m a bit of everything. But none of it makes up a school” (Alfaro, 2016: 253 & 367). In 1917, while isolated in Manhufe, art historians agree that Amadeo produced his most cohesive and innovative works of art, mastering all his materials and techniques, Figure 1.9 (França, 1992; Gonçalves, 2006; Freitas, 2008b).

Amadeo died on the 25th of October of 1918, only thirty years old, a victim of the Spanish flu, never achieving his wish to return to Paris. Although young, he left an extensive and extraordinary art production with a glimpse of what could have been his exceptional future as an artist (Freitas, 2008b).

1.3.2. The artist’s materials and techniques: an overview

Amadeo’s materials and techniques have been the subject of an ongoing study at the DCR FCT NOVA since 2008. Thirty-two paintings attributed to Amadeo have been studied together with one of the artist’s palettes, one artist’s box which was also used as a palette (both belonging to the CAM collection) and one artist’s box with thirty oil paint tubes found at the Manhufe house. These materials together with twenty-one paintings thoroughly selected by Helena de Freitas, were studied for the second volume of the *Catalogue Raisonné*²⁶ (Vilarigues *et al.*, 2008; Melo *et al.*, 2009). Six paintings were studied in the framework of the PhD of Cristina Montagner²⁷ at the DCR FCT NOVA (Montagner, 2015) and four paintings belonging to Amadeo’s family²⁸, as well as another from a private collection were analysed for authentication purposes. A selection of Amadeo’s paintings is shown in Figure 1.8 (from the period between 1913 and 1916) and in Figure 1.9 (from c.1917).

All paintings were investigated using a multi-analytical approach. First, surface examinations were performed using macrophotography (visible, UV and IR) and X-radiography. These techniques mainly allow the detection of underdrawings, texture (e.g. *impasto*) and previous interventions (e.g. inpainting or overpaint). The manner in which the colours were mixed and the brushstrokes were revealed by photography using the stereo-microscope. Secondly, the paintings were analysed in situ by μ -EDXRF, FORS and μ -Raman. Micro-samples, including cross-sections, were taken for analysis by μ -FTIR, μ -Raman and where necessary, by SEM-EDS, HPLC-DAD and microspectrofluorimetry. All of these techniques combined enabled a full characterisation of the materials present in the paintings.

²⁶ The twenty-one paintings studied were: *Quadro G*, c.1912, cat. n° P41; untitled (*O Jockey*), c.1913, cat. n° P58; untitled, c.1913, cat. n° P74; untitled, c.1913, cat. n° P75; untitled, 1914, cat. n° P83; untitled, c.1914, cat. n° P85; untitled, 1914, cat. n° P88; untitled, c.1914, cat. n° P96; untitled (*Cabeça*), c.1914, cat. n° P117; untitled, c.1914, cat. n° P121; untitled, c.1914, cat. n° P122; untitled, c.1914, cat. n° P138; *Ar livre nú*, c.1914, cat. n° P139; untitled, c.1914, cat. n° P140; *Paysagem figura negra*, c.1914-1915, cat. n° P153; *Janellas do pescador*, c.1915-1916, cat. n° P168; *Mucha*, c.1915-1916, cat. n° P172; untitled, c.1917, cat. n° P199; untitled (unfinished work), cat. n° P.AP.I; untitled (case study 1) and untitled (case study 2).

²⁷ Four paintings are included in the *Catalogue Raisonné*: untitled (*BRUT 300 TSF*), c.1917, cat. n° P196; untitled, c.1917, cat. n° P197; untitled (*Entrada*), c.1917, cat. n° P200; untitled (*Coty*), c.1917, cat. n° P201. Two paintings are not included in the *Catalogue Raisonné* but as a result of their technical investigation these may be attributed to Amadeo de Souza-Cardoso.

²⁸ Two paintings are included in the *Catalogue Raisonné*: untitled, c.1908-1910, cat. n° P12; *Luto cabeça boquilha*, c.1914-1915, cat. n° P119, and two paintings: *Teatro* and *As Bretãs* were not included in the *Catalogue Raisonné* at the time.

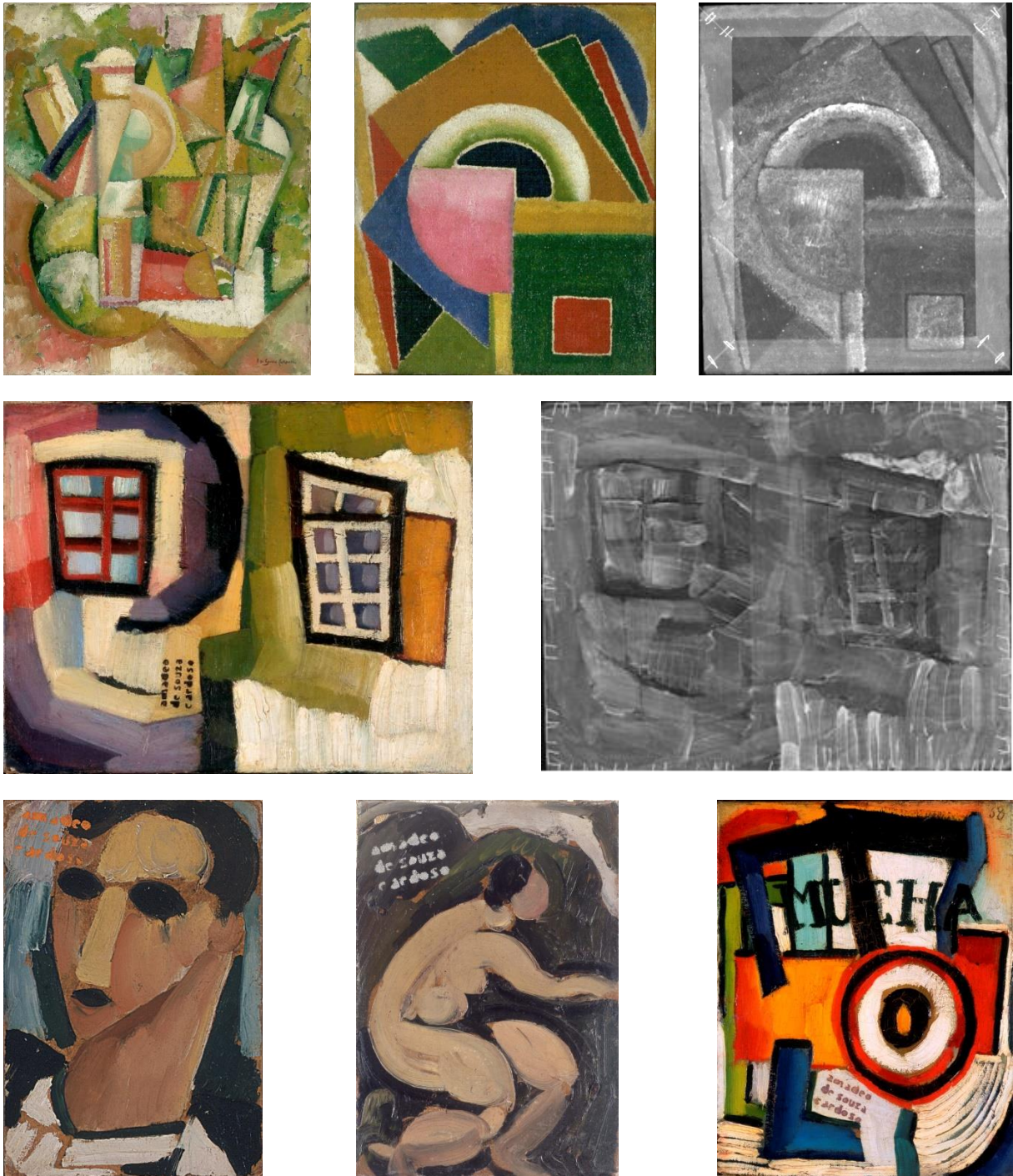


Figure 1.8. Amadeo de Souza-Cardoso paintings, from left to right, top to bottom: untitled (*O Jockey*), c.1913, 61 x 50 cm, cat. nº P58 (Freitas, 2008: 209); untitled, c.1913, 34.4 x 28.2 cm, cat. nº P75 (Freitas, 2008: 229) and the X-radiograph (Melo *et al.*, 2009); *Janellas do pescador*, c.1915-1916, 27.4 x 34.8 cm, cat. nº P168 (Freitas, 2008: 318) and the X-radiograph (Vilarigues *et al.*, 2008: 98); untitled, c.1914, 18.7 x 12.8 cm, cat. nº P122 (Freitas, 2008: 269); *Ar livre nú*, c.1914, 18.8 x 13 cm, cat. nº P139 (Freitas, 2008: 286); *Mucha*, c.1915-1916, 27.3 x 21.4 cm, cat. nº P172 (Freitas, 2008: 322) © FCG & DCR FCT NOVA.

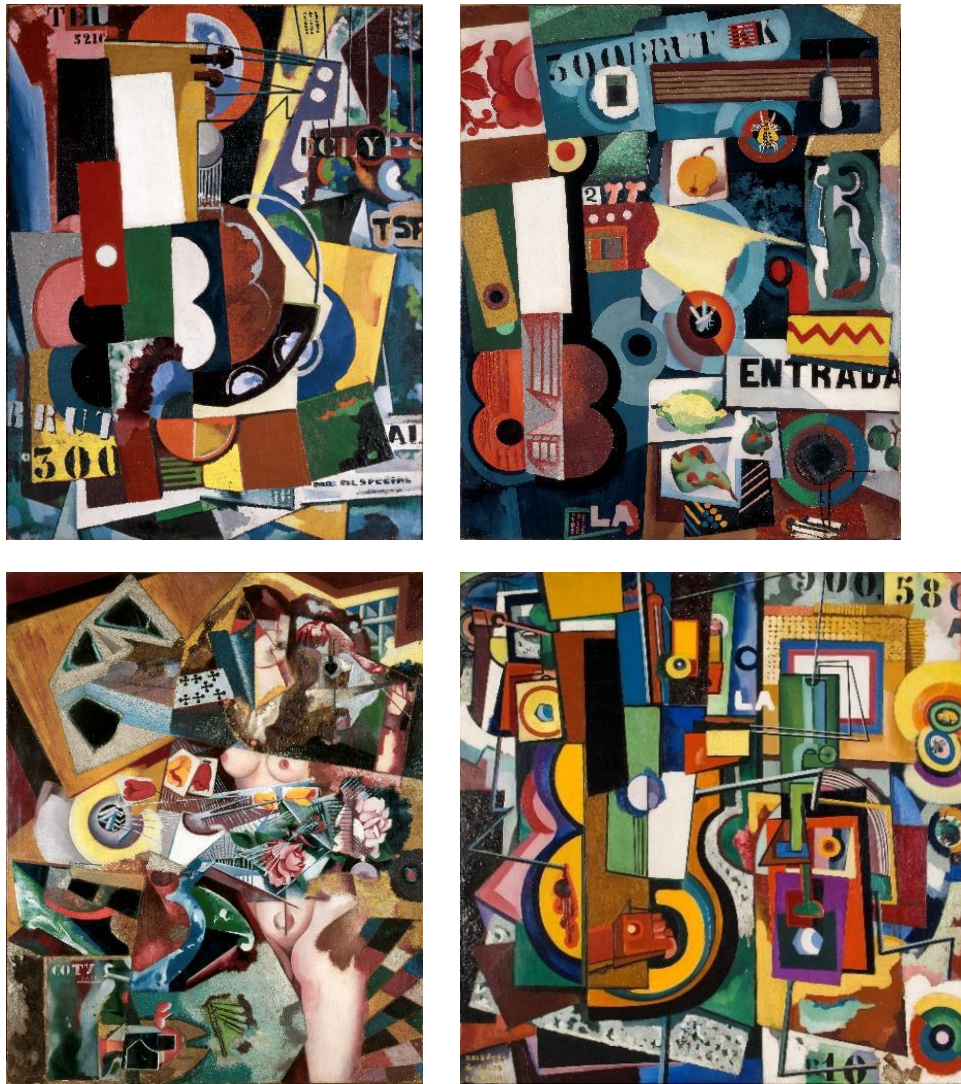


Figure 1.9. Amadeo de Souza-Cardoso paintings, from left to right, top to bottom: untitled (*BRUT 300 TSE*), c.1917, 85.8 x 66.2 cm, cat. n° P196 (Freitas, 2008: 356); untitled (*Entrada*), c.1917, 93.5 x 75.5 cm, cat. n° P200 (Freitas, 2008: 364); untitled (*Coty*), c.1917, 94 x 76 cm, cat. n° P201 (Freitas, 2008: 367); untitled, c.1917, 93.5 x 93.5 cm, cat. n° P197 (Freitas, 2008: 358) © FCG (photos by Cristina Montagner).

From this investigation it appears that Amadeo painted directly onto his canvases without prior preparation. Almost no underdrawings were detected (by infrared photography) nor were corrections or overlapping figures visible (by X-radiography, see Figure 1.8). Interestingly, adding support to the idea that Amadeo painted directly, there are few examples of sketches that could be considered studies for his paintings (Vilarigues *et al.*, 2008; Melo *et al.*, 2009; Montagner, 2015).

Texture along with colour is a key element in Amadeo's paintings. The painting's *impasto* is clearly seen through the X-radiographs, as shown in Figure 1.8. The brushstrokes are thick, apparently rapidly applied and can be found juxtaposed, overlapped or mixed while wet. His main technique is the application of paint in two ways here described as "wet-on-wet", where an overlap occurs when a brush of paint is applied over another not completely dried, and "wet-in-wet", where a juxtaposition of colours happens in a single stroke when the colours are applied only slightly mixed. To define shapes, he used large and differentiated patches of colour (*taches*) (Vilarigues *et al.*, 2008).

Paintings produced near the end of his life (Figure 1.9) are thought to form a homogeneous nucleus (França, 1992; Freitas, 2008) using similar techniques to what observed previously, however, with the creative use of unconventional materials such as glasses, mirrors, sand and matches. Moreover, there is the use of golden and silver tones, only previously identified on the *La Légende de St Julien L'Hospitalier* and never before used in his oil paintings (Melo *et al.*, 2009; Montagner, 2015; Silva, 2018).

As supports for his paintings, Amadeo chose canvas fixed on wooden stretchers as well as cardboard in small dimensions. A white preparation layer was found on most of the paintings; the preparation layer on the canvases was consistently composed of chalk (calcium carbonate), lead white (basic lead carbonate) and/or barytes (barium sulfate), presumably in an oil binder, whereas the preparation layers found on the cardboards consisted predominantly of lead white. In some cases, cardboard without a preparation layer was found where Amadeo had made use of the cardboard colour as part of the composition (Vilarigues *et al.*, 2008; Melo *et al.*, 2009; Montagner, 2015). It is important to note that in the 19th century it was common to buy prepared supports in standard formats (Carlyle, 2001: 185).

The results obtained by Maria João Melo's team allowed the determination of the pigments most used by Amadeo throughout his life, Table 1.1 (Vilarigues *et al.*, 2008; Melo *et al.*, 2009), and used more frequently in his last paintings, c.1917, Table 1.2 (Montagner, 2015). The majority of these pigments belong to the impressionist palette as described by Bomford *et al.*, 1990. Amadeo was knowledgeable about his materials. In the recent exhibition *Amadeo de Souza-Cardoso, Porto-Lisboa, 1916-2016*, a notebook belonging to the artist was revealed for the first time, containing personal and professional notes²⁹, including excerpts from the late 19th century book *La science de la peinture*³⁰ by the French academic painter Jehan-Georges Vibert³¹ (1840-1902) about the durability, composition, properties and application of 19th century painting materials (Vibert, 1891).

The blue pigment which most often appears in Amadeo's work was **cobalt blue**, a cobalt aluminate that was discovered in 1802 by L. J. Thénard (published in 1803) following previous researches (Harley, 1982: 56; Eastaugh *et al.*, 2004: 112). Bomford *et al.* attribute its popularity to its "pure blue colour" and chemical qualities and for that reason state that it was quickly made available to painters (Bomford *et al.*, 1990: 56). Amadeo used cobalt blue pure and it was also found in mixtures with cerulean blue, synthetic ultramarine blue and Prussian blue, all of which were also found pure (Vilarigues *et al.*, 2008; Montagner, 2015).

Prussian blue, a ferric ferrocyanide compound, was invented between 1704 and 1707. Harley credits Diesbach, a German colourmaker, for its discovery and Dippel an alchemist, for supplying the raw materials. According to her, details of the manufacturing process were only published in 1724, with the result that it was only broadly available to painters after this time (Harley, 1982: 71). **Ultramarine blue** has an aluminosilicate matrix with a sodalite structure containing entrapped sulfur

²⁹ The book was kindly shown by Marta Soares, curator of the exhibition *Amadeo de Souza-Cardoso, Porto-Lisboa, 1916-2016*.

³⁰ The excerpts are transcribed in Appendix I (p. 157).

³¹ *La science de la peinture* is a 19th century authoritative source on painting materials of that period. It discusses the materials and their application from a 'scientific' and practical point of view, containing a list of the colours and/or pigments Vibert considered 'good' and 'bad' (Vibert, 1891; Carlyle, 2001: 11 & 329).

groups. Its mineral form is called lazurite. Before the 19th century, this exquisite pigment was obtained from the semi-precious stone lapis lazuli. As mentioned above, extensive research was undertaken and in 1828, J. B. Guimet found a method to synthesise it with high quality and lower costs. Its synthetic form was called French Ultramarine (Plester, 1993; Eastaugh *et al.*, 2004: 375). **Cerulean blue** is a cobalt stannate whose origin is unclear from the literature, as noted by Eastaugh *et al.*, but they mention the existence of precursors since late 18th century (Eastaugh *et al.*, 2004: 90). According to Carlyle it was introduced as an artists' material in the 1860's (Carlyle, 2001: 472).

Table 1.1. Amadeo's main pigments: common names and chemical formulas (Melo *et al.*, 2009; Montagner, 2015).


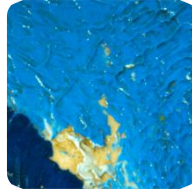
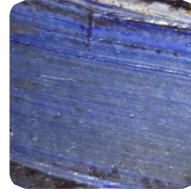
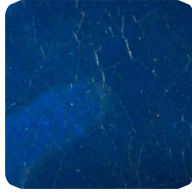
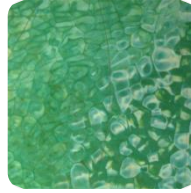
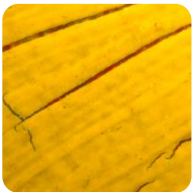


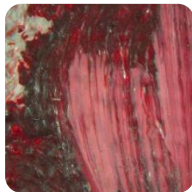

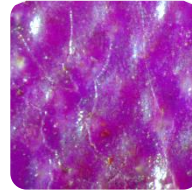

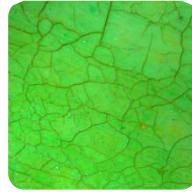


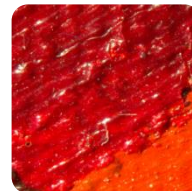

				
Cobalt blue $\text{CoO} \cdot \text{Al}_2\text{O}_3$	Cerulean blue $\text{CoO} \cdot n\text{SnO}_2$	Ultramarine blue $\text{Na}_8[\text{Al}_6\text{Si}_6\text{O}_{24}]\text{S}_n$	Prussian blue $\text{Fe}_4[\text{Fe}(\text{CN})_6]_3$	Viridian $\text{Cr}_2\text{O}_3 \cdot 2\text{H}_2\text{O}$
				
Chrome yellow PbCrO_4	Cadmium Yellow CdS	Vermilion HgS	Carmine Lake	Lead white $2\text{PbCO}_3 \cdot \text{Pb}(\text{OH})_2$

Table 1.2. Other pigments used in the paintings of c.1917 (Figure 1.9): common names and chemical formulas (Montagner, 2015).

			
Cobalt violet $\text{Co}_3(\text{AsO}_4)_2$	Eosin based lake ³²	Emerald green $\text{Cu}(\text{C}_2\text{H}_3\text{O}_2)_2 \cdot 3\text{Cu}(\text{AsO}_2)_2$	
			
Strontium yellow SrCrO_4	Cobalt yellow $\text{K}_3[\text{Co}(\text{NO}_2)_6] \cdot 3\text{H}_2\text{O}$	β-naphthol red	Zinc white ZnO

³² No image is shown because the eosin based lake found in Amadeo's painting (BRUT 300 TSF) has faded (Montagner, 2015).

In his last paintings, Figure 1.9, Amadeo also used **cobalt violet** in the form of a cobalt arsenate. It was introduced in the middle of the 19th century and was available in other compositions as magnesium cobalt arsenate and cobalt phosphate (Carlyle, 2001: 503; Corbeil *et al.*, 2002).

The introduction of new chemically produced pigments also introduced new greens in the 19th century painters' palette, for example viridian and emerald green, which were used by Amadeo. Until this time, the greens were mainly prepared as mixtures of blues with yellows sometimes adding some malachite (Vilarigues *et al.*, 2008). **Viridian**³³ is a hydrated chromium (III) oxide, reported to be a pigment of great transparency and durability, offered for sale in the 19th century (Carlyle, 2001: 492). It was first prepared by a French colourmen, Pannetier around 1838, following the discovery of the dull green chromium (III) oxide by L. N. Vauquelin in 1809, but its synthesis was only patented in 1859 by Guignet (Vauquelin, 1809; Newman, 1997). Amadeo used viridian pure, but it was also found in his work with chrome yellow, strontium yellow and cadmium yellow (producing light green tones) and with Prussian blue which produced darker green tones (Vilarigues *et al.*, 2008; Montagner, 2015). **Emerald green**³³ is a copper acetoarsenite first manufactured commercially in Germany in 1814 by Wilhelm Sattler and Friedrich Russ but its synthesis was only published in 1822 by J. von Liebig and Braconnot, separately (Harley, 2001).

Judging from an analysis of Amadeo's palette from the paintings studied (Vilarigues *et al.*, 2008; Montagner, 2015), the yellow pigment which appears most often in his work, throughout his artistic life, was **chrome yellow**, (thoroughly described below in Chapters 3 & 4). Another yellow chromate based pigment, **strontium yellow** (described in Chapter 3.6, p. 70), was found in his work, although less frequently (Vilarigues *et al.*, 2008; Montagner, 2015). **Cadmium yellow** appears most often in mixtures, but it was also found pure in Amadeo's last paintings (Vilarigues *et al.*, 2008; Montagner, 2015). It is a cadmium sulfide that was only commercially available after the 1840's due to the scarcity of the metal. It was considered a bright and durable pigment (Harley, 1982: 103; Carlyle, 2001: 523). Another yellow found in Amadeo's work, although less commonly than cadmium (Montagner, 2015) was **cobalt yellow** or Aureolin, a tripotassium hexanitrocobalt (III) first synthesised by N.W. Fischer in 1831 and made available as an artist's pigment in 1851, it was reported to lack opacity (Cornman, 1986; Carlyle, 2001: 525).

Vermilion, a traditional pigment of a bright opaque red, was also found in Amadeo's paintings. An extremely toxic material consisting of mercury sulfide. During Amadeo's time, this pigment was synthetically produced by the so-called wet process (Gettens *et al.*, 1993a). The traditional and light-sensitive natural **red lake pigments** such as cochineal and madder based lake pigments were also found in his paintings (Vilarigues *et al.*, 2008). Since ancient times, the cochineal red dye is obtained from the eggs of the female insect (*Dactylopius coccus*, *Porphyrophora polonica* L. and *Porphyrophora hamelii*) and the madder colour extracted from the roots of plants from the *Rubiaceae* family. The main chromophores of these dyes/pigments³⁴ are derived from the anthraquinone

³³ The hydrated chromium (III) oxide is called viridian in modern English and Portuguese, however, is named *vert émeraude* in French. The copper acetoarsenite is called emerald green in modern English and Portuguese and *vert Véronèse*, *vert de Vienne* and *vert de Brunswick* in French (Carlyle, 2001: 492-494).

³⁴ A dye or a pigment may be inorganic or organic; their distinction is related to their solubility in the applied medium: a dye is soluble, and a pigment is insoluble during their application (Herbst & Hunger, 2004).

molecule, namely carminic acid for cochineal and alizarin plus purpurin for madder, Figure 1.10 (Cardon, 2007; Melo, 2009).

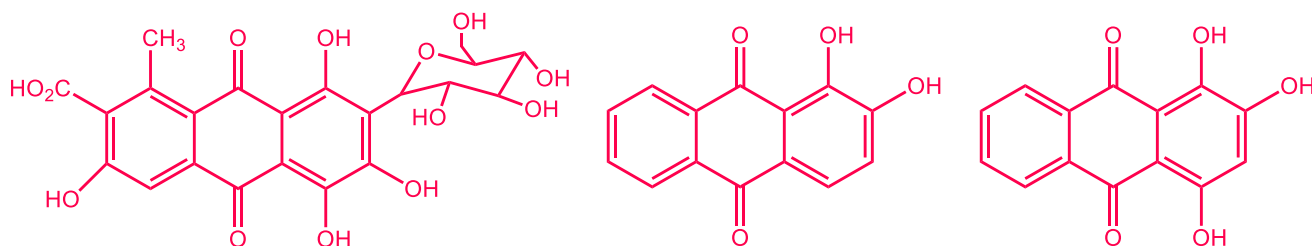


Figure 1.10. Molecular structures of carminic acid (left), alizarin (middle) and purpurin (right).

In his last paintings, two synthetic organic pigments were found (Montagner, 2015): a **β -naphthol red pigment**, and an **eosin based lake**, Figure 1.11. The β -naphthol red pigments consist of monoazo compounds which were discovered as early as 1869 by Schaeffer, but only entered the market as pigments in 1889 (Keijzer, 1999). The eosin based lakes have a hydroxy-phthalein structure which makes them extremely light-sensitive, therefore they quickly fade. Fluorescein was the first to be synthesised in 1860 by the German chemist Adolf Baeyer, followed by eosin in 1873 (Geldof *et al.*, 2013b).

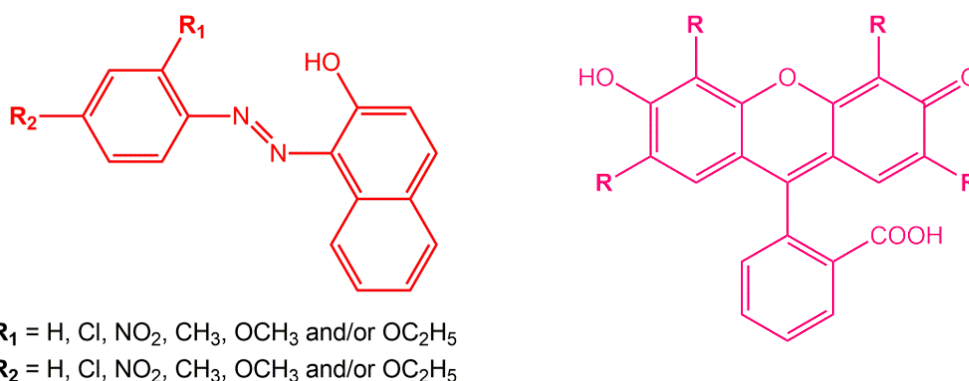


Figure 1.11. Molecular structures of β -naphthol pigments (left) and eosin based lakes (right): fluorescein ($R = \text{H}$), eosin ($R = \text{Br}$) and erythrosin ($R = \text{I}$).

Lead white was the white pigment most frequently found in Amadeo's paintings, it was present alone or mixed with barytes (barium sulfate) (Melo *et al.*, 2009; Montagner, 2015). Carlyle reports that barium sulfate was often added to lead white (Carlyle, 2001: 514). **Zinc white** appears mainly in his last paintings (Montagner, 2015). Lead white, a traditional white pigment very dense, consists of a basic lead carbonate (Gettens *et al.*, 1993b). Zinc white is a zinc oxide introduced in the late 18th century as an alternative to the toxic lead white (Carlyle, 2001: 516; Eastaugh *et al.*, 2004: 72).

Amadeo's brown tones were obtained by mixing reds, greens and yellows, with ochre pigments rarely appearing. As for his blacks they are predominantly mixtures of Prussian blue, ultramarine, viridian, chrome yellow and vermilion (Vilarigues *et al.*, 200; Melo *et al.*, 2009; Montagner, 2015).

The binding medium found in Amadeo's paintings was predominately oil (Vilarigues *et al.*, 2008; Melo *et al.*, 2009; Montagner, 2015). Amadeo wrote about using it in a letter to Sonia Delaunay in May of 1916 “(...) *j'aime mieux l'huile, c'est plus dans mon temperament*” (I prefer oil, it suits my temperament better) (Alfaro, 2016: 234 & 365).

Individual oil paint tubes which have been attributed to Amadeo (Vilarigues *et al.*, 2008) were also fully characterised using the same analytical techniques as were used for the paintings. The pigment compositions found correlate well with those identified in Amadeo's paintings, adding weight to their attribution to Amadeo. The collection of thirty oil paint tubes, mainly labelled Lefranc, Bourgois and Winsor & Newton, were dated according to the information on their labels and their overall shape. With the exception of three, the tubes could be dated to before 1914³⁵ (Vilarigues *et al.*, 2008; Melo *et al.*, 2009). It has been established through Amadeo's correspondence that between 1914 and 1918, he bought his materials from Araújo & Sobrinho, a stationer in Porto which had been selling W&N products since at least the end of the 19th century (Ferreira, 1981).

³⁵ This information was kindly provided by Jessica Montgomery, from W&N (Vilarigues *et al.*, 2008).

Chapter 2

The Winsor & Newton 19th Century Archive Database



Image of the manuscript books included in the W&N 19th Century Archive Database © Mark Clarke

M. Vilarigues, V. Otero. 2018. *Magic lantern hand-painted slides and the 19th century artists' colourmen Winsor & Newton*. In: S. Dellmann, F. E. Kessler, eds. Proceedings of the International conference A Million Pictures: History, Archiving, and Creative Re use of Educational Magic Lantern Slides, *in press*.

T. Vitorino, V. Otero, L. Carlyle, M. J. Melo, A. J. Parola, M. Picollo. 2017. *Nineteenth-century cochineal lake pigments from Winsor & Newton: insight into their methodology through reconstructions*. In: J. Bridgland ed. ICOM-CC 18th Triennial Conference Preprints, Copenhagen, art. 0107.

Chapter 2. The Winsor & Newton 19th Century Archive Database

The Winsor & Newton (W&N) 19th century archive is a unique primary documentary source covering handwritten formulation instructions and workshop notes for pigments, paints, grounds and varnishes, together with shop floor accounts (time and pricing for manufacturing their products). Access to these records gives a rare insight into W&N's true concern for the quality, durability and reliability of their products. To date, no other comprehensive historical archive of detailed instructions for the manufacture of artists' materials is available for researchers (Woodcock, 1995; Clarke & Carlyle, 2005a & 2005b; Clarke, 2008; Carlyle *et al.*, 2011).

The W&N 19th century archive has been available as a page-image database since 2006³⁶. It is an innovative database that associates a computer based indexing system with high resolution digitalized images from each page of a manuscript³⁷. These two components can be viewed individually or simultaneously in two windows, as will be described below. The contents of the archive are thus available without requiring full transcription or complex editing, allowing researchers easy, fast and flexible access to the archive, avoiding the need for visiting it, and most importantly handling such rare manuscripts (Clarke & Carlyle, 2005a & 2005b).

Access to the complete version of the database is only possible at the parent company, ColArt Fine Art & Graphics Ltd. (UK). An index providing general information on the content of the database may be consulted on-line and it is currently possible to view the first page-image corresponding to a database record (Winsor & Newton Archive, 2018). This will also be further discussed below. For this work, the Researcher's Edition (RE) of the database was consulted. It contains restricted records³⁸ (see below) due to their commercial sensitivity at the time of its construction. Presently, the Researcher's Edition is available in five locations³⁹ (Carlyle *et al.*, 2011).

2.1. Introduction to the Archive Database

The W&N 19th Century Archive Database comprises a summary index linked to digitalized page-images of 85 manuscript books (corresponding to a total of 16.648 page-images) and a digital

³⁶ This project was initiated by Leslie Carlyle and undertaken with Mark Clarke. It was originally begun as a Pilot project within the 'De Mayerne Programme' (2002-2006) which was funded by the Nederlandse Organisatie voor Wetenschappelijk Onderzoek (NWO) from 2003 to 2005. The Database resulting from the Pilot Project, named the Researcher's Edition is currently hosted in five locations, see note 4 below. Work to expand and add detail to the Researcher's edition was continued under the direction of Mark Clarke. This work took place thanks to Ian McClure's kind reception for it, at the Hamilton Kerr Institute, and was funded by the Arts and Humanities Research Council (AHRC) from 2006 to 2008 (Winsor & Newton Archive, 2009).

³⁷ The database was built in a FileMaker™ Pro 6.0, by Filemaker Inc. and the digital images were taken with a Canon Powershot S60 and a Canon EOS 1Ds mkII with an Esprit Gemini EM500 flash kit (Clarke & Carlyle, 2005a & 2005b; Winsor & Newton Archive, 2009).

³⁸ It is expected that the full unrestricted edition of the database will come on-line within the near future. Contact the Hamilton Kerr Institute, Cambridge University, UK, for more information (<http://www.hki.fitzmuseum.cam.ac.uk/archives/winsor-and-newton>).

³⁹ The locations are: in the Netherlands, the Rijksbureau voor Kunsthistorische Documentatie (RKD); in the UK, The Hamilton Kerr Institute, University of Cambridge; The Conservation and Technology Department, Courtauld Institute of Art, University of London; Department of Conservation, Tate Britain; and in Portugal, the Department of Conservation and Restoration, Faculty of Sciences and Technology, NOVA University of Lisbon.

collection of 47 W&N 19th century trade and retail catalogues. The Researcher's Edition consists of 15,003 database records with 3,579 inaccessible (restricted) due to the commercial sensitivity of the information at the time the database was completed (Carlyle *et al.*, 2011; Clarke, 2012).

Each database record presents a Unique Recipe Code (URC), which was developed by Mark Clarke such that the code incorporates the individual book, the page and the line number of the first line on the page where the recipe is found. Each book has a 2-character code and each page is designated by a P with a 3-digit page number, plus either A or B for recto and verso, where necessary (see below). The numbering of the first line of the record is necessary because there can be more than one record on a page (Clarke & Carlyle, 2005a; Clarke, 2012).

An example of a database record for a Damp Lake (URC: 08P042L01) and the corresponding page-image is shown in Figure 2.1 and 2.2, respectively. This example is available at the Winsor & Newton Archive website (Winsor & Newton Archive, 2009).

The screenshot displays the database interface for the 'Damp Lake' record (URC: 08P042L01). The interface is divided into several sections:

- Name Area:** Contains the original recipe name 'Damp Lake' and the interpreted name 'damp lake'. It also shows the restriction 'unrestricted', book '08', first page 'P042', first line '01', and the unique recipe code '08P042L01'.
- Topic Area:** Lists topics such as 'pigment manufacture notes' and 'damp lake'. A green box identifies the database as 'Winsor & Newton 19th Century Recipe Database, Researcher Edition 2008'.
- Material Area:** Features an 'INGREDIENTS TABLE' with columns for materials (original and interpreted names), qualifiers, units, quantities, and SI units. The table lists ingredients like Carb Ammo, water, aqua, alum, and W&N Liquor.
- Form Section:** Includes fields for 'equipment materials', 'Recipe date', 'Inferred MS date range', 'specifies costs or prices', 'marginal numbering', 'misc references', 'preparation summary', and 'transcription'. It also has checkboxes for 'discusses durability', 'discusses quality', 'illustration', and 'sample attached'.
- Navigation and Search:** A sidebar on the left contains a 'View Image' button, navigation arrows, 'Show All Records', 'Go to URC ...', a 'Find' section with search options, and buttons for 'Dictionary', 'MS Information', and 'Catalogues'.

Figure 2.1. Database window. Example: Damp Lake, URC: 08P042L01 © Winsor & Newton (ColArt Fine Art & Graphics Ltd.) (Winsor & Newton Archive, 2009; Clarke, 2012).

On the right side of the database window, there are three main field areas relating to the record, that is, the record name (original and interpreted), the topics associated with it and the materials (including quantities) referred to in the record. Other possible fields can include the date of the record, equipment, prices, companies referred to and a transcription of the record, see Figure 2.1. The information currently available was entered by the database project teams (discussed further below). On the left side, fields indicate the possibilities for consultation, these include the trade catalogues, information on individual books and a dictionary containing definitions and/or interpretations of abbreviated terms and obsolete terminology. The inbuilt dictionary is based on data from the archive and external technical literature (Winsor & Newton Archive, 2009; Clarke, 2009 & 2012).

Damp Lake small trial Oct 23/96
 2^{lb} Carb Ammo diss^d in a mixture of
 2 Gals hot & 2 Gals cold Wg - put into
 250 Gals Wg.
 5^{lb} ~~Al~~ Al Sphered in as usual
 add
 2 Gals Wg Purif^d 25 or Lig
 Produces 11^{lb} or X at 10^{lb} Damp
 make a fair cheap common lake

Gamboge dissolved in Carb Soda by boiling in
 water - then evaporated to dryness is
 soluble by standing in Spirits of Wine
 The Soda is here doubtless in a caustic state
 this view is confirmed by the effervescence
 discernable while the solution in Carb Soda
 is taking place, the Gamboge performs the part
 of an acid to the Soda
 This solution of Gamboge in Spirits of wine will
 bear dilution with water without the resin
 being thrown down -
 Perhaps it need not be evaporated, but the

Figure 2.2. Corresponding page image of the Damp Lake database record on Figure 2.1 © Winsor & Newton (ColArt Fine Art & Graphics Ltd.) (Winsor & Newton Archive, 2009).

The database can be used according to general or specific subjects. A term can be searched anywhere in the database by using the All Fields search button. It is possible to use a number of symbols which restrict the search, such as searching recipes within a date range. Individual Fields can be searched, one or more at a time, such as the original title of the recipe or the recipe name interpreted (the subject or title of the recipe expressed in modern terminology), topics, sub-topics, or an ingredient in its original or modern terminology. The search can be limited or extended between the individual fields and it can be presented in chronological or alphabetical order (Winsor & Newton Archive, 2009; Clarke, 2012).

2.2. The content of the Database

Within the framework of this thesis, a survey of the content of the historic catalogues and the manuscript books was conducted with special emphasis given to yellow chromate and cochineal lake pigments.

2.2.1. Winsor & Newton's catalogues

A comprehensive study of W&N's 19th century catalogues was carried out by Leslie Carlyle, who researched all available catalogues in their archive to establish what they offered throughout the 19th century in terms of oils, mediums, driers, varnishes, supports and colours in powder and in oil (Carlyle, 2001). Within this thesis, the objective is to discuss the catalogues currently available in the database and call attention to details which justify W&N's fast growth through ingenious and solid work together with good dissemination strategies.

As noted above, the database includes a digital collection of 47 W&N's 19th century catalogues covering the period between c.1835 and 1900. Although by far the majority of the collection are not complete catalogues (see Table 2.1), the seven marked in bold are complete (see also Table II.1.1 (p. 161)).

Table 2.1. Estimated dates of W&N's 19th century catalogues (included by Mark Clarke in the database). For the dates highlighted in bold, these catalogues are complete. See also Table II.1.1. (p. 161).

c.1835	1841	1850	1861	c.1870	1883	1892
	1842	1851	1863	1874	c.1884	1896[#]
	1846	1856	c.1864	1876	1885	1898
	1849	1857	1865		1886	1900
			1868		1887	
			c.1869		1888 [#]	
					1889	

[#] French catalogue available.

As previously noted, W&N became one of the leading artists' colourmen in Britain and ultimately, by the end of the 19th century, around the world. As will be seen, their archive reveals that they were committed to producing high quality products. In their catalogue from c.1835 (Figure 1.4), they list their newly developed moist watercolours. In total they were selling 51 colours "prepared in spirits, in impalpable powder, for oil or water colour painting; also in Bladders, finely ground in oil". Throughout the 19th century, W&N's catalogues bear evidence of a continually expanding range of materials. Their c.1870 catalogue consists of 205 pages and includes watercolours (in diverse containers such as cakes, pans and tubes), oil colours in tubes, pigments, oils, varnishes, inks, canvas and millboards, as well as a range of brushes and painter's boxes.

W&N's catalogues also demonstrate their efforts to promote their materials and their company. Their catalogues detail the medals they were awarded, and care is taken to inform customers of their successes, for example in their 1849 catalogue they state: "Fifteen years experience has now tested the qualities of THE MOIST COLOURS, and the very large and rapidly increasing demand, as well as the very flattering Testimonials received by Messrs. Winsor & Newton from Continental and English Artists, are evidence of the high estimation in which they are held" (p. 3).

Aside from the catalogues, further evidence of their dedication to quality and responsible manufacturing practices for artists' materials is their document on the composition and permanence of their colours, which was released in October of 1892 (and was included in their catalogues from this time and forwards). In this document, W&N clarified their position as artists' colourmen and their commitment to artists. For them, "manufacturing businesses exist, as a rule, not for the enforcement of moral laws on their customers, but for the satisfaction of the demands which those customers make; and while, for instance, we continue to be asked for *Magenta* and *Geranium Lake*, so long shall we continue to supply them. The Artist is, in our opinion, the sole judge of his right to employ such pigments; and we, who use our best efforts to supply him with all he requires, have no intention of excluding them from our list of manufactures. We do not assert that such colours are durable; all we do assert is that they are as durable as they can be made. (...) We propose, however, in the following pages, to classify colours in the order of their permanence, (...) because we shall thus, once and for all, dissipate the notion that we affirm all colours to be durable. (...) We, for our part, attach now little importance, as far as the success of business is concerned, to any concealment of the chemical composition of our colours and media; although we necessarily attach very considerable importance to maintaining the secrecy of those methods which long experience has taught us (...) but have always entertained the greatest reluctance to take any step whereby we might render unnecessary assistance to enterprising competitors." This document is fully transcribed in Appendix II.2 (p. 175). The composition and permanence of their pigments as analysed and studied by them, may be consulted.

2.2.2. Winsor & Newton's manuscript books

The majority of the 85 manuscript books indexed in the Researcher's Edition (RE) database consist of miscellaneous information (35 books), which can range from medical recipes, notes on suppliers and customers, as well as comments by chemists and colourmen and transcribed notes from

chemical periodicals and patents (Winsor & Newton Archive, 2009). There are also twenty books which primarily cover watercolour manufacture. Table 2.2 presents all books distributed according to their content. Data on their estimated date, number of pages and database records may be consulted in Table II.1.2 (p. 162).

Restrictions are mainly found in the books concerning watercolour and madder lake pigment manufacture (e.g. the book MA is completely restricted in the RE database).

Table 2.2. General content of the 85 books (codes as in the database). Highlighted in bold is the book belonging to Henry Charles Newton, and bold+underlined to Arthur Henry Newton. See also Table II.1.2 (p. 162).

	Miscellaneous information	Watercolours Manufacture	Pigment Manufacture	Oil paint Manufacture	Graining	Varnish	Others*
Book codes	01-29 [#]	2C C1 M2	2P P1 X5	DR	G1	V1	ES
	AC	2M C2 MT	3P P2 X6	GR	G2	V2	LP
	EN	A1 C3 WW	4P P3 X7	KT	G3		MA
	IN	A2 C4 X1	7P P4 [†] X8				P8
	NA	A3 C5 X3	9P PM				
	OG	A4 CP X4	A5 SE				
	RE [‡]	A7 HS	A6 X2				

[#] These books are entitled “*Omnium Gatherum*” and are the smaller books of the archive.

* ES stands for Estimated Costs, LP for Lead Pencil, MA for Madder and P8 concerns the preparation of spirit colours.

[‡] This book is entitled “A Relic of Old Times” being the earliest book of the archive dated 1833.

[†] This book also has contributions by Arthur Henry Newton.

Eighteen books cover pigment manufacture from 1834 to 1893. Two of these are private copies of processes belonging to the founder Henry Charles Newton and six of them belonged to his son Arthur Henry Newton, who worked with his father in the company⁴⁰. These books bear evidence of their commitment to the quality of their artists’ materials⁴¹.

Some of the books are numbered in chronological order and, most importantly, in some books the recipes are numbered and can be tracked using these numbers in other recipes, even in a different book (e.g. comparison between batches or a pigment used in a watercolour recipe; as detailed in Clarke, 2008). A set of books on pigment manufacture with numbered recipes throughout and largely dated are labelled P1, P2, P3 and 4P; these belonged to Arthur Henry Newton.

The RE database contains 202 general topics such as the manufacture of different artists’ materials, quality development and prices, see Table II.1.3 (p. 163) and 523 specific sub-topics such as the pigments that W&N was producing and selling, see Table II.1.4 (p. 166).

⁴⁰ The name of the authors is found inside the books, for example in book 7P there is the notation: “Private Copy of Processes belonging to H. C. Newton” and in book 9P: “This book is the private property of A H Newton”.

⁴¹ In book P2 belonging to Arthur Henry Newton, is the note: “In Father’s opinion this is a much safer color to use in oil than Chromate of Strontia” He was referring to a mixture of lemon yellow (barium chromate) with citron yellow (zinc potassium chromate) which appears under the recipe name: Strontian Yellow: No. 2 for Oil, dated 23/11/1859 (URC: P2P264AL07). In W&N’s 1892 declaration (Appendix II.2, p. 175), this mixture appears under the name Primrose Yellow and it is described as “similar in colour to the old ‘Strontian Yellow’ (Chromate of Strontium) but keeps its colour better” (Carlyle, 2001: 526).

An initial assessment of the content of the RE database can be made through its topics and sub-topics. For example, Carlyle *et al.* reported that 24% of the database records correspond to pigment manufacture, which provides an overview of the weight given to this activity in these records (Carlyle *et al.*, 2011). In this work, the sub-topics associated with a colour were also evaluated, which helped to reveal their significance to W&N. Although there are sub-topics in the RE database which are incorrectly attributed and others which are overlapping (this will be discussed below in Chapter 2.3), for this initial assessment, all pigment sub-topics relating to a colour were included and are highlighted in Table II.1.4 (p. 166). This shows the general distribution of the archive content in relation to W&N's colours and/or pigments. From a total of 8593 database records referring to pigments, 39% correspond to red/purple lake pigments and 19% to yellow/orange⁴² pigments, as may be seen in Figure 2.3. This indicates that these were the colours W&N was investigating and developing the most during the 19th century (to be discussed further below).

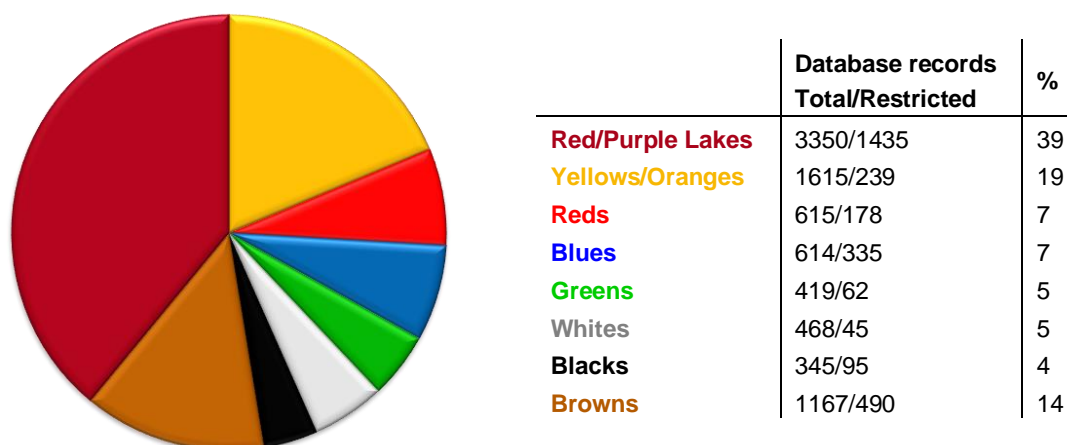


Figure 2.3. Distribution of pigment sub-topics relating to a colour in the W&N 19th Century Archive Database.

2.2.3. Winsor & Newton's yellow chromate and cochineal products

In W&N c.1870 catalogue, they describe once again their concern for and dedication to the quality of their products. In this passage, they specifically refer to their chrome yellows and cochineals: "The high standard of excellence sought by Winsor and Newton entirely set aside all common recipes and pernicious compounds, and rendered indispensable the aid of Chemical Science. Therefore perfectly appointed Chemical Works were established by them in 1844, with steam apparatus and all the appliances auxiliary to modern Chemical Art. The advantageous results of the establishment of these Works were apparent in the production of colours totally different from those of all the other manufacturing colour houses. The old colours were improved and new ones introduced. (...) Take, for instance, the **Cochineal Products**, the Carmines, the Crimson, Scarlet, and Purple Lakes, wherein stability is all but secured by the elimination of acids, and those other foreign matters necessary to the primary production of the pigment, but which, if not removed, or neutralized, before the ulterior

⁴² The orange fraction was included in the yellow because it is very small consisting of just 104 database records. Due to their low significance, the manufacturing processes of orange-red chromate based pigments were not included in the systematic study presented in Chapter 3.

preparation of the colour, act very prejudicially to its durability. Again, **Chromes** - Yellow, Deep, Orange or Scarlet - are, by the peculiar treatment applied to them by this House, made most valuable additions to the palette, *and this may be said of nearly all the chemically made colours*. The attainment of such effects can only be assured by the aid of the most perfect laboratory arrangements; and, certainly, none but those who devote themselves exclusively to the study and production of colours for artistic use, can hope to pursue the manufacture with any considerable measure of success" (p. 2-3).

Table 2.3 presents the colour names which appeared in W&N's catalogues throughout the 19th century associated with yellow chromate and cochineal lake pigments in powder, watercolour and oil paint. This data provides extra information to that already published by Carlyle in 2001 (Appendix 26, Table 6, p. 533-536), such as the availability of colours in watercolours, the colour names used in the French catalogues, periods of unavailability and additional variations in colour names introduced throughout the 19th century.

From their earliest c.1835 catalogue, watercolours were sold in cakes and in pans (named 'moist' watercolours) and after 1863 were also available in collapsible tubes. In the early catalogues from 1840's, oil colours were still listed in bladders, although oil paint tubes were also available. After 1846, only oil colours in collapsible tubes were available. The range of yellow chromate and cochineal lake watercolours listed throughout the 19th century rarely changed in contrast to other materials listed in Table 2.3.

W&N sold lead chromate based artists' materials under the trade names **Chrome Yellow** and **Chrome Deep** from their earliest catalogues from c.1835 and 1841, respectively (Carlyle, 2001: 536). Variations in colour names appear in the catalogues (Table 2.3), for example **Chrome Lemon** was introduced in the latter part of the century, appearing for the first time in W&N's 1886 catalogue listed in the oil colours (Carlyle, 2001: 536). In their declaration of 1892 (Appendix II.2; p. 175), **Chrome Yellow** is described as pure lead chromate, while **Chrome Deep** is given as pure lead chromate, more or less basic, and finally **Chrome Lemon** is presented as a combination of chromate and sulfate of lead. In the same document, all lead chromate pigments were classified as moderately permanent colours in water and in oil, standing well in the combined action of light, oxygen and moisture, but susceptible to darken under the influence of hydrogen sulfide.

Other yellow chromate based pigments were sold under the trade names **Lemon Yellow** (barium chromate), **Citron Yellow** (zinc potassium chromate) and **Strontian Yellow** (strontium chromate), the first available since c.1835 and the latter two appearing for the first time in the catalogue from 1861 as an oil colour (Carlyle, 2001: 536; Clarke, 2009: 164-66) and never sold as a watercolour. Variations of **Lemon Yellow**, **Pale** and **Deep**, were introduced in the catalogue from 1863 as powders and as oil colours. By the end of the 19th century, there was also available a **Permanent Yellow**, which in the declaration of 1892 (Appendix II.2; p. 175) is described as a preparation of barium chromate and zinc white, and a **Primrose Yellow**, a combination of zinc and barium chromates (Carlyle, 2001: 526). In W&N's 1892 declaration only the Lemon Yellow was considered a permanent colour in water and in oil. Permanent Yellow was given as permanent in oil and Citron Yellow together with Primrose Yellow were reported to be fugitive colours in oil.

Table 2.3. Availability of colours associated with yellow chromate and cochineal lake pigments in powder, watercolour and oil colour** throughout the 19th century from W&N, adapted from Carlyle, 2001, Appendix 26, Table 6, p. 533-536.

	Colour		Powder	Water Colours	Oil Colours
	English name	French name (in 1896)			
Yellow Chromate	Chrome Yellow	<i>Jaune de chrôme</i>	1835 - 1900*	1835 - 1900‡	1835 - 1900 [§] ^
	Chrome Deep	<i>Jaune de chrôme foncé</i>	1841 - 1900*	1842 - 1900 [‡] ^	1841 - 1900 [§]
	Chrome Lemon	<i>Jaune de chrôme citron</i>	1889 - 1900	1896 - 1900	1886 - 1900
	Lemon Yellow	<i>Jaune de citron</i>	1835 - 1861	1835 - 1900	1835 - 1900 [◇]
	Lemon Yellow, Pale	<i>Jaune de citron clair</i>	1863 - 1900	---	1863 - 1900
	Lemon Yellow, Deep	<i>Jaune de citron foncé</i>	1863 - 1900	---	1863 - 1876
	Citron Yellow	<i>Jaune citron</i>	---	---	1861 - 1900 [×]
	Strontian Yellow	<i>Jaune de strontian</i>	1863 - 1868	---	1861 - 1896 [×]
	Permanent Yellow	<i>Jaune permanent</i>	---	---	1886 - 1900
	Primrose Yellow	<i>Jaune primevère</i>	---	---	1896 - 1900
Cochineal Lake	Carmine	<i>Carmin</i>	1835 - 1887 [‡]	1835 - 1900	1835 - 1900 [⊙]
	Burnt Carmine	<i>Carmin brûlé</i>	1841 - 1900	1842 - 1900	1841 - 1900
	Carmine, Ordinary	---	1863 - 1876	---	---
	Carmine, Fine	<i>Carmin fin</i>	1863 - 1900 [•]	---	---
	Carmine, Finest Orient	<i>Carmin surfin d'orient</i>	1863 - 1900	---	---
	Carmine, No. 2	<i>Carmin fin 2</i>	---	---	1869 - 1900
	Carmine, Finest	<i>Carmin</i>	---	---	1886 - 1892
	Crimson Lake	<i>Laque carminée</i>	1835 - 1900	1835 - 1900	1835 - 1900
	Crimson Lake. Extra	<i>Laque carminée, extra</i>	1857 - 1900 [⊘]	---	---
	Purple Lake	<i>Laque pourpre</i>	1835 - 1900	1835 - 1900	1835 - 1900
	Scarlet Lake	<i>Laque écarlate</i>	1835 - 1900	1835 - 1900	1835 - 1900
	Indian Purple	<i>Pourpre indien</i>	1857 - 1868	1863 - 1900	1886 - 1900

** No data on powders is available for the catalogues from 1842, 1849, 1850, 1856 and 1888; on water colours for the years 1841, 1846, 1850, 1851, 1856, 1857, 1861, c.1864, 1865, 1868, c.1869, 1874, 1876, 1883, 1887, 1889 and 1892; on oil colours for the year 1889.

◇ In the catalogues from 1863, 1864, 1865 and 1868 the name used was Chrome Pale.

* In the catalogues from 1841, 1846, 1851, 1857 the name used was Deep Chrome.

‡ Carmine powder was not available in the catalogues from the period 1863-1876.

• Carmine, Fine powder was not available in the catalogues from the period 1883-1887.

⊘ Crimson Lake. Extra powder was not available in the catalogues from the period 1883-1887 and after 1889 it was available as Crimson Lake. Extra Fine.

‡ In the catalogues from 1842 and 1849, lead chromate based water colours were sold under the names Chrome Yell., 1, 2 & 3.

^ In the catalogues from 1863 and 1870 the name used was Deep Chrome.

§ In the catalogue from 1846, lead chromate based oil colours were sold under the names Chrome Yell., 1, 2 & 3.

^ In the catalogues from 1869, 1870, 1874 and 1876 the name used was Chrome Yellow, Pale.

◇ Lemon Yellow oil colour was not available in the catalogues from the period 1863-1876.

× Citron Yellow and Strontian Yellow oil colours were not available in the catalogues from the period 1869-1876.

⊙ Carmine oil colour was not available in the catalogues from the period 1887-1892.

W&N sold cochineal based products mainly under the names **Carmine**, **Crimson Lake**, **Scarlet Lake** and **Purple Lake**, listed since their earliest catalogue from c.1835, and **Burnt Carmine** since 1841. Furthermore, variations of carmine were introduced throughout the second part of the 19th century as powders and as oil colours (Carlyle, 2001: 535) as may be seen in Table 2.3. A **Crimson Lake Extra** was also available as a powder after 1857 and an additional colour, **Indian Purple** was available as powder between 1857 and 1868, as watercolour after 1863 and as an oil colour after 1886 (Carlyle, 2001: 535). In the declaration of 1892 (Appendix II.2; p. 175), W&N defines Indian Purple as a copper based cochineal lake for watercolours and a mixture of madder lake and French ultramarine for oil colours (Carlyle, 2001: 502). Moreover, in the same document all cochineal based lake pigments were classified as fugitive colours in water and in oil, with the exception of Burnt Carmine and Indian Purple, which were considered permanent colours. Interestingly, Scarlet Lake was listed among the permanent colours in oil.

It is also relevant to note that in the declaration of 1892, chrome yellow pigments were also found in mixtures with other pigments to produce particular colours: **Jaune Brillant** described as a moderately permanent oil colour was a mixture of chrome yellow and white lead; **Kings' Yellow** also reported to be a moderately permanent oil colour, was a mixture of chrome yellow and zinc white; **Chrome Greens** and **Cinnabar Greens** moderately permanent oil colours were preparations of chrome yellow and Prussian blue. Carlyle (2001) reports on this as well in pages 492, 526 and 530. Research using the W&N Archive Database on-line (Winsor & Newton Archive, 2018) under these names reveals one inaccuracy in the data available in their 1892 declaration. In book 9P and page P208, contrary to what is described, Jaune Brillant is referred to as "Naples Yellow, some white tinted with Extra Deep Cadmium", while King's Yellow is described as a mixture of chrome yellow and white, which is in agreement with the declaration. In a chrome green oil paint formulation dated 21/02/1871 (URC: GRP013AL13), a mixture of Lemon Chrome, Deep Chrome, Prussian blue and white earth⁴³ is ground in a mixture of linseed and poppy oil. No record is found for Cinnabar Green.

W&N's dedication to their yellows and red/purple lake colours, especially their chromes and cochineal products is also evidenced by their significant number of records for these colours as may be seen in Figure 2.4. From a total of 1511 database records for yellows, 34% correspond to yellow chromate pigments with 23% relating to lead chromate and 11% to other chromate based pigments (barium, zinc, strontium chromate and mixed chromates). W&N was also adding chrome yellow pigments to their other yellows, specifically the lakes, ochres and Naples yellow presumably to improve their colours (Carlyle, 2001; Clarke, 2009). There are 3350 database records concerning red/purple lake colours, with the majority pertaining to cochineal lakes (59%). The relevance of these pigments in the W&N archive also prompted attention to these colours in this research. In Chapter 3, a systematic investigation of the W&N 19th century manufacturing processes of yellow lead chromates, commonly known as chrome yellow pigments, and of the other yellow chromates is described. A thorough study of W&N's 19th century manufacture of cochineal red lake pigments is also being carried out in collaboration with Tatiana Vitorino at the DCR FCT NOVA & IFAC-CNR (Vitorino *et al.*, 2017).

⁴³ White earth is "precipitated from potash alum and pearl ash" (e.g. URC: P1P138AL06) (quote from Clarke, 2009: 167).

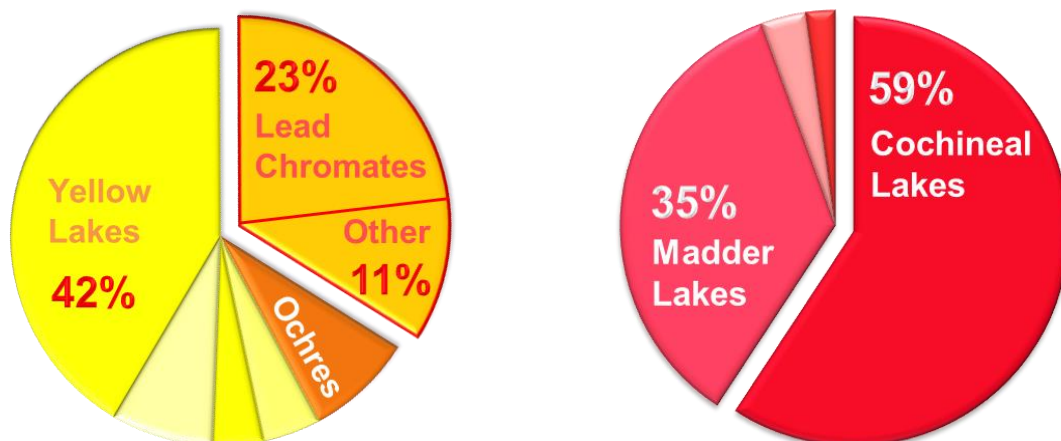


Figure 2.4. Distribution of the yellow (left) and red/purple lakes (right) in the pigment sub-topics from W&N's RE database. For the yellows, 42% are yellow lakes, 23% are lead chromate pigments, and 11% consist of other yellow chromate pigments. The percentage of yellow ochres is 8%, 4% of cadmium yellows, 4% of Naples yellows and 8% of other yellow pigments. The red/purple lake includes 59% of cochineal lakes, 35% of madder lakes, 2% of lac lakes and 4% of other lake pigments.

2.3. Advantages and limitations of the RE Archive Database

As stated above, the W&N RE database allows straightforward and time-saving access to a unique source of information on 19th century artists' materials, from their trade to their manufacture. The current restrictions in the Researcher's Edition comprise its main limitation. The restricted records are mainly focused on the manufacture of madder lake pigments and watercolours (Carlyle *et al.*, 2011) which are not the subject of this thesis⁴⁴. Fortunately, almost no restrictions were found for the work developed on the W&N 19th century manufactures of their yellow chromate and cochineal lake pigments.

The prime advantage of the W&N database is the simultaneous viewing of the indexed component and the correspondent digitalized page-image from the manuscript. As discussed by Clarke and Carlyle, this feature allows researchers to have their own interpretation of the original text and figures, since they do not have to depend solely on data inserted by the first compilers of the database (Clarke & Carlyle, 2005a & 2005b). Researchers can go forward and back within a particular book with the ability to zoom in with high resolution and can also adjust the brightness and contrast of the digitalized page image according to their needs (Carlyle *et al.*, 2011).

For the researchers, the indexed part of the database also displays very useful technical features which were initially designed by Leslie Carlyle and Mark Clarke⁴⁵, such as the summary fields, which enables an overall assessment of the archive content or of a particular subject under study. In the case of manufacturing processes, thanks to Mark Clarke, the ingredients table (when filled in) shows both the original and interpreted names of the ingredients together with the original quantities and measures which are also translated into SI units (Figure 2.1). This feature is particularly important as it

⁴⁴ However, it is important to note that during this research restricted page-images were found which were not marked as such in the database.

⁴⁵ Information on the responsibility for individual features of the database was provided in a personal communication by Leslie Carlyle.

immediately allows proportions to be calculated, which quickly reveals paint formulations and facilitates scaling down the quantities to a laboratory experience. Mark Clarke also developed the field for the interpretation of the original ingredient names and provided background information justifying these interpretations based on data from the archive itself and from other documentary sources (the 'authority' feature, as described in Carlyle *et al.*, 2011).

Within the comprehensive investigation for this work (described in Chapter 3), inconsistencies detected previously (Carlyle *et al.*, 2011) within the fields' content and topic groupings were found. Since no other researcher has worked as closely with the RE database since its completion, there has been no previous opportunity to test the data-entry in practice to this extent.

The difficulty with finding all relevant records for a given material became evident in the initial approach to the RE database (Carlyle *et al.*, 2011; Otero *et al.*, 2012), where a search for chrome yellow pigment recipes through the sub-topic 'chrome yellow' and the topic 'pigment manufacture' resulted in 115 database records, of which only 79 were actual manufacturing processes. However, as will be described further in Chapter 3, the yellow lead chromate production records actually appear under a variety of sub-topics besides the main search term 'chrome yellow'. These sub-topics include 'deep chrome', 'lemon chrome', 'middle chrome' and 'pale chrome' (Table II.1.4; p. 166), which are, in fact, the most common manufacturing names in the archive. Although some overlap and there are records with more than one sub-topic, there are others without any sub-topic and even others incorrectly attributed, as previously noted (Carlyle *et al.*, 2011). From the investigation conducted, it was possible to find an extra 104 records pertaining to chrome yellow pigment manufacture, a total of 183 production records as compared to the original search which only revealed 79.

When evaluated, the records for the manufacture of yellow lead chromates actually result in a limited number of recipes. For clarity, a distinction has been made in this research between the terms database record and production record. This was important since in a database record (data from the RE database) the corresponding archive page can contain more than one production record, Figure 2.5, whereas production records (manufacturing data from the actual W&N archive) are not always indexed in the database.

This work also revealed records with incomplete fields and occasional typing errors. Furthermore, abbreviations are frequently used through the manuscript books and their original interpretation by the project team is sometimes unclear. Table II.1.5 (p. 173) provides a corrected list of abbreviations and original names translated to modern terminology which is based not only on the original database interpretation but also on the knowledge acquired throughout this investigation. This work adds practical knowledge to that published by Clarke in 2009 on the W&N terminology based on his work with the archive to build the database (Clarke, 2009).

The existence of such irregularities is understandable when considering the database was built from an enormous and diverse amount of data by a small team with limited time. Furthermore, data was removed when the restrictions of the Researcher's Edition were implemented⁴⁶. In fact, the original design was intended to be a dynamic and flexible database that would allow updates by researchers who could contribute with corrections, additional data, other fields of interest and new

⁴⁶ This information was provided in a personal communication by Mark Clarke.

cross-referencing links (Carlyle *et al.*, 2011). Unfortunately, the result of the restrictions on the RE database by W&N during data-entry was a non-changeable database⁴⁷. Hopefully, in the upcoming unrestricted on-line version which has been promised by the Hamilton Kerr Institute, it will be possible to incorporate new entries and to make corrections based on the findings in this work.

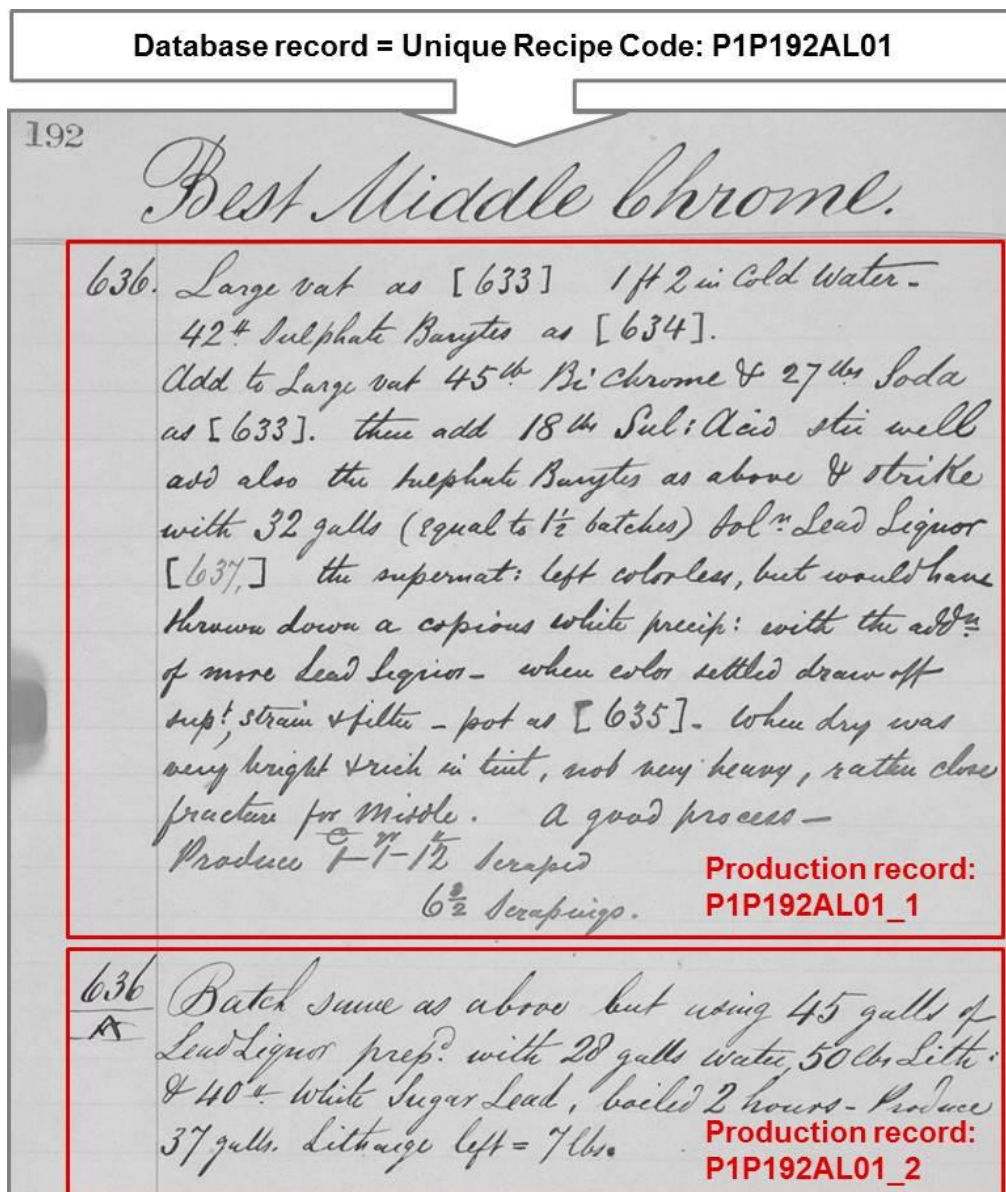


Figure 2.5. Page image of the Best Middle Chrome database record P1P192AL01, where two production records were identified; available on-line © 2009-2016 Hamilton Kerr Institute, University of Cambridge.

At the time of writing, the current on-line version is completely unrestricted, which is exceptionally valuable, however, it is not user friendly and it is time consuming. It is based on the elementary on-line index initially made by the first compilers which was designed to only provide an outline of the complete information of the database (Winsor & Newton Archive, 2018). This on-line version only allows access to the first page-image of a database record, which may not correspond to its complete

⁴⁷ This information was provided in a personal communication by Leslie Carlyle.

text. As it is, it will perpetuate the irregularities mentioned above and may lead to inaccurate investigations.

2.4. Conclusions

The Winsor & Newton 19th Century Archive Database in the Researcher's Edition is an invaluable research tool, especially for art technological source research that would benefit tremendously from an interactive on-line version where researchers could introduce peer-reviewed outcomes from their investigations. This would advance global knowledge on the study of artists' materials contributing to the establishment of better conservation strategies, provenance and authenticity problems.

As will be shown in the coming Chapter, the close study of the archive's content undertaken as part of this research (which included the W&N 19th century catalogues and manuscript books) clearly demonstrates that W&N did have a strong commitment to the development, quality and durability of their artists' materials, in particular to their yellow chromate pigments. The lead chromate pigments were mainly sold under the trade names **Chrome Yellow** and **Chrome Deep**, and the barium, zinc and strontium chromates under **Lemon Yellow**, **Citron Yellow** and **Strontian Yellow**, respectively. The red/purple cochineal lakes appeared mainly under the trade names **Carmine**, **Crimson Lake**, **Scarlet Lake** and **Purple Lake**⁴⁸. These colours account for the majority of the database records, adding relevance to the study of their manufacture.

⁴⁸ For more on the W&N's 19th century manufacture of cochineal red lake pigments please consult Vitorino *et al.*, 2017.

Chapter 3

Chrome yellow: the HART approach



Detail from painting *Entrada* by Amadeo de Souza-Cardoso, c.1917, Modern Collection / Calouste Gulbenkian Museum @ FCG

V. Otero, M. F. Campos, J. V. Pinto, M. Vilarigues, L. Carlyle, M. J. Melo. 2017. *Barium, zinc & strontium yellows in late 19th-early 20th century oil paintings*. *Herit. Sci.* 5:46.

V. Otero, J. V. Pinto, L. Carlyle, M. Vilarigues, M. Cotte, M. J. Melo. 2017. *Nineteenth century chrome yellow and chrome deep from Winsor & NewtonTM*. *Stud. Conservat.* 62 (3), 123-149.

V. Otero, M. Vilarigues, L. Carlyle, M. J. Melo. 2016. *Winsor & Newton's nineteenth century manufacture of yellow chromate-based pigments*. In: Sigrid Eyb-Green, Joyce Townsend, Kathrin Pilz, Stefanos Kroustallis & Idelette van Leeuwen eds. *Sources in Art Technology: Back to Basics*, London: Archetype Publications, Proceeding from the 6th symposium of the ICOM-CC Working Group Art Technological Source Research, pp. 149-150.

Chapter 3. Chrome yellow: the HART approach

The following Chapter presents the systematic study of the W&N 19th century manufacturing processes for yellow chromate based pigments. There are 286 yellow chromate based production records in the W&N 19th century archive. The majority pertain to different hues of lead chromate, $\text{PbCr}_{1-x}\text{S}_x\text{O}_4$ (64%) but production records for the manufacture of other yellow chromate pigments based on barium chromate, BaCrO_4 , (25%), zinc potassium chromate, $4\text{ZnCrO}_4 \cdot \text{K}_2\text{O} \cdot 3\text{H}_2\text{O}$, (9%), and strontium chromate, SrCrO_4 , (2%) were also found. The production records selected for this work are transcribed in Appendix II.3 (p. 187) and detailed in Appendix III and IV (p. 205-231). Pigment reconstructions synthesised in accordance to W&N recipes were characterised with complementary analytical techniques (μ -EDXRF, FORS, μ -Raman, μ -FTIR, XRD and SEM-EDS) and compared with samples from historic W&N oil paint tubes and micro-samples from Amadeo's paintings. The experimental section, including the synthesis methods and the experimental conditions of the analytical equipment used, is detailed in Appendix V (p. 233).

3.1. Introduction

3.1.1. The pigment's history of manufacture and use

Chrome yellow pigments are composed of pure lead chromate (PbCrO_4) or mixed crystals⁴⁹ (or mixed-phase crystals) of lead chromate and lead sulfate with the general formula $\text{PbCr}_{1-x}\text{S}_x\text{O}_4$ ⁵⁰. They are registered in the *Colour Index* as C.I. Pigment Yellow 34:77600 and 77603, respectively (Eastaugh *et al.*, 2004: 99; Brandt, 2005). The colour range of these pigments varies from greenish-yellow (containing more lead sulfate) to yellow-orange (pure lead chromate) (Harley, 1982: 100; Erkens *et al.*, 2001). Today, the orange-red hues are based on mixed crystals or mixed-phase crystals of lead chromate, lead sulfate and lead molybdate ($\text{Pb}(\text{Cr},\text{Mo},\text{S})\text{O}_4$), commonly known as molybdate orange and red (C.I. Pigment Red 104: 77605) (Brandt, 2005). These were discovered in the 1930s (Keijzer, 2001), substituting the traditional formulations of chrome orange and red pigments, composed of basic lead chromate with the general formula $\text{PbCrO}_4 \cdot x\text{PbO}$. The traditional chrome orange occurs in nature as the mineral phoenicochroite (Pb_2CrO_5) (Kühn & Curran, 1986; Burnstock *et al.*, 2003).

Currently, there are three types of chrome yellow pigments classified in accordance with ASTM⁵¹ International standard D211 - 67(2012), Table 3.1 (ASTM, 2018) and under the REACH⁵² European regulation (Commission Regulation (EU) No 301/2014), their circulation and commercialisation are only possible with approval by the European authorities (EUR-Lex, 2018).

⁴⁹ A mixed crystal is a solid solution, i.e., is a crystal structure where one or more atoms are substituted by others that can assume the same geometry, without changing the structure (Klein, 2002; Brandt, 2005; IUPAC, 2018).

⁵⁰ These pigments are also referred to as lead sulfochromate pigments (Brandt, 2005; ECHA, 2018a).

⁵¹ ASTM is the acronym for American Society for Testing and Materials (ASTM, 2018).

⁵² REACH stands for Registration, Evaluation, Authorisation and Restriction of Chemicals (ECHA, 2018b).

Table 3.1. Compositional classification of the three modern types of chrome yellow, adapted from Kühn & Curran, 1986: 193 (in accordance to ASTM D211 - 67(1977)).

	Name	Composition (% of PbCrO ₄)
Type I	Primrose Chrome Yellow	> 50%
Type II	Lemon Chrome Yellow	> 65%
Type III	Medium Chrome Yellow	> 87%



Figure 3.1. Red crystals of crocoite © DCR FCT NOVA.

Lead chromate is found in nature as the reddish mineral crocoite (Figure 3.1), discovered in Siberia around the 1770's (Kühn & Curran, 1986; Erkens *et al.*, 2001). However, its chemical composition was only unveiled in 1797 by L. N. Vauquelin when he isolated and identified the chromium element. In 1809, Vauquelin published his work on lead chromate, demonstrating that process modifications would influence the colour, e.g.,

different hues resulted according to the pH during manufacture: an 'orange yellow' resulted in neutral conditions (pure lead chromate, PbCrO₄), 'a yellowish red or sometimes a beautiful deep red' in alkaline conditions (basic lead chromate, Pb₂CrO₅) and a 'deep lemon yellow' in acidic solutions (mixed crystals of lead chromate and lead sulfate, PbCr_{1-x}S_xO₄) (Vauquelin, 1809; Harley, 1982: 100; Ball, 2008: 175). Since then, large-scale production of chrome yellow has followed Vauquelin's essential steps. It is synthesised by adding a solution of a lead salt (e.g. nitrate or acetate) to a chromate or dichromate (e.g. sodium or potassium) solution (Brandt, 2005).

Although recognized earlier as a colouring material, its commercial production was not immediate due to the scarcity of the raw material (Harley, 1982: 100; Kühn & Curran, 1986). In the beginning of the 19th century, the only known chromite (FeO.Cr₂O₃) mines were in the Var region in France. Other chrome mines were later found in the Shetland Islands (Scotland) and in the Pennsylvania-Maryland region (USA) (Kühn & Curran, 1986; Harley, 1982: 100). Harley mentions Dr. Bollman (1769-1821) as the first to manufacture chrome yellow in England, using chrome ore from the USA. He also worked with George Field doing experiments to improve the pigment properties (Harley, 1982: 101). Interestingly, chrome yellow was detected in Thomas Lawrence's (1769-1830) *Portrait of a Gentleman*, which has been dated to before 1810 (Kühn & Curran, 1986).

From the mid-19th century onwards, chrome yellow pigments were reported to be enthusiastically used by artists, in watercolours and oil paints, even when its use was deemed inadvisable (Kühn & Curran, 1986; Bomford *et al.*, 1990; Cove, 1991; Townsend, 1993; Kirby *et al.*, 2003; Vilarigues *et al.*, 2008; Geldof *et al.*, 2013a). Carlyle reports on the concerns regarding the use of chrome yellow by 19th century authorities on painters' materials, namely George Field, Jean Francois Mérimée,

Laughton Osborn, George Arnald and Sir Arthur Church⁵³ (Carlyle, 2001: 521). Carlyle quotes from Mérimée who pointed out that chrome yellow "... is not however, a permanent colour... in a few years its brightness goes off, and it becomes like yellow ochre" (transl. 1839, p. 94-6, as cited in Carlyle, 2001, p. 521). For Vibert, lead based pigments such as chrome yellow were "...more or less bad..." and would "...get black or decompose" (as cited in Vibert, 1892, transl. by Percy Young, p. 166). The general opinion was that these pigments were of poor stability with a great tendency to fade and discolour on exposure to light and sulfurous atmospheres. However, the "beauty and brilliancy of their colours"⁵⁴ contributed to their continued use as an artists' material (Field, 1835; Harley, 1982: 102; Carlyle, 2001: 521). The darkening of chrome yellow observed in paintings is still an object of study and this subject is further developed in Chapter 4 (p. 85).

Throughout the 19th century, chrome yellow pigments also appeared under other names: mineral yellow, Cologne yellow, Leipzig yellow, Vienna yellow, Paris yellow, king's yellow, new yellow and lemon yellow (also the name of other chromate pigments, namely barium or strontium chromate) (Kühn & Curran, 1986; Carlyle, 2001: 521). The availability of colours associated with lead chromate from W&N is described in Table 2.3. Carlyle also details its availability in powder and oil colours from Rowney: Chrome Yellow Nos 1, 2, 3 [lemon, yellow, orange]⁵⁵, and from Reeves: Chrome Yellow 1, 2, 3 [or pale, middle & deep]⁵⁶ (Carlyle, 2001: 533-543). The lack of reliability of 19th century artists' materials labels has been covered by Carlyle (1993 & 2001) and Townsend *et al.* (1995).

The high tinting strength of chrome yellow pigments was known since the beginning of its commercialisation, allowing the manufacturers to extend their pigments and paints by incorporating other inorganic materials such as chalk, gypsum, barytes, clay, lithopone and alumina, either to make them cheaper or to improve their mechanical properties or shade (Kühn & Curran, 1986; Townsend *et al.*, 1995; Burnstock *et al.*, 2003). Furthermore, chrome yellow was also mixed with other pigments such as ochres, Naples yellow, lead and zinc white to improve their hue and with viridian and Prussian blue to produce greens⁵⁷ (Townsend *et al.*, 1995; Carlyle, 2001).

During the first half of the 20th century, pigment manufacturers concentrated their research on developing and improving the durability of chrome yellow, without sacrificing its colouristic properties. Stabilizing after-treatments such as surface treatments (also called coating and encapsulation treatments) were developed (Gray, 1988; Erkens *et al.*, 2001; Brandt, 2005). These treatments consist

⁵³ George Field (1777-1854) was the author of "*Chromatography; or A Treatise on Colours and Pigments, and of their Powers in Painting & c.*" (1835) (Carlyle, 2001, p. 299). Jean Francois Mérimée (1757-1836) was the author of "*De la peinture a l'huile, ou des procédés matériels employés dans ce genre de peinture, depuis Hubert et Jean Van-Eyck jusqu'a nos jours*" (1839) (Carlyle, 2001, p. 312). Laughton Osborn (1809-78) was the author of "*An American Artist. Handbook of young artists and amateurs in oil painting, being chiefly a condensed compilation from the celebrated manual of Bouvier, with additional matter selected from the labors of Mérimée, De Montabert and other distinguished continental writers in the Art, in seven parts. The whole adapted by the method of its arrangements and the completeness of its detail as well for a textbook in academies of both sexes as for self instruction. Appended a new explanatory and critical vocabulary*" (1845) (Carlyle, 2001, p. 317). George Arnald (1763-1841) was the author of "*A practical treatise on landscape painting in oil; illustrated by various diagrams, and with two original studies in oil, painted on the principles given in the treatise*" (1839) (Carlyle, 2001, p. 285). Sir Arthur Church (1834-1915) was the author of "*The chemistry of paints and painting*" (1890) (Carlyle, 2001, p. 291).

⁵⁴ George Field in "*Chromatography; or, A treatise on Colours and Pigments, and of their Powers in Painting*", 1835, p. 77.

⁵⁵ Rowney sold Chrome Yellow 1, 2, 3 3 in oil paint tubes after 1849 and in powder after c.1855. In the latter year, they also added a No. 4 'deep' (Carlyle, 2001: 543).

⁵⁶ Reeves sold Chrome Yellow 1, 2, 3 in oil paint tubes after 1852 and in powder probably after 1856 (Carlyle, 2001: 540).

⁵⁷ As previously noted, W&N acknowledged some of these mixtures in their 1892 declaration, Appendix II.2 (p. 175).

of coating the individual pigment particles with inorganic materials (e.g. amorphous silica) or organic compounds of low solubility. This is achieved by precipitating these materials onto the particle surface, limiting the chemical interactions between the pigment and the binder (Brandt, 2005).

From the 1970s onwards, lead chromate pigment production has been reduced due to the restrictive legislation concerning health and environmental hazards associated with lead and chromium (VI) compounds (Cowley, 1986; Gray, 1988). As of 2001, Pyle & Pierce report that the modern chrome yellow hue oil paints from W&N (Colart Fine Art & Graphics, Ltd.) are organic based (Pyle & Pierce, 2001). Nevertheless, owing to its exceptional price-performance ratio, lead chromate pigments are still produced by the paint industry under the REACH European regulation, as mentioned above (Erkens *et al.*, 2001; ECHA, 2018b).

3.1.2. The pigment's colour and chemistry

The chromate^{VI} ion (CrO_4^{2-}) is the chromophore responsible for the colour of lead chromate. It is a transition metal oxoanion with the d^0 electronic configuration. The colour is due to charge-transfer (CT) transitions from the ligand to the metal, involving $p\pi(\text{O}) \rightarrow d\pi(\text{Cr})$ electronic transitions. Two main absorption bands are observed at approximately 275 nm and 375 nm (ultraviolet). The edge of the latter band reaches the visible region at around 480 nm (blue), giving rise to the yellow colour of all chromate compounds (Weyl, 1999; Bartecki & Burgess, 2000). However, the assignment of these bands is not straightforward. According to Bartecki & Burgess (2000), Wolfsberg & Helmholz (1952) described it as resulting from the transitions $t_1 \rightarrow 3t_2$ and $2t_2 \rightarrow 3t_2$, whereas Ballhausen & Liehr (1958) state that it results from the transitions $t_1 \rightarrow 2e$ and $t_1 \rightarrow 3t_2$ (Bartecki & Burgess, 2000).

When in solution, the yellow chromate^{VI} ion (CrO_4^{2-}) is in an acid-base equilibrium with the orange dichromate^{VI} ion ($\text{Cr}_2\text{O}_7^{2-}$) (Cotton *et al.*, 1999; Shriver & Atkins, 1999). Its general equation is shown in Figure 3.2:

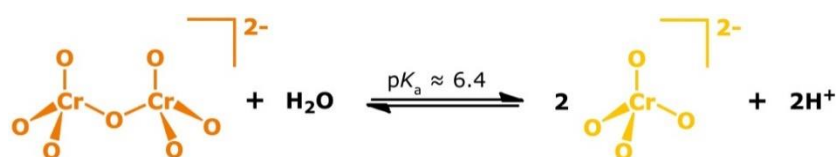
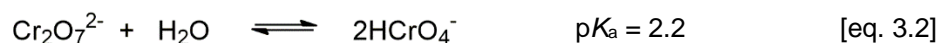


Figure 3.2. Acid-base equilibrium established in the range $1 < \text{pH} < 11$ between chromate ion (CrO_4^{2-}) and dichromate ion ($\text{Cr}_2\text{O}_7^{2-}$) (Shriver & Atkins, 1999).

However, there is a series of labile equilibria between both ions. In acidic conditions below pH 2, the main species are H_2CrO_4 , between pH 2 and 6 the species HCrO_4^- and $\text{Cr}_2\text{O}_7^{2-}$ are in equilibrium and, above pH 6 the main species are CrO_4^{2-} (Greenwood & Earnshaw, 1984; Cotton *et al.*, 1999; Lide, 2006). The equilibria are as follows:



As noted above, the pH-dependent equilibria are considered very labile and the addition of cations such as Ba^{2+} , Pb^{2+} and Ag^+ , leads to the formation of insoluble chromates. Additionally, these equilibria are only established if nitric (HNO_3) or perchloric acid (HClO_4) is used. If hydrochloric (HCl) or sulfuric (H_2SO_4) are used, other compounds are formed: chlorochromate ion and a sulfate complex, respectively (Cotton *et al.*, 1999), as follows:

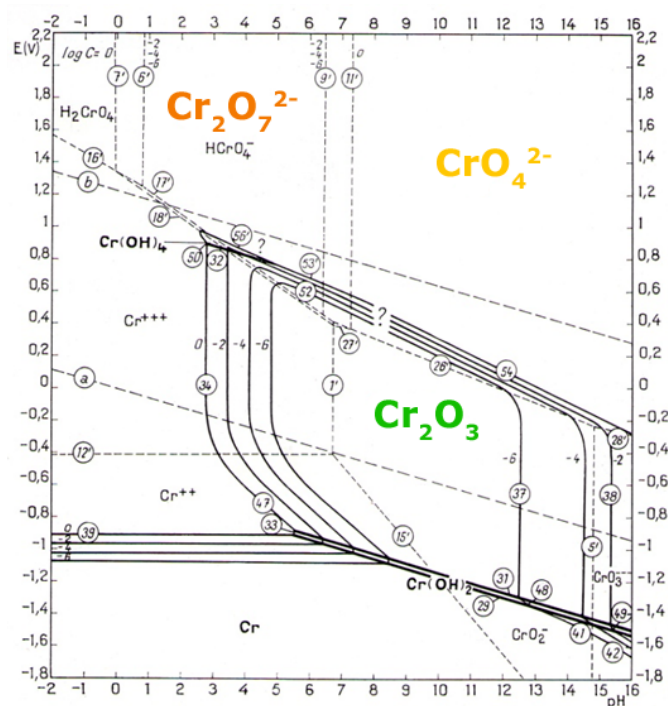
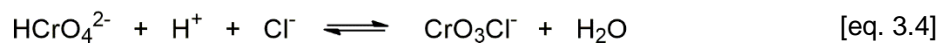
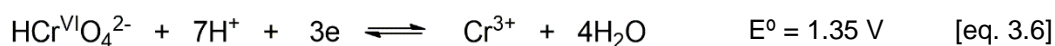


Figure 3.3. Pourbaix diagram of the Cr-H₂O system at 25°C adapted from Pourbaix (1963).

The pH also influences the redox potential of the chromate species, as demonstrated by the Pourbaix diagram of chromium (Cr), presented in Figure 3.3. It expresses the chromium speciation as a function of pH and potential, showing the regions where each species is thermodynamically stable. The vertical lines separate species that undergo chemical reactions involving H^+ , such as the chromate^{VI} species (independent of the potential but dependent on the pH), the horizontal lines separate species that undergo electrochemical reactions not involving H^+ (dependent on the potential but independent of the pH) and the oblique lines separate species that undergo electrochemical reactions involving H^+ (dependent both on the potential and the pH) (Pourbaix, 1963). Under acidic conditions, chromate species are strong oxidizing agents, commonly used in organic chemistry, being reduced to chromium (III) species, with chromium (V) and (IV) species forming as intermediates (Cotton *et al.*, 1999; Smith & March, 2007):



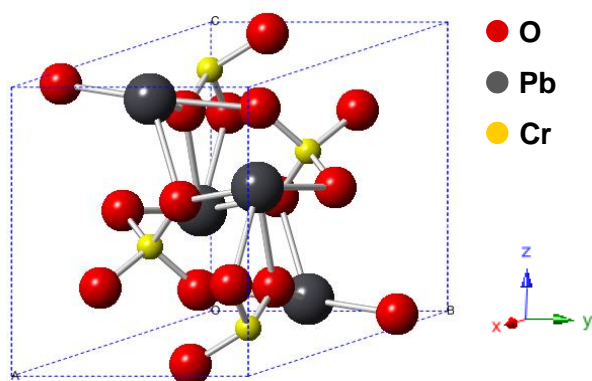


Figure 3.4. Monoclinic structure of lead chromate (PbCrO_4 , mineral form crocoite) (Quareni & Pieri, 1965).

Lead chromate (PbCrO_4) exists in three crystal structures, a stable reddish yellow monoclinic structure (space group $P2_1/n$), Figure 3.4, an unstable orange-red tetragonal structure (space group $I4_1/a$), and an unstable greenish yellow orthorhombic structure (space group $Pnma$). When the latter crystals are formed, they usually convert to the monoclinic structure, especially in acidic conditions and with high temperatures (Gray, 1988; Erkens *et al.*,

2001; Crane *et al.*, 2001). According to literature data, the orthorhombic lead chromate is thermodynamically less stable with a higher solubility product constant at 25°C ($\Delta_r G^0 = -813.2 \pm 0.9 \text{ kJ mol}^{-1}$; $K_{ps} = 10^{-10.71}$) in comparison to the monoclinic form ($\Delta_r G^0 = -824 \text{ kJ/mol}$; $K_{ps} = 10^{-12.6}$) (Martell & Smith, 1982; Crane *et al.*, 2001).

As shown in Figure 3.4, in lead chromate structure lead atoms are bound to the oxygen atoms with a square-antiprismatic geometry (coordination number of 8), linking six chromate ions with a tetrahedral geometry (coordination number of 4) (Quareni & Pieri, 1965; Liang *et al.*, 2005; Frost, 2004).

Mixed crystals or solid solutions of lead chromate and lead sulfate ($\text{PbCr}_{1-x}\text{S}_x\text{O}_4$) form when sulfate ions are incorporated in the lead chromate crystal lattice. According to Mentzen *et al.*, the lead environment hardly changes with substitution of chromium (Cr) by sulfur (S) cations, while the cation-oxygen bond distances expand to accommodate the larger cations. The valence state of lead cations remains +2 and of chromium and sulfur atoms remains +6. Only when sulfate ions are introduced in sufficient quantities in a mixed crystal with chromate ions, does a phase transition from the monoclinic to an orthorhombic structure take place, producing lighter tones (Mentzen *et al.*, 1984; Erkens *et al.* 2001). For Crane *et al.* the monoclinic structure prevails until 60 mol % of chromate. Below this quantity, the orthorhombic structure of lead sulfate appears and initiates a two-phase region. The orthorhombic structure of lead sulfate dominates below 10 mol % of chromate (Crane *et al.*, 2001).

3.2. The W&N 19th century manufacture of lead chromate pigments













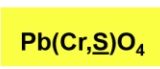




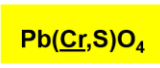




























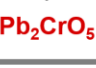


A thorough investigation of the W&N RE Database revealed 183 production records for yellow lead chromates. They include the following names: Primrose Chrome, Lemon Chrome, Pale Chrome, Middle Chrome and Deep Chrome⁵⁸. These names are further modified with adjectives including, Best, Genuine, Fine, Super, Pure, No 1. Despite this variety, W&N's retail catalogues from the 19th century listed only three chrome yellows: Chrome Yellow, Chrome Deep and Chrome Lemon, as shown in Table 2.3. No explanation for this has been found yet, but it is notable that their archive

⁵⁸ There are 20 records that present different names, nevertheless, they were included as process variations and detailed in the tables presented in Appendix III (p. 205); they are highlighted in *italic*.

recipes for oils encompassed the same level of detail and variety which was also omitted in the trade catalogues (Carlyle *et al.*, 2011).

A systematic evaluation of all production records for yellow lead chromates showed that there were in fact a limited number of variations for synthesising the pigments. Assuming that the higher the number of entries, the more frequently the process was carried out, the main synthetic pathways judged to be the most significant in W&N's commercial production are presented in Table 3.2. The full range of their process variations is represented in Appendix III along with details on the ingredients, their order of addition, and the respective number of production records for each manufacturing process. Table 3.2 and the tables in the Appendix III (p. 205) also highlight the pattern of experimentation made by W&N (to be discussed below).

Table 3.2. W&N's chrome yellow key ingredients, main synthetic pathways and final pigment formulations.

Key Ingredients									
Chromate Source	Sulfate Source		Lead Source		Additives/Extenders				
									
K ₂ Cr ₂ O ₇ + Na ₂ CO ₃	H ₂ SO ₄	Na ₂ SO ₄	Pb(NO ₃) ₂	Pb(Ac) ₂ ·2Pb(OH) ₂	PbSO ₄	BaSO ₄	CaCO ₃	CaSO ₄ ·2H ₂ O	
W&N production record name	Code [§]	Order of addition				Final pigment formulation [‡]			
PRIMROSE	PR1a								
LEMON/PALE	L1#*								
	L2a								
MIDDLE	M1a [#]								
	M2a [‡]								
DEEP	D1b								
	D2a [¥]							 	

[§] Codes refer to variations in the manufacturing processes, see Appendix III (p. 205).

[‡] Solubility product of PbCrO₄, $K_{sp} = 1.8 \times 10^{-14}$; of PbCO₃, $K_{sp} = 7.4 \times 10^{-14}$; of PbSO₄, $K_{sp} = 2.53 \times 10^{-8}$; BaSO₄, $K_{sp} = 1.08 \times 10^{-10}$, of CaCO₃, $K_{sp} = 3.36 \times 10^{-9}$ and of CaSO₄·2H₂O, $K_{sp} = 3.14 \times 10^{-5}$ (Chang, 1994; Lide, 2006).

[#] L1 and M1a both produce PbCO₃ as by-product.

* Acid is provided by the lead sulfate pulp which has an acidic pH.

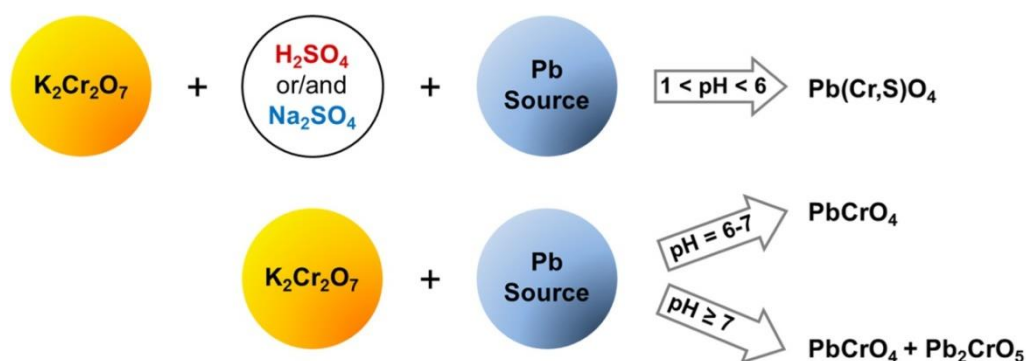
[‡] In M2a, the addition of lead subacetate may form a small amount of Pb₂CrO₅.

[¥] In D2a, CaSO₄·2H₂O may disappear with the addition of sulfuric acid.

Table 3.2 shows that for producing the W&N yellow lead chromates, a solution of lead nitrate or subacetate [$\text{Pb}(\text{NO}_3)_2$ or $\text{Pb}(\text{Ac})_2 \cdot 2\text{Pb}(\text{OH})_2$] was added to a chromate solution (CrO_4^{2-}). The yellow lead chromates as produced, can be described chemically as: *i*) mixed crystals of lead chromate and lead sulfate (light lemony yellows) and *ii*) pure lead chromate monoclinic phase (yellow) as seen in Figure 3.5 and Scheme 3.1. In the deep hues, basic lead chromate may also be found.



Figure 3.5. The final colour is modulated by pH during manufacture. On the left: the lemony mixed crystals of lead chromate and lead sulfate that precipitate at low pH; centre: the yellow pure lead chromate monoclinic phase (PbCrO_4) at neutral pH; on the right: an orange/red basic lead chromate (Pb_2CrO_5) formed in basic media.



Scheme 3.1. The main ingredients for the production of *i*) mixed crystals of lead chromate and lead sulfate and *ii*) pure monoclinic lead chromate crystals. The type of lead source greatly influences the final pH (and colour): lead subacetate ($\text{Pb}(\text{Ac})_2 \cdot 2\text{Pb}(\text{OH})_2$) is usually employed for neutral or close to neutral pH, and lead nitrate ($\text{Pb}(\text{NO}_3)_2$) is used when acidic solutions are required. Additives are not represented.

3.2.1. The main ingredients and their role in W&N's formulations

The **chromate** solution was obtained by adding sodium carbonate (Na_2CO_3) to a dichromate solution. The pH of the chromate solution was controlled from the beginning by the quantity of Na_2CO_3 added, which acts as a buffer (Otero *et al.*, 2012). The chromate solution is the only common ingredient to all their manufacturing processes (see Table 3.2).

Lead nitrate ($\text{Pb}(\text{NO}_3)_2$) and lead subacetate ($\text{Pb}(\text{Ac})_2 \cdot 2\text{Pb}(\text{OH})_2$) were prepared by adding lead(II) oxide (PbO) to an aqueous solution of nitric acid (HNO_3) or lead acetate ($\text{Pb}(\text{CH}_3\text{CO}_2)_2 \cdot 3\text{H}_2\text{O}$), respectively (synthesis described in Table V.2.1.1.2, p. 234). As will be discussed in greater detail

below, both lead sources were used to produce Lemon/Pale and Middle, but for the Deep which initially requires a higher pH, only lead subacetate was used, see Scheme 3.1. Characterisation of both lead sources was carried out and may be consulted in Appendix VII (p. 273).

Sulfate and Lead sources as pairs. As Lemon, Pale and Middle were precipitated at neutral to low pH values, the pairs of lead nitrate/sodium sulfate (Na_2SO_4) and lead subacetate/sulfuric acid (H_2SO_4) were the most frequently found. The paired $\text{Pb}(\text{NO}_3)_2/\text{Na}_2\text{SO}_4$ induces the mixed crystals formation in low pH conditions⁵⁹ and was most used for the Lemon/Pale. Likewise, the paired $\text{Pb}(\text{Ac})_2 \cdot 2\text{Pb}(\text{OH})_2/\text{H}_2\text{SO}_4$, at a neutral pH, was used for the formation of the Deep. For the very low pH's observed in some Primrose formulations, the more unusual pairing of $\text{Pb}(\text{NO}_3)_2/\text{H}_2\text{SO}_4$ was found.

The crystal structure modifiers, which transform the pure lead chromate monoclinic phase into a solid solution (mixed crystals) of lead chromate and lead sulfate $\text{PbCr}_{1-x}\text{S}_x\text{O}_4$ ⁶⁰ were Na_2SO_4 and/or H_2SO_4 , but these are only effective at low pH. To obtain lighter hues, a high amount of lead sulfate in the crystal structure, *i.e.*, a high proportion of sulfate over chromate in the mixed crystal is required. This was confirmed in W&N's formulations.

Other materials were added in solution. The main additives in W&N's formulations, which may have acted as extenders (also called fillers⁶¹), were plaster of Paris ($\text{CaSO}_4 \cdot \frac{1}{2}\text{H}_2\text{O}$), which would be previously converted into gypsum ($\text{CaSO}_4 \cdot 2\text{H}_2\text{O}$), barytes (BaSO_4), lead sulfate (PbSO_4), and chalk (CaCO_3). Besides these, experiments with China clay ($\text{Al}_2\text{Si}_2\text{O}_5(\text{OH})_4$), terra alba (finely powdered $\text{CaSO}_4 \cdot 2\text{H}_2\text{O}$), alum ($\text{AlK}(\text{SO}_4)_2 \cdot 12\text{H}_2\text{O}$), magnesium sulfate (MgSO_4) and potassium sulfate (K_2SO_4) were also carried out.

Recently, Sanches *et al.* have demonstrated that the main fillers used by W&N in their chrome yellow pigment formulations resulted in oil paints with a similar thermomechanical behavior, which means W&N carefully chose the fillers and their combination in order to obtain oil paints with the same viscoelastic properties (Sanches *et al.*, 2017).

3.2.2. The W&N 19th century manufacturing processes and experiments

W&N's books reveal thorough and informed testing of the ingredients (sources for chromate, sulfate and lead as well as additives) and their order of addition. Once the main ingredients (chromate, lead ion and crystal structure modifiers) had been established (which was to pair the chromate with either $\text{Pb}(\text{NO}_3)_2/\text{Na}_2\text{SO}_4$ or $\text{Pb}(\text{Ac})_2 \cdot 2\text{Pb}(\text{OH})_2/\text{H}_2\text{SO}_4$ as explained above), their next most significant tests centered primarily on the additives: gypsum, barytes, lead sulfate and chalk. All possible combinations were tested, but only the ones that afforded a good quality product were selected by

⁵⁹ In L1, the lead sulfate pulp must have a low pH for the successful formation of the mixed crystals.

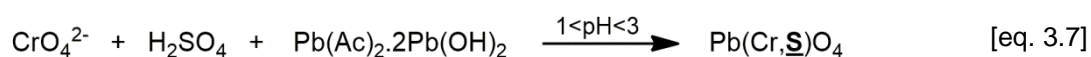
⁶⁰ A set of references for $\text{PbCr}_{1-x}\text{S}_x\text{O}_4$ crystals was synthesised and characterised by μ -Raman, μ -FTIR and XRD enabling a better characterisation of the reconstructed pigments described below. The results may be consulted in Appendix VIII (p. 275).

⁶¹ According to ISO 3262-1, a "filler is a substance consisting of particles which is practically insoluble in the application medium and is used to increase volume or to improve technical properties and/or to influence optical properties" (quote from Gysau, 2006: 16).

W&N (surmised from the frequency of their appearance in the production records). There are records with notes on the quality of the hue achieved and the stability of the pigments after some years, for example in one process to produce Deep Chrome (D1*b*, see Table 3.2) was the note: "*Kept its colour in oil, on palette, very well when examined Sept 1870*"⁶². The diversity found in the extenders may reflect either a search for a better product, a better process (high quality and lower price) or perhaps the availability of the raw materials.

3.2.2.1. Primrose Chrome

There were only 8 production records for Primrose Chrome, which can be reduced to 3 synthesis methods (Appendix III.1, p. 205). These cover the period from 1846 to 1880. The majority of these records date to the 1850s and pertain to the process coded as PR1*a*, Table 3.2 and eq. 3.7⁶³.



This pigment class is characterised by a high amount of lead sulfate in the crystal structure as a consequence of the addition of a higher quantity of sulfuric acid when compared to Lemon/Pale Chrome. This led W&N to choose lead subacetate as the lead source (likely because it is much easier to control the precipitation pH). The most frequent pair $\text{Pb}(\text{Ac})_2 \cdot 2\text{Pb}(\text{OH})_2/\text{H}_2\text{SO}_4$, produces the low pH (< 3.5) necessary to obtain, with high yield, the lemony $\text{PbCr}_{1-x}\text{S}_x\text{O}_4$ crystals displaying a high sulfate to chromate ratio. There is only one record for PR1*b*, probably because the pH is much more difficult to control with the pair $\text{Pb}(\text{NO}_3)_2/\text{H}_2\text{SO}_4$. This affects the reproducibility of the process (during synthesis it was found that a very small variation of the sulfate or lead content results in $\text{PbCr}_{1-x}\text{S}_x\text{O}_4$ crystals with different compositions).

Interestingly, no extenders were used in any of the Primrose Chrome processes, however, in PR2 and PR3 manufacturing processes, MgSO_4 and K_2SO_4 were experimented with as additional sulfate sources, respectively.

As will be further explained in Chapter 4, Monico *et al.* reports that pigments with a high amount of sulfur in the $\text{PbCr}_{1-x}\text{S}_x\text{O}_4$ crystals are more prone to degradation (Monico *et al.*, 2013b). In support of the evidence for W&N's commitment to durability, it is notable that there was a low number of production records found for Primrose Chrome and that the quantity of ingredients used was not of an industrial scale. These factors, together with the lack of a corresponding trade name in the W&N catalogues⁶⁴, suggests that W&N was not selling this product on a large scale either wholesale or retail⁶⁵.

⁶² This was one and half years after the pigment manufacture on the 26/02/1869. Citation from Best Deep Chrome; URC: P3P054AL01. See Appendix II.3.1 (p. 187).

⁶³ Equations 3.7 to 3.10 are given to help the reader to interpret the role played by the main ingredients and by pH. These chemical reactions are not presented as balanced chemical equations, and only the sources for chromate, sulfate and lead are depicted.

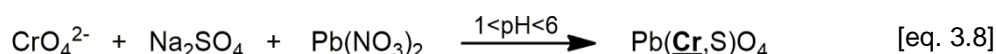
⁶⁴ As mentioned in Chapter 2.2.3., W&N was selling a Primrose Yellow by the end of the 19th century, but in accordance to their 1892 declaration (Appendix II.2; p. 175), it was a combination of zinc and barium chromates. This was confirmed by research in the RE database (discussed further below).

⁶⁵ However, it is possible that Primrose pigments were made available through special orders.

3.2.2.2. Lemon/Pale Chrome

In the books there are 46 production entries corresponding to Lemon and 51 for Pale Chrome, accounting for 53% of all yellow lead chromate production records. These can be reduced to 4 main synthesis methods for Lemon and 11 for Pale Chrome. All manufacturing processes are depicted in Appendix III.2 (p. 207). Most of the production records cover the period from 1846 to 1893, with the earliest records dated 1846.

Since the reaction scheme and final products are very similar for both Lemon and Pale entries, they were grouped into a single class. Five of the manufacturing processes, including the ones with the most entries, are expressed by the same synthetic pathway: L1/P1⁶⁶, L3a/P3a⁶⁷, L3b/P3b⁶⁸, L4a/P4a⁶⁹ and L4b/P4b⁷⁰ (see Appendix III.2.1; p. 209 and III.2.2; p. 212). Presently, it is still unclear why these records were given separate names but it may be related to their final use. The main synthetic pathways are L1 and L2a, Table 3.2 and eq. 3.8. The pathway L2a is only found in the Lemon records.



These processes are characterised by the pair $\text{Pb}(\text{NO}_3)_2/\text{Na}_2\text{SO}_4$. The majority of the manufacturing processes are based on adding the sulfate ions to the chromate solution before the addition of the lead source, resulting in the formation of mixed crystals at low to neutral pH ($1 \leq \text{pH} \leq 6$). These pigments form a paler yellow when compared with pure lead chromates (Figure 3.5). In L1, the low pH is produced with the lead sulfate pulp and, in L2a, by sulfuric acid (Table 3.2). In L1, sodium carbonate is used as a buffer, and lead carbonate ($K_{\text{sp}} = 7.4 \times 10^{-14}$) forms as by-product since its solubility product is very similar to lead chromate ($K_{\text{sp}} = 1.8 \times 10^{-14}$) (Chang, 1994; Lide, 2006). The resulting mixed crystals present different proportions of lead sulfate, but the monoclinic structure of lead chromate is preserved (Figure 3.6B). W&N described the synthesised L2a as displaying a "fine colour" and in their notes report that it was "*sent to Reynolds Co, N.Y.*"⁷¹; L1 is described as a "*Bright lemon tint, (...): light in weight*"⁷².

⁶⁶ Both L1 and P1 present a high number of entries. The production records for L1 show a consistent proportion of starting materials from 1853 to 1859. P1 presents the same proportion of starting materials as L1 from 1846 to 1858, but this changes from 1865 to 1880.

⁶⁷ L3a and P3a show the same synthetic pathway with relatively the same proportion of the starting materials from 1846 to 1858, presenting one and three production records, respectively.

⁶⁸ L3b only has one production record from the period 1846-58, whereas P3b presents eleven production records from 1846 to 1874. However, the proportion of the starting materials varied between production records. This may be related to the control of the pH during the synthesis.

⁶⁹ L4a and P4a present three and five production records, respectively, with relatively the same proportion of the starting materials, from the period 1846-58.

⁷⁰ L4b presents four production records from the period 1846-58, whereas P4b has only one from the period 1862-64. Here, the proportion of the starting materials also varied between production records. This may also be related to the control of the pH during the synthesis.

⁷¹ Citations from Best Lemon Chrome; URC: A5P028AL01 and Best Lemon Chrome; URC: 4PP102AL01, respectively. See Appendix II.3.1 (p. 187).

⁷² Citation from Best Lemon Chrome; URC: X6P240L11. See Appendix II.3.1 (p. 187).

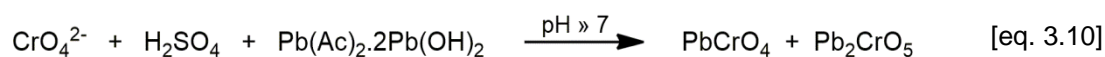
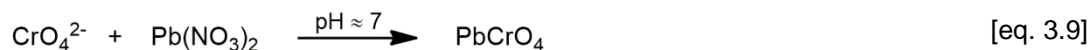
Barium sulfate (barytes) and lead sulfate were added in the two main processes (Table 3.2), presumably acting as extenders. The addition of sulfate compounds (gypsum was also used in L4a and P2, together with barium sulfate) contributes to the shift of the equilibrium reaction towards the mixed crystals formation. Chalk was never found in a Lemon/Pale process, probably because it would act as a buffer not allowing the lower pH values necessary for the formation of the mixed crystals.

It is also important to note the process variations L2b and L3b where no extenders are added (see Appendix III.2; p. 207). As in L1, lead carbonate also forms during L3b synthesis, showing a spectral fingerprint very similar to L1 (see Figure X.2.1, p. 298, and Figure X.2.5, p. 302). There are a significant number of production records for these two variations: 12% for L3b and 5% for L2b⁷³.

In 16% of the manufacturing processes lead subacetate is used with sulfuric acid (as found in the production of Primrose) which should result in mixed crystals of lead chromate and lead sulfate producing a very bright yellow with a lemony hue.

3.2.2.3. Middle/Deep Chrome

Middle and Deep Chromes are found in 40 and 38 entries respectively, representing 43% of all the yellow lead chromate production records. These can be reduced to 8 synthetic methods for Middle and 10 for Deep. All variations are depicted in Appendix III.3 (p. 216) and III.4 (p. 220). Most of the production records are found in books ranging from 1834 to 1882, with the earliest record dating from December 1852.



In general, all of the Middle and Deep manufacturing processes produce lead chromate at a neutral pH (eqs. 3.9 and 3.10). Middle can be obtained with either lead nitrate or lead subacetate (eqs. 3.9 and 3.10). A good example is the manufacturing process M1a (Table 3.2) where chalk is mixed with the chromate solution followed by the addition of lead nitrate. In this case, lead carbonate also forms as by-product. As stated in their record, "*When dry was very bright and rich in tint, not very heavy, rather close fracture for middle. A good process*"⁷⁴. The other main process for Middle, M2a (Table 3.2), is described as a "*Very good rich color in Oil & Kept a bright full tint in Oil*"⁷⁵. In this case, lead subacetate was used and in order to lower the pH, sulfuric acid was added prior to precipitation, shifting the system towards the pure lead chromate formation (although a small amount of basic lead chromate may also be formed). The process M2a is very similar to Deep (D1b), the only difference being the order of addition of the ingredients. For the Deep (eq. 3.10), lead subacetate is added to the chromate solution and precipitation occurs at a basic pH prompting the formation of basic lead

⁷³ The percentage values given correspond to the sum of the Lemon and Pale production records.

⁷⁴ Citation from Best Middle Chrome; URC: P1P192AL01. See Appendix II.3.1 (p. 187).

⁷⁵ Citation from Best Middle Chrome; URC: P2P386AL01. See Appendix II.3.1 (p. 187).

chromate; sulfuric acid is then added afterwards in order to lower the pH to neutral. This control of the pH enabled W&N to switch from a yellow coloured pure lead chromate to an orange/red basic lead chromate (Figure 3.5).

Individual experiments with Deep were conducted by mixing lead nitrate with the chromate solution (methods D3 and D4, Appendix III.4; p. 220) and with dichromate without the addition of the sodium carbonate buffer (D6, D9 and D10a, Appendix III.4; p. 220). In the case of methods D3 and D9, the addition of Plymouth lime (interpreted as CaO) replaces the carbonate, introducing the alkalinity necessary to produce basic lead chromate.

For the extender, depending on the pH desired, either chalk or barytes was used. However, in the main process D2a, gypsum was added together with barytes, both acting as extenders. The colour obtained is described as "*nice close & good fracture & texture & light in weight - tint good*"⁷⁶. The addition of gypsum with barytes also appears in D1a and M3a.

3.2.2.4. Other experiments

W&N also performed experiments with other ingredients detailed in Appendix III (p. 205). As noted above they were essentially using a buffered chromate solution with sodium carbonate, but potassium carbonate was also found substituting the sodium carbonate in 11 production records for Middle and Deep and, in 4 others where no buffer was used and dichromate appears alone. In 2 records, alum was also experimented with as a buffer for Middle together with chalk. Lead acetate was tested as a lead source in 10 production records: 4 for Pale and 6 for Middle. In these experiments, the formation of the less stable orthorhombic form of lead chromate (Gray, 1988; Crane *et al.*, 2001) is more likely with the use of lead acetate (pH \approx 6). They also experimented with lead white in 5 records for Deep and in 2 of these hydrochloric acid had been previously added. The pigment resulting from the single production record coded D5a, where lead white was added to a chromate solution with hydrochloric acid was considered "very powdery"⁷⁷. In 1846, they also refer testing the use of lead chloride for Pale.

China clay with terra alba were used as additives in one production record for Pale and another for Deep, while, as noted above, magnesium sulfate was used in a manufacturing process for Primrose and, potassium sulfate in another two records for Primrose and for Deep.

3.3. The characterisation of W&N's lead chromate pigment reconstructions

Pigment reconstructions were synthesised following selected⁷⁸ production records transcribed in Appendix II.3.1 (p. 187) and highlighted in Appendix III (p. 205). The synthesis methods are described in Appendix V.2.1.1 (p. 233) and the pH measurements throughout the syntheses are showed in

⁷⁶ Citation from Best Deep Chrome; URC: P3P106AL01. See Appendix II.3.1 (p. 187).

⁷⁷ Citation from Golden Chrome - Rich tint; URC: P1P427AL09.

⁷⁸ The selection of the individual production records was based on their representativeness and the amount of detail provided in the records.

Appendix IX.1 (p. 287). The main synthesis methods were reproduced more than once to verify their reproducibility. The reconstructed pigments were characterised by Energy Dispersive X-Ray Fluorescence Spectrometry (μ -EDXRF), UV-Vis Fibre Optic Reflectance Spectroscopy (FORS), Colourimetry, μ -Raman Spectroscopy (μ -Raman), μ -Fourier Transform Infrared Spectroscopy (μ -FTIR), X-Ray Diffraction (XRD) and Scanning Electron Microscopy (SEM). Selected pigments were also analysed by micro X-ray Absorption Near-Edge Structure (Cr K-edge μ -XANES), which will be further discussed in Chapter 4 (p. 85). The experimental conditions for the analytical equipment used are detailed in Appendix V.3. (p. 239). Spectral and SEM data of reference compounds may be found in Appendix VI (p. 243). Full characterisation of representative lead chromate pigment reconstructions is presented in Appendix X (p. 293).

$L^*a^*b^*$ colour coordinates, inflection point of the reflectance (FORS) spectra⁷⁹ and the composition of the reconstructed pigments depicted in Table 3.2 are presented in Table 3.3. Table 3.4 details other pigments synthesised due to the relevance of their synthetic pathways and pigment formulations. The a^* coordinate clearly shows the increase in red proceeding from Primrose ($a^* \approx 0$) to Pale/Lemon ($a^* = 10-15$) through to Middle/Deep ($a^* = 20-30$), which is also evident in Figure 3.5 and by the FORS data in Figure 3.6A.

Spectral data of the pigments' chromophores are described below and the infrared fingerprints of the pigments from the main synthetic pathways are shown in Figures 3.7 and 3.9. Identification of additional material, both by-products resulting during synthesis and deliberate additions, is straightforward by combining infrared, Raman spectroscopy and X-ray diffraction. The spectral assignments were made in accordance with the spectra and band assignments shown in Appendix VI.3 (p. 245) and VI.4 (p. 256).

Table 3.3. $L^*a^*b^*$ colour coordinates, inflection point (λ_{IP} , nm) of the reflectance (FORS) spectra and composition of pigments representative of the main synthetic pathways.

	PR1a	L1	L2a	M1a**	M2a**	D1b	D2a
Final pH[§]	≈ 3.5	≈ 6	≈ 1	≈ 6.5	≈ 7		
L^*	90.5 ± 0.3	86.7 ± 0.6	87.1 ± 0.5	84.8 ± 0.3	76.1 ± 0.7	73.7 ± 0.8	74.4 ± 1.0
a^*	1.0 ± 0.5	12.5 ± 1.9	9.3 ± 0.3	19.8 ± 0.2	28.5 ± 1.1	31.3 ± 1.4	31.4 ± 0.4
b^*	80.2 ± 1.5	89.7 ± 3.6	84.4 ± 1.1	81.1 ± 2.5	69.8 ± 2.7	67.0 ± 2.4	69.8 ± 2.3
λ_{IP} (nm)	505	517	514	523	528	528	530
Composition[¥]	$PbCr_{0.3}S_{0.7}O_4$	$PbCr_{0.8}S_{0.2}O_4$ $PbCO_3$ $PbSO_4$	$PbCr_{0.6}S_{0.4}O_4$ $BaSO_4$	$PbCrO_4$ $CaCO_3$ $PbCO_3$	$PbCrO_4$ $BaSO_4$ Pb_2CrO_5	$PbCrO_4$ $BaSO_4$ Pb_2CrO_5	$PbCrO_4$ $BaSO_4$ $CaSO_4 \cdot 2H_2O$ Pb_2CrO_5

[§] Final pH was measured at the end of the precipitation.

[¥] The molar fractions of $PbCr_{1-x}S_xO_4$ are approximate values resulting from comparison of the infrared spectrum and diffraction pattern of the pigments with the reference set of $PbCr_{1-x}S_xO_4$ synthesised in the laboratory (see Appendix VIII, p. 275 and Appendix X, p. 293).

⁷⁹ The wavelength of the inflection points was obtained through calculation of the first derivative of the FORS spectra.

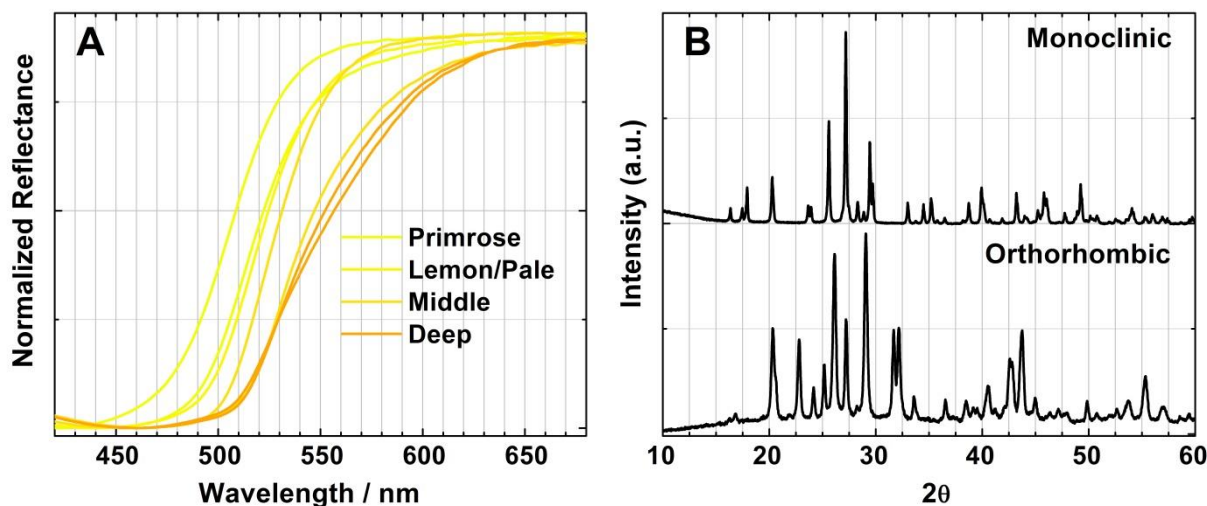


Figure 3.6. A) Normalized FORS spectra of the pigments representative of the main synthetic pathways and B) diffraction pattern of lead chromate, monoclinic and orthorhombic crystal structure.

Table 3.4. L*a*b* colour coordinates, inflection point (λ_{IP} , nm) of the reflectance (FORS) spectra and composition of pigments representative of other synthetic pathways.

	PR1b [#]	L2b	L3a	L3b	M1b	D1a
Final pH [§]	≈ 1	≈ 2	≈ 6		≈ 4	≈ 7
L*	88.5 ± 0.1	86.2 ± 0.1	86.6 ± 0.1	84.6 ± 0.3	80.3 ± 0.02	82.7 ± 0.02
a*	5.3 ± 0.04	12.7 ± 0.9	10.9 ± 0.1	15.4 ± 0.1	23.7 ± 0.03	20.9 ± 0.02
b*	68.0 ± 0.1	87.7 ± 2.1	79.4 ± 0.1	81.5 ± 0.4	85.4 ± 0.1	72.1 ± 0.1
λ_{IP} (nm)	514	518	516	519	523	530
Composition [¥]	PbCr _{0.4} S _{0.6} O ₄	PbCr _{0.6} S _{0.4} O ₄	PbCr _{0.8} S _{0.2} O ₄ CaSO ₄ ·2H ₂ O PbCO ₃	PbCr _{0.8} S _{0.2} O ₄ PbCO ₃	PbCrO ₄ PbCO ₃	PbCrO ₄ CaSO ₄ ·2H ₂ O BaSO ₄ PbCO ₃

[§] Final pH was measured at the end of the precipitation.

[¥] The molar fractions of PbCr_{1-x}S_xO₄ are approximate values resulting from comparison of the infrared spectrum and diffraction pattern of the pigments with the reference set of PbCr_{1-x}S_xO₄ synthesised in the laboratory (see Appendix VIII, p. 275 and Appendix X, p. 293).

[#] Here the L*a*b* colour coordinates and composition of a PR1b pigment reconstruction with a high proportion of sulfur over chromium, Figure X.1.2 (p. 294), is presented. For the photochemical study developed in Chapter 4, three other reconstructions with a lower proportion of sulfur were prepared, Figures X.1.3 to X.1.5 (p. 295-297).

3.3.1. Middle/Deep Chrome

Pure monoclinic lead chromate was detected for all Middle and Deep pigment reconstructed (see Appendix X.3, p. 305). Their infrared spectra show an intense and broad band at 854 cm⁻¹ (shoulders at 831 and 820 cm⁻¹) assigned to the CrO₄²⁻ asymmetric stretching mode, as shown in Figure 3.7. Their Raman spectra present an intense band at 839 cm⁻¹, assigned to the CrO₄²⁻ symmetric stretching mode, and a series of bands at 325, 337, 357, 375, 399 cm⁻¹, which are assigned to the

CrO_4^{2-} bending modes, Figure 3.10. Only the pure monoclinic phase of lead chromate was found by XRD (ICDD card⁸⁰: 00-073-1332) and the orthorhombic phase was never detected (ICDD card: 00-038-1363), Figure 3.6B.

As may be seen in Figure 3.7 and 3.11, in the M1a pigments the presence of chalk causes an overlap between the CrO_4^{2-} asymmetric stretching band and the CO_3^{2-} asymmetric bending band at 875 cm^{-1} . As noted above, M2a and D1b processes are very similar and consequently the composition of the resulting pigments is close, presenting mainly lead chromate and barytes, as may be seen below in Figure 3.16D and Figures X.3.3 and X.3.5 (p. 307 and 309).

Where present in low amounts, basic lead chromate is not easily detected by FTIR since its band at 849 cm^{-1} overlaps with the CrO_4^{2-} asymmetric stretching bands of lead chromate, Figure VI.4.1. (p. 256) (Roncaglia *et al.*, 1985). However, in larger amounts it is possible to observe a slight shift to lower wavenumbers and the CrO_4^{2-} asymmetric stretching band becomes sharper. Nevertheless, the Raman spectrum for basic lead chromate is distinct from lead chromate, Figure VI.3.1. (p. 245). Basic lead chromate shows three very strong bands at 825 cm^{-1} , 837 and 846 cm^{-1} , assigned to CrO_4^{2-} symmetric stretching modes. In the bending region, the Raman spectra display bands at 322 , 341 , 355 , 379 and 399 cm^{-1} , attributable to the CrO_4^{2-} bending modes (Roncaglia *et al.*, 1985). Its presence is also easily detected by XRD; diffraction peaks are indexed to the monoclinic phase of basic lead chromate (ICDD card: 00-076-0861). The infrared spectrum of the D2a pigment reconstruction, Figure 3.7, shows a sharper CrO_4^{2-} asymmetric stretching band due to the presence of basic lead chromate, confirmed by Raman and XRD. As noted above, the identification of gypsum and barytes is very straightforward.

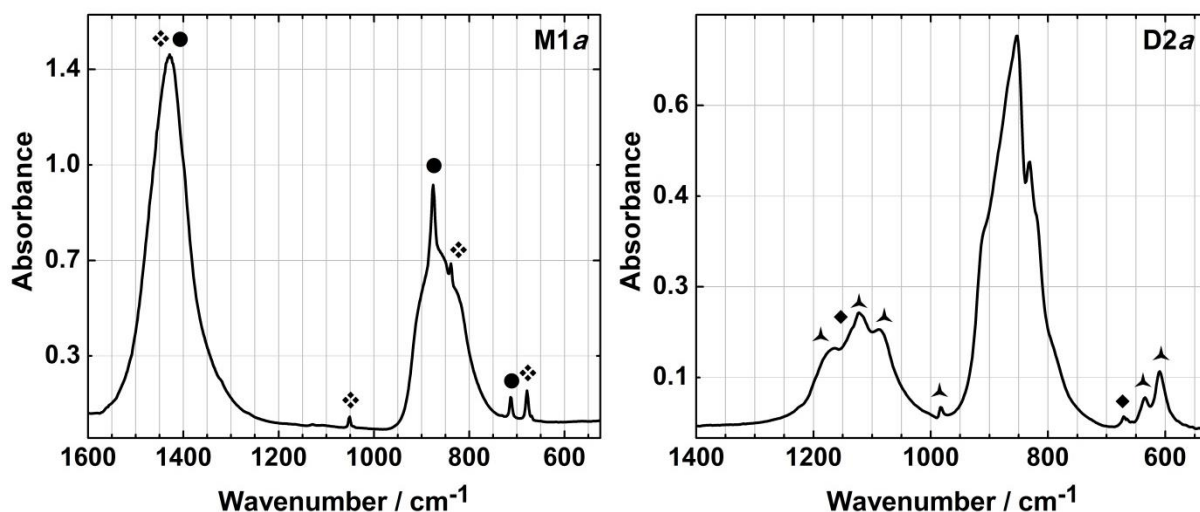


Figure 3.7. Infrared spectra of pigment reconstructions for Middle (M1a) and Deep (D2a); (●) CaCO_3 , (◇) PbCO_3 , (▲) BaSO_4 , (◆) $\text{CaSO}_4 \cdot 2\text{H}_2\text{O}$.

⁸⁰ Identification cards from the International Centre for Diffraction Data (ICDD).

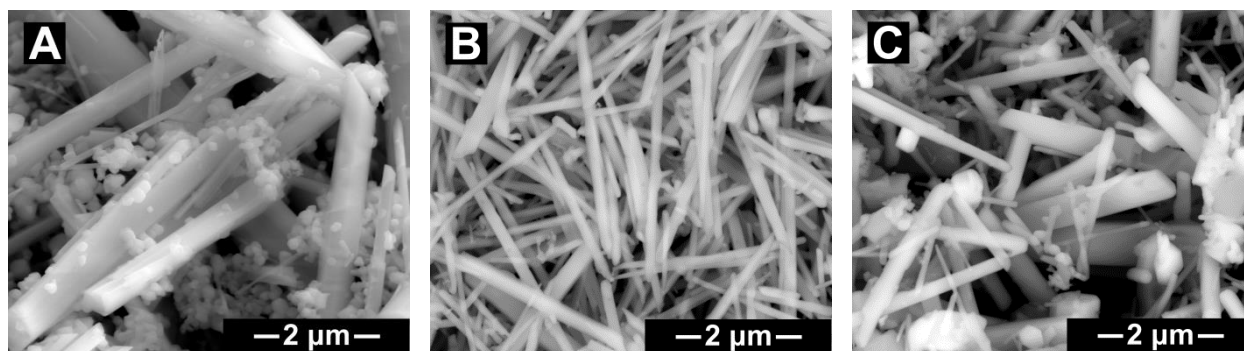


Figure 3.8. SEM images of pigment reconstructions for **A)** Primrose (PR1a), **B)** Lemon (L1) and **C)** Middle (M2a).

SEM images of all the reconstructed pigments show the characteristic rod-like particles of lead chromate (Figure VI.2.1, p. 244). However, as may be seen in Figure 3.8 and in Appendix X (p. 293), the various production methods result in different rod-like particle sizes ranging from 1 μm to 4 μm in length, and 0.1 μm to 1 μm in width. In general, the particles produced are longer than those reported by Burnstock *et al.*, where lead chromate rod-like particles with a maximum length of 1 μm were observed (Burnstock *et al.*, 2003; Otero *et al.* 2012). This is most probably related to the precipitation conditions, namely the concentration of the ingredients, the pH and the reaction times (Gray, 1988; Xiang *et al.*, 2004; Lau, 2005). Liang *et al.* (2005) report on the effect of pH on the synthesis of lead chromate nanorods, relating the pH with the morphology of the particles. Their results show a morphology evolution from particle-like to rod-like structure with increasing pH. According to them, pH 7 is the optimal condition for the formation of rod-like particles (Liang *et al.*, 2005). From the reconstructed pigments, the lower pHs corresponds to the W&N Primrose and Lemon/Pale processes, which result in larger rod-like particles, but smaller particle-like structures are also visible (Figure 3.8A). In accordance with the literature, the rod-like particles correspond to monoclinic phases and the particle/globular-like structures to orthorhombic phases (Xiang *et al.*, 2004; Monico *et al.*, 2013a). However, at pH almost neutral (Figure 3.8B) only rod-like particles are detected, and at higher pHs (particularly in the synthesis methods where lead subacetate is used) the particle-like structures are most probably basic lead chromate particles (Figure 3.8C). It is also noteworthy that the length of the rod-like particles produced decreases from Primrose to Deep pigment reconstructions.

3.3.2. Primrose and Lemon/Pale Chrome

Mixed crystals (or mixed-phase crystals) of lead chromate and lead sulfate, $\text{PbCr}_{1-x}\text{S}_x\text{O}_4$, can be detected by FTIR, Raman and XRD, as detailed in Appendix VIII (p. 275). In summary, as the content of sulfur increases in the crystal structure, a shift from the characteristic spectral and diffraction features of pure monoclinic lead chromate is observed. When the SO_4^{2-} molar fraction (x) is between 0.5 and 0.8, the diffraction peaks of both monoclinic lead chromate and orthorhombic lead sulfate phases are detected, shifted from the features of the pure compounds. A complete change to the orthorhombic structure of lead sulfate only occurs when the SO_4^{2-} molar fraction ≥ 0.9 (Crane *et al.*, 2001).

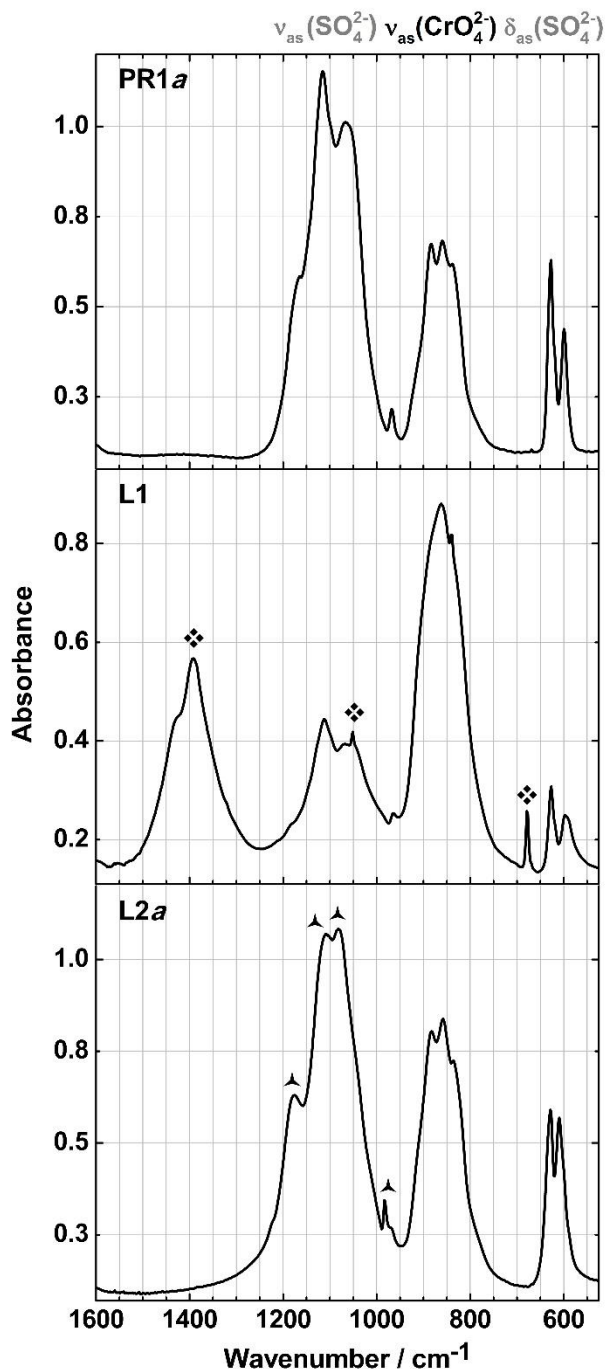


Figure 3.9. Infrared spectra of pigment reconstructions for Primrose (PR1a) and Lemon/Pale (L1 and L2a); (❖) PbCO_3 , (▲) BaSO_4 .

As may be observed in Figure 3.9, the presence of these crystals is easily detected by FTIR due to the appearance of the SO_4^{2-} bands and the shifted CrO_4^{2-} band. These are distinctive even in the presence of lead and barium sulfate, where an overlap of their infrared SO_4^{2-} asymmetric stretching and bending bands occurs, Figures 3.9 and 3.11. With the reference set of $\text{PbCr}_{1-x}\text{S}_x\text{O}_4$ described in Appendix VIII (p.275), it was possible to create calibration curves of the ratio $A_{\nu_{\text{as}}(\text{SO}_4^{2-})}/A_{\nu_{\text{as}}(\text{CrO}_4^{2-})}$ as a function of the SO_4^{2-} molar fraction, Figure 3.10. There is a calibration curve for pigments with SO_4^{2-} molar fraction ≤ 0.5 (with a ratio < 1) and another one for those with a higher content of SO_4^{2-} . This enabled the semi-quantification of the SO_4^{2-} molar fraction for these compounds found in the absence of other sulfate compounds, due to the overlapping of their infrared SO_4^{2-} asymmetric stretching. When other sulfate compounds are present in the pigment formulation, it is essential to complement the analysis with the XRD data.

In the reconstructed pigments, a complete change in the crystal structure was never observed. Pale-like pigments (PR1a) present both monoclinic lead chromate and orthorhombic lead sulfate phases with a SO_4^{2-} molar fraction of approximately 0.7, Figure 3.10. For Lemon/Pale pigments, no phase transition or the lead sulfate phase was detected, and the mixed crystals obtained had a SO_4^{2-} molar fraction ≤ 0.4 ⁸¹. The diffraction patterns were indexed to a pure monoclinic phase of lead chromate. Again, the orthorhombic lead chromate was never detected.

⁸¹ Exceptions were found in L2b pigment reconstructions where the orthorhombic lead sulfate phase may be detected but the main phase was still the monoclinic lead chromate.

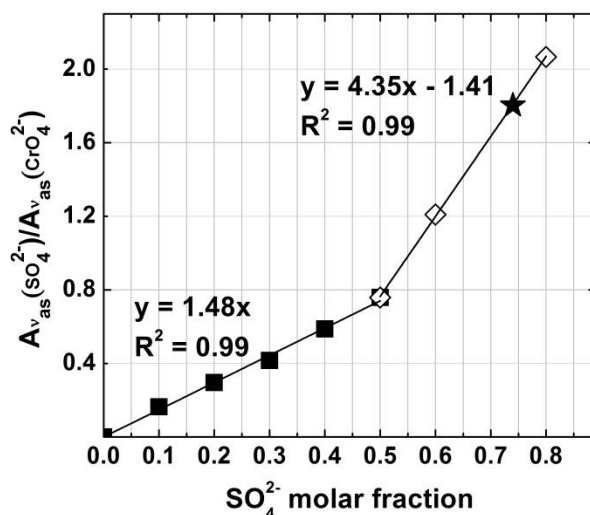


Figure 3.10. Variation of the $A_{v_{as}}(\text{SO}_4^{2-})/A_{v_{as}}(\text{CrO}_4^{2-})$ as a function of the SO_4^{2-} molar fraction. The ratio was calculated using the absorbance of $\nu_{as}(\text{SO}_4^{2-})$ at 1100 cm^{-1} normalized to the $\nu_{as}(\text{CrO}_4^{2-})$ at 853 cm^{-1} after baseline correction. (★) molar fraction of the Primrose pigment reconstruction (PR1a).

3.4. Comparison with historic paint tubes

Comparisons were made with samples from two W&N oil paint tubes labelled **Chrome Deep** and **Chrome Yellow** (Figure 3.11) which were reported to have belonged to the Portuguese painter, Columbano Bordalo Pinheiro (1857-1929) and are thought to date between 1882 and 1905 according to their labels and tube shape; a tube of W&N **Chrome Deep** oil paint from a private collection⁸²; as well as a **Jaune de Chrome foncé** oil paint from the French producer Lefranc, and a tube labelled **Jaune de Chrome foncé - tempera farge**, which were found in the studio of Amadeo de Souza-Cardoso at the Manhufe house⁸³ (1887-1918), Table 3.5. These paints tubes were characterised using the same approach of complementary analytical techniques used for the pigment reconstructions. Infrared and Raman spectra are shown in Figures 3.11 and 3.12 (spectral assignments were made in accordance with those shown in Appendix VI.3 (p. 245) and VI.4 (p. 256). SEM images of the W&N **Chrome Yellow** and **Chrome Deep** oil paint tubes belonging to Columbano are also presented in Figure 3.13. Additional data (μ -EDXRF, FORS, XRD and SEM) may be seen in Appendix XI (p. 311).

⁸² The private collection is composed of late 19th century W&N oil paint tubes, dated according to the data on the labels by Marta Félix Campos (personal communication). The oil paint tubes were characterised with complementary analytical techniques in the framework of the PhD of Marta Félix Campos at the DCR FCT NOVA (Campos, forthcoming).

⁸³ See note 35 in page 24.

Table 3.5. Historic chrome yellow paint tubes: description, composition, L*a*b* colour coordinates and inflection point (λ_{IP} , nm) of the reflectance (FORS) spectra.

Name on tube label	<i>Chrome Deep</i> (W&N)	<i>Chrome Deep</i> (W&N)	<i>Chrome Yellow</i> (W&N)	<i>Jaune de Chrome foncé</i> (Lefranc)	<i>Jaune de Chrome - tempera farge</i> [#]
Paint tube provenance	Private collection (@DCR FCT NOVA)	Columbano (MNAC collection)		Amadeo (@DCR FCT NOVA)	
Composition [‡]	PbCrO ₄ (50%) CaCO ₃ (50%) MgCO ₃ .xH ₂ O [§]	PbCrO ₄ (50%) CaCO ₃ (50%) MgCO ₃ .xH ₂ O [§]	PbCr _{0.6} S _{0.4} O ₄ (80%) BaSO ₄ (20%) MgCO ₃ .xH ₂ O [§] <i>zinc linoleate</i> [†]	PbCrO ₄ <i>lead azelate</i> [†]	PbCr _{0.8} S _{0.2} O ₄ PbCO ₃
L*	70.7 ± 0.04	70.4 ± 0.1	72.7 ± 0.1	67.1 ± 0.03	-
a*	22.3 ± 0.1	20.2 ± 0.01	11.5 ± 0.1	20.6 ± 0.02	-
b*	78.1 ± 0.03	69 ± 0.1	68.9 ± 0.1	71 ± 0.1	-
λ_{IP} (nm)	530	530	518	530	-

[#] Unidentified colourman due to the degraded state of the tube. XRD analysis was not carried out due to the lack of quantity.

[‡] The semi-quantification of the compounds was obtained by XRD. The molar fractions of PbCr_{1-x}S_xO₄ are approximate values resulting from comparison of the infrared spectrum and diffraction pattern of the pigments with the reference set of PbCr_{1-x}S_xO₄ synthesised in the laboratory (see Appendix VIII, p. 275 and Appendix X, p. 293).

[§] MgCO₃.xH₂O was not accounted for in the XRD semi-quantification because it was not detected by this technique; it is most probably in its amorphous form.

[†] Zinc and lead carboxylates were only detected by μ -FTIR, see Figure VI.4.7 (p. 262).

The W&N oil paint tube labelled **Chrome Yellow** is composed of mixed crystals, barytes and magnesium carbonate (MgCO₃.xH₂O), Figure 3.11. The latter compound, designated as spar⁸⁴ (Eastaugh *et al.*, 2004: 246), was not listed in any W&N's chrome yellow pigment production entry. However, magnesium carbonate does appear in some of W&N's oil paint formulations under the term "spar", as revealed by a search in the on-line W&N Archive Database under the book code GR (entitled 'Oil Grinding at New Factory, various colours at different dates')⁸⁵. Interestingly, magnesium carbonate was only detected by μ -FTIR and not by XRD, which means it is most probably in its amorphous form. Although the quantity of barytes detected is significantly smaller than that added in the L2a pigment reconstruction (Figure 3.9), a good match was found between the pigment in the tube paint and a L2b pigment's infrared fingerprint, Figure 3.11. As stated above, L2b is a process variation of L2a where no BaSO₄ is added, nonetheless the chromophores are similar (Tables 3.3 and 3.4). Furthermore, L*a*b* colour coordinates also correlate well. This supports the assumption that W&N's Lemon/Pale manufacturing processes were used to produce their Chrome Yellow oil paint.

The W&N oil paint tubes labelled **Chrome Deep** contain a high amount of chalk together with pure lead chromate, Figure 3.11, and magnesium carbonate. As noted above, the presence of chalk is characteristic of W&N's Middle Chrome formulations, which support the hypothesis that these were used to produce their Chrome Deep colour (L*a*b* colour coordinates also corroborate this, see

⁸⁴ The authority for this attribution is given by the Recipe name: Spar in Oil (Artists'), URC: P2P097AL07, where carbonate of magnesia (MgCO₃) is ground in poppy oil. This record is only available on-line (Winsor & Newton Archive, 2018).

⁸⁵ Carlyle reported on its use by W&N in their 19th century oil paints formulations in the HART Report (Carlyle, 2005, Chapter 4).

Tables 3.3 and 3.4). The pigment in the *Chrome Deep* tube paints correlates best with an M1a production variation, Figure 3.7, where sodium carbonate was not added. As lead carbonate was not detected in the tube, this variation is likely since the lack of sodium carbonate ensures that lead carbonate does not form as a by-product. It is possible that by the end of the 19th century, W&N had chosen to stop using sodium carbonate as a buffer in their M1a syntheses to avoid the formation of lead carbonate given that there was a widespread distrust of lead compounds in artists' materials at that time (Carlyle, 2001: 41-46).

The tube of Lefranc's **Jaune de Chrome foncé** (yellow chrome deep) is composed of pure lead chromate, Figure 3.11, obtained from adding lead to a chromate source not buffered by the addition of a carbonate compound. There is only one record where W&N experimented with this simple process. That W&N chose more complex formulations incorporating significant proportions of additives that were chemically compatible is easily understood when considering a note in W&N's archive referring to this pigment's body and high tinting strength: "*no colour affords perhaps a greater opportunity for adulteration⁸⁶ than chrome yellow. When pure it is of such a powerful body and has such strong qualities for staining that it may be adulterated to a great extent without much injuring its appearance as a saleable article (...)*" (quote from book G3 dated post 1844 (page P018).

On the other hand, the other tube labelled **Jaune de Chrome foncé - tempera farge** from an unidentified colourman, is composed of mixed crystals with a low sulfate to chromate ratio and a high amount of lead carbonate, Figure 3.12. A very good correlation is made with an L3b pigment reconstruction (Table 3.4). As noted above, lead carbonate forms as a secondary product during the pigment synthesis. Although this formulation was not one of W&N's main synthetic pathways, it still represents 12% of all their Lemon/Pale production records (Appendix III.2, p. 207).

Interestingly, magnesium carbonate (spar) was only detected in W&N's oil paint tubes. As further evidence, from the thirty oil paint tubes found in Amadeo's studio, only W&N's paints present magnesium carbonate in their composition: nine out of fourteen W&N oil paint tubes. On the private collection of late 19th century W&N oil paint tubes deposited at the DCR FCT NOVA, ten tubes out of thirty-five present magnesium carbonate in their composition⁸⁷. This suggests that magnesium carbonate may also be used as a marker for W&N's oil paints⁸⁸. Silvester *et al.* have associated the presence of this compound to the water sensitivity of certain 20th century oil paints. Their results point to the formation of magnesium sulfite and sulfates hydrates from the reaction of magnesium carbonate with atmospheric sulfur dioxide (SO₂), especially under high RH conditions (Silvester *et al.*, 2014). It is important to refer that no magnesium-sulfur compounds were identified in the historic oil paint tubes studied.

The metal carboxylates detected in the historic oil paint tubes may have been intentionally added as additives to the oil paint or may result from the reaction between free carboxylic acids (formed

⁸⁶ In this context the use of the term "adulteration" is more likely to mean "extention" since there is ample evidence that W&N were seeking a high quality durable pigment.

⁸⁷ This information was provided in a personal communication by Marta Félix Campos (Campos, forthcoming).

⁸⁸ Monico *et al.* also identified the presence of magnesium carbonate in two historic (end of 19th century) oil paint tubes (Elsens, Brussels), which according to the labelling, one is a light chrome yellow and the other is a darker tone. Both belong to the Royal Academy of Fine Arts of Antwerp (Monico *et al.*, 2011a). However, the origin of its manufacture is unclear.

during the drying of the oil paint, detailed below in p. 90) and compounds of lead or zinc added as driers during the preparation of the oil paints (Carlyle, 2001: 41 & 154-156).

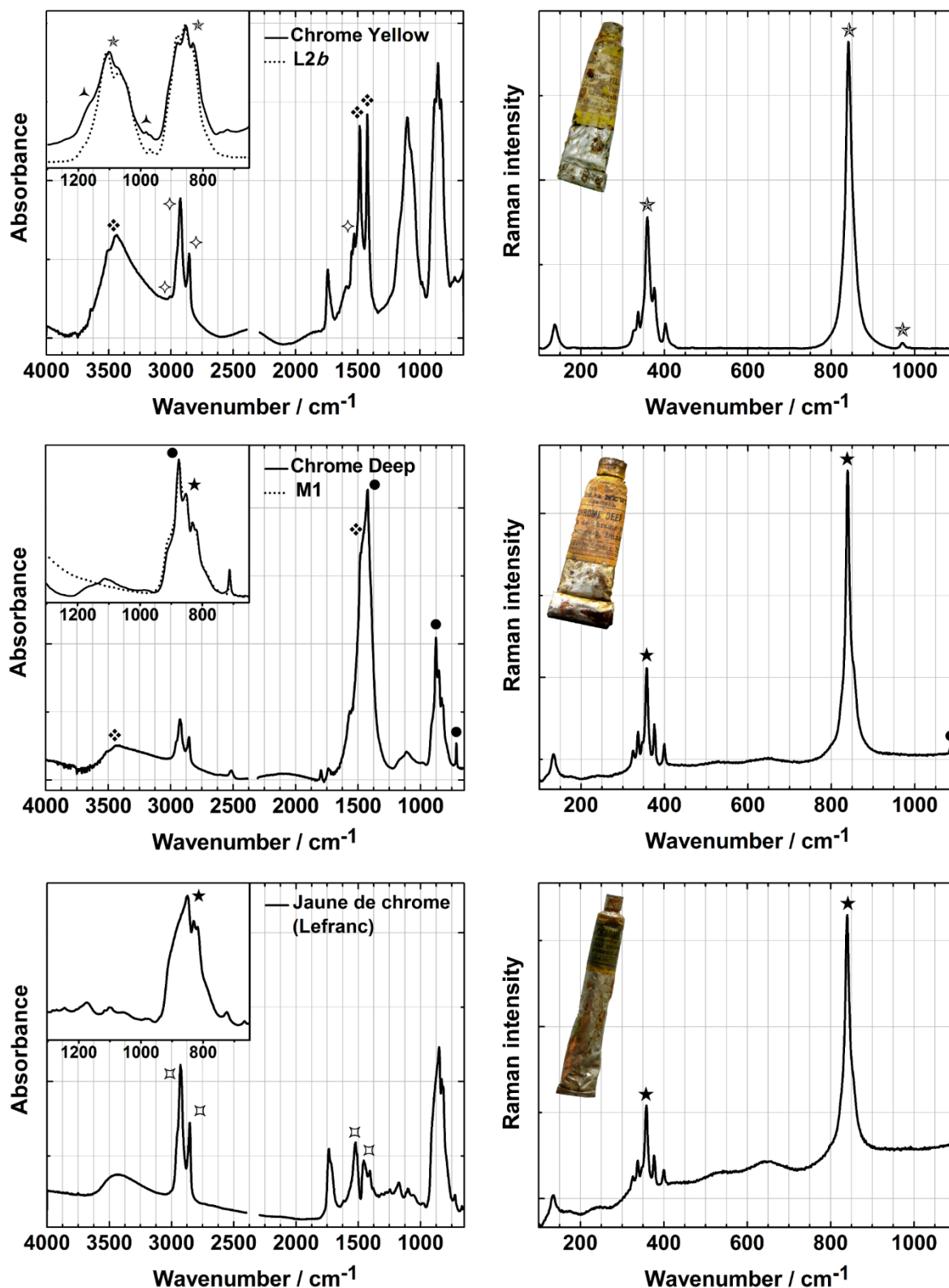


Figure 3.11. Infrared (left) and Raman (right) spectra of the W&N *Chrome Yellow* and *Chrome Deep* oil paint tubes belonging to Columbano. In the inset, comparison with the matching pigment reconstructions, L2b and M1, for 1300-650 cm^{-1} . Also shown is the spectrum from Lefranc's *Jaune de Chrome foncé* oil paint tube. (\blacktriangle) BaSO_4 , (\blacklozenge) $\text{MgCO}_3 \cdot x\text{H}_2\text{O}$, (\blacktriangledown) zinc linoleate, (\bullet) CaCO_3 , (\square) lead azelate, (\star) PbCrO_4 and (\star) $\text{PbCr}_{0.6}\text{S}_{0.4}\text{O}_4$.

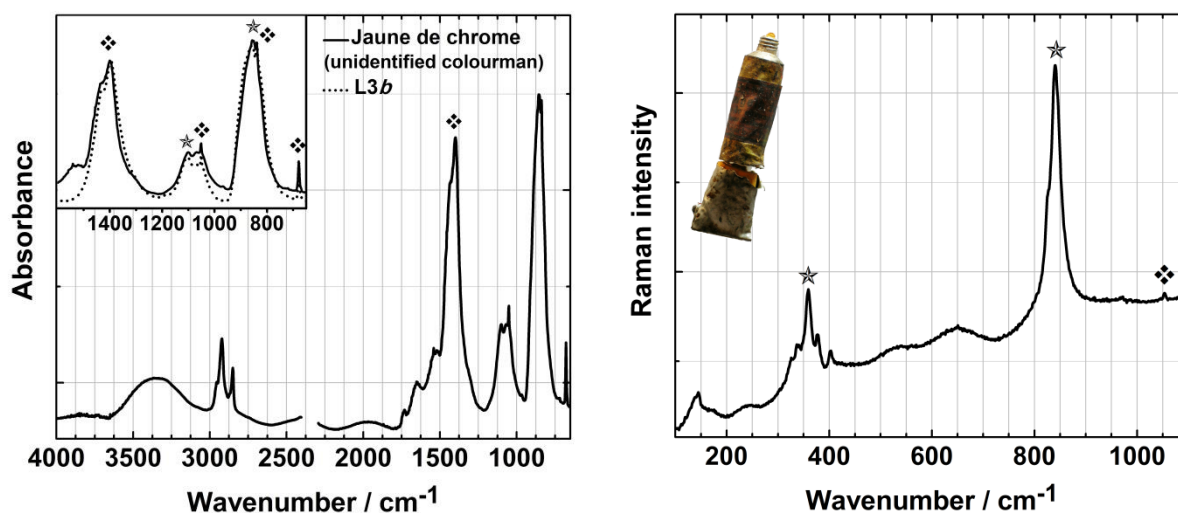


Figure 3.12. Infrared (left) and Raman (right) of the *Jaune de Chrome foncé - tempera farge* paint tube belonging to Amadeo. In the inset, comparison with the matching pigment reconstruction, L3b, for 1600-650 cm^{-1} . (*) $\text{PbCr}_{0.8}\text{S}_{0.2}\text{O}_4$, (♠) PbCO_3 .

In terms of morphology, Figure 3.13, the size of the lead chromate rod-like particles in the pigment reconstructions is similar to that found in the historic W&N's oil paint tubes. It is noteworthy that these particles are generally longer and thinner than those found in the historic Lefranc oil paint (Figure XI.2, p. 308). SEM analysis also showed that W&N was using natural chalk (calcium carbonate) in their Chrome Deep pigment formulation since coccoliths arranged in a coccosphere, resulting from organogenic sedimentation were clearly seen, and indicate a natural source of chalk (Gysau, 2006). Coccoliths were also found in Amadeo's painting *Entrada* (Montagner, 2015: 102).

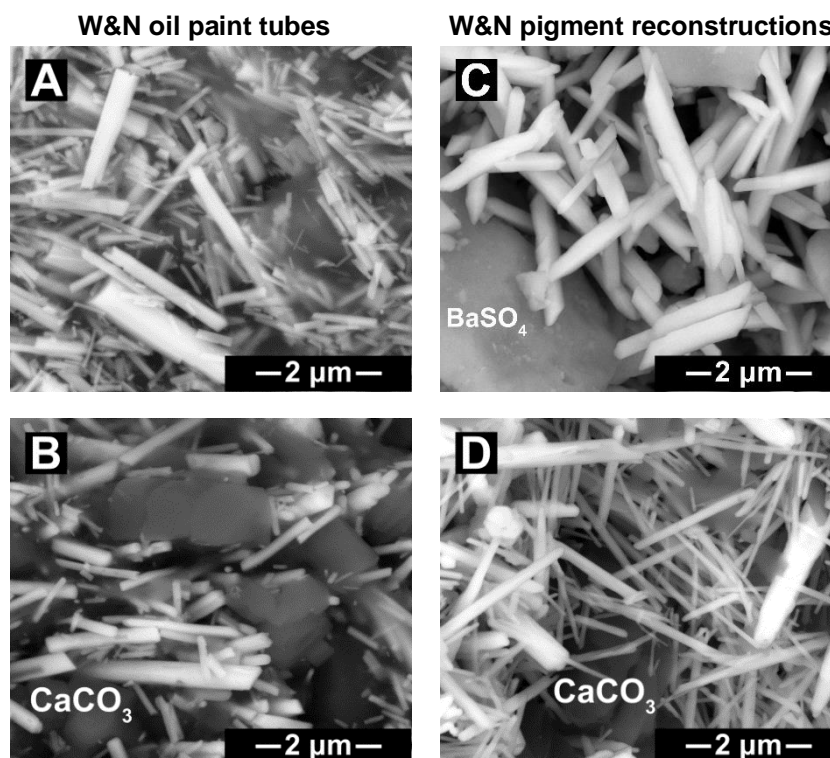


Figure 3.13. SEM images of historic W&N A) *Chrome Yellow* and B) *Chrome Deep* oil paint tubes, C) L2a and D) M1a pigment reconstructions.

Considering the results summarized in Table 3.2 and this comparison with the historic paint tubes, it is proposed that the Pale and Lemon formulations were used to produce the W&N's Chrome Yellow hue and, the Middle plus Deep were used to obtain their Chrome Deep hue. However, there is an interesting discrepancy with W&N's declaration of pigments' composition of 1892 (Appendix II.2; p. 175) where, as mentioned in Chapter 2.2.3 (p. 33), Chrome Yellow is described as pure lead chromate, Chrome Deep is given as pure lead chromate, more or less basic, and it is Chrome Lemon that is presented as a combination of chromate and sulfate of lead. Whether this actually denotes a change in terminology, formulation or an inaccuracy in the technical information provided can only be answered with the analysis of other W&N oil paint tubes, including the Chrome Lemon variety.

3.5. Chrome yellow in Amadeo's paintings

As previously mentioned, in the ongoing study supervised by Maria João Melo, chrome yellow has been widely found in oil paintings by Amadeo (Vilarigues *et al.*, 2008; Melo *et al.*, 2009; Montagner, 2015).

In the context of this thesis, a more in-depth characterisation by μ -Raman was performed on cross-sections previously sampled and mounted⁸⁹, from selected paintings by Amadeo where chrome yellow was detected (see Appendix XII, p. 313). Chrome yellow was identified as a single colour and in the darker and lighter greens, mainly mixed with Prussian blue and viridian, respectively. It was also detected in greens consisting of emerald green and in blues made with ultramarine blue.

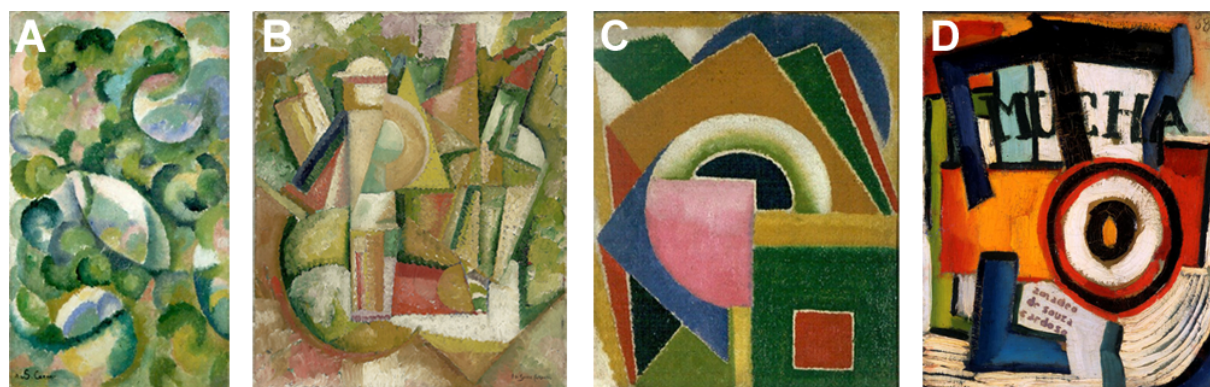


Figure 3.14. Amadeo de Souza-Cardoso paintings: **A)** *Gemälde G / Quadro G*, c.1912, 51 x 29.5 cm, cat. n° P41 (Inv. 77P2; Freitas, 2008: 182); **B)** *Untitled (O Jockey)*, c.1913, 61 x 50 cm, cat. n° P58 (Inv. 77P5; Freitas, 2008: 209); **C)** *Untitled*, c.1913, 34.4 x 28.2 cm, cat. n° P75 (Inv. 92P209; Freitas, 2008: 229) and **D)** *Mucha*, c.1915-1916, 27.3 x 21.4 cm, cat. n° P172 (Inv. 86P21; Freitas, 2008: 322) © FCG.

⁸⁹ The cross-sections were sampled and mounted by Sara Babo (Melo *et al.*, 2009). These resin-embedded cross-sections were prepared in Technovit 2000LC resin (Appendix V.2.5, p. 238). The cross-sections were re-polished and new Optical Microscope images were taken with the support of Isabel Pombo Cardoso (DCR & LAQV-REQUIMTE NOVA).

Based on the previous results, a new set of yellow and green micro-samples were taken⁹⁰ from the same areas as the cross-sections from the paintings: *Quadro G* (Figure 3.14A), *Untitled - O Jockey* (Figure 3.14B), *Untitled* (Figure 3.14C) and *Mucha* (Figure 3.14D). These samples and cross-sections were further studied by μ -XRF, μ -FTIR, μ -Raman, and where possible, by SEM-EDS and SR based techniques, namely μ -XRF, μ -FTIR mapping and μ -XANES. Their full characterisation is presented in Appendix XIII (p. 319) and was based on the reference data available in Appendix VI (p. 243). This approach allowed complementary analysis of the samples revealing not only their composition but also the morphology and distribution of the components, as shown by the example given in Figure 3.15 of a green cross-section taken from the painting *O Jockey* (Figure 3.15B).

Following the work by Monico *et al.*, selected micro-samples were studied by SR based techniques to assess the actual conservation state of the chrome yellow oil paints in Amadeo's paintings (Monico *et al.*, 2011a & 2011b). The combined use of SR μ -XRF maps obtained at different energies along the XANES spectrum allows the detection of the chromium element in its different oxidation state. SR μ -XRF maps obtained at 5.993 keV for the detection of Cr^{6+} and at 6.1 keV for other Cr species such as Cr^{3+} (Figures 3.15A and 3.15D), together with μ -XANES acquired at the Cr K-edge, enabled the determination that no degradation due to the reduction of the Cr^{6+} from the lead chromate pigments to other Cr species is currently occurring. This methodology is further explained in Chapter 4.1.1. (p. 88).

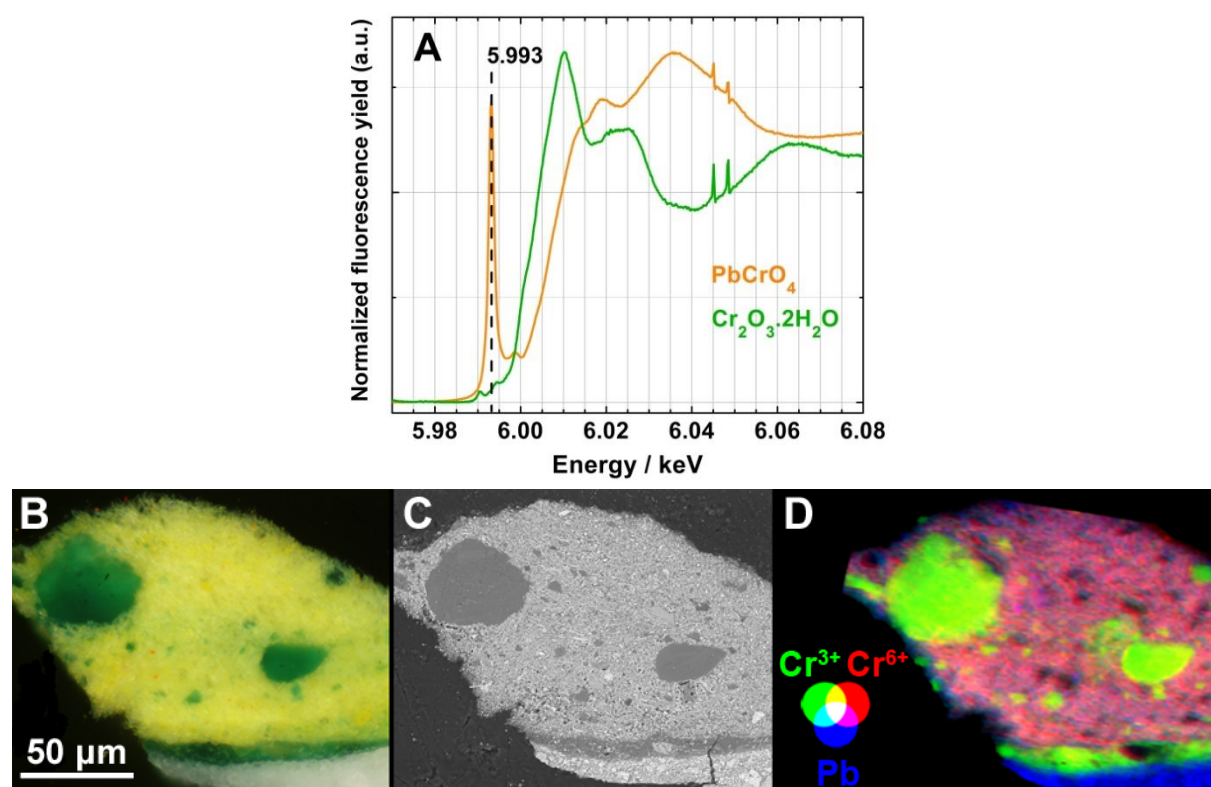


Figure 3.15. A) Cr K-edge μ -XANES spectra of lead chromate (PbCrO_4) and viridian ($\text{Cr}_2\text{O}_3 \cdot 2\text{H}_2\text{O}$). Complementary analysis of a green cross-section from Amadeo's painting *O Jockey* (c.1913, cat. n° P58) by B) visible light microscope image (50x), C) SEM image (1500x) and D) SR μ -XRF elemental maps at 5.993 keV of Cr^{6+} and Pb and at 6.1 keV for other Cr species such as Cr^{3+} (map size: $170 \times 116 \mu\text{m}^2$, with $1 \times 1 \mu\text{m}^2$ pixel size).

⁹⁰ The micro-samples were taken from the paintings at the Calouste Gulbenkian Museum, in April of 2013. The team members were: Maria João Melo, Márcia Vilarigues, Cristina Montagner and Vanessa Otero. The micro-sampling procedure is explained in Appendix V.2.2 (p. 237).

Table 3.6 presents W&N chrome yellow pigment formulations from the reconstructions correlated to the pigments found in Amadeo's paintings, based on a comparison of their infrared fingerprints, see Figure 3.16. Full characterisation of the samples from Amadeo's paintings by μ -FTIR was achieved in accordance with the reference spectra and band assignments shown in Appendix VI.4 (p. 256). Data from Montagner (2015) was included in order to complement the data acquired in the framework of this thesis.

Table 3.6. Correlation of W&N chrome yellow pigment formulations with pigments found in μ -samples from paintings by Amadeo, analysed by μ -FTIR. See also Appendix XIII, p. 319.

	W&N Formulation	Amadeo's paintings	
Lemon	L2a PbCr _{0.6} S _{0.4} O ₄ BaSO ₄	- <i>Quadro G</i> , c.1912 (μ 2, μ 3) - <i>O Jockey</i> , c.1913 (μ 1, μ 2, μ 3, μ 4, μ 5, μ 6, μ 8) - <i>Untitled</i> , c.1913 (μ 1, μ 2) - <i>BRUT 300 TSF</i> , c.1917 (μ 3, μ 16) [‡] - <i>Untitled</i> , c.1917 (μ 1) [‡]	Figure 3.16A
	L2b PbCr _{0.6} S _{0.4} O ₄	- <i>Mucha</i> , c.1915-1916 (μ 3) - <i>Entrada</i> , c.1917 (μ 17) [‡]	Figure 3.16B
Middle	M1a PbCrO ₄ CaCO ₃	- <i>Mucha</i> , c.1915-1916 (μ 1) - <i>Entrada</i> , c.1917 (μ 8, μ 19, μ 32, μ 37) [‡] - <i>Untitled</i> , c.1917 (μ 29, μ 40) [‡]	Figure 3.16C
	M2a PbCrO ₄ BaSO ₄	- <i>Quadro G</i> , c.1912 (μ 1, μ 5)	Figure 3.16D

[‡] For more information, please consult Montagner (2015, p. 101). Note that the codes presented here are different from those presented in Montagner: L2a, L2b and M1a correspond to L3a, L3b and M3a, respectively. The codes changed in the course of this work.

It was possible to relate four W&N 19th century chrome yellow pigment formulations with the pigments found in the paintings by Amadeo studied. Three of them belong to W&N's main formulations described in Table 3.2. The formulation found most often in Amadeo's work corresponds to the L2a synthesis method, which is composed of mixed crystals of lead chromate and lead sulfate with barytes, Figure 3.16A. This is also the same formulation of W&N **Chrome Yellow** oil paint tube (described above). The W&N formulation without the barytes, derived from L2b synthesis method was also found in Amadeo's yellow and green paint samples, Figure 3.16B. Samples from Amadeo's paintings could also be related to the formulation found in W&N's **Chrome Deep** oil paint tube, composed of pure lead chromate and chalk, Figure 3.16C. The formulation from M2a synthesis method made of pure lead chromate and barytes was also discovered, Table 3.6 and Figure 3.16D.

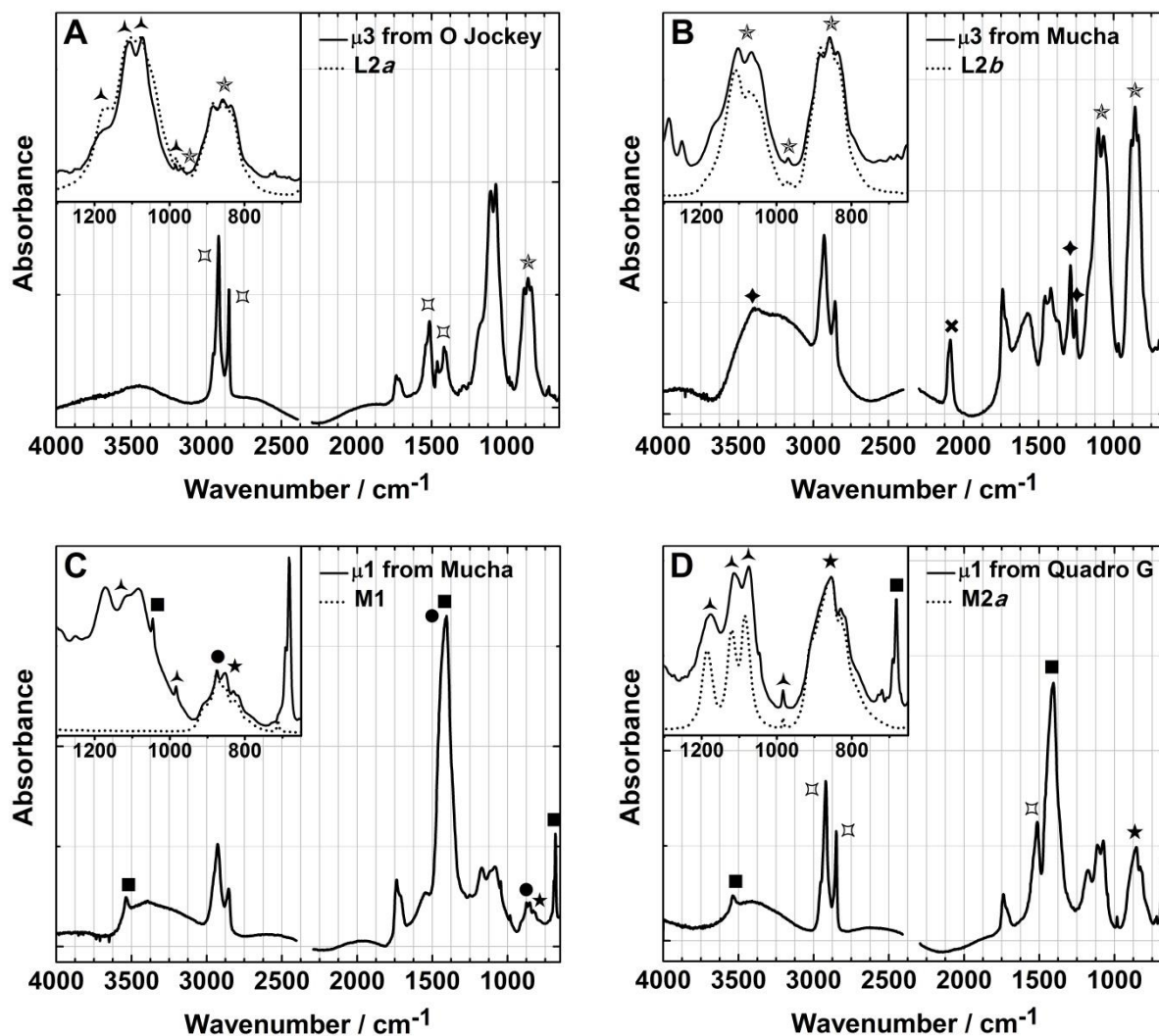


Figure 3.16. Infrared spectra (inset between 1000-750 cm^{-1}) of μ -samples taken from Amadeo's paintings and matching pigment reconstructions: **A)** μ_3 from *O Jockey* (c.1913, cat. n° P58) and L2a pigment reconstruction; **B)** μ_3 from *Mucha* (c.1915-1916, cat. n° P172) and L2b pigment reconstruction; **C)** μ_1 from *Mucha* and M1a pigment variation; **D)** μ_1 from *Quadro G* (c.1912, cat. n° P41) and M2a pigment reconstruction. (★) $\text{PbCr}_{0.6}\text{S}_{0.4}\text{O}_4$, (☆) PbCrO_4 , (■) $2\text{PbCO}_3 \cdot \text{Pb(OH)}_2$, (⊠) lead soap, (▲) BaSO_4 , (●) CaCO_3 , (◆) $\text{Cr}_2\text{O}_3 \cdot 2\text{H}_2\text{O}$ and (✕) $\text{Fe}_4[\text{Fe(CN)}_6]_3$.

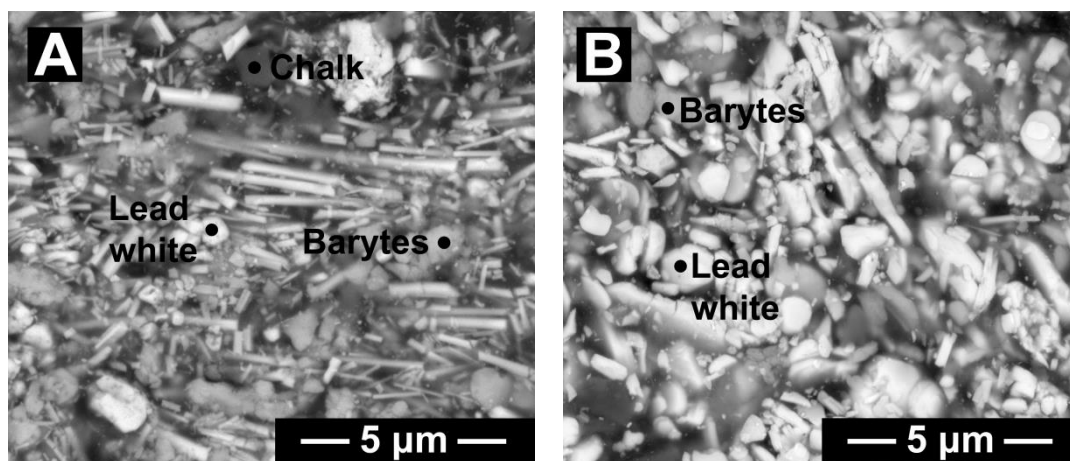


Figure 3.17. SEM images of yellow colours from Amadeo's paintings **A)** *O Jockey* (c.1913, cat. n° P58) and **B)** *Quadro G* (c.1912, cat. n° P41).

It is also important to note that the chrome yellow formulations identified by μ -FTIR were not only found as a single component paint but also mixed with other pigments such as lead white, cobalt yellow, yellow ochres and cadmium yellow, and/or with additives, namely lead carbonate, chalk, gypsum, kaolin, quartz, magnesium carbonate, strontium and magnesium sulfate, Figure 3.16. This is in agreement with the SEM images, where the characteristic lead chromate rod-like particles are observed together with particles of other compounds such as lead white, chalk and barytes, Figure 3.17 (see also Appendix XIII, p. 319, and Montagner, 2015). Interestingly, the formulations discovered in the greens that were analysed, mainly consisting of viridian and/or emerald green, were always mixed with the Lemon formulations composed of mixed crystals of lead chromate and lead sulfate. The particular mixtures of pigments found could have been supplied by a manufacturer other than W&N⁹¹ or may have been mixed by Amadeo himself.

3.6. Other yellow chromate pigments

As noted previously W&N also produced, to a lesser extent, other yellow chromate pigments based on barium (BaCrO_4), zinc ($4\text{ZnCrO}_4 \cdot \text{K}_2\text{O} \cdot 3\text{H}_2\text{O}$) and strontium chromate (SrCrO_4), which they designated as Lemon, Citron and Strontian Yellow, respectively. They also experimented with variations, especially of mixed chromate pigments, i. e., mixed crystals and/or mixed-phase crystals of the different yellow chromates⁹².

3.6.1. Introduction to barium, zinc and strontium chromate pigments

Vauquelin's discovery of chromium in 1797 and the differently coloured compounds derived from it, led to the development of a range of new yellow pigments, the most popular being chrome yellow (lead chromate) as noted above in Chapter 3 (Vauquelin, 1809). In addition, three yellow chromates based on barium, zinc and strontium were introduced. While not as popular with artists, these three new yellows were nevertheless adopted throughout the 19th century (Kühn & Curran, 1986; Bomford *et al.*, 1990; Carlyle, 2001: 521-523; Kirby *et al.*, 2003). Burnstock *et al.* identified these compounds in 19th to 20th century pigments and paints using X-Ray Diffraction (XRD) and Scanning Electron Microscopy (SEM) with elemental analysis (Burnstock *et al.*, 2003). Correia *et al.* also detected barium and strontium chromate using μ -Raman in oil paintings by the Portuguese Naturalist Henrique Pousão (1859-1884) (Correia *et al.*, 2007). They are still in use today, especially as anticorrosive pigments⁹³, also under the REACH European regulation (EUR-Lex, 2018). Their anticorrosive properties are based on their higher water solubility, K_{sp} (Table 3.7), which allows the migration of part of the chromate ions onto the metal surface, leading to the formation of passive layers (Krieg, 2005). Table

⁹¹ There are no evidences of W&N producing oil paints with these mixtures of pigments, neither in the W&N's 19th Century Archive Database nor in the W&N's 1892 declaration (Appendix II.2; p. 175).

⁹² The synthesis and characterisation of these mixed chromate pigments was outside the scope of this work due to their low relevance in the archive.

⁹³ The use of barium chromate as anticorrosive pigment was limited, and it is currently out of use (Krieg, 2005).

3.7 includes their common and chemical names, chemical formula, Colour Index (C.I.) numbers and other characteristics.

Table 3.7. Chrome, barium, zinc and strontium yellow pigments: common and chemical names, chemical formula, Colour Index number (C.I.), refractive index, solubility product constants (K_{sp} at 25°C), crystal structure and space group (Chang, 1994; Liang *et al.*, 2005; Lide, 2006; Cameo, 2016).

Common name	Chrome yellow	Barium yellow Lemon yellow*	Zinc yellow Citron yellow	Strontium yellow Strontian yellow
Chemical name	Lead chromate	Barium chromate	Zinc potassium chromate hydrate	Strontium chromate
Chemical formula	PbCrO ₄	BaCrO ₄	4ZnCrO ₄ ·K ₂ O·3H ₂ O	SrCrO ₄
C.I. Pigment Yellow	34:77600	31:77103	36:77955	32:77839
Refractive index	2.3 - 2.65	1.94 - 1.98	1.84 - 1.9	1.92 - 2.01
K_{sp}	1.8×10^{-14}	1.17×10^{-10}	3.3×10^{-11} #	3.5×10^{-5}
Crystal structure	Monoclinic	Orthorhombic	Monoclinic	Monoclinic
Space group	P2 ₁ /n	Pnma	P2 ₁ /n	P2 ₁ /n

* The designation "lemon yellow" was also used for zinc and strontium chromates (Carlyle, 2001: 521-523) but herein it will only refer to barium chromate.

The solubility product constant of zinc yellow is not tabulated. It was calculated using the data from Simonsen *et al.* (2017).

Barium chromate (BaCrO₄), first synthesised and analysed by Vauquelin, resulted from adding a solution of barium nitrate to a chromate or dichromate (e.g. sodium or potassium) solution (Vauquelin, 1809). Barium chloride may also be used as an alternative source of barium (Kühn & Curran, 1986; Alía *et al.*, 1999). Throughout the 19th century, barium chromate was known under several different names including: barium yellow, lemon yellow, ultramarine yellow, baryta yellow and Steinbühl yellow (Kühn & Curran, 1986; Eastaugh *et al.*, 2004: 36). In Field's 1st edition of *Chromatography*, in 1835, the entry for lemon yellow corresponds to a variation of platina yellow⁹⁴ (p. 81), but in the edition of 1869, edited by Thomas W. Salter, it was identified as chromate of baryta (p. 101) (Field, 1835; Carlyle, 2001: 522). Furthermore, Carlyle (2001) notes that by the end of the 19th century, Reeves was selling a Pale hue of Lemon Yellow composed of barium chromate and a Deep hue composed of barium and strontium chromate, the latter being less lightfast, as stated in their catalogue from c.1898 (Carlyle, 2001: 522).

Zinc chromate with the approximate composition of 4ZnCrO₄·K₂O·3H₂O also appeared in the beginning of the 19th century, and the origin of its discovery is unclear (Kühn & Curran, 1986). Recently, Simonsen *et al.* have determined its structure as KZn₂(CrO₄)₂H₂O(OH) by single-crystal X-ray crystallography (Simonsen *et al.*, 2017). There is another formula which was patented in 1941, with the composition ZnCrO₄·4Zn(OH)₂ (zinc chromate hydroxide) (Kühn & Curran, 1986; Eastaugh *et al.*, 2004: 408). This type of pigment is formed by precipitation when a solution of a zinc salt is added to a chromate (e.g. sodium or potassium) solution, in the presence of potassium ions (Kühn & Curran, 1986). During the 19th century, the most common names for zinc chromate were zinc yellow and citron

⁹⁴ Field did not reveal the composition of the platina yellow pigment, however in 1837, G. H. Bachhoffner (British chemist; 1810-1879) suggested it was a potassium chloroplatinate (K₂PtCl₆) (Field, 1835; Harley, 1982: 102).

yellow but it was also labelled as ultramarine yellow, yellow button of gold and permanent yellow (Kühn & Curran, 1986; Carlyle, 2001: 523; Eastaugh *et al.*, 2004: 408).

It is also uncertain who synthesised strontium chromate (SrCrO₄) for the first time (Kühn & Curran, 1986, Eastaugh *et al.*, 2004: 354). Presently it is obtained when a solution of strontium chloride is added to a sodium dichromate solution (Krieg, 2005). During the 19th century onwards, it appears variously as: strontian yellow, strontaine yellow, lemon yellow and ultramarine yellow (as noted, the last two names could also refer to barium chromate) (Kühn & Curran, 1986; Carlyle, 2001: 522; Eastaugh *et al.*, 2004: 354).

The availability of colours associated with these yellow chromate pigments throughout the 19th century from W&N is described in Table 2.3 (p. 35) and from Reeves and Rowney in Table 3.8 (Carlyle, 2001: 533-543). They were also mixed with other pigments, especially with Prussian blue and chromium oxide to provide new colours (Kühn & Curran, 1986).

Table 3.8. Dates of the first appearance of colours associated with Lemon (barium chromate), Citron (zinc potassium chromate) and Strontian (strontium chromate) Yellow in powder and oil colour in the 19th century from Reeves and Rowney. From Carlyle (2001, Appendix 26, Table 7, p. 540 & Table 8, p. 543).

Colour	Reeves		Rowney	
	Oil paint tube	Powder	Oil paint tube	Powder
Lemon Yellow	1852	(1856)	1849	1849
Citron Yellow	c.1896	<i>not in powder</i>	<i>not available</i>	
Strontian Yellow	1872	1872*	c.1885	c.1885

* Reeves stop selling Strontian Yellow in powder in 1892.

Of the three yellow chromate pigments, barium chromate is considered the most lightfast, nevertheless, it is reported to turn green after long exposure to light (Kühn & Curran, 1986). This agrees with the reactivity model suggested by Monico and Tan *et al.*, that relates the tendency to degrade with the solubility of the pigments, see Table 3.7 (Monico *et al.*, 2013a; Tan *et al.*, 2013). There is only one dedicated study concerning the degradation of these pigments; it is focused on the darkening of zinc chromate (4ZnCrO₄·K₂O·3H₂O), which has been observed in Georges Seurat's paintings including *A Sunday on La Grande Jatte – 1884* (Kirby *et al.*, 2003; Casadio *et al.*, 2008 & 2011; Zanella *et al.*, 2011). Casadio *et al.* studied the darkening of oil paints prepared with a modern zinc yellow (DuPont, Y-539-D; PS-83109) and cold pressed linseed oil (W&N), and subjected to artificial aging under combined environmental conditions: light/dark, air humidity (50% and 90% RH) and acidic gases (SO₂ and CO₂). Colour changes were observed in all aging experiments, but the highest degree of darkening occurred in the presence of light, SO₂ and 90% RH. By means of Electron Energy Loss Spectroscopy (EELS) and XANES, they determined that the darkening is related to the reduction of the original Cr(VI) in zinc yellow pigment to Cr(III) species such as the green chromium oxide (Cr₂O₃). Orange Cr(VI) dichromate species were also detected in the samples aged under light, SO₂ and 50% RH (Casadio *et al.*, 2008 & 2011; Zanella *et al.*, 2011).

3.6.2. The W&N 19th century manufacture of other yellow chromate pigments

Research into W&N's pigment manufacture using the W&N 19th Century Archive Database resulted in the identification of 103 production records for other yellow chromate pigments based on barium, zinc and strontium. There are 71 production records for Lemon Yellow (also under the names Chromate Barytes and Permanent Primrose) corresponding to barium chromate, 26 for Citron Yellow (or Chromate of Zinc) which correspond to zinc potassium chromate, and 6 for Strontian Yellow (or Chromate Strontia) resulting in strontium chromate. Contrary to the wide range of names used for lead chromate pigments in W&N's production records, further variations on naming for these three pigments were not found in the W&N archive.

The names in the production records correlate well to their trade names from the W&N 19th century catalogues shown in Table 2.3 (p. 35) and the pigment composition is in agreement with W&N's declaration of their pigment compositions from 1892 (Appendix II.2; p. 175). **Lemon Yellow** is described as chromate of barium and **Citron Yellow** is given as chromate of zinc. On the other hand, it is notable that **Strontian Yellow** is not included in W&N's 1892 declaration. Its absence is likely because it was considered too fugitive for W&N and may explain why there are so few records for the production of strontium chromate. Evidence for this assumption appears in a book belonging to Arthur Henry Newton, already mentioned in Chapter 2 (p. 32). Associated with a recipe for a physical mixture of Lemon Yellow (barium chromate) with Citron Yellow (zinc potassium chromate) which appears under the name: "Strontian Yellow: No. 2 for Oil", dated 23/11/1859, is a note: "In Father's opinion this is a much safer color to use in oil than Chromate of Strontia" (W&N Database Unique Recipe Code: P2P264AL07). In W&N's 1892 declaration (Appendix II.2, p. 175), this physical mixture appears under the name **Primrose Yellow**⁹⁵ and is described as "similar in colour to the old 'Strontian Yellow' (Chromate of Strontium) but keeps its colour better". Despite this observation both Citron Yellow and Primrose Yellow were nevertheless designated fugitive in oil in W&N's 1892 declaration, with only Lemon Yellow considered permanent in oil. Interestingly, this is contrary to the position of Jehan-Georges Vibert, a 19th century authority on painting materials and supplier as well as consultant to the 19th century artists' colourman Lefranc & Co. (Bomford *et al.*, 1990; Carlyle, 2001: 329). He placed strontium chromate in a list of permanent or "good" pigments, together with zinc chromate whereas barium chromate belonged to the list of "bad" pigments (he declared lead chromate pigments "more or less bad") (Vibert, 1891: 98 & 285).

There are 15 additional production records where W&N experimented with methods of producing yellow mixed chromate pigments, mainly of combinations of two different chromates at a time⁹⁶: lead and barium chromate, lead and strontium chromate, lead and zinc chromate, barium and strontium chromate and, barium and zinc chromate, see Appendix IV.4, p. 231. From these, it is noteworthy to refer the production records for **Permanent Yellow** based on the addition of zinc white and barium chloride to a solution of potassium dichromate. This correlates to what is published in the W&N's 1892 declaration under Permanent Yellow.

⁹⁵ Interestingly, no production record was found in the W&N database under Primrose Yellow.

⁹⁶ The synthesis and characterisation of the mixed chromate pigments was outside the scope of this work due to their low relevance in the archive.







3.6.2.1. The W&N 19th century manufacturing processes and experiments for barium, zinc and strontium chromate pigments









As found to be the case for the lead chromate pigments (Chapter 3.2, p. 48), once all the production records were analysed for barium, zinc and strontium chromates, it was evident that the company was using a limited number of methods for synthesis. Their main synthetic pathways are described in Table 3.9. The full range of process variations for these pigments is presented in Appendix IV (p. 225) along with details on the ingredients, the order of addition, as well as the respective number of production records and date range for each manufacturing process.

The core difference between W&N's 19th century manufacture of barium, zinc and strontium chromate (Table 3.9) and lead chromate pigments (Table 3.2, p. 49) is the degree of experimentation. For the lead chromates, W&N extensively tested sources for chromate, sulfate and lead as well as additives such as extenders and fillers. In the manufacture of barium, zinc and strontium chromate pigments, experimentation was reduced to the choice of the chromate and metal ion source. No extenders or fillers were tested likely because these pigments present a lower tinting strength, see Table 3.10. Interestingly, Burnstock *et al.* did not find extenders in paint samples where these pigments were detected (Burnstock *et al.*, 2003).

Table 3.9 shows that to produce W&N's Lemon, Citron and Strontian Yellow, solutions of barium chloride, zinc nitrate and strontium nitrate were respectively added to a chromate solution (CrO₄²⁻). In the case of Citron Yellow, potassium carbonate was added as a buffer but may also act as an extra source of potassium. The resulting pigments present lighter yellow hues compared with pure lead chromate pigments, see Figure 3.18.

Table 3.9. W&N's Lemon, Citron and Strontian Yellow: key ingredients, main synthetic pathways and final pigment formula.

Key Ingredients					
Chromate Source		Potassium Source	Barium Source	Zinc Source	Strontium Source
					
K ₂ Cr ₂ O ₇ + Na ₂ CO ₃	K ₂ Cr ₂ O ₇	K ₂ CO ₃	BaCl ₂	Zn(NO ₃) ₂	Sr(NO ₃) ₂

W&N production record name	Code [§]	Order of addition			Final pigment formula [†]
LEMON YELLOW	LY1a				BaCrO₄
CITRON YELLOW	CY1a			 	4ZnCrO₄·K₂O·3H₂O
STRONTIAN YELLOW	SY1a				SrCrO₄

[§] Codes refer to variations in the manufacturing processes, see Appendix IV (p. 225).

[†] See table 3.7, p. 71.

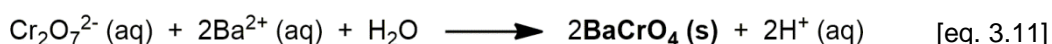


Figure 3.18. The final colour of Lemon Yellow (BaCrO_4), Strontian Yellow (SrCrO_4), Citron Yellow ($4\text{ZnCrO}_4 \cdot \text{K}_2\text{O} \cdot 3\text{H}_2\text{O}$), and pure chrome yellow (PbCrO_4) manufactured following W&N 19th century recipes.

3.6.2.1.1. Lemon Yellow (barium chromate, BaCrO_4)

The 71 production records found for Lemon Yellow cover the period from 1838 to 1880. These can be reduced to 3 main methods of synthesis. All manufacturing processes are depicted in Appendix IV.1 (p. 225).

The majority of the Lemon Yellow productions records (64) pertain to the process coded LY1a, Table 3.9 and eq. 3.11.



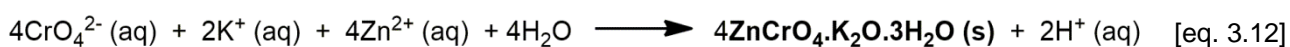
This is the only chromate pigment method of synthesis where W&N chose to use potassium dichromate alone without the addition of a buffer (in the form of a carbonate). This results in a very acidic final pH (Table 3.10). Of these three chromates, barium chromate is the only that precipitates regardless of the pH (as does lead chromate), hence the absence of the buffer.

Four production records were found where a buffered chromate solution (potassium dichromate with potassium carbonate) was used. A single experiment with potassium chromate alone (this would result in a basic final pH) was also conducted. Barium nitrate was also tried in two production records to substitute for barium chloride.

3.6.2.1.2. Citron Yellow (zinc potassium chromate, $4\text{ZnCrO}_4 \cdot \text{K}_2\text{O} \cdot 3\text{H}_2\text{O}$)

Twenty-six production records were found for zinc potassium chromate under the name Citron Yellow and Chromate of Zinc. These cover the period from 1834 to 1893 with the majority of the records dated in the 1850s. There are only 3 main methods of synthesis. All variations are presented in Appendix IV.2 (p. 227).

Most of the Citron Yellow productions records (18) correspond to the process coded CY1a, Table 3.9 and eq. 3.12.



For the manufacture of their Citron Yellow, W&N primarily used potassium dichromate as the chromate source. Potassium carbonate was added to play three functions: to shift the dissociation

reaction of dichromate into chromate, and to act as a buffer and an additional potassium source. This particular reaction results in a pigment formula different from the common chemical formula of yellow chromates, $M\text{CrO}_4$ ($M = \text{Pb, Ba and Sr}$), since potassium ion (K) and “hydroxo aqua” ions are present in the crystal structure together with the zinc ion (Zn), eq. 3.12 (Simonsen *et al.*, 2017). For this particular formula to precipitate, the buffered chromate solution needs to be around pH 6 (achieved by the addition of the potassium carbonate) when the zinc nitrate is added. Precipitation does not occur in acidic conditions. There are 5 production records where potassium dichromate was used with sodium carbonate. W&N also experimented with zinc sulfate and zinc acetate as zinc sources. In addition, they performed a test with potassium dichromate and zinc sulfate, but it is unlikely that this resulted in pigment precipitation, due to the low pH of the potassium dichromate solution.

3.6.2.1.3. Strontian Yellow (strontium chromate, SrCrO_4)

Few production records were found for Strontian Yellow: just 6, all dated in the 1850s. There were 3 methods of synthesis, which are depicted in Appendix IV.3 (p. 229). As noted above, the low number of production records suggests that W&N was not producing and consequently not selling strontium chromate on a large scale.

The majority of the Strontian Yellow productions records (4) pertain to the process coded SY1a, Table 3.9 and eq. 3.13.



In addition to the main synthetic pathway, there is one production record where the pathway is very similar to CY1a, with the addition of potassium carbonate before and during pigment precipitation, and another record where potassium chromate is used alone. As observed for zinc potassium chromate, when potassium dichromate is used, a carbonate compound must be added to shift the dissociation reaction of dichromate into chromate, enabling the precipitation to occur at $\text{pH} > 6$. No other sources of strontium were tested.

3.6.3. The characterisation of W&N’s barium, zinc and strontium chromate pigment reconstructions




Pigment characterisation followed the same methodology adopted for lead chromate pigments presented in Chapter 3.3. (p. 55). Pigment reconstructions were synthesised following selected production records⁹⁷ (transcribed in Appendix II.3.2, p. 200, and highlighted in Appendix IV, p. 225). Syntheses are detailed in Appendix V.2.1.2 (p. 236) and the pH measurements throughout the syntheses are detailed in Appendix IX.2 (p. 291). These were reproduced more than once to confirm their reproducibility. The reconstructed pigments were characterised by μ -EDXRF, FORS, Colourimetry, μ -Raman, μ -FTIR and XRD. The experimental conditions for the analytical equipment

⁹⁷ The selection of the representative production records was based on their prominence within the whole set for that pigment and the amount of detail provided.

are detailed in Appendix V.3 (p. 239). Full characterisation of representative pigment reconstructions is presented in Appendix XIV (p. 343).

$L^*a^*b^*$ colour coordinates and the inflection point (λ_{IP} , nm) of the reflectance (FORS) spectra are shown in Table 3.10. Lemon and Strontian Yellows (b^* around fifty) present a more greenish tone (a^* negative) than Citron Yellow (a^* positive). As shown in Fig. 3.19, their reflectance spectra present distinctive inflection points enabling their in situ identification by FORS. However, Citron Yellow presents the inflection point of the reflectance spectra closer to that observed for the lighter hues of lead chromate pigments (Table 3.3 and 3.4, p. 56-57).

Table 3.10. Reconstructions of W&N's Lemon (LY1a), Citron (CY1a) and Strontian (SY1a) Yellow pigments following their main synthetic pathways: final pH, $L^*a^*b^*$ colour coordinates, relative tinting strength (% TS) and inflection point (λ_{IP} , nm) of the reflectance spectra.

	Final pH [#]	L^*	a^*	b^*	% TS [§]	λ_{IP} (nm)
 LY1a	≈ 1	89.9 ± 3.2	-7.7 ± 0.5	52.1 ± 0.8	92	450
 CY1a	≈ 5	86.9 ± 0.4	5.1 ± 0.4	88.5 ± 0.8	65	510
 SY1a	≈ 8	94.1 ± 1.1	-11.4 ± 0.2	55.2 ± 0.2	78	483 (445, sh)

[#] Final pH was measured at the end of the precipitation.

[§] The relative tinting strength was calculated using the ASTM Standard Test Method D4838 - 88(2003) and pure lead chromate was used as the standard (100% TS). For more details see Appendix V.2.3. (p. 237).

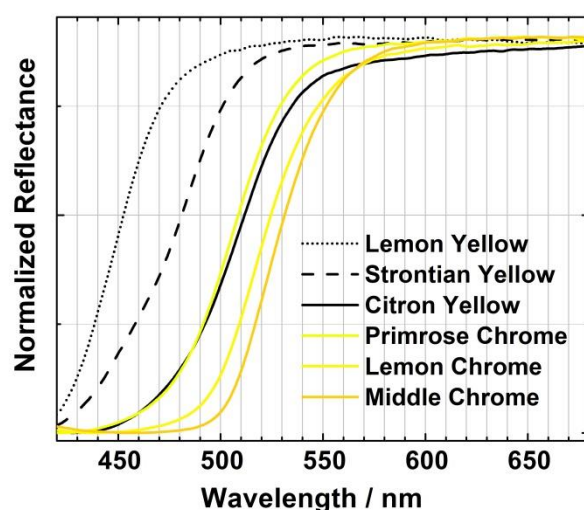


Figure 3.19. Normalized FORS spectra of all yellow chromate pigments representative of the main synthetic pathways shown in Table 3.2 and Table 3.9.

The identification of these yellow chromate pigments is very straightforward by μ -FTIR, μ -Raman and XRD. Their distinctive infrared and Raman spectral fingerprints are shown in Figure 3.20 (μ -EDXRF spectra and diffraction patterns may be consulted in Appendix XIV, p. 343).

The characteristic infrared and Raman bands of the pigments' chromophores are detailed in Table 3.11 and the spectral assignments were made in accordance to the literature (Alía *et al.*, 1999; Hummel, 2002; Stoilova *et al.*, 2005; Liang *et al.*, 2005; Correia *et al.*, 2007; Simonsen *et al.*, 2017; Nakamoto, 2009). As may be seen in Fig. 3.20 and Table 3.11, their infrared spectra present distinctive spectral profiles assigned to the CrO_4^{2-} asymmetric stretching mode (between 1000-700 cm^{-1}). On the other hand, their Raman spectra display differences in their main band assigned to the CrO_4^{2-} symmetric stretching mode, which together with the CrO_4^{2-} asymmetric stretching bands (in the region 850-950 cm^{-1}) allows a complete differentiation between these pigments. This is particularly important when these pigments are found together.

Table 3.11. Reconstructions of W&N's Lemon (LY1a), Citron (CY1a) and Strontian (SY1a) Yellow pigments: pigment composition, ICDD diffraction cards, Raman and infrared characteristic bands (Alía *et al.*, 1999; Hummel, 2002; Stoilova *et al.*, 2005; Liang *et al.*, 2005; Correia *et al.*, 2007; Simonsen *et al.*, 2017; Nakamoto, 2009) (the main bands appear in bold).

	Lemon Yellow (LY1a)		Citron Yellow (CY1a)		Strontian Yellow (SY1a)	
Pigment Composition	BaCrO ₄ orthorhombic		4ZnCrO ₄ ·K ₂ O·3H ₂ O monoclinic		SrCrO ₄ monoclinic	
ICDD diffraction card	00-078-1401		00-008-0202		00-035-0743	
Infrared bands (cm⁻¹)						
ν(OH)	-		3442		-	
ν _{as} (CrO ₄ ²⁻)	885	s	881	s	911	s
	855	sh	951, 809	sh	888, 874, 843	sh
Raman bands (cm⁻¹)						
δ(CrO ₄ ²⁻)	349, 360, 403, 427	w-m	342, 408	w-m	338, 348, 374, 400	w-m
ν _s (CrO ₄ ²⁻)	862	s	872	s	866	s
ν _{as} (CrO ₄ ²⁻)	872, 898, 906	w-m	892	sh	894	m
			940	m	916, 930	w-m

w-m: weak to medium; m: medium; s: strong; sh: shoulder.

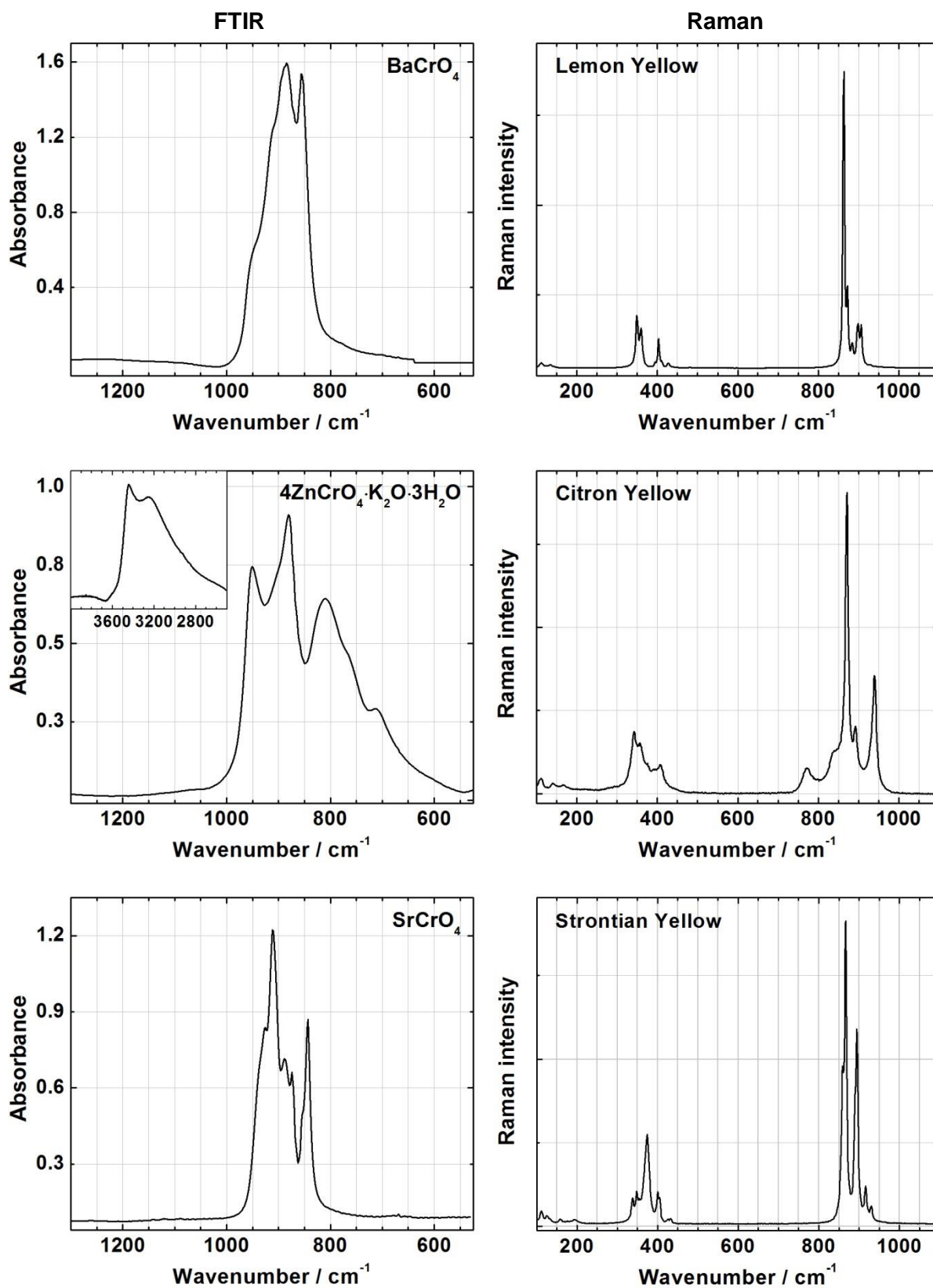


Figure 3.20. Infrared (left) and Raman (right) spectra of pigment reconstructions for W&N's Lemon (LY1a), Citron (CY1a) and Strontian (SY1a) Yellows.

3.6.4. Comparison with historic oil paint tubes and Amadeo's paintings

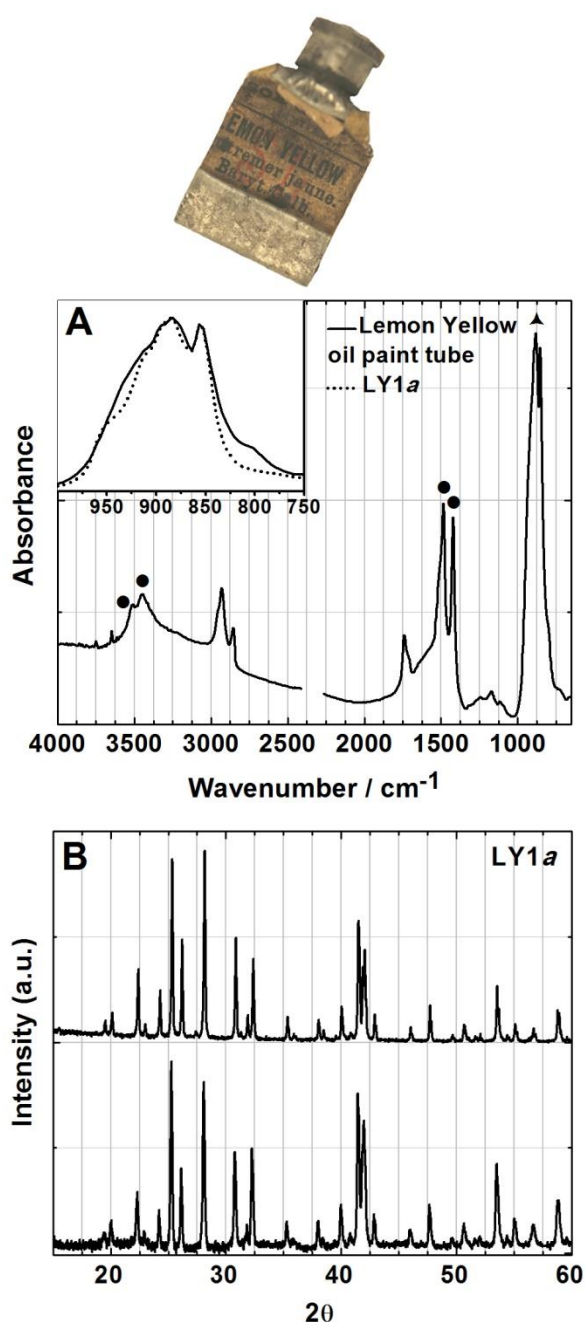


Figure 3.21. A) Infrared spectra (inset between 1000 and 750 cm⁻¹) and B) diffraction pattern of the W&N *Lemon Yellow* oil paint (private collection @ DCR FCT NOVA) compared with a LY1a pigment reconstruction; (▲) BaCrO₄, (●) MgCO₃·xH₂O.

A comparison was made with a late 19th century W&N oil paint tube labelled **Lemon Yellow** from the private collection deposited at DCR FCT NOVA⁹⁸. The pigment in the tube is composed of barium chromate and the additive magnesium carbonate (MgCO₃·xH₂O) was also found, Fig. 3.21. As observed for the 19th century W&N lead chromate oil paint tubes (p. 61), magnesium carbonate was only detected by μ-FTIR, not by XRD, which indicates it is most probably in its amorphous form. As seen in Fig. 3.21, the infrared (between 1000 and 750 cm⁻¹) and diffraction pattern of the pigment in the *Lemon Yellow* oil paint tube presents a very good match with the pigment reconstruction for W&N's *Lemon Yellow* (LY1a, barium chromate). Additional data (μ-EDXRF, FORS, Colourimetry, μ-Raman) on the *Lemon Yellow* oil paint tube may be seen in Appendix XV (p. 347).

The identification of magnesium carbonate in another W&N oil paint tube supports that this additive was part of W&N's oil paint formulation and strengthens the earlier suggestion that it may be a good marker for W&N's oil paints.

⁹⁸ As previously noted, the private collection is composed of late 19th century W&N oil paint tubes studied by Marta Félix Campos; they were dated according to the data on the label (Campos, forthcoming).

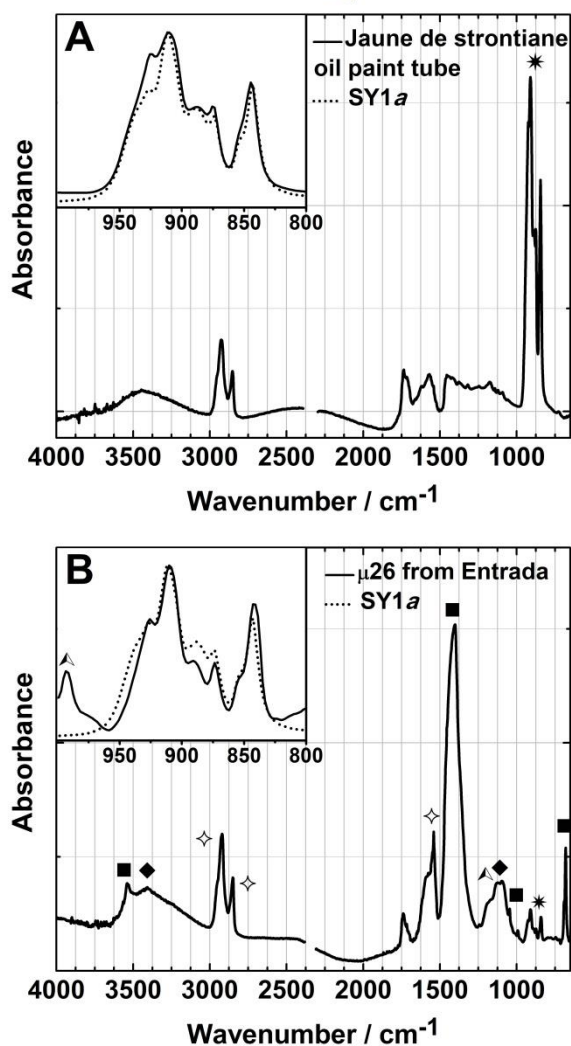


Figure 3.22. Infrared spectra (inset between 1000 and 800 cm^{-1}) of **A)** Lefranc's *Jaune de Strontiane* oil paint tube, **B)** μ -sample 26 from Amadeo's painting *Entrada* (c.1917, cat. n° P200), compared with a SY1a pigment reconstruction; (*) SrCrO_4 , (■) $2\text{PbCO}_3 \cdot \text{Pb(OH)}_2$, (▲) SrSO_4 , (◆) $\text{CaSO}_4 \cdot 2\text{H}_2\text{O}$, and (◇) zinc palmitate.

A historic oil paint tube labelled **Jaune de Strontiane** (Strontian Yellow) from the French producer Lefranc was also found in the studio of Amadeo de Souza-Cardoso at the Manhufe house⁹⁹. It is only composed of strontium chromate, Fig. 3.22A. This yellow pigment was identified only in Amadeo's last paintings¹⁰⁰: as a single colour in the painting *Entrada*, Fig. 3.22B, and mixed with viridian in the painting *Untitled* (Figure 1.9, p. 19). A direct match with the CrO_4^{2-} infrared stretching fingerprint spectral profile of a pigment reconstruction for W&N's Strontian Yellow (SY1a, strontium chromate) is presented in Fig. 3.22. In the painting *Entrada*, strontium chromate was found together with lead white, strontium sulfate and gypsum, Fig. 22B. The presence of the latter extenders suggests that this particular yellow paint was most probably prepared by Amadeo himself.

The identification of strontium chromate in the Strontian Yellow oil paint tube from Lefranc and not from W&N is very interesting and supports the above mentioned. It is most probable that Lefranc was selling it as such because their consultant Jehan-Georges Vibert considered it a permanent pigment. Whereas W&N was not selling strontium chromate by the end of the 19th century since it was considered too fugitive for them.

⁹⁹ See note 35 in page 24.

¹⁰⁰ As previously mentioned, the paintings by Amadeo *Entrada* and *Untitled* were studied in the framework of the PhD of Cristina Montagner at the DCR FCT NOVA. For more information, please consult Montagner, 2015.

3.7. Conclusions

Access to the production records from W&N's 19th century archive made it possible to carry out a comprehensive study of their manufacturing processes for yellow chromate pigments. Two hundred and eighty-six production records covering the period from 1834 to 1893 were found for the manufacture of chrome yellow (lead chromate; 64%), lemon yellow (barium chromate, 25%), citron yellow (zinc potassium chromate, 9%) and strontian yellow (strontium chromate, 2%).

Despite the high number of production records, in fact only a limited number of different recipes were used for their main pigment formulations. Nevertheless, W&N investigated a very wide range of possible formulations, experimenting with different manufacturing conditions such as varying the starting materials and/or adding different extenders. The pH was a key factor controlled by W&N, particularly to achieve precipitation of zinc potassium and strontium chromate pigments. This demonstrates a thorough and systematic investigation into the chemical processes during manufacture; a testament to W&N's determination to produce the best quality and most stable product possible.

Tests with extenders were conducted only in relation to the manufacture of their chrome yellow pigments (excluding the Primrose formulations). During the manufacture of their other chromate pigments (Lemon, Citron and Strontian Yellow) extenders were not added. This may infer that for W&N, extenders were primarily present to adjust mechanical properties, tinting strength or hue, rather than functioning predominantly as a means to reduce the cost of materials.

All 183 production records for W&N's yellow lead chromate pigments could be grouped into distinct pathways resulting in three types of pigments: Lemon/Pale, Middle and Deep. Lemon/Pale pigments are composed of mixed crystals of lead chromate and lead sulfate $\text{PbCr}_{1-x}\text{S}_x\text{O}_4$ with $x \leq 0.4$; Middle pigments are mainly pure lead chromate $[\text{PbCrO}_4]$ and Deep have a mixture of the latter with basic lead chromate. Of the few records for Primrose pigments, the composition found was $\text{PbCr}_{1-x}\text{S}_x\text{O}_4$ with a higher SO_4^{2-} molar fraction ($x > 0.6$).

The low number of production records for Primrose Chrome composed of a high SO_4^{2-} molar fraction and for strontium chromate, together with their absence from the W&N's declaration of pigments' composition of 1892, indicates that W&N was not selling these products on a large scale¹⁰¹. This provides further evidence to support the conclusion that W&N had a strong commitment to the durability of their products.

The unique spectral fingerprints of the reconstructed pigments produced in accordance with W&N's main manufacturing processes correlate very well with those detected in samples from historic W&N oil paint tubes and Amadeo's oil paintings.

According to the findings in this research, it appears that the pigments in the historic W&N oil paint tubes labelled **Chrome Yellow** and **Chrome Deep** were made in accordance to their production records entitled Lemon/Pale and Middle/Deep, respectively. For the processes which appear most frequently, W&N was relying on barytes as an extender. Only for the pure monoclinic lead chromate (Middle Chrome) was a preference for chalk found. Because of this clear preference, this research also suggests that the presence of chalk in Chrome Deep oil paint could point to it being a W&N

¹⁰¹ However, it is possible that these pigments were made available through special orders.

product. Furthermore, a correspondence between the historic W&N oil paint tube labelled **Lemon Yellow** and W&N's formulations for Lemon Yellow (barium chromate) was also found.

Another possible marker for W&N oil paint is the presence of magnesium carbonate (identified as "spar" in their records), which has only been detected in W&N oil paint tubes. Comparative analysis with oil paint formulations of other contemporary colourmen will be necessary to confirm this hypothesis.

The study of the chrome yellow samples from Amadeo's oil paintings show that he mainly used the Lemon/Pale formulations, however, Middle formulations were also identified. Most importantly, regardless of the pigment formulation, it was possible to determine by SR based techniques that no degradation related to the reduction of the Cr⁶⁺ from the lead chromate pigments to Cr³⁺ species is currently occurring on Amadeo's oil paintings.

Chapter 4

Chrome yellow: the photochemical study



Image of a chrome yellow paint before and after Xenon irradiation @ DCR FCT NOVA

V. Otero, M. Vilarigues, L. Carlyle, M. Cotte, W. De Nolf, M. J. Melo. 2018. *A little key to oxalate formation in oil paints: protective patina or chemical reactor?* Photochem Photobiol Sci. 17, 266-270.

Chapter 4. Chrome yellow: the photochemical study

This Chapter presents the photochemical study of the degradation of chrome yellow pigments. The investigation presented in Chapter 3 (p. 41) allowed the selection of the pigment formulations expected to be more prompt to degradation (Monico *et al.*, 2013b). Oil and poly(vinyl acetate) (PVAc) paints were prepared with reconstructed pigments following W&N's manufacturing processes, air-dried and then irradiated in a Xenon-light apparatus ($\lambda_{\text{irr}} > 300 \text{ nm}$). PVAc was chosen as an additional binder for it contains ester groups as the oil binder with the advantage of quickly air-drying on exposure to air. Samples from the historic lead chromate oil paint tubes described in Chapter 3.4 (p. 61) were also irradiated in order to compare any degradation with the comprehensive set of reconstructed pigments. The degradation processes were studied by Colourimetry, FORS, μ -Raman, μ -FTIR, XRD, SEM-EDS and Synchrotron Radiation (SR) techniques including μ -XRF, μ -FTIR, μ -XRD and μ -XANES (Cr, S and Ca K-edge). The description of the irradiation experiment, including the preparation of the paints, and the experimental conditions of equipments used are described in Appendices V.2.4 (p. 237) and V.3 (p. 239), respectively.

This Chapter shows that an integrated approach is crucial for predicting the stability of chrome yellow paints, as all paint components, from the pigment's crystalline structure to the additives and binders, are determining factors for the degradation mechanisms, intermediates formed and final products. It is important to add that to effectively compare the photostability of the lead chromate pigments it would be necessary to measure the light absorption by the reactive species, i.e., determine the quantum yields of the reactions, however, this was outside the scope of this work.

4.1. Introduction

4.1.1. The degradation of chrome yellow

As mentioned in Chapter 3, since the beginning of their use, chrome yellow pigments were considered unstable (Carlyle, 2001: 521). Evidence of the adoption of these pigments by 19th century artists has been reported, for example in the works by the following artists: J. W. Turner (1775-1851) see Townsend (1993); John Constable (1776-1837) see Cove (1991); Paul Cézanne (1839-1906) see Butler (1984); Paul Gauguin (1848-1903) see Monico *et al.* (2013a); Vincent Van Gogh (1853-1890) see Geldof *et al.* (2013a); Georges Seurat (1859-1891) see Fiedler (1984); and Amadeo de Souza-Cardoso (1887-1918) see Vilarigues *et al.* (2008), Melo *et al.* (2009) and Montagner (2015). Darkening due to the degradation of chrome yellow has been observed in the paintings by Vincent van Gogh and it has been extensively studied by Monico *et al.* by means of SR based techniques (Monico *et al.*, 2011a & 2011b, 2013a & 2013b, 2014b, 2015a & 2015b & 2015c, 2016; Tan *et al.*, 2013). As noted in Chapter 3.5 (p. 66), no degradation of chrome yellow is presently detected in Amadeo's paintings.

Cowley and Erkens *et al.* note that the first studies of the darkening of lead chromate suggested that it resulted from the reduction of Cr^{6+} to Cr^{3+} , more specifically of lead chromate (PbCrO_4) to lead chromite ($\text{Pb}(\text{CrO}_2)_2$) or chromium trioxide (Cr_2O_3) (Cowley, 1986; Erkens *et al.*, 2001). In the 1940s, Lashof investigated the electrical properties of lead chromate and proposed that lead chromate

dissociates to lead chromite ($\text{Pb}(\text{CrO}_2)_2$), elementary lead (Pb^0) and oxygen (O_2) (Lashof, 1943). Later, Watson & Clay analysed several types of lead chromate irradiated with a mercury-vapour lamp. They supported Lashof's theory that the blackening of lead chromate was due to photochemical reduction but for they surmised that the oxygen formed is in the atomic form, and not molecular oxygen (Watson & Clay, 1955). However, no experimental evidence was offered at the time.

Through the complementary use of bench and portable (in situ) XRF, Raman, FTIR and XRD, Monico *et al.* studied samples from historic chrome yellow oil paint tubes (Monico *et al.* 2011a, 2013a; Tan *et al.*, 2013) and from altered and unaltered chrome yellow areas in paintings by Vincent Van Gogh and Paul Gauguin (Monico *et al.* 2011b, 2013a, 2014a, 2014b, 2015a, 2015c). They reported the identification of pure lead chromate and solid solutions of lead chromate and lead sulfate with a SO_4^{2-} molar fraction between 0.1 and 0.5 on the paintings (Monico *et al.*, 2013a, 2014a). Very recently, this characterisation has also been possible in situ by chemical mapping using Macroscopic X-ray powder diffraction (MA-XRPD) (Vanmeert *et al.*, 2018). A higher content of SO_4^{2-} molar fraction with a complete change to the orthorhombic lead sulfate phase, 0.9, was solely detected in a historic oil paint tube belonging to the Flemish Fauvist Rik Wouters (1882-1913). However, this tube was also composed of other phases; its full composition was revealed by XRD: 58% of solid solutions of orthorhombic lead sulfate and lead chromate ($\text{PbCr}_{0.1}\text{S}_{0.9}\text{O}_4$), 41% of solid solutions of orthorhombic lead chromate and lead sulfate ($\text{PbCr}_{0.8}\text{S}_{0.2}\text{O}_4$) and 1% of solid solutions of monoclinic lead chromate and lead sulfate ($\text{PbCr}_{0.6}\text{S}_{0.4}\text{O}_4$)¹⁰². Interestingly, this was the only case study where the orthorhombic form of lead chromate was detected (Monico *et al.*, 2013a). Darkening of chrome yellow was found regardless of the lead chromate composition (Monico *et al.*, 2011b, 2014b, 2015a, 2015c).

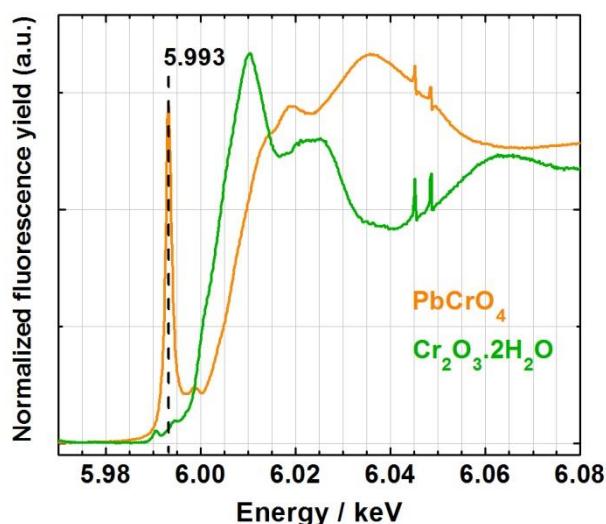


Figure 4.1. Cr K-edge μ -XANES spectra of lead chromate (PbCrO_4) and viridian ($\text{Cr}_2\text{O}_3 \cdot 2\text{H}_2\text{O}$).

et al., 2016; Cotte *et al.*, 2017b). As may be seen in Figure 4.1, Cr K-edge μ -XANES spectrum of Cr^{6+} compounds such as lead chromate, presents a characteristic and well-defined pre-edge peak around

Following the methodology developed for the study of the degradation of the zinc yellow pigment ($4\text{ZnCrO}_4 \cdot \text{K}_2\text{O} \cdot 3\text{H}_2\text{O}$) in Georges Seurat's *A Sunday on La Grande Jatte—1884* (Casadio *et al.*, 2008 & 2011; Zanella *et al.*, 2011), experiments by Monico *et al.* demonstrated for the first time, that the degradation of chrome yellow pigments results from the reduction of the original oxidation state Cr^{6+} to Cr^{3+} (Monico *et al.*, 2011a & 2011b).

As previously mentioned in Chapter 3.5 (p. 67), the combined use of SR μ -XRF and μ -XANES enables the study of the distribution of chemical species at different oxidation states with micrometric resolution (Janssens

¹⁰² The sulfur and chromium abundances were calculated as a weighted average for the mass fraction of orthorhombic and monoclinic phases. The chemical composition of the oil paint tube was estimated as $\text{PbCr}_{0.4}\text{S}_{0.6}\text{O}_4$ (Monico *et al.*, 2013a).

5.993 keV due to a dipole-forbidden transition $\text{Cr}(1s) \rightarrow 3d(t_2)$, related to their noncentrosymmetric tetrahedral geometry. On the other hand, Cr^{3+} compounds show two very low intensity pre-edge peaks around 5.990 and 5.993 keV assigned to the electron transitions $1s \rightarrow 3d(t_{2g})$ and $1s \rightarrow 3d(e_g)$, related to their centrosymmetrical octahedral geometry (Pantelouris *et al.*, 2004; Monico *et al.*, 2011a). By acquiring SR μ -XRF maps at 5.993 keV for the detection of Cr^{6+} and at 6.1 keV for other Cr species such as Cr^{3+} it is possible to obtain species-specific maps (Janssens *et al.*, 2016; Cotte *et al.*, 2017b).

Monico *et al.* investigated the degradation of chrome yellow paints by studying artificially aged samples from historic late 19th century chrome yellow oil paint tubes and from oil paint models prepared with linseed oil and synthesised pigments of solid solutions of lead chromate and lead sulfate $\text{PbCr}_{1-x}\text{S}_x\text{O}_4$ with increasing x values¹⁰³ (80:20 weight ratio) (Monico *et al.*, 2011a, 2013a, 2013b, 2014b, 2015a, 2015b, 2016; Tan *et al.*, 2013). Samples from altered chrome yellow areas from Van Gogh's paintings were also studied (Monico *et al.*, 2011b, 2014b, 2015a). The degradation processes were followed by UV-Vis, μ -Raman, μ -FTIR, XRD, SR μ -XRF, SR μ -XRD, S and Cr K-edge μ -XANES, Scanning Transmission Electron Microscopy coupled to Energy Electron Loss Spectroscopy (STEM-EELS) and Electron Paramagnetic Resonance (EPR) spectroscopy. They established that degradation results from the surface reduction (thickness around 2-3 μm) of the original oxidation state Cr^{6+} to Cr^{3+} with the formation of Cr^{3+} compounds such as Cr_2O_3 , $\text{Cr}_2\text{O}_3 \cdot 2\text{H}_2\text{O}$, $\text{Cr}(\text{OH})_3$, $\text{Cr}_2(\text{SO}_4)_3 \cdot \text{H}_2\text{O}$, $\text{CrK}(\text{SO}_4) \cdot 12\text{H}_2\text{O}$ and/or Cr^{3+} organometallic compounds (Monico *et al.*, 2011a, 2011b, 2013b, 2014b, 2015a, 2016; Tan *et al.*, 2013). They also demonstrated that solid solutions of lead chromate and lead sulfate richer in lead sulfate orthorhombic phase are more prone to degradation, especially under UV ($240 \leq \lambda \leq 400 \text{ nm}$), UV-Vis ($\lambda \geq 300 \text{ nm}$) and blue light ($335 \leq \lambda \leq 525 \text{ nm}$)¹⁰⁴. According to them, this is due to their higher solubility¹⁰⁵ which enables more chromate ions to be available for redox reactions. Consequently, the solid solutions dominated by the lead chromate monoclinic phase are less susceptible to darkening (Monico *et al.*, 2013b).

Monico *et al.* also showed the first evidence of the presence of Cr^{5+} species by EPR spectroscopy, which are intermediates of the $\text{Cr}^{6+}/\text{Cr}^{3+}$ redox reaction responsible by the darkening of chrome yellow paints (Monico *et al.*, 2015b, 2016). Furthermore, they also studied the influence of the environmental conditions (e.g., light, temperature, humidity) and observed that for oil paints prepared with $\text{PbCr}_{0.2}\text{S}_{0.8}\text{O}_4$ pigments, the photo-reduction reaction is accelerated at higher moisture levels and with thermal treatment. The presence of lead carboxylates was also detected, including in the naturally aged historic oil paint tube belonging to the painter Rik Wouter (described above), most probably as a result of the reaction of the pigment with the oil binder (Monico *et al.*, 2016).

By means of STEM-EELS, Tan *et al.* studied at the nanoscale level the historic oil paint tube belonging to the painter Rik Wouter before and after artificial ageing. They proposed a model of the

¹⁰³ The syntheses followed the method reported by Crane *et al.* (2001) where a solution of lead nitrate ($\text{Pb}(\text{NO}_3)_2$) was added drop by drop to a solution of variable concentrations of potassium chromate (K_2CrO_4) and potassium sulfate (K_2SO_4), always mixed under agitation. pH measurements of 10 mL of water equilibrated with 1-2 mg of the prepared pigments revealed pH's between 4.5 and 6 (Monico *et al.*, 2013a).

¹⁰⁴ Recently, Lunz *et al.* also studied the impact of different light spectra on the degradation of an oil paint model prepared with a $\text{PbCr}_{0.2}\text{S}_{0.8}\text{O}_4$ pigment. They determined the wavelength dependence of the pigment discoloration and proposed a method to optimize LED sources with a particular spectrum (Hue) able to reduce light induce damage (Lunz *et al.* 2017).

¹⁰⁵ The solubility of lead sulfate ($K_{sp} = 2.53 \times 10^{-8}$) is greater than lead chromate ($K_{sp} = 1.8 \times 10^{-14}$) (Lide, 2006).

degradation process, which starts via an initial dissolution of the chromate ions, leading to the oxidation of the organic binder and the formation of Cr³⁺ compounds (Tan *et al.*, 2013; Janssens *et al.*, 2016). However, it is important to refer that the particular pigment composition of this oil paint (detailed above) was never found in paintings by Van Gogh's and his contemporaries (Monico *et al.*, 2013a)¹⁰⁶.

To study the electronic properties of chrome yellow pigments, Amat *et al.* applied first principles Density Functional Theory (DFT) calculations on reference structures of pure monoclinic lead chromate, orthorhombic lead chromate, orthorhombic lead sulfate and of solid solutions with variable compositions. Their results suggest that in a purely electronic picture and contrary to what has been published by Monico *et al.*, the pure lead chromate is more prone to reduction than the pigments with high sulfate content or with an orthorhombic phase (Amat *et al.*, 2016). The same method was explored by Muñoz-García *et al.* to investigate the role of the bulk properties of the chrome yellow pigments composed of solid solutions richer in the sulfate phase (Muñoz-García *et al.*, 2016). As observed by Amat *et al.*, their results also show that the band gap increases with increasing sulfate content and when in the orthorhombic phase. An increase in the band gap is associated with a lower photo-reactivity. However, they suggest that the degradation results from an initial local segregation of lead sulfate, which absorbs UV light providing the necessary energy to reduce the chromate ions. No experimental evidence has been found to support this hypothesis (Muñoz-García *et al.*, 2016; Janssens *et al.*, 2016).

Recently, Rahemi *et al.* have complemented first-principles calculations with photo-electrochemical measurements demonstrating that the lower lightfastness of the solid solutions which are richer in lead sulfate orthorhombic phase is due to an increase of the photo absorption current regardless of the higher band gap observed for this type of pigment (Rahemi *et al.*, 2017).

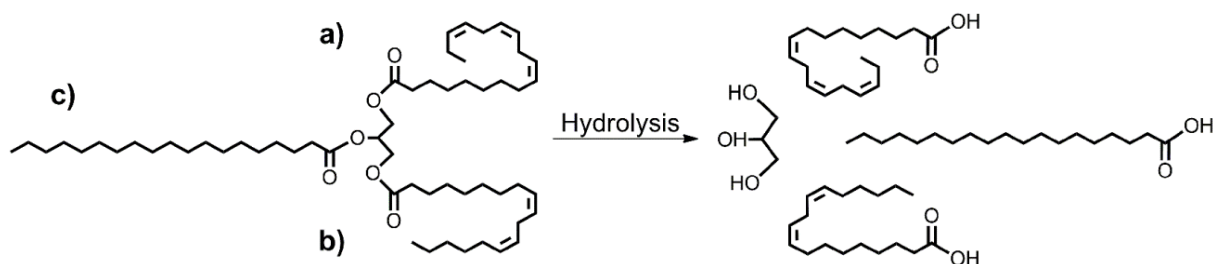
The results of this thesis will add a new insight into the factors influencing the photostability of chrome yellow pigments and, in addition to the published results noted, this thesis work will demonstrate that the manufacturing conditions and the final pigment formulation, which includes additives, as well as the binder, also play a key role in their tendency to degrade.

4.1.2. The oil paint system

In the last two decades, major breakthroughs in the study of the oil paint system have greatly expanded the understanding of its nature, its chemical formation and the degradation processes which occur. The contribution by Jaap J. Boon and his paintings research groups in the MOLART Programme (Molecular Aspects of Ageing in Art, 1995-2002) and the De Mayerne Programme (Molecular Studies in Conservation and Technical Studies in Art History, 2002-2006) initiated important advances in this field which have continued in the subsequent PAinT Project (Paint Alterations in Time, 2012-2016) led by Katrien Keune and Annelies van Loon (De Mayerne Programme, 2006; S4a-Paint, 2016).

¹⁰⁶ It was also not encountered in paintings by Amadeo de Souza-Cardoso (Chapter 3.5, p. 66).

Traditional oil paints were prepared with drying oils such as linseed, poppy and nut oil due to their ability to chemically dry to form hard films upon exposure to air (Carlyle, 2001; Van den Berg, 2002). A drying oil is a natural product mainly composed of poly-unsaturated triglyceride moieties (TAGs), i.e. esters of glycerol linked to three long-chain carboxylic acids (Scheme 4.1). The fatty acid portion of the drying oils generally used in oil paint is mostly composed of C18 polyunsaturated acids: oleic acid (C18:1¹⁰⁷), linoleic (C18:2) and linolenic (C18:3); and a small percentage of saturated fatty acids with 12–18 carbon atoms, e.g. palmitic (C16:0) and stearic (C18:0) (Lazzari & Chiantore, 1999; Van den Berg, 2002).



Scheme 4.1. Hydrolysis of a triglyceride composed of two unsaturated acids, (a) linolenic and (b) linoleic, and one saturated acid, (c) stearic, adapted from Solomons & Fryhle (2000) (Otero *et al.*, 2014).

Drying of the oil predominantly results from oxidative polymerisation via autoxidation and photoxidation reactions. The reactivity of the double bonds of the unsaturated fatty acids promotes the initiation of these reactions, Figure 4.2A (Meilunas *et al.*, 1990; Boon *et al.*, 1997; Mallégo *et al.*, 1999; Van den Berg, 2002; Van der Weerd *et al.*, 2005; Cotte *et al.*, 2006a). This process may be catalysed by the presence of metal ions from pigments and driers (e.g. lead oxide or acetate) (Osawa, 1988; Tumosa *et al.*, 2005), Figure 4.2B. The end result is a complex three-dimensional polyanionic network based on the glycerol ester with a crosslinked fraction of carboxylate anions stabilised by metal cations, Figure 4.2C (Boon *et al.*, 1997; Van den Berg, 2002; Van der Weerd *et al.*, 2005). The paint system has been characterised as capable of self-repair, preventing paint failure (Boon, 2006; Boon *et al.*, 2007). The diacids, such as azelaic acid (C9), contribute to the stabilisation of the network due to their chain building ability in three dimensions (Boon, 2006; Boon *et al.*, 2007).

The autoxidation reactions form hydroperoxides (R-O-OH) and radicals such as peroxy (ROO[•]) and alkoxy (RO[•]), especially in the presence of metal-ion catalysts, which are then free to promote further radical reactions (Boon *et al.*, 1997; Lazzari *et al.*, 1999; Van den Berg, 2002; Burnstock & Van den Berg, 2014). Simultaneous to these reactions, oxidative degradation of the triglyceride components takes place resulting in the formation of free low molecular weight molecules such as aldehydes, ketones, alcohols, carboxylic acids and hydrocarbons. Although some of these compounds evaporate, there is a fraction that remains in the oil matrix, susceptible to oxidation reactions (Boon *et al.*, 1997; Lazzari *et al.*, 1999; Van den Berg, 2002; Burnstock & Van den Berg, 2014).

A microkinetic model of the autoxidative curing of an oil-based paint system has been recently proposed by Oakley *et al.* based on the elementary steps for the cobalt-catalyzed autoxidative curing

¹⁰⁷ In the nomenclature C_n:_m, C stands for carbon, n corresponds to the number of carbon atoms in the chain and m refers to the number of double bonds (degree of unsaturation).

of an ethyl linoleate up to the formation of single cross-links. Promising results were obtained and a good correlation with the actual increase of the peroxide content and oxygen uptake was found, however, the formation of secondary products was not straightforward (Oalkey *et al.*, 2015).

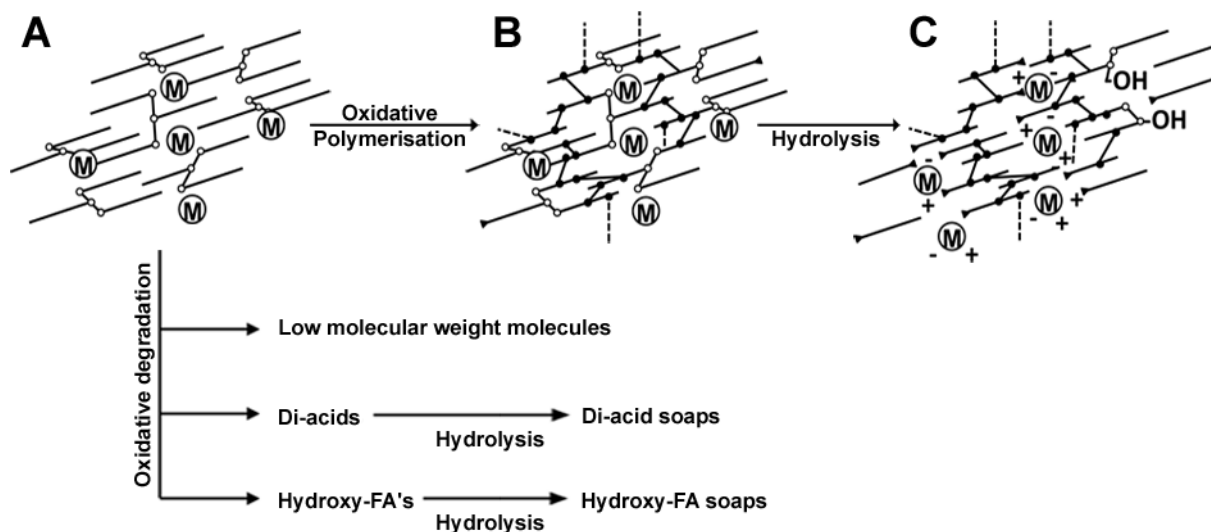


Figure 4.2. The oil paint model adapted from Boon *et al.* (1997) and Burnstock & Van den Berg (2014). **A**) ‘fresh oil’ paint in the presence of metal ions (M), **B**) polyanionic network (after curing), and **C**) after hydrolysis of the ester bond (after maturation).

Mono and dicarboxylic acids that are not incorporated in the polyanionic network may migrate to react with metal cations, leading to the formation of an increased proportion of metal carboxylates (metal soaps). In some cases, metal soaps form aggregates within the paint film. Their formation is still not fully understood, but it appears that aggregation depends on the paint composition (pigments, extenders and driers), the availability of free fatty acids, the build-up of the layers, the environmental conditions (temperature, relative humidity, etc.) and the conservation history of the painting (Robinet & Corbeil, 2003; Plater *et al.*, 2003; Van der Weerd *et al.*, 2005; Boon, 2006; Boon *et al.*, 2007; Keune & Boon, 2007; Cotte *et al.*, 2007 & 2017a; Spring *et al.*, 2008; Ferreira *et al.*, 2011; Keune *et al.*, 2014). The presence of metal soap aggregates in high proportions can negatively influence the appearance of oil paintings (Boon *et al.*, 2002; Noble *et al.*, 2005; Centeno & Mahon, 2009; Keune *et al.*, 2013; Osmond *et al.*, 2014).

The identification of metal soaps in oil paintings has been achieved mainly with the use of μ -FTIR and mass spectrometry (Robinet & Corbeil, 2003; Plater *et al.*, 2003; Van der Weerd *et al.*, 2005; Boon, 2006; Boon *et al.*, 2007; Keune & Boon, 2007; Cotte *et al.*, 2007 & 2017a; Spring *et al.*, 2008; Ferreira *et al.*, 2011) but the complementary analysis by μ -Raman has also proven its value (Otero *et al.*, 2014).

Recently, Hermans *et al.* have provided new insights into “the understanding of the structure of metal soaps and the polymerised oil network in various stages of oil paint ageing” (in Hermans, 2017, p. 143; Hermans *et al.*, 2015, 2016a, 2016b). They studied the transition from amorphous to crystalline fatty acid and/or metal soap by Differential Scanning Calorimetry (DSC) and Attenuated Total Reflection Fourier Transform Infrared Spectroscopy (ATR-FTIR) and concluded that this phenomenon is spontaneous and irreversible and occurs due to the low solubility of the metal soaps. They highlight

the fundamental role played by the oil paint's properties such as the presence of microscopic fractures in the paint, and environmental factors on the crystal nucleation and growth kinetics of the metal soap's crystallisation (Hermans *et al.*, 2016a). Furthermore, by means of ATR-FTIR and Small-Angle X-ray Scattering (SAXS) measurements they propose that an interaction between carboxylic species and the surface of the pigments occurs enabling the migration of the metal ions into the polymeric medium through the carboxylate groups. This leads to the formation of a metal carboxylate ionomeric polymer network similar to more classical ionomer system described in literature (Hermans *et al.*, 2016b). Banti *et al.* have also suggested that the nature of the ionomeric/polymeric network also plays a determining role in the development of the water sensitivity of modern oil paints (Banti *et al.*, 2018).

4.1.3. An overview of the presence of metal oxalates in artworks

Metal oxalates are chemically formed by reaction of oxalic acid (ethanedioic acid) with metal cations. The dissociation reactions and constants of oxalic acid are described as follows (Chang, 1994; Lide, 2006):



Metal oxalates are regularly encountered in artworks, especially in those exposed outdoor such as stone artifacts (Cariati *et al.*, 2000; Rampazzi *et al.*, 2004; Maravelaki-Kalaitzaki, 2005; Bordignon *et al.*, 2008) but they can also be found in polychrome objects. **Calcium** oxalates are the most commonly found in paintings (Salvadó *et al.*, 2002, 2009, 2013; Lluveras *et al.*, 2008; Van der Snickt *et al.*, 2011; Monico *et al.*, 2013c; Beltran *et al.*, 2015) but **copper** (Castro *et al.*, 2008; Nevin *et al.*, 2008; Cotte *et al.*, 2008; Švarcová *et al.*, 2009; Lluveras *et al.*, 2010; Salvadó *et al.*, 2013; Beltran *et al.*, 2015; Prati *et al.*, 2016), **lead** (Salvadó *et al.*, 2009), **zinc** (Miliani *et al.*, 2008; Poli *et al.*, 2014) and **cadmium** (Van der Snickt *et al.*, 2012; Mass *et al.*, 2013; Pouyet *et al.*, 2015) have also been detected.

Calcium oxalates have been identified in paintings in the dihydrate form ($\text{CaC}_2\text{O}_4 \cdot 2\text{H}_2\text{O}$, weddellite) (Salvadó *et al.*, 2002 & 2013; Lluveras *et al.*, 2008), in the monohydrated form ($\text{CaC}_2\text{O}_4 \cdot \text{H}_2\text{O}$, whewellite) (Beltran *et al.*, 2015; Sotiropoulou *et al.*, 2016) and together (Salvadó *et al.*, 2009; Van der Snickt *et al.*, 2011; Monico *et al.*, 2013c). The stability and phase transformation between weddellite and whewellite has been studied by Conti *et al.* and their results suggest that their structural stability is influenced by their "internal" water molecules and that weddellite is more stable in dry conditions. Furthermore, "external" water molecules influence their transformation and in the presence of humidity, weddellite converts to whewellite. The latter is considered to be the most stable in normal environmental conditions. However, other factors can hinder this transformation since weddellite is found in sites with significant moisture such as the surfaces of monuments (Conti *et al.*, 2010 & 2014).

The identification of these compounds is very straightforward by X-ray diffraction, FTIR and Raman spectroscopies. The use of synchrotron radiation based techniques enables higher spatial resolution and lower detection limits providing better insights into their presence and origin (Salvadó *et al.*, 2002, 2009 & 2013; Lluveras *et al.*, 2008 & 2010; Cotte *et al.*, 2008; Van der Snickt *et al.*, 2012; Mass *et al.*, 2013; Beltran *et al.*, 2015; Pouyet *et al.*, 2015). Nevertheless, the use of μ -FTIR mapping has allowed the identification of metal oxalates and contributed to a better understanding of their origin, distribution and formation pathways (Prati *et al.*, 2016; Sotiropoulou *et al.*, 2016 & 2018).

The use of in situ techniques is also of great value, particularly when monitoring and evaluating the conservation state of artworks, where oxalates are considered degradation products (Ricci *et al.*, 2006; Miliani *et al.*, 2008, 2010; Kahrim *et al.*, 2009; Van der Snickt *et al.*, 2011). In particular, Monico *et al.* have made available a comprehensive infrared spectral database of metal oxalates of calcium (II), magnesium (II), iron (II), iron (III), zinc (II), cadmium (II), sodium (II), copper (II), lead (II) and chromium (III) (Monico *et al.*, 2013c).

The formation of these compounds continues to be the subject of great discussion; the determining factor being the origin of the oxalic acid. It can be related to microbiological activity from which the oxalic acid results (Castro *et al.*, 2008; Švarcová *et al.*, 2009; Miliani *et al.*, 2010), it can result from the interaction with the environment (Salvadó *et al.*, 2013; Monico *et al.*, 2013c; Beltran *et al.*, 2015), and it can also derive from the oxidative degradation of organic materials, including all types of binders, waxes, resins and chiefly those introduced as surface coatings (Cariati *et al.*, 2000; Salvadó *et al.*, 2002 & 2009; Rampazzi *et al.*, 2004; Maravelaki-Kalaitzaki, 2005; Ricci *et al.*, 2006; Bordignon *et al.*, 2008; Lluveras *et al.*, 2008 & 2010; Kahrim *et al.*, 2009; Van der Snickt *et al.*, 2011 & 2012; Mass *et al.*, 2013; Poli *et al.*, 2014; Pouyet *et al.*, 2015).

The formation of oxalate films on carbonate surfaces by bacterial and fungal activity has been investigated and its role as either a degradative or possibly a protective “patina” is still subject of discussion (Bonaventura *et al.*, 1999; Sturm *et al.*, 2015). The efficiency of artificial oxalate protection treatments on marble has also been studied and optimized (Doherty *et al.*, 2007; Burgos-Cara *et al.*, 2017).

Few authors have investigated oxalate formation in artworks based on the oxidative degradation of organic materials and no mechanism pathways have been offered. Cariati *et al.* studied the oxidative degradation of different binders over a calcium carbonate substrate, which always led to the formation of calcium oxalate monohydrate and of calcium oxalate dihydrate in the case of irradiated H₂O₂ (Cariati *et al.*, 2000). More recently, Poli *et al.* have investigated the interaction of natural resins, shellac in particular, with pigments under different ageing conditions. They found that the most reactive pigments were zinc white (ZnO) and smalt (a cobalt potassium silicate glass) promptly forming resin acids carboxylates and oxalates (Poli *et al.*, 2014 & 2017). Zoppi *et al.* studied pigment reactivities in the presence of oxalic acid by Raman spectroscopy, concluding that calcite and verdigris are very reactive followed by azurite, malachite and lead white, and that ultramarine blue shows poor reactivity (Zoppi *et al.*, 2010). A relationship between the formation of metal oxalates and carboxylates has also been suggested by Salvadó *et al.* and further discussed by Prati *et al.* (Salvadó *et al.*, 2009; Prati *et al.*, 2016). Sotiropoulou *et al.* studied samples from ancient wall paintings to identify their original organic binder through the detection of its degradation compounds. They detected metal

carboxylates and oxalates at the interface of free fatty acids and pigment particles (Sotiropoulou *et al.*, 2016). In another study, Voras *et al.* by means of Time-of-Flight Secondary Ion Mass Spectrometry (ToF-SIMS) imaging suggested that oxalate ions may result from acid hydrolysis of the binding medium, due to the depletion of long-chain fatty acids where cadmium oxalates were also identified (Pouyet *et al.*, 2015; Voras *et al.*, 2015).

4.2. Photochemical study using lead chromate paint reconstructions

The photochemical study of the degradation of chrome yellow was carried out by irradiation of samples from historic lead chromate oil paint tubes (Chapter 3.4, p. 61) and paints prepared with oil¹⁰⁸ or PVAc binders with reconstructed pigments following W&N's manufacturing processes. The syntheses of the reconstructed pigments and the pH measurements throughout are detailed in Appendix V.2.1.1 (p. 233) and Appendix IX.1 (p. 287), respectively. The paint preparation is described in Appendix V.2.4.1 (p. 237).

As previously mentioned, the experimental sample set, Figure 4.3, was designed to contain paints mainly prepared with different pigment formulations expected to be more susceptible to degradation (Monico *et al.*, 2013b). The experimental sample set was composed of 6 oil paints: one was prepared with a lead chromate (monoclinic form) reference pigment; one with a reconstructed pigment based on pure lead chromate monoclinic phase (here designated as Middle¹⁰⁹); and another with a reconstructed pigment based on mixed crystals of lead chromate and lead sulfate (here designated as Lemon¹¹⁰). Included in the set of six were three lead chromate oil paints taken from historic oil paint tubes. For comparison, there were also 9 paints of reconstructed pigments with a PVAc binder. The full characterisation of the reconstructed pigments used is presented in Appendix X (p. 293) and of the historic oil paint tubes in Chapter 3.4 (p. 61) and Appendix XI (p. 311).

The irradiation experiment was carried out in a Xenon-light apparatus ($\lambda_{\text{irr}} > 300 \text{ nm}$; 800 W/m^2) as detailed in Appendix V.2.4.2 (p. 238), and monitored by Colourimetry, UV-Vis Fibre Optic Reflectance Spectroscopy (FORS), μ -Raman spectroscopy (μ -Raman), μ -Fourier Transform Infrared spectroscopy (μ -FTIR), X-Ray Diffraction (XRD) and Scanning Electron Microscopy with X-ray microanalysis (SEM-EDS). SR based techniques were also used, including μ -FTIR, μ -XRD, micro X-Ray Fluorescence spectrometry (μ -XRF) and micro X-ray Absorption Near-Edge Structure (Cr, S and Ca K-edge μ -XANES). The experimental conditions are described in Appendix V.3 (p. 239).

The oil paints prepared with the reconstructed pigments were irradiated for the longest period of time: 11000h (31643 MJ/m^2). The sample from W&N's oil paint tube labelled *Chrome Deep*, was irradiated for 10000h (28766 MJ/m^2) and the samples from the other historic oil paint tubes, W&N's

¹⁰⁸ The oil used was an untreated single seed source linseed oil, see Appendix V.2.4.1 (p. 237).

¹⁰⁹ The Middle pigment reconstruction was a variation of the L3a synthesis method where a lower quantity of lead nitrate was used resulting in a Middle pigment composed of pure lead chromate (and not a Lemon pigment with mixed crystals as expected). The L3a* synthesis method is described in p. 231.

¹¹⁰ The Lemon pigment reconstruction was a variation of the PR1b synthesis method where a lower quantity of sulfuric acid was used resulting in a Lemon pigment composed of mixed crystals of lead chromate and lead sulfate, the first being the dominant phase (monoclinic). The PR1b* synthesis method is described in p. 231.

Chrome Yellow and Lefranc's *Jaune de Chrome* were irradiated for 8500h (24451 MJ/m²). Samples from the oil paints were collected at different irradiation times (detailed in Appendix V.2.4.2, p. 238). Samples from the PVAc paints were removed at intervals of 1500h up to a total of 8500h (24451 MJ/m²) irradiation time. The oil paint with the lead chromate reference pigment was only irradiated for 1500h (4315 MJ/m²) since by this time it was determined to be more lightfast than the other oil paints.

The results obtained with complementary analyses will be discussed in detail below.

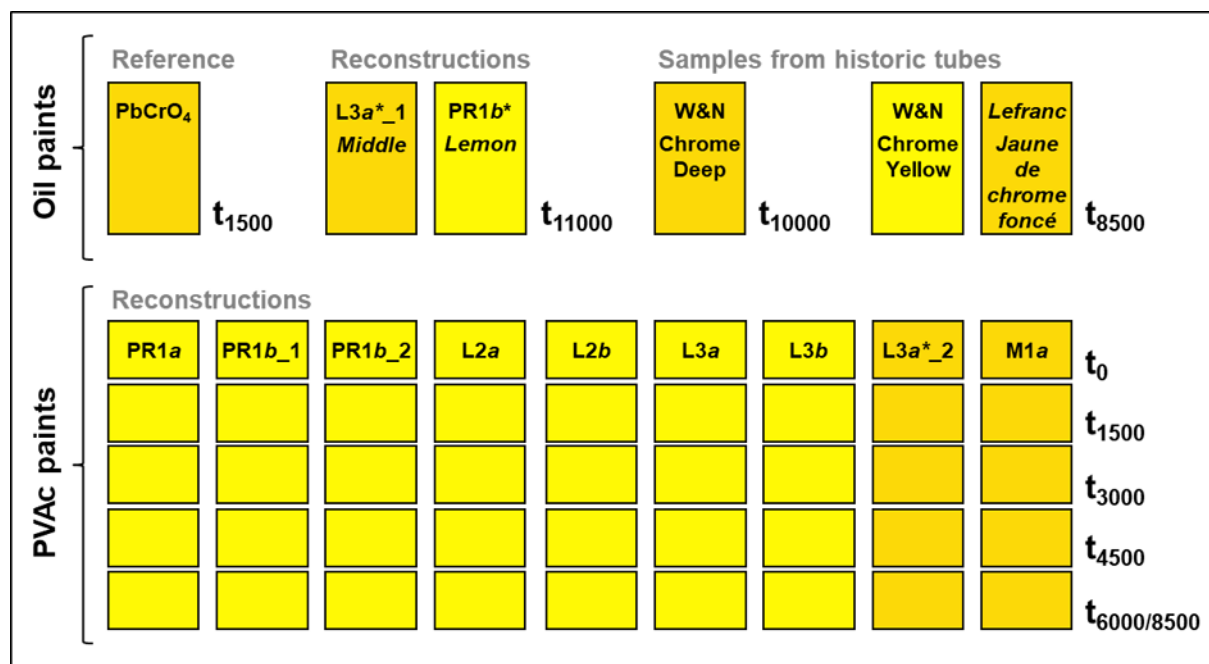


Figure 4.3. Experimental sample set for the irradiation experiment carried out under a Xenon lamp, $\lambda_{\text{irr}} > 300$ nm. The codes of the reconstructed pigments presented refer to variations in the manufacturing processes as described in Chapter 3.2 (p. 48), see also Appendix III (p. 205). The pigments composed of $\text{PbCr}_{1-x}\text{S}_x\text{O}_4$ with variable ratio of sulfate to chromate and pure PbCrO_4 monoclinic phase are highlighted in yellow and orange, respectively.

4.2.1. A multi-analytical approach













The first evidence for pigment degradation appears as a variation in colour. The $L^*a^*b^*$ colour coordinates throughout the irradiation time and the ΔE^* observed for the oil and PVAc paints are presented in Table 4.1 and 4.2, respectively. Colourimetric values for all irradiation times are shown in Appendix XVI (p. 349). There is a general decrease of L^* (lightness) and b^* (yellow/blue component).

For both sets of paints, the greatest changes in ΔE^* are observed for the reconstructed pigment formulation made of pure monoclinic lead chromate admixed with two extenders (chalk, CaCO_3 and gypsum, $\text{CaSO}_4 \cdot 2\text{H}_2\text{O}$), coded L3a^*_1 (Middle oil paint) and L3a^*_2 (Middle PVAc paint). This was unexpected considering the work by Monico *et al.* (2013b) but is in agreement with the results presented by Amat *et al.* (2016) and Muñoz-García *et al.* (2016).

For the set of oil paints, Table 4.1, the reference sample of pure monoclinic lead chromate was the most lightfast at the lowest irradiation time (1500h). At higher irradiation times, the historic oil paint tube (W&N's *Chrome Deep*) composed of pure monoclinic lead chromate and chalk showed the least

colour change. Unfortunately, the sample from the tube of Lefranc's *Jaune de Chrome*, also composed of pure monoclinic lead chromate was very small and therefore it was not possible to collect colourimetric measurements. However, it is important to note that this sample was aged in ambient conditions for 6 years and already showed signs of degradation (a change to brownish hue) prior to the irradiation experiment. W&N's *Chrome Yellow* and *Lemon* oil paints, composed of mixed crystals of lead chromate and lead sulphate with a SO_4^{2-} molar fraction of 0.4, showed a greater decrease in a^* , which may be related to the appearance of a green degradation product such as Cr_2O_3 (Newman, 1997).

Table 4.1. Oil paints before and after irradiation with a Xenon lamp ($\lambda_{\text{irr}} > 300 \text{ nm}$): pigment formulation, $L^*a^*b^*$ colour coordinates and ΔE^* .

Pigment code & formulation [§]	$t_{\text{irr}} / \text{h}$	L^*	a^*	b^*	ΔE^*
PbCrO₄	 0	63.9 ± 0.4	18.2 ± 0.1	67.6 ± 0.6	
	 1500	60.2 ± 0.2	17.9 ± 0.1	59.5 ± 0.2	8.9
W&N CD oil paint	0	70.7 ± 0.04	22.3 ± 0.1	78.1 ± 0.03	
PbCrO ₄ (50%)	 1500	65.2 ± 0.1	18.9 ± 0.02	67.03 ± 0.1	12.8
CaCO ₃ (50%)	 3000	64.2 ± 0.1	18.4 ± 0.02	63.9 ± 0.1	16.1
MgCO ₃ .xH ₂ O [¶]	10000	63.1 ± 0.2	17.7 ± 0.1	62.0 ± 0.2	17.6
W&N CY oil paint	0	77.2 ± 0.04	13.4 ± 0.24	78.5 ± 0.1	
PbCr _{0.6} S _{0.4} O ₄ (80%)	 1500	66.5 ± 0.1	7.7 ± 0.03	57.3 ± 0.03	24.4
BaSO ₄ (20%), MgCO ₃ .xH ₂ O [¶]	 3000	65.6 ± 0.3	6.7 ± 0.04	56.3 ± 0.6	25.9
Zinc linoleate	8500	64.7 ± 0.1	4.4 ± 0.05	56.9 ± 0.04	26.6
Lemon	0	70.1 ± 0.04	17.7 ± 0.07	82.5 ± 0.07	
PR1b*	 1500	59.9 ± 0.2	7.2 ± 0.2	56.9 ± 0.4	29.5
PbCr _{0.6} S _{0.4} O ₄	 3000	57.9 ± 0.2	5.8 ± 0.3	54.9 ± 0.9	32.4
	 7750	54.9 ± 0.04	3.9 ± 0.02	47.2 ± 0.4	40.8
	11000	54.3 ± 0.1	2.8 ± 0.02	46.4 ± 0.1	42.1
Middle	0	64.8 ± 0.1	24.9 ± 0.05	73.4 ± 0.2	
L3a*_1	 1500	48.1 ± 0.1	14.3 ± 0.1	39.9 ± 0.2	38.9
PbCrO ₄ (15%)	 3000	46.6 ± 0.2	13.8 ± 0.1	38.2 ± 0.4	41.1
CaCO ₃ (54%)	 7750	44.7 ± 0.1	11.1 ± 0.05	31.7 ± 0.2	48.2
CaSO ₄ .2H ₂ O (31%)	11000	43.2 ± 0.2	11.7 ± 0.04	34.6 ± 0.04	46.3

[§] Characterisation of the reconstructed pigments following original W&N recipes, and of the historic oil paint tubes may be consulted in Appendix X (p. 293) and XI (p. 311), respectively. As mentioned, the semi-quantification of the compounds was obtained by XRD. The molar fractions of $\text{PbCr}_{1-x}\text{S}_x\text{O}_4$ are approximate values resulting from comparison of the infrared spectrum and diffraction pattern of the pigments with the reference set of $\text{PbCr}_{1-x}\text{S}_x\text{O}_4$ synthesised in the laboratory (see Appendix VIII, p. 275 and Appendix X, p. 293).

[¶] $\text{MgCO}_3 \cdot x\text{H}_2\text{O}$ was not accounted for in the XRD semi-quantification because it was not detected by this technique.

^{||} Zinc linoleate was only detected by μ -FTIR, see Figure VI.4.7 (p. 262).

As may be seen in Table 4.2, the set of PVAc paints showed a general decrease in lightfastness as the ratio of sulfate to chromate increases in the $\text{PbCr}_{1-x}\text{S}_x\text{O}_4$, regardless of the presence of the extenders used, which is in line with the results by Monico *et al.* (2013b). However, exceptions are found, not only for the above mentioned L3a*_2 Middle paint, but it is also interesting to note that paints with very similar pigment composition such as PR1b_2, PR1b_1 and L2b, $\text{PbCr}_{0.5}\text{S}_{0.5}\text{O}_4$, present very different colour variations after irradiation, the first being the most lightfast of the set and the other two belonging to the group of paints most light-sensitive.

By means of μ -XANES at the Cr K-edge, this thesis work offers for the first time a Light Susceptibility Index (LSI) based on the ratio of the Cr K pre-edge intensity after/before irradiation, which decreases as a function of irradiation time, as the quantity of Cr^{3+} degradation species increases. This will be fully described in Chapter 4.2.1.1.

As mentioned above, all samples were analysed by FORS, μ -Raman and μ -FTIR. XRD and SEM-EDS were only carried out on cross-sections¹¹¹ of the oil paints before and after selected irradiation times. In order to gain spatially resolved evidence of photodegradation intermediates and final products, the paints that revealed the highest colour change were further studied by SR μ -XRF and μ -FTIR. It was only possible to perform SR μ -XRD on the most aged oil paints. To identify the presence of Cr^{3+} species, μ -XANES spectra at the Cr K-edge were collected on all paint samples. Furthermore, S K-edge μ -XANES measurements were also acquired on the samples containing sulfur species and Ca K-edge μ -XANES analysis was performed on the Middle oil paint (L3a*_1) irradiated for 11000h. XANES spectra of reference compounds were also obtained and may be consulted in Appendix VI.5. (p. 267). In order to combine all available SR based techniques, the preparation of embedding-free thin cross-sections was tested following the “sample enclosing system” (SES) developed by Pouyet *et al.* (2014)¹¹². Details on the methodology may be found in Appendix V.2.6. (p. 238).

The set that showed the most relevant molecular changes throughout the irradiation experiment was that of the oil paints. The results obtained through the multi-analytical approach are fully described for each oil paint¹¹³ in Chapters 4.2.1.2 and 4.2.1.3. For the PVAc paints it was not possible to detect significant molecular changes¹¹⁴. The FORS, μ -FTIR and Cr K-edge μ -XANES spectra of all PVAc paints before and after 8500h of irradiation are shown in Appendix XVII (p. 353). μ -Raman only detected the pigment and additives spectral fingerprint, see Appendix X, p. 293. The SR μ -XRF and μ -FTIR maps of PR1a PVAc paint after 5250h of irradiation are shown as examples in Appendix XVIII (p. 359).

















¹¹¹ The preparation of the resin-embedded cross-sections is described in Appendix V.2.5. (p. 238).

¹¹² To perform SR μ -FTIR analysis in transmission mode, the embedding-free thin cross-sections were mounted horizontally on a BaF_2 window or between two BaF_2 windows.

¹¹³ With the exception of the oil paint prepared with the reference of monoclinic lead chromate, which as noted was the most lightfast of the set; its FORS and μ -FTIR spectra before and after irradiation may be consulted in Figure XIX.1 and the Cr K-edge μ -XANES spectra in Figure XIX.2 (p. 361).

¹¹⁴ Unfortunately, it was not possible to obtain good embedding-free thin cross-sections of the PVAc paints. This was most probably due to the original low thickness of the paints ($\approx 50 \mu\text{m}$).

Table 4.2. PVAc paints before and after irradiation with a Xenon lamp ($\lambda_{\text{irr}} > 300 \text{ nm}$): pigment formulation, $L^*a^*b^*$ colour coordinates and ΔE^* .

Pigment code & formulation [§]		$t_{\text{irr}} / \text{h}$	L^*	a^*	b^*	ΔE^*
PR1b_2 PbCr _{0.5} S _{0.5} O ₄		0	80.5 ± 0.02	2.4 ± 0.1	83.8 ± 0.2	
		8500	73.9 ± 0.05	2.7 ± 0.05	71.1 ± 0.1	14.4
M1a PbCrO ₄ (30%) CaCO ₃ (40%) PbCO ₃ (30%)		0	79.2 ± 0.03	20.2 ± 0.1	88.3 ± 0.04	
		8500	70.6 ± 0.06	17.7 ± 0.05	74.4 ± 0.03	16.6
L3a PbCr _{0.8} S _{0.2} O ₄ (20%) CaSO ₄ ·2H ₂ O (45%) PbCO ₃ (35%)		0	80.3 ± 0.1	14.5 ± 0.1	88.1 ± 0.1	
		8500	70.6 ± 0.01	12.7 ± 0.03	70.5 ± 0.02	20.2
L3b PbCr _{0.8} S _{0.2} O ₄ (40%) PbCO ₃ (60%)		0	79.8 ± 0.4	15.2 ± 0.6	88 ± 0.1	
		8500	69.6 ± 0.2	13 ± 0.03	69.6 ± 0.05	21.1
PR1b_1 PbCr _{0.5} S _{0.5} O ₄		0	83 ± 0.1	6.4 ± 0.03	91.2 ± 0.1	
		8500	71.5 ± 0.04	4 ± 0.1	70.2 ± 0.2	24.0
PR1a PbCr _{0.3} S _{0.7} O ₄		0	84.5 ± 0.05	0.3 ± 0.01	84.6 ± 0.1	
		8500	72.2 ± 0.01	-2.5 ± 0.1	61.5 ± 0.2	26.2
L2a PbCr _{0.6} S _{0.4} O ₄ (50%) BaSO ₄ (50%)		0	80.8 ± 0.05	9.2 ± 0.02	89.6 ± 0.1	
		8500	66.4 ± 0.05	7 ± 0.04	65.3 ± 0.1	28.4
L2b PbCr _{0.5} S _{0.5} O ₄		0	81.6 ± 0.04	13 ± 0.1	89.6 ± 0.1	
		8500	68.3 ± 0.03	9.6 ± 0.04	63.4 ± 0.02	29.5
L3a*_2 (Middle) PbCrO ₄ (34%) CaCO ₃ (54%) CaSO ₄ ·2H ₂ O (12%)		0	74.4 ± 0.04	25.6 ± 0.1	82.1 ± 0.04	
		8500	52.1 ± 0.1	16.6 ± 0.02	43.1 ± 0.03	45.8

[§] Characterisation of the reconstructed pigments following original W&N recipes, and of the historic oil paint tubes may be consulted in Appendix X (p. 293) and XI (p. 307), respectively. As mentioned, the semi-quantification of the compounds was obtained by XRD. The molar fractions of PbCr_{1-x}S_xO₄ are approximate values resulting from comparison of the infrared spectrum and diffraction pattern of the pigments with the reference set of PbCr_{1-x}S_xO₄ synthesised in the laboratory (see Appendix VIII, p. 275 and Appendix X, p. 293).

4.2.1.1. Development of a Light Susceptibility Index using μ -XANES

As previously mentioned, Monico *et al.* established that the degradation of chrome yellow pigments results from the reduction of the original Cr^{6+} to Cr^{3+} with the formation of Cr^{3+} species such as the green Cr_2O_3 , Cr^{3+} sulfates and/or organo compounds (Monico *et al.*, 2011a & 2011b). μ -XANES acquired at the Cr K-edge clearly distinguish between Cr^{6+} and Cr^{3+} compounds, Figure 4.1 (p. 88). The reduction of Cr^{6+} to Cr^{3+} is detected by μ -XANES due to the intensity decrease of Cr^{6+} well-defined pre-edge peak around 5.993 keV and a shift of the absorption edge to lower energies (Zanella *et al.*, 2011; Monico *et al.*, 2011a & 2011b), Figure 4.4. Cr K-edge μ -XANES spectra were acquired at 5 to 10 different points on surface sections at selected irradiation times for all paint formulations under study (Figure 4.3). The treatment of these spectra is described in Appendix V.3 (p. 239). The intensity values of the Cr K pre-edge peak at 5.993 keV for all irradiation times studied for each sample are presented in Appendix XVI (p. 349).

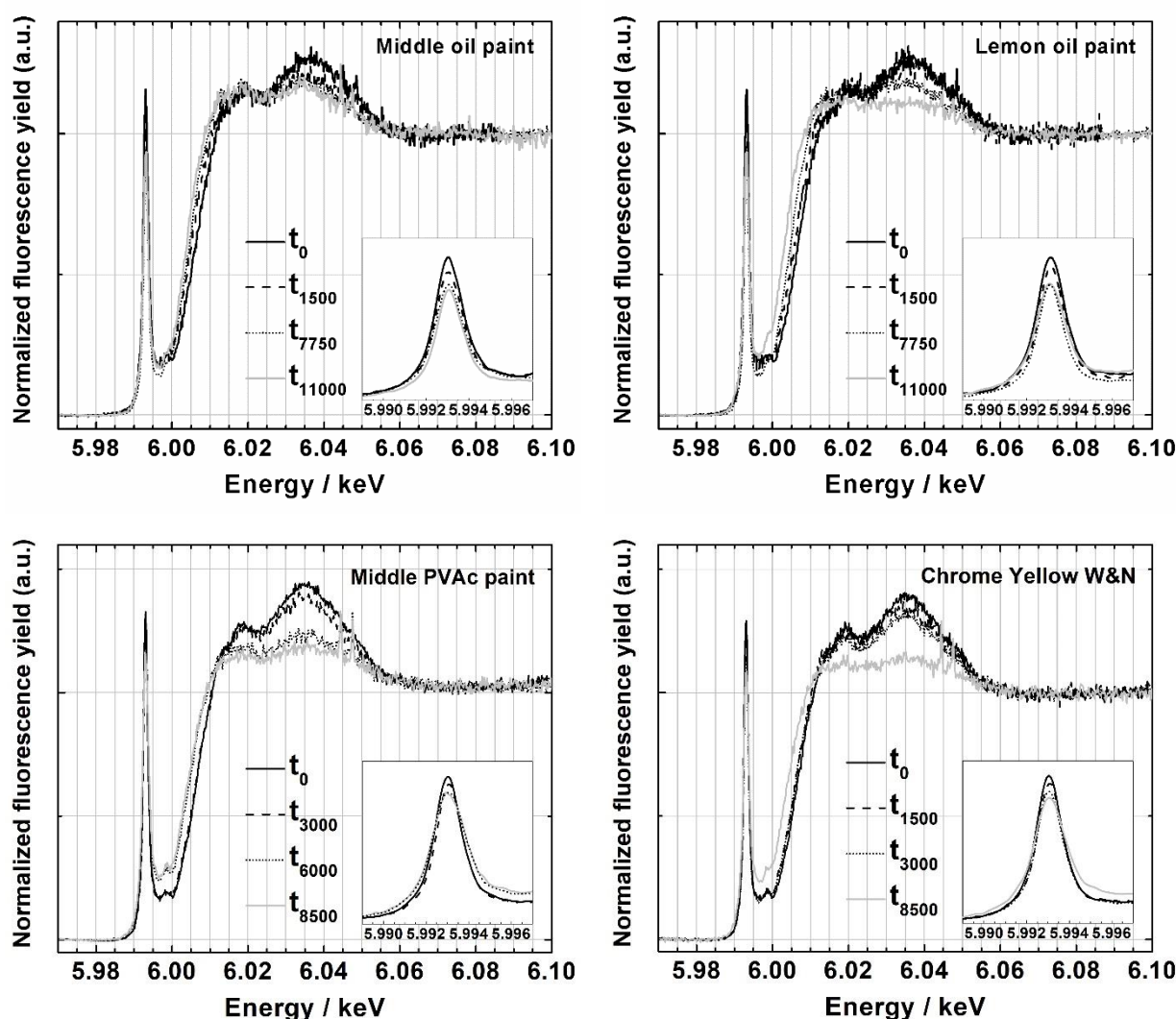


Figure 4.4. Normalized Cr K-edge μ -XANES spectra of the Middle, Lemon and the historic W&N *Chrome Yellow* oil paints and Middle (L3a*_2) PVAc paint before and after irradiation with a Xenon lamp ($\lambda_{\text{irr}} > 300$ nm).

The plot of the ratio of Cr K pre-edge intensity after/before irradiation of the oil and PVAc paints throughout irradiation time is shown in Figure 4.5 and 4.6, respectively. This ratio reports the rate of Cr³⁺ that is being formed from Cr⁶⁺. This data led to the development of a Light Susceptibility Index (LSI) which relates to the photostability of the different paint formulations. The LSI values given by the slope of the regression lines, for both the set of oil and PVAc paints are in agreement with the colour variations observed, as may be seen in Table 4.3 and 4.4, respectively. However, it is relevant to add that colour variation may not result solely from the formation of Cr³⁺ compounds and the presence of additional degradation products will most certainly influence it.

Higher degradation rates are observed for the oil paints. The linear regression model between the ratio of Cr K pre-edge intensity after/before irradiation plotted against time was only established for the first 3000h in the case of the oil paints. These samples present higher LSI values, whereas for the PVAc paints it was possible to fit the model for longer irradiation times. This most likely occurred because the oil binder degrades in the conditions of irradiation, resulting in the formation of more reactive compounds such as carboxylic acids, which, as will be explained below, play a determinant role in the degradation mechanisms. In contrast, PVAc binder has proven to be very stable when irradiated at $\lambda \geq 300$ nm and no degradation compounds have been detected (Ferreira *et al.*, 2010). This explains why no significant molecular changes were detected by μ -FTIR in the PVAc paints after irradiation, see Appendix XVII (p. 353). However, in the most degraded PVAc paints (see Figures XVIII.2 and XVIII.3, p. 359-360), the higher spatial resolution and lower detection limits of SR μ -FTIR allowed the identification of molecular changes in the C-H stretching bands profile (3000-2900 cm⁻¹) and an increase/broadening of the C=O stretching band at 1738 cm⁻¹ to lower wavenumbers, which suggests the formation of other compounds such as acids. Acetic acid is a known photodegradation product resulting from chain scission and crosslinking of PVAc binder (Ferreira *et al.*, 2010; Wei *et al.*, 2012). Furthermore, different degradation rates were obtained for the different chrome yellow pigment formulations, which suggest distinctive interactions with the PVAc binder.

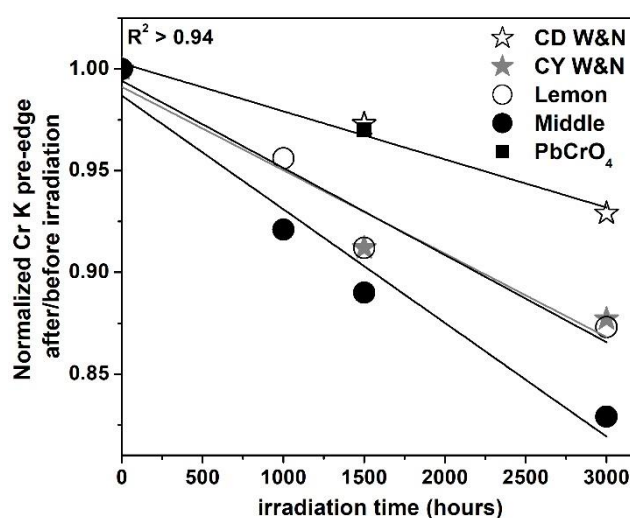


Figure 4.5. Normalized Cr K pre-edge intensity before and after irradiation of the oil paint samples: historic W&N oil paint tubes, *Chrome Deep* (☆) and *Chrome Yellow* (★); Lemon (○) and Middle (●) oil paint reconstructions; and lead chromate reference oil paint (■) (see Table 4.3).

Figure 4.5 and Table 4.3 show three degrees of photostability for the lead chromate oil paint formulations studied: 1) LSI \approx 2 for pure monoclinic lead chromate, PbCrO_4 ; 2) LSI \approx 4 for mixed crystals of monoclinic lead chromate and lead sulfate, $\text{PbCr}_{0.6}\text{S}_{0.4}\text{O}_4$; and 3) LSI \approx 6 for pure monoclinic lead chromate, PbCrO_4 , admixed with two extenders, CaCO_3 and $\text{CaSO}_4 \cdot 2\text{H}_2\text{O}$, here designated as the Middle oil paint reconstruction. Most importantly, it was possible to successfully relate the photodegradation behaviour of the Lemon oil paint reconstruction with the historic W&N *Chrome Yellow* oil paint, both composed of $\text{PbCr}_{0.6}\text{S}_{0.4}\text{O}_4$. They display similar ratios throughout irradiation time, which result in very close LSI values. Additionally, the ratios for the monoclinic lead chromate reference and the historic W&N *Chrome Deep* oil paints are also very similar after 1500h of irradiation (representative Cr K-edge μ -XANES spectra in Figure XIX.2, p. 361).

Table 4.3. Historic W&N oil paint tubes and lead chromate oil paint reconstructions: total colour variation (ΔE^*) and Light Susceptibility Index (LSI).

Paint label	Pigment Composition	ΔE^* (t_{3000h})	LSI ($\times 10^{-5}$)
W&N oil paint <i>Chrome Deep</i>	PbCrO_4 (50%) CaCO_3 (50%) $\text{MgCO}_3 \cdot x\text{H}_2\text{O}$	16.1	2.4
W&N oil paint <i>Chrome Yellow</i>	$\text{PbCr}_{0.6}\text{S}_{0.4}\text{O}_4$ (80%) BaSO_4 (20%) $\text{MgCO}_3 \cdot x\text{H}_2\text{O}$ Zinc linoleate	25.9	4.1
Lemon (PR1b*)	$\text{PbCr}_{0.6}\text{S}_{0.4}\text{O}_4$	32.4	4.3
Middle (L3a*_1)	PbCrO_4 (15%) CaCO_3 (54%) $\text{CaSO}_4 \cdot 2\text{H}_2\text{O}$ (31%)	41.1	5.6

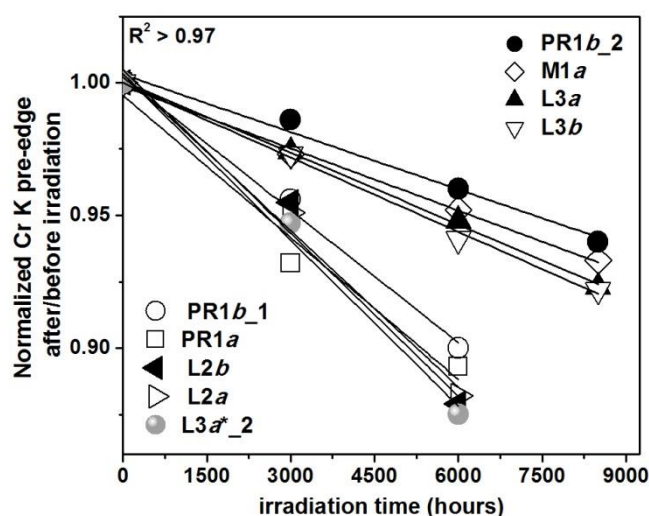


Figure 4.6. Normalized Cr K pre-edge intensity before and after irradiation of the PVAc paint samples (see Table 4.4).

Overall, the degradation trends found for the PVAc paint set follow those of the oil paint set. In Figure 4.6 and Table 4.4 it is possible to identify two degrees of photostability for the lead chromate PVAc paint formulations: 1) LSI \approx 1 for pigments composed of $\text{PbCr}_{x-1}\text{S}_x\text{O}_4$ with $0 \leq x \leq 0.2$, and 2) LSI \approx 2 for pigments composed of $\text{PbCr}_{x-1}\text{S}_x\text{O}_4$ with $x \geq 0.4$; also found in this group is the L3a*_2 paint composed of pure monoclinic lead chromate, PbCrO_4 , admixed with CaCO_3 and $\text{CaSO}_4 \cdot 2\text{H}_2\text{O}$, with a LSI of 2.1, being the most light-sensitive of the PVAc paint set. Considering what was observed for the oil paint set, an even higher LSI value for the latter formulation was expected, however, the results may be explained not only by the lower reactivity of the PVAc binder but also by the lower quantity of extenders present in the pigment used in this paint: L3a*_2 contains 66% extenders whereas L3a*_1 is composed of 85% of extenders. The degradation pathway of this particular formulation is related to the presence of these extenders and will be further explained below in Chapter 4.2.1.2.1.

Table 4.4. PVAc paint set prepared with lead chromate pigment reconstructions: total colour variation (ΔE^*) and Light Susceptibility Index (LSI).

Paint label	Pigment Composition	ΔE^* (t_{6000h})	LSI ($\times 10^{-5}$)
PR1b_2	$\text{PbCr}_{0.5}\text{S}_{0.5}\text{O}_4$	12.6	0.7
M1a	PbCrO_4 (30%) CaCO_3 (40%) PbCO_3 (30%)	15.0	0.8
L3a	$\text{PbCr}_{0.8}\text{S}_{0.2}\text{O}_4$ (20%) $\text{CaSO}_4 \cdot 2\text{H}_2\text{O}$ (45%) PbCO_3 (35%)	18.1	0.9
L3b	$\text{PbCr}_{0.8}\text{S}_{0.2}\text{O}_4$ (40%) PbCO_3 (60%)	19.3	0.9
PR1b_1	$\text{PbCr}_{0.5}\text{S}_{0.5}\text{O}_4$	21.8	1.7
PR1a	$\text{PbCr}_{0.3}\text{S}_{0.7}\text{O}_4$	24.5	1.8
L2b	$\text{PbCr}_{0.5}\text{S}_{0.5}\text{O}_4$	25.8	2
L2a	$\text{PbCr}_{0.6}\text{S}_{0.4}\text{O}_4$ (50%) BaSO_4 (50%)	26.5	2
L3a*_2 (Middle)	PbCrO_4 (34%) CaCO_3 (54%) $\text{CaSO}_4 \cdot 2\text{H}_2\text{O}$ (12%)	42.1	2.1

An interesting exception is found for the PR1b_2 PVAc paint formulation, which is composed of $\text{PbCr}_{0.5}\text{S}_{0.5}\text{O}_4$ and it is the most lightfast of this set with a LSI of 0.7. The other formulations with the

same relative composition, PR1*b*_1 and L2*b*, present higher values for the LSI as expected. This indicates that in addition to the importance of the lead chromate pigment's crystalline structure when sulfate ions are present (Monico *et al.*, 2013b), the manufacturing processes also play a determining role in the photostability of these pigments. As explained in Chapter 3 (p. 41), the pigments coded PR correspond to a Primrose process, in which lead nitrate was added to a solution of chromate ions buffered with sodium carbonate and acidified with sulfuric acid. For the L2*b* process, lead nitrate was added to a solution of chromate and sulfate ions in a carbonate buffering system, which was immediately acidified with sulfuric acid. As previously noted, when working with the pair $\text{Pb}(\text{NO}_3)_2/\text{H}_2\text{SO}_4$ it is more difficult to control the pH, a key factor that influences the morphology of the lead chromate particles (Liang *et al.*, 2005). As shown in Figure 4.7, the pigments PR1*b*_2, PR1*b*_1 and L2*b* present different lead chromate rod-like particles. Those of PR1*b*_2 appear longer and thinner, more similar to lead chromate rod-like particles obtain at neutral pH (Figure 3.8, p. 59); a small percentage of globular-like particles are also detected, most likely from orthorhombic structures (Xiang *et al.*, 2004; Monico *et al.*, 2013a). This probably resulted from the pH at which the precipitation started, and not necessary to the final pH, before filtration, that was acidic for all syntheses. The PR1*b*_2 synthesis was the only one where the $\text{PbCr}_{x-1}\text{S}_x\text{O}_4$ crystals started to precipitate at acidic conditions, which is considered to be the most effective conditions for their formation.

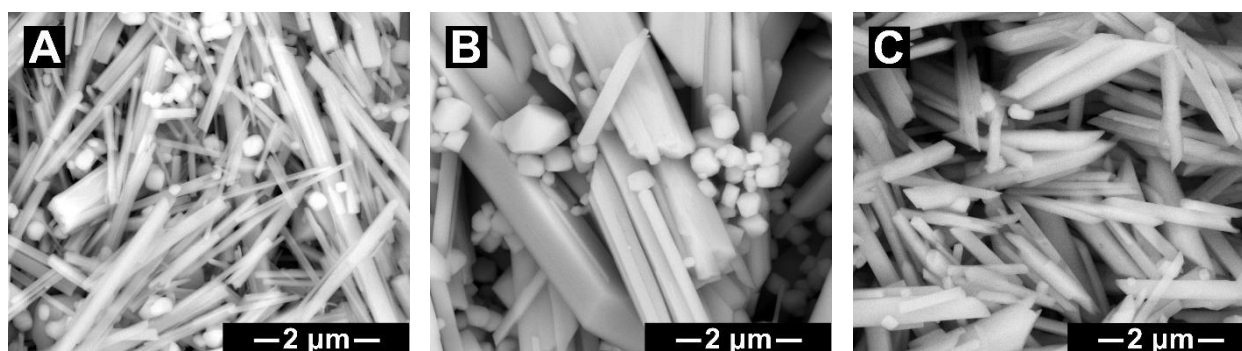


Figure 4.7. SEM images of the lead chromate pigment reconstructions composed of $\text{PbCr}_{0.5}\text{S}_{0.5}\text{O}_4$; **A)** PR1*b*_2, **B)** PR1*b*_1 and **C)** L2*b*.

In general, the Light Susceptibility Index developed shows a decrease in photostability when the lead chromate monoclinic phase saturates in the structure of the mixed crystals, i. e., when the SO_4^{2-} molar fraction $\geq 0.4/0.5$ (see Appendix VIII, p 275). This is in agreement with the results by Monico *et al.* (2013b) that correlate this lower photostability to the higher solubility¹¹⁵ of the $\text{PbCr}_{x-1}\text{S}_x\text{O}_4$ crystals, which enables more chromate ions to be available for redox reactions with the binder and/or other additives present. The work carried out for this research demonstrates that the manufacturing conditions of the $\text{PbCr}_{x-1}\text{S}_x\text{O}_4$ crystals also play a key role in their formation, which most likely influences their solubility. In addition, this work confirms the findings by Monico *et al.*, that pigments composed of pure monoclinic lead chromate are the most lightfast (Monico *et al.*, 2013b), except when in presence of a high content of CaCO_3 and $\text{CaSO}_4 \cdot 2\text{H}_2\text{O}$. As the current research results show,

¹¹⁵ The solubility of lead sulfate ($K_{\text{sp}} = 2.53 \times 10^{-8}$) is greater than lead chromate ($K_{\text{sp}} = 1.8 \times 10^{-14}$) (Lide, 2006).

different degradation pathways must be considered for each pigment formulation, including the lead chromate crystal structure and the presence of extenders.

4.2.1.2. The lead chromate oil paint reconstructions

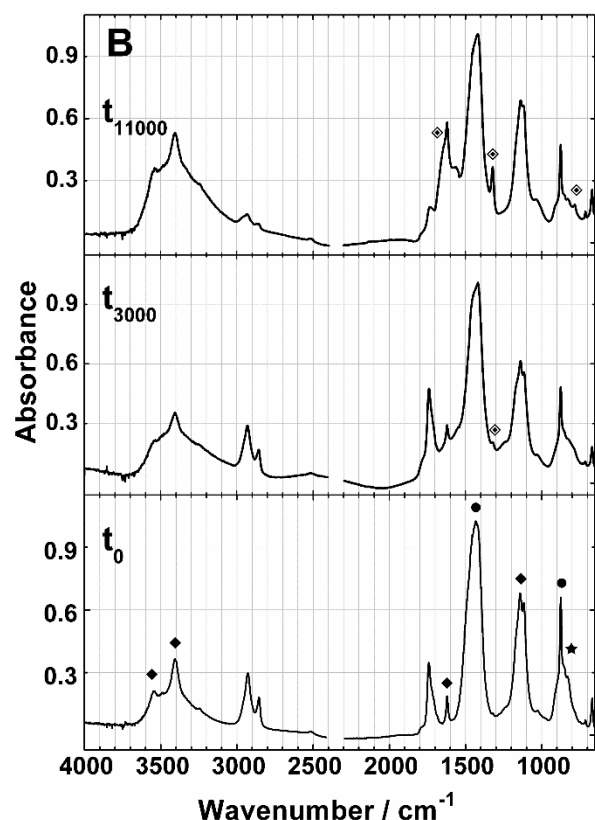
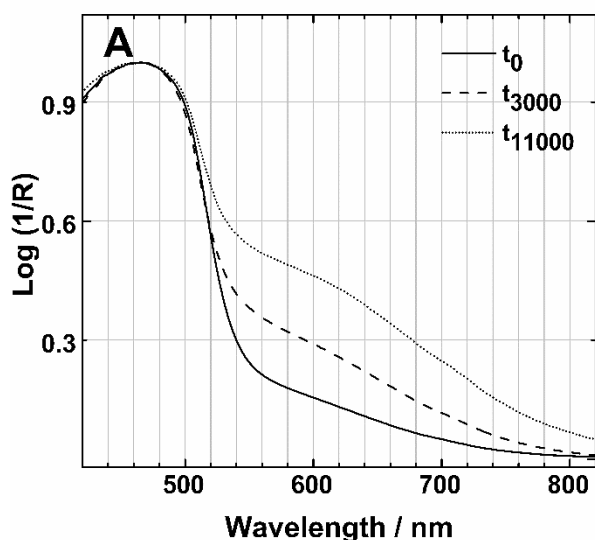


Figure 4.8. A) Normalized FORS and B) infrared spectra of the Middle oil paint before and after irradiation with a Xenon lamp ($\lambda_{\text{irr}} > 300$ nm); (★) PbCrO_4 , (●) CaCO_3 , (◆) $\text{CaSO}_4 \cdot 2\text{H}_2\text{O}$ and (◇) $\text{CaC}_2\text{O}_4 \cdot x\text{H}_2\text{O}$.

As previously mentioned, the oil paint reconstructions were prepared with selected lead chromate pigment formulations following W&N's recipes and untreated linseed oil. They were applied onto glass slides with a palette knife and air-dried in ambient conditions for two and a half years before being irradiated ($\lambda_{\text{irr}} > 300$ nm) (Appendix V.2.4, p. 237). The photodegradation experiment was followed by a multi-analytical approach and the results obtained are fully described below.

4.2.1.2.1. The Middle oil paint

As noted, the Middle oil paint composed of pure monoclinic lead chromate, PbCrO_4 , admixed with chalk (CaCO_3) and gypsum ($\text{CaSO}_4 \cdot 2\text{H}_2\text{O}$) (15, 54 and 31%, respectively), was the formulation where the highest change in colour was observed, Table 4.1 (p. 97), presenting the highest LSI value, Figure 4.5 (p. 101) and Table 4.3 (p. 102). FORS and infrared spectra before and after irradiation of the Middle oil paint¹¹⁶ are shown in Figure 4.8. The degradation leads to the formation of a shoulder with a maximum around 600 nm, which relates to the appearance of a blue component. The infrared spectra shows that the pigment to oil ratio changes throughout the irradiation time. An increase and broadening of the C=O stretching band at 1741 cm^{-1} assigned to the

¹¹⁶ The full characterisation of the pigment used in the Middle oil paint is presented in p. 303.

ester bond of the oil is observed, together with a small deviation to lower wavenumbers, which indicates an increase in the carboxylic acid content (Van der Weerd *et al.*, 2005). After 3000h of irradiation, a band around 1320 cm^{-1} started to appear, assigned to the COO^- symmetric stretching of calcium oxalate¹¹⁷, whose presence became more straightforward to identify after 7750h of irradiation, due to the appearance of its COO^- asymmetric stretching band around $1650\text{-}1620\text{ cm}^{-1}$ and COO^- bending band at 782 cm^{-1} . However, a clear identification of the type of calcium oxalate, whewellite ($\text{CaC}_2\text{O}_4\cdot\text{H}_2\text{O}$) or weddellite ($\text{CaC}_2\text{O}_4\cdot 2\text{H}_2\text{O}$), was not possible due to the overlapping of the COO^- symmetric stretching band and the bending mode of water at 1621 cm^{-1} , characteristic of gypsum. After 7750h of irradiation it was possible to detect the additional presence of anhydrous calcium sulfate (CaSO_4 , $K_{\text{sp}} = 4.93 \times 10^{-5}$; Lide, 2006) near a gypsum aggregate due to the appearance of its SO_4^{2-} symmetric stretching band at 1016 cm^{-1} , together with the unaltered Raman fingerprint of monoclinic lead chromate described in p. 57, Figure 4.9. Anhydrous calcium sulfate was not identified by infrared spectroscopy. No further changes were found, which includes an analysis with XRD, performed on a sample after 7750h of irradiation. This XRD analysis matched the pigment's diffraction pattern shown in Figure X.2.6, p.303.

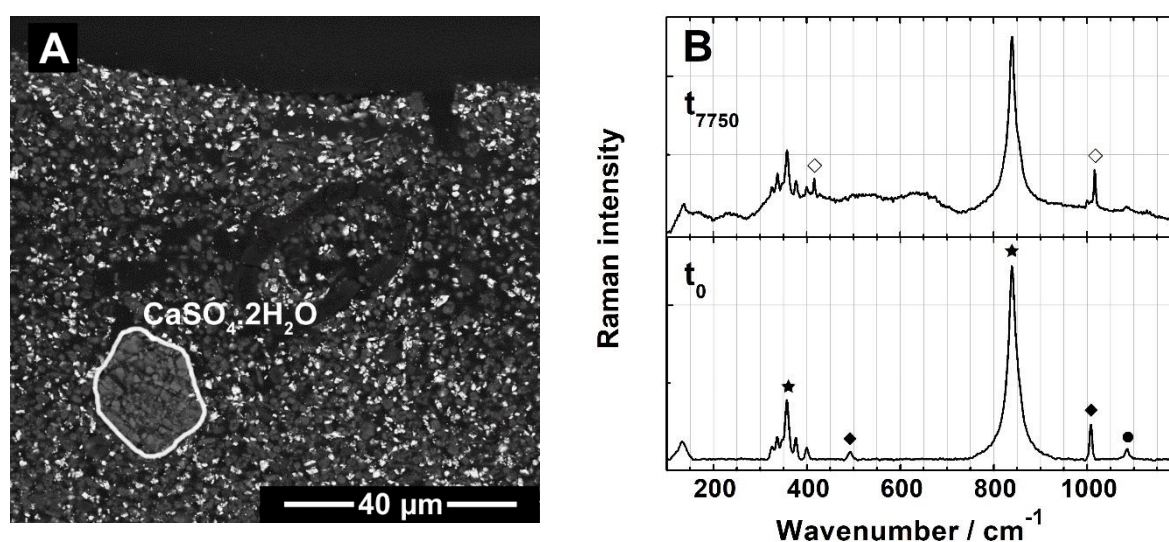


Figure 4.9. **A)** SEM image of a cross-section from the Middle oil paint after 7750h of irradiation and **B)** Raman spectra acquired at the interface of the gypsum aggregate outlined in the SEM image; (★) PbCrO_4 , (●) CaCO_3 , (◆) $\text{CaSO}_4\cdot 2\text{H}_2\text{O}$ and (◇) CaSO_4 .

Embedding-free thin cross-sections of the Middle oil paint were successfully prepared with a thickness of 1 to 4 μm , enabling the combined characterisation by SR μ -FTIR, μ -XRF, μ -XANES (at the Cr, S and Ca K-edge) and μ -XRD. μ -XANES at Ca K-edge and μ -XRD were carried out for an irradiation time of 11000h¹¹⁸. This data allowed access to the distribution of the different paint components and degradation products. The results obtained after 7750h and 11000h of irradiation are presented in Figures 4.10 through to 4.14 (see also Figures XIX.4 to XIX.7, p. 362-364).

¹¹⁷ It is important to note that neither microorganisms were found in the irradiated Middle oil paint nor were conservation treatments applied.

¹¹⁸ SR μ -XRD was only operational at ID 21 (ESRF facility) for the 11000h of irradiation.

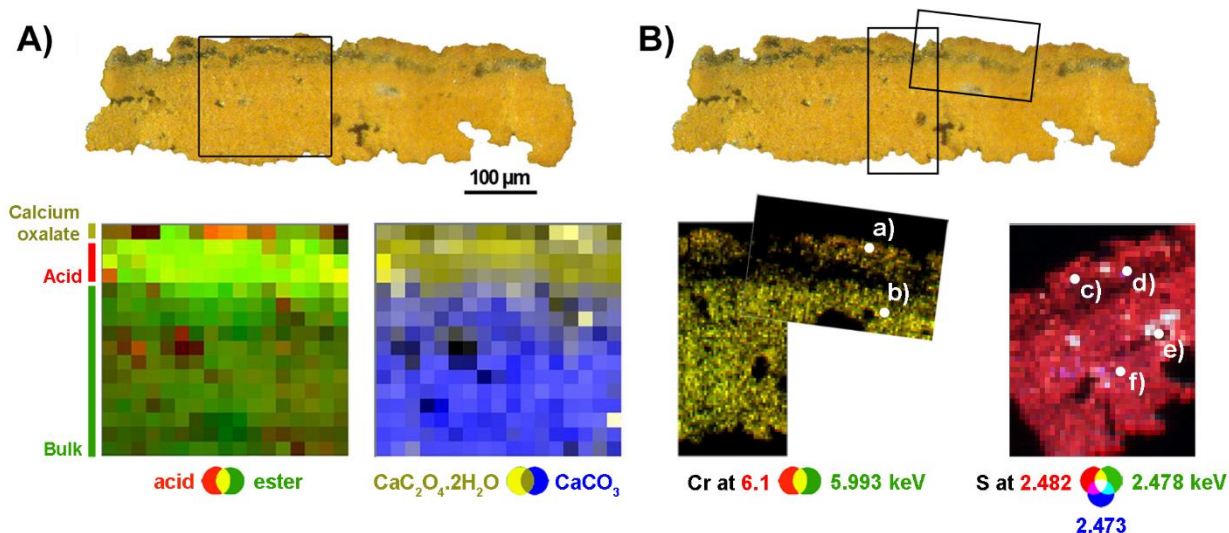


Figure 4.10. Optical microscope image of an embedding-free thin cross-section of the Middle oil paint after 7750h of irradiation (analysed areas outlined in black). **A)** SR μ -FTIR chemical maps (size: $170 \times 160 \mu\text{m}^2$, with $10 \times 10 \mu\text{m}^2$ step size), ROI: acids ($1718\text{-}1700 \text{ cm}^{-1}$), esters ($1755\text{-}1720 \text{ cm}^{-1}$), calcium oxalate ($1340\text{-}1300 \text{ cm}^{-1}$), calcium carbonate ($1520\text{-}1350 \text{ cm}^{-1}$); **B)** SR μ -XRF maps around Cr K-edge at 5.993 and 6.1 keV (vertical map size: $92 \times 192 \mu\text{m}^2$ and diagonal map size: $152 \times 100 \mu\text{m}^2$, with $2 \times 2 \mu\text{m}^2$ step size) and around S K-edge at 2.473, 2.478 and 2.842 keV (size: $185 \times 220 \mu\text{m}^2$, with $5 \times 5 \mu\text{m}^2$ step size). The points labelled a) through to f) represent the location of μ -XANES spectra presented in Fig. 4.11. See also Figure XIX.4 (p. 362).

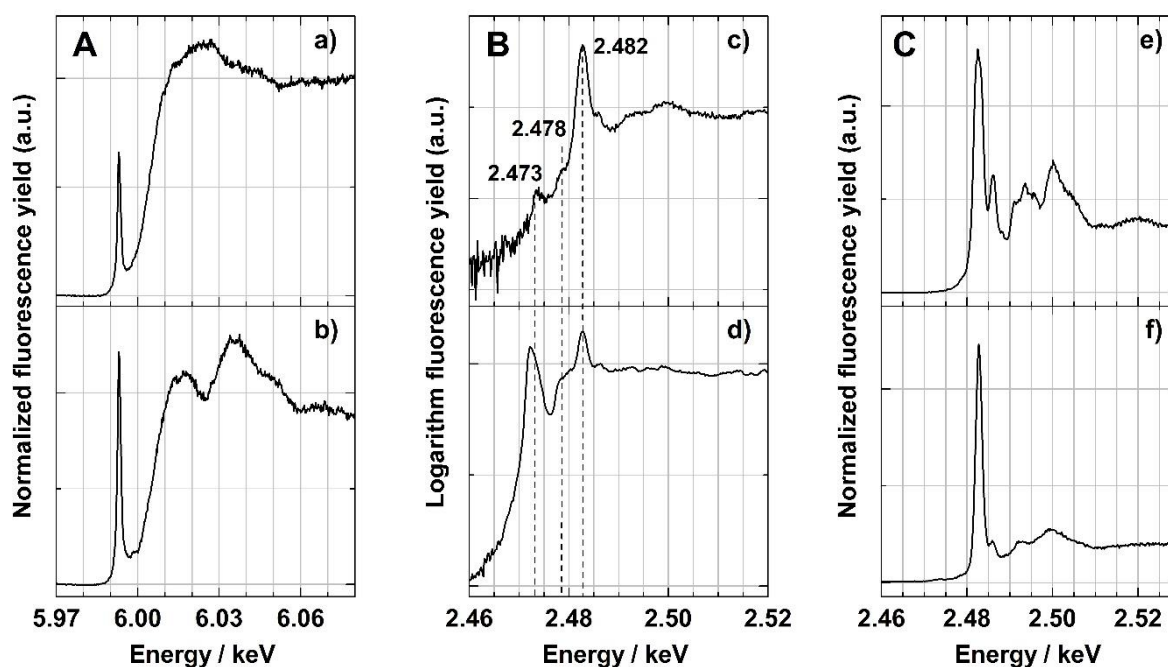


Figure 4.11. **A)** Normalized Cr K-edge, **B)** & **C)** S K-edge μ -XANES spectra of the points in Figure 4.10.

As may be seen in Figure 4.10, after 7750h of irradiation, the Middle oil paint presents a clear three-layer stratigraphy in which the two most superficial layers ($20 \mu\text{m}$) can be differentiated from the bulk ($130 \mu\text{m}$). This was not observed in the paint before irradiation¹¹⁹, as shown in Figure XIX.3 (p. 362).

SR μ -FTIR mapping clearly identified calcium oxalate through its COO^- symmetric stretching band at 1320 cm^{-1} . It was formed due to the depletion of calcium carbonate, detected by its CO_3^{2-}

¹¹⁹ Naturally aged for two and a half years.

asymmetric stretching band at 1422 cm^{-1} , in the presence of an enriched layer of carboxylic acids (broadening of the C=O stretching band at 1741 cm^{-1}) resulting from the photochemical degradation of the linseed oil described above (p. 90). Below these two layers characterised by a higher content of calcium oxalate and carboxylic acids, the bulk paint is reached and with it, largely unaltered chrome yellow oil paint, in which disperse altered regions can be observed; calcium oxalate is also found near chalk-rich areas in the bulk paint (see also Figure XIX.4, p. 362). The presence of this unaltered bulk is proof of a photochemical reaction from light penetration into the paint and demonstrates a limiting factor due to the degree of light absorption/penetration.

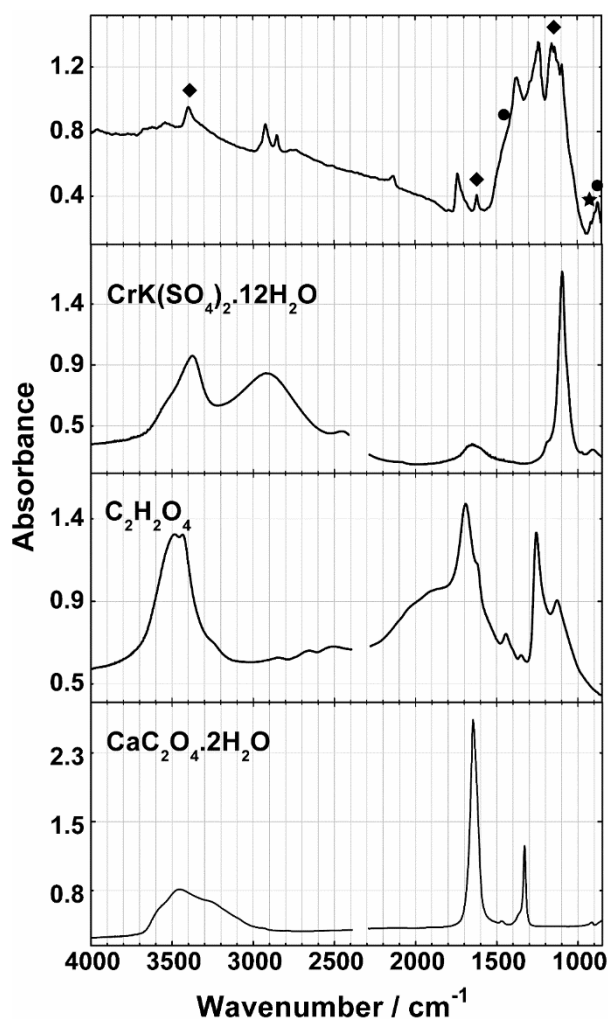


Figure 4.12. SR infrared spectrum obtained on the surface of an embedding-free thin cross-section of the Middle oil paint after 7750h of irradiation and 3 reference compounds: chromium potassium sulfate $\text{CrK}(\text{SO}_4)_2 \cdot 12\text{H}_2\text{O}$, oxalic acid ($\text{C}_2\text{H}_2\text{O}_4$), calcium oxalate dihydrate ($\text{CaC}_2\text{O}_4 \cdot 2\text{H}_2\text{O}$, weddellite)¹²⁰; (◆) $\text{CaSO}_4 \cdot 2\text{H}_2\text{O}$, (●) CaCO_3 and (★) PbCrO_4 . See also Figure XIX.5 (p. 363).

¹²⁰ The infrared spectrum of $\text{CaC}_2\text{O}_4 \cdot 2\text{H}_2\text{O}$ was kindly provided by Letizia Monico and Costanza Miliani (Monico *et al.*, 2013c).

¹²¹ The presence of potassium ions most probably resulted from the starting reagent, potassium dichromate. Residues from this reagent have also been detected in the study by Casadio *et al.* (2011).

¹²² Interestingly, when SR μ -XANES at the S K-edge was performed on surface sections of the Middle oil paint, no S^{6+} reduction was observed and only the spectral feature of gypsum was detected (Figure VI.5.6, p. 270).

This work provides, for the first time, the molecular identification of a Cr^{3+} degradation compound by infrared spectroscopy: a chromium potassium sulfate ($\text{CrK}(\text{SO}_4)_2 \cdot 12\text{H}_2\text{O}$)¹²¹ characterised by a sharp band at 1097 cm^{-1} assigned to its SO_4^{2-} asymmetric stretching mode, Figure 4.12 (see also Figure XIX.5, p. 363). The loss of monoclinic lead chromate pigment is also evident in the low intensity of the CrO_4^{2-} asymmetric stretching band at 854 cm^{-1} .

SR μ -XRF and μ -XANES at the Cr K-edge performed with even higher spatial resolution corroborated that in the superficial layer where calcium oxalate is present, the reduction of Cr^{6+} from lead chromate is also observed, Figure 4.10B and 4.11A. However, a complete conversion of Cr^{6+} to Cr^{3+} was not detected by Cr K-edge μ -XANES, and a clear identification of the Cr^{3+} species by this technique was not possible.

SR μ -XRF and μ -XANES at the S K-edge were also carried out, Figure 4.10B and 4.11B and C, showing signs of S^{6+} reduction¹²², particularly near gypsum-rich areas characterised by an intense white line at 2.482 keV due to an electronic $s \rightarrow p$ transition (Cotte *et al.*, 2006b; Monico *et al.*,

2014b); see point f) in Figure 4.11C. As may be seen in Figure 4.11B, low intensity bands appear at 2.473 and 2.478 keV, indicating the presence of sulfite S^{4+} and sulfide S^{2-} species, respectively. The most reduced point observed was found at the surface of the Middle oil paint, corresponding to the presence of sulfide S^{2-} species; see point d) in Figure 4.11B. No other S species with different oxidation states were identified. Furthermore, it was also possible to detect the spectral feature of another sulfate compound, $CaSO_4$, as shown in point e) in Figure 4.11C, which is in agreement with the findings obtained by μ -Raman described above. However, the presence of $CrK(SO_4)_2 \cdot 12H_2O$ was not identified.

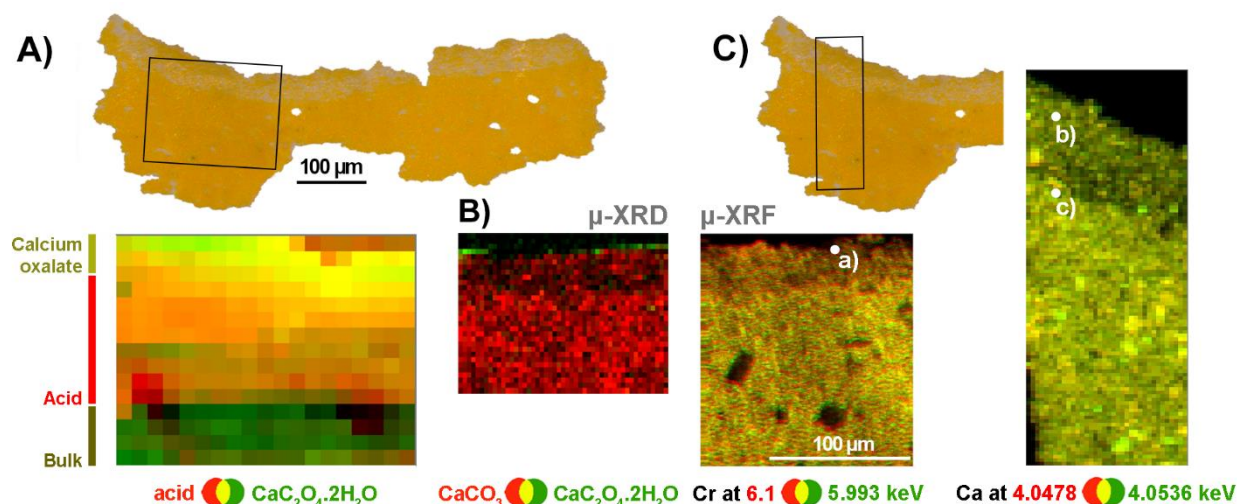


Figure 4.13. Optical microscope image of an embedding-free thin cross-section of the Middle oil paint after 11000h of irradiation (analysed areas outlined in black). **A)** SR μ -FTIR chemical map (size: $190 \times 150 \mu m^2$, with $10 \times 10 \mu m^2$ step size), ROI: acids ($1718-1700 \text{ cm}^{-1}$) and calcium oxalate ($1340-1300 \text{ cm}^{-1}$); **B)** SR μ -XRD map (size: $173 \times 90 \mu m^2$, with $2 \times 2 \mu m^2$ step size), red = Rietveld scaling factor of calcite, green = intensity of the (200) Bragg peak of weddellite), and SR μ XRF map around Cr K-edge at 5.993 and 6.1 keV (size: $150 \times 180 \mu m^2$, with $1 \times 1 \mu m^2$ step size); **C)** SR μ -XRF map around Ca K-edge at 4.0478 and 4.0536 keV (size: $72 \times 222 \mu m^2$, with $2 \times 2 \mu m^2$ step size). The points a), b) & c) represent the location of μ -XANES spectra presented in Fig. 4.14. See also Figures XIX.6 and XIX.7 (p. 364).

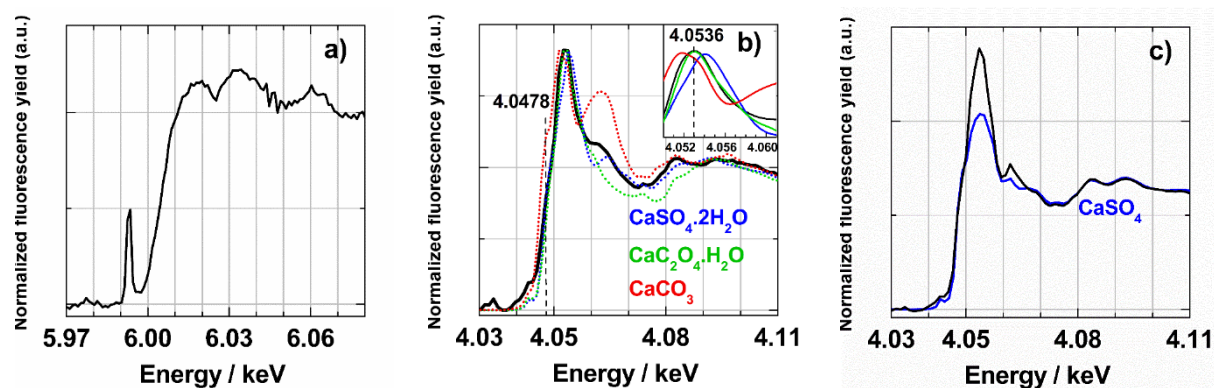
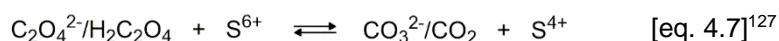
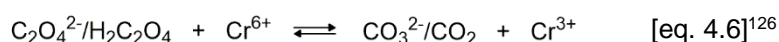
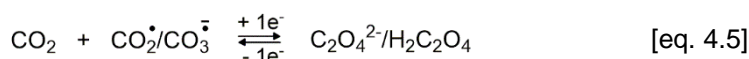
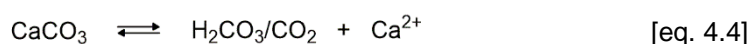
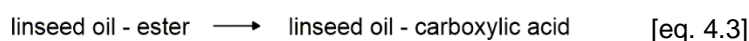


Figure 4.14. a) Normalized Cr K-edge, b) & c) Ca K-edge μ -XANES spectra of the points in Figure 4.13, and the references compounds: chalk ($CaCO_3$), calcium oxalate monohydrate ($CaC_2O_4 \cdot H_2O$) gypsum ($CaSO_4 \cdot 2H_2O$) and calcium sulfate anhydrous ($CaSO_4$), see also Figure VI.5.7, p. 271.

Finally, SR μ -XRD was performed on an embedding-free thin cross-section of the Middle oil paint after 11000h of irradiation, clearly identifying calcium oxalate in the dihydrate form ($\text{CaC}_2\text{O}_4 \cdot 2\text{H}_2\text{O}$, weddellite, $K_{\text{sp}} \approx 10^{-9}$; Hummel *et al.*, 2005)¹²³ and confirming the depletion of calcium carbonate in this top layer, Figure 4.13. At this irradiation time, a higher content of calcium oxalate, carboxylic acids and reduction of Cr^{6+} is observed by SR μ -FTIR and μ -XANES, nevertheless, no clear identification of a Cr^{3+} compound was possible, Figure 4.14a. Further reduction of S^{6+} from gypsum to sulfite S^{4+} and sulfide S^{2-} species was also detected, Figure XIX.7 (p. 364).

SR μ -XRF and μ -XANES at the Ca K-edge also show the depletion of calcium carbonate, identified due to its characteristic white line at 4.0511 keV (with a shoulder at 4.0478 keV and a sub-peak at 4.0625 keV; see Figure XIX.7C, p. 364) assigned to $1s \rightarrow 4p$ transitions (Asokan *et al.*, 2001; Veiga *et al.*, 2008; Hesse *et al.*, 2016). More importantly, it was also possible to detect in the upper layer of the paint, a XANES spectral feature with a white line at 4.0536 eV, supporting the presence of Ca^{2+} oxalates¹²⁴, Figure 4.14.b. Additionally, it also confirmed the formation of CaSO_4 , Figure 4.14c.

Considering the results obtained, it is suggested that the degradation pathway following light absorption follows eqns. 4.3 to 4.6¹²⁵:



In a first step the ester triglycerides are hydrolysed into carboxylic acids (Mallécol *et al.*, 1999) and, therefore locally, the oil binder is acidified. Consequently, the extender CaCO_3 , through its acid-base equilibria¹²⁹, is converted into H_2CO_3 or CO_2 (depending on the pH of the medium), eq. 4.3 and 4.4. In an oil paint system, upon light absorption, the excited states that are formed are more active

¹²³ No Cr^{3+} compound was detected by SR μ -XRD.

¹²⁴ It matches with the white line of calcium oxalate monohydrate (Figure VI.5.7, p. 271); the Ca K-edge μ -XANES spectrum of the calcium oxalate dihydrate was not available.

¹²⁵ The skeletal equations are a qualitative summary of the chemical reactions occurring; they are not written as balanced chemical equations.

¹²⁶ $E^\circ(\text{Cr}^{6+}/\text{Cr}^{3+}) = 1.35 \text{ V}$; for $E^\circ(\text{H}_2\text{CO}_3/\text{H}_2\text{C}_2\text{O}_4) = -0.39 \text{ V}$, $\Delta E^\circ = 1.7 \text{ V}$; for $E^\circ(\text{CO}_2/\text{H}_2\text{C}_2\text{O}_4) = -0.47 \text{ V}$, $\Delta E^\circ = 1.8 \text{ V}$; for $E^\circ(\text{CO}_3^{2-}/\text{C}_2\text{O}_4^{2-}) = 0.48 \text{ V}$, $\Delta E^\circ = 0.9 \text{ V}$ (Bard *et al.*, 1985). Full reduction equations may be found in Appendix XX (p. 369).

¹²⁷ $E^\circ(\text{S}^{6+}/\text{S}^{4+}) = 0.17 \text{ V}$; for $E^\circ(\text{H}_2\text{CO}_3/\text{H}_2\text{C}_2\text{O}_4) = -0.39 \text{ V}$, $\Delta E^\circ = 0.56 \text{ V}$; for $E^\circ(\text{CO}_2/\text{H}_2\text{C}_2\text{O}_4) = -0.47 \text{ V}$, $\Delta E^\circ = 0.64 \text{ V}$ (Bard *et al.*, 1985). Full reduction equations may be found in Appendix XX (p. 369).

¹²⁸ $\Delta E^\circ = 1.18 \text{ V}$ (Bard *et al.*, 1985).

¹²⁹ $\text{CaCO}_3(\text{s}) \rightleftharpoons \text{Ca}^{2+}(\text{aq}) + \text{CO}_3^{2-}(\text{aq})$; $\text{CO}_3^{2-}(\text{aq}) + \text{H}_3\text{O}^+ \rightleftharpoons \text{HCO}_3^-(\text{aq}) + \text{H}_2\text{O}$ (pK_a 10.33); $\text{HCO}_3^-(\text{aq}) + \text{H}_3\text{O}^+ \rightleftharpoons \text{H}_2\text{CO}_3(\text{aq}) + \text{H}_2\text{O}$ (pK_a 6.35); $\text{H}_2\text{CO}_3(\text{aq}) \rightleftharpoons \text{CO}_2(\text{g}) + \text{H}_2\text{O}$ (Chang, 1994; Lide, 2006).

oxidizing and reducing agents; this together with the availability of Ca^{2+} makes the formation of calcium oxalate possible through a redox reaction, eq. 4.5 (Pina *et al.*, 1985). For this reaction, the redox pair may be an excited species or a radical such as HO^{\bullet} (resulting from the binder's photodegradation). In the presence of oxalate species, Cr^{6+} from chrome yellow is transformed into Cr^{3+} as depicted in eq. 4.6¹³⁰. Westheimer refers to experiments that have shown that chromic acid (HCrO_4^-) oxidations can be accelerated by light (Westheimer, 1949). Furthermore, oxalate can also reduce the S^{6+} from gypsum to S^{4+} (SO_3^{2-}) as described in eq. 4.7. These species can be easily oxidised by Cr^{6+} , especially in acidic conditions, adding to the formation of Cr^{3+} compounds, eq. 4.8. S^{6+} species can also be further reduced in the presence of oxalate via $\text{S}^{4+}/\text{S}^0/\text{S}^{2-}$ intermediate species¹³¹, see Table XX.1 (p. 369).

The transformation of oxalate, following light absorption, into CO_2 and CO_2^{\bullet} is well documented in the literature (Pina *et al.*, 1985). The formation of oxalate via CO_2 radicals has also been previously studied (Amatore & Savéant, 1981). As depicted in eq. 4.5 and 4.6, the presence of CO_2^{\bullet} or CO_3^{\bullet} will depend on the pH. This is supported by the fact that it was possible to identify, in the altered regions, both calcium oxalate and oxalic acid, Figures 4.12.

The high content of calcium carbonate in this Middle formulation may also contribute to its higher reactivity, since calcium carbonate is capable of scattering and reflecting light between 300-350 nm within the paint matrix, increasing light absorption by both pigment and binder and thus accelerating the photochemical reactions (Ferreira *et al.*, 2010).

The importance of the binder in the formation of oxalates in both tempera and oil paintings, and as such the interdependence of eq. 4.3 and 4.5, is well documented in the literature (Cariati, *et al.*, 2000; Salvadó *et al.*, 2009). Oxalic acid is generally considered an end-product of the oxidation of the more complex carboxylic acids (Benner *et al.*, 2000). The persistence of calcium oxalate over geological timescales on Earth is well documented and is associated with its stability to light, in both strongly oxidizing conditions and in acidic media. Oxalic acid and metal-oxalates have even been proposed to be “stable under the pressure and ultraviolet irradiation environment of the surface of Mars” (Applin *et al.*, 2015). It is possible that in certain chrome yellow paint formulations the conversion of the oil binder and carbonate compounds into calcium oxalate is driven by light and results in the formation of a very thin superficial layer at the surface of the oil paint. This may act as a protective surface which acts to inhibit light absorption by the bulk paint and as such, works as a *molecular patina*. The protective role of calcium oxalate on chrome yellow paints will be further addressed below.

4.2.1.2.2. The Lemon oil paint

The Lemon oil paint is composed solely of mixed crystals of lead chromate and lead sulfate, $\text{PbCr}_{0.6}\text{S}_{0.4}\text{O}_4$, dominated by the lead chromate monoclinic phase. A significant change in colour was observed, Table 4.1 (p. 97), and a shoulder with a maximum around 600 nm also appears in the FORS spectra throughout the irradiation time, Figure 4.15A, as seen for the Middle oil paint, Figure 4.8A.

¹³⁰ The solubility of chrome yellow pigment is influenced by the pH; a rough estimate predicts an enhancement from K_{sp} (pH 1) $\approx 10^{-10}$ to K_{sp} (pH 3) $\approx 10^{-12}$.

¹³¹ Unfortunately, no evidence for the presence of S^0 species was found.

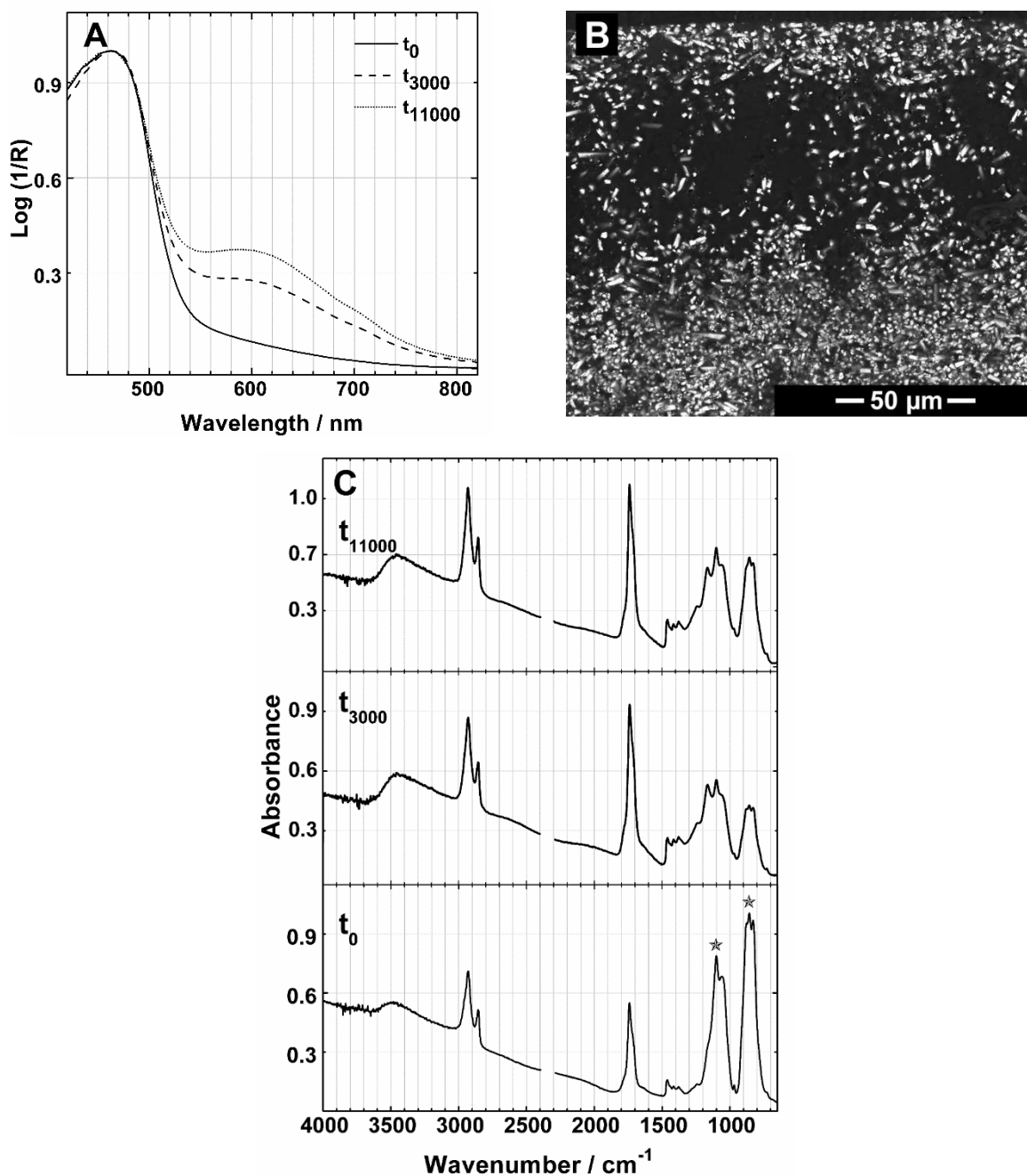


Figure 4.15. **A)** Normalized FORS, **B)** SEM image of a cross-section ($t_{\text{irr}} = 7750\text{h}$), and **C)** infrared spectra of the Lemon oil paint before and after irradiation with a Xenon lamp ($\lambda_{\text{irr}} > 300\text{ nm}$); (*) $\text{PbCr}_{0.6}\text{S}_{0.4}\text{O}_4$.

For this particular formulation, oil separation occurred near the surface of the paint, which is clearly visible in the SEM image of a sample taken after 7750h of irradiation, Figure 4.15B. Carlyle has studied this phenomenon on oil paint reconstructions and it appears to be related to the oil treatment, pigment type and substrate as well as the paint application method (brush or palette knife) (Carlyle, 2005 & 2012b). In Carlyle's work, a greater separation between the oil and the pigment was visible in SEM-BSE images of cross-sections of paint made with water washed oil applied to non-porous substrates (i.e. glass or polyester) and where the paint was applied with a palette knife versus a brush

(Carlyle, 2005). As noted above, the Lemon paint¹³² was prepared with untreated linseed oil and applied onto a glass slide with a palette knife. However, oil separation was not observed in the paint undergoing normal aging in ambient conditions¹³³. Throughout the irradiation time, infrared spectra show an increase in the oil's spectral features (main bands: $\nu(\text{CH})$ at 2926 and 2855 cm^{-1} ; $\nu(\text{C}=\text{O})$ at 1741 cm^{-1} ; (C-O) ester bonds at 1240, 1168 and 1099 cm^{-1} ; Van der Weerd *et al.*, 2005), Figure 4.15C. Additionally, an increase and a broadening of the C=O stretching band at 1741 cm^{-1} to lower wavenumbers is also observed indicating a higher content of carboxylic acids. A shoulder at lower wavenumbers also points to the presence of other low molecular weight carbonyl compounds such as aldehydes and ketones. Moreover, there is an increase of the broad O-H stretching band around 3460 cm^{-1} which is assigned to hydroxyl oxidation products such as alcohols and/or hydroperoxides (Van der Weerd *et al.*, 2005). However, no changes were found by μ -Raman or XRD, which was performed on a sample exposed to 7750h of irradiation and these analyses matched the pigment's Raman fingerprint and diffraction pattern shown in Figure X.1.3, p.295.

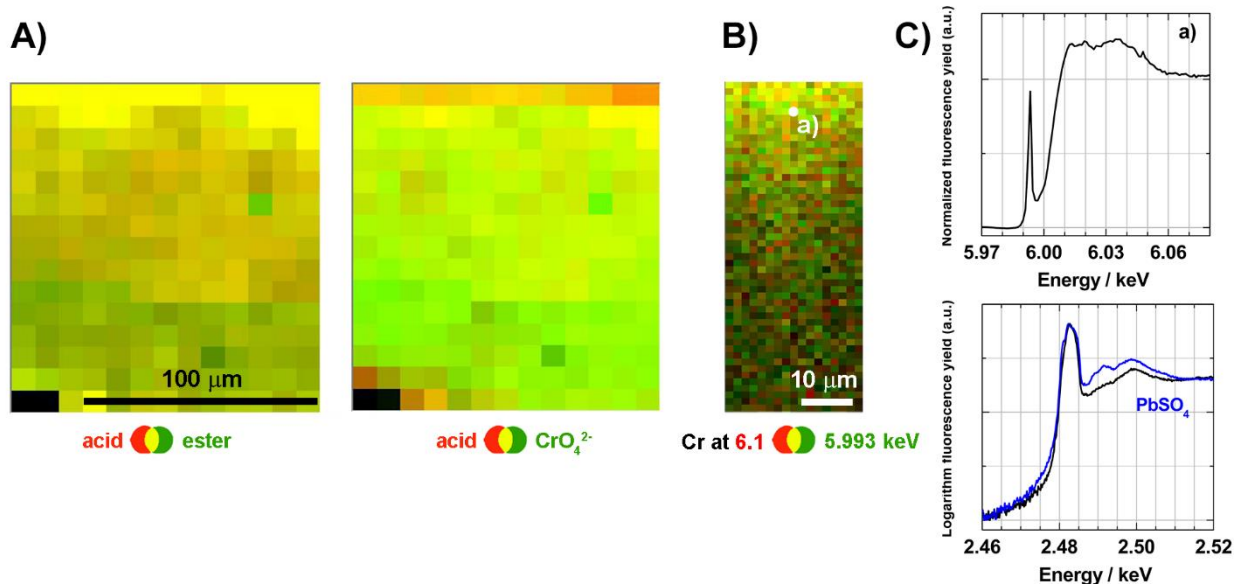


Figure 4.16. **A)** SR μ -FTIR chemical maps (size: $130 \times 150 \mu\text{m}^2$, with $10 \times 10 \mu\text{m}^2$ step size), ROI: acids ($1718\text{-}1700 \text{ cm}^{-1}$), esters ($1755\text{-}1720 \text{ cm}^{-1}$), chromate ($920\text{-}800 \text{ cm}^{-1}$); **B)** SR μ -XRF map around Cr K-edge at 5.993 and 6.1 keV (map size: $26 \times 100 \mu\text{m}^2$, with $1.5 \times 1.5 \mu\text{m}^2$ pixel size); **C)** normalized Cr K-edge XANES spectrum at a), and S K-edge μ -XANES spectrum acquired at the surface of a cross-section from the Lemon oil paint after 7750h of irradiation. See also Figure XIX.8 (p. 365).

As may be seen in Figure 4.16 (see also Figure XIX.8, p. 365), the combined characterisation by SR μ -FTIR, μ -XRF and Cr K-edge μ -XANES of the Lemon oil paint after 7750h of irradiation shows that the degradation pathway was induced by light. Like the Middle oil paint, the uppermost layer is rich in carboxylic acids (broadening of the C=O stretching band at 1741 cm^{-1}) due to the photodegradation of the oil binder and is rich in Cr^{3+} species which is due to a depletion of the original lead chromate fingerprint signals, namely the CrO_4^{2-} broad asymmetric stretching band between 920-

¹³² The full characterisation of the pigment used in the Lemon oil paint is presented in p. 295.

¹³³ Naturally aged for two and a half years.

800 cm^{-1} and the Cr^{6+} well-defined pre-edge peak at 5.993 keV. A complete conversion of Cr^{6+} to Cr^{3+} was not detected by μ -XANES, Figure 4.16C. However, after 11000h of irradiation it was possible to identify at the surface of an embedding-free thin cross-section, the degradation product $\text{CrK}(\text{SO}_4)_2 \cdot 12\text{H}_2\text{O}$ by SR μ -FTIR, through its SO_4^{2-} characteristic asymmetric stretching band at 1097 cm^{-1} , Figure 4.17. This degradation product was found together with a low chromate signal and a high content of carboxylic acids. The presence of oxalic acid is strongly suggested by the low intensity band at 1257 cm^{-1} , assigned to the COH bending mode and the broadening of the C=O stretching band to lower wavenumbers, Figure XIX.8 (p. 365).

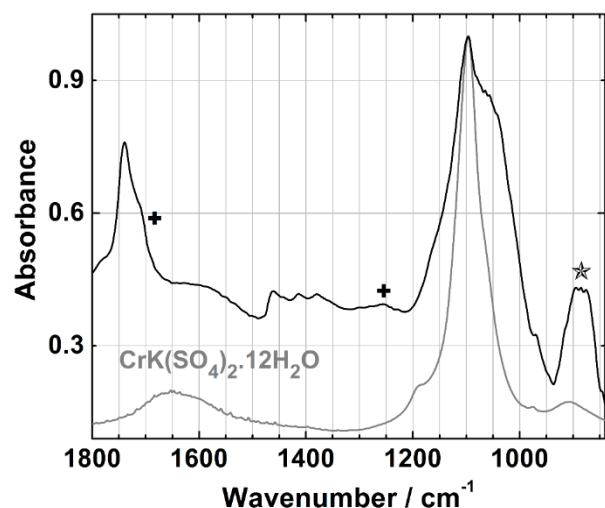
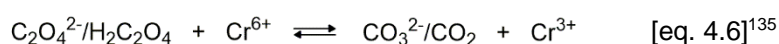
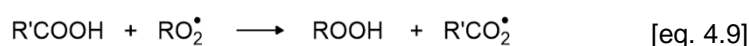
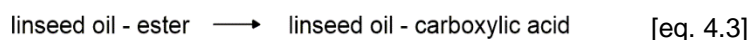


Figure 4.17. SR infrared spectrum obtained on the surface of an embedding-free thin cross-section of the Lemon oil paint after 11000h of irradiation and of the reference compound chromium potassium sulfate $\text{CrK}(\text{SO}_4)_2 \cdot 12\text{H}_2\text{O}$; (*) $\text{PbCr}_{0.6}\text{S}_{0.4}\text{O}_4$, (+) oxalic acid ($\text{C}_2\text{H}_2\text{O}_4$). See also Figure XIX.8 (p. 365).

Contrary to what was found for the Middle oil paint, no signs of S^{6+} reduction were detected for the Lemon oil paint. As shown in Figure 4.16C (bottom), the S K-edge μ -XANES spectra acquired at the surface of the paint are very similar to that of lead sulfate presenting a white line at 2.482 keV but with no pre-edge at 2.481 keV or post-edge bands. This corresponds to the spectral feature of mixed crystals of lead chromate and lead sulfate (Monico *et al.*, 2013a). The presence of additional sulfate compounds such as $\text{CrK}(\text{SO}_4)_2 \cdot 12\text{H}_2\text{O}$ was not detected by S K-edge μ -XANES.

No additional data was obtained with the SR analyses performed after 11000h, not even by SR μ -XRD (Figure XIX.9, p. 365).

The degradation pathway following light absorption of the Lemon oil paint is necessarily different from that of the Middle oil paint since there is no calcium carbonate nor calcium sulfate dihydrate to react. However, the role played by carbon dioxide to form oxalate ions can still be considered via decarboxylation of carboxylic acids, as may be seen in the following eqns.¹³⁴:



¹³⁴ The skeletal equations are a qualitative summary of the chemical reactions occurring; they are not written as balanced chemical equations.

¹³⁵ $E^\circ(\text{Cr}^{6+}/\text{Cr}^{3+}) = 1.35 \text{ V}$; for $E^\circ(\text{H}_2\text{CO}_3/\text{H}_2\text{C}_2\text{O}_4) = -0.39 \text{ V}$, $\Delta E^\circ = 1.7 \text{ V}$; for $E^\circ(\text{CO}_2/\text{H}_2\text{C}_2\text{O}_4) = -0.47 \text{ V}$, $\Delta E^\circ = 1.8 \text{ V}$; for $E^\circ(\text{CO}_3^{2-}/\text{C}_2\text{O}_4^{2-}) = 0.48 \text{ V}$, $\Delta E^\circ = 0.9$ (Bard *et al.*, 1985). Full reduction equations may be found in Appendix XX (p. 369).

As described for the Middle oil paint, the first step involves the hydrolysis of the ester triglycerides into carboxylic acids (Mallégol *et al.*, 1999). In an oil matrix, free carboxylic acids can easily react with metal ions to form metal carboxylates (Van der Weerd *et al.*, 2005), however, this was not observed in the Lemon oil paint, excluding their role as intermediates in the degradation mechanism. On the other hand, while chromic acid is known to be an oxidizing agent, the literature does not report its activity regarding the oxidation of long-chain carboxylic acids (Westheimer, 1949; Cotton *et al.*, 1999). The hypothesis proposed in this work is the oxidation of carboxylic acids via decarboxylation, which has been the subject of study, in particular when in an excited state (Mittal *et al.*, 1973; Coyle, 1978; Kaiser *et al.*, 1978, Smith & March, 2007; Denisov & Shestakov, 2013). The formation of peroxy radicals RO_2^* occur through common radical chain reactions during the ageing of an oil paint (Van den Berg, 2002). Denisov & Shestakov have discussed the reaction of radicals with the carboxyl group of carboxylic acids and the formation of carbon dioxide as a result of the action of the peroxy radical on the carboxyl group via cleavage of the α -CH₂ group, as depicted in eq. 4.9 and 4.10 (Denisov & Shestakov, 2013). This is more prone to happen in the excited state (Coyle, 1978; Kaiser *et al.*, 1978). Furthermore, light can also influence these reactions (Mittal *et al.*, 1973) as can the presence of a strong oxidizing agent such as $HCrO_4^{2-}$, in acidic conditions. Following the formation of CO_2 , oxalate ions can be formed as described in eq. 4.11 (Amatore & Savéant, 1981) and then react with Cr^{6+} species from chrome yellow leading to the formation of Cr^{3+} compounds, eq. 4.6.

4.2.1.3. The historic lead chromate oil paints

Samples from the historic oil paint in tubes, Lefranc's *Jaune de Chrome* and W&N's *Chrome Deep* and *Chrome Yellow* (Chapter 3.4, p. 61) were applied onto glass slides with a palette knife and air-dried for six years (Lefranc) and four months (W&N), before being irradiated ($\lambda_{irr} > 300$ nm), Appendix V.2.4 (p. 237). This photodegradation experiment was followed by the same analytical methodology used for the oil paint reconstructions; the results obtained are detailed below.

4.2.1.3.1. W&N's *Chrome Yellow* oil paint

According to the LSI values obtained, the degradation rate of the W&N *Chrome Yellow* oil paint is very similar to that of the Lemon oil paint reconstruction (LSI ≈ 4 for $t_{irr} = 3000h$). Both are composed of $PbCr_{0.6}S_{0.4}O_4$ dominated by the lead chromate monoclinic phase¹³⁶, Figure 4.4 (p. 101) and Table 4.1 (p. 102). However, at the highest irradiation times, these paints presented different colour changes (Table XVI.1, p. 349) and as may be seen in the FORS spectra, Figure 4.18A, the absorption shoulder with a maximum around 600 nm is less intense for the W&N *Chrome Yellow* oil paint. This may be explained by the fact that no oil separation was observed at the surface of the W&N oil paint. The lack of observed oil separation in this paint may have had a significant impact on the degradation rate at

¹³⁶ The W&N *Chrome Yellow* oil paint also contains 20% of the extender barium sulfate ($BaSO_4$), and the presence of magnesium carbonate ($MgCO_3 \cdot xH_2O$) and zinc linoleate was also detected.

the higher irradiation times, since a higher content of photodegradation products from the oil binder will most certainly accelerate degradation reactions.

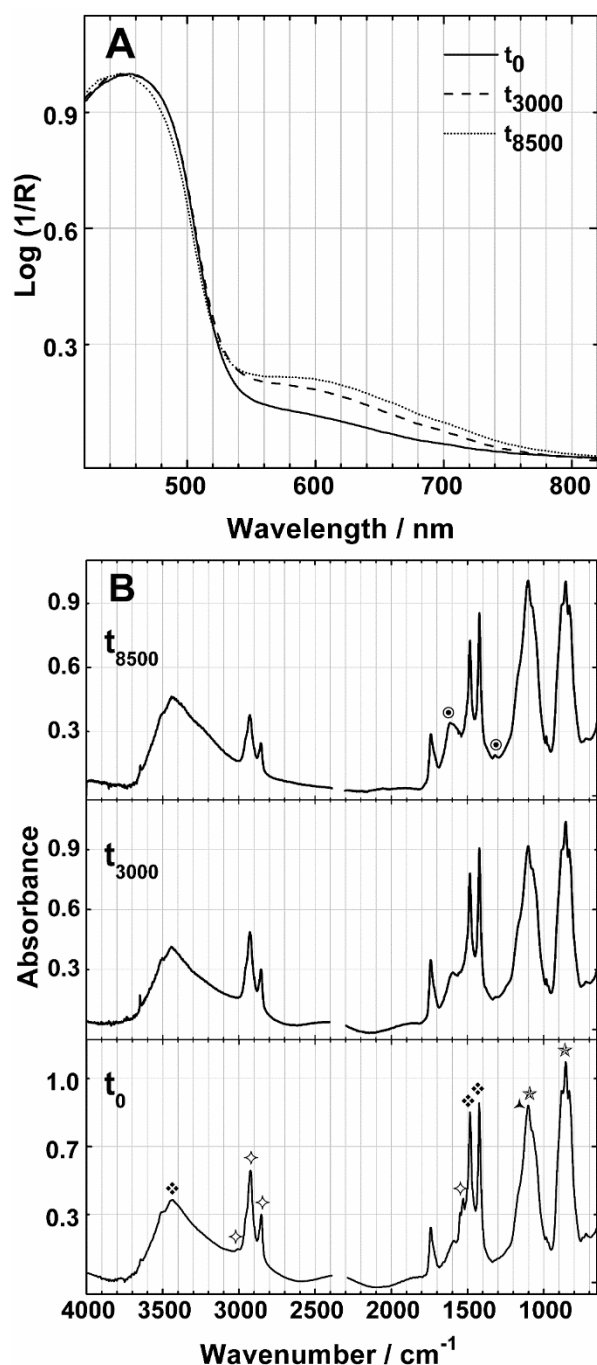


Figure 4.18. A) Normalized FORS and B) infrared spectra of the historic W&N *Chrome Yellow* oil paint before and after irradiation with a Xenon lamp ($\lambda_{\text{irr}} > 300$ nm); (*) $\text{PbCr}_{0.6}\text{S}_{0.4}\text{O}_4$, (\blacktriangle) BaSO_4 , (\blacklozenge) $\text{MgCO}_3 \cdot x\text{H}_2\text{O}$, (\blacklozenge) zinc linoleate, (\odot) oxalate compound.

The infrared spectra throughout the time of irradiation is shown in Figure 4.18B. The presence of zinc linoleate in the paint was detected due to its unequivocal COO^- asymmetric stretching doublet band at $1547/1527 \text{ cm}^{-1}$ and C=C-H stretching band at 3007 cm^{-1} (Otero *et al.*, 2014). These bands disappear with irradiation time and new ones appear at 1320 and 1615 cm^{-1} , which can be attributed to the COO^- symmetric and asymmetric stretching bands of oxalates compounds. An accurate identification of the type of oxalate was not possible but it is suggested that it may be zinc oxalate even if its COO^- symmetric band at 1364 cm^{-1} does not appear (Monico *et al.*, 2013c). The absence of this band may be due to a different crystalline formation of zinc oxalates in such a complex matrix as an oil paint, when compared with reference compounds. Changes in the ratio of sulfate to chromate infrared absorption bands were also detected; the intensity of the SO_4^{2-} asymmetric stretching region, which has contributions from the mixed crystals and BaSO_4 , increases, which may be associated with the presence of the degradation compound, chromium potassium sulfate ($\text{CrK}(\text{SO}_4)_2 \cdot 12\text{H}_2\text{O}$).

No changes could be verified by μ -Raman or XRD, which were performed on a sample after 5250h of irradiation; the analysis matched the Raman fingerprint and diffraction pattern of the oil paint before irradiation (Figure 3.11, p. 64; Figure XI.1, p. 307).

SR μ -FTIR, μ -XRD, μ -XRF and μ -XANES at the Cr and S K-edge were performed on cross-sections taken after

5250h and 8500h of irradiation to gain a better understanding of the degradation pathway of the historic W&N *Chrome Yellow* oil paint. Figure 4.19 shows the formation of a three-layer stratigraphy very similar to that observed for the Middle oil paint, composed of oxalate compounds (~ 20 μm), carboxylic acids and the unaltered bulk paint.

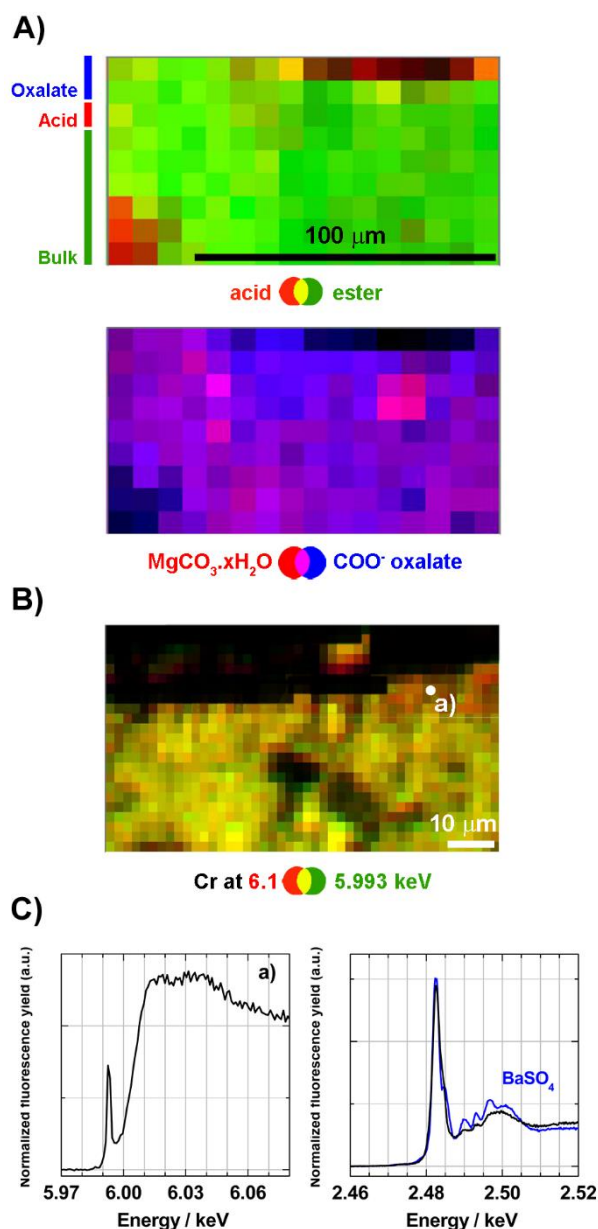


Figure 4.19. **A)** SR μ -FTIR maps (size: $136 \times 72 \mu\text{m}^2$, with $8 \times 8 \mu\text{m}^2$ step size), ROI: acids ($1718\text{-}1700 \text{ cm}^{-1}$), esters ($1755\text{-}1720 \text{ cm}^{-1}$), oxalate compounds ($1620\text{-}1570 \text{ cm}^{-1}$), magnesium carbonate ($3480\text{-}3410 \text{ cm}^{-1}$); **B)** SR μ XRF map around Cr K-edge at 5.993 and 6.1 keV (map size: $92 \times 46 \mu\text{m}^2$, with $2 \times 2 \mu\text{m}^2$ step size); **C)** Cr K-edge μ -XANES spectra acquired at a) and S K-edge μ -XANES spectra acquired at the surface, of cross-sections from the W&N *Chrome Yellow* oil paint after 5250h (for μ -FTIR maps) and 8500h of irradiation. See also Figures XIX.10 and XIX.11 (p. 366).

SR μ -FTIR mapping, Figure 4.19A (see also Figure XIX.10, p. 366), detected the presence of oxalate compounds at the paint surface through the broad band around 1615 cm^{-1} . While a clear characterisation was not possible, it is proposed that it may consist of zinc oxalate, as noted above. This top layer also presents a high content of carboxylic acids (broadening of the C=O stretching band at 1741 cm^{-1} to lower wavenumbers) due to the photodegradation of the oil binder. More importantly, SR μ -FTIR also shows the light induced depletion of the magnesium carbonate ($\text{MgCO}_3 \cdot x\text{H}_2\text{O}$, $K_{\text{sp}} \approx 10^{-6}$; Lide, 2006) characterised by a CO_3^{2-} asymmetric stretching doublet band at $1483/1420 \text{ cm}^{-1}$ and a characteristic $\nu(\text{OH})$ spectral profile at 3648 , 3511 and 3447 cm^{-1} . Unfortunately, SR μ -XRD mapping was not able to identify the type of oxalate compound nor other degradation products (Figure XIX.11, p. 366).

As noted above, the relationship between metal carboxylates and oxalates have been discussed in the literature (Salvadó *et al.*, 2009; Prati *et al.*, 2016). However, in the case of the W&N *Chrome Yellow* oil paint, the oxalate compounds do not appear to derive from zinc linoleate, originally in the paint before irradiation, since, as may be seen in Figure XIX.10 (p. 366) no correlation was found. The decomposition of zinc linoleate by the action of light is easily explained by the high reactivity of the existing double bonds (Van den Berg, 2002). The resulting free zinc ions become available to form zinc oxalates.

SR μ -XRF and μ -XANES at the Cr K-edge, Figure 4.19B and C, show the reduction of Cr^{6+} from lead chromate in the upper layer of the paint, though no full conversion was observed. On the other hand, no reduction of the S^{6+} compounds, $\text{PbCr}_{0.6}\text{S}_{0.4}\text{O}_4$ and BaSO_4 , was detected by μ -XANES at the S K-edge, Figure 4.19C. The spectra obtained appear to be a combination of both sulfate compounds, where it is possible to perceive the post-edge bands of BaSO_4 together with the S^{6+} characteristic white line at 2.482 keV (Cotte *et al.*, 2006b).

Considering the results presented here, it is proposed that the degradation gradient induced by light in the W&N *Chrome Yellow* oil paint is the same as the Middle oil paint reconstruction and follows eqns. 4.3 to 4.6 (p. 110). The lower degradation rate in the W&N *Chrome Yellow* oil paint is most possibly due to the lower proportion of carbonate vs chromate ions and the absence of the $\text{CaSO}_4 \cdot 2\text{H}_2\text{O}$. It is noteworthy that BaSO_4 did not show the same catalytic behaviour as $\text{CaSO}_4 \cdot 2\text{H}_2\text{O}$ in the Middle oil paint. It would be interesting to investigate if a higher quantity of BaSO_4 will affect the degradation rate.

4.2.1.3.2. W&N's *Chrome Deep* oil paint

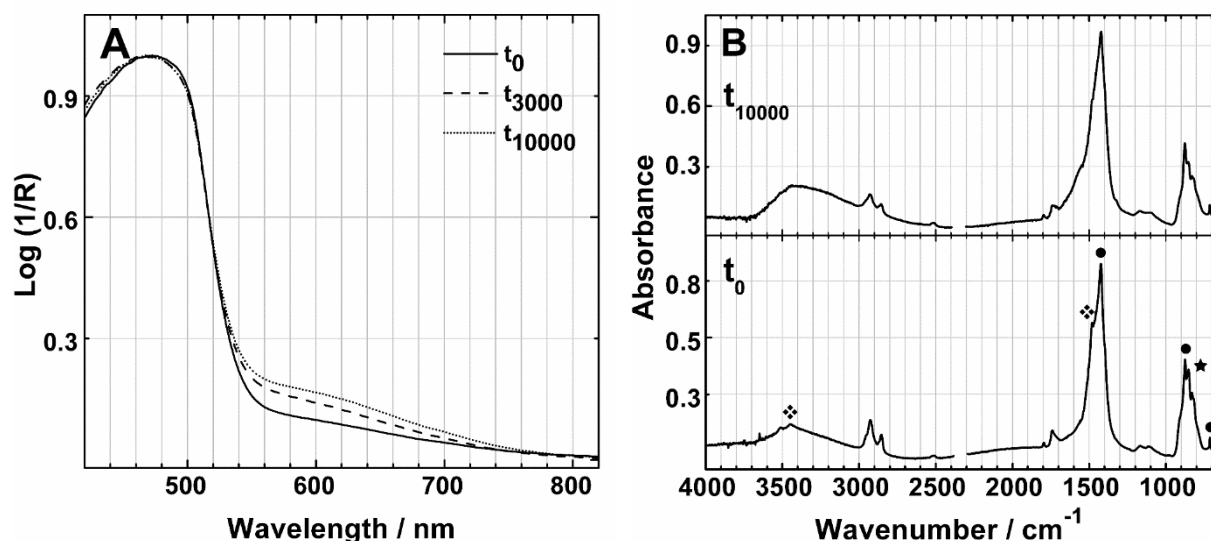


Figure 4.20. A) Normalized FORS and B) infrared spectra of the W&N *Chrome Deep* oil paint before and after irradiation with a Xenon lamp ($\lambda_{\text{irr}} > 300 \text{ nm}$); (★) PbCrO_4 , (●) CaCO_3 and (❖) $\text{MgCO}_3 \cdot x\text{H}_2\text{O}$.

The historic W&N *Chrome Deep* oil paint tube is composed of pure monoclinic lead chromate (PbCrO_4) and calcium carbonate (CaCO_3) in a proportion of approximately 50:50, admixed with magnesium carbonate ($\text{MgCO}_3 \cdot x\text{H}_2\text{O}$). Of the oil paints studied, it was the least light-sensitive oil paint with the lowest colour variation and LSI value, Figure 4.4 (p. 101) and Table 4.1 (p. 102). The FORS and μ -FTIR spectra over irradiation time are shown in Figure 4.20 and present very small differences when compared with the oil paint before irradiation (see also Figure 3.11, p. 64). After 10000h of irradiation it was possible to observe a slight change in the pigment to oil ratio and a broadening of the CO_3^{2-} asymmetric stretching band at 1422 cm^{-1} , which may suggest the appearance of oxalate compounds through their COO^- asymmetric ($1650\text{-}1580 \text{ cm}^{-1}$) and symmetric ($1360\text{-}1290 \text{ cm}^{-1}$)

stretching bands. A small shoulder also appears at 780 cm^{-1} that may be assigned to the oxalates COO^- bending band. The infrared bands for the additive $\text{MgCO}_3 \cdot x\text{H}_2\text{O}$, namely its CO_3^{2-} asymmetric stretching bands and the OH stretching bands of the hydration waters, tend to disappear. No alterations were detected after irradiation by μ -Raman or XRD (Figure 3.11, p. 64; Figure XI.1, p. 307).

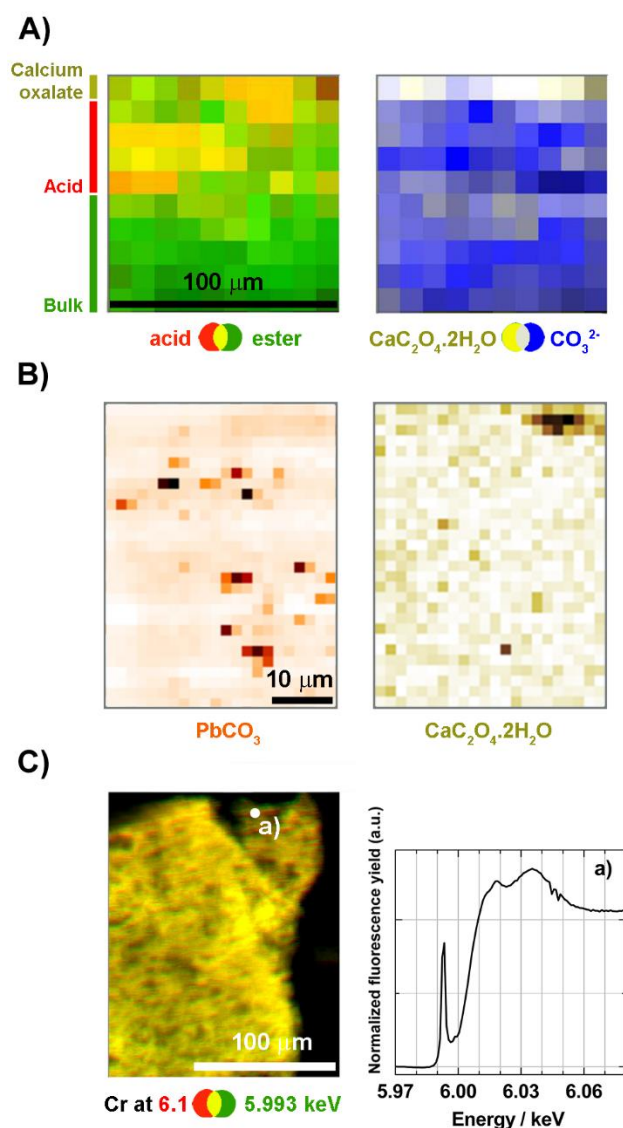


Figure 4.21. **A)** SR μ -FTIR maps (size: $100 \times 100\ \mu\text{m}^2$, with $10 \times 10\ \mu\text{m}^2$ step size), ROI: acids ($1718\text{-}1700\text{ cm}^{-1}$), esters ($1755\text{-}1720\text{ cm}^{-1}$), calcium oxalate ($1615\text{-}1555\text{ cm}^{-1}$), carbonate compounds ($1520\text{-}1350\text{ cm}^{-1}$); **B)** SR μ -XRD maps (size: $49 \times 54\ \mu\text{m}^2$, with $1.5 \times 1.5\ \mu\text{m}^2$ step size) of cerussite (intensity of the (111) Bragg peak) and weddellite (Rietveld scaling factor); **C)** SR μ -XRF map around Cr K-edge at 5.993 and 6.1 keV (map size: $140 \times 200\ \mu\text{m}^2$, with $1 \times 1\ \mu\text{m}^2$ step size) and the Cr K-edge μ -XANES spectra acquired at a), of cross-sections from the W&N Chrome Deep oil paint after 10000h of irradiation. See also Figures XIX.12 and XIX.13 (p. 367).

110), Figure 4.21A. A high content of carboxylic acids (from the photochemical degradation of the oil,

Figure 4.21 presents the combined results obtained by SR μ -FTIR, μ -XRD, μ -XRF and Cr K-edge μ -XANES analysis of cross-sections from the W&N Chrome Deep oil paint after 10000h of irradiation (Figures XIX.12 and XIX.13, p. 367). It is very interesting to observe the same light-induced phenomenon as previously found, which leads to the formation of a three-layer stratigraphy, (Figure 4.10, p. 107): a very thin superficial layer of calcium oxalate ($\sim 5\ \mu\text{m}$) in an acidic media ($\sim 40\ \mu\text{m}$), followed by the mainly unaltered bulk of the paint. However, it is important to note that the altered top layer in the W&N Chrome Deep oil paint is much thinner than what was observed above in the W&N Chrome Yellow and the oil paint reconstructions.

Evidence of the presence of calcium oxalate was found by SR μ -FTIR mapping through a broad shoulder between $1615\text{-}1555\text{ cm}^{-1}$ attributed to its COO^- asymmetric stretching mode, Figure 4.21A. The COO^- symmetric stretching band at 1320 cm^{-1} was not detected. Its unambiguous identification was achieved by SR μ -XRD mapping in its dihydrate form ($\text{CaC}_2\text{O}_4 \cdot 2\text{H}_2\text{O}$, weddellite), Figure 4.21B.

As previously observed, after irradiation calcium oxalate appeared to be formed at the expense of the carbonate additives, CaCO_3 and $\text{MgCO}_3 \cdot x\text{H}_2\text{O}$ ¹³⁷, that degrade into H_2CO_3 or CO_2 by the action of light in an acidic media, eq. 4.4 and 4.5 (p.

¹³⁷ It is important to refer that no magnesium sulfate was detected in any of the irradiated W&N oil paint samples. These have been identified as degradation products resulting from the decomposition of magnesium carbonate (Silvester *et al.*, 2014).

eq. 4.3) was again identified by μ -FTIR mapping. In the top layer of the paint, the depletion of the Cr^{6+} from lead chromate is clear in the SR μ -XRF mapping at different energies, 5.993 keV for Cr^{6+} and 6.1 for other Cr species such as Cr^{3+} (dark yellow region), and by Cr K-edge μ -XANES, Figure 4.21C. No Cr^{3+} compounds were characterised in this sample.

The degradation pathway ends with the reduction of Cr^{6+} promoted by oxalic acid and/or oxalate ions, eq. 4.6. The reduction rate for the W&N *Chrome Deep* oil paint was the lowest of the oil paints studied. The determination of the LSI values demonstrated this, Table 4.1 (p. 102). The significant difference in lightfastness between the W&N *Chrome Deep* and the other chrome yellow oil paints is most likely related to the lower content of $\text{CaCO}_3/\text{MgCO}_3 \cdot x\text{H}_2\text{O}$ and the absence of the catalytic $\text{CaSO}_4 \cdot 2\text{H}_2\text{O}$. As well the lower solubility of pure lead chromate (in comparison with mixed crystals; Monico *et al.*, 2013b) in the W&N *Chrome Deep* oil paint formulation also accounts for its great stability. It is possible that the quantity of carbonate compounds present in this paint is just sufficient to produce a very thin superficial layer of calcium oxalate, which, as proposed above, may act as a protective layer, a *molecular patina*, that prevents light absorption by the bulk paint. The high stability of W&N's *Chrome Deep* reinforces the evidence that W&N was looking to provide the most durable and lightfast products possible.

It is notable that in the sample of W&N's *Chrome Deep* which underwent 10000h of irradiation, SR μ -XRD also identified lead carbonate in the cerussite form, Figure 4.21B. This degradation product is thought to result from the dissolution of the carbonate compounds ($\text{CaCO}_3/\text{MgCO}_3 \cdot x\text{H}_2\text{O}$) in acidic media followed by the prompt precipitation of the carbonate ions with lead (PbCO_3 , $K_{\text{sp}} = 7.4 \times 10^{-14}$; Lide, 2006) which was available from the degradation of lead chromate. The formation of this new compound then competes with the formation of oxalate ions and consequently with the Cr^{6+} reduction.

4.2.1.3.3. Lefranc's *Jaune de Chrome* oil paint

As noted above, a paint-out from Lefranc's lead chromate oil paint tube labelled *Jaune de Chrome* was already presenting signs of degradation before being irradiated. The paint-out had been exposed to ambient conditions for a period of 6 years before analysis. The visual degradation was clearly evident by the darkening of the colour and the shoulder observed at 600 nm in the FORS spectrum¹³⁸, Figure 4.22A. The infrared spectrum from the paint-out shows the presence of pure monoclinic lead chromate (CrO_4^{2-} asymmetric stretching profile at 854/831/820 cm^{-1}) and lead azelate (COO^- asymmetric and symmetric stretching bands at 1513 and 1404/1406 cm^{-1} ; Otero *et al.*, 2014). Considering the results described above, it was unexpected that an oil paint solely composed of pure monoclinic lead chromate, in the absence of CaCO_3 and $\text{CaSO}_4 \cdot 2\text{H}_2\text{O}$ (the formulation which is the most light-sensitive), would exhibit such significant degradation.

After 8500h of irradiation, while it was still possible to encounter unaltered regions at the surface of the paint, the most common spectra found is presented in Figure 4.22Bb¹³⁹. The degradation of the

¹³⁸ Unfortunately, the paint-out exposed to ambient conditions for 6 years which was available for the photodegradation experiment was too small to perform accurate colourimetric measurements throughout the irradiation time.

¹³⁹ This heterogeneous behaviour was also observed in the 6 year old paint-out, before irradiation.

oil binder is evident in the transformation of the CH stretching profile between 3010-2810 cm^{-1} , the high intensity and broadening of the C=O stretching band deviated to 1722 cm^{-1} and the broad band centred at 3435 cm^{-1} which relates to the presence of hydroxyl oxidation products. There is also an increase in the lead carboxylate content (see also SEM images in Figure XIX.14, p. 368). The COO^- asymmetric band appears deviated to higher wavenumbers, most probably due to the overlap with bands from carbonyl oxidation products. Also visible are the infrared bands of an oxalate compound ($\nu_{\text{as}}(\text{COO}^-)$ at 1620 cm^{-1} ; ($\nu_{\text{s}}(\text{COO}^-)$ at 1312 cm^{-1} ; ($\delta(\text{COO}^-)$ at 780 cm^{-1}) however its precise characterisation is not possible¹⁴⁰. The loss of lead chromate is also distinctive as evidenced by the low intensity of its characteristic band.

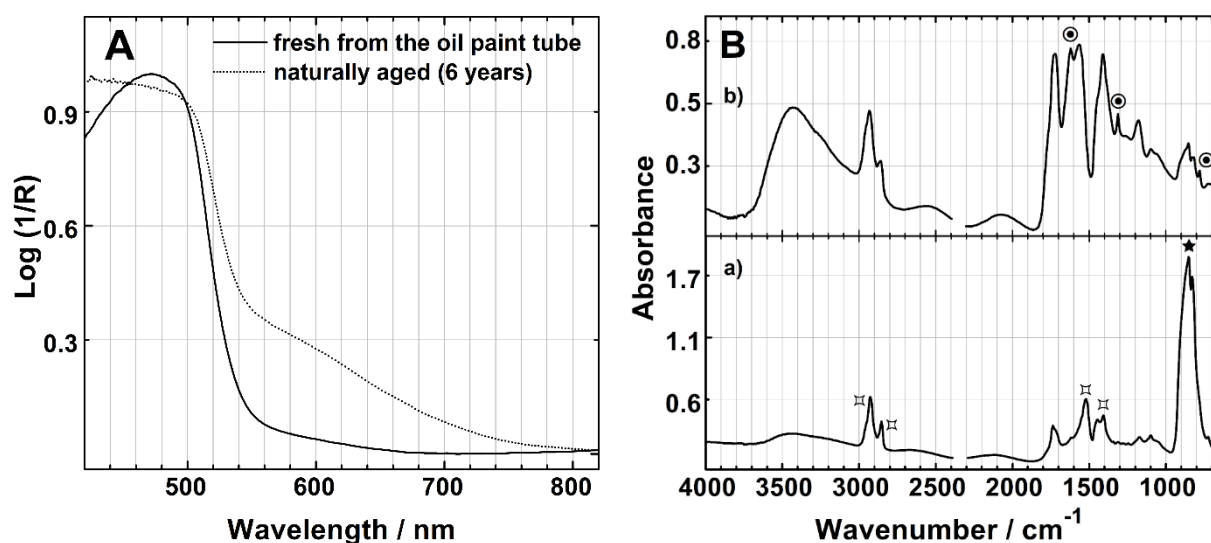


Figure 4.22. A) Normalized FORTS and B) infrared spectra of the historic *Lefranc Jaune de Chrome* oil paint a) fresh taken from the oil paint tube and b) exposed to ambient conditions for 6 years then exposed to irradiation with a Xenon lamp ($\lambda_{\text{irr}} > 300 \text{ nm}$); (★) PbCrO_4 , (⊐) lead azelate and (⊙) oxalate compound.

SR μ -FTIR, μ -XRF and Cr K-edge μ -XANES analysis were carried out on cross-sections of the non-irradiated sample from the 6 year old paint-out and on a sample after 5250h of irradiation with a Xenon Lamp, Figure 4.23. SR μ -XRD mapping of a cross-section after 8500h only revealed the presence of pure monoclinic lead chromate at the surface of the oil paint, Figure XIX.15 (p. 368).

The heterogeneous degradation described above was also observed by SR based techniques on the same sample, before and after irradiation. As may be seen in Figure 4.23A, SR μ -XRF mapping¹⁴¹ shows the heterogeneous distribution of chromium and lead in the non-irradiated sample. The regions where only lead is detected are most probably those rich in oil/lead azelate. Interestingly, Cr K-edge μ -XANES analysis performed on these regions shows a higher reduction of Cr^{6+} from lead chromate, however no Cr^{3+} species were identified by any of the techniques used, even after irradiation.

¹⁴⁰ The infrared bands are similar to those of calcium and lead oxalate. The presence of calcium ions was not detected by XRF.

¹⁴¹ The SR μ -XRF maps at different energies, 5.993 keV for Cr^{6+} and 6.1 for other Cr species such as Cr^{3+} are not shown here because the maps did not show any trends.

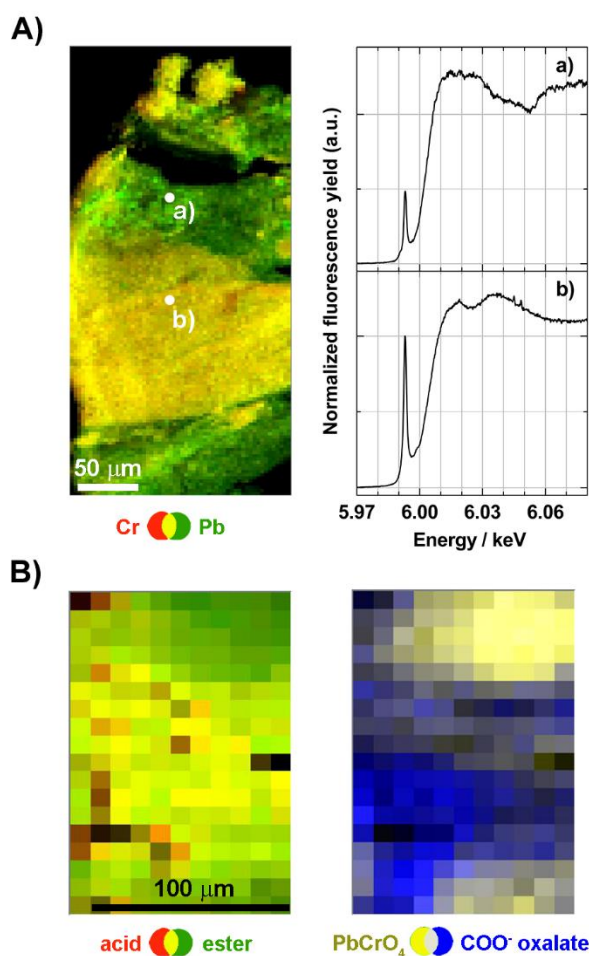


Figure 4.23. A) SR μ -XRF maps at 5.993 keV of Cr and Pb (map size: $171 \times 426 \mu\text{m}^2$, with $3 \times 3 \mu\text{m}^2$ step size) and the Cr K-edge μ -XANES spectra acquired at a) and b) of a cross-section from the *Lefranc Jaune de Chrome* oil paint before irradiation (aged in ambient conditions for 6 years); B) SR μ -FTIR maps (size: $180 \times 110 \mu\text{m}^2$, with $10 \times 10 \mu\text{m}^2$ step size) of an embedding-free cross-section from the *Lefranc Jaune de Chrome* oil paint after 5250h of irradiation, ROI: acids ($1718\text{-}1700 \text{ cm}^{-1}$), esters ($1755\text{-}1720 \text{ cm}^{-1}$), oxalate compounds ($1615\text{-}1555 \text{ cm}^{-1}$), lead chromate ($920\text{-}800 \text{ cm}^{-1}$); see also Figures XIX.15 and XIX.16 (p. 368).

4.2. Conclusions

This is the first study of the photochemical degradation of chrome yellow that successfully combines the use of historically accurate reconstructions as references with the analytical power of Synchrotron Radiation based techniques. This complementary approach enabled the discovery at the micro-scale, of the nature and distribution of the degradation products and intermediaries, thereby disclosing the sequence of steps that result in the degradation of chrome yellow oil paints. It also demonstrates that the photostability of chrome yellow pigments, in addition to the reported factors of

Figure 4.23B shows the uneven distribution of the oil paint components and oxalate compounds by μ -FTIR mapping. Likely due to the initial heterogeneity of the sample prior to irradiation, no gradient induced by light can be identified and the role of the photochemical exposure of the binder on the degradation pathway cannot be confirmed. However, due to the acidification of the binder, it can be proposed that the formation of oxalate compounds may follow the mechanism previously described by eqns. 4.9 to 4.11 (p. 114). Moreover, it is possible to see that there is almost no overlap between the lead chromate and oxalate regions, which may suggest that also in this case, one reacts with the other leading to the reduction of Cr^{6+} as depicted in eq. 4.6 (p. 110). No correlation with the degradation phenomenon was found with the presence of lead azelate, Figure XIX.16 (p. 368), nevertheless, it seems that the presence of azelate may accelerate the degradation rate of this oil paint formulation. Further photochemical studies of the *Lefranc Jaune de Chrome* oil paint must be undertaken in order to understand what are the triggers for such a rapid degradation.

crystalline structure and environmental conditions (light, temperature and humidity), is influenced by their manufacturing conditions, in particular the pH during the production of the $\text{PbCr}_{x-1}\text{S}_x\text{O}_4$ crystals.

By means of micro X-ray Absorption Near-Edge Structure (μ -XANES), a Light Susceptibility Index was developed for chrome yellow formulations based on the ratio of the Cr K pre-edge intensity after/before irradiation. This ratio decreases as the quantity of Cr^{3+} degradation species increases. Three degrees of lightfastness were identified: 1) $\text{PbCr}_{1-x}\text{S}_x\text{O}_4$ with $0 \leq x \leq 0.4/0.5$, 2) $\text{PbCr}_{1-x}\text{S}_x\text{O}_4$ with $x \geq 0.4/0.5$ and 3) PbCrO_4 admixed with a high quantity of the extenders chalk (CaCO_3) and gypsum ($\text{CaSO}_4 \cdot 2\text{H}_2\text{O}$), the latter being the most light-sensitive formulation. This tool will allow the prediction of light-sensitivity of chrome yellow paints in works of art.

The high spatial resolution provided by SR based techniques allowed the detection of a photochemically induced gradient that revealed a fundamental piece of evidence concerning the degradation of chrome yellow paints: the role played by oxalate ions. This work proposes that oxalates are formed due to the decomposition of carbonate compounds (CaCO_3 and/or $\text{MgCO}_3 \cdot x\text{H}_2\text{O}$, present as pigment/paint additives), in acidic media or via decarboxylation of carboxylic acids from the oil. Triggered by the photodegradation of the oil binder, oxalic acid and metal oxalates are able to induce the reduction of Cr^{6+} from lead chromate to Cr^{3+} compounds. Oxalic acid and metal oxalates were detected by infrared spectroscopy. The identification of calcium oxalate in the weddellite form ($\text{CaC}_2\text{O}_4 \cdot 2\text{H}_2\text{O}$) was achieved by SR X-ray diffraction but Ca K-edge XANES also suggested its presence. For the first time, SR μ -FTIR was used for the unambiguous identification of the Cr^{3+} degradation product, chromium potassium sulfate ($\text{CrK}(\text{SO}_4)_2 \cdot 12\text{H}_2\text{O}$).

It was found that the degradation rate is closely dependent on the pigment and paint formulations, which necessarily include their additives. For the Middle oil paint, composed of pure monoclinic lead chromate and a high percentage of CaCO_3 and $\text{CaSO}_4 \cdot 2\text{H}_2\text{O}$, the latter compounds extensively promote the reduction of Cr^{6+} to Cr^{3+} and a thick layer of calcium oxalate in the weddellite form is formed at the surface of the paint, negatively impacting its colour. In this case, $\text{CaSO}_4 \cdot 2\text{H}_2\text{O}$ acts as a catalyst; its decomposition by the reduction of S^{6+} was detected by S K-edge XANES and the presence of S^{4+} species induces the formation of Cr^{3+} . The formation of the S^{6+} compound, CaSO_4 , was detected by μ -Raman and S K-edge XANES in the irradiated samples. The formulation of the historic W&N *Chrome Deep* oil paint composed of calcium carbonate and pure monoclinic lead chromate in a proportion of approximately 50:50 (with an additional percentage of magnesium carbonate) was the most lightfast of the oil paints studied. After irradiation, this paint presented a very thin superficial layer of calcium oxalate, which may be considered a protective coating: a *molecular patina*. The combination of CaCO_3 and $\text{CaSO}_4 \cdot 2\text{H}_2\text{O}$ was never found in W&N 19th century production records for their chrome yellow pigments, which demonstrates their commitment to supply the most durable products possible. For the W&N *Chrome Yellow* oil paint made of mixed crystals of lead chromate and lead sulfate ($\text{PbCr}_{0.6}\text{S}_{0.4}\text{O}_4$) with the addition of barium sulfate, the same degradation mechanism, described above, was observed due to the decomposition of magnesium carbonate, added as a paint additive. The presence of metal carboxylates was identified by μ -FTIR, however, no evidence of a correlation between them and the formation of metal oxalates was found.

The degraded samples now provide valuable reference materials for the development of new conservation-restoration treatments.

Chapter 5

General conclusions & Future research



Detail from painting *Untitled* by Amadeo de Souza-Cardoso, c.1917, Modern Collection / Calouste Gulbenkian Museum @ FCG

Chapter 5. General conclusions & Future research

This doctoral work demonstrates how art technological research can contribute to and strengthen chemical studies of the degradation of artists' materials. The use of highly characterised historically accurate reconstructions enabled an assessment of the original appearance of yellow chromate pigments and contributed to new knowledge regarding the photostability as well as the mechanisms leading to the degradation of chrome yellow (lead chromate) pigments in oil paint.

The W&N 19th Century Archive Database proved to be a unique source of information on the 19th century trade and manufacture of artists' materials. To further research overall in the technical investigation of historical artists materials, it is essential that this database is available to the community of professionals concerned with the conservation of cultural heritage. Access to their 19th century production records made it possible to carry out a thorough study of their manufacturing processes for yellow chromate pigments based on lead ($\text{PbCr}_{1-x}\text{S}_x\text{O}_4$; 64%), barium (BaCrO_4 ; 25%), zinc ($4\text{ZnCrO}_4 \cdot \text{K}_2\text{O} \cdot 3\text{H}_2\text{O}$; 9%) and strontium (SrCrO_4 ; 2%). Despite the high number of production records (286), an analysis of their records revealed that their main pigment formulations resulted from a limited number of synthetic pathways. This research showed that W&N's use of extenders in the production of their yellow chromate pigments was restricted to the lead chromates; most likely because these colours present a higher relative tinting strength compared with their other yellow chromate pigments. Furthermore, it was possible to infer from their production records that W&N was not manufacturing the less stable Primrose type of lead chromate (characterised by a pigment formulation composed of sulfur-rich $\text{PbCr}_{1-x}\text{S}_x\text{O}_4$) and strontium chromate pigments. Throughout this research, both in the analysis of the records and in the reconstruction of their pigments it became evident that W&N carried out systematic research to find the best manufacturing processes that resulted in the most durable products possible.

This investigation also determined that the pigments in historic oil paint tubes from W&N labelled *Chrome Yellow* and *Chrome Deep* were prepared in accordance to their production records entitled Lemon/Pale (composed of mixed crystals of lead chromate and lead sulphate, $\text{PbCr}_{1-x}\text{S}_x\text{O}_4$, with $x \leq 0.4$), and Middle/Deep (composed of pure lead chromate, PbCrO_4) respectively; together with extenders such as barytes (BaSO_4) pure or admixed with gypsum ($\text{CaSO}_4 \cdot 2\text{H}_2\text{O}$), and calcium carbonate (CaCO_3) specifically for Chrome Deep. In this study and in other investigations of the W&N 19th century archive the name given to the material in the production record was not always the same as names for products in their sales catalogues. This was the case for the chrome yellow pigments, hence the importance of the findings in this thesis which correlates the name of a paint on the label with the formula for the pigment manufacture in their archive. Full and straightforward access to the complete version of the W&N 19th century database, in particular to their pigment and paint manufacturing processes, will allow comprehensive investigation and research on the relationship between pigment formulations and paint formulation, from watercolour to oil. Reference samples, of the quality and detail as those created for this research are needed to further investigations into the authenticity and the degradation of artist's materials in historical cultural objects.

This research suggests that the presence of calcium carbonate in the W&N *Chrome Deep* pigment formulation and of magnesium carbonate ($\text{MgCO}_3 \cdot x\text{H}_2\text{O}$) in W&N's oil paints may be used as markers for W&N 19th century products. Further research must be conducted on 19th century manufacturing processes and products from other contemporary colourmen, such as Lefranc and Bourgeois, in order to confirm this hypothesis.

The historical accuracy of the pigment reconstructions carried out for this work was successfully validated by comparison with analyses of samples from paintings by Amadeo de Souza-Cardoso and from historic oil paints.

This work has resulted in physical reference materials (the reconstructed pigments and paints) and a library of analytical reference data including the spectral, morphological and crystal structure of the main yellow chromate pigment formulations used by W&N in the 19th century. This data is now available for more accurate characterisations of 19th century pigments and paints and may be used to develop the characterisation of W&N particular materials. Already the reconstructed pigments have proven to be valuable reference materials for the work of other researchers in support of their investigations¹⁴².

The photostability of lead chromate pigment formulations was assessed using colourimetry which was successfully correlated to the Light Susceptibility Index (LSI) developed for this thesis. This LSI is based on the ratio of the Cr K pre-edge intensity after/before irradiation, which decreases as the quantity of Cr^{3+} degradation species increases. Using the LSI it was possible to determine three degrees of lightfastness: 1) $\text{PbCr}_{1-x}\text{S}_x\text{O}_4$ with $0 \leq x \leq 0.4/0.5$, 2) $\text{PbCr}_{1-x}\text{S}_x\text{O}_4$ with $x \geq 0.4/0.5$ and 3) PbCrO_4 admixed with a high quantity of the extenders chalk (CaCO_3) and gypsum ($\text{CaSO}_4 \cdot 2\text{H}_2\text{O}$). This research also demonstrated that the pH at which the precipitation of the $\text{PbCr}_{x-1}\text{S}_x\text{O}_4$ crystals begins may play a determining role in their stability. Further studies of the manufacture of the $\text{PbCr}_{x-1}\text{S}_x\text{O}_4$ crystals and how the manufacturing conditions influence their crystal structure and solubility must be carried out. A more precise quantitative characterisation of these compounds will also be necessary and on that note, the complementary analysis by μ -FTIR and SR XRD is currently underway.

The degradation mechanisms that lead to the darkening of lead chromate paints were investigated using complementary techniques, the combination of which contributed new knowledge to the study of this phenomenon. In particular, the high spatial resolution given by synchrotron light allowed to uncover which paint and pigment components contribute to degradation in lead chromate pigments and oil paints. A degradation gradient induced by light was discovered and oxalic acid/metal oxalates were identified at the surface of oil paints where altered lead chromate pigment and reduced Cr^{3+} were also found. The role of an acidic environment resulting from the hydrolysis of the oil binder due to photodegradation was elucidated. This work demonstrated that in the presence of oxalate species, Cr^{6+} from lead chromate is transformed into Cr^{3+} species. The oxalic acid/metal oxalates result from the decomposition of the carbonate additives, calcium carbonate and/or magnesium carbonate, in acidic media or via decarboxylation of carboxylic acids. Although no other intermediaries capable of suffering oxidation and forming oxalic acid in contact with Cr^{6+} were detected, the latter

¹⁴² Samples from the lead chromate historically accurate reconstructions have been made available to the Van Gogh Museum and used in their investigation (Kirchner *et al.*, 2018; Geldof *et al.*, 2018).

degradation pathway still needs further evidences. For the set of oil paints studied, no correlation between the presence of metal carboxylates and the formation of metal oxalates was found, however, as demonstrated in this work, depending on the paint and pigment formulations, other degradation pathways may take place. The role of metal carboxylates is still unclear, and more pigment and paint formulations must be studied in order to fully evaluate all possible degradation pathways.

Most importantly, in order to fully establish the stability of the lead chromate pigment formulations, further experiments to determine the quantum yields for the photochemical reactions and verify how these may be influenced by external factors such as the pH should be performed.

These new findings on the intermediaries and final products of the degradation of chrome yellow paints will enhance the understanding of the mechanisms that lead to the degradation of these important artist's colours. The LSI promises to provide a method for predicting the stability of current pigments and paints which can lead to improved conditions for their display and storage. Furthermore, the degraded samples resulting from the photodegradation experiment are now available to be used as testing materials for new conservation treatments.

References



Image of historic paint tubes @ DCR FCT NOVA

References

- Alfaro, C. 2016. Fotobiografia. In Freitas, H., ed. *Catálogo Raisoné. Amadeo de Souza-Cardoso. Fotobiografia*. Lisbon: Calouste Gulbenkian Foundation, 2nd edition, pp. 19-326 (translated to English by Kennis Translations: Geoffrey Chan, Sandra Laranjeiro, Andrew Miller, José António Oliveira and Nicola Whyte in pp. 339-382).
- Alía, J. M., Edwards, H. G. M., Fernández, A., Prieto, M. 1999. *Fourier Transform Raman Spectroscopic Study of Ba(SO₄)_x(CrO₄)_{1-x} Solid Solution*. Journal of Raman Spectroscopy, 30, 105-114.
- Amat, A., Miliani, C., Fantacci, S. 2016. *Structural and Electronical Properties of the PbCrO₄ Chrome Yellow Pigment and of Its Light Sensitive Sulfate-Substituted Compounds*. RSC Advances, 6, 36336-36344.
- Amatore, C. & Savéant, J.-M. 1981. *Mechanism and Kinetic Characteristics of the Electrochemical Reduction of Carbon Dioxide in Media of Low Proton Availability*. Journal of the American Chemical Society, 103, 5021-5023.
- Andrade, S. C. 2009. *Jaime Isidoro, o pintor-divulgador que fez a vanguarda no Porto*. Accessed on the 10 June 2018. Available at: <http://www.publico.pt/culturaipsilon/jornal/jaime-isidoro-o-pintor-divulgador-que-fez--a-vanguarda-no-porto-292364>.
- Applin, D. M., Izawa, M. R. M., Cloutis, E. A., Goltz, D., Johnson, J. R. 2015. *Oxalate minerals on Mars?* Earth and Planetary Science Letters, 420, 127-139.
- Asokan, K., Jan, J. C., Chiou, J. W., Pong, W. F., Tseng, P. K., Lin, I. N. 2001. *X-ray absorption spectroscopy studies of Ba_{1-x}Ca_xTiO₃*, Journal of Synchrotron Radiation, 8, 839-841.
- ASTM. 2018. Accessed on the 10 June 2018. Available at: <http://www.astm.org/ABOUT/overview.html>.
- Atkins, P. W. & Jones, L. 1997. *Chemistry: Molecules, Matter, and Change*. New York: W. H. Freeman and Co., pp. 50 & 566-567.
- Ball, P. 2008. *Bright Earth: Art and the Invention of Color*. 3rd ed. London: Vintage, pp. 165-221.
- Ballhausen, C. J. & Liehr, A. D. 1958. *Intensities in Inorganic Complexes* Part II. Tetrahedral Complexes*. Journal of Molecular Spectroscopy, 2, 342-360.
- Banti, D., La Nasa, J., Tenorio, A. L., Modugno, F., van den Berg, K., Lee, J., Ormsby, B., Burnstock, A., Bonaduce, I. 2018. *A molecular study of modern oil paintings: investigating the role of dicarboxylic acids in the water sensitivity of modern oil paints*. RSC Advances, 8, 6001-6012.
- Bard, A. J., Parsons, R., Jordan, J. eds. 1985. *Standard Potentials in Aqueous Solution*. 1st ed. USA: CRC Press, 189-197 and 453-461.
- Bartecki, A. & Burgess, J. 2000. *The Colour of Metal Compounds*. Amsterdam: Gordon and Breach Science Publishers, pp. 63-67.

- Beltran, V., Salvadó, N., Butí, S., Cinque, G. 2015. *Micro infrared spectroscopy discrimination capability of compounds in complex matrices of thin layers in real sample coatings from artworks*. *Microchemical Journal*, 118, 115-123.
- Benner, S. A., Devine, K. G., Matveeva, L. N., Powell, D. H. 2000. *The missing organic molecules on Mars*. *Proceedings of the National Academy of Sciences*, 97, 2425-2430.
- Biblioteca de arte (FCG). 2018. Accessed on the 10 June 2018. Available at: <http://www.biblartepac.gulbenkian.pt/ipac20/ipac.jsp?session=144K3P063B195.76169&profile=ba&menu=tab13&ts=1444320637195#>.
- Bomford, D., Kirby, J., Leighton, J., Roy, A. 1990. *Art in the making, Impressionism*. National Gallery Publications Ltd. pp. 32-43, 51-72.
- Bonaventura, M. P., Gallo, M., Cacchio, P., Ercole, C., Lepidi, A. 1999. *Microbial Formation of Oxalate Films on Monument Surfaces: Bioprotection or Biodeterioration?* *Geomicrobiology Journal*, 16, 55-64.
- Boon, J. J., Peulvé, S., Van den Brink, O. F., Duursma, M. C., Rainford, D. 1997. Molecular aspects of mobile and stationary phases in ageing tempera and oil paint films. In: Bakkenist, T., Hoppenbrouwers, R., Dubois, H. eds. *Early Italian Paintings, Techniques and Analysis*. Limburg Conservation Institute, pp. 35-56.
- Boon, J.J., Van der Weerd, J., Keune, K., Noble, P., Wadum, J. 2002. Mechanical and chemical changes in Old Master paintings: dissolution, metal soap formation and remineralization processes in lead pigmented ground/intermediate paint layers of 17th century paintings. In: Vontobel, R. ed. *Preprints of the ICOM-CC 13rd Triennial Meeting, Rio de Janeiro*, vol. 1, pp. 401-406.
- Boon, J. J. 2006. Processes inside paintings that affect the picture: chemical changes at, near and underneath the paint surface. In Boon, J. J., Ferreira, E. S. B. eds. *Reporting Highlights of the De Mayerne Programme*. The Netherlands: Netherlands Organisation for Scientific Research (NWO), pp. 21-32.
- Boon, J. J., Hoogland, F. G., Keune, K. 2007. Chemical processes in aged oil paints affecting metal soap migration and aggregation. In: Mar Parkin, H. ed. *AIC paintings specialty group postprints*. Washington: AIC, pp. 16-23.
- Bordignon, F., Postorino, P., Dore, P., Tabasso, M. L. 2008. *The Formation of Metal Oxalates in the Painted Layers of a Medieval Polychrome on Stone, as Revealed by Micro-Raman Spectroscopy*. *Studies in Conservation*, 53 (3), 158-169.
- Brandt, K. 2005. Chromate Pigments. In: Buxbaum, G. & Pfaff, G. eds. *Industrial Inorganic Pigments*. 3rd ed. Weinheim: Wiley-VCH Verlag GmbH & Co KGaA, pp. 128-135.
- Burgos-Cara, A., Ruiz-Agudo, E., Rodriguez-Navarro, C. 2017. *Effectiveness of oxalic acid treatments for the protection of marble surfaces*. *Materials and Design*, 115, 82-92.
- Burnstock, A. R., Jones, C. G., Cressey, G. 2003. *Characterisation of Artists' Chromium-Based Yellow Pigments*. *Zeitschrift für Kunsttechnologie und Konservierung*, 17 (74), 74-84.

- Burnstock, A. & Van den Berg, K. J. 2014. Twentieth Century Oil Paint. The Interface between science and conservation and the challenges for modern oil paint research. In: Van den Berg, K. J., Burnstock, A., de Keijzer, M., Krueger, J., Learner, T., de Tagle, A., Heydenreich, G. eds. *Proceedings of the Issues in Contemporary Oil Paint Symposium*. Switzerland: Springer International Publishing, pp. 1-19.
- Butler, M. H. 1984. An Investigation of the Materials and Techniques Used by Paul Cezanne. *Preprints of the 12th Annual Meeting of the American Institute for Conservation*, pp. 20-33.
- Cameo. 2016. Accessed on the 29 February 2016. Available at: http://cameo.mfa.org/wiki/Main_Page.
- Campos, M. F. *forthcoming*. *Materials and techniques of the Portuguese Naturalism: the cases of Silva Porto and Marques de Oliveira*. PhD dissertation. Department of Conservation and Restoration (FCT NOVA).
- Cardon, D. 2007. *Natural Dyes. Sources, Tradition, Technology and Science*. London: Archetype Publications.
- Cariati, F., Rampazzi, L., Toniolo L., Pozzi. A. 2000. *Calcium Oxalate Films on Stone Surfaces: Experimental Assessment of the Chemical Formation*. *Studies in Conservation*, 45 (3), 180-188.
- Carlyle, L. 1993. *Authenticity and adulteration: What materials were 19th century artists really using?*. *The Conservator*, 17, 56-60.
- Carlyle, L. 2001. *The Artist's Assistant: Oil Painting Instruction Manuals and Handbooks in Britain, 1800-1900, with Reference to Selected Eighteenth-century Sources*. London: Archetype Publications.
- Carlyle, L. & Witlox, M. 2005. Historically accurate reconstructions of artists' oil painting materials. In: Clarke, M., Townsend J. & Stijnman, A. eds. *Art of the Past - Sources and Reconstructions*. London: Archetype Publications, pp. 53-59.
- Carlyle, L., with contributions by Witlox, M., Pilz, K., Chavannes, M., Baade, B. 2005. *HART Report, De Mayerne Programme 2002-2005* (unpublished).
- Carlyle, L., Boon, J. J., Haswell, R., Witlox, M. 2008. Historically accurate ground reconstructions for oil paintings. In: Townsend, J. H., Doherty, T., Heydenreich, G., Ridge, J. eds. *Preparation for Painting. The artist's choice and its consequences*. London: Archetype Publications, pp. 110-122.
- Carlyle, L., Alves, P., Otero, V., Melo, M. J., Vilarigues, M. 2011. A question of scale and terminology, extrapolating from past practices in commercial manufacture to current laboratory experience: the Winsor & Newton 19th century artists' materials archive database. In: Bridgland, J. ed. *Preprints of the ICOM-CC 16th Triennial Meeting*, Lisbon, Paper 0102.
- Carlyle, L. 2012a. Practical Considerations for Creating Historically Accurate Reconstructions. In: Kroustallis, S. & Del Egido, M. eds. *Fatto d'Archimia – Los Pigmentos Artificiales en las Técnicas Pictóricas*. Espana: Ministerio de Educacion, Cultura y Deporte, Villena Artes Gráficas, pp. 105-117.
- Carlyle, L. 2012b. Exploring the grammar of oil paint through the use of historically accurate reconstructions. In Stoner, J. H. & Rushfield, R. eds. *Conservation of Easel Paintings*. 1st ed. Abingdon, Oxon [England], New York, NY: Routledge, pp. 33-38.

- Carneiro, A. 2006. *Elementos da história da química do século XVIII. Boletim da sociedade Portuguesa de Química*, 102, 25-31.
- Casadio, F., Fiedler, I., Gray, K. A., Warta, R. 2008. Deterioration of zinc potassium chromate pigments: elucidation the effects of paint composition and environmental conditions on chromatic alteration. In: Bridgland, J. ed. *Preprints of the ICOM-CC 15th Triennial Meeting*, New Delhi, Allied Publishers, pp. 572-580.
- Casadio, F., Xie, S., Rukes, S. C., Myers, B., Gray, K. A., Warta, R., Fiedler, I. 2011. *Electron energy loss spectroscopy elucidates the elusive darkening of zinc potassium chromate in Georges Seurat's A Sunday on La Grande Jatte-1884*. *Analytical and Bioanalytical Chemistry*, 399, 2909-2920.
- Castele, K. V., Geiger, H., De Loose, R., Van Sumere, C. F. 1983. *Separation of some anthocyanidins, anthocyanins, proanthocyanidins and related substances by reversed-phase high-performance liquid chromatography*. *Journal of Chromatography*, 259, 291-300.
- Castro, K., Sarmiento, A., Martínez-Arkarazo, I., Madariaga, J. M., Fernández L. A. 2008. *Green Copper Pigments Biodegradation in Cultural Heritage: From Malachite to Moolooite, Thermodynamic Modeling, X-ray Fluorescence, and Raman Evidence*. *Analytical Chemistry*, 80, 4103-4110.
- Chang, R. 1994. *Química*. 5th ed. Portugal: McGraw-Hill, pp. 757-759.
- Clarke, M. & Carlyle, L. 2005a. Page-image recipe databases, a new approach for accessing art technological manuscripts and rare printed sources: the Winsor & Newton archive prototype. In: Bridgland, J. ed. *Preprints of the ICOM-CC 14th Triennial Meeting*, The Hague, vol. I. London: James & James, pp. 24-29.
- Clarke, M. & Carlyle, L. 2005b. Page-image Recipe Databases: A New Approach to Making Art Technological Manuscripts and Rare Printed Sources Accessible. In: Clarke, M., Townsend J. & Stijnman, A. eds. *Art of the Past - Sources and Reconstructions*. London: Archetype Publications, pp. 49-52.
- Clarke, M. 2008. Nineteenth-century English artists' colourmen's archives as a source of technical information. In Kroustallis, S., Townsend, J., Bruquetas, E., Stijnman, A., Moya, M. S. A. eds. *Art Technology - Sources and Methods*. London: Archetype Publications, pp. 75-84.
- Clarke, M. 2009. A nineteenth-century colourman's terminology. *Studies in Conservation*, 54, 160-169.
- Clarke, M. 2012. *Software User Guide for the Winsor & Newton 19th Century Archive Database* (unpublished).
- Centeno, S. A.; Mahon, D. 2009. *The Chemistry of Aging in Oil Paintings: Metal Soaps and Visual Changes*. *The Metropolitan Museum of Art Bulletin, New Series*, vol. 67, pp. 12-19.
- ColArt. 2015. Accessed on the 13 November 2015. Available at: <http://www.colart.com/group-operations/>
- Constantin, S. 2001. *The Barbizon Painters: A Guide to Their Suppliers*. *Studies in Conservation*, 46 (1), 49-67.

- Conti, C., Brambilla, L., Colombo, C., Dellasega, D., Gatta, G. D., Realini, M., Zerbi, G. 2010. *Stability and transformation mechanism of weddellite nanocrystals studied by X-ray diffraction and infrared spectroscopy*. Physical Chemistry Chemical Physics, 12, 14560-14566.
- Conti, C., Casati, M., Colombo, C., Realini, M., Brambilla, L., Zerbi, G. 2014. *Phase transformation of calcium oxalate dihydrate–monohydrate: Effects of relative humidity and new spectroscopic data*. Spectrochimica Acta Part A: Molecular and Biomolecular Spectroscopy, 128, 413-419.
- Corbeil, M. C., Charland J. P., Moffatt, E. 2002. *The characterization of cobalt violet pigments*. Studies in Conservation, 47, 237-249.
- Cornman, M. 1986. Cobalt Yellow (Aureolin). In Feller, R. L. ed. *Artists' Pigments. A Handbook of their History and Characteristics*, 1st ed. Cambridge: Cambridge University Press and Washington: National Gallery of Art., vol. 1, pp. 37-46.
- Correia, A. M., Clark, R. J. H., Ribeiro, M. I. M., Duarte, M. L. T. S. 2007. *Pigment Study by Raman microscopy of 23 paintings by the Portuguese artist Henrique Pousão (1859-1884)*. Journal of Raman Spectroscopy, 38 (11), 1390-1405.
- Cotte, M., Checroun, E., Susini, J., Dumas, P., Tchoreloff, P., Besnard, M., Walter, Ph. 2006a. *Kinetics of oil saponification by lead salts in ancient preparations of pharmaceutical lead plasters and painting lead mediums*. Talanta, 70, 1136-1142.
- Cotte, M., Susini, J., Metrich, N., Moscato, A., Gratziu. C., Bertagnini, A., Pagano, M. 2006b. *Blackening of Pompeian Cinnabar Paintings: X-ray Microspectroscopy Analysis*. Analytical Chemistry, 78, 7484-7492.
- Cotte, M., Checroun, E., Susini, J., Walter, Ph. 2007. *Micro-analytical study of interactions between oil and lead compounds in paintings*. Applied Physics A, 89, 841-848.
- Cotte, M., Susini, J., Sole, V., Taniguchi, Y., Chillid, J., Checroun, E., Walter, P. 2008. *Applications of synchrotron-based micro-imaging techniques to the chemical analysis of ancient paintings*. Journal of Analytical Atomic Spectrometry, 23, 820-828.
- Cotte, M., Checroun, E., Nolf, W., Taniguchi, Y., Viguerie, L., Burghammer, M., Walter, P., Rivard, C., Salomé, M., Janssens, K., Susini, J. 2017a. *Lead soaps in paintings: Friends or foes?*. Studies in Conservation, 62 (1), 2-23.
- Cotte, M., Pouyet, E., Salomé, M., Rivard, C., De Nolf, W., Castillo-Michel, H., Fabris, T., Monico, L., Janssens, K., Wang, T., Sciau, P., Verger, L., Cormier, L., Dargaud, O., Brun, E., Bugnazet, D., Fayard, B., Hesse, B., Pradas del Real, A. E., Veronesi, G., Langlois, J., Balcar, N., Vandenberghe, Y., Solé, V. A., Kieffer, J., Barrett, R., Cohen, C., Cornu, C., Baker, R., Gagliardini, E., Papillon, E., Susini, J. 2017b. *The ID21 X-ray and infrared microscopy beamline at the ESRF: status and recent applications to artistic materials*. Journal of Analytical Atomic Spectrometry, 32, 477-493.
- Cotton, F. A., Wilkinson, G., Murillo, C. A., Bochmann. M. 1999. *Advanced Inorganic Chemistry*. 6th ed. New York: John Wiley & Sons, pp. 736-756.
- Cove, S. 1991. Constable's Oil Painting Materials and Techniques. In Parris, L. and Fleming-Williams, I., ed. *Constable, exhibition catalogue*. London: Tate Gallery, pp. 493-529.

- Cowley, A. C. D. 1986. *Lead Chromate – That Dazzling Pigment*. Coloration Technology: Review of Progress in Coloration and Related topics, Society of Dyers and Colourists, vol. 1, issue 1, 16-24.
- Coyle, J. D. 1978. *Photochemistry of Carboxylic Acid Derivatives*. Chemical Reviews, 78, 2, 97-123.
- Crane, M. J., Leverett, P., Shaddick, L. R., Williams, P. A., Kloprogge, J. T., Frost, R. L. 2001. *The PbCrO₄-PbSO₄ System and its Mineralogical Significance*. Neues Jahrbuch für Mineralogie-Monatshefte, 11, 505–519.
- Cruz, A. J. 2005. *A pintura de Columbano Segundo as suas Caixas de Tintas e Pincéis*. Conservar o Património, Associação Profissional de Conservadores-Restauradores de Portugal, nº 1, 5-19.
- De Mayerne Programme. 2006. Accessed on the 17 June 2018. Available at:
http://assets.kennislink.nl/upload/181089_391_1193921849265-HighlightsMayerne.pdf
- De Nolf, W., Vanmeert, F., Janssens, K. 2014. *XRDUA: crystalline phase distribution maps by two-dimensional scanning and tomographic (micro) X-ray powder diffraction*. Journal of Applied Crystallography, 47, 1107-1117.
- Denisov, E. T. & Shestakov, A. F. 2013. *Free-Radical Decarboxylation of Carboxylic Acids as a Concerted Abstraction and Fragmentation Reaction*. Kinetics and Catalysis, 2013, 54, 1, 22-33.
- Doherty, B., Pamplona, M., Selvaggi, R., Miliani, C., Matteini, M., Sgamellotti, A., Brunetti, B. *Efficiency and resistance of the artificial oxalate protection treatment on marble against chemical weathering*. Applied Surface Science, 253, 4477-4484.
- Eastaugh, N., Walsh, V., Chaplin, T. Siddall, R. 2004. *The Pigment Compendium, a Dictionary of Historical Pigments*. 1st ed. Oxford: Elsevier Butterworth-Heinemann.
- ECHA. 2018a. Accessed on the 10 June 2018. Available at:
https://echa.europa.eu/substance-information/-/substanceinfo/100.014.267#OTHER_NAMEScontainer
- ECHA. 2018b. Accessed on the 10 June 2018. Available at:
<http://echa.europa.eu/regulations/reach/understanding-reach>
- Erkens, L. J. H., Hamers, H., Hermans, R. J. M., Claeys, E., Bijnens, M. 2001. *Lead chromates: A review of the state of the art in 2000*. Surface Coatings International Part B: Coatings Transactions, 84 (3), 169-176.
- EUR-Lex. 2018. Accessed on the 10 June 2018. Available at: <http://eur-lex.europa.eu/legal-content/EN/TXT/?uri=CELEX%3A32014R0301>.
- Fairbairn, L., Beal, M., Winsor & Newton 1982. *Paint & painting: An exhibition and working studio sponsored by Winsor & Newton to celebrate their 150th anniversary*. London: Tate Gallery.
- FCT. 2009. Accessed on the 10 June 2018. Available at:
https://www.fct.pt/apoios/projectos/consulta/vglobal_projecto.phtml.en?idProjecto=113612&idElemConcurso=3665.
- Ferraz, A. 2018. *Materiais e técnicas da pintura a óleo em Portugal (1836-1914): Estudo das fontes documentais*. PhD dissertation. Department of Conservation and Restoration (FCT NOVA).

- Ferreira, E. S. B., Boon, J. J., Stampanoni, M., Marone, F. 2011. Study of the mechanism of formation of calcium soaps in an early 20th century easel painting with correlative 2D and 3D microscopy. In: Bridgland, J. ed. *Preprints of the ICOM-CC 16th Triennial Meeting, Lisbon*, Paper 1604.
- Ferreira, J. L., Melo, M. J., Ramos, A. M. 2010. *Poly(vinyl acetate) paints in works of art: A photochemical approach. Part 1*. *Polymer Degradation and Stability*, 95, 453-461.
- Ferreira, P. 1981. *Correspondance de quatre artistes portugais. Almada Negreiros, José Pacheco, Souza Cardoso, Eduardo Viana, avec Robert et Sonya Delaunay*. 2nd ed. Lisbon: Calouste Gulbenkian Foundation.
- Fiedler, I. 1984. Materials Used in Seurat's La Grande Jatte, Including Color Changes and Notes on the Evolution of the Artist's Palette. *Preprints of the 12th Annual Meeting of the American Institute for Conservation*, pp. 43–51.
- Field, G. 1835. *Chromatography or a Treatise on Colours and Pigments and of their Powers in Painting, &c*. London: Tilt, 1835.
- França, J. A. 1956. *Amadeo de Souza-Cardoso*. Lisbon: Editorial Sul.
- França, J. A. 1960. *Amadeo de Souza-Cardoso 1887-1918*. Lisbon: Artis.
- França, J. A. 1986. *Amadeo & Almada*. Lisbon: Bertrand Editora.
- França, J.A. 1992. *As últimas pinturas de Amadeo de Souza-Cardoso*. In *Amadeo de Souza-Cardoso 1887-1918*. Porto: Ed. Fundação de Serralves, pp. 23-26.
- França, J. A. 2009. *A Arte em Portugal no século XX (1911-1961)*. 4th ed. Lisbon: Livros Horizonte.
- Freitas, H. (coord.) 2006. *Amadeo de Souza-Cardoso, Diálogo de vanguardas*. Lisbon: Calouste Gulbenkian Foundation.
- Freitas, H. (coord.) 2007. *Catálogo Raisonné. Amadeo de Souza-Cardoso. Fotobiografia*. Volume 1. Lisbon: Assírio & Alvim and Calouste Gulbenkian Foundation.
- Freitas, H. (coord.) 2008. *Catálogo Raisonné. Amadeo de Souza-Cardoso. Pintura*. Volume 2. Lisbon: Assírio & Alvim and Calouste Gulbenkian Foundation.
- Freitas, H. 2008a. Elements on the critical reception of Amadeo de Souza-Cardoso. In Freitas, H., ed. *Catálogo Raisonné. Amadeo de Souza-Cardoso. Pintura*. Volume 2. Lisbon: Assírio & Alvim and Calouste Gulbenkian Foundation, pp. 441-444.
- Freitas, H. 2008b. Amadeo de Souza-Cardoso - 1887-1918. In Freitas, H., ed. *Catálogo Raisonné. Amadeo de Souza-Cardoso. Pintura*. Volume 2. Lisbon: Assírio & Alvim and Calouste Gulbenkian Foundation, pp. 17-37, 422-435.
- Freitas, H. (coord.) 2016. *Amadeo de Souza-Cardoso*. Exhibition catalogue. Paris: Réunion des musées nationaux-Grand Palais and Calouste Gulbenkian Foundation.
- Frost, R. L. 2004. *Raman microscopy of selected chromate minerals*. *Journal of Raman Spectroscopy*, 35 (2), 153-158.

- Fuller, W. R. 1968. Inorganic Chemical Color Pigments. Lead Chromate Yellows and Oranges. In *Federation Series on Coatings Technology – Inorganic Color Pigments*, Unit Eight, Pennsylvania: Federation of Societies for Paint Technology, pp. 35-36.
- Gage J. 2001. *A Romantic Colourman: George Field and British art*. Walpole Society, vol. 63, pp.1-73.
- Garfield, S. 2000. *Mauve: How One Man Invented a Colour that Changed the World*. London: Faber and Faber.
- Gautier, G. Bezur, A., Muir, K., Casadio, F., Fiedler, I. 2009. *Chemical Fingerprinting of Ready-Mixed House Paints of Relevance to Artistic Production in the First Half of the Twentieth Century. Part I: Inorganic and Organic Pigments*. *Journal of Applied Spectroscopy*, 63 (6), 597-603.
- Geldof, M., Megens, L., Salvant, J. 2013a. Van Gogh's Palette in Arles, Saint-Rémy and Auvers-sur-Oise. In Vellekoop, M., Geldof, M., Hendriks, E., Jansen, L., Tagle, A. de. eds. *Van Gogh Studio Practice*, Brussels: Mercatorfonds. pp. 238-255.
- Geldof, M., Keijzer de, M., Bommel van, M., Pilz, K., Salvant J., Keulen van, H., Megens, L. 2013b. Van Gogh's Geranium lake. In Vellekoop, M., Geldof, M., Hendriks, E., Jansen, L., Tagle, A. de. eds. *Van Gogh Studio Practice*, Brussels: Mercatorfonds. pp. 268-289.
- Geldof, M., Gaibor, A. N. P., Ligterink, F., Hendriks, E., Kirchner, E. 2018. *Reconstructing Van Gogh's palette to determine the optical characteristics of his paints*. *Heritage Science*, 6:17.
- Gettens, R. J., Feller, R. L., Chase, W. T. 1993a. Vermillion and Cinnabar. In Roy, Ashok, ed. *Artists' Pigments. A Handbook of Their History and Characteristics*, 1st ed. New York: Oxford University Press, Washington: National Gallery of Art, vol. 2, pp. 159-182.
- Gettens, R. J., Kühn, H, Chase, W. T. 1993b. Lead White. In Roy, Ashok, ed. *Artists' Pigments. A Handbook of Their History and Characteristics*, 1st ed. New York: Oxford University Press, Washington: National Gallery of Art, vol. 2, pp. 67-81.
- Gibson, C. S. & Matthews, E. 1985. LXXIX. – Lead Subacetate Solution ("Goulard's Extract") and its Reaction with Phenols. *Journal of the Chemical Society*, 596 – 601.
- Gonçalves, R. M. 2006. *Amadeo de Souza-Cardoso, a ânsia da originalidade*. In Almeida, B. P. (dir.) *Caminhos da Arte Portuguesa no século XX*. Lisbon: Editorial Caminho.
- Gray, A. 1988. Lead Chrome Pigments. In Lewis, P. A. ed. *Pigments Handbook. Properties and economics*. vol. 1. New York: Wiley-Interscience Publication, 2nd ed., pp. 315-325.
- Greenwood, N. N. & Earnshaw, A. 1984. *Chemistry of the Elements*. London: Butterworth Heinemann, pp. 1167-1178.
- Gysau, D. 2006. *Fillers for Paints: Fundamentals and Applications*. Hannover: Vincentz Network, p. 21.
- Harley, R. D. 1971. *Oil colour containers: Development work by artists and colourmen in the nineteenth century*. *Annals of Science*, 27, 1-12.
- Harley, R. D. 1975. Background & development of the Artist Colourmen. In *A brief history of Winsor & Newton*. Harrow: Winsor & Newton, Ltd., pp. 3-5.

- Harley, R. D. 1982 & 2001. *Artists' Pigments c. 1600–1835: A Study in English Documentary Sources*, the 2001 edition is reprinted from the second revised edition, 1982, with an additional article on new watercolours in the nineteenth century, London: Archetype publications Ltd.
- Herbst, W. & Hunger, K. 2004. *Industrial Organic Pigments*. 3rd ed. Weinheim: Wiley-VCH Verlag GmbH & Co KGaA, pp. 1.
- Hermans, J. J., Keune, K., Van Loon, A., Iedema, P. D. 2015. *An infrared spectroscopic study of the nature of zinc carboxylates in oil paintings*. *Journal of Analytical Atomic Spectrometry*, 30, 1600-1608.
- Hermans, J. J., Keune, K., Van Loon, A., Iedema, P. D. 2016a. *The crystallization of metal soaps and fatty acids in oil paint model systems*. *Physical Chemistry Chemical Physics*, 18, 10896-10905.
- Hermans, J. J., Keune, K., Van Loon, A., Corkery, R. W., Iedema, P. D. 2016b. *Ionomer-like structure in mature oil paint binding media*. *RSC Advances*, 6, 93363-93369.
- Hermans, J. J. 2017. *Metal Soaps in Oil Paint - Structure, Mechanisms and Dynamics*. PhD dissertation. University of Amsterdam.
- Hesse, B., Salome, M., Castillo-Michel, H., Cotte, M., Fayard, B., Sahle, C. J., De Nolf, W., Hradilova, J., Masic, A., Kanngießer, B., Bohner, M., Varga, P., Raum, K., Schrof, S. 2016. *Full-Field Calcium K-Edge X-ray Absorption Near-Edge Structure Spectroscopy on Cortical Bone at the Micron-Scale: Polarization Effects Reveal Mineral Orientation*, *Analytical Chemistry*, 88, 3826-3835.
- Homburg, E. 1992. The emergence of research laboratories in the dyestuffs industry, 1870-1900. In *Organic Chemistry and High Technology, 1850-1950*. *The British Journal for the History of Science*, 25, 65-90.
- Hornix, W. J. 1992. From process to plant: innovation in the early artificial dye industry. In *Organic Chemistry and High Technology, 1850-1950*. *The British Journal for the History of Science*, 25, 65-90.
- Hummel, D. O. 2002. *Atlas of Plastics Additives. Analysis by Spectrometric Methods*. Berlin: Springer-Verlag.
- Hummel, W., Anderegg, G., Rao, L., Puigdomènech, I., Tochiyama, O. 2005. Chemical Thermodynamics of compounds and complexes of U, Np, Pu, Am, Tc, Se, Ni and Zr with selected organic ligands (review). In F. J. Mompean, M. Illemassène, OECD Nuclear Energy Agency Data Bank, eds. *Chemical Thermodynamics*. Vol. 9. North Holland Elsevier Science Publishers B. V., Amsterdam, The Netherlands, pp. 164-177.
- IUPAC, 2018. Accessed on the 10 June 2018. *Compendium of Chemical Terminology*, 2nd ed. (the "Gold Book"). Compiled by A. D. McNaught and A. Wilkinson. Blackwell Scientific Publications, Oxford (1997). XML on-line corrected version: <http://goldbook.iupac.org> (2006-) created by M. Nic, J. Jirat, B. Kosata; updates compiled by A. Jenkins.
- Janssens, K., Van der Snickt, G., Vanmeert, F., Legrand, S., Nuyts, G., Alfeld, M., Monico, L., Anaf, W., De Nolf, W., Vermeulen, M., Verbeeck, J., De Wael, K. 2016a. *Non-Invasive and Non-Destructive Examination of Artistic Pigments, Paints, and Paintings by Means of X-Ray Methods*. *Topics in Current Chemistry (Z)*, 374, 81.

- Kahrim, K., Daveri, A., Rocchi, P., de Cesare, G., Cartechini, L., Miliani, C., Brunetti, B.G., Sgamellotti A. 2009. *The application of in situ mid-FTIR fibre-optic reflectance spectroscopy and GC-MS analysis to monitor and evaluate painting cleaning*. *Spectrochimica Acta Part A*, 74, 1182-1188.
- Kaiser, T., Grossi, L., Fischer, H. 1978. *Free Radical Formation from Excited States of Aliphatic Carboxylic Acids and Esters in Solution as Studied by Electron Spin Resonance*. *Helvetica Chimica Acta*, 61, 16, 223-233.
- Katlan, A. W. 1987. *American Artists' Materials Suppliers Directory: Nineteenth Century, New York 1810-1899, Boston 1823-1887*. Park Ridge, N. J.: Noyes Press.
- Keijzer, M. 1999. A survey of red and yellow modern synthetic organic artist's pigments discovered in the 20th century and used in oil colours. *Preprints of the ICOM-CC 12th Triennial Meeting, Lyon*. vol. I. London: James & James. pp. 369-380.
- Keijzer, M. 2001. The history of modern synthetic inorganic and organic artists' pigments. In Mosk, J. A. & Tennant, N. H. eds. *Contributions to Conservation: Research in Conservation at the Netherlands Institute for Cultural Heritage (ICN)*, London: James and James, pp. 42-54.
- Keune, K. & Boon, J. J. 2007. *Analytical Imaging Studies of Cross-Sections of Paintings Affected by Lead Soap Aggregate Formation*. *Studies in Conservation*, 52, 161-176.
- Keune, K., Boon, J. J., Boitelle, R., Shimadzu, Y. 2013. *Degradation of Emerald green in oil paint and its contribution to the rapid change in colour of the Descente des vaches (1834-1835) painted by Théodore Rousseau*. *Studies in Conservation*, 58, 199-210.
- Keune, K. & Boevé-Jones, G. 2014. Its Surreal: Zinc-Oxide Degradation and Misperceptions in Salvador Dalí's Couple with Clouds in Their Heads, 1936. In: Van den Berg, K. J., Burnstock, A., de Keijzer, M., Krueger, J., Learner, T., de Tagle, A., Heydenreich, G. eds. *Proceedings of the Issues in Contemporary Oil Paint Symposium*. Switzerland: Springer International Publishing, pp. 283-294.
- Killik, W. E. 1925. *A short history of the house of Winsor & Newton Ltd*. Winsor & Newton Library (Turner Room), typescript.
- Kirby, J., Stonor, K., Roy, A., Burnstock, A., Grout, R., White, R. 2003. *Seurat's Painting Practice: Theory, Development and Technology*. National Gallery Technical Bulletin, 28, pp. 4-37.
- Kirchner, E., van der Lans, I., Ligterink, F., Geldof, M., Megens, L., Meedendorp, T., Pilz, K., Hendriks, E. 2018. *Digitally reconstructing Van Gogh's Field with Irises near Arles part 3: Determining the original colors*. *Color Research & Application*, 43, 311-327.
- Klein, C. 2002. *Manual of Mineral Science*, 22nd ed, New York, Chichester, Weinheim, Brisbane, Singapore, Toronto: John Wiley & Sons, Inc., pp. 91-92. & 428.
- Kortright, J. B., Thompson, A. C. 2009. X-ray Emission Energies. In: Thompson, A., Lindau, I., Attwood, D., Liu, Y., Gullikson, E., Pianetta, P., Howells, M., Robinson, A., Kim, K., Scofield, J., Kirz, J., Underwood, J., Kortright, J., Williams, G., Winick, H. eds. *X-Ray Data Booklet*. 3rd ed. California: Berkeley, University of California, Lawrence Berkeley National Laboratory, pp. 1-9-13.

- Krieg, S. 2005. Anticorrosive pigments. In: Buxbaum, G. & Pfaff, G. eds. *Industrial Inorganic Pigments*. 3rd ed. Weinheim: Wiley-VCH Verlag GmbH & Co KGaA, pp. 212-214.
- Kühn, H. & Curran, M. 1986. Chrome Yellow and Other Chromate Pigments. In Feller, R. L. ed. *Artists' Pigments. A Handbook of their History and Characteristics*, 1st ed. Cambridge: Cambridge University Press and Washington: National Gallery of Art., vol. 1, pp. 187-200, 208-211.
- Labreuche, P. 2018. *Guide historique des fournisseurs de matériel pour artistes à Paris 1790 - 1960*. Accessed on the 10 June 2018. Available at: <http://www.labreuche-fournisseurs-artistes-paris.fr/>.
- Lashof, T. W. 1943. *The Electrical Conductivity of Lead Chromate*. Journal of Chemical Physics, 11, 196-202.
- Lau, Joanne. 2005. *An investigation into the effects of manufacturing conditions on the particle morphology of lead chromate and madder lake pigments* (part of The Pigmentum Project). Master dissertation. Forensic & Drug Monitoring School of Life Sciences. King's College London.
- Lazzari, M. & Chiantore, O. 1999. *Drying and oxidative degradation of linseed oil*. Polymer Degradation and Stability, 65, 303-313.
- Leal, J. C. 2010. *Amadeo de Souza-Cardoso*. Accessed on the 10 June 2018. Available at: <http://gulbenkian.pt/cam/artist/amadeo-de-souza-cardoso/>.
- Levere, T. H. 2001. *Transforming Matter: A History of Chemistry from Alchemy to the Buckyball*. Baltimore and London: Johns Hopkins University Press.
- Liang, J., Peng, Q., Wang, X., Zheng, X., Wang, R., Qiu, X., Nan, C., Li, Y. 2005. *Chromate Nanorods/Nobelts: General Synthesis, Characterization, and Properties*. Inorganic Chemistry, 44, 9405-9415.
- Lide, D. R., ed. 2006. *CRC Handbook of Chemistry and Physics*. 87th ed. USA: CRC Press.
- Lindéngruppen, 2018. Accessed on the 10 June 2018. Available at: <http://lindengruppen.com/businesses/colart>
- Lliveras, A., Boularand, S., Roqué, J., Cotte, M., Giráldez, P., Vendrell-Saz M. 2008. *Weathering of gilding decorations investigated by SR: development and distribution of calcium oxalates in the case of Sant Benet de Bages (Barcelona, Spain)*. Applied Physics A, 90 (1), 23-33.
- Lliveras, A., Boularand, S., Andreotti, A., Vendrell-Saz M. 2010. *Degradation of azurite in mural paintings: distribution of copper carbonate, chlorides and oxalates by SRFTIR*. Applied Physics A, 99, 363-375.
- Lunz, M., Talgorn, E., Baken, J., Wagemans, W., Veldman, D. 2017. *Can LEDs help with art conservation? - Impact of different light spectra on paint pigment degradation*. Studied in Conservation, 62, 294-303.
- Mallécol, J., Gardette, J.-L., Lemaire, J. 1999. *Long-Term Behavior of Oil-Based Varnishes and Paints I. Spectroscopic Analysis of Curing Drying Oils*. Journal of the American Oil Chemists' Society, 76, 967-976.

- Mass, J. L., Opila, R., Buckley, B., Cotte, M., Church, J., Mehta, A. 2013. *The photodegradation of cadmium yellow paints in Henri Matisse's Le Bonheur de vivre (1905–1906)*. Applied Physics A, 111, 59-68.
- Maravelaki-Kalaitzaki, P. 2005. *Black crusts and patinas on Pentelic marble from the Parthenon and Erechtheum (Acropolis, Athens): characterization and origin*. Analytica Chimica Acta, 532, 187-198.
- Martell, A. E. & Smith, R. M. eds. 1982. *Critical Stability Constants, Volume 5: First Supplement*. Springer Science+Business Media New York (originally published by Plenum Press, New York), pp. 398.
- Mayo, D., Miller, F., Hannah, R. eds. 2004. *Course Notes on the Interpretation of Infrared and Raman Spectra*. John Wiley & Sons, Inc., Hoboken, New Jersey.
- Meilunas, R. J., Bentsen, J. G., Steinberg, A. 1990. *Analysis of aged paint binders by FTIR spectroscopy*. Studies in Conservation, 35, 33-51.
- Melo, M. J. 2009. History of Natural Dyes in the Ancient Mediterranean World. In *Handbook of Natural Colorants*. John Wiley & Sons: Hoboken, NJ, USA, pp. 3-20.
- Melo, M. J., Vilarigues, M., Babo, S., Alfaro, C., Freitas, H. and Sandu, I. 2009. *Estudo dos materiais e técnicas de Amadeo de Souza-Cardoso*. Technical report. Department of Conservation and Restoration (FCT NOVA).
- Mentzen, B. F., Latrach, A., Bouix, J. 1984. *The Crystal Structure of $PbO.PbXO_4$ ($X = S, Cr, Mo$) at 5K by Neutron Powder Profile Refinement*. Materials Research Bulletin, 19 (5), 549-554.
- Miliani, C., Sgamellotti, A., Kahrim, K., Brunetti, B.G., Aldrovandi, A., Van Bommel, M. R., Van den Berg, K. J., Janssen, H. 2008. MOLAB, a mobile facility suitable for non-invasive in-situ investigations of early and contemporary paintings: case study - Victory Boogie Woogie (1942-1944) by Piet Mondrian. In Bridgland J. ed. *Proceedings of the 15th Triennial Conference ICOM Committee for Conservation*, New Delhi, Allied Publishers, vol. 2, 244-251.
- Miliani, C., Daveri, A., Spaabaek, L., Romani A., Manuali, V., Sgamellotti, A., Brunetti B. G. 2010. *Bleaching of red lake paints in encaustic mummy portraits*. Applied Physics A, 100, 703-711.
- Mittal, L. J., Mittal, J. P., Hayon E. 1973. *Photo-Induced Decarboxylation of Aliphatic Acids and Esters in Solution. Dependence upon State of Protonation of the Carboxyl Group*. The Journal of Physical Chemistry, 77, 12, 1482-1487.
- Monico, L., Van der Snickt, G., Janssens, K., Nolf, W., Miliani, C., Verbeeck, J., Tian, H., Tan, H., Dik, J., Radepon, M., Cotte, M. 2011a. *Degradation Process of Lead Chromate in Paintings by Vincent van Gogh Studied by Means of Synchrotron X-ray Spectromicroscopy and Related Methods. 1. Artificially Aged Model Samples*. Analytical Chemistry, 83, 1214-1223.
- Monico, L., Van der Snickt, G., Janssens, K., Nolf, W., Miliani, C., Verbeeck, J., Tian, H., Tan, H., Dik, J., Radepon, M., Hendriks, E., Geldof, M., Cotte, M. 2011b. *Degradation Process of Lead Chromate in Paintings by Vincent van Gogh Studied by Means of Synchrotron X-ray Spectromicroscopy and Related Methods. 2. Original Paint Layer Samples*. Analytical Chemistry, 83, 1224-1231.

- Monico, L., Janssens, K., Miliani, C., Brunetti, B. G., Vagnini, M., Vanmeert, F., Falkenberg, G., Abakumov, A., Lu, Y., Tian, H., Verbeeck, J., Radepont, M., Cotte, M., Hendriks, E., Geldof, M., Loeff, L., Salvant, J., Menu, M. 2013a. *Degradation Process of Lead Chromate in Paintings by Vincent van Gogh Studied by Means of Spectromicroscopic Methods. 3. Synthesis, Characterization, and Detection of Different Crystal Forms of the Chrome Yellow Pigment*. Analytical Chemistry, 85, 851-859.
- Monico, L., Janssens, K., Miliani, Van der Snickt, G., C., Brunetti, B. G., Guidi, M., Radepont, M., Cotte, M. 2013b. *Degradation Process of Lead Chromate in Paintings by Vincent van Gogh Studied by Means of Spectromicroscopic Methods. 4. Artificial Aging of Model Samples of Co-Precipitates of Lead Chromate and Lead Sulfate*. Analytical Chemistry, 85, 860-867.
- Monico, L., Rosi, F., Miliani, C., Daveri, A., Brunetti, B. G. 2013c. *Non-invasive identification of metal-oxalate complexes on polychrome artwork surfaces by reflection mid-infrared spectroscopy*. Spectrochimica Acta Part A, 116, 270-280.
- Monico, L. Janssens, K., Hendriks, E., Brunetti, B. G., Miliani, C. 2014a. *Raman study of different crystalline forms of $PbCrO_4$ and $PbCr_{1-x}S_xO_4$ solid solutions for the noninvasive identification of chrome yellows in paintings: a focus on works by Vincent van Gogh*. Journal of Raman Spectroscopy, 45, 1034-1045.
- Monico, L., Janssens, K., Vanmeert, F., Cotte, M., Brunetti, B. G., Van der Snickt, G., Leeuwestein, M., Plisson, J. S., Menu, M., Miliani, C. 2014b. *Degradation Process of Lead Chromate in Paintings by Vincent van Gogh Studied by Means of Spectromicroscopic Methods. Part 5. Effects of Nonoriginal Surface Coatings into the Nature and Distribution of Chromium and Sulfur Species in Chrome Yellow Paints*. Analytical Chemistry, 86, 10804-10811.
- Monico, L., Janssens, K., Alfeld, M., Cotte, M., Vanmeert, F., Ryan, C. G., Falkenberg, G., Howard, D. L., Brunetti, B. G., Miliani, C. 2015a. *Full spectral XANES imaging using the Maia detector array as a new tool for the study of the alteration process of chrome yellow pigments in paintings by Vincent van Gogh*. Journal of Analytical Atomic Spectrometry, 30, 613-626.
- Monico, L., Janssens, K., Cotte, M., Romani, A., Sorace, L., Grazia, C., Brunetti, B. G., Miliani, C. 2015b. *Synchrotron-based X-ray spectromicroscopy and electron paramagnetic resonance spectroscopy to investigate the redox properties of lead chromate pigments under the effect of visible light*. Journal of Analytical Atomic Spectrometry, 30, 1500-1510.
- Monico, L., Janssens, K., Hendriks, E., Vanmeert, F., Van der Snickt, G., Cotte, M., Falkenberg, G., Brunetti, B. G., Miliani, C. 2015c. *Evidence for Degradation of the Chrome Yellows in Van Gogh's Sunflowers: A Study Using Noninvasive In Situ Methods and Synchrotron-Radiation-Based X-ray Techniques*. Angewandte Chemie International Edition, 54, 13923-13927.
- Monico, L., Janssens, K., Cotte, M., Sorace, L., Vanmeert, F., Brunetti, B. G., Miliani, C. 2016. *Chromium speciation methods and infrared spectroscopy for studying the chemical reactivity of lead chromate-based pigments in oil medium*. Microchemical Journal, 124, 272-282.

- Monico, L., Chieli, A., De Meyer, S., Cotte, M., De Nolf, W., Falkenberg, G., Janssens, K., Romani, A., Miliani, C. 2018. Role of the Relative Humidity and the Cd/Zn Stoichiometry in the Photooxidation Process of Cadmium Yellows (CdS/Cd_{1-x}Zn_xS) in Oil Paintings. *Chemistry A European Journal*, 24, 1584-11593.
- Montagner, C. 2015. *The brushstroke and materials of Amadeo de Souza-Cardoso combined in an authentication tool*. PhD dissertation. Department of Conservation and Restoration (FCT NOVA). Available on-line at: <http://hdl.handle.net/10362/14777>.
- Montagner, C., Jesus, R., Correia, N., Vilarigues, M., Macedo, R., Melo, M. J. 2016. *Features combination for art authentication studies: brushstroke and materials analysis of Amadeo de Souza-Cardoso*. *Multimedia Tools and Applications*, 75 (7), 4039-4063.
- Moya, M. S. A., Fernández-Villa, S. G. 2008. Patents as a source of documentation for studying art technology. In Kroustallis, S., Townsend, J., Bruquetas, E., Stijnman, A., Moya, M. S. A. eds. *Art Technology - Sources and Methods*. London: Archetype Publications, pp. 64-74.
- Muñoz-García, A., Massaro, A., Pavone, M. 2016. *Ab Initio Study of PbCr_(1-x)S_xO₄ Solid Solution: an Inside Look at Van Gogh Yellow Degradation*. *Chemical Science*, 7, 4197-4203.
- MUHNAC. 2012. Accessed on the 10 March 2012. Available at: <http://www.mc.ul.pt/patrimonio/laboratorio-chimico/galeria/historicas>.
- Myers, R. J. 2010. *One-Hundred Years of pH*. *Journal of Chemical Education*, 87 (1), 30-32.
- Nakamoto, K. 2009. *Infrared and Raman Spectra of Inorganic and Coordination Compounds, Theory and Applications in Inorganic Chemistry*, 6th ed. Wiley-Interscience.
- Nevin, A., Melia, J. L., Osticioli, I., Gautier, G., Colombini, M. P. 2008. *The identification of copper oxalates in a 16th century Cypriot exterior wall painting using micro FTIR, micro Raman spectroscopy and Gas Chromatography-Mass Spectrometry*. *Journal of Cultural Heritage*, 9, 154-161.
- Newman, R. 1997. Chromium Oxide Greens. Chromium Oxide and Hydrated Chromium Oxide. In Fitzhugh, E. W., ed. *Artists' Pigments. A Handbook of their History and Characteristics*, 1^a ed. Cambridge: Cambridge University Press and Washington: National Gallery of Art, vol. 3, pp. 273-293.
- Noble, P., Van Loon, A., Boon, J. J. 2005. Chemical changes in old master paintings II: darkening due to increased transparency as a result of metal soap formation processes. In Bridgland, J. ed. *Preprints of the ICOM-CC 14th Triennial Meeting, The Hague*, vol. 1, pp. 496-503.
- Oakley, L. H., Casadio, F., Shull, K. R., Broadbelt, L. J. 2015. *Microkinetic modeling of the autoxidative curing of an alkyd and oil-based paint model system*. *Applied Physics A*, 121, 869-878.
- Orna, M. V. 1980. *Chemistry and Artists' Colors. Part III. Preparation and properties of artist pigments*. *Journal of Chemical Education*, vol. 57, n^o 4, 267-269.
- Osawa, Z. 1988. *Role of Metals and Metal-Deactivators in Polymer Degradation*. *Polymer Degradation and Stability*, 20, 203-236.
- Osmond, G. Ebert, B., Drennan, J. 2014. *Zinc oxide-centred deterioration in 20th century Vietnamese paintings by Nguyễn Trọng Kiệm (1933–1991)*. *AICCM Bulletin*, 34, 4-14.

- Otero, V., Carlyle, L., Vilarigues, M., Melo, M. J. 2012. *Chrome yellow in nineteenth century art: historical reconstructions of an artists' pigment*. RSC Advances, 2 (5), 1798-1805.
- Otero, V., Sanches, D., Montagner, C., Vilarigues, M., Carlyle, L., Lopes, J. A., Melo, M. J. 2014. *Characterisation of metal carboxylates by Raman and infrared spectroscopy in works of art*. Journal of Raman Spectroscopy, 45, 1197-1206.
- Panopticon Lavoisier. 2018. Accessed on the 10 June 2018. Available at: <http://moro.imss.fi.it/lavoisier/>.
- Pantelouris, A., Modrow H., Pantelouris M., Hormes J., Reinen D. 2004. *The influence of coordination geometry and valency on the K-edge absorption near edge spectra of selected chromium compounds*. Chemical Physics, 300, 13-22.
- Pavey, D. & Staples, P. 1984. *The artists' colourmen's story. A guide to the history of artists' colourmen of London as illustrated in the artists' colourmen's room at the Winsor & Newton Colour Works at Wealdstone*. Wealdstone: Reckitt & Colman Leisure Limited.
- Perthue, A., Thérias, S., Gardette, J.-L., Boyer, D. & Boutinaud, P. 2013. *Photodegradation of down-converting composites for application as coatings for organic solar cells*. Poster presented at the International Symposium Frontiers in Polymer Science. 21–23 May, Sitges, Spain, [P3.111].
- Pina, F., Mulazzani, Q. G., Venturi, M., Ciano, M., Balzani, V. 1985. *Photochemistry of Co(sep)³⁺-Oxalate Ion Pairs: A Novel System for Dihydrogen Evolution from Aqueous Solutions*. Inorganic Chemistry, 24, 848-851.
- Plater, M. J., De Silva, B., Gelbrich, T., Hursthouse, M. B., Higgitt, C. L., Saunders, D. R. 2003. *The characterisation of lead fatty acid soaps in 'protrusions' in aged traditional oil paint*. Polyhedron, 22, 3171-3179.
- Poli, T., Piccirillo, A., Zoccali, A., Conti, C., Nervo, M., Chiantore, O. 2014. *The role of zinc white pigment on the degradation of shellac resin in artworks*. Polymer Degradation and Stability, 102, 138-144.
- Poli, T., Piccirillo, A., Nervo, M., Chiantore, O. 2017. *Interactions of natural resins and pigments in works of art*. Journal of Colloid and Interface Science, 503, 1-9.
- Pourbaix, M. 1963. *Atlas d'équilibres électrochimiques*. Paris: Gauthier-Villars & Cie, pp. 256-271.
- Pouyet, E., Lluveras-Tenorio, A., Nevin, A., Saviello, D., Sette, F., Cotte, M. 2014. *Preparation of thin-section of painting fragments: Classical and innovative strategies*. Analytica Chimica Acta, 822, 51-59.
- Pouyet, E., Cotte, M., Fayard, B., Salomé, M., Meirer, F., Mehta, A., Uffelman, E. S., Hull, A., Vanmeert, F., Kieffer, J., Burghammer, M., Janssens, K., Sette, F., Mass, J. 2015. *2D X-ray and FTIR micro-analysis of the degradation of cadmium yellow pigment in paintings of Henri Matisse*. Applied Physics A, 121, 967-980.
- Prati, S., Bonacini, I., Sciutto, G., Genty-Vincent, A., Cotte, M., Eveno, M., Menu, M., Mazzeo, R. 2016. *ATR-FTIR microscopy in mapping mode for the study of verdigris and its secondary products*. Applied Physics A, 122: 10.

- Pyle, D. & Pearce, E. eds. 2001. *The Oil Colour Book: A comprehensive resource for painters*. Middlesex (England): Winsor & Newton, Colart Fine Art and Graphics Limited, pp. 1-91.
- Quareni, S. & De Pieri, R. 1965. *A three-dimensional refinement of the structure of crocoite, PbCrO₄*. *Acta Crystallographica*, 19, 287-289.
- Rahemi, V., Sarmadian, N., Anaf, W., Janssens, K., Lamoen, D., Partoens, B., De Wael, K. 2017. *Unique opto-electronic structure and photo reduction properties of sulfur doped lead chromates explaining their instability in paintings*. *Analytical Chemistry*, 89 (6), 3326-3333.
- Rampazzi, L., Andreotti, A., Bonaduce, I., Colombini, M. P., Colombo, C., Toniolo, L. 2004. *Analytical investigation of calcium oxalate films on marble monuments*. *Talanta*, 63, 967-977.
- Ricci, C., Miliani, C., Brunetti, B. G., Sgamellotti, A. 2006. *Non-invasive identification of surface materials on marble artifacts with fiber optic mid-FTIR reflectance spectroscopy*. *Talanta*, 69 (5), 1221-1226.
- Roncaglia, D. I., Botto, I. L., Baran, E. J. 1985. *Vibrational spectrum of Pb₂CrO₅*. *Journal of Materials Science Letters*, 4 (11), 1427-1428.
- Roth-Meyer, C. 2005. *Les marchands de couleurs à Paris au XIXe siècle*. Thèse doctorat: Histoire de l'art, Paris 4, 2004. Université Paris-Sorbonne. Lille: Atelier national de Reproduction des Thèses.
- RSC Periodic Table. 2018. Accessed on the 10 June 2018. Available at: <http://www.rsc.org/periodic-table>.
- S4a-Paint. 2016. Accessed on the 04 May 2016. Available at: <http://www.s4a-paint.uva.nl/>.
- Salvadó, N., Pradell, T., Pantos, E., Papiz, M. Z., Molera, J., Seco, M., Vendrell-Saz, M. 2002. *Identification of copper-based green pigments in Jaume Huguet's Gothic altarpieces by Fourier transform infrared microspectroscopy and synchrotron radiation X-ray diffraction*. *Journal of Synchrotron Radiation*. 9, 215-222.
- Salvadó, N., Butí, S., Nicholson, J., Emerich, H., Labrador, A., Pradell T. 2009. *Identification of reaction compounds in micrometric layers from gothic paintings using combined SR-XRD and SR-FTIR*. *Talanta*, 79, 419-428.
- Salvadó, N., Butí, S., Cotte, M., Cinque, G., Pradell, T. 2013. *Shades of green in 15th century paintings: combined microanalysis of the materials using synchrotron radiation XRD, FTIR and XRF*. *Applied Physics A*, 111, 47-57.
- Sanches, D., Ramos, A. M., Coelho, J. F. J., Costa, C. S. M. F., Vilarigues, M., Melo, M. J. 2017. *Correlating thermophysical properties with the molecular composition of 19th century chrome yellow oil paints*. *Polymer Degradation and Stability*, 138, 201-211.
- Santos, S. B. 2011. Pigmentos Vermelhos na Pintura Portuguesa no Século XIX: Análise da Literatura Técnica e Estudo Comparativo de Preços no Fim do Século. In Calvo, A. & Casto, L. coord. *Através da Pintura: Olhares sobre a Matéria. Estudos sobre pintores no Norte de Portugal*. Porto: Clássica - Artes Gráficas, S.A. pp. 128 and 134.

- Salomé, M., Cotte, M., Baker, R., Barrett, R., Benseny-Cases, N., Berruyer, G., Bugnazet, D., Castillo-Michel, H., Cornu, C., Fayard, B., Gagliardini, E., Hino, R., Morse, J., Papillon, E., Pouyet, E., Rivard, C., Solé, V. A., Susini, J., Veronesi, G. 2013. *The ID21 Scanning X-ray Microscope at ESRF*. Journal of Physics: Conference Series, 425 (18), 182004.
- Shriver, D. F. & Atkins, P. W. 1999. *Inorganic Chemistry*. 3rd ed. OUP Oxford, pp. 329.
- Silva, A. M. 2018. *History, materials and techniques of an artists' book: La Légende de Saint Julien l'Hospitalier by Amadeo de Souza-Cardoso*. PhD dissertation. Department of Conservation and Restoration (FCT NOVA). Available on-line at: <http://hdl.handle.net/10362/31764>.
- Silvester, G., Burnstock, A., Megens, L., Learner, T., Chiari, G., Van den Berg, K. J. 2014. *A cause of water-sensitivity in modern oil paint films: The formation of magnesium sulphate*. Studies in Conservation, 59, 38-51.
- Simon, J. 2018. *British artists' suppliers, 1650-1950. Winsor & Newton*. Accessed on the 10 June 2018. Available at: <http://www.npg.org.uk/research/programmes/directory-of-suppliers/w>
- Simonsen, K. P., Christiansen, M. B., Vinum, M. G., Sanyova, J., Bendix, J. 2017. *Single crystal X-ray structure of the artists' pigment zinc yellow*. Journal of Molecular Structure, 1141, 322-327.
- Smith, M. B. & March, J. 2007. *March's Advanced Organic Chemistry. Reactions, Mechanisms and Structure*. 6th ed. Hoboken, New Jersey: John Wiley & Sons, Inc., pp. 1727, 1772.
- Solé, V.A., Papillon, E., Cotte, M., Walter, P., Susini, J. 2007. *A multiplatform code for the analysis of energy-dispersive X-ray fluorescence spectra*. Spectrochimica Acta B 62, 63-68.
- Solomons, T. W. G., Fryhle, C. B. 2000. *Organic Chemistry*. 7th ed. John Wiley & Sons, pp. 368.
- Sotiropoulou, S., Papiakia, Z. E., Vaccari, L. 2016. *Micro FTIR imaging for the investigation of deteriorated organic binders in wall painting stratigraphies of different techniques and periods*. Microchemical Journal, 124, 559-567.
- Sotiropoulou, S., Scitutto, G., Tenorio, A. L., Mazurek, J., Bonaduce, I., Prati, S., Mazzeo, R., Schilling, M., Colombini, M. P. 2018. *Advanced analytical investigation on degradation markers in wall paintings*. Microchemical Journal, 139, 278-294.
- Sousa, M. M., Melo, M. J., Parola, A. J., Morris, P. J. T., Rzepa, H. S., Melo, J. S. S. 2008. *A study in mauve. Unveiling Perkin's Dye in Historic Samples*. Chemistry A European Journal, 14, 8507-8513.
- Spring, M., Ricci, C., Peggie, D., Kazarian, S. 2008. *ATR-FTIR imaging for the analysis of organic materials in paint cross sections: case studies on paint samples from the National Gallery, London*. Analytical and Bioanalytical Chemistry, 392, 37-45.
- Stoilova, D., Georgiev, M., Marinova, D. 2005. *Infrared study of the vibrational behavior of CrO₄²⁻ guest ions matrix-isolated in metal (II) sulfates (Me = Ca, Sr, Ba, Pb)*. Journal of Molecular Structure, 738, 211-215.
- Sturm, E. V., Frank-Kamenetskaya, O., Vlasov, D., Zelenskaya, M., Sazanova, K., Rusakov, A., Kniep, R. 2015. *Crystallization of calcium oxalate hydrates by interaction of calcite marble with fungus Aspergillus niger*. American Mineralogist, 100, 2559-2565.

- Susini, J., Scheidt, K., Cotte, M., Dumas, P., Polack, F., Chubar, O. 2005. *Why infrared spectromicroscopy at the ESRF?*, ESRF Newsletter, 41, 24-25.
- Švarcová, S., Hradil, D., Hradilová, J., Kočí, E., Bezdička, P. 2009. *Micro-analytical evidence of origin and degradation of copper pigments found in Bohemian Gothic murals*. Analytical and Bioanalytical Chemistry, 395, 2037-2050.
- Tan, H., Tian, H., Verbeeck, J., Monico, L., Janssens, K. & Tendeloo, G. 2013. *Nanoscale Investigation of the Degradation Mechanism of a Historical Chrome Yellow Paint by Quantitative Electron Energy Loss spectroscopy Mapping of Chromium Species*. Angewandte Chemie International Edition, 52, 11360-11363.
- Travis, A. S. 2006. *Decadence, Decline and Celebration: Raphael Meldola and the Mauve Jubilee of 1906*. History and Technology: An International Journal, 22, 131-152.
- Townsend, J. H. 1993. *The Materials of J. M. W. Turner: Pigments*. Studies in Conservation, 38 (4), 231-254.
- Townsend, J. H., Carlyle, L., Khandekar, N., Woodcock, S. 1995. *Later nineteenth century pigments: Evidence for additions and substitutions*. The Conservator, 19, 65-78.
- Townsend, J. H. 2002. *The materials used by British oil painters throughout the nineteenth century*. Reviews in Conservation, 3, 46-55.
- Tumosa, C. S. & Mecklenburg, M. F. 2005. *The influence of lead ions on the drying of oils*. Reviews in Conservation, 6, 39-47.
- Van den Berg, J. D. J. 2002. *Analytical chemical studies on traditional linseed oil paints*. (MolArt; 6), University of Amsterdam, pp. 9-52.
- Van der Snickt, G., Miliani, C., Janssens, K., Brunetti, B. G., Romani, A., Rosi, F., Walter, P., Castaing, J., De Nolf, W., Klaassen, L., Labarque, I., Wittermann R. 2011. *Material analyses of 'Christ with singing and music-making Angels', a late 15th-C panel painting attributed to Hans Memling and assistants: Part I. non-invasive in situ investigations*. Journal of Analytical Atomic Spectrometry, 26, 2216-2229.
- Van der Snickt, G., Janssens, K., Dik, J., De Nolf, W., Vanmeert, F., Jaroszewicz, J., Cotte, M., Falkenberg, G., Van der Loeff, L. 2012. *Combined use of Synchrotron Radiation Based Micro-X-ray Fluorescence, Micro-X-ray Diffraction, Micro-X-ray Absorption Near-Edge, and Micro-Fourier Transform Infrared Spectroscopies for Revealing an Alternative Degradation Pathway of the Pigment Cadmium Yellow in a Painting by Van Gogh*. Analytical Chemistry, 84, 10221-10228.
- Van der Weerd, J., Van Loon, A., Boon, J. J. 2005. *FTIR Studies of the Effects of Pigments on the Aging of Oil*. Studies in Conservation, 50, 3-22.
- Vanmeert, F., Hendriks, E., Van der Snickt, G., Monico, L., Dik, J., Janssens, K. 2018. *Chemical mapping by Macroscopic X-ray Powder Diffraction (MA-XRPD) of Van Gogh's Sunflowers: Identification of areas with higher degradation risk*. Angewandte Chemie International Edition, 130, 1-6.

- Vasconcelos, M. J. (coord.) 2016. *Amadeo de Souza-Cardoso, 2016-1916, Porto-Lisboa*. Porto: Museu Soares dos Reis & Blue Book.
- Vauquelin, L. N. 1809. *Mémoire sur la meilleure méthode pour décomposer le chrômate de fer, obtenir l'oxide de chrôme, préparer l'acide chrômique, et sur quelques combinaisons de ce dernier*. Annales de Chimie, 70, 70-94.
- Veiga, J. P. & Figueiredo, M. O. 2008. Calcium in ancient glazes and glasses: a XAFS study. Applied Physics A, 92, 229-233.
- Vibert, J.-G. 1891. *La Science de la Peinture*. Paris: Paul Ollendorff, p. 98, 285.
- Vibert, J.-G. 1892. *The Science of Painting*. Translated by Percy Young. London: Percy Young.
- Vilarigues, M., Melo, M. J., Babo, S., Alfaro, C., Freitas, H., Sandu, I. 2008. A Hand full of colours, the 20th century and the dawn of modern art. In Freitas, H., ed. *Catálogo Raisoné. Amadeo de Souza-Cardoso. Pintura*. Volume 2. Lisbon: Assírio & Alvim and Calouste Gulbenkian Foundation, pp. 81-104, 445-455.
- Vitorino, T., Melo, M. J., Carlyle, L., Otero, V. 2015. *New insights into brazilwood manufacture through the use of historically accurate reconstructions*. Studies in Conservation, 61 (5), 255-273.
- Vitorino, T., Otero, V., Carlyle, L., Melo, M. J., Parola, A. J., Picollo, M. 2017. Nineteenth-century cochineal lake pigments from Winsor & Newton: insight into their methodology through reconstructions. In *ICOM-CC 18th Triennial Conference Preprints*, Copenhagen, 2017, ed. J. Bridgland, art. 0107. Paris: International Council of Museums.
- Voras, Z. E., deGhetaldi, K., Wiggins, M. B., Buckley, B., Baade, B., Mass, J., Beebe Jr. T. P. 2015. *ToF-SIMS imaging of molecular-level alteration mechanisms in Le Bonheur de vivre by Henri Matisse*. Applied Physics A, 121, 1015-1030.
- Xiang, J., Yu, S., Xu, Z. 2004. *Polymorph and Phase Discrimination of Lead Chromate Pigments by Facile Room Temperature Precipitation Reaction*. Crystal Growth & Design, 4 (6), 1311-1315.
- Watson, V. & Clay, H. F. 1955. *The lightfastness of lead chrome pigments*. Journal of the Oil and Colour Chemists' Association, 38, 167-175.
- Watts Collection. 2018. Accessed on the 10 June 2018. Available at: <https://www.npg.org.uk/research/archive/collected-archives/the-watts-collection/>.
- Wei, S., Pintus, V., Schreiner, M. 2012. *Photochemical degradation study of polyvinyl acetate paints used in artworks by Py-GC/MS*. Journal of Analytical and Applied Pyrolysis, 97, 158-163.
- Westheimer, F. H. 1949. *The Mechanisms of Chromic Acid Oxidations*. Chemical Reviews, 45, 419-451.
- Wetering, E. Van de 1995. Reflections on the Relation between Technique and Style: The Use of the Palette by the Seventeenth-Century Painter. In Wallert, A., Hermens, E., Peek, M. eds. *Historical Painting Techniques, Materials, and Studio Practice: Preprints of a Symposium Held at the University of Leiden, the Netherlands, 26-29 June, 1995*. Marina Del Rey, CA: Getty Conservation Institute, pp. 196-203.
- Weyl, W. A. 1999. *Coloured Glasses*. United Kingdom: Society of Glass Technology, pp. 136.

- Winsor & Newton Archive. 2009. Accessed on the 10 June 2018. Available at: <http://webapps.fitzmuseum.cam.ac.uk/wn/index.php>. See also: http://english.rkd.nl/Collections/Technical_Documentation/Winsor__Newton_database
- Winsor & Newton Archive. 2018. Accessed on the 10 June 2018. Available at: <http://webapps.fitzmuseum.cam.ac.uk/wn/search.php>.
- Winsor & Newton. 2014. *The Winsor & Newton Story (1832-2007)*. Accessed on the 30 January 2014. Available at: <http://www.winsornewton.com/about-us/our-history/>.
- Winsor & Newton. 2018. *Royal Warrant*. Accessed on the 10 June 2018. Available at: <http://www.winsornewton.com/row/discover/about-us/the-royal-warrant>.
- Wolfsberg, M. & Helmholz, L. 1952. *The Spectra and Electronic Structure of the Tetrahedral Ions MnO_4^- , CrO_4^{2-} , and ClO_4^-* . *Journal of Chemical Physics*, 20, 837-843.
- Woodcock, S. 1995. The Roberson Archive: content and significance. In Wallert, A., Hermens, E., Peek, M. eds. *Historical Painting Techniques, Materials, and Studio Practice: Preprints of a Symposium Held at the University of Leiden, the Netherlands, 26-29 June, 1995*. Marina Del Rey, CA: Getty Conservation Institute, pp. 30-37.
- Woodcock, S. 1996. *Leighton and Roberson: An Artist and His Colourman*. *The Burlington Magazine*, 138 (1121), pp. 526-528.
- Zanella, L., Casadio, F., Gray, K. A., Warta, R., Ma, Q., & Gaillard, J. 2011. *The darkening of zinc yellow: XANES speciation of chromium in artist's paints after light and chemical exposures*. *Journal of Analytical Atomic Spectrometry*, 26, 1090-1097.
- Zoppi, A., Lofrumento, C., Mendes, N. F. C., Castellucci, E. M. 2010. *Metal oxalates in paints: a Raman investigation on the relative reactivities of different pigments to oxalic acid solutions*. *Analytical and Bioanalytical Chemistry*, 397, 841-849.
- Zumbuehl, S., Scherrer, N. C., Berger A., Eggenberger, U. 2009. *Early Viridian Pigment Composition Characterization of a (Hydrated) Chromium Oxide Borate Pigment*. *Studies in Conservation*, 54, 149-159.

'(...) to evolve is a proof of life.'

Amadeo de Souza-Cardoso

1912

(Letter to Uncle Francisco)

Appendices



Image of a box with oil paint tubes with Amadeo's inscription, found at the Manhufe house, Amadeo's family collection @ Manhufe

Appendix I. Excerpts from *La science de la peinture* found in Amadeo's notebook

French version by Jehan-Georges Vibert (1891)	English version translated by Percy Young (1892)																					
<p><i>p. 47</i></p> <p>Cramoisi..... -----</p> <p>ROUGE..... ----- 1 impaire.</p> <p>Rouge-orange... -----</p> <p>ORANGE..... ----- 2 paire.</p> <p>Jaune-orange... -----</p> <p>JAUNE..... ----- 3 impaire.</p> <p>Jaune-vert..... ✖ point fixe.</p> <p>VERT..... ----- 4 paire.</p> <p>Bleu-vert..... -----</p> <p>BLEU..... ----- 5 impaire.</p> <p>Bleu-outremer... -----</p> <p>OUTREMER..... ----- 6 paire.</p> <p>Violet..... -----</p>	<p><i>p. 36</i></p> <p>Crimson..... -----</p> <p>Red..... ----- 1 odd.</p> <p>Red-orange..... -----</p> <p>Orange..... ----- 2 even.</p> <p>Yellow-orange... -----</p> <p>Yellow..... ----- 3 odd.</p> <p>Yellow-green..... ✖ fixed point.</p> <p>Green..... ----- 4 even.</p> <p>Bleu-green..... -----</p> <p>Bleu..... ----- 5 odd.</p> <p>Bleu-ultramarine -----</p> <p>Ultramarine..... ----- 6 even.</p> <p>Violet..... -----</p>																					
<p><i>p. 49</i></p> <p>Le moyen le plus simple de trouver tout de suite la complémentaire d'une couleur, c'est d'ajouter le nombre 3 au numéro qu'elle porte dans le spectre jusqu'au vert, et, à partir du vert, de retrancher au contraire ce nombre 3.¹⁴³</p>	<p><i>This sentence was not translated to the english version.</i></p>																					
<p><i>p. 50</i></p> <p><i>Exemple :</i></p> <p>La complémentaire</p> <table style="width: 100%; border-collapse: collapse;"> <thead> <tr> <th style="width: 30%;"></th> <th style="width: 10%; text-align: center;">Numéros</th> <th style="width: 60%;"></th> </tr> </thead> <tbody> <tr> <td>du rouge</td> <td style="text-align: center;">1</td> <td>est $1 + 3 = 4$ vert.</td> </tr> <tr> <td>de l'orange</td> <td style="text-align: center;">2</td> <td>est $2 + 3 = 5$ bleu.</td> </tr> <tr> <td>du jaune</td> <td style="text-align: center;">3</td> <td>est $3 + 3 = 6$ outremer.</td> </tr> <tr> <td>du vert</td> <td style="text-align: center;">4</td> <td>est $4 - 3 = 1$ rouge.</td> </tr> <tr> <td>du bleu</td> <td style="text-align: center;">5</td> <td>est $5 - 3 = 2$ orange.</td> </tr> <tr> <td>de l'outremer</td> <td style="text-align: center;">6</td> <td>est $6 - 3 = 3$ jaune.</td> </tr> </tbody> </table>		Numéros		du rouge	1	est $1 + 3 = 4$ vert.	de l'orange	2	est $2 + 3 = 5$ bleu.	du jaune	3	est $3 + 3 = 6$ outremer.	du vert	4	est $4 - 3 = 1$ rouge.	du bleu	5	est $5 - 3 = 2$ orange.	de l'outremer	6	est $6 - 3 = 3$ jaune.	<p><i>p. 37</i></p> <p><i>Example :</i></p> <p>The complement of red..... No. 1 is $1 + 3 = 4$, green.</p> <p>“ “ orange “ 2 “ $2 + 3 = 5$, blue.</p> <p>“ “ yellow “ 3 “ $3 + 3 = 6$, ultramarine.</p> <p>“ “ green “ 4 “ $4 - 3 = 1$, red.</p> <p>“ “ blue “ 5 “ $5 - 3 = 2$, orange.</p> <p>“ “ ultramarine 6 “ $6 - 3 = 3$, yellow.</p>
	Numéros																					
du rouge	1	est $1 + 3 = 4$ vert.																				
de l'orange	2	est $2 + 3 = 5$ bleu.																				
du jaune	3	est $3 + 3 = 6$ outremer.																				
du vert	4	est $4 - 3 = 1$ rouge.																				
du bleu	5	est $5 - 3 = 2$ orange.																				
de l'outremer	6	est $6 - 3 = 3$ jaune.																				

¹⁴³ In the notebook, Amadeo translated to Portuguese: *A maneira mais simples de achar a complementar duma cor é de juntar o número 3 ao número que ela tem no espectro até ao verde e a partir do verde... número 3.*

French version by Jehan-Georges Vibert (1891)	English version translated by Percy Young (1892)
<p>p. 65-67</p> <p>CONTRASTE DES COULEURS JUXTAPOSÉES</p> <p>Lorsque deux couleurs, qui se suivent dans l'ordre du spectre, sont placées côte à côte, elles prennent de plus en plus, à mesure qu'elles se rapprochent Tune de l'autre, l'aspect de la couleur qui les précède ou qui les suit.</p> <p><i>Exemple</i> : Rouge et orange; le rouge qui touche à l'orange se rapproche de la couleur cramoisi qui le précède; l'orange qui touche au rouge se rapproche de la couleur jaune qui le suit. Le jaune à côté du vert devient plus orange, le vert à côté du jaune plus bleu; le bleu à côté de l'outremer devient plus vert, l'outremer à côté du bleu plus violet, le violet à côté du cramoisi plus outremer, le cramoisi à côté du violet plus rouge, etc.</p> <p>Lorsque deux couleurs séparées par une autre, dans l'ordre du spectre sont juxtaposées, ce sont encore les mêmes résultats.</p> <p><i>Exemple</i> : Rouge à côté du jaune devient plus cramoisi, jaune à côté du rouge plus vert, etc.</p> <p>Lorsque deux couleurs sont séparées par deux autres, dans l'ordre du spectre, elles sont, comme nous l'avons dit, complémentaires; alors elles ne changent pas lorsqu'elles sont juxtaposées, mais elles s'exaltent.</p> <p><i>Exemple</i> : Rouge à côté du vert augmente d'intensité, il paraît rouge plus vif; vert à côté du rouge paraît vert plus vif, de même pour toutes les couleurs avec leurs complémentaires.</p> <p>Lorsque deux couleurs séparées par plus de deux autres, dans l'ordre du spectre, sont juxtaposées, elles se rapprochent chacune de la complémentaire de l'autre.</p> <p><i>Exemple</i> : Rouge à côté du bleu se rapproche de l'orange, complémentaire du bleu, il devient plus orange ; le bleu à côté du rouge se rapproche du vert, complémentaire du rouge, il devient plus vert.</p> <p>Le rouge et outremer. Le rouge à côté de l'outremer se rapproche du jaune, complémentaire de l'outremer, il devient plus orange; l'outremer à côté du bleu se rapproche du vert, complémentaire du rouge, il devient plus bleu.</p> <p>L'orange et outremer. L'orange à côté de l'outremer se rapproche du jaune, complément taire de l'outremer, il devient plus jaune ; l'outremer à côté de l'orange se rapproche du bleu, complémentaire de l'orange, il devient plus bleu, etc.</p> <p>Après ces explications, il est facile de comprendre comment on peut modifier l'aspect d'une couleur sans la changer. Lorsque vous aurez épuisé toutes les res sources de la palette pour rendre une couleur intense, vous pourrez encore augmenter son éclat en l'entourant adroitement d'objets de sa couleur complémentaire ; si, au contraire, vous trouvez qu'une couleur est trop prononcée, vous pouvez l'atténuer en l'entourant d'objets de la même couleur, plus intense.</p>	<p>p. 45-46</p> <p><i>Contrast of Colours in Juxtaposition</i></p> <p>When two colours which follow each other in the order of the spectrum are placed side by side, they take more and more, in proportion as they approach each other, the aspect of the colour which precedes or follows them.</p> <p><i>Example:-</i> Red and orange : the red which verges on orange approaches the crimson colour which precedes it; the orange which verges on red approaches the yellow colour which follows it. Yellow beside green becomes more orange; green beside yellow more blue; blue beside ultramarine becomes greener; ultramarine beside blue more violet; violet beside crimson more ultramarine; crimson beside violet redder, etc.</p> <p>When two colours separated by another in the order of the spectrum are in juxtaposition, the same results are obtained.</p> <p><i>Example:-</i> Red beside yellow becomes more crimson; yellow beside red greener, etc.</p> <p>When two colours are separated by two others in the other of the spectrum they are, as has been said, complementary; then they do not change when in juxtaposition, but they intensify.</p> <p><i>Example:-</i> Red beside green increases in intensity - it becomes a brighter red; green beside red appears a brighter green, as do all the colours with their complements.</p> <p>When two colours separated by more than two others in the order of the spectrum are in juxtaposition, each approaches the complement of the other.</p> <p><i>Example:- Red and blue.</i> Red beside blue verges on orange, complementary to blue it becomes more orange; blue beside red verges on green, complementary to red it becomes greener. <i>Red and ultramarine</i> - Red beside ultramarine verges on yellow, complementary to ultramarine it becomes more orange; ultramarine beside blue verges on green, complementary to red it becomes bluer. - <i>Orange and ultramarine.</i> Orange beside ultramarine verges on yellow, complementary to ultramarine it becomes yellower; ultramarine beside orange verges on blue, complementary to orange it becomes bluer, etc.</p> <p>After these explanations, it is easy to understand how the aspect of a colour may be modified without changing it.</p> <p>When you have exhausted all the resources of the palette to make a colour intense, you can still increase its brilliancy by cleverly surrounding it with objects of its complementary colour; if, on the contrary, you find that a colour is too pronounced, you can soften it by surrounding it with objects of the same colour, more intense.</p>

French version by Jehan-Georges Vibert (1891)	English version translated by Percy Young (1892)
<p><i>p. 114</i></p> <p>L'huile de lin est la plus siccativante des deux, elle acquiert plus de dureté et reste plus transparente en séchant que l'huile d'oeillette; mais elle est plus visqueuse et devient plus facilement acide.¹⁴⁴</p>	<p><i>p. 73</i></p> <p>Linseed oil is the more siccativante of the two; it acquires greater hardness and remains more transparent whilst drying than poppy oil; but it is more viscous and gets more easily sour.</p>
<p><i>p. 115</i></p> <p>L'emploi des couleurs broyées avec des huiles acidifiées est même une des principales causes qui font germer les tableaux.</p> <p>On doit donc avoir bien soin, avant de broyer les couleurs, de s'assurer au moyen du papier de tournesol que l'huile n'est pas acide : ce qui arrive très souvent après les opérations qu'on lui fait subir, soi-disant pour l'épurer et la rendre plus siccativante.</p> <p style="text-align: center;">LE BROYAGE DES COULEURS</p>	<p><i>p. 74</i></p> <p>The use of colours ground with acidified oils is one of the principal reasons why pictures crack.</p> <p>We should always be careful, before grinding the colours, to assure ourselves by means of litmus paper that the oil is not sour; which often happens after submitting it to operations said to be for purifying it and rendering it siccativante.</p> <p style="text-align: center;">THE GRINDING OF COLOURS</p>
<p><i>p. 119-120</i></p> <p>(...) En ne broyant les couleurs qu'avec la quantité d'huile strictement nécessaire, cela permet d'y introduire d'autres substances utiles (...par exemple) résine soluble dans l'huile, à froid, nous augmenterons à volonté la transparence de quelques-unes, laissant à d'autres toute leur opacité.</p>	<p><i>p. 76</i></p> <p>(...) By grinding colours with only the quantity of oil strictly necessary, we are able to introduce other useful substances (... for example) resin soluble in oil, cold, we shall increase at will the transparency of some, leaving to others all their opacity.</p>
<p><i>p. 97</i></p> <p>Nous donnons (page 280) des explications détaillées sur les couleurs bonnes et mauvaises; mais pour ceux que ces détails peuvent ennuyer, voici la liste de celles que l'on peut employer en toute sûreté.¹⁴⁵</p> <p>Blanc de plomb (carbonate de plomb).</p> <p>Blanc de zinc (oxyde de zinc).</p> <p>Jaunes de cadmium (sulfure de cadmium).</p> <p>Jaune de strontiane (chromate de strontiane).</p> <p>Jaune de zinc (chromate de zinc).</p> <p>Laque de fer (oxyde de fer fixé sur alumine).</p> <p>Vermillon (sulfure de mercure).</p> <p>Laques de garance (teinture de garance fixée sur alumine).</p> <p>Bleu de cobalt (oxyde de cobalt fixé sur alumine).</p> <p>Outremer (sulfure de sodium et silicate d'alumine).</p> <p>Vert de cobalt (oxyde de cobalt fixé sur oxyde de zinc).</p> <p>Vert-émeraude (oxyde de chrome).</p> <p>Violet minéral (phosphate de manganèse).</p> <p>Violet de cobalt (phosphate de cobalt).</p>	<p><i>p. 64</i></p> <p>We give (Appendix - "Good and Bad Colours") detailed explanations on good and bad colours; but for those whom these details may tire, here is the list of the colours which may be used with perfect certainty:-</p> <p>White lead (carbonate of lead).</p> <p>Zinc white (oxide of zinc).</p> <p>Cadmium yellows (sulphide of cadmium).</p> <p>Strontia yellow (chromate of strontia).</p> <p>Zinc yellow (chromate of zinc).</p> <p>Iron lake (oxide of iron on aluminium basis).</p> <p>Vermilion (sulphide of mercury).</p> <p>Madder lakes (madder dye on aluminium basis).</p> <p>Cobalt blue (oxide of cobalt on aluminium basis).</p> <p>Emerald green (oxide of chrome).</p> <p>Mineral violet (phosphate of manganese).</p> <p>Cobalt violet (phosphate of cobalt).</p>

¹⁴⁴ Before this sentence, Amadeo wrote: "L'huile d'olive ne sèche pas. L'huile de Lin ou d'oeillette sont les préférées pour la peinture" (translation to English: The olive oil does not dry. Linseed or poppyseed oils are preferred for painting).

¹⁴⁵ In the notebook, Amadeo wrote in Portuguese: *Cores que se podem empregar com toda a segurança* (translation to English: Colours to be employed with complete safety).

French version by Jehan-Georges Vibert (1891)	English version translated by Percy Young (1892)
<p><i>p. 98</i></p> <p>De plus, toutes les ocres naturelles et brûlées, toutes les terres naturelles et brûlées qui ont l'oxyde de fer pour base (...) ainsi que toutes les couleurs de mars qui sont de l'oxyde de fer (...) fixé sur l'alumine. Quant aux noirs, ils sont tous bons, sauf le noir de fumée (...).</p> <p>De cette liste nous excluons toutes les couleurs à base de plomb, comme les jaunes de chrome (chromate de plomb). Les jaunes de Naples et d'antimoine, le massicot et le minium qui sont du blanc de plomb plus ou moins calciné, parce que ces combinaisons métalliques sont sujettes à noircir au contact de l'air (...) cependant on-peut s'en servir en prenant quelques précautions (...) du vert Veronèse.</p>	<p><i>p. 64-65</i></p> <p>Further, all the natural and burnt ochres, all natural and burnt earths having oxide of iron for basis, are equally good, as well as all the mars colours, which are oxide of iron at different degrees of calcination on aluminium basis. As for blacks, they are all good except lampblack (...).</p> <p>From this list we exclude all colours on lead bases, such as chome yellows (chromate of lead), Naples and antimony yellows, massicot and minium, which are white lead more or less calcined, because those metallic combinations are liable to get black when brought in contact with the air, and they may be replaced by others; still they may be used if certain precautions are taken, and also Veronese green.</p>

Appendix II. Winsor & Newton 19th Century Archive Database

II.1. A survey of selected database contents

Table II.1.1. Estimated dates and number of pages available for each of the 47 W&N's 19th century catalogues (included by Mark Clarke in the database). For the dates highlighted in bold, these catalogues are complete. The letter T stands for Trade, R for Retail and F for French.

Catalogue code	Estimated date	Number of pages [#]	Catalogue code	Estimated date	Number of pages [#]
P1835	1832 [§]	5	P1883T	1883	13
P1840T	1841	13	1884	1884T	147
P1842	1842	9	P1885	1885	16
P1846	1846T	5	1886N	1886T	181
P1849T	1849	7	1886P	1886T	141
1849	1849	33	1886T	1886	90
P1850	1850	1	P1887R	1887	2
P1851T	1851	9	P1887U	1887	7
PPost1851	1851	*	1888F	1888	66
1856	1856	15	P1889	1898	16
P1857	1857	7	P1889R	1889	8
P1861T	1861	8	P1889T	1889	4
1863R	1863	109	PUnknown [†]	1892	16
1863T	1863	106	P1892R	1892	*
P1864	1864	8	P1892T	1892	18
P1864T	1864	14	1896	1896R	147
P186xT	1864T	3	1896F	1896	99
P1865T	1865	12	1896R	1896	151
P1866T	1866	*	1896T	1896	164
P1868R	1868	6	P1896	1896	8
P1869R	1869	14	PUSA	1896	18
1870T	1870	315	1900T	1900	144
P1874	1874	19	Pc1900	1900	9
P1876	1876	11			

[#] The number corresponds to the number of pages of the pdf file, frequently with recto and verso pages.

[§] The estimated date should be c. 1835, since it was in this year that W&N introduced their moist watercolours, already mentioned in this catalogue as the "newly enbented moist water colours".

* The pdf file does not open.

[†] This file corresponds to the W&N declaration on the composition and permanence of their colours from 1892, which is transcribed in Appendix II.2 (p. 175).

Table II.1.2. Inferred manuscript (MS) date range (included by Mark Clarke in the database), pages and number of records for each of the 85 manuscript books.

Book code	Inferred MS date range	Pages	Database records	Book code	Inferred MS date range	Pages	Database records
01	1843	40	219	A1	1875-79	162*	143
02	1843-44	44	183	A2	1878-79	176*	167
03	1844	44	130	A3	1874-79	201*	198
04	1844	44	109	A4	1862-77	210*	95
05	1845	44	128	A5	1864-80	170*	59
06	1846	44	103	A6	1861-81	174*	58
07	1846	52	120	A7	1864-81	210*	45
08	1846	44	113	AC	1849-54	141	32
09	1846-47	44	73	C1	1856 ?	920	770
10	1847-48	44	114	C2	1873 ?	366*	265
11	1848-49	44	107	C3	1872 ?	366*	338
12	1850	44	93	C4	1873-77	366	342
13	1850	44	76	C5	1872-78	372*	282
14	1850 or 1832-4	40	81	CP	1835-38	141	42
15	1850-51	40	65	DR	1890-1926	462*#	162
16	1851-53	44	105	EN	1843 ?	16	35
17	1853-55	44	84	ES	1871	44*	23
18	1846-56	40	85	G1	post 1844	44	56
19	1856-57	20	52	G2	post 1844	44	57
20	1857-58	36	87	G3	post 1844	44	52
21	1858-59	40	101	GR	1866-71	40*	85
22	1859	40	74	HS	1834-36	208	228
23	1859-60	40	99	IN	1843-44	4	2
24	1860-62	40	119	KT	1850-56	349	326
25	1862-65	40	91	LP	1846-48	44	23
26	1865-67	40	90	M2	1872 ?	660*	766
27	1868-69	26	64	MA	1846-54	40	38
28	1869-70	20	53	MT	c. 1889 ?	964**	1358
29	1871-72	16	58	NA	post 1844 ? w/m	44	6
2C	1838-43 ?	269	160	OG	Undated w/m 1832	40	102
2M	1839 ?	181	205	P1	1846-58	950*	485
2P	1834-35	78*	51	P2	1848-65	950*	598
3P	1837-39	364	260	P3	1867-73	260*	165
4P	post 1874	364*	186	P4	1834-93	350#	248
7P	1842-48	352	224	P8	1870-78	376*	230
9P	1844-56	242	349	PM	1862-82	351	158

* Books with recto (A) and verso (B) pages.

Book incomplete with blank pages.

‡ From the 964 pages, not all were digitalised.

Table II.1.2. (continued).

Book code	Inferred MS date range	Pages	Database records	Book code	Inferred MS date range	Pages	Database records
RE	1833	49	125	X3	1854-59	363	361
SE	1848-49	44	37	X4	1854-55	420	293
V1	1836-51	456	325	X5	1862-64	240*	115
V2	1850-63	535	326	X6	1852-56	528	501
WW	post 1837	44	24	X7	1848-59	183	117
X1	1878	160*#	54	X8	1854-60	176	168
X2	1844-48	281	207	85 Manuscript Books			15.003

* Books with recto (A) and verso (B) pages.

Book incomplete with blank pages.

Table II.1.3. W&N database topics by alphabetical order.

Topics	Records (total/restricted)	Topics	Records (total/restricted)
accounts	43/12	cleaning	18/0
[accounts]	1/0	colour quality	270/93
address	5906/	comparison between recipies	118/55
adhesives	10/2	comparison with other manufactures	65/15
adulteration	87/40	complains	3/0
advertisement (2 ref)	27/1	conservation treatment	3/0
agricultural notes	3/0	[costing]	476/46
architecture	2/0	cover page	78/0
art theory	11/0	crayon	28/1
binder manufacture	5/1	crayon manufacture	25/0
book	25/1	customer complaints	2/0
breaking sorting & picking	16/7	customers [people supplied TO]	110/15
brush	3/0	dates	10/7
burning pigment	43/8	dates of production	8/7
calculation	2/0	[DIAGRAM]	1/0
canvas	65/1	diary entry	2/0
canvas preparation	40/0	[diary entry]	1/0
care and maintenance	5/0	dimensions	3/0
chemical composition	18/3	discussion of quality	1/1
chemical formulae	56/2	discussion of variations	4/2
chemical properties	45/6	drawing	38/1
chemical solubility	7/0	dryers	89/1
chemical test	54/5	dryers ?	<i>Invalid criteria</i>
chemistry of oil	2/0*	drying oil	83/1
chemistry of pigment	39/1	dye	32/0

* 1 not marked.

Table II.1.3. (continued).

Topics	Records (total/restricted)	Topics	Records (total/restricted)
equipment design	163/11	miniatures	3/0
experiment	810/160	miscellaneous materials	935/93
experiment [?]	1/0	miscellaneous processes	72/4
fixative	6/1	mixed pigments	537/153
flattening	2/1	mixing	89/34
food colour manufacture	1/0	mixing instructions	88/34
for coachmakers	1/0	moist colours	131/30
frames	1/0	not	4571/1393
gilding	39/0	note on fermenting	1/1
graining	134/2	notes	4388/1372
grinding time	16/10	notes on drying	129/43
grounds	26/0	notes on grinding	1386/549
gum	84/51	notes on heating	242/60
house decorating	3/1	notes on hydrocarbon distillates	2/0
house painters	22/2	notes on material sources	4/1
household recipe	4/0	notes on moulding	46/16
idea for design	32/0	notes on paint retail	4/0
illuminating	18/0	notes on patents	17/3
index	107/5	[notes on patents]	2/2
ink (2 ref)	97/27	notes on people or companies	951/82
ink [?]	1/0	[notes on people or companies]	15/0
interior decoration	106/0	notes on quality	1326/766
Japanning	67/0	notes on soaking	167/42
labour costs	281/27	notes on solvents	3/0
lake manufacture	4/3	notes on storage	70/40
light	1/0	notes on use	113/23
lithography	11/0	notes on varnish	41/0
manufacturer	108/17	notes on washing	73/33
maps	1/0	notes on watercolour	1754/1078
marbelling	27/2	[notes]	25/0
marbelling [?]	1/0	[observations]	24/3
materials definition	103/12	oil : misc.	179/2
materials source	18/1	oil paint manufacture	862/182
measures	21/3	oil treatment	34/1
medical recipe	102/1	oil varnish	5/0
medical remedy	4/0	other material manufacture	51/1
medium manufacture	71/26	packaging	3/0
medium properties	17/8	paint for special use	51/3
metal leaf	21/0	painting technique	104/1

Table II.1.3. (continued).

Topics	Records (total/restricted)	Topics	Records (total/restricted)
panel	11/0	[section heading]	11/1
paper	43/2	size	21/0
paper support	8/0	sizing	3/0
patent	36/3	spirit colours	156/43
pencils	58/1	spirit varnish	7/0
photography	3/0	storage of materials	22/7
physical properties	10/0	suggested modifications	178/64
pigment	3967/743	suppliers	287/29
pigment manufacture	3673/623	synonyms	4/1
pigment manufacture ??	<i>Invalid criteria</i>	terminology defined	72/23
pigment manufacture [?]	4/0	textiles	1/0
pigment properties	55/15	theory	13/0
pigment selection	80/23	tools, equipment	84/20
pigment test	35/6	tubes	1908/281
plaster	4/0	UNCLEAR	100/9
powder colours	5/2	unrelated drawing	11/0
premises & services (eg water,	20/0	[unrelated drawing]	2/0
preparing additives (misc.)	4/1	unrelated material	415/1
prices, not W&N	119/3	[unrelated material]	12/0
printing	47/2	varnish	514/1
process description	45/7	varnish manufacture	494/1
process variations	165/25	wallpaper	2/0
purification	21/3	water washing with carbonic gas	1/0
purification process	4/0	watercolour	5889/2741
quality evaluation	791/295	watercolour cakes	2138/1199
quantities	1088/558	water colour cakes ?	<i>Invalid criteria</i>
query	40/6	water colour cakes [?]	1/0
question posed (not answered)	129/30	watercolour paint manufacture	274/83
quotation from publication	75/6	watercolour paint manufacture ?	<i>Invalid criteria</i>
quotation from publication ?	<i>Invalid criteria</i>	watercolour paint manufacture§	2/1
quotation from publication (?)	1/0	watercolour, moist	1682/1146
quotation from publication [?]	2/0	watercolour, pans	4/4
[quotation from publication] (2 ref)	17/0	watercolour, tubes	225/58
recycling or reuse	57/18	waxes	25/2
reference to other literature	182/5	weather/time of year	36/20
rel	793/383	wood : structure	7/0
related recipies	792/383	working properties	3/0

Table II.1.4. W&N database sub-topics by alphabetical order.

Sub-topics	Records (total/restricted)	Sub-topics	Records (total/restricted)
1862 Exhibition	3/1	black lake	12/7
acetate of alumina	4/1	black pigments	28/2
acid	20/2	black-brown organics	65/4
acroter	1/0	blue black	14/6
albúmen	8/3	blue pigments	19/1
alcohol	32/10	blue verditer	1/0
alizarin lake	1/0	body	88/2
alkaline earths	1/0	bone black	6/0
alkanet (<i>Anchusa tinctoria</i>)	1/0	bone brown	14/0
alum	116/11	borax	20/3
alumina	61/3	brazil	4/0
aluminium	1/0	bread	2/0
amber	5/0	Bristol Pink	1/0
ammonia	29/2	brown lake	28/10
aniline	5/0	brown madder	139/138
antimony	13/0	brown ochre	19/4
Antwerp blue	15/8	brown pigments	20/1
apothecaries	1/0	brown pink	61/5
arnatto	4/0	Brunswick black	4/0
arrowroot	1/0	Brunswick green	22/2
"arsenate of potassium"	2/0	Brunswick green [?]	1/0
arsenic	8/1	brushes	16/1
artificial gall	8/0	burnishing	1/0
artificial malachite	10/0	burnt carmine	12/6
artificial Sienna yellow	9/0	burnt lake	6/3
artificial ultramarine	20/11	burnt ochre	19/6
asphalt	34/2	burnt Roman ochre	12/6
asphaltum	12/0	burnt Sienna	106/44
aureolin	11/10	burnt terre verte	10/0
autobiographical	2/0	burnt umber	55/24
barium carbonate	3/0	cadmium	87/27
barium chromate lemon yellow	6/0	cadmium orange	10/8
barium sulphate	14/0	cadmium yellow	67/22
barytes	52/0	camphor	3/1
barytic white	35/0	canvas	8/0
benzoic acid	2/0	Cappah brown	18/1
bistre	13/5	carbon black	2/0
bitumen	9/0	carbonate of ammonia	5/0
black : Japan	9/0	carmine	392/117

Table II.1.4. (continued).

Sub-topics	Records (total/restricted)	Sub-topics	Records (total/restricted)
"carmine" (2 ref)	392/117	cochineal ?	<i>Invalid criteria</i>
carpenter	2/0	cochineal [?]	2/0
carriage	6/0	cochineal dregs/grouts	22/1
Cassel earth	5/0	cochineal lake pigment	125/2
catechu	1/0	cochineal liquor	50/0
ceiling painting	2/0	cochineal perhaps	1/0
cerulean blue	6/5	Cologne earth	31/9
chalk	15/0	cone mill	1/1
charcoal	12/0	constant white	4/0
charcoal powder	2/0	copal	58/0
China blue	4/1	copper	37/1
Chinese blue (Prussian blue)	25/4	copper carbonate	1/0
Chinese red	9/0	copper greens	8/0
Chinese white	74/28	copperas	8/0
chlorine	1/0	cork black	5/2
[?] chrome	15/0	crayon	3/1
chrome	526/36	cream of tartar	1/1
chrome [?]	15/0	cremnitz white	2/1
chrome green	40/7	crimson lake	231/27
chrome green ?	<i>Invalid criteria</i>	crimson liquor	3/0
chrome liquor	11/0	crimson madder	8/8
chrome orange (=orange chrome)	67/5	crop madder	5/4
chrome oxide	8/1	curdled gum solution	83/45
chrome red	27/1	curdled plain gum arabic solution	26/11
chrome red [?]	8/0	dammar	11/0
chrome yellow	176/12	damp lake	88/1
chrome yellow ??	<i>Invalid criteria</i>	dark ground	1/0
cire savon	2/1	deep chrome	53/4
citron yellow	4/0	distemper	7/0
clay	6/0	dragon's blood	3/1
Coagulated Glycerine	1/1	drawing	3/0
coal	5/0	drier	3/0
cobalt	123/61	drop green lake	2/0
cobalt [blue?]	9/4	drop lake	8/1
cobalt blue	51/29	drop yellow lake	4/1
cobalt green	3/0	dryers	30/0
cobalt pigment	25/4	Dutch pink	6/0
cobalt stannate blue	6/3	earths	7/0
cochineal (2 ref)	679/13	egg white	4/1

Table II.1.4. (continued).

Sub-topics	Records (total/restricted)	Sub-topics	Records (total/restricted)
Egyptian blue	1/0	gum solution	85/46
emerald green	75/2	gum water	23/22
encaustic	4/0	gumtion	5/1
English carmine	1/0	gypsum	2/0
fixative	26/2	Hooker's green	17/9
flake white	5/1	hops	1/0
framing	1/0	imports	2/0
French blue	26/21	incompatability	1/0
french carmine	2/1	indelible black ink	2/0
French cobalt	1/1	indelible brown ink	8/0
French ochre	4/0	India rubber	8/1
French polish	30/0	Indian ink	22/20
fresco	6/2	Indian lake	16/3
fuchsin	1/0	Indian purple	10/8
fustic	1/0	Indian red	80/36
galls	5/3	Indian red/ivory black mixture	2/0
gallstone	4/3	Indian yellow	102/37
gamboge	171/66	indigo	89/48
Garance brown	1/1	intense blue	4/2
Garance purple	1/1	iodene	2/0
gas	5/0	iodine	13/0
gelatine	5/0	iodine scarlet	4/0
Gilmartin Lime	1/0	iron	50/0
glass	16/0	iron oxide	18/0
glue	6/0	iron oxide : Mars	8/0
glycerine	69/51	iron pigment	24/0
gold	49/2	iron pigment [?]	2/0
gold ochre	13/0	iron red	13/0
gold paper	2/0	iron red ??	<i>Invalid criteria</i>
gold size	19/0	iron yellows	4/0
"gold" ink [bronze]	11/2	isinglass	1/0
graphite	1/0	Italian pink	68/9
gray pigments	1/0	ivory	64/15
green pigments	32/0	ivory black	53/14
green ultramarine	1/1	Japanese varnish	17/0
grinding stone	4/0	Jaune de Mars	1/0
grouts	36/1	jellied glycerine	1/1
gum	199/92	jet	1/0
gum arabic	29/13	kings yellow	3/1

Table II.1.4. (continued).

Sub-topics	Records (total/restricted)	Sub-topics	Records (total/restricted)
lac	56/21	madder liquor	2/1
lac [?]	1/0	madder orange (=orange madder)	14/14
lacquer	1/0	madder pigment	16/16
lake	1110/118	madder pink	21/18
lake base	11/0	madder purple	97/95
lake liquor	87/0	madder root paste	1/1
lamp black	83/53	madder rose	81/79
lapis lazuli	2/2	madder yellow	8/5
lead	214/5	magnesium	7/0
lead acetate	29/0	malachite	18/1
lead chromate	2/0	malt	1/0
lead chromate [accidental product]	1/0	manganese	6/0
lead liquor	15/0	marble	19/0
lead pigments	31/2	Mars orange	6/5
lead sulphate	13/0	Mars pigments	47/6
lead white	83/2	mars yellow	9/2
Leitch's blue	1/0	mastic	48/0
Leitch's brown	2/2	mastic varnish	30/0
lemon chrome	51/1	mauve	5/4
lemon yellow	97/8	medicinal herbs	1/0
lemon yellow : barytic	11/0	megilp	33/4
lemon yellow : strontium	2/0	megilp ?	Invalid criteria
levigation	3/0	mercury	11/0
lichen extract	3/0	middle Brunswick green	1/0
light red	14/9	middle chrome	11/0
lime	36/1	milk	5/0
limescale	1/0	mineral green	3/0
linen	1/0	miniature painting	1/0
linseed oil	52/7	moist composition	3/0
liquid ammonia fortis	1/1	moists	17/5
list of pigments	4/0	morinda	1/0
litharge	10/0	mull madder	1/1
lithography	8/0	muller	1/0
loaf of sugar	2/1	mummy	3/0
madder	622/613	munjiet	1/0
madder "carmine"	71/68	muriate of barytes	11/0
madder "crimson"	8/8	muriate of tin	5/0
madder brown	139/138	muriatic acid	1/1
madder lake	49/47	myrbane	12/4

Table II.1.4. (continued).

Sub-topics	Records (total/restricted)	Sub-topics	Records (total/restricted)
Naples yellow	43/3	"paper varnish"	17/0
"Naples yellow" [mixed pigment]	16/0	Paris white	7/2
Naptha	4/0	Parisian lake	1/0
neutral orange	4/4	paste	13/4
neutral tartar potash	4/2	patent dryers	15/0
neutral tint	24/13	patent yellow	12/0
new blue	7/6	Payne's grey	20/12
"new yellow"	1/0	pearl white	3/0
nitrate of iron	1/0	pencil lead	3/0
nitrate of lead	9/0	permanent white	9/0
nitrate of lime	1/0	Persian red	3/0
nitrate of tin	3/0	picture cleaning	2/0
nitric acid	4/0	picture lining	2/0
nitro-muriate of tin	2/0	plaster	2/0
[notes on quality]	1/1	platina	9/0
nut tannin	1/0	platina yellow	8/0
oak	10/0	poison	1/1
ochres	48/9	poppy oil	37/8
oil	139/13	porphyry	1/0
oil bottoms	1/0	potash	48/2
oil gilding	4/0	potassium chromate [?]	7/0
oil grinding	2/0	potassium silicate [?]	1/0
olive green	20/14	potassium tartrate [?]	1/0
olive tint	2/0	precipitates	35/2
orange chrome	67/5	preservative	6/0
orange lead	2/0	proteinous solution	1/0
orange madder	14/14	Prouts brown	4/0
orange ochre	3/0	Prussian black (burnt Prussian	4/0
orange orpiment (realgar)	1/0	Prussian blue	114/39
orange vermilion	11/9	Prussian brown	2/1
orpiment	11/1	Prussian green	23/5
ox gall	47/0	pumice	3/0
Oxford ochre	20/1	pure scarlet	16/0
oxide of barytes and zinc	2/0	[purple carmine]	1/1
oxide of chromium	14/7	purple lake	101/18
paint pot	1/0	purple madder	97/95
painting support	4/0	"purple madder" [lac]	19/18
pale Chinese blue	2/0	purple of Cassius	3/0
pale chrome	47/2	putty	2/0

Table II.1.4. (continued).

Sub-topics	Records (total/restricted)	Sub-topics	Records (total/restricted)
Quaker's Green	2/0	silica	6/0
quercitron / Rhamnus yellow	32/1	silver	20/1
quercitron yellow	146/1	silver white	9/0
quercitron yellow (probably)	16/0	sissing	1/0
quercitron yellow (probably)	1/0	size	67/2
raw Sienna	53/4	smalt	24/11
raw umber	38/13	soap	12/0
realgar	2/0	soda	6/0
red carmine shreds	6/1	soft woods	2/0
red lead	42/0	solubility	81/3
red ochre	33/11	solution of gum ammoniac	1/0
red pigments	29/0	some copper green	1/0
Rembrandt's madder	1/1	Spanish brown	1/0
resin	2/0	Spanish Mahogany	1/0
Rhamnus / Persian Berries	4/0	"spar"	12/12
Roman ochre	44/10	spermaceti	5/0
Roman sepia	5/3	spirit varnish	21/0
rose madder	81/79	spirits of wine	1/0
Rose pink	8/4	starch paste	6/0
rose wood	1/0	stone slabs	2/0
rosin	8/2	strontium	13/0
rough purple	3/1	strontium yellow (chromate)	10/0
rubber	10/1	sugar of lead	14/1
safflower	2/0	sugar solution	3/0
sal ammoniac	1/0	sulphuric acid	9/1
salt	3/0	sumach	3/0
saltpetre	1/0	sunshine green	1/0
samples	1/0	Tabach	2/0
sandarac	6/0	tallow	1/0
sap green	24/9	tannin	2/0
scarlet	170/25	tartar	33/2
scarlet earth (vermilion)	21/8	terre verte	36/3
scarlet lake	130/17	tin	73/14
scarlet pink	1/1	tin solution for carmine	2/0
scent	3/0	transparent moist composition TM	1/1
sepia	77/44	trial	41/7
shell	22/0	Troy	1/0
shellac	19/0	turmeric	9/0
Sienna yellow	18/0	turpentine	21/0

Table II.1.4. (continued).

Sub-topics	Records (total/restricted)	Sub-topics	Records (total/restricted)
twisted grain	1/0	wax	33/1
ultramarine	121/91	weights	2/0
ultramarine ashes	31/30	weld	12/1
umber	90/37	West Calder Lime	1/0
[unclear, zinc hydroid:?]	1/0	white copperas	3/0
[unclear]	31/0	white earth	21/1
Vandyke Brown	119/18	white pigments	25/1
Vandyke Brown ?	<i>Invalid criteria</i>	whiting	8/0
varnish alteration	32/1	wine vessel	1/0
varnish disposal	3/0	wood	19/0
vegetable oil	1/0	wood stain	1/0
venetian brown	1/1	yeast	13/0
Venetian red	73/25	yellow lake/ivory black mixture	2/0
verdigris	29/1	yellow lakes	121/15
verditer	3/0	yellow ochre	71/2
verm	242/79	yellow pigments	60/2
vermilion	241/79	[yellow pigments]	13/0
vermilion ???	<i>Invalid criteria</i>	zinc	149/11
Vernal Green	1/0	zinc chromate	24/0
Verona brown	2/0	zinc green deep	1/0
violet carmine	15/10	zinc green middle	1/0
Violet lake	3/0	zinc green pale	1/0
viridian	11/0	zinc nitrate	6/0
vivianite	1/0	zinc oxide	9/0
wallpaper	1/0	zinc sulphate	7/0
water purification	11/0	zinc white	72/9
water washing with carbonic gas	3/0	zinc yellow	17/1
watercolour grinding mills	1/0		

Table II.1.5. W&N abbreviations, from original to modern terminology¹⁴⁶.

Material original name	Material interpreted name	Material original name	Material interpreted name
A		Chro: Zinc	Zinc chromate
A. H. N.	Arthur Henry Newton	Coch	Cochineal
Aq.; aqua	Water	Crim Lake; Cr Lake	Crimson Lake
Al; A*	Alum	E	
A*	Pearlash	Etain	Tin
(or Potash; P: Ash; P. A.)	Potassium carbonate	Exp ^t	Experiment
Ac Alu	Aluminium acetate	F	
Ac Ac; acet: acid	Acetic acid	F	Ferment Patent Yeast
Ac Pl.	Lead acetate	G	
(or sugar lead; sug lead; G. S. Lead; G:S:L:)		Grout	Dregs
Ac Zinc	Zinc acetate	H	
Alu in P	Alumina in Caustic Potash	H. C. N.	Henry Charles Newton
A la Mon.	Monro's method of boiling cochineal	L	
Ammo	Ammonia	Lem Yell	Lemon yellow (barium chromate)
B		Lead Liquor; Lead Liq ^{re} (or Sub Ac.)	Lead subacetate solution
Bi Chromate; Bi Ch Pot;	Potassium dichromate	Li.	Quick lime
Bi Chrome; Bi Chro; B. C.		Liqr	Liquor = solution
Bi tartrate potash; Bi T P;	Cream Tartar	Lith; L.	Litharge (lead oxide)
BTP; Cr Tart; C T.	Potassium Bitartrate	L S; S*	Loaf Sugar
Bor Soda or B S.	Borax	M	
Boracic Tartar; B: T:	Sodium Borate (borax) + Potassium Bitartrate	Muriatic acid; Mur ac.	Hydrochloric acid
C		Mur: Barytes; Mur B.;	Barium chloride
Cit. ac.; C. ac.; C. A.*	Citric acid	Mu Bary	
Carb acid gas	Carbon dioxide	Muriat Soda	Sodium chloride
Carb ammo; C. A.*	Ammonium carbonate	Muriat Lead	Lead chloride
C. Am.; Amm carb		N	
Carb Baryt	Barium carbonate	N T P	Neutral Tartar Potassa
Carb Lead	Lead carbonate	Nitrate Barytes; Nit Baryt	Barium nitrate
Caustic potash	Potassium hydroxide	Nit. Lead; Nit. L; N. Lead;	Lead nitrate
China Clay; Ch Cl	Kaolin	Nit Pl; N. L.	
Chi W ⁱ ; Z: W:	Chinese white; zinc oxide	Nit strontia; Nit stront	Strontium nitrate
Chro: Lead	Lead chromate	Nit Zinc; Nit Z	Zinc nitrate
Chro: Potash	Potassium chromate	Nitros acid	Nitric acid
Chro: Stront	Strontium chromate	N W	New milk

¹⁴⁶ There is a database record on abbreviations, URC: 7PF05L01. As noted, Clarke also reports on the W&N terminology (Clarke, 2009).

Table II.1.5. (continued).

Material original name	Material interpreted name	Material original name	Material interpreted name
O		Sul Acid; Sul Ac; S.O.3	Sulfuric acid
O G.	Ox Gall	Sulphate Barytes; Sul Bar;	Barium sulfate
P		Sul Baryt; W. S. B.	Barytes
Plymouth lime	Calcium oxide	Sulp Magnesia	Magnesium sulfate
P verm; P. V.	Pale vermilion	(or Epsom salts)	
Prec; Pcp; pp	Precipitate	Sulphate Soda; Sulp Sod;	Sodium sulfate
Plaster Paris	Calcium sulfate	Sul Soda; SO3 Sod; S. S	
Superf Plaster; Superf. P P	hemihydrate	S.O.3.S; Gaulber salts	
Hydrated sulphate lime		Sulp: Copper; Sul Cup	Copper sulfate
Q		Sul: Iron	Iron sulfate
Quer B ^K	Quercitron Bark	Sul: Zinc; Sul Z; S Z;	Zinc sulfate
R		zinc sulp	
R. Carm	Rough Carmine	Sul White; Sul Lead; Sul Pl	Lead sulfate
R. L.; O. L.	Orange Lead	Pulp Sulp. L.; Pulp S. L.	
S		Sup ^t	Supernant
Sct Lake	Cochineal Scarlet Lake	T	
Scarlet liquor	Cochineal scarlet liquor	Terra alba	Finely ground gypsum
Soda; Sod.; S.*	Sodium carbonate	W	
(or Carb Soda)		Whiting	Chalk
Sol	Solution	(or Paris White; P. W.)	Calcium carbonate
Spar	Magnesium carbonate	W ^t S ^t	White Starch
Sub C P; S. C. P.	Potassium Bicarbonate		
Sub carb potassa			
Potassa carb: PLN		ΔL. alcohol	Spirits Wine

* The context of the production record is extremely important. Note that A may stand for alum or potassium carbonate, C. A. may stand for citric acid or ammonium carbonate, and S may stand for loaf sugar or sodium carbonate.

Table II.1.6. Conversion of measures, adapted from Carlyle, 2001. *The Artist's Assistant*. Appendix 27 (pp. 545-546).

Units used by 19 th c. W&N	Modern SI units
Liquid measures	
1 gallon	4.546 l
1 pint	0.568 l
1 gill	0.142 l
Weight measures	
1 hundredweights (cwt)	50.8 kg
1 pound (lb)	0.454 kg
1 ounce (oz)	0.028 kg
Metric measures	
1 foot (ft)	0.3048 m
1 inch (in)	0.0254 m

II.2. Transcription of the W&N's declaration on their pigments permanence (1892)

INTRODUCTION

Two Criticisms are often levelled by thoughtless people at the heads of Artists' Colourmen, and of these we have decided, as one of the leading English firms, to take some practical notice. It is alleged:-

- i. That Artists' Colourmen are in the habit of selling Colours which are not permanent; and
- ii. That they keep Artists in ignorance of the Chemical Composition of the Colours they sell.

The answer to the first of these two Criticisms seems obvious enough. Manufacturing businesses exist, as a rule, not for the enforcement of moral laws on their customers, but for the satisfaction of the demands which those customers make; and while, for instance, we continue to be asked for *Magenta* and *Geranium Lake*, so long shall we continue to supply them. The Artist is, in our opinion, the sole judge of his right to employ such pigments; and we, who use our best efforts to supply him with all he requires, have no intention of excluding them from our list of manufactures. We do not assert that such colours are durable; all we do assert is that they are as durable as they can be made.

We have not hitherto deemed it incumbent on us to publish any information relating the permanence of pigments. Instruction on this subject has always been attainable in *Field's Chromatography*, published by us, - a work which, in its various editions, has for more than half a century maintained its reputation as the standard authority on pigments.¹⁴⁷ Lectures on the Chemistry of Painting have also long formed at the Royal Academy (as they should form everywhere) a part of the training of every art student. Indeed, we do not think it has ever been seriously suggested that it is the function of Artists' Colourmen to give such information as we are referring to.

We propose, however, in the following pages, to classify colours in the order of their permanence, because answering questions on this topic has involved us in a considerable amount of correspondence; and because we shall thus, once and for all, dissipate the notion that we affirm all colours to be durable.

The important question now presents itself:- What experimental tests shall form the basis of classification, and by whom shall they be made? It may seem rather a naïve idea for a manufacturer to publish his own test of his own colours; but everybody who has had to deal with the subject knows that it is really the only thing at present to be done. For, even supposing the tests hitherto conducted by scientific men to have been properly performed, there is (and can be for obvious reasons) no published guarantee that the colours upon which they experimented were identical in chemical structure or mode of preparation with those which any particular house is in the habit of selling.

We believe, however, it is a matter of opinion whether there are at present any satisfactorily organized investigations before the public; because those which so far been published have all been based on the principle of exposure to direct sunshine. The value of these sunshine tests when used to

¹⁴⁷ Within the last few years much attention has been paid to the scientific study of artists' colours, and the literature of the subject has received two most important accessions. In the report by Dr. Russell and Captain Abney, on the Action of Sunlight on Water-Colour Pigments, accurate and exhaustive investigations on this subject by scientific experts of high calibre have for the first time been given to the world; and in the treatise of Prof. Church, subsequently published, on the Chemistry of Paintings, we possess a work which eclipses everything that has so far been written on painting from the chemical side. The time-honoured *Field's Chromatography* is, therefore, although we hope as valuable as ever, no longer the only treatise in vogue.

prove anything more than the pros of permanence is a matter of the gravest doubt. Adverse criticisms of the reasoning which, in this particular, constituted the only weak point in the otherwise admirable report of Dr. Russell and Captain Abney have been endorsed by no less an authority on Light than Prof. G. G. Stokes, the President of the Royal Society. Prof. Church, of the Royal Academy, has also thrown his vote in the opposing scale. So that there seems to be more or less general consensus of opinion that pigments can only be satisfactorily tested by exposure to diffused daylight alone; and that sunshine exposures, though useful in their way as conferring special hall-marks of permanence, should be put out of court for being used as arguments against the durability of a colour. No person who values a painting ever dreams of exposing it to the direct blaze of sunlight, and, with the proviso already specified, no experimenter should therefore carry out his investigations under conditions other than those which obtain in the ordinary life history of a properly kept picture.

At the North London Colour Works careful testing of the durability of our colours has always gone hand in hand with colour manufacture, and it is by this method of daylight exposure that the pigments have always been tried. A well-lighted room with a northerly aspect was many years ago set apart for this purpose by the founders of the business, and from the results of experiments made in this manner we have arranged the classified lists.

* * * * *

The reply to Criticism No. 2 - that Artists' Colourmen keep Artists in ignorance of the composition of their Colours - is no less obvious than to the first. It is impossible, in these days of analytical chemistry, for the secrets of colour-making to consist to any great extent in the chemical composition of the colours. We, for our part, attach now little importance, as far as the success of business is concerned, to any concealment of the chemical composition of our colours and media; although we necessarily attach very considerable importance to maintaining the secrecy of those methods which long experience has taught us (as long experience alone can teach) are best adapted for the manufacture of the above-named commodities. We have, in fact, invariably been willing to divulge the composition of our pigments and vehicles to *bonâ fide* artists, but have always entertained the greatest reluctance to take any step whereby we might render unnecessary assistance to enterprising competitors, and thus enable them to reap the benefit of knowledge which we have ourselves often only acquired by much expenditure of time and capital.

Artists will no doubt see how difficult it has hitherto been for us to give them information which we wished to safeguard effectually from other sources of enquiry, and they will no doubt therefore also see the common sense of the conclusion to which our experience has forced us - the conclusion that we cannot treat artists in one way and the world at large in another: all must be treated alike.

We have, therefore, decided to make a second new departure, and to obviate further misunderstanding as well as to lessen our private correspondence, by publishing a statement of the nature of our colours and vehicles. Our position, broadly stated, is therefore this:- That we make no concealment of the chemical structure of our pigments and mediums, but reserve to ourselves only

those details which have reference to the manner in which these pigments and mediums are made.¹⁴⁸ In plain words, we reserve to ourselves no more than is necessary for any business conducted by private enterprise¹⁴⁹ in these present times. From artists themselves we wish we could have no concealment at all; but only in a more ideal age can such things as this be possible. Nevertheless, with the Artists' Colourmen in such a position as we have here endeavoured to define, the painter has little cause for regret. He is in possession, if not of all the interesting, yet of all the *essential*, information relating to the manufacture of those materials which, manifold in their variety and application, pass from his palette to constitute in his picture the physical basis of his craft. He knows, in fact, everything that may help him in compassing stability, as far as may be, for the complex fabric of his work; and there are no more earnest wishes than ours that success may attend him in his efforts to endow the fleeting aspects of Nature and the ephemeral creations of Imagination with the "living hues of Art".

WINSOR & NEWTON, Ltd.

October, 1892

COMPOSITION OF PIGMENTS PREPARED BY WINSOR & NEWTON, LIMITED,
and used by them in the manufacture of their oil and water colours,

<i>Alizarin Crimson</i>	A Lake prepared from artificial Alizarin. The Lakes prepared from this colouring matter do not approach in beauty of colour those obtained from the genuine Madder Root.
<i>Antwerp Blue</i>	A weak variety of Prussian Blue containing Alumina.
<i>Asphaltum</i>	Mineral Pitch obtained from Egypt.
<i>Aureolin</i>	Double Nitrite of Cobalt and Potassium. This colour, introduced by us, has always been a speciality of ours.
<i>Aurora Yellow</i>	An opaque and brilliant variety of Sulphide of Cadmium introduced by us in 1889, and peculiar to ourselves. It vies with genuine Ultramarine in its combination of exquisite beauty with unflinching durability.
<i>Bistre</i>	A brown soot obtained from Wood, and used inly in Water Colour.
<i>Bitumen</i>	Synonymous with Asphaltum.
<i>Black Lead</i>	Prepared Graphite.
<i>Blue Black</i>	A variety of Carbon Black, prepared by charring woody issue.
<i>Bone Brown</i>	Charred Bone Dust.
<i>Brilliant Ultramarine</i>	The finest brand of French Ultramarine obtainable.

¹⁴⁸ We have carried out this principle even in the case of those of our colours which are imitative mixtures, and about which if we tell anything we tell all; because so far from having anything to fear from a publication of their composition, we feel sure that the attempts which they represent to replace fugitive pigments by more permanent substitutes will gain some credit for the maligned Artists' Colourmen. Although our action in this case may to some extent check the sale of these colours, yet we believe that the intimate manner in which they are blended, the careful choice of proportions of their constituents, and the unvarying constancy of their composition, will always recommend them for the artist's adoption.

¹⁴⁹ "It is my conviction that if the Royal Academy or the Government were to establish a laboratory for the manufacture and manipulation of pigments, the products would not compare more advantageously with those of private enterprise that do ships, or ordnance, or weapons," - Thos. J. Gullick ("Oil Painting on Glass").

Bronze	A mixed Chrome Green.
Brown Madder	Lake prepared from the Madder Root.
Brown Ochre	Native Earth. This colour is valued for its rough appearance by water-colour artists.
Brown Pink	Lake made from Quercitron Bark.
Burnt Carmine	A colour obtained by charring Cochineal Carmine.
Burnt Lake	Formely obtained by heating Crimson Lake; a more permanent variety is now prepared from Madder Lake.
Burnt Roman Ochre	Calcined Native Earth.
Burnt Sienna	Calcined Raw Sienna.
Burnt Umber	Calcined Raw Umber.
Cadmium Yellow Pale	} Different varieties of Sulphide of Cadmium. They differ from Aurora Yellow in possessing a certain amount of transparency.
Cadmium Yellow	
Cadmium Orange	
Caledonian Brown	The original Caledonian Brown being no longer obtainable, a close imitation is prepared from Sienna and Vandyke Brown.
Cappagh Brown	A native earth containing Manganese in notable quantity. Many years ago the mine was exhausted, and the whole of the market was bought, up at the time by Messrs. Winsor and Newton, who now hold a large and valuable stock of this magnificently-drying colour.
Carmine	} Lakes prepared from Cochineal.
Carmine, No^o 2	
Cassel Earth	Synonymous with Vandyke Brown.
Chinese Blue	Synonymous with Prussian Blue.
Cerulean Blue	Stannate of Cobalt. Originally introduced to the public by Messrs. Rowney & Co.
Charcoal Grey	The composition of this colour is expressed by its name.
Chinese Vermilion	The genuine article imported from China.
Chinese White	A specially dense variety of Oxide of Zinc, used only in Water Colour. Chinese White was first introduced by us and is still one of our great specialities. It should be noted that ordinary Zinc White is often sold as Chinese White; buyers should therefore test it for covering power on a piece of black paper.
Chrome greens	Preparation of Chrome Yellow and Prussian Blue.
Chrome Lemon	A combination of Chromate and Sulphate of Lead.
Chrome Yellow	Normal Chromate of Lead.
Chrome Deep	} Chromates of Lead, more or less basic. Our Chromes are specially distinguished by the capital way in which they keep their colour on exposure.
Chrome Orange	
Chrome Red	
Cinnabar Greens	Similar in composition to Chrome Greens; but a deeper variety of Chrome Yellow is employed.
Citron Yellow	Chromate of Zinc.
Cobalt Blue	Alumina tintured with Oxide of Cobalt. Our Cobalt Blue is unusually free from a tendency to become greenish on exposure.
Cobalt Green	Zinc Oxide tintured with Oxide of Cobalt.

Cologne Earth	Calcined Vandyke Brown.
Constant White	Barium Sulphate. Used only in Water Colour.
Cork Black	A variety of Carbon Black, obtained by charring cork.
Cremnitz White	Basic Carbonate of Lead.
Crimson Lake	A Lake prepared from Cochineal.
Crimson Madder	A Lake prepared from the Madder Root.
Dragons' Blood	The genuine Dragons' Blood (a resin) being fugitive, an imitative pigment is now prepared, for use in Water Colour only, from Burnt Sienna, Cochineal Lake and Gamboge.
Emerald Green	Aceto-Arsenite of Copper.
Extract of Vermilion	Now synonymous with Scarlet Vermilion.
Field's Orange Vermilion	A specially levigated variety of Orange Vermilion.
Flake White	Basic Carbonate of Lead.
French Blue	} Artificial Ultramarines.
French Ultramarine	
French Vermilion	A variety of Sulphide of Mercury.
French Veronese Green	Synonymous with Viridian.
Gamboge	A preparation of the gum resin known under this name.
Geranium Lake	An extremely fugitive Lake prepared from an artificial dye.
Green Lake Light	} Combinations of Quercitron Lake and Prussian Blue.
Green Lake Deep	
Hooker's Green, No. 1	} Water Colour, pigments, prepared from Prussian Blue and Gamboge.
Hooker's Green, No. 2	
Indian Lake	A Lake obtained from Lac.
Indian Purple	This pigment, for use in Water Colour, is a Cochineal Lake with a base of copper. For use in oil an excellent substitute for this fugitive pigment is now manufactured from Madder Lake and French Ultramarine.
Indian Red	A variety of Iron Oxide.
Indian Yellow	Prepared "Purree" imported from India. A good deal of the permanence of this colour depends on its careful purification.
Indigo	A vegetable Blue extracted from the Indigo Plant.
Intense Blue	An extract of Indigo, used only as a Water Colour.
Italian Pink	Lake obtained from Quercitron Bark.
Ivory Black	Carbon Black, prepared by charring Ivory.
Jaune Brillant	A variety of Naples Yellow prepared from Chrome Yellow and White Lead.
Kings' Yellow	In Water Colour the original Sulphide of Arsenic is used. In Oil a tolerably permanent imitation of this fugitive pigment is made from Chrome Yellow and Zinc White.
Lamp Black	A variety of Carbon Black obtained by the imperfect combustion of hydro carbons.
Leitch's Blue	A combination of Prussian Blue and Cobalt.

Lemon Yellow Pale	}	Preparations of Chromate of Barium. It may be well to state that a more brilliant, but more fugitive preparation of Chromate of Strontium is sold by some houses under the name of "Lemon Yellow".
Lemon Yellow		
Light Red		Calcined Yellow Ochre.
Madder Carmine	}	Lakes prepared from the Madder Root.
Madder Carmine Extra		
Madder Lake		A synonym for Rose Madder.
Magenta		An Aniline Lake.
Malachite Green		Native Carbonate of Copper carefully prepared. We find the genuine Malachite stands much better than the artificial Carbonate of Copper often sold as Malachite Green.
Mars Brown	}	Earths containing Oxide of Iron as the essential colouring constituent, and differing mainly in the temperature to which they have been subjected.
Mars Orange		
Mars Red		
Mars Violet		
Mars Yellow		
Mauve	}	Aniline Lakes, Mauve No. 2 being the bluer variety.
Mauve, No. 2		
Mineral Grey		A very admirable pigment, prepared from the inferior grades of genuine Ultramarine. It has lately been much improved by us, and has a beautiful translucent quality and dries capitally. Some makes we have met with are the veriest rubbish, and appear to be mere crude Lapis Lazuli ground to powder.
Monochrome Tints Warm		Intimate combinations of Flake White and Umber.
Monochrome Tints Cool.		Combinations of Carbon Black and Flake White.
Naples Yellow		In Water Colour this consists of a combination of Zinc White and Cadmium Yellow. In Oil it is obtained by blending Lead White and Cadmium with a dash of Ochre.
Naples Yellow French		Is prepared solely as an Oil Colour, and is similar in composition to Naples Yellow - only differing in the proportions of the ingredients.
Neutral Tint		In Water Colour is made from Indigo, Cochineal Lake, and Carbon Black, according to the old formula. In Oil this has been replaced by an intimate combination of Carbon Black, Ochre, and French Ultramarine - a thoroughly durable mixture. Neutral Tint, both in Water and Oil, differs from Payne's Gray only in the proportions of its constituents.
Neutral Orange		A mixture of Cadmium Yellow and Venetian Red.
New Blue		A pale variety of French Ultramarine.
Nottingham White		Synonymous with Flake White.
Olive Green		In Water Colour this consists of a combination of Indian Yellow, Umber, and Indigo. In Oil it is prepared from Quercitron Lake and Prussian Blue.
Olive Lake		Quercitron Lake and Bone Brown blended with Ultramarine.
Orange Vermilion		Sulphide of Mercury.
Orient Yellow		An opaque variety of Cadmium Yellow, similar in quality to Aurora Yellow, but of a much deeper hue.
Orpiment		Synonymous with Kings' Yellow.

<i>Oxide of Chromium</i>	Is, as is suggested by its name, Chromium Sesquioxide. No praise can be too high for this most durable and unassumingly beautiful pigment.
<i>Oxide of Chromium, Transparent</i>	A hydrated variety of Chromium Sesquioxide.
<i>Oxford Ochre</i>	Synonymous with Yellow Ochre.
<i>Payne's Gray</i>	In Water Colour this compound pigment is still prepared from Indigo, Cochineal Lake and Carbon Black. In Oil we make it, as already stated, from Carbon Black, Ochre and French Ultramarine, and find, as is the case with Neutral Tint, that it stands like a rock compared with makes which are composed of the original ingredients.
<i>Permanent Blue</i>	A variety of French Ultramarine.
<i>Permanent Violet</i>	A new mineral pigment introduced by us in 1890, and containing Manganese as its tinctorial constituent.
<i>Permanent White</i>	Synonymous with Zinc White in Oil, and with Chinese White in Water Colour.
<i>Permanent Yellow</i>	A preparation of Chromate of Barium and Zinc White.
<i>Pink Madder</i>	A variety of Rose Madder leaning towards Pink.
<i>Primrose Aureolin</i>	A very pale and delicate variety of Aureolin, introduced by us in 1889. It is, if anything, more permanent than ordinary Aureolin.
<i>Primrose Yellow</i>	A combination of the Chromates of Zinc and Barium. Similar in colour to the old "Strontian Yellow" (Chromate of Strontium) but keeps its colour better.
<i>Prussian Blue</i>	Ferrocyanide of Iron.
<i>Prussian Brown</i>	Prepared from Prussian Blue by calcination.
<i>Prussian Green</i>	A mixture of Gamboge and Prussian Blue in Water Colour, and of Italian Pink and Prussian Blue in Oil.
<i>Pure Scarlet</i>	Mercury Iodide. Used only as a Water Colour.
<i>Purple Lake</i>	A purple modification of Crimson Lake.
<i>Purple Madder</i>	} Lakes prepared from the Madder Root.
<i>Purple Madder Extra</i>	
<i>Primrose Yellow</i>	A combination of the Chromates of Zinc and Barium. Similar in colour to the old "Strontian Yellow" (Chromate of Strontium) but keeps its colour better.
<i>Raw Sienna</i>	The native earth carefully prepared for artistic use.
<i>Raw Umber</i>	Native Umber of very fine quality, and possessing the greenish cast of colour which is so much prized by Artists.
<i>Rembrandt's Madder</i>	Lakes prepared from the Madder Root.
<i>Roman Ochre</i>	} Prepared native earths.
<i>Roman Ochre Cool</i>	
<i>Roman Sepia</i>	Sepia tinted with a little Sienna; it is used only in Water Colour.
<i>Rose Doree</i>	A variety of Rose Madder inclining to Scarlet.
<i>Rose Lake</i>	A new colour somewhat similar in composition to Geranium Lake; but possessing a rather opaque quality. It is, however, considerably more rosy in hue than Geranium Lake. No guarantee can be given of the permanence of this colour.
<i>Rose Madder</i>	A lake of exquisite beauty prepared from the Madder Root. Our Rose Madder has long been renowned for its delicate bloom, transparency, and the clearness of its tint with white. This favourite colour is consequently a great speciality with us

Rubens' Madder	This beautiful Lake is also prepared from the Madder Root, and resembles the Orange-brown Lake which is so well known to those who are familiar with Rubens' pictures.
Sap Green	In Water Colour is a mixture of the genuine Sap Green (a concrete vegetable juice) with Green Lake. In Oil the colour is a combination of Quercitron Lake, Ultramarine, and Bone Brown.
Scarlet Lake	An intimate combination of Vermilion and Alizarin Crimson. This mixture has, after careful trial, been introduced to supersede the much more fugitive compound hitherto made from Vermilion and Crimson Lake.
Scarlet Madder	A beautiful but rather weak variety of Rose Madder. It gives exquisite tints with white.
Scarlet Vermilion	Sulphide of Mercury.
Sepia	In Water Colour the genuine cuttlefish bags are prepared for painting. In Oil the natural pigment is ineligible, and an imitative mixture of Carbon Black and Vandyke Brown passes under the name.
Silver White	Synonymous with Cremnitz White.
Sky Blue	A cheap imitation of Cobalt, consisting of Ultramarine with a trace of Lemon Yellow.
Smalt	Silicate of Cobalt. Used only as a Water Colour.
Terra Rosa	As artificial earth tintured with Sesquioxide of Iron.
Terra Verte	} The native earths carefully selected.
Transparent Gold Ochre	
Ultramarine Genuine	The choicest extract of <i>Lapis Lazuli</i> . A speciality with us; as also is
Ultramarine Ash	The second quality of blue obtained from Lapis Lazuli. We have, of late, much improved this pigment, which excels particularly in the beauty and translucency of its colour. Ultramarine Ash dries well, and it altogether one of the most admirable pigments we know. These remarks of course apply equally well to genuine Ultramarine; but expense debars many artists from using the latter.
Vandyke Brown	The native earth prepared for painting.
Venetian Red	Artificially-prepared Sesquioxide of Iron.
Verdigris	Subacetate of Copper.
Vermilion Pale	} Varieties of Mercuric Sulphide.
Vermilion	
Verona Brown	A native ferruginous earth calcined.
Violet Carmine	A Lake obtained from the root of the "Anchusa Tinctoria".
Viridian	A hydrated and very transparent variety of Chromium Sesquioxide, originally introduced by our house.
Warm Sepia	A Water Colour pigment, prepared by tinting Sepia with Cochineal Lake and Sienna.
Yellow Carmine	A concentrated Lake prepared from Quercitron Bark. It is sometimes called "Yellow Madder".
Yellow Lake	A Lake prepared from Quercitron Bark.
Yellow Ochre	The native earth carefully prepared.
Zinc White	Oxide of Zinc. Although not possessing the body of White Lead, this beautiful white keeps its colour better. It has unfortunately a tendency to crack.

COMPOSITION OF WINSOR AND NEWTON'S VEHICLES

Amber Varnish	Genuine Amber dissolved in drying oil, and thinned with turpentine. "Pale Amber Varnish" is prepared with a special view to paleness of colour, but is otherwise similar in composition.
Oil-Copal Varnish	Similar in preparation to the above, but containing Copal in place of Amber. No guarantee, however, is given as to which of the many varieties of Copal enters into its composition. It is a very elastic and durable Varnish, but rather slow in drying. "Picture Copal" is a paler Varnish than "Oil-Copal": it is manufactured specially for Artists, and is guaranteed to be made only with the finest Sierre Leone Copal. Picture Copal Varnish dries much more rapidly than "Oil-Copal".
Manganesed Linseed Oil	Purified Linseed Oil containing a small percentage of Oxide of Manganese. The oil is thus rendered highly siccative.
Manganesed Poppy Oil	A precisely similar preparation made with Poppy Oil.
Mastic Varnish	A solution of Genuine Gum Mastic in purified turpentine. "Picture Mastic" is a thinner Varnish than the ordinary "Mastic", the latter being used only for making Megilp.
Medium	A carefully prepared composition of Drying Oil, Mastic Varnish, and Copal Varnish.
Megilp	A combination of Pale Drying Oil and Mastic Varnish.
Pale Drying Oil	Linseed Oil prepared with Oxide of Lead.
Petroleum, or "Essence de Petrole"	A volatile spirit obtained from Petroleum or "Rock Oil", and specially prepared for use by Artists as a substitute for Turpentine. It is thinner, and more penetrating in its nature than the latter, evaporates more rapidly, and leaves no sticky residue. It is also destitute of the pungent odour which renders turpentine so distasteful to many Painters.
CAUTION. - <i>Petroleum is highly inflammable, and neither the liquid nor its vapour must be allowed to come in contact with a light.</i>	
Purified Linseed Oil	Linseed Oil clarified by two or three years' exposure to sunlight.
Purified Poppy Oil	Poppy Oil clarified by two or three years' exposure to sunlight.
Strong Drying Oil	Linseed Oil prepared with Oxides of Lead and Manganese.
Turpentine	The best re-distilled turpentine prepared in England.

A NOTE ON THE PERMANENCE OF COLOURS

The word "Permanence" is capable of such broad signification that it seemed desirable to define with some exactitude what is meant in the following Classification Lists by the permanence of a colour.

(i.) By the permanence of a Water Colour we mean its durability when washed in Whatman paper and exposed freely, under a glass frame, for a series of years, to ordinary daylight; no special precaution (other than the usual pasting of the back of the frame) being taken to prevent the access of an ordinary town atmosphere. By an ordinary town atmosphere we signify an atmosphere containing normally, as the active change-producing constituents, oxygen, moisture, and a small percentage of carbonic acid, together with chronic traces of sulphur acids, spasmodic traces of sulphuretted hydrogen, and a certain amount of dust and organic matter in suspension.

(ii.) By the permanence of an Oil Colour we mean its durability when laid on ordinary prepared canvas and exposed freely, for a series of years, in an open room (as far as possible dust-proof) to ordinary daylight and the above-described town atmosphere. The action of the oil medium - sometimes reducing, sometimes oxidizing - has also in this case to be taken into consideration, and the white lead priming of the prepared canvas must likewise be regarded as having in many instances, an important bearing on the result.

It will be seen from the above definitions that our colours are tested under conditions which are as nearly as possible the same as those which obtain in the ordinary practice of picture-painting and picture-exposure. This we regard as a point of some importance; as it is, for instance, of little use to test the durability of oil-colours on glass or porcelain, while the artists of the day paint, practically without exception, on canvas or panel coated with a preparation of white lead. Parallel tests on inert backgrounds are, however, useful in determining the bearing of the orthodox preparation on the question of permanence.

With regard to our method of arranging the colours in three classes, it is of course impossible to draw any hard and fast line between a Permanent and Moderately-Permanent, or a Moderately-Permanent and a Fugitive Colour. The arrangement is an arbitrary one, and made only for convenience. Finally, it should be pointed out that one very important consideration which comes into play in the case of actual pictures - the mutual action of mixed colours - is not taken into account at all in our lists, which have reference only to colours exposed *per se*. We hope, however, in future issues of our catalogue, to give some account of the durability of certain selected mixtures, and also to correct and modify our present lists, which must be regarded as only provisional.

A CLASSIFICATION OF WINSOR & NEWTON'S WATER-COLOURS, In three Degrees of Permanence

CLASS I. - PERMANENT COLOURS

Alizarin Crimson	Cerulean Blue	Lemon Yellow	Raw Sienna
Aureolin	Charcoal Grey	Light Red	Raw Umber
Aurora Yellow	Chinese White	Madder Carmine	Roman Ochre
Black Lead	Cobalt Blue	Mars Orange	Roman Sepia
Blue Black	Cologne Earth	Mars Yellow	Rose Madder
British Ink	Constant White	Naples Yellow	Scarlet Madder
Brown Madder	French Blue	Neutral Orange	Sepia
Brown Ochre	Genuine Ultramarine	New Blue	Smalt
Burnt Carmine	Indian Purple	Oxide of Chromium	Terre verte
Burnt Sienna	Indian Red	Permanent Violet	Ultramarine Ash
Burnt Umber	Indian Yellow	Pink Madder	Venetian Red
Cadmium Orange	Ivory Black	Primrose Aureolin	Viridian
Cadmium Yellow, Pale	Lamp Black	Purple Madder	Yellow Ochre
Cadmium Yellow			

CLASS II. - MODERATELY PERMANENT COLOURS

Antwerp Blue	Chrome Deep ¹⁵⁰	Emerald Green	Prussian Blue
Bistre	Chrome Lemon ¹⁵⁰	Field's Orange Vermilion	Rubens' Madder
Bronze	Chrome Orange ¹⁵⁰	Leitch's Blue	Scarlet Vermilion
Brown Pink	Chrome Yellow ¹⁵⁰	Orange Vermilion	Vandyke Brown Vermilion

CLASS III. - FUGITIVE COLOURS

Carmine	Hooker's Green, No. 1 ¹⁵¹	Neutral Tint ¹⁵¹	Rose Lake
Carmine Lake	Hooker's Green, No. 2 ¹⁵¹	Olive Green ¹⁵¹	Sap Green
Crimson Lake	Indigo	Payne's Gray ¹⁵¹	Scarlet Lake ¹⁵¹
Dragons' Blood ¹⁵¹	Intense Blue	Prussian Green ¹⁵¹	Violet Carmine
Flake White ¹⁵²	Italian Pink	Pure Scarlet	Warm Sepia ¹⁵¹
Gamboge	Kings' Yellow	Purple Lake	Yellow Carmine Yellow Lake

A CLASSIFICATION OF WINSOR & NEWTON'S OIL-COLOURS, In three Degrees of Permanence

CLASS I. - PERMANENT COLOURS

Alizarin Crimson	Burnt Umber	Crimson Madder	Light Red
Aureolin	Cadmium Orange	Extra Madder Carmine	Madder Carmine
Aurora Yellow	Cadmium Yellow, Pale	Extra Purple Madder	Mars Brown
Black Lead	Caledonian Brown	Field's Orange Vermilion	Mars Orange
Blue Black	Cappagh Brown	French Ultramarine	Mars Red
Bone Brown	Cassel Earth	French Vermilion	Mars Violet
Brilliant Ultramarine	Cerulean Blue	Genuine Ultramarine	Mars Yellow
Brown Madder	Chinese Vermilion	Indian Purple	Mineral Gray
Brown Ochre	Cobalt Blue	Indian Red	Neutral Tint
Burnt Carmine	Cobalt Green	Ivory Black	New Blue
Burnt Lake	Cologne Earth	Lamp Black	Orange Vermilion
Burnt Roman Ochre	Cool Roman Ochre	Lemon Yellow, Pale	Orient Yellow
Burnt Sienna	Cork Black	Lemon Yellow	Oxford Ochre
Oxide of Chromium	Primrose Aureolin	Rubens' Madder	Transparent Gold Ochre

¹⁵⁰ These stand well the combined action of light, oxygen and moisture, but are liable to darken under the influence of sulphuretted hydrogen.

¹⁵¹ These mixed colours do not fade right out, but only fade in respect of their fugitive constituents. Inasmuch, however, as the strength of a chain is only that of its weakest link, we have been compelled to class them with the fugitive colours.

¹⁵² Stands light, oxygen, and moisture well, but goes black in time, being extremely sensitive to the action of sulphuretted hydrogen.

Oxide of Chromium, Transp ^t	Prussian Brown	Scarlet Lake	Ultramarine Ash
Pale Vermilion	Purple Madder	Scarlet Madder	Vandyke Brown
Payne's Gray	Raw Sienna	Scarlet Vermilion	Venetian Red
Permanent Blue	Raw Umber	Sepia	Vermilion
Permanent Violet	Rembrandt's Madder	Sky Blue	Verona Brown
Permanent Yellow	Roman Ochre	Terra Rosa	Viridian
Pink Madder	Rose Madder	Terre Verte	Yellow Ochre
			Zinc Whit

CLASS II. - MODERATELY PERMANENT COLOURS

Antwerp Blue	Chrome Lemon ¹⁵⁵	Cremnitz White ¹⁵³	Malachite Green ¹⁵⁴
Asphaltum	Chrome Orange ¹⁵⁵	Emerald Green ¹⁵⁴	Monochrome Tints, Cool, Nos. 1, 2 and 3 ¹⁵³
Brown Pink	Chrome Red ¹⁵⁵	Flake White ¹⁵³	Monochrome Tints, Warm, Nos. 1, 2 and 3 ¹⁵³
Chrome Deep ¹⁵⁵	Chrome Yellow ¹⁵⁵	Indian Yellow	Naples Yellow ¹⁵³
Chrome Green, No. 1 ¹⁵⁵	Cinnabar Green, Light ¹⁵⁵	Jaune Brillant ¹⁵³	Naples Yellow, French ¹⁵³
Chrome Green, No. 2 ¹⁵⁵	Cinnabar Green, Mid ¹⁵⁵	Kings' Yellow ¹⁵³	Prussian Blue
Chrome Green, No. 3 ¹⁵⁵	Cinnabar Green, Deep ¹⁵⁵	Leitch's Blue	

CLASS III. - FUGITIVE COLOURS

Carmine, Orient	Green Lake, Deep	Mauve	Purple Lake
Carmine, No. 2	Green Lake, Light	Mauve, No. 2	Sap Green
Citron Yellow ¹⁵⁶	Indian Lake	Olive Green	Verdigris ¹⁵⁷
Crimson Lake	Indigo	Olive Lake	Violet Carmine
Gamboge	Italian Pink	Primrose Yellow ¹⁵⁶	Yellow Carmine
Geranium Lake	Magenta	Prussian Green	Yellow Lake

N.B. - Some of these fugitive colours are often supposed to be much more fleeting in ordinary daylight than is really the case. Thus, Orient Carmine, Carmine No. 2, Crimson Lake, Gamboge, the Green Lakes, Indigo, Italian Pink, Olive Lake and Yellow Lake experience very little alteration, even after two or three years' exposure, and without any protection whatever from varnish.

¹⁵³ Permanent on exposure to light, etc., but sullied in an atmosphere containing sulphuretted hydrogen, and yellowed by reaction with the oil medium.

¹⁵⁴ Permanent to light, etc., but darkened by sulphuretted hydrogen, the change being facilitated by the slight solubility of these pigments in oil.

¹⁵⁵ These stand light, oxygen, and moisture fairly well, but are reduced by the oil of the medium, and by the action of sulphuretted hydrogen.

¹⁵⁶ Reduced and turned green in contact with an oil medium, or with sulphuretted hydrogen.

¹⁵⁷ Soluble in oil and blackened by sulphuretted hydrogen. In every way a bad colour under the present conditions of oil-painting.

Geranium Lake is the most fugitive oil-colour made, and fades quickly in an ordinary wall-light. The Mauve and Magenta become redder in hue and have tendency to blacken; but do not fade rapidly. Purple Lake and Indian Lake also redden considerably; but otherwise stand tolerably well. Olive Green and Sap Green become bluer. Verdigris becomes much yellower. Violet Carmine turns quite black.

The above remarks apply, of course, only to the colours exposed *per se*. When, however, they are diluted with Zinc White, or White Lead, in the formation of tints, the changes are, as a rule, greatly accelerated.

II.3. Transcription of selected W&N production records

The identification data and the transcriptions of the production records reproduced from the W&N 19th century database are described below.

II.3.1. Lead chromate pigments

● Primrose Chrome PR1a

Original Recipe Name	URC	Marginal numbering	Date
Primrose Chrome	P1P235AL04	[718A] & [718B]	1846-58

Transcription:

Primrose Chrome

[718A] Take 30 galls Cold Aq. dissolve & add to it

1 1/2 lbs Bi Chrome

1 1/4 lbs Soda. add 3 lbs Sul Acid

strike with 4 1/4 galls Lead Liquor¹⁵⁸, left supernat^t quite free of Bi Chrome & in excess of acid_ leave till next day_ draw off supernat^t liquor & wash the chrome 4 times. Produce 8 3/4 lbs nett.

[718B] Take 25 galls Cold Aq dissolve & add to it 1 1/2 lbs Bi Chro: 1 1/4 lbs Soda. The temperature of the liquor is 50°. add 2 lbs Sul Ac (sp gr 1850) strike with 2 1/2 galls Lead Liquor_ stir well all the time_ left supernat^t in excess of acid_ take out stick & leave till next day_ draw off supernatant which is still in excess of acid_ strain & put on filters. no washing

So very light & spongy_ doesn't shrink much

Page B:

[718B] Produce Scraped 6 1/2 lbs Scrap⁹ 1/4 lb Total 6 3/4 lbs

Light in weight, rich & bright Lemon tint

has a coarse fracture

¹⁵⁸ The lead liquor production record reconstructed is described below.

● **Primrose Chrome PR1b**

Original Recipe Name	URC	Marginal numbering	Date
Primrose Chrome	P1P235AL04	[718C]	1846-58

Transcription:

[718C] The usual chrome liqr & salts [as prep^d for Pure Lemon Chrome] with Sulp:Acid added & precipitated when cold with a solution of Nitrate of Lead¹⁵⁹_ affords a very bright & lemoney tint_ some made this way, after washing & drying off turned to a usual Lemon. (?) to keep it pale, the acid must be left in excess, & the color left under the supernatant all night & next morn⁹ filtered without washing at all.

● **Lemon Chrome L1**

Original Recipe Name	URC	Marginal numbering	Date
Super Lemon Chrome	X6P235L15	a174	30-12-1853

Transcription:

Super Lemon Chrome a174

30/12/53

Large vat 1 foot Cold aq add cist Chro: Liq made with 25# Bi Chro' 28# Soda & 30# S.O.3.S as usual see p87 Sept 19/53. add 10# more S.O.3.S diss in hot aq & stir well up & have till next day

In the mean time a batch of Sul PI (hydr state) was taken (this was the Sul PI precip of the making of S. M. C. page 145 & supposed to be equal to 30# dry Sul PI) after it has been washed abt 8 times add 1# S.O.3 to the last washing, stirring well up from the bottomm of the tub.

31/12/53

Draw off the water from the white & let a person stir it up well & constantly all the while the large vat is being struck

stir up the large vat and strike as quickly as poss with 23 galls Nit PI: Solⁿ (that had been made as usual) have supernat free from yell but do not strike down the white (S.O.3S Solⁿ) as it makes the color poor & moreover it increases the expenses of the Chrome, as Sul PI made by that means is too dear

When the large vat is struck, bale in the white passed thro' a sieve & stir constantly till all is in, then continue to stir 1/2 hour longer.

Then leave to settle, draw off as soon as you can, & put on filters passing the chro thro a wire sieve. Pot in large size moulds. When dry cakes kept tog' well, close facture & a fine Lemon Tint rather above the ordinary quality

Mem. Took a whole batch of Nit PI Solⁿ all but 1 gallon. made with 73# Acid Nitros 90# Litharge (all the Lith was not quite taken up)

was marked "super"

For Oil grinding as for Xtra quality for sale.

¹⁵⁹ The lead nitrate production records reconstructed are described below.

Original Recipe Name	URC	Marginal numbering	Date
Best Lemon Chrome	X6P240L11	a291	31-05-1854

Transcription:

a291 Best Lemon Chrome

May 31/1854

Take 1 Batch Sul White that had been made as usual from the sup^t V & precip with 20# S.O.3 & washed 6 times. (mem. had been made a month or two)

Put this white into a clean tub & fill up with cold aq add 1/2# S.O.3 stirred in.

Large vat 1 foot Cold aq add to it 1/2 cist Chrome liq made as at page 273 (may 22/54)

Dissolve in a tub 40# S.O.3 S in 14 galls boiling water then abt 16 galls Cold aq & leave till next day to get quite cold

June 1/54

Add to the Large vat the diss^d S.O.3.S. then add the washed White (the supernat liq having been previously drawn off) & strike immediately with galls of nit PI Solⁿ quite clear & cold as made at page 132. All the Bi Chro is struck down leaving the supernat in excess of salts. stir well for 1/2 hour, leave to settle draw off & strain on to filters

Next day pot large size

Bright lemon tint, close fracture med: light in weight

● **Lemon Chrome L2a**

Original Recipe Name	URC	Marginal numbering	Date
Best Lemon Chrome	4PP102AL01	[2813]	03-08-1872

Transcription:

Best Lemon Chro:

P/5570. Aug 3.1872

[2813] In 1000 Gln Back put

1 ft 6 Cold Aq

84 lbs S: S: ref^d [H&S]

stir occasionally till diss^d

[2814] Get ready

120 lbs W: S: B: []

soaked in Aq.

[2815] Get ready in "7 plug" tub

40 gallons Sol: N: L: [2676/9]

[2816] Get ready

3 x 2 lbs SO3 that has each been added to 1 gall cold aq

[2817] 8 Aug 72 The Strike:--

50 gallons Chrome Liquor [2178] add the WSB [2814] thro' 70 hole sieve, strike at once with Sol:N:L [2815]

supernat^t colorless & in excess of precipitant, add the dil: SO₃ [2816] sup^t now affords moderate white precip: with more Sol:N:L: but none whatever with Solⁿ:B:C Continue stirr^g 1/2 hour longer & leave.

Next day, leave undisturbed to "Lemonize".

Day after that, draw off colorless sup^t This affords very faint turbidness with both Sol:N:L & Sol:B:C:

I believe this sup^t to be neutral as possible, draw it off.

Wash settled Colour = 4 times Cold Aq. Last sup^t afforded no acid re-action on Litmus, draw off, strain, filter well, pot on tiles & dry off @ 90° a 100°

Sent 2.1.25 nett to Reynolds Co, N. Y.

Original Recipe Name	URC	Marginal numbering	Date
Best Lemon Chrome	A5P028AL01	7548	06-10-1879

Transcription:

Best Lemon Chrome

7548. Oct 6. 1879

1 ft 6 Cold Aq

84 lbs S: S: ref: [1/3/77] same as [7547]

Get ready

120 lbs W: S: B: [] washed over into 300 gln Back filled to within 9 in of top with Cold aq. add 1 qt SO₃, stir constantly for 1 hour, then stir up well hourly during the day.

Next day, draw off & wash 2^{ce} Cold aq.

To 1200 gln Back set with the Aq & S: S: add the washed & settled WSB. add 50 galls Chrome Liq [6959]

strike at once with galls Sol: Nit: Lead [] sup^t as bef. add 4 x 2 lbs SO₃ as before

stir 1/2 hour _ leave _

wash 5 times

Worked as [7547]

Page B:

Fine colour & very soft.

● **Lemon Chrome L2b**

Original Recipe Name	URC	Marginal numbering	Date
Super Lemon Chrome	P2P358AL01	M/4181	09-07-68

Transcription:

M/4181. 9/7/68 Batch made with

1 ft 9 Cold Aq

80 lbs S: S: stir occasionally till diss^d

20/7/68 38 Glns Sol: N: Lead [] in 4 plug tub

" 4 lbs SO₃ added to 2 glns Cold Aq.

21/7/68 50 Glns Chro Liq [1232A] thro' hair sieve & added to Large vat cont^g the Aq & SS.

Strike with the Sol N Lead at once, finish with 10 glns more Sol: N: L, sup^t in slight excess of precipitant, add immediately the dil So₃ stir 1/2 hr leave. sup^t now affords no precip with Sol BC & very slight white pp wi Sol N L

The clear sup^t faint buff color, yields strong acid re-action on litmus.

23/7/68 Draw off sup^t affording acid re-action on litmus

no precip wi either Sol N L, or Bi Chro. Wash 6 dry off as usual.

Pilot beautiful rich lemon tint.

● **Lemon Chrome L3a**

Original Recipe Name	URC	Marginal numbering	Date
Super Lemon Chrome	P1P433AL01	[1163]	1846-58

Transcription:

Super Lemon Chrome

[1163] 1/2 cistern soda chrome liquor_ 35 lbs sulphate of soda diss' in aq_ added to the chrome liquor & left to get cold before using.

[1164] 73 lbs Litharge }
75 lbs nitros acid } dissolved cold and the clear solution drawn off for use

[1165] Large tub set with 1 ft 10 in of aq _ put in the chrome and salts solution [1163] and strike with the nitrate of lead which it took the whole.

[1166] Work the tub for a full hour after it is struck, stirring continually

[1167] Have 35^{lbs} Plaster Paris (at 10/cwt) when all mixed with about 140 galls aq stir the plaster in solution for 2 hours unremittingly then leave to subside_ wash twice before using.

[1168] When the struck Chrome has subsided in the large tub_ then add the plaster solution pouring its thro' the fine wire sieve & stir till intimately mixed together.

There were more scrapings than ought have been

The batch should have produced 1 cwt scraped colour

Page B:

This batch was a particularly clear and pure lemon and rather light_ it shrank very much in drying on account of its not having been potted on chalk if it had it would I think have been very light indeed, very excellent batch.

● **Lemon Chrome L3b**

Original Recipe Name	URC	Marginal numbering	Date
Pale Lemon Chrome	P1P424AL01	[1137]	1846-58

Transcription:

Pale Lemon Chrome

very Pale Best quality. small assay.

[1137] 5 galls Chrome Liq (made with 50^{lbs} Red Salt, 56^{lbs} soda, 150 galls Aq.)

6 1/2 galls usual sulph soda solⁿ sp:gr: 1070.

This takes to precipitate it

3 1/2 galls Solⁿ Nitrate of Lead_ sp:gr: 1400.

Leave all night_ next day wash.

Produce 17[#] 3/4

3[#] to Cooke & Rowley

● **Middle Chrome M1a**

Original Recipe Name	URC	Marginal numbering	Date
Best Middle Chrome	P1P245AL01	[735]	1846-58

Transcription:

Best Middle Chro: Light in weight & close fracture

[735] The large vat set going with 1 ft 2 cold aqua

45 lbs Bi Chrome & 27 lbs soda [433]

[736] Serve 56 lbs Whiting same as [433]

[737] Prepare nit lead sol as follows:

In the new (stout) 64 galls tub put 16 galls of cold aqua make it boil by means of the steam pipe (the tin one) Take the steam pipe out of the water and add to the boil^g water 73 lbs acid nitros _ now sprinkle in by degrees 90 lbs litharge _ another stir all the time. when all in, add 16 galls more aqua (this time it would be better to add hot, but cold would do) and now screw on the steam pipe again and make the liquor boil for 1 hour* Then take off the pipe & leave for the liquor to deposit its sediments. Produce 36 galls.

* during this hour, it must be constantly stirred.

[738] To the liquor in Lg vat [735] add the white [736] and precipitate with 33 gallons of nit lead

Left the supernatant a little yellow (chrome) fill up vat with aqua. Then draw off and wash 1^{ce} dry of as usual.

This batch is quite as rich and bright as [433A] for oil, but there is a slight difference altho' hardly perceptible, in the dry state in favour of [433].

Page B:

This costs nearly 3^d lb less than [433].

for a still cheaper formula vide [433A].

Original Recipe Name	URC	Marginal numbering	Date
Best Middle Chrome	P2P211AL01	[1663]	28-07-58

Transcription:

Best Middle Chrome 28/7/58

[1662] Large Vat 1 ft 2 in Cold Aq.

Dissolve & add separately 45lb Bi Chrome 30lb Soda.

Into a tub wash over 60lbs Whiting

Strike:- Pass the whiting thro' 70 hole sieve into the liq^r in large vat & stir well together, now precip^t with

42 galls Nit Lead Solⁿ syphoned in & stirred all the time _ the whole of the yellow color was precip^d stir 1/2 hour after precipⁿ draw off supernatant when color settled, wash twice filter same day. was bulky on filters.

Page B: Notes:- Is best to leave the supernatant liq^r rather in excess of chrome, a mere tint _ I see no objection to its standing till next day for this color _ and probably the slight tint left in the supernatant would be lapped up by that time.

I find that Paris White is freer from fluff than whiting, therefore substitute the former for the latter.

Original Recipe Name	URC	Marginal numbering	Date
Best Middle Chrome	P2P386AL01	[2010A]	02-11-66

Transcription:

K/3678 2/11/66

[2010A] Chro liq made as at [2010] but using 90 lbs Bi Chro (White's)

60 lbs Soda make up with cold aq to 2 feet when done.

[2010B] Bright lig [2010A] in L^g vat measured

6 1/2 inches = 100 glns. add of cold aq

6 1/2 " making 13 in altogether

[2010C] 120 lbs Paris White [19/5/66] soak^d in 14 glns Cold Aq & pass^d thro' 70 hole sieve into [2010B] strike as usual, (?) 40 glns Sol: N: Lead [2156] sup^t colorless & in excess of salts, stir well at intervals during 4 hours, strain & filters same day....

Very good rich color in Oil & Kept a bright full tint in Oil when dry on tile.

● **Middle Chrome M1b**

Original Recipe Name	URC	Marginal numbering	Date
Super Middle Chrome	X5P078AL01	5842	1862-64

Transcription:

Super Middle Chrome 5842
 In N^o 2 Back put
 2 ft Cold Aq:
 50 galls Chro: Liquor
 Precip with 20 galls Nit Lead Sol:
 Draw off, wash 1^{ce}
 Strain filter, pot & dry off as usual
 Produce 3 grs 18 1/4 lbs nett

This is made for Water Colours, and in the Cake & Mst Processes is sometimes termed "Pure" It however has to be crushed well washed and dried again

● **Middle Chrome M2a**

Original Recipe Name	URC	Marginal numbering	Date
Best Middle Chrome	X6P251L01	a206	22-02-1854

Transcription:

Best Middle Chrome a206
 Feb 22/54
 Large Butt 1 ft 10 in Cold aq diss 30[#] Bi Chro in 18 galls Boiling Aq add 18[#] Soda when diss^d
 strain into large vat & leave
 Lead Liq made as usual with 50[#] Grey Sug Lead & 50[#] Litharge. Produce 30 galls
 28[#] Sul Barytes washed over into tub next day drawn off supt aq.
 Feb 23/54
 To Large vat add 12[#] S.O.3 stir well, tint the Sul Baryt with 30 galls of the Chro Liq out of the vat & strike with 2 galls Lead Liq. left sup^t little in excess of Chro_ stir all the while the Large Vat is being struck.
 Strike the large vat with 20 galls Lead Liq, left off when all the Bi Chro' had been struck down, add the tinted white thro' sieve to the chrome in vat & continue to stir well for 1/2 hour after it is all in, when settled draw off & put on filters. Lead Liquor left 8 gallons

of a very rich bright - a goldeny chrome
 tol light in weight, rather richer in tint than 198

Original Recipe Name	URC	Marginal numbering	Date
Best Middle Chrome	P1P192AL01	[636]	1846-58

Transcription:

Best Middle Chrome

[636] Large vat as [633] 1 ft 2 in Cold water.

42 lbs sulphate Barytes as [634].

Add to large vat 45 lbs Bi Chrome and 27 lbs Soda as [633]. Then add 18 lbs Sul:acid stir well add also the sulphate Barytes as above & strike with 32 galls (equal to 1 ½ batches) solⁿ Lead Liquor [637] The supernat: left colorless, but would have thrown down a copious white precip: with the addⁿ of more Lead Liquor _ when color settled draw off sup^t strain & filter _ pot as [635] _ when dry was very bright and rich in tint, not very heavy, rather close fracture for middle. A good process

Would Carb: Lead or Sulphate of lead be a good base for Chrome?

Page B:

Notes: vide page 106 for a process where the chrome is softer to grind in oil.

This formula [636] is for a somewhat cheaper article for sale.

● **Deep Chrome D1a**

Original Recipe Name	URC	Marginal numbering	Date
No. 1 Deep Chrome	X8P059L17	B462	21-11-1854

Transcription:

B462 No 1 Deep Chrome

1854

Nov 21 Wash over 56[#] Sul Baryt then sift into 28[#] Plaster Paris (super) sifted in dry as usual, while another person stirring well all the time (takes 2 hours

good stirring, add aq as required until the butt is full

Dissolves 30[#] Bi Chrome

10[#] Soda

} together in 18 galls Boiling aq

Strain it into large butt_ containing 1 foot 10 in Cold Aq

Add to large butt

2 lbs S. O3 (sp:gr: 1850) now add the above sponged white thro' sieve & at the same time strike with stirring the whole time

32 galls Lead Liquor_ left sup^t trifle in excess of Chrome stir 1/4 hour & occasionally until it becomes as orange as it will. Then add 7 lbs S. O. 3 (sp:gr: 1850) diluted by pouring it into 2 galls cold aq stir up the color & occasionally until the proper tint is obtained then take out stick & leave to settle till next day.

Draw off strain & filter : seems tolerably bulky

Good rich tint, rather more orange in hue than B458 = rather closer in fracture than that batch_ abt the same in bulk. Perhaps B458 is the best tint.

Note!! This is considered by Mr HCN to be the best tint for deep.

● **Deep Chrome D1b**

Original Recipe Name	URC	Marginal numbering	Date
Best Deep Chrome	P1P190AL01	[633]	1846-58

Transcription:

Best Deep Chrome

[633] In 500 gallon (butt) put 1 foot cold water. Dissolve and add to it 45 lbs Bi Chromate of Potash and 27 lbs of Soda, diss' separately.

[634] Wash over thro' a sieve into cold water 42 lbs sulphate of Barytes _ when whit has settled draw the water off.

[635] Add to [633] 9 lbs Sulphuric acid (concentrated) stir well _ add also the washed Barytes [634] stir well and strike with 24 galls Lead Liquor [] (equal to 1 batch composed of 56 lbs grey sugar of lead and 50 lbs litharge). Left supernant.^t little tinted with chrome _ stir well for 20 minutes _ leave to settle _ draw off the supernant.^t and strain chrome, put on filters and pot in circular tin moulds like fig which is open top and bottom _ it is 5 ½ or 6 inches in diam^r and 3 inches deep. This mould is to be placed on the chalk stones with linen placed between and the colour filled into it, then left until suff^t of the water has absorbed into the chalk when the mould be removed and the color is left to set firmer before it is removed to be finally drier off on absorbent or any flat tiles, in the drying room.

When dry produced 1 – 0 – 17 scraped chrome

By scraping – is meant cleaning the surface of the cakes with a Hare's foot and rubbing over a piece of wire stretched over a hollow box _ by these means all dirt and dark crusty parts on surface of the cakes are removed.

The color produced was rich in tint, but very heavy.

Original Recipe Name	URC	Marginal numbering	Date
Best Deep Chrome	P3P054AL01	M/4387	26-02-1869

Transcription:

Best Deep Chro:

M/4387

26/2/69

[2307] In 300 gln Vat put 1 ft 2 in Cold Aq

50 gln Chrome Liq^r [2308]

Wash over thro' 70 hole sieve

56 lbs W:S:B [] strike at once with

80 glns Lead Liquor [] sup^t yellow, add 8 lb So3

1/3/69

next day, draw off colorless sup^t add to settled color

2/3/69

4 lb SO₃ stir well, fill up with cold aq. Draw off colorless sup^t having slight acid re-action on litmus add to settled color 4 lb SO₃ stir well in, fill up with Cold Aq

3/3/69

Draw off colorless sup^t same as before, wash settled color until no acid re-action is observed when tried with litmus. strain & filter

Pot & dry off

Kept its colour in oil, on palette, very well when examined Sept 1870.

● Deep Chrome D2a

Original Recipe Name	URC	Marginal numbering	Date
Best Deep Chrome	P3P106AL01	O/4917	24-08-1870

Transcription:

Best Deep Chrome

O/4917. Aug 24. 1870

[2468] In 500 gln Chrome vat put 2 ft cold aq

45 lbs B.C. diss^d in 12 glns Boil^g Aq

7 1/2 lb S: diss^d in 3 gln " "

each diss^d separately.

[2469] In 300 gln vat put 1 ft 6 cold aq

Dry sift in thro' fine wire sieve 21 lb superf: P: P: [Bellman's 18/8/70]

21 lb W:S:B: []

this latter (viz the W:S:B: is soaked in aq & wash^d thro' 70 hole sieve into the Superf: P: P: diffused in the Aq. continue the constant stirring (from the first) to the expiration of 1 hour after all the WSB is in then leave to settle. Draw off.

[2470] 25/8/70

To vat set as [2468] add the settled white [2469] thro' 70 hole sieve, strike with 30 glns Lead Liquor [] by 2 glns at a time.

22 glns Lead Liquor [] by 1 gln at a time stirring constantly. supt pale yellow, stir occasionally add 5 lbs So₃ - sup^t now colorless.

Draw off, wash 3 times cold aq. Last supt no acid re-action on litmus. Strain settled color, filter, & pot on tiles & dry off.

Instead of leaving it all night to redded as much as it would, the So₃ was put in in an hour or two after fin^d striking with the Lead Liq^r.

In the washing up, Fletcher remarked that it was much more bulky in the Butt than usual.

Nice close & good fracture & texture & light in weight - tint good.

Original Recipe Name	URC	Marginal numbering	Date
Best Deep Chrome	4PP038AL01	[2631]	10-1871

Transcription:

Best Deep Chrome.

P/5304. Oct 1871.

[2631] In "Back" (capable of holding about 10 or 12 hundred gallons of liquor)

2 feet Cold Aq

60 lbs Bi Chro: diss^d in Boil^g Aq

10 lbs Sod: diss^d in Boil^g Aq

when all in the "Back" make up to

2 ft 6 with sufft Cold Aq.

[2632] In "2nd size" (abt 300 glns) put 2 feet Cold Aq 28 lbs Superf: P: P: [23/10/71] dry sift it thro' fine wire sieve, ano^r stirring all the time, then wash over into it thro' 70 hole sieve 28 lbs W: S: B: [] stirred as before, now continue the stirring for 1 hour longer, adding Cold Aq as the white thickens, until the vat is full. next day, draw off transp^t sup^t

[2633] Strike the vat set as [2631] with sufft Lead Liquor [2611] run in by very fine stream & stirred well all the time left sup^t very pale yellow

leave 4 hours to redden as much as it will, stirring occasionally, add the settled white [2632] stir^g well all the time, add 6 lbs SO₃, stir well, leave.

[2634] Draw off colorless sup^t having no acid re-action on litmus.

Wash settled color 2^{ce} Cold Aq.

Draw off, strain & filter When well filter^d, pot on tiles, & dry off as usual.

● **Lead Liquor (Lead Subacetate)**

Original Recipe Name	URC	Marginal numbering	Date
Lead Liquor	P1P193AL01	[637]	1846-58

Transcription:

Lead Liquor or Sub-Acetate of Lead Solⁿ

[637] Put 15 gallons Cold water, make this boil by means of a steam pipe (tin) conveying high pressure steam into the above cold water.

when the water boils or nearly so, add 56 (lbs) Grey Sugar of Lead, when dissolved add by degrees 50 (lbs) flake litarge, shed over the boiling liquor by scoop pulls at a time & continue stirring for 2 hours. The whole or the greater portion of the litharge should be by this time dissolved_ The solution assumes a greenish hue, perhaps owing to its being done in a copper vessel.

would not an iron pot be better?

The produce of the batch when cold was 24 gallons.

Original Recipe Name	URC	Marginal numbering	Date
Lead Liquor	A5P037AL01		1864-80

Transcription:

[6855] In 132 gln Lead Lined Tub with Leaden steam worm put 112 galls Cold Aq, when 212° slaken steam & add at a simmer only,

1 cwt Grey Sug: Lead, when dissolved, add

1 cwt Litharge slowly sprinkled in & well stirred, when all in, get up the heat to a good steady boil & Boil 2 hours at a steady bubble, adding aq as required to bring up too 112 galls.

Turn off steam & leave 1 hour for sed^{ts} to subside.

then run off the bright into the stone Back for use.

● **Lead Nitrate**

Original Recipe Name	URC	Marginal numbering	Date
Nitrate Lead Solution	P2P198AL01	[1645] & [1645A]	1846-58

Transcription:

Nitrate Lead Solution

[1645] 19/7/59

In usual tub put

32 galls cold aq

73 lbs Acid Nitros [C Foot & Co 18/7/59]

76 lbs Litharge [10/5/59]

not enough water, added 8 galls more aq - when all the Lith is in stir 1 hour.

21/7/59

Draw off clear liq from sediments.

Produce 41 galls bright Litharge left = 4 1/2[#].

[1645A] Another formula

40 galls Cold Aq

73[#] Acid Nitros [18/7/59]

73[#] Litharge [19/5/59] Stir 2 1/2 hrs

Produce 42 galls bright -

This quy of Litharge exatly diss^d in the acid making the quantity necessary.

Original Recipe Name	URC	Marginal numbering	Date
Sol: Nit: Lead	P2P442BL12	[2156]	12-10-66

Transcription:

Sol: Nit Lead.

K/3667. 12/10/66

[2156] In pan or tub put 26 glns Boil⁹ Aq

196 lbs Ac: Nit [Huskisson's 10/10/66

238 lbs Litharge [16/1/65]

add carefully for fear of coming over be particularly cautions towards the end of the operation takes from 1/2 to 3/4 hrs to get all the Lith in. add

20 glns more Boil⁹ Aq, stir well 1/2 hr

bale into pan, Produce hot = 57 Glns.

sp: gr: cold 1455 = Lith left abt 20 lbs

II.3.2. Other yellow chromate pigments

● **Lemon Yellow**

Original Recipe Name	URC	Marginal numbering	Date
Lemon Yellow	X6P154L20	a232	06-04-1854

Transcription:

a232 Lemon Yellow

April 6/54

Middle Copper with Purif Aq boiling

13 1/2 galls Boiling Aq in large Pan, passed thro' sieve

1 1/2[#] Bi Chro diss in a stone Pan (not lead glazed) with boiling aq

pass thro sieve into large Pan

strike immediately with 2 1/4 gall Soln. Mur: Baryt (made as at page 68) stir well some minutes & leave to settle 1 hour, draw off supernat liq & wash 3 times with cold Purif Aq. filter chalk & dry off

Original Recipe Name	URC	Marginal numbering	Date
Lemon Yellow	X8P076L11	B599	06-1855

Transcription:

Lemon Yellow B599

June

1st Batch 10 galls Boiling Purif^d Aq

1[#] Bi: Chro: diss^d in 2 galls aq

- | 1 gallon of the strong Mur: Baryt soln sp:gr: made at A199
- | 1 gallon cold purif^d aq

[added together before striking] the Bi: Chro: _ when struck leave 1 hour. draw off the supernat & wash clean with purif^d aq cold

Produce = 1 lb 8 1/4 oz nett

very bright, Pale & rich color transpt in Oil Pale color & rich in tint. marked for water

● Barium Chloride

Original Recipe Name	URC	Marginal numbering	Date
Muriate Barytes Solution	X6P042AL01	a68	07-1853

Transcription:

a68 Mu. Bar. Sol. making July 1853

Take of Mu Ac. 213[#] nett (2 ? 23/7/53)

add 26 1/2 galls clean cold aq

add by degrees for fear of coming over 213[#] Powered Stone (Carb Bar)

Soak the quantity of powdered stone that remained in the pan from last making & washed away the dirt iron &c and then made up the quantity (viz 213[#]) with fresh stone for this present batch. the last of the stone was put in July 24th 1853 continued to stir up every day until (abt) latter end of oct/53 then take out stick scrape down sides & leave covered over for all sediments & impurities to subside.

Jan 54 Draw off clear liq into another pan & put the bottoms into another small pan to settle. Take 2 galls of this clear Mu Bar Solⁿ precip with suff^t P. Ash in hot aq

wash 4 times add to the bulk of Mu Bar Solⁿ in large pan stir up every day for 6 days then leave quiet to settle & brighten from Mar 17/54 until Oct 23/54 when it was draw off from sedimts & put into clear pan for any further deposit.

● Citron Yellow

Original Recipe Name	URC	Marginal numbering	Date
Chromate of Zinc	X6P385L15	B460	20-11-1854

Transcription:

B460 Chromate of Zinc

1854 Nov 20

10 galls Aq

6 lbs Bi Chrome

3[#] 1/2 oz P. Ash

44 lbs Nit Z Solⁿ (p452) = to 3 galls

2[#] 1/2 oz P Ash

washed 3 times

Produce = 8 lbs 4 1/2 oz nett

as the produce is only 8 1/4# the cost of this batch (?) lb is 16 for materials only

Nov 21

10 galls Aq

6 lbs Bi Chrome

3# 1/2 oz P. Ash

3 galls Nit Z Solⁿ

2# 1/2 oz P Ash

washed 4 times

Produce = 8 lbs 6 oz nett

X 16 lb rather under mat^{ls} only

good bright color. soft

● Zinc Nitrate

Original Recipe Name	URC	Marginal numbering	Date
Nitrate of Zinc	X6P376L10	B452	17-11-1854

Transcription:

Nitrate of Zinc B452

1854

Nov 17

9 galls boiling aq

36 lbs Nitros Acid

15 lbs Chi W^t (CW)

prep^d as usual

Nov 18

Sp:gr:1210 clear & fit for use

Produce 9 galls clear solⁿ

Estimate of cost p gallon x 2/gall

● Strontian Yellow

Original Recipe Name	URC	Marginal numbering	Date
Strontian Yellow	P1P197BL10	[645A]	1846-58

Transcription:

Strontian Yellow. another form

[645A] Take 2 lbs Nit Stront: dissd in only just sufft boilg aq.

[646A] Take 1 quart Chro: Liq: that had been prepd as follows; In a 15 gallon iron pan half full of aq boiling, add 12# 1/2 Bi Chromte Pot: when dissd, add 12# soda by degress_ this quantity of Sod: was sufft to neutralize the liquor; boil 1 hour after all in. the finish by filling up the pot with cold water.

[647A] Strike the 1 qt Chro Liq prepd [646A] with the whole of the Nit Stront [645A] adding abt a 1/9th part at each addn & stirg now leave till the next day. the supernat left nearly neutral, perhaps of the two there was a very slight excess of chrome. The supernatt was tinted a pale yellow, approaching to a stran colour, but would not have been less tinted had there been more Nit: Stront added.

Next day draw off supernat liqr which is very weak in tint of yellow. filter the colour, drop on chalk with linen & blotting paper placed between the colour & the chalk. dry off in drying room. Produce 2 3/4 ozs. was not washed at all, for we found that washing only brought out a strongly tinted yellow color, of a beautiful hue which if repeated would deprive the pigment of its strength & brilliancy. Zinc white might be precipitated in the Chromate of Strontia

Strontian Yellow for Oil.

Pale Lemon Yellow, & Zinc Citron Yellow mixed well together in dry state. makes a very good color for oil grinding only.

Appendix III. Full description of all W&N 19th century manufacturing processes for lead chromate pigments

Table III.1. Codes for the ingredients used by W&N.

Chromate source		Sulfate source		Lead source			Additives/Extenders		
a	b	a	b	a	b	c	a	b	c
$K_2Cr_2O_7 + Na_2CO_3$	$K_2Cr_2O_7$	H_2SO_4	Na_2SO_4	$Pb(NO_3)_2$	$Pb(Ac)_2 \cdot 2Pb(OH)_2$	$Pb(Ac_3)_2$			
$PbSO_4$	$BaSO_4$	$CaCO_3$	$CaSO_4 \cdot 2H_2O$	China Clay Terra alba	$MgSO_4$	K_2SO_4	K_2CO_3	Plymouth Lime (CaO)	

III.1. Primrose Chrome

Table III.1.1. W&N Primrose Chrome (PR) manufacturing processes.

PR1a	a	a	b						PR1b	a	a	a
PR2	b	a	b									
PR3	b											

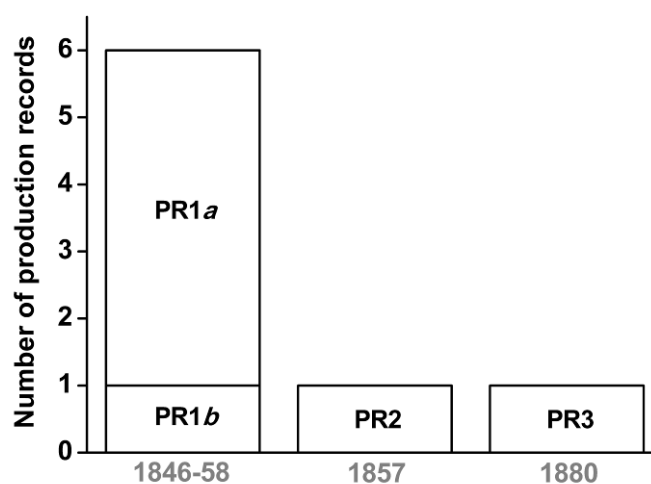


Figure III.1.1. Number of production records and date range for each of the Primrose Chrome manufacturing processes.

Table III.1.2. PR1a production records: molar proportions between the chromate ion and the other ingredients used, their Unique Recipe Code (URC), name and date. The production record reproduced is highlighted.

Na_2CO_3	H_2SO_4	$\text{Pb}(\text{Ac})_2 \cdot 2\text{Pb}(\text{OH})_2$	URC	Name	Date
1.2	4.0	4.5 [◇]	X8P123L01	Primrose Chrome Xpt	01-12-54
1.2	3.0	3.8 [◇]	X8P043L04	Primrose Chrome	04-12-54
1.2	3.0	3.8 [◇]	X8P043L19	Primrose Chrome	08-12-54
1.2	3.0	3.8 [◇]	P1P235AL04_1	Primrose Chrome	1846-58
1.2	2.0	2.2 [◇]	P1P235AL04_2	Primrose Chrome	1846-58

[◇] Assuming $[\text{Pb}(\text{Ac})_2 \cdot 2\text{Pb}(\text{OH})_2] = 0.3 \text{ M}$. This value is not clear since the lead liquor recipe is not given but a correlation with a frequent recipe is made.

Table III.1.3. PR1b production record: molar proportions between the chromate ion and the other ingredients used, its URC, name and date.

Na_2CO_3	H_2SO_4	$\text{Pb}(\text{NO}_3)_2$	URC	Name	Date
1.2	-	-	P1P235AL04_3	Primrose Chrome	1846-58

Table III.1.4. PR2 production record: molar proportions between the chromate ion and the other ingredients used, its URC, name and date.

H_2SO_4	$\text{Pb}(\text{Ac})_2 \cdot 2\text{Pb}(\text{OH})_2$	K_2CO_3	MgSO_4	URC	Name	Date
4.1	4.8	0.5	1.2	P1P382AL01	Primrose Chrome	11-12-57

Table III.1.5. PR3 production record: molar proportions between the chromate ion and the other ingredients used, its URC, name and date.

K_2CO_3	K_2SO_4	$\text{Pb}(\text{NO}_3)_2$	URC	Name	Date
0.5	1.7	2.1 [◇]	A6P008AL01	Genuine Primrose Chrome	09-03-80

[◇] Assuming $[\text{Pb}(\text{NO}_3)_2] = 0.8 \text{ M}$. This value is not clear since the lead nitrate recipe is not given but a correlation with a frequent recipe is made.

III.2. Lemon/Pale Chrome

Table III.2.1. W&N **Lemon (L)** and **Pale (P) Chrome** manufacturing processes.

L1 [§]	a	b	a	a			
L2a [#]	a	b	b	a	a	L2b	a b a a
L3a	a	b	a	d		L3b	a b a
L4a	a	a	b	d	b	L4b	a a b
P1 [§]	a	b	a	a			
P2	a	b	b	a	d		
P3a	a	b	a	d		P3b	a b a
P4a	a	a	b	d	b	P4b	a a b
P5a	a	a	b	d		P5b	a a b e
P6	b	a	b				
P7a	a	b	c			P7b	a c
P8	a	PbCl ₂	a				
P9	a	a+b	a	a			
P10	a	a	d	b			
P11	a	b	a				

[§] This order of addition of the ingredients corresponds to the majority of the productions records, however, there are also production records where lead sulfate is added after precipitation, as may be seen below in tables III.2.1.1 and III.2.2.1.

[#] Two production records vary the order of addition with the chromate solution added afterwards to the sodium sulfate and barytes solution, as may be seen below in table III.2.1.2.

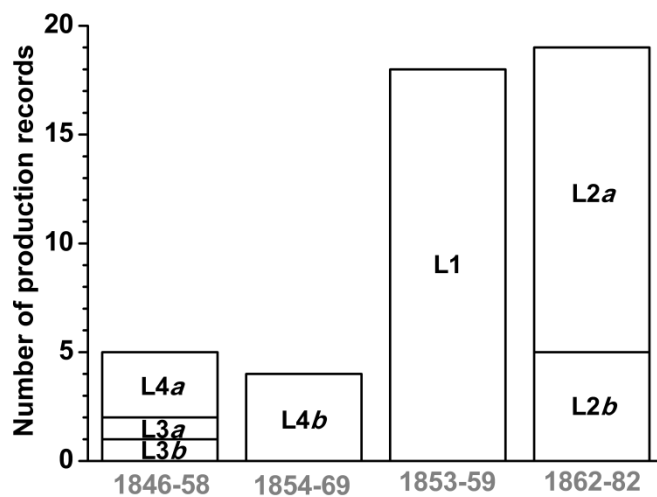


Figure III.2.1. Number of production records and date range for each of the Lemon (L) Chrome manufacturing processes.

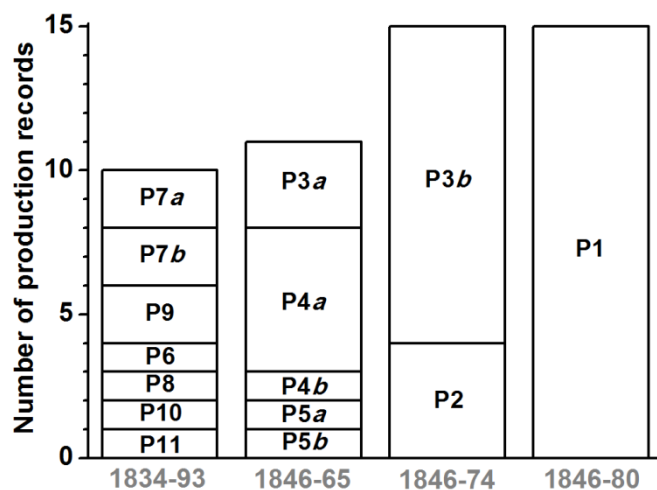


Figure III.2.2. Number of production records and date range for each of the Pale (P) Chrome manufacturing processes.

III.2.1. Lemon Chrome

Table III.2.1.1. L1 production records: molar proportions between the chromate ion and the other ingredients used, their URC, name and date. The production records reproduced are highlighted.

Na ₂ CO ₃	Na ₂ SO ₄	PbSO ₄	Pb(NO ₃) ₂	URC	Name	Date
1.6	1.2	- [⊕]	2.3	X6P233L20	Best Pale Chrome marked as "Best Lemon Chrome"	19-09-53
1.6	1.7	- [⊕]	2.1	X6P234L15	Best Pale Chrome marked as "Best Lemon Chrome"	09-53
1.6	1.7	0.6 [⊕]	2.2	X6P235L15	Super Lemon Chrome	30-12-53
1.6	1.7	0.6 [⊕]	1.8	X6P237L17	Super Lemon Chrome	26-01-54
1.6	1.7	- [^]	2.2	X6P239L01	Best Lemon Chrome	15-03-54
1.6	1.7	- [^]	2.2 [⊕]	X6P240L11	Best Lemon Chrome	31-05-54
1.6	1.7	- [^]	2.3	X6P241L11	Best Lemon Chrome	14-06-54
1.6	1.7	- [⊗]	2.5	X6P244L19	Best Lemon Chrome	04-07-54
1.6	1.7	- [^]	1.8	X8P044L08	Best Lemon Chrome	08-55
1.6	1.7	- [^]	2.1	X8P046L01	Best Lemon Chrome	09-55
1.6	1.7	- [^]	2.4	X8P047L15	Best Lemon Chrome	04-01-56
1.6	1.7	- [^]	2.1	X8P048L05	Best Pale Lemon Chrome or Primrose Chrome	01-02-56
1.6	1.7	- [^]	1.6	X8P050L01	Best Lemon Chrome	02-02-56
1.6	1.7	- [^]	-	P1P198AL11	Best Lemon Chrome	1848-58
1.3	1.7	-	1.5 or 2.2	P2P202AL01	Best Lemon Chrome	27-03-58
1.6	1.7	- [⊕]	1.5 or 2.3	P2P253AL01_1	Best Lemon Chrome	29-08-59
1.6	1.7	- [^]	1.5 or 2.3	P2P253AL01_2	Best Lemon Chrome	29-08-59
1.6	1.7	- [⊗]	1.9	P2P262AL01	Best Lemon Chrome (1741)	08-09-59

⊕ Tinted white added to pigment. ⊕ White added after precipitation. ^ White added before precipitation. ⊗ Tinted white added after main precipitation.

⊕ Assuming [Pb(NO₃)₂] = 1.6 M. This value is not clear since the lead nitrate recipe is not given but a correlation with similar production records from the same book is made.

Table III.2.1.2. L2a production records: molar proportions between the chromate ion and the other ingredients used, their URC, name and date. The production record reproduced is highlighted.

Na ₂ CO ₃	Na ₂ SO ₄	BaSO ₄	Pb(NO ₃) ₂	H ₂ SO ₄	URC	Name	Date
1.2 ^Δ	1.7	1.5	2.0	0.2	X5P016AL01	Best Lemon Chrome	1862-64
1.2 ^Δ	1.7	2	2.0	0.1	X5P057AL01	No 1 Lemon Chrome	1862-64
1.2	1.7	1.5	2.1	0.2	P2P405AL01_1	Best Lemon Chrome	27-02-65
1.2	1.7	1.5	0.9	0.1	P2P405AL01_2	Best Lemon Chrome	05-01-72
1.2	1.7	1.5	2.2	0.1	P2P383AL01	Best Lemon Chrome	02-03-65
1.2	1.7	2.0	2.1	0.1	P2P401AL01_1	Lemon Chrome	24-10-65
1.2	1.7	2.0	2.1	0.1	P2P401AL01_2	Lemon Chrome	19-08-69
1.2	1.7	1.5	2.1	0.1	P2P430AL01_1	Best Lemon Chrome	17-06-66
1.2	1.7	1.5	2.1	0.1	P2P430AL01_2	Best Lemon Chrome	18-09-66
1.2	1.7	1.5	1.9 or 2.0 [◇]	0.1	4PP025AL01	Best Lemon Chrome	07-06-71
1.2	1.7	1.5	1.9 or 2.0 [◇]	0.2	4PP102AL01	Best Lemon Chrome	03-08-72
1.2 [⊕]	1.7	1.5	1.8 or 2.0 [◇]	0.1	4PP113AL01	Best Lemon Chrome	10-10-72
1.2	1.7	1.5	-	0.2	A5P025AL01	Best Lemon Chrome	29-09-79
1.2	1.7	1.5	-	0.2	A5P028AL01	Best Lemon Chrome	06-09-79

^Δ The quantities of potassium dichromate and sodium carbonate are not given but a correlation with similar production records is made. Also in these records, the chromate solution is added to the sodium sulfate solution with the barytes.

[◇] Assuming [Pb(NO₃)₂] = 1.6 or 1.7 M. This value is not clear since the lead nitrate recipe is not given but a correlation with similar production records is made.

[⊕] This value is assumed considering the reference to 4PP102AL01.

Table III.2.1.3. L2b production records: molar proportions between the chromate ion and the other ingredients used, their URC, name and date. The production record reproduced is highlighted.

Na ₂ CO ₃	Na ₂ SO ₄	Pb(NO ₃) ₂	H ₂ SO ₄	URC	Name	Date
1.2	1.7	2.0	0.1	X5P083AL01	Super Lemon Chrome	1862-64
1.2	1.7	1.9	0.1	P2P358AL01_1	Super Lemon Chrome	19-03-64
1.2	1.7	1.1	0.1	P2P358AL01_2	Super Lemon Chrome	09-07-68
1.2	1.7	1.8 [◇]	0.1	P3P007AL01	Super Lemon Chrome	01-07-67
1.2	-	-	-	PMP124L01	Super Lemon Chrome	1862-82

[◇] Assuming [Pb(NO₃)₂] = 1.6 M. This value is not clear since the lead nitrate recipe is not given but a correlation with similar production records is made.

Table III.2.1.4. L3a production record: molar proportions between the chromate ion and the other ingredients used, its URC, name and date.

Na ₂ CO ₃	Na ₂ SO ₄	Pb(NO ₃) ₂	CaSO ₄ .1/2H ₂ O	URC	Name	Date
1.6	1.4	1.9 [◇]	1.4	P1P433AL01	Super Lemon Chrome	1846-58

[◇] Assuming [Pb(NO₃)₂] = 0.8 M. This value is not clear since the lead nitrate recipe is not given but a correlation with a frequent recipe is made.

Table III.2.1.5. L3b production record: molar proportions between the chromate ion and the other ingredients used, its URC, name and date.

Na ₂ CO ₃	Na ₂ SO ₄	Pb(NO ₃) ₂	URC	Name	Date
1.6	-	2.4 [◇]	P1P424AL01	Pale Lemon Chrome	1846-58

[◇] Assuming [Pb(NO₃)₂] = 0.8 M. This value is not clear since the lead nitrate recipe is not given but a correlation with a frequent recipe is made.

Table III.2.1.6. L4a production records: molar proportions between the chromate ion and the other ingredients used, their URC, name and date.

Na ₂ CO ₃	H ₂ SO ₄	Pb(Ac) ₂ .2Pb(OH) ₂	BaSO ₄	CaSO ₄ .1/2H ₂ O	URC	Name	Date
1.2	1.2	-	1.5	1.2*	P1P442AL01	No 1 Lemon Chrome	1846-58
1.2	1.9	2.6 [◇]	1.5	1.2*	X6P246L16	No 1 Lemon Chrome	18-07-54
1.2	1.9	2.4 [◇]	1.5	1.2*	X6P248L01	No 1 Lemon Chrome	24-07-54

* Tinted white added after main precipitation.

[◇] Assuming [Pb(Ac)₂.2Pb(OH)₂] = 0.4 M. This value is not clear since the lead liquor recipe is not given but a correlation with a frequent recipe is made.

Table III.2.1.7. L4b production records: molar proportions between the chromate ion and the other ingredients used, their URC, name and date.

Na ₂ CO ₃	H ₂ SO ₄	Pb(Ac) ₂ .2Pb(OH) ₂	URC	Name	Date
1.2	2.0	2,9 [◇]	X8P121L01	Pure Lemon Chrome	21-11-54
1.2	2.0	3.2 [◇]	X8P042L01	Genuine Lemon Chrome	23-11-54
			P1P104BL01	Genuine Lemon Chrome	
1.2 [△]	1.7	2.3	X5P072AL01	Fine Lemon Chrome	1862-64
1.2	2.4	3.1	P3P029AL01	Fine Lemon Chrome	11-02-69

[◇] Assuming [Pb(Ac)₂.2Pb(OH)₂] = 0.4 M. This value is not clear since the lead liquor recipe is not given but a correlation with a frequent recipe is made.

[△] The quantities of potassium dichromate and sodium carbonate are not given but a correlation with similar production records is made.

III.2.2. Pale Chrome

Table III.2.2.1. P1 production records: molar proportions between the chromate ion and the ingredients used, their URC, name and date.

Na ₂ CO ₃	Na ₂ SO ₄	PbSO ₄	Pb(NO ₃) ₂	URC	Name	Date
1.6	0.6	-	-	04P021L01	<i>Chromes / Midgley's</i>	01-1846
1.6	-	1.1 [⊙]	1.5	P2P001AL01	Best Pale Chrome #118	08-01-49
1.6	1.2	- [⊙]	1.9 [◇]	X6P231L15	Best Pale Chrome	06-09-53
1.6*	1.7*	- [^]	2.6 [◇]	X5P001AL01	Best Pale Chrome	1862-64
1.6	-	- [◇]	1.6 [◇]	P1P416AL01	Pale Chrome	1846-58
1.6	-	- [^]	1.5 [◇]	P1P430AL01	Pale Chrome	1846-58
1.2	1.2	- [^]	1.4	P2P392AL01	Best Pale Chrome	08-08-65
1.2	1.3	- [^]	1.8	P2P431AL01	Best Pale Chrome	22-05-66
1.2	1.2	- [^]	1.8	P3P002AL01	Best Pale Chrome	08-04-67
1.2	1.2	- [^]	1.7	4PP011AL01	Best Pale Chrome	13-04-71
1.2	0.6	- [^]	1.0 [◇]	A6P072BL01_1	Pale Chrome	27-03-77
1.2	0.6	- [^]	1.0 [◇]	A6P072BL01_2	Pale Chrome	27-03-77
1.2	-	-	-	PMP136L01	Pale Chrome	1879(?)
1.2	0.6	- [^]	1.1 [◇]	A6P016AL01	Pale Chrome	15-05-80
1.2	0.6	- [^]	1.1 [◇]	A6P017AL01	Pale Chrome	21-09-80

⊙ Tinted white added after main precipitation. ^ White added before precipitation. ◇ White added after precipitation.

◇ Assuming [Pb(NO₃)₂] = 1.6 M. This value is not clear since the lead nitrate recipe is not given but a correlation with similar production records is made.

Table III.2.2.2. P2 production records: molar proportions between the chromate ion and the ingredients used, their URC, name and date.

Na ₂ CO ₃	Na ₂ SO ₄	Pb(NO ₃) ₂	BaSO ₄	CaSO ₄ .1/2H ₂ O	URC	Name	Date
1.6*	1.2*	1.4 [◇]	1.4** [^]	2.3** [◇]	X5P032AL01	No 1 Pale Chrome	1862-64
1.6*	1.2*	2.4 [◇]	1.1** [^]	1.7** [^]	P3P111AL01	No 1 Pale Chrome	29-10-70
1.6	1.2	1.4 [◇]	1.1 [^]	1.7 [◇]	4PP097AL01_1	No 1 Pale Chrome	20-07-72
1.6	1.2	1.4 [◇]	1.4 [^]	2.3 [◇]	4PP097AL01_2	No 1 Pale Chrome	27-07-72

* These quantities are not clear but a correlation with similar production records is made.

^ White added before precipitation. ◇ White added after precipitation.

◇ Assuming [Pb(NO₃)₂] = 1.6 M. This value is not clear since the lead nitrate recipe is not given but a correlation with a frequent recipe is made.

Table III.2.2.3. P3a production records: molar proportions between the chromate ion and the ingredients used, their URC, name and date.

Na ₂ CO ₃	Na ₂ SO ₄	Pb(NO ₃) ₂	CaSO ₄ .1/2H ₂ O	URC	Name	Date
1.6	-	2.0 [◇]	1.6	P1P392AL01	Pale Chrome with Sulphate Lime Base	1846-58
1.6*	-	1.3 [◇]	1.0 [✕]	P1P419AL09	Pale Chrome (best with Terra Alba)	1846-58
1.6	-	-	1.6	P1P440AL07	Pale Chrome Plaster Base	1846-58

[◇] Assuming [Pb(NO₃)₂] = 1.6 M. This value is not clear since the lead nitrate recipe is not given but a correlation with a frequent recipe is made.

* This quantity is not clear but a correlation with similar production records is made.

[✕] The white used was *Terra Alba*, i.e., finely ground gypsum.

Table III.2.2.4. P3b production records: molar proportions between the chromate ion and the ingredients used, their URC, name and date.

Na ₂ CO ₃	Na ₂ SO ₄	Pb(NO ₃) ₂	URC	Name	Date
-	-	-	P1P424AL10	Pure Pale Chrome	07-46
1.6	1.2	2.0 [◇]	X6P232L23	Pure Pale Chrome	16-09-53
1.6	2.1	1.8	X6P238L01	Pure Pale Chrome	01-02-54
1.6*	1.2*	1.6 [◇]	X5P096AL01	Super Pale Chrome	1862-64
1.4	2.1	1.3	P1P102AL01_1	Pure Pale Chrome	1846-58
1.6	1.2	1.4	P1P102AL01_2	Pure Pale Chrome	1846-58
1.3	1.7	1.5 or 2.2	P2P224AL01	Pure Pale Chrome	26-04-58
1.2	1.2	1.7	A5P056AL01	Super Pale Chrome	29-05-67
1.2	1.4	1.8	A5P052AL01	Super Pale Chrome	08-05-74
1.2	1.2	1.6	A5P053AL01	Super Pale Chrome	18-05-74
-	-	-	PMP126L01	Super Pale Chrome	1879(?)

[◇] Assuming [Pb(NO₃)₂] = 1.6 M. This value is not clear since the lead nitrate recipe is not given but a correlation with a frequent recipe is made.

* These quantities are not clear but a correlation with similar production records is made.

Table III.2.2.5. P4a production records: molar proportions between the chromate ion and the ingredients used, their URC, name and date.

Na ₂ CO ₃	H ₂ SO ₄	Pb(Ac) ₂ .2Pb(OH) ₂	BaSO ₄	CaSO ₄ .1/2H ₂ O	URC	Name	Date
1.1	1.2	1.4 [◇]	1.4	1.1 [⊙]	X6P230L01	No 1 Pale Chrome	29-07-53
1.2	1.2	1.5 [◇]	1.5	1.2 [⊙]	X6P243L01	No 1 Pale Chrome	01-07-54
1.2	1.2	1.8 [◇]	1.5	1.2 [◇]	X6P245L16	No 1 Pale Chrome	14-07-54
1.2	1.2	1.5 [◇]	1.5	1.2 [⊙]	P1P343AL01_1	No 1 Pale Chrome	1846-58
1.2	1.9	2.5 [◇]	1.5	1.2 [⊙]	P1P343AL01_2	No 1 Pale Chrome	1846-58

[◇] Assuming [Pb(Ac)₂.2Pb(OH)₂] = 0.4 M. This value is not clear since the lead liquor recipe is not given but a correlation with a frequent recipe is made.

[⊙] Tinted white added after main precipitation. [◇] Tinted white added to pigment.

Table III.2.2.6. P4b production record: molar proportions between the chromate ion and the ingredients used, its URC, name and date.

Na ₂ CO ₃	H ₂ SO ₄	Pb(Ac) ₂ .2Pb(OH) ₂	URC	Name	Date
1.2	1.5	2.7 [‡]	X5P073AL01	Fine Pale Chrome	1862-64

[‡] Assuming [Pb(Ac)₂.2Pb(OH)₂] = 0.4 M. This value is not clear since the lead liquor recipe is not given but a correlation with a frequent recipe is made.

Table III.2.2.7. P5a production record: molar proportions between the chromate ion and the ingredients used, its URC, name and date.

Na ₂ CO ₃	H ₂ SO ₄	Pb(Ac) ₂ .2Pb(OH) ₂	CaSO ₄ .1/2H ₂ O	URC	Name	Date
1.2	1.2	1.8	1.2	P2P009AL01	<i>Best Yellow Chrome</i>	02-1857

Table III.2.2.8. P5b production record: molar proportions between the chromate ion and the ingredients used, its URC, name and date.

Na ₂ CO ₃	H ₂ SO ₄	Pb(Ac) ₂ .2Pb(OH) ₂	China clay	URC	Name	Date
0.8	0.6	0.2 [‡]	-	P2P006AL09	Common Pale Chrome	1848-65

[‡] Assuming [Pb(Ac)₂.2Pb(OH)₂] = 0.4 M. This value is not clear since the lead liquor recipe is not given but a correlation with a frequent recipe is made.

Table II.2.2.9. P6 production record: molar proportions between the chromate ion and the ingredients used, its URC, name and date.

H ₂ SO ₄	Pb(Ac) ₂ .2Pb(OH) ₂	URC	Name	Date
0.7	3.9	P1P428AL13	Pale Chrome Experiment	1846-58

Table III.2.2.10. P7a production records: molar proportions between the chromate ion and the ingredients used, their URC, name and date.

Na ₂ CO ₃	Na ₂ SO ₄	Pb(Ac) ₂	URC	Name	Date
1.6	1.2	1.0	9PP189L12	<i>Pure Chrome for Oil</i>	28-02-1853
1.6	1.4	1.0	9PP190P01	<i>Pure Chrome for Painter's Oxford Ochre</i>	03-1853

Table III.2.2.11. P7b production records: molar proportions between the chromate ion and the ingredients used, their URC, name and date.

Na ₂ CO ₃	Pb(Ac) ₂	URC	Name	Date
1.6	-	9PP191L12	<i>Pure Chrome for Painter's Oxford Ochre</i>	09-03-1853
-*	-	P4P071L06	Very Pale Chrome	1834-93

* There is a reference to the use of potassium carbonate as alternative.

Table III.2.2.12. P8 production record: URC, name and date.

Na_2CO_3	PbCl_2	H_2SO_4	URC	Name	Date
-	-	-	08P002L01	<i>Chrome Experiment</i>	1846

Table III.2.2.13. P9 production records: molar proportions between the chromate ion and the ingredients used, their URC, name and date.

Na_2CO_3	Na_2SO_4	H_2SO_4	PbSO_4	$\text{Pb}(\text{NO}_3)_2$	URC	Name	Date
1.2	0.7	0.1	- [^]	1.0	A6P057BL01	Best Pale Chrome	14-03-77
1.2	0.7	0.1	- [^]	1.0	A6P059B	Best Pale Chrome	14-03-77

[^] White added before precipitation.

Table III.2.2.14. P10 production record: molar proportions between the chromate ion and the ingredients used, its URC, name and date.

Na_2CO_3	$\text{Pb}(\text{NO}_3)_2$	BaSO_4	$\text{CaSO}_4 \cdot 1/2\text{H}_2\text{O}$	URC	Name	Date
1.6	0.7 [◇]	0.6	1.0	P1P425AL01	No 1 Pale Chrome. Small Batch	1846-58

[◇] Assuming $[\text{Pb}(\text{NO}_3)_2] = 1.6 \text{ M}$. This value is not clear since the lead nitrate recipe is not given but a correlation with a frequent recipe is made.

Table III.2.2.15. P11 production record: molar proportions between the chromate ion and the ingredients used, its URC, name and date.

Na_2CO_3	$\text{Pb}(\text{Ac})_2 \cdot 2\text{Pb}(\text{OH})_2$	H_2SO_4	URC	Name	Date
0.2	2.1 [◇]	0.4	P3P102AL01	<i>Super Golden Chrome</i>	06-04-1870

[◇] Assuming $[\text{Pb}(\text{Ac})_2 \cdot 2\text{Pb}(\text{OH})_2] = 0.4 \text{ M}$. This value is not clear since the lead liquor recipe is not given but a correlation with a frequent recipe is made.

III.3. Middle Chrome

Table III.3.1. W&N Middle Chrome (M) manufacturing processes.

M1a	a	c	a		M1b	a	a		
M2a [#]	a	a	b	b	M2b	a	a	b	
M3a	a	a	b	d	b	M3b	a	b	
M4	b	a	b						
M5a	a	c	d		M5b	b	d	c	
M6	b	c	Alum	c					
M7a	b		a	d	a	M7b	b		a
M8	b		c						

[#] In three production records, barytes is added before precipitation, as may be seen below in table III.3.1.3.

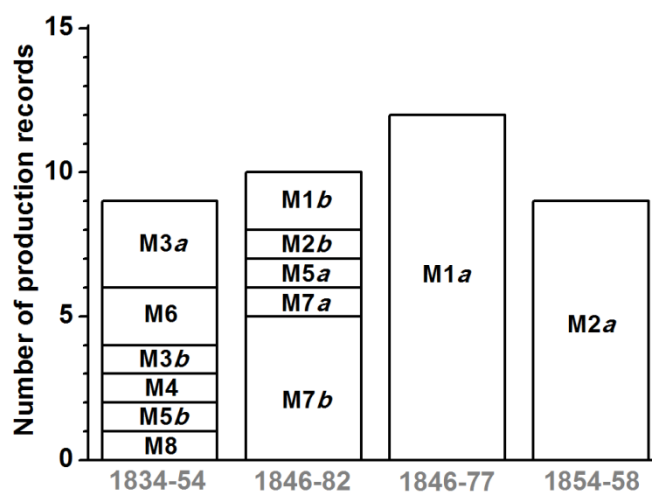


Figure III.3.1. Number of production records and date range for each of the Middle Chrome manufacturing processes.

Table III.3.1.1. M1a production records: molar proportions between the chromate ion and the ingredients used, their URC, name and date. The production records reproduced are highlighted.

Na ₂ CO ₃	CaCO ₃	Pb(NO ₃) ₂	URC	Name	Date
0.8	1.4 [^]	-	P1P106AL14	Best Middle Chrome for Oil	1846-58
0.8	2.0 [^]	-	P1P107BL14	Best Middle Chrome for Oil	1846-58
0.8	1.8 [^]	1.2	P1P245AL01	Best Middle Chrome	1846-58
0.9	2.0 [^]	1.1 [◇]	P2P211AL01_1	Best Middle Chrome	28-07-58
0.9	2.0 [^]	1.2	P2P211AL01_2	Best Middle Chrome	03-08-60
0.9	2.0 [^]	2.4	P2P386AL01_1	Best Middle Chrome	04-04-65
0.9	2.0 [^]	2.2	P2P386AL01_2	Best Middle Chrome	02-11-66
0.9	2.0 [^]	-	X5P031AL01	Best Middle Chrome	1862-64
0.9	2.6 [^]	1.3	P2P415AL01	Best Middle Chrome	1848-65
0.9	2.0 [^]	-	P3P115AL01	Best Middle Chrome	30-11-70
0.9	- [^]	1.0	4PP101AL01	Best Middle Chro	01-08-72
1.4	2.5 [◇]	1.1	A5P081AL01	Best Middle Chro	08-01-77

[^] White added before precipitation. [◇] White added after precipitation.

[◇] Assuming [Pb(NO₃)₂] = 0.8 M. This value is not clear since the lead nitrate recipe is not given but a correlation with similar production records is made.

Table III.3.1.2. M1b production records: molar proportions between the chromate ion and the ingredients used, their URC, name and date.

Na ₂ CO ₃	Pb(NO ₃)	URC	Name	Date
-	-	X5P078AL01	Super Middle Chrome	1862-64
1.2	-	PMP128L01	Super Middle Chrome	1862-82

Table III.3.1.3. M2a production records: molar proportions between the chromate ion and the ingredients used, their URC, name and date. The production records reproduced are highlighted.

Na ₂ CO ₃	H ₂ SO ₄	Pb(Ac) ₂ .2Pb(OH) ₂	BaSO ₄	URC	Name	Date
0.8	0.6	-	0.6 [®]	X6P250L01	Best Middle Chrome	20-02-54
0.8	0.6	0.4	0.6 [®]	X6P251L91	Best Middle Chrome	22-02-54
0.8	0.6	-	0.6 [®]	X6P252L01	Best Middle Chrome	28-07-54
0.8	0.6	0.4 [◇]	0.6 [®]	X8P051L01	Best Middle Chrome	27-10-54
0.8	0.6	0.4 [◇]	0.6 [®]	X8P052L19	Best Middle Chrome	31-10-54
0.8	0.6	0.4	0.6 [®]	X8P054L01	Best Middle Chrome	01-11-54
0.8	0.6	0.5	0.6 [^]	X8P055L01	Best Middle Chrome	27-02-56
0.8	0.6	0.5	0.6 [^]	P1P192AL01_1	Best Middle Chrome	1846-58
0.8	0.6	0.4	0.6 [^]	P1P192AL01_2	Best Middle Chrome	1846-58

[®] Tinted white added after main precipitation. [^] White added before precipitation.

[◇] Assuming [Pb(Ac)₂.2Pb(OH)₂] = 0.4 M. This value is not clear since the lead liquor recipe is not given but a correlation with similar production records is made.

Table III.3.1.4. M2b production record: URC, name and date.

Na_2CO_3	H_2SO_4	$\text{Pb}(\text{Ac})_2 \cdot 2\text{Pb}(\text{OH})_2$	URC	Name	Date
-	-	-	X5P074AL01	Fine Middle Chrome	1862-64

Table III.3.1.5. M3a production records: molar proportions between the chromate ion and the ingredients used, their URC, name and date.

Na_2CO_3	H_2SO_4	$\text{Pb}(\text{Ac}_3)_2 \cdot 2\text{Pb}(\text{OH})_2$	BaSO_4	$\text{CaSO}_4 \cdot 1/2\text{H}_2\text{O}$	URC	Name	Date
1.2	1.2	-	1.5	1.2 [®]	X6P024L01	No 1 Middle Chrome	05-53
0.5	0.4	0.4 [‡]	1.2	0.9 [®]	X6P252L22	No 1 Middle Chrome	29-07-54
0.8	0.6	0.5 [‡]	1.2	0.9 [®]	X6P253L20	No 1 Middle Chrome	02-08-54

[®] Tinted white added after main precipitation.

[‡] Assuming $[\text{Pb}(\text{Ac})_2 \cdot 2\text{Pb}(\text{OH})_2] = 0.4 \text{ M}$. This value is not clear since the lead liquor recipe is not given but a correlation with a frequent recipe is made.

Table III.3.1.6. M3b production record: molar proportions between the chromate ion and the ingredients used, its URC, name and date.

Na_2CO_3	$\text{Pb}(\text{Ac}_3)_2 \cdot 2\text{Pb}(\text{OH})_2$	URC	Name	Date
1.3	0.4	PMP129	<i>no name</i>	no date

Table III.3.1.7. M4 production record: molar proportions between the chromate ion and the ingredients used, its URC, name and date.

H_2SO_4	$\text{Pb}(\text{Ac}_3)_2 \cdot 2\text{Pb}(\text{OH})_2$	CaO	URC	Name	Date
0.9	-	-	P1P434AL01	<i>Chrome Making - Proceeds for Middle</i>	21-09-1846

Table III.3.1.8. M5a production record: URC, name and date.

Na_2CO_3	$\text{Pb}(\text{Ac}_3)_2$	$\text{CaSO}_4 \cdot 1/2\text{H}_2\text{O}$	URC	Name	Date
-	-	-	P1P419AL01	Middle Chrome - Cheap - Experiment	1846-58

Table III.3.1.9. M5b production record: URC, name and date.

$\text{CaSO}_4 \cdot 1/2\text{H}_2\text{O}$	$\text{Pb}(\text{Ac}_3)_2$	URC	Name	Date
-	-	05P026L01	<i>Low Chrome Body</i>	1845

Table III.3.1.10. M6 production records: molar proportions between the chromate ion and the ingredients used, their URC, name and date.

CaCO ₃	Alum	Pb(Ac ₃) ₂	URC	Name	Date
2.9	0.2	0.5	2PP025BL01	<i>Chromes</i>	1834-35
0.4	1.2	1.8	3PP012L01	<i>Chrome Yellow</i>	1837-39

Table III.3.1.11. M7a production record: molar proportions between the chromate ion and the ingredients used, its URC, name and date.

K ₂ CO ₃	Pb(NO ₃) ₂	PbSO ₄	CaSO ₄ .1/2H ₂ O	URC	Name	Date
0.9	-	-	0.5	P1P385AL01	Middle Chrome. (Midgeley's)	1846-58

Table III.3.1.12. M7b production records: molar proportions between the chromate ion and the ingredients used, their URC, name and date.

K ₂ CO ₃	Pb(NO ₃) ₂	URC	Name	Date
0.5	-	X6P249L01	<i>Pure Chrome or Chro: Lead</i>	12-12-53
0.4	1.2	P1P105AL15	Pure Middle Chrome	1846-58
0.7	-	P2P339AL01	Pure Middle Chrome	08-08-63
0.7	-	A5P058AL01	Super Middle Chrome	15-11-66
0.7	-	4PP031AL01	Super Middle Chrome	02-08-71

Table III.3.1.13. M8 production records: molar proportions between the chromate ion and the ingredients used, their URC, name and date.

K ₂ CO ₃	Pb(Ac ₃) ₂	URC	Name	Date
1.1	1.2	3PP240L01	<i>Chrome Yellow n°2</i>	10-1838

III.4. Deep Chrome

Table III.4.1. W&N Deep (D) Chrome manufacturing processes.

D1a	a	a	d	b	b	a	D1b [§]	a	b	b	a
D2a [†]	a	b	d	b	a		D2b	a	b	a	
D3	a	e	a								
D4	a	a	a								
D5a [#]	a	HCl	LW				D5b	a	LW		
D6a	b	HCl	LW				D6b	b	LW		
D7	b		LW								
D8	b		g	b							
D9	b	a	b								
D10a	b	a	d				D10b	b	a		

[§] In three production records, barytes is added before precipitation, as may be seen below in table III.4.1.2.

[†] In three production records, barytes is added before precipitation, as may be seen below in table III.4.1.3.

[#] LW = Lead White ($2\text{PbCO}_3 \cdot \text{Pb}(\text{OH})_2$). HCl = Hydrochloric acid. These are only used in Deep chrome experimental processes.

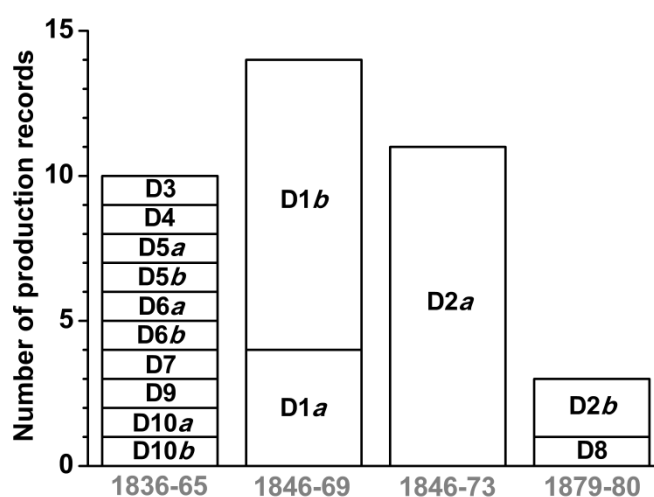


Figure III.4.1. Number of production records and date range for each of the Deep Chrome manufacturing processes.

Table III.4.1.1. D1a production records: molar proportions between the chromate ion and the ingredients used, their URC, name and date. The production record reproduced is highlighted.

Na ₂ CO ₃	H ₂ SO ₄	CaSO ₄ .1/2H ₂ O	BaSO ₄	Pb(Ac) ₂ .2Pb(OH) ₂	H ₂ SO ₄	URC	Name	Date
0.5	0.1	0.9	1.2	-	0.3	9PP179L14	No 1 Deep Chrome	29-12-52
0.5	0.1	0.9	1.2	-	0.3	X8P058L10	No 1 Deep Chrome	20-11-54
0.5	0.1	0.9	1.2	-	0.3	X8P059L17	No 1 Deep Chrome	21-11-54
0.5	0.1	0.9	1.2	-	0.3	P1P357AL01	Deep Chrome No 1	1846-58

Table III.4.1.2. D1b production records: molar proportions between the chromate ion and the ingredients used, their URC, name and date. The production records reproduced is highlighted.

Na ₂ CO ₃	BaSO ₄	Pb(Ac) ₂ .2Pb(OH) ₂	H ₂ SO ₄	URC	Name	Date
0.5	0.6 [®]	-	0.3	X8P056L01	Best Deep Chrome	06-11-54
0.5	0.6 [®]	-	0.5	X8P057L01	Best Deep Chrome	14-11-54
0.8	0.6 [^]	0.4	0.3 [#]	X8P062L14	Best Deep Chrome	14-03-56
0.8	0.6 [^]	0.4	0.3 [#]	P1P190AL01_1	Best Deep Chrome	1846-58
0.5	0.6 [®]	-	0.5	P1P190AL01_3	Best Deep Chrome	1846-58
0.5	0.6 [^]	-	0.5	P2P355AL01_1	Best Deep Chrome	08-01-64
0.5	0.6 [^]	-	0.5	P2P355AL01_2	Best Deep Chrome	1848-65
1.1	0.7 [^]	-	0.5	P3P054AL01	Best Deep Chrome	26-02-69
0.4	1.0 [^]	-	0.5	P3P074AL01_1	Deep Chrome	19-08-69
0.4	1.0 [^]	-	-	P3P074AL01_2	Deep Chrome	19-08-69

[®] Tinted white added after main precipitation, [^] White added before precipitation, [#] Added before precipitation.

Table III.4.1.3. D2a production records: molar proportions between the chromate ion and the ingredients used, their URC, name and date. The production records reproduced is highlighted.

Na ₂ CO ₃	Pb(Ac) ₂ .2Pb(OH) ₂	CaSO ₄ .1/2H ₂ O	BaSO ₄	H ₂ SO ₄	URC	Name	Date
0.5	0.6 [◇]	0.5 [#]	0.3 [#]	0.5	X8P061L03	Best Deep Chrome	09-08-55
0.5	-	0.9	1.2	0.4	X8P063L08	No 1 Deep Chrome	1854-60
0.5	0.6 [◇]	0.5	0.3	0.5	P1P190AL01_2	Best Deep Chrome	1846-58
0.7	-	0.6	0.3	0.2	X5P007AL01	Best Deep Chrome	1862-64
0.2	-	0.9	0.6	0.05	X5P052AL01	No 1 Deep Chrome	1862-64
0.5	0.4	0.5 [#]	0.3 [#]	0.4	P2P425AL01	Deep Chrome Best	12-04-66
0.2	0.7 [◇]	0.5 [#]	0.3 [#]	0.2	P3P106AL01	Best Deep Chrome	24-08-70
0.2	-	0.5	0.3	0.1	4PP038AL01	Best Deep Chrome	10-71
0.2	0.1	0.5	0.3	0.1	4PP082AL01	Best Deep Chrome	09-07-72
0.2	0.1	0.5	0.3	0.2	4PP093AL01	Best Deep Chrome	20-07-72
0.7	-	0.6	0.3	0.2	A5P031AL01	Best Deep Chrome	23-04-73

[◇] Assuming [Pb(Ac)₂.2Pb(OH)₂] = 0.4 M. This value is not clear since the lead liquor recipe is not given but a correlation with similar production records is made.

[#] White added before precipitation.

Table III.4.1.4. D2b production records: molar proportions between the chromate ion and the ingredients used, their URC, name and date.

Na_2CO_3	$\text{Pb}(\text{Ac})_2 \cdot 2\text{Pb}(\text{OH})_2$	H_2SO_4	URC	Name	Date
0.7	0.5	0.2	A5P011AL01_1	Super Deep Chrome	11-79
0.7	0.5	0.2	A5P011AL01_2	Super Deep Chrome	11-79

Table III.4.1.5. D3 production record: molar proportions between the chromate ion and the ingredients used, its URC, name and date.

Na_2CO_3	$\text{CaSO}_4 \cdot 2\text{H}_2\text{O}$	$\text{Al}_2\text{Si}_2\text{O}_5(\text{OH})_4$	$\text{Pb}(\text{NO}_3)_2$	CaO	URC	Name	Date
1.6	15.3	1.3	1.8	1.7	P1P171AL01	Deep Chrome No 2 quality	1846-58

Table III.4.1.6. D4 production record: URC, name and date.

Na_2CO_3	PbSO_4	$\text{Pb}(\text{NO}_3)_2$	URC	Name	Date
-	-	-	P1P431AL01_2	Deep Chrome	1846-58

Table III.4.1.7. D5a production record: URC, name and date.

Na_2CO_3	HCl	$2\text{PbCO}_3 \cdot \text{Pb}(\text{OH})_2$	URC	Name	Date
-	-	-	P1P427AL09	<i>Golden Chrome</i>	1846-58

Table III.4.1.8. D5b production record: URC, name and date.

Na_2CO_3	$2\text{PbCO}_3 \cdot \text{Pb}(\text{OH})_2$	URC	Name	Date
-	-	08P003L01	<i>Chrome Experiment</i>	1846

Table III.4.1.9. D6a production record: URC, name and date.

HCl	$2\text{PbCO}_3 \cdot \text{Pb}(\text{OH})_2$	URC	Name	Date
-	-	P1P426AL14	Middle or Deep Chrome Expt	1846-58

Table III.4.1.10. D6b production record: molar proportions between the chromate ion and the ingredients used, its URC, name and date.

$2\text{PbCO}_3 \cdot \text{Pb}(\text{OH})_2$	URC	Name	Date
3.0	P4P071L01	<i>Pink Chrome</i>	04/1836

Table III.4.1.11. D7 production record: URC, name and date.

K_2CO_3	$2PbCO_3 \cdot Pb(OH)_2$	URC	Name	Date
-	-	06P034L16	<i>Cheap Chrome</i>	1846

Table III.4.1.12. D8 production record: molar proportions between the chromate ion and the ingredients used, its URC, name and date.

K_2CO_3	K_2SO_4	$Pb(Ac)_2 \cdot 2Pb(OH)_2$	URC	Name	Date
0.5	1.7	-	A6P015ABL01	Deep Chrome	03-80

Table III.4.1.13. D9 production record: molar proportions between the chromate ion and the ingredients used, its URC, name and date.

H_2SO_4	$Pb(Ac)_2 \cdot 2Pb(OH)_2$	CaO	URC	Name	Date
1.2	-	-	P1P434AL01	<i>Chrome Making - Proceeds for Middle</i>	21-09-1846

Table III.4.1.14. D10a production record: molar proportions between the chromate ion and the ingredients used, its URC, name and date.


$Pb(NO_3)_2$	$CaSO_4 \cdot 2H_2O$	URC	Name	Date
-	11.4	P2P030AL01	<i>Chinese Yellow</i>	1848-65

Table III.4.1.15. D10b production record: URC, name and date.

$Pb(NO_3)_2$	CaO	URC	Name	Date
-	-	P1P431AL01_1	Deep Chrome	1846-58

Appendix IV. Full description of all W&N 19th century manufacturing processes for other yellow chromate pigments

Table IV.1. Codes for the ingredients used by W&N.

Chromate source			Buffer	Barium source		Zinc source			Strontium source
a	b	c		a	b	a	b	c	a
$K_2Cr_2O_7 + Na_2CO_3$	$K_2Cr_2O_7$	K_2CrO_4	K_2CO_3	$BaCl_2$	$Ba(NO_3)_2$	$Zn(NO_3)_2$	$ZnSO_4$	$Zn(Ac)_2$	$Sr(NO_3)_2$

IV.1. Lemon Yellow

Table IV.1.1. W&N Lemon Yellow (LY) manufacturing processes.













LY1a			LY1b			
LY2a			LY2b			
LY3						



Figure IV.1.1. Number of production records and date range for each of the Lemon Yellow manufacturing processes.

Table IV.1.2. LY1a production records: molar proportions between the chromate ion and barium chloride used, their URC, name and date. The production records reproduced are highlighted.

BaCl ₂ [†]	URC	Name	Date	BaCl ₂ [†]	URC	Name	Date
-	3PP200L01	Lemon Yellow	06-1838	4.4	X6P157	Lemon Yellow	19-07-1854
-	P4P056L09	Chro Baryt	1834-93	4.4	X6P155L06_4 th	Lemon Yellow	22-07-1854
-	7PP120L01*	Lem Yell	08-1845	5.9	X8P075L13_1 st	Lemon Yellow	24-04-1855
5.9	7PP242L01#_1 st	Lem Yell	06-12-1847	4.7	X8P075L13_2 nd	Lemon Yellow	24-04-1855
7.9	7PP242L01#_2 nd	Lem Yell	06-12-1847	3.9	X8P075L13_3 rd	Lemon Yellow	25-04-1855
7.9	7PP242L01#_3 rd	Lem Yell	06-12-1847	5.9	X8P076L11_1 st	Lemon Yellow	06-1855
6.7	7PP242L01#_4 th	Lem Yell	06-12-1847	5.9	X8P076L11_2 nd	Lemon Yellow	06-1855
6.7	7PP242L01#_5 th	Lem Yell	06-12-1847	5.9	X8P076L11_3 ^r	Lemon Yellow	06-1855
5.9	7PP242L01#_6 th	Lem Yell	06-12-1847	5.9	X8P076L11_4 th	Lemon Yellow	06-1855
5.9	7PP242L01#_7 th	Lem Yell	06-12-1847	5.9	X8P076L11_5 th	Lemon Yellow	06-1855
5.9	7PP242L01#_8 th	Lem Yell	06-12-1847	5.9	P1P161AL01	Lemon Yellow	1846-58
5.9	7PP242L01#_9 th	Lem Yell	06-12-1847	6.6	X8P078L22_1 st	Lemon Yellow	10-1855
5.9	7PP242L01#_10 th	Lem Yell	06-12-1847	5.9	X8P078L22_2 nd	Lemon Yellow	10-1855
5.9	7PP242L01#_11 th	Lem Yell	06-12-1847	6.6	X8P078L22_3 rd	Lemon Yellow	10-1855
5.9	7PP242L01#_12 th	Lem Yell	06-12-1847	6.6	X8P078L22_4 th	Lemon Yellow	10-1855
5.2	7PP242L01#_13 th	Lem Yell	06-12-1847	6.6	X8P078L22_5 th	Lemon Yellow	10-1855
5.9	7PP242L01#_14 th	Lem Yell	06-12-1847	6.6	X8P078L22_6 th	Lemon Yellow	10-1855
5.2	7PP242L01#_15 th	Lem Yell	06-12-1847	6.6	X8P078L22_7 th	Lemon Yellow	10-1855
8.8	X7P096L01	Lemon Yellow	01-1850	5.9	P2P171AL01	Lemon Yellow	01-01-1859
4.4	X6P018L01	Lemon Yellow	05-1853	5.9	P2P171AL18	Lemon Yellow	1848-65
4.4	X6P039L01_1 st	Lemon Yellow	06-07-1853	5.4	P2P172AL01	Lemon Yellow	1848-65
4.4	X6P039L01_2 nd	Lemon Yellow	25-07-1853	4.9	P2P172AL07	Lemon Yellow	1848-65
4.4	X6P039L01_3 rd	Lemon Yellow	28-07-1853	5.9	P2P172AL12	Lemon Yellow	1848-65
5.9	X6P153L01	Lemon Yellow	05-08-1853	6.4	P2P172AL18	Lemon Yellow	1848-65
5.9	X6P153L13_1 st	Lemon Yellow	09-12-1853	6.9	P2P173AL01	Lemon Yellow	1848-65
8.8	X6P153L13_2 nd	Lemon Yellow	17-12-1853	7.9	P2P173AL04	Lemon Yellow	1848-65
8.8	X6P153L13_3 rd	Lemon Yellow	19-12-1853	8.8	P2P173AL09	Lemon Yellow	1848-65
8.8	X6P154L20	Lemon Yellow	06-04-1854	2.9 [‡]	P2P173AL12	Lemon Yellow	02-01-1863
8.8	X6P156L23	Lemon Yellow	04-07-1854	1.4 [◇]	X5P087AL01	Lemon Yellow	1862-64
5.9	X6P155L06_1 st	Lemon Yellow	15-07-1854	1.9 [◇]	P2P433AL01_1 st	Lemon Yellow	22-06-1866
4.4	X6P155L06_2 nd	Lemon Yellow	15-07-1854	1.4 [◇]	P2P433AL01_2 nd	Lemon Yellow	27-11-1866
3.7	X6P155L06_3 rd	Lemon Yellow	19-07-1854	1.4 [◇]	4PP026AL01	Lemon Yellow	08-06-1871

[†] The values shown consider a [BaCl₂] = 4 M. This is an average value considering all W&N's recipes available for "muriate of barytes" (barium chloride).

* A copy of this production record is found in X2P102L01.

A copy of this production record is found in 9PP112L19 and X2P208L01.

[‡] This value considers a [BaCl₂] = 1.9 M.

◇ In these production records, the barium chloride is added in solid state.

Table IV.1.3. LY1b production records: molar proportions between the chromate ion and the ingredients used, their URC, name and date.

K_2CO_3	$BaCl_2$	URC	Name	Date
0.5	-	A6P020BL01_2	Permanent Primrose	16-03-1880
0.5	-	A6P031BL01	Permanent Primrose	08-04-1880

Table IV.1.4. LY2a production records: URC, name and date.

$Ba(NO_3)_2$	URC	Name	Date
-	ACP057L01	Lemon Yellow	1849-54
-	P1P011AL07	Lemon Yellow	1846-58

Table IV.1.5. LY2b production records: molar proportions between the chromate ion and the ingredients used, their URC, name and date.

K_2CO_3	$Ba(NO_3)_2$	URC	Name	Date
0.9*	1.3	P1P394AL01	Chromate Barytes or Permanent Primrose	1846-58
0.7	1.8	P1P422AL01	Chromate Barytes, or Perm ^l Primrose	1846-58













* There is a reference to the use of sodium carbonate as alternative.

Table IV.1.6. LY3 production records: URC, name and date.

$BaCl_2$	URC	Name	Date
-	A6P020BL01_1	Permanent Primrose	15-03-1880

IV.2. Citron Yellow

Table IV.2.1. W&N Citron Yellow (CY) manufacturing processes.

CY1a					CY1b		
CY2							
CY3							

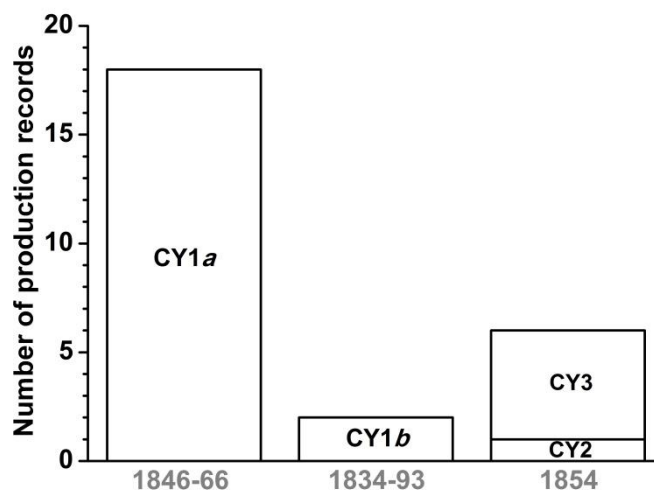


Figure IV.2.1. Number of production records and date range for each of the Citron Yellow manufacturing processes.

Table IV.2.2. CY1a production records: molar proportions between the chromate ion and the ingredients used, their URC, name and date. The production record reproduced is highlighted.

K_2CO_3	$Zn(NO_3)_2$	URC	Name	Date
1.1	1.1	X6P379L07_1 st	Chromate of Zinc	11-11-1854
1.2	1.1	X6P379L07_2 nd	Chromate of Zinc	11-11-1854
1.2	1.1	X6P379L07_3 ^d	Chromate of Zinc	11-11-1854
1.3	1.1	X6P381L12_4 th	Chromate of Zinc	13-11-1854
1.3	1.5	X6P382L03_6 th	Chromate of Zinc	15-11-1854
1.6	-	X6P382L03_7 th	Chromate of Zinc	15-11-1854
1.3	1.7	X6P382L03_8 th	Chromate of Zinc	15-11-1854
1.0	1.1	X6P383L07	Chromate of Zinc	16-11-1854
1.0	1.4	X6P384L01_1	Chromate of Zinc	18-11-1854
0.9	1.5	X6P385L15_1	Chromate of Zinc	20-11-1854
0.9	1.5	X6P385L15_2	Chromate of Zinc	21-11-1854
1.8	-	X8P082L01_1 st	Citron Yellow	25-11-1854
1.0	1.3	P1P159AL12_1	Citron Yellow	1846-58
1.0	1.2	P1P159AL12_2	Citron Yellow	1846-58
1.2	1.0	P1P159AL12_3	Citron Yellow	1846-58
1.0	-	P1P159AL12_4	Citron Yellow	1846-58
1.2	2.2	P2P288AL01	Citron Yellow	25-07-66
1.0	1.1	X5P102AL01	Citron Yellow	1862-64

Table IV.2.3. CY1b production records: URC, name and date.

ZnSO ₄	URC	Name	Date
-	P4P064L01	Chro Zinc	1834-93
-*	P4P075L01	Chro Zinc	1834-93

* In this production record there is also the addition of ammonia.

Table IV.2.4. CY2 production record: URC, name and date.

K ₂ CO ₃	Zn(Ac) ₂	URC	Name	Date
-	-	X6P381L12_5 th	Chromate of Zinc	13-11-1854

Table IV.2.4. CY3 production records: molar proportions between the chromate ion and the ingredients used, their URC, name and date.

Na ₂ CO ₃	Zn(NO ₃) ₂	URC	Name	Date
1.6	-	X6P378L01_1	Chromate of Zinc	08-11-1854
1.6	-	X6P378L01_2	Chromate of Zinc	09-11-1854
1.6	-	X6P378L20	Chromate of Zinc	09-11-1854
1.6	-	X8P120L01_1	Chromate of Zinc Xpts	27-10-1854
1.6	-	X8P120L01_2	Chromate of Zinc Xpts	11-1854

IV.3. Strontian Yellow

Table IV.3.1. W&N Strontian Yellow (SY) manufacturing processes.









SY1				
SY2				
SY3				



Figure IV.3.1. Number of production records and date range for each of the Strontian Yellow manufacturing processes.

Table IV.3.2. SY1 production records: molar proportions between the chromate ion and the ingredients used, their URC, name and date. The production record reproduced is highlighted.

Na ₂ CO ₃	Sr(NO ₃) ₂	URC	Name	Date
1.3	0.4	P1P197BL10	Strontian Yellow	1846-58
1.6	-	X6P145L01	Chromate Strontia	28-09-1854
1.6	-	X6P145L10	Chromate Strontia	04-10-1854
1.6	-	X6P146L08	Chromate Strontia	10-1854

Table IV.3.3. SY2 production record: URC, name and date.

K ₂ CO ₃	Sr(NO ₃) ₂	URC	Name	Date
-	-	P1P447BL09	Mems: - Chromate of Strontia	1846-58










Table IV.3.4. SY3 production record: molar proportions between the chromate ion and the strontium nitrate used, its URC, name and date.

Sr(NO ₃) ₂	URC	Name	Date
0.1	P1P197AL08*	Strontian Yellow	03-01-1856

* A copy of this production record is found in X8P086L01.

IV.4. Other experiments

Table IV.4.1. Data on other experimental production records: order of ingredients (using the codes of tables III.1 and IV.1), URC, name and date.

Order of ingredients*	URC	Name	Date
	X6P167L01	Xpt with Nitrate Barytes	1852-56
	X6P168L01	Xpt with Strontia Nitrate	28-09-1854
	X8P119L01	Constant Yellow Xpt	26-10-1854
	X6P384L01_2	Chromate of Zinc (Expt 3) [‡]	18-11-1854
	X8P082L01_2 nd	Citron Yellow	25-11-1854
	X8P082L01_3 rd	Citron Yellow	25-11-1854
	P2P174AL01_1	Palest Lemon Yellow. Exp [†]	26-01-1859
	P2P174AL01_2	Palest Lemon Yellow. Exp [†]	26-01-1859
	P2P326AL01	Permanent Yellow No. 2	05-01-1863
	P2P331AL01_1	Permanent Yellow No. 1	16-01-1863
	P2P331AL01_2	Permanent Yellow No. 1	01-11-1866
	X5P084AL01	Permanent Yellow	1862-64
	X5P085AL01	Pale Lemon Yellow	1862-64
	P2P443BL13	Pale Lemon Yellow	02-01-1867
	P1P363AL15	Buff Yellow Experiment	1846-58

* When two ingredients are presented together, it means it is a solution of both ingredients that is added.

[‡] Although the addition of the zinc source is not mentioned, it was probably added considering the other reported experiments.

Appendix V. Experimental section

V.1. Materials and suppliers

All reagents and solvents were of analytical grade, and Millipore water was used. Only chalk from Kremer Pigmente (Leicht Natürlich) and barytes from Sibelco were of mineral origin.

List of Suppliers

Laborspirit, Estrada de Pintéus 15, Fracção P, 2660-194 Santo Antão do Tojal, Loures, Portugal, supplied all chemicals from **Sigma-Aldrich**, **Panreac**, **Riedel-de Haën** and **Roig Farma**.

Kremer Pigmente: Hauptstr. 41 – 47, DE 88317 Aichstetten, Germany.

Sibelco: SCR-Sibelco N.V. Plantin Moretuslei 1A, B-2018 Antwerp, Belgium.

V.2. Experimental methods

V.2.1. Pigment synthesis methods

The solutions used in the pigment syntheses were always mixed under agitation. The pH measurements throughout the syntheses are presented in Appendix IX (p. 287). All pigments were thoroughly washed, dried and then ground to a powder.

The synthesis methods following the W&N production records transcribed in Appendix II.3 (p. 187) were based on the data available in Table II.1.5 (p. 173), on the proportional scale down of the starting ingredients and on the 'pH data'¹⁶⁰ provided in the production records.

V.2.1.1. Lead chromate pigments

The summary of the conditions used for the synthesis of lead chromate references (Orna, 1980; Xiang *et al.*, 2004) is described in Table V.2.1.1.1, for the main synthetic pathways listed in Table 3.2 (p. 49) in Table V.2.1.1.2 and for other synthetic pathways in Table V.2.1.1.3.

Table V.2.1.1.1. Summary of the conditions used for the synthesis of lead chromate references.

	Synthesis
PbCrO₄ Monoclinic	1.75 g of K ₂ CrO ₄ in 25 ml of H ₂ O + 3 g of Pb(NO ₃) ₂ in 25 ml of H ₂ O
PbCrO₄ Orthorhombic	18.96 g of Pb(Ac) ₂ ·3H ₂ O dissolved in 250 ml of H ₂ O + AcOH until pH = 5 + 1.94 g of K ₂ CrO ₄ dissolved in 50 ml of H ₂ O (maintain the pH = 5)
Pb₂CrO₅	1.9 of Pb(Ac) ₂ ·3H ₂ O in 25 ml of H ₂ O + NaOH until pH = 12 + 0.97 g of K ₂ CrO ₄ in 50 ml of H ₂ O

¹⁶⁰ The concept of pH was only developed in 1909 (Myers, 2010), however, as explained in Carlyle *et al.* (2011), the behaviour of acid, neutral and basic materials was appreciated in the 19th century and the W&N production records clearly attest to this. For example, in Recipe: Primrose Chrome, URC: P1P235AL04, there is mentioned the need for excess of acid (see p. 187) and in Recipe: Best Lemon Chrome, URC: 4PP102AL01, there is reference to the use of litmus paper (see p. 190).

Table V.2.1.1.2. Summary of the conditions used for the lead chromate main synthetic pathways (Table 3.2, p. 49).

	Synthesis
PR1a	708 ml of H ₂ O + 3.53 g of K ₂ Cr ₂ O ₇ dissolved in 40 ml of H ₂ O + 2.94 g of Na ₂ CO ₃ dissolved in 20 ml of H ₂ O + 3.8 ml of H ₂ SO ₄ + 100 ml of Pb(Ac) ₂ ·2Pb(OH) ₂ [§] (leave till next day)
L1	60 ml of H ₂ O + 2.94 g of K ₂ Cr ₂ O ₇ + 3.29 g of Na ₂ CO ₃ (stir till no effervescence takes place; 1.5 h boiling; leave the solution to get cold) + 4.71 g of Na ₂ SO ₄ dissolved in 35.5 ml of H ₂ O + 3.53 g of PbSO ₄ in acidic solution (0.2 ml of H ₂ SO ₄ /10 ml of H ₂ O) + 27 ml of Pb(NO ₃) ₂ [¶] (stir for ½ hour)
L2a	250 ml of H ₂ O + 9.89 g of Na ₂ SO ₄ + 60 ml of boiling H ₂ O + 5.88 g of K ₂ Cr ₂ O ₇ + 4.94 g of Na ₂ CO ₃ (boil and stir for 1/2 h; add water to fill 60 ml) + 14.12 g of BaSO ₄ (natural source; Sibelco) + 47 ml of Pb(NO ₃) ₂ [¶] + 3 ml of H ₂ SO ₄ in 4 ml of H ₂ O (stir for ½ hour; leave till next day)
M1a	100 ml of H ₂ O + 5.88 g of K ₂ Cr ₂ O ₇ dissolved in 50 ml of H ₂ O + 3.92 of Na ₂ CO ₃ dissolved in 35 ml of H ₂ O + 7.84 g of CaCO ₃ (natural source; Kremer) + 55 ml of Pb(NO ₃) ₂ [¶] (stir for ½ hour)
M2a	100 ml of H ₂ O + 2.65 g of K ₂ Cr ₂ O ₇ dissolved in 25 ml of boiling H ₂ O + 1.59 of Na ₂ CO ₃ dissolved in 25 ml of boiling H ₂ O + 0.6 ml of H ₂ SO ₄ + 18.8 ml of Pb(Ac) ₂ ·2Pb(OH) ₂ [‡] + 2.47 g of BaSO ₄ (natural source; Sibelco) (stir for 20 min, wash and leave to air dry until next day)
D1b	100 ml of H ₂ O + 2.65 g of K ₂ Cr ₂ O ₇ dissolved in 25 ml of boiling H ₂ O + 1.59 of Na ₂ CO ₃ dissolved in 25 ml of boiling H ₂ O + 2.47 g of BaSO ₄ (natural source; Sibelco) + 18.8 ml of Pb(Ac) ₂ ·2Pb(OH) ₂ [‡] + 0.6 ml of H ₂ SO ₄ (stir for 20 min, wash and leave to air dry until next day)

[§] 118 ml of boiling H₂O + 12.95 g of Pb(Ac)₂·2H₂O + 12.95 g of PbO (Boil and stir for 2 hours and then fill up to make 118 ml).

[¶] 150 ml of boiling H₂O + 32.3 ml of HNO₃ + 53.5 g of PbO (Boil and stir for 2 hours and then fill up to make 150 ml).

[‡] 50 ml of boiling H₂O + 5.24 g of Pb(CH₃COO)₂·2H₂O + 5.24 g of PbO (Boil and stir for 2 hours and then fill up to make 50 ml).

Table V.2.1.1.2. (continued).

D2a	100 ml of H ₂ O + 2.65 g of K ₂ Cr ₂ O ₇ dissolved in 25 ml of boiling H ₂ O + 0.88 of Na ₂ CO ₃ dissolved in 25 ml of boiling H ₂ O + 18.8 ml of Pb(Ac) ₂ ·2Pb(OH) ₂ [‡] + 2.22 g of CaSO ₄ ·½H ₂ O (Vaz Pereira) + 1.24 g of BaSO ₄ (natural source; Sibelco) sifted into 70 ml of H ₂ O and stirred for 1 h + H ₂ SO ₄ till neutral (stir for ½ hour, wash and leave to air dry until next day)
------------	---

[‡] 50 ml of boiling H₂O + 5.24 g of Pb(CH₃COO)₂·2H₂O + 5.24 g of PbO (Boil and stir for 2 hours and then fill up to make 50 ml)

Table V.2.1.1.3. Summary of the conditions used for other lead chromate synthetic pathways.

	Synthesis
PR1b	491 ml of H ₂ O (5°C) + 5.88 g of K ₂ Cr ₂ O ₇ dissolved in 20 ml of boiling H ₂ O + 4.90 g of Na ₂ CO ₃ dissolved in 20 ml of boiling H ₂ O + Pr1b: 4 ml of H ₂ SO ₄ in 40 ml of H ₂ O Pr1b_1: 1.1 ml of H ₂ SO ₄ in 40 ml of H ₂ O Pr1b_2: 1.5 ml of H ₂ SO ₄ in 40 ml of H ₂ O + 108 ml of Pb(NO ₃) ₂ [§] (leave till next day)
PR1b*	110 ml of H ₂ O (5°C) + 1.32 g of K ₂ Cr ₂ O ₇ dissolved in 4.5 ml of boiling H ₂ O + 1.10 g of Na ₂ CO ₃ dissolved in 4.5 ml of boiling H ₂ O + 0.25 ml of H ₂ SO ₄ in 9 ml of H ₂ O + 24.3 ml of Pb(NO ₃) ₂ [§] (leave till next day)
L2b	250 ml of H ₂ O + 9.41 g of Na ₂ SO ₄ + 60 ml of boiling H ₂ O + 5.88 g of K ₂ Cr ₂ O ₇ + 4.94 g of Na ₂ CO ₃ (boil and stir for ½ h; add water to fill 60 ml) + 57 ml of Pb(NO ₃) ₂ [¥] + 1.7 ml of H ₂ SO ₄ in 2 ml of H ₂ O (stir for ½ hour)
L3a*¹⁶¹	222 ml of H ₂ O + 5.88 g of K ₂ Cr ₂ O ₇ dissolved in 55 ml of boiling H ₂ O + 6.59 g of Na ₂ CO ₃ dissolved in 55 ml of boiling H ₂ O + 8.24 g of Na ₂ SO ₄ in 55 ml of H ₂ O + 43 ml of Pb(NO ₃) ₂ [‡] (always stirring for 1 hour) + 8.24 g of CaSO ₄ ·1/2H ₂ O sifted into 329 ml of H ₂ O and stirred for 2 hours

[§] 110 ml of boiling H₂O + 17.9 ml of HNO₃ + 28.46 g of PbO (Boil and stir for 1 hour and then fill up to make 110 ml).

[¥] 150 ml of boiling H₂O + 32.3 ml of HNO₃ + 53.5 g of PbO (Boil and stir for 2 hours and then fill up to make 150 ml).

[‡] 150 ml of boiling H₂O + 8.1 ml of HNO₃ + 13.37 g of PbO (Boil and stir for 1 hour and then fill up to make 150 ml).

¹⁶¹ This recipe is a variation of the L3a synthesis method presented in the next page; a lower quantity of lead nitrate was used.

Table V.2.1.1.3. (continued).

	Synthesis
L3a	222 ml of H ₂ O + 5.88 g of K ₂ Cr ₂ O ₇ dissolved in 55 ml of boiling H ₂ O + 6.59 g of Na ₂ CO ₃ dissolved in 55 ml of boiling H ₂ O + 8.24 g of Na ₂ SO ₄ in 55 ml of H ₂ O + 121 ml of Pb(NO ₃) ₂ [‡] (always stirring for 1 hour) + 8.24 g of CaSO ₄ ·1/2H ₂ O sifted into 329 ml of H ₂ O and stirred for 2 hours
L3b	222 ml of H ₂ O + 5.88 g of K ₂ Cr ₂ O ₇ dissolved in 55 ml of boiling H ₂ O + 6.59 g of Na ₂ CO ₃ dissolved in 55 ml of boiling H ₂ O + 8.24 g of Na ₂ SO ₄ in 55 ml of H ₂ O + 121 ml of Pb(NO ₃) ₂ [‡] (always stirring for 1 hour)
M1b	50 ml of H ₂ O + 1.32 g of K ₂ Cr ₂ O ₇ dissolved in 12.5 ml of H ₂ O + 0.79 g of Na ₂ CO ₃ dissolved in 12.5 ml of H ₂ O + 9.7 ml of Pb(NO ₃) ₂ [¥] (stir for ½ hour)
D1a	20 ml of H ₂ O + 1.32 g of K ₂ Cr ₂ O ₇ dissolved in sufficient H ₂ O + 0.44 of Na ₂ CO ₃ dissolved in sufficient H ₂ O + 0.05 ml of H ₂ SO ₄ + 2.47 g of BaSO ₄ + 1.24 g of CaSO ₄ ·½H ₂ O (Vaz Pereira) sifted into 30 ml of H ₂ O and stirred for 2h + Pb(Ac) ₂ ·2Pb(OH) ₂ [‡] till neutral + 0.2 ml of H ₂ SO ₄ (stir for ¼ hour)

[‡] 300 ml of boiling H₂O + 32.3 ml of HNO₃ + 53.5 g of PbO (Boil and stir for 1 hour and then fill up to make 300 ml).

[¥] 150 ml of boiling H₂O + 32.3 ml of HNO₃ + 53.5 g of PbO (Boil and stir for 2 hours and then fill up to make 150 ml).

[‡] 50 ml of boiling H₂O + 5.24 g of Pb(CH₃COO)₂·2H₂O + 5.24 g of PbO (Boil and stir for 2 hours and then fill up to make 50 ml).

V.2.1.2. Other yellow chromate pigments

The summary of the conditions used for the main synthetic pathways listed in Table 3.9 is presented in Table V.2.1.2.1.

Table V.2.1.2.1. Summary of the conditions used for the other yellow chromate main synthetic pathways.

	Synthesis
LY1a	100 ml of boiling H ₂ O + 1.32 g of K ₂ Cr ₂ O ₇ dissolved in 13 ml of H ₂ O + 10 ml of BaCl ₂ * (stir for 10 min and leave to settle 1 hour).
CY1a	50 ml of boiling H ₂ O + 2.94 g of K ₂ Cr ₂ O ₇ + 0.3 g of K ₂ CO ₃ + 50 ml of Zn(NO ₃) ₂ [†] + 0.05 g of K ₂ CO ₃ (stir for 10 min).
SY1a	25 ml of chromate solution* + 1.1 g of Sr(NO ₃) ₂ dissolved in 25 ml of boiling H ₂ O (stir for 10 min; leave till next day).

* 5 g of BaCl₂ dissolved in 30 ml of H₂O.
[†] 2.97 g of Zn(NO₃)₂ dissolved in 50 ml of H₂O.
* 25 ml of boiling H₂O + 0.75 g of K₂Cr₂O₇ + Na₂CO₃ until neutral pH (boil and stir for 1 h; add water to fill 25 ml)

V.2.2. Micro-sampling

Micro-sampling was carried out using a micro-chisel from *Ted Pella* microtools under a Leica MZ16 stereomicroscope (7.1× to 115× zoom range), equipped with a Leica ICD digital camera and a fibre-optic light Leica system (Leica KI 1500 LCD).

V.2.3. Calculation of the tinting strength of yellow chromate pigments

The relative tinting strength was calculated using the ASTM Standard Test Method D4838 - 88(2003). Poly(vinyl acetate) paints were prepared with the reconstructed pigments and barium sulfate, which was added until a maximum reflectance between 35% to 45% was obtained. A poly(vinyl acetate) paint of lead chromate and barium sulfate was used as the standard. The reflectance spectra were acquired in paint drawdowns applied with a thickness of 100 μm. The relative tinting strength calculated does not account for differences in hue and chroma.

V.2.4. Irradiation experiment

V.2.4.1. Paint preparation

Oil paints of the references and the reconstructed pigments (Appendix X, p. 293) were prepared in 2011 by hand-grinding with a glass muller on a glass slab a mixture of 33.3% of untreated linseed oil (HART project seed lot Electra, extracted in 2005) to pigment by weight. Paints were applied onto glass slides with a palette knife.

PVAc paints with reconstructed pigments (Appendix X, p. 293) were prepared in 2014 by hand-grinding with a pestle on an agate mortar a mixture of 0.5 ml of PVAc solution (20% (w/v) in acetone) to 0.5 g of pigment. Paints were applied onto glass slides with a Zehntner GmbH applicator ZAF 2010.6050 (50 μm).

V.2.4.2. Accelerated ageing

The irradiation experiment was carried out in a CO.FO.ME.GRA accelerated aging apparatus (SolarBox 3000e) equipped with a Xenon-arc light source ($\lambda_{\text{irr}} > 300 \text{ nm}$) with constant irradiation of 800 W/m^2 and black standard temperature of 50°C , cooled with air conditioning (inside the camera temperature was maintained at approximately 30°C and RH at 40%; Ferreira *et al.*, 2010).

The oil paints prepared with the reconstructed pigments were irradiated for a period of 11000h (total irradiance = 31643 MJ/m^2); they were analysed and samples were taken after 1000h, 1500h, 3000h, 4000h, 5500h, 7750h and 9000h. The sample from the W&N's *Chrome Deep* was irradiated for 10000h (total irradiance = 28766 MJ/m^2); it was analysed and samples were taken after 1500h, 3000h, 4500h and 8500h. The samples from the historic oil paints W&N's *Chrome Yellow* and Lefranc's *Jaune de Chrome* together with the PVAc paints were irradiated for a period of 8500h (total irradiance = 24451 MJ/m^2); they were analysed and samples were taken after 1500h, 3000h, 4500h, 5250h, 6000h and 8500h. The lead chromate reference oil paint was only irradiated for a period of 1500h (total irradiance = 4315 MJ/m^2).

V.2.5. Preparation of resin-embedded cross-sections

Resin-embedded cross-sections were prepared in two different ways: by embedding i) in Technovit 2000LC resin and ii) in Cristal polyester resin with catalyzer (MR Dinis dos Santos). The cross-sections were then dry polished using Micromesh sheets (with micron graded silicon carbide crystals) with a final polish using a 12000 sheet.

V.2.6. Preparation of embedding-free thin cross-sections

Embedding-free thin cross-sections were prepared using the "sample enclosing system" (SES) approach (Pouyet *et al.*, 2014). In this system, the sample is placed on a transparent polycarbonate foil ($5 \times 8 \text{ cm}^2$), which is then covered by another polycarbonate foil of the same size. The "sandwiched" sample is put into a commercial sample holder for microtoming (Pouyet *et al.*, 2014). Microtoming was performed under dried conditions, using a motorized rotary Leica RM2265 microtome with binoculars for examination under magnification. Carbide tungsten blades were used and thin cross-sections with thickness between 1 to $4 \mu\text{m}$ were obtained.

V.3. Equipment and data acquisition

Colourimetry

For measuring colour, a portable spectrophotometer colourimetry Data Color International was used. Its measuring head's optical system uses diffuse illumination from a pulsed Xenon arc lamp over the 8mm-diameter measuring area, with 0° viewing angle geometry. Colour coordinates were calculated defining the D65 illuminant and the 10° observer. The calibration was performed with a white bright standard plate and a total black standard. Colour, as perceived by the human eye, may be represented in a three dimensional system. The colour data are presented in the CIE-Lab system. In the Lab cartesian system, L*, relative brightness, is represented by the z-axis. Variations in relative brightness range from white (L*=100) to black (L*=0). The (a*, b*) pair represents the hue of the object. The red/green y-axis plots a* ranging from negative values (green) to positive (red). The yellow/blue x-axis reports b* going from negative (blue) to positive numbers (yellow). Total colour variation (ΔE^*) was calculated according to the expression $\Delta E^* = [(\Delta L^*)^2 + (\Delta a^*)^2 + (\Delta b^*)^2]^{1/2}$.

FORS

Reflectance spectra were acquired with Ocean Optics equipment composed by a single-beam dispersive fibre optic spectrometer (model MAYA 2000 PRO) equipped with 2048 linear silicon CCD array detector (Hamamatsu). The MAYA 2000 PRO has a spectral response from 200 nm to 1050 nm. The illumination is an Ocean Optics HL-2000-HP with 20 Watt halogen light source in a single optical path covering the 360-2400 nm range. Spectra were obtained with an integration time of 8 ms and 15 scans to average. The measuring head, in a 45°/45° (illumination/acquisition angles) configuration, gives a diameter of analysis of about 2 mm. As reference a Spectralon® standard was used. FORS spectra were acquired in reflectance and the wavelength of the inflection points was obtained through calculation of their first derivative. However, in the main text of this thesis, the spectra are presented as apparent absorbance, $A' = \text{Log}_{10}(1/R)$.

Optical microscopy

Optical microscopy (OM) images were obtained using an Axioplan 2ie Zeiss microscope equipped with a transmitted and incident halogen light illuminator (tungsten light source, HAL 100); UV light (mercury light source, HBO 100 illuminator); and a digital Nikon camera DXM1200F, with Nikon ACT-1 application program software. Samples were analysed with 10x ocular lenses and 5x/10x/20x/50x objective Epiplan lenses (giving total optical magnification of 50x, 100x, 200x, and 500x). For the incident and transmitted light (normal light) the samples were analysed under crossed polars – polariser and analyser filters; and for UV light the Zeiss filter set 2 [BP300-400, FT 395, LP 420] was used. The scales for all objectives were calibrated within the Nikon ACT-1 software.

Micro-EDXRF

Micro-EDXRF analyses were performed on an ArtTAX spectrometer of Intax GmbH, equipped with a molybdenum (Mo) anode and a Xflash detector refrigerated by the Peltier effect (Sidrift). The primary X-ray beam is focused to a diameter of 70 μm by means of polycapillary X-ray mini lens. The characteristic x-rays emitted by the sample are detected by a silicon drift electro-thermally cooled detector with a resolution of 160 eV at Mn-K α . The X-ray emission lines are described in Appendix VI.1 (p. 243). The experimental parameters used were: 40 kV of voltage, 600 μA of intensity and between 100 to 200 seconds of acquisition time. Measurements were carried out in helium atmosphere when necessary to detect lower elements such as aluminium (Al).

SEM-EDS

SEM images were obtained using a FEI Quanta 400 FEG ESEM, with a Schottky emitter field emission gun, operating at low vacuum conditions and at 15 kV, equipped with an EDAX Genesis X4M detector. Images were acquired using a backscattered (BSE) electron detector. SEM was performed within the Portuguese microscopy network REM, at CEMUP (Centro de Materiais, Universidade do Porto). SEM images in BSE mode of reference compounds are shown in Appendix VI.2 (p. 244).

Micro-Raman

Raman microscopy was carried out using a Labram 300 Jobin Yvon spectrometer, equipped with a HeNe laser 17mW operating at 632.8nm. Spectra were recorded as an extended scan. The laser beam was focused with 50x Olympus objective lens. The laser power at the surface of the samples was varied with the aid of a set of neutral density filters. All samples were analysed using 15 s laser exposure time for 5 scans. Raman spectra of reference compounds are presented in Appendix VI.3 (p. 245).

Micro-FTIR

Infrared analyses were carried out with a Nicolet Nexus spectrophotometer coupled to a Continuum microscope (15x Objective) with a MCT-A detector cooled by liquid nitrogen. The pigments were prepared as KBr pellets, and spectra were collected in transmission mode, with a resolution of 4 cm^{-1} and 64 scans. For the micro-samples from oil paints and paintings, spectra were obtained in transmission mode, 4000–650 cm^{-1} , with a resolution of 4 cm^{-1} and 128 scans, using a *Thermo* diamond anvil compression cell. The spectra are shown here as acquired, without corrections or any further manipulations, except for the removal of the CO₂ absorption at ca. 2300–2400 cm^{-1} . Infrared spectra of reference compounds are presented in Appendix VI.4 (p. 256).

XRD

X-ray diffraction patterns were acquired with a PANalytical X'Pert PRO diffractometer equipped with a X'Celerator detector and using CuK α radiation in the $10 < 2\theta < 80$ range with a step width of 0.02°, at the CENIMAT/i3N – Centro de Investigação de Materiais/Instituto de Nanoestruturas, Nanomodelação e Nanofabricação of the Universidade NOVA de Lisboa.

X-ray diffraction patterns were also acquired with a RIGAKU X-ray diffractometer MiniFlex II using CuK α radiation (30 kV/15 mA) in the $10 < 2\theta < 80$ range with a 1° step size, at the REQUIMTE Analysis Laboratory (FCT NOVA).

SR-based techniques¹⁶² were performed at the X-ray microscopy beamline, ID21, at the European Synchrotron Radiation Facility (ESRF, Grenoble, France) (Susini *et al.*, 2005; Salomé *et al.*, 2013; Pouyet *et al.*, 2015). The scanning X-ray microscope has a tunable energy ranging from 2.1 to 9.1 keV and is optimized for very low background and low detection limits. The fluorescence excitation is stimulated with a highly monochromatic beam by means of a fixed-exit, double crystal Si(111) monochromator, located upstream of the microscope, and which provides an energy resolution of $\Delta E/E=10^{-4}$.

Micro-XRF and **micro-XANES** analyses were performed in vacuum (10^{-5} mbar). A collimated beam of 200 μm diameter and a focused beam of ca. $0.3 \times 0.8 \mu\text{m}^2$ (horizontal \times vertical) obtained by means of a Fresnel zone plate were used for sample irradiation. The XRF signal was collected in the horizontal plane perpendicular to the incident beam direction by using a single energy-dispersive silicon drift detector (Xflash 5100-Bruker). The energy resolution of this detection system is 130 eV at 6 keV. The detection limit for elements ranging from Fe to P is around 10 ppm. The sample surface was oriented vertically and at an angle of 69° relative to the incident beam. During the μ -XRF mapping experiments, the fluorescence signals were generated by employing a monochromatic primary beam of fixed energy (around 5.989 keV at the Cr K-edge, 2.472 keV at the S K-edge and 4.053 keV at the Ca K-edge). During the μ -XANES energy scans, the position of the primary beam was maintained stable within 1 μm . μ -XANES spectra were acquired by scanning the primary energy around the Cr K-edge (5.97-6.1 keV), the S K-edge (2.46-2.53 keV) and Ca K-edge (4.03-4.12 keV) with a step size of 0.2, 0.3 and 0.18 eV, respectively. The energy calibrations were performed using a metallic Cr foil and a $\text{CaSO}_4 \cdot 2\text{H}_2\text{O}$ reference powder. μ -XANES spectra of reference compounds are shown in Appendix VI.5 (p. 267).

For the calculation of the Light Susceptibility Index, Cr K-edge XANES spectra were acquired with a macro-beam (200 μm) at 5 to 10 different points on surface sections at selected irradiated samples. Normalisation of all XANES spectra were made by means of ATHENA software and the same energy range and polynomial type of the pre- and post-edge lines were used (Monico *et al.*, 2011a; Zanella *et al.*, 2011). Using between 3 to 10 normalized Cr K-edge XANES spectra, an average value of the intensity of the Cr⁶⁺ pre-edge peak at 5.993 keV was obtained for each surface section.

Ca K-edge XANES spectra were also normalized below the pre-peak and above the post-edge structure, set to zero and one, respectively, by means of the ATHENA software (Hesse *et al.*, 2016).

Micro-FTIR analyses were performed using a spectro-microscope based on a commercial instrument composed of a Thermo Nicolet Nexus FTIR bench associated with a Thermo Continuum microscope. The infrared beam is emitted at the edges of a bending magnet. In the microscope, two

¹⁶² The team members of SR-experiments HG-28 (2014), HG-53 (2015) and HG-80 (2016) were: Maria João Melo, Márcia Vilarigues and Vanessa Otero. Cristina Montagner was a team member of SR-experiment HG-28. The local contact of all experiments was Marine Cotte.

×32 Schwarzschild objectives were used in a confocal mode and an aperture defines the spot size of the beam. The embedding-free thin cross-sections were mounted horizontally, deposited on a 10×10×0.2 mm³ BaF₂ window or between two BaF₂ windows, allowing spectra acquisition in transmission mode. The μ-samples were analysed using a diamond anvil compression cell and μ-FTIR maps of resin-embedded cross-sections were acquired in ATR mode. The beam size and step size was 10×10 μm² or 8×8 μm². Spectra were acquired as a sum of 100 scans, with a spectral resolution of 8 cm⁻¹, over the 4000-750 cm⁻¹ range.

μ-XRF and μ-FTIR maps were analysed using the PyMca software. The X-ray emission lines are described in Appendix VI.1. The infrared regions of interest used for μ-FTIR mapping are shown below in Table V.3.1. For μ-FTIR analyses, the OMNIC software was also used (Solé *et al.*, 2007; Pouyet *et al.*, 2015).

Micro-XRD experiments were performed at the new μXRD end-station, at ID21, in transmission geometry. The primary beam energy was tuned by single fixed monochromatic energy of 8.53 keV and focused down to 0.7×1.0 μm² (vertical×horizontal). The transmitted diffraction patterns were recorded using a 2D taper FReLoN CCD and the XRF signal was collected using a Ketek 80mm² Silicon Drift Diode. Both μ-XRD and μ-XRF signals were collected in continuous scan (zap) mapping mode. The resulting μXRD maps were analysed using the XRDUA package (De Nolf *et al.*, 2014).

Table V.3.1. Regions of interest used for μ-FTIR mapping with PyMca software (see Appendix VI.4, p.256).

Region of interest (ROI)	From	To	Region of interest (ROI)	From	To
Quartz ν(Si-O)	807	790	Lead white ν _{as} (CO ₃ ²⁻)	1480	1340
Lead carbonate δ _{as} (CO ₃ ²⁻)	850	825	Chalk ν _{as} (CO ₃ ²⁻)	1520	1350
Chalk δ _{as} (CO ₃ ²⁻)	890	860	Zinc soap broad ν _{as} (COO ⁻)	1560	1525
Chromate ν _{as} (CrO ₄ ²⁻)	920	800	Magnesium carbonate ν _{as} (CO ₃ ²⁻)	1540	1450
Mixed crystals ν _s (SO ₄ ²⁻)	975	960	Metal soaps ν _{as} (COO ⁻)	1600	1475
Barium sulfate ν _s (SO ₄ ²⁻)	990	975	Oxalates ν _{as} (C=O)	1650	1600
Strontium sulfate ν _s (SO ₄ ²⁻)	1005	980	Gypsum δ(H ₂ O)	1635	1600
Barium sulfate ν _{as} (SO ₄ ²⁻)	1150	1050	Acid ν(C=O)	1718	1700
Quartz ν _{as} (Si-O-Si)	1170	1157	Ester ν(C=O)	1755	1720
Gypsum ν _{as} (SO ₄ ²⁻)	1190	1090	PVAc ν(C=O)	1770	1710
Lead sulfate ν _{as} (SO ₄ ²⁻)	1200	1140	Prussian Blue ν(C≡H)	2130	2050
Viridian	1270	1240	ν(CH)	2980	2830
Viridian	1300	1270	Gypsum ν(OH)	3460	3360
Oxalates ν _s (C=O)	1340	1300	Magnesium carbonate ν(OH)	3480	3410
Cobalt Yellow ν _s (NO ₂)	1360	1300	Lead White ν(OH)	3580	3500
Cobalt Yellow ν _{as} (NO ₂)	1440	1360	Kaolin ν(OH)	3720	3610
Magnesium carbonate ν _{as} (CO ₃ ²⁻)	1450	1380			

Appendix VI. Spectral and SEM data of reference compounds

VI.1. X-ray Emission Lines

Table VI.1.1. Photon energies, in keV, of principal K-, L-, and M-shell emission lines, adapted from Kortright & Thompson, 2009. X-Ray Data Booklet, Table 1-2.

Element	K α	K β	L α	L β_1	L β_2	L γ_1	M α
¹³ Al	1.486	1.553					
¹⁴ Si	1.739	1.829					
¹⁵ P	2.013	2.139					
¹⁶ S	2.308	2.464					
¹⁷ Cl	2.622	2.815					
¹⁸ Ar	2.957	3.190					
¹⁹ K	3.312	3.589					
²⁰ Ca	3.690	4.012					
²¹ Sc	4.090	4.460					
²² Ti	4.510	4.932					
²³ V	4.952	5.427					
²⁴ Cr	5.414	5.946					
²⁵ Mn	5.893	6.489					
²⁶ Fe	6.396	7.057					
²⁷ Co	6.922	7.648					
²⁸ Ni	7.477	8.264					
²⁹ Cu	8.040	8.904					
³⁰ Zn	8.630	9.570					
³¹ Ga	9.251	10.264					
³² Ge	9.886	10.982					
³³ As	10.543	11.725					
³⁴ Se	11.207	12.492					
³⁵ Br	11.924	13.291					
³⁸ Sr	14.164	15.834					
⁴⁷ Ag			2.984	3.150	3.347	3.519	
⁴⁸ Cd			3.133	3.316	3.528	3.716	
⁵⁰ Sn			3.443	3.662	3.904	4.131	
⁵⁶ Ba			4.467	4.828	5.156	5.531	
⁷⁹ Au			9.713	11.442	11.584	13.381	
⁸⁰ Hg			9.987	11.823	11.923	13.828	
⁸² Pb			10.550	12.812	12.621	14.782	2.342

VI.2. SEM images

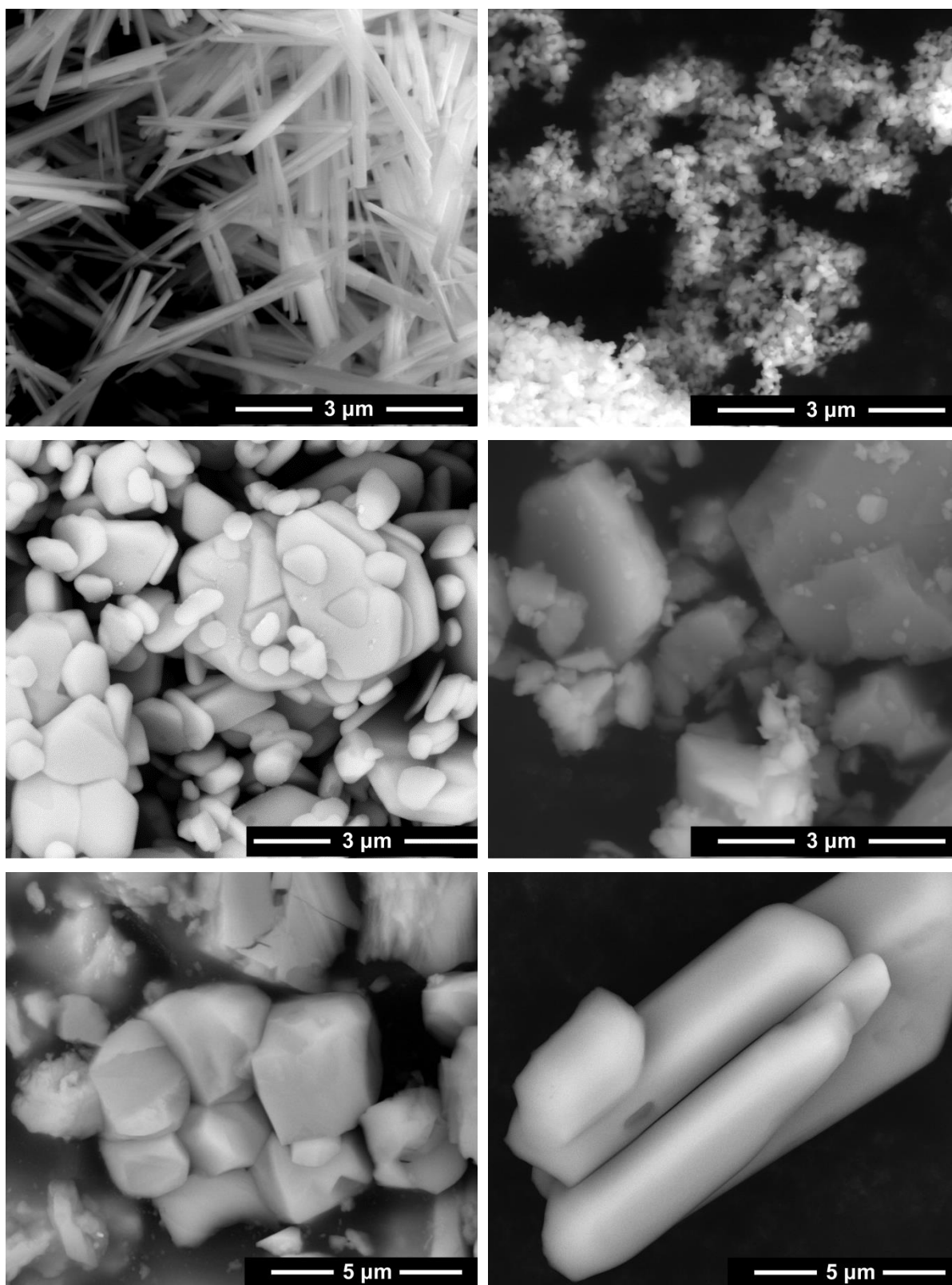


Figure VI.2.1. SEM image of lead chromate (lead chromate (PbCrO_4 , monoclinic crystal structure); lead chromate (PbCrO_4 , orthorhombic crystal structure); lead white¹⁶³ obtained by the stack process ($2\text{PbCO}_3 \cdot \text{Pb(OH)}_2$); barium sulfate (BaSO_4), calcium carbonate¹⁶³ (CaCO_3) and calcium sulfate dihydrate ($\text{CaSO}_4 \cdot 2\text{H}_2\text{O}$).

¹⁶³ SEM images kindly provided by Diogo Sanches.

VI.3. μ -Raman spectra

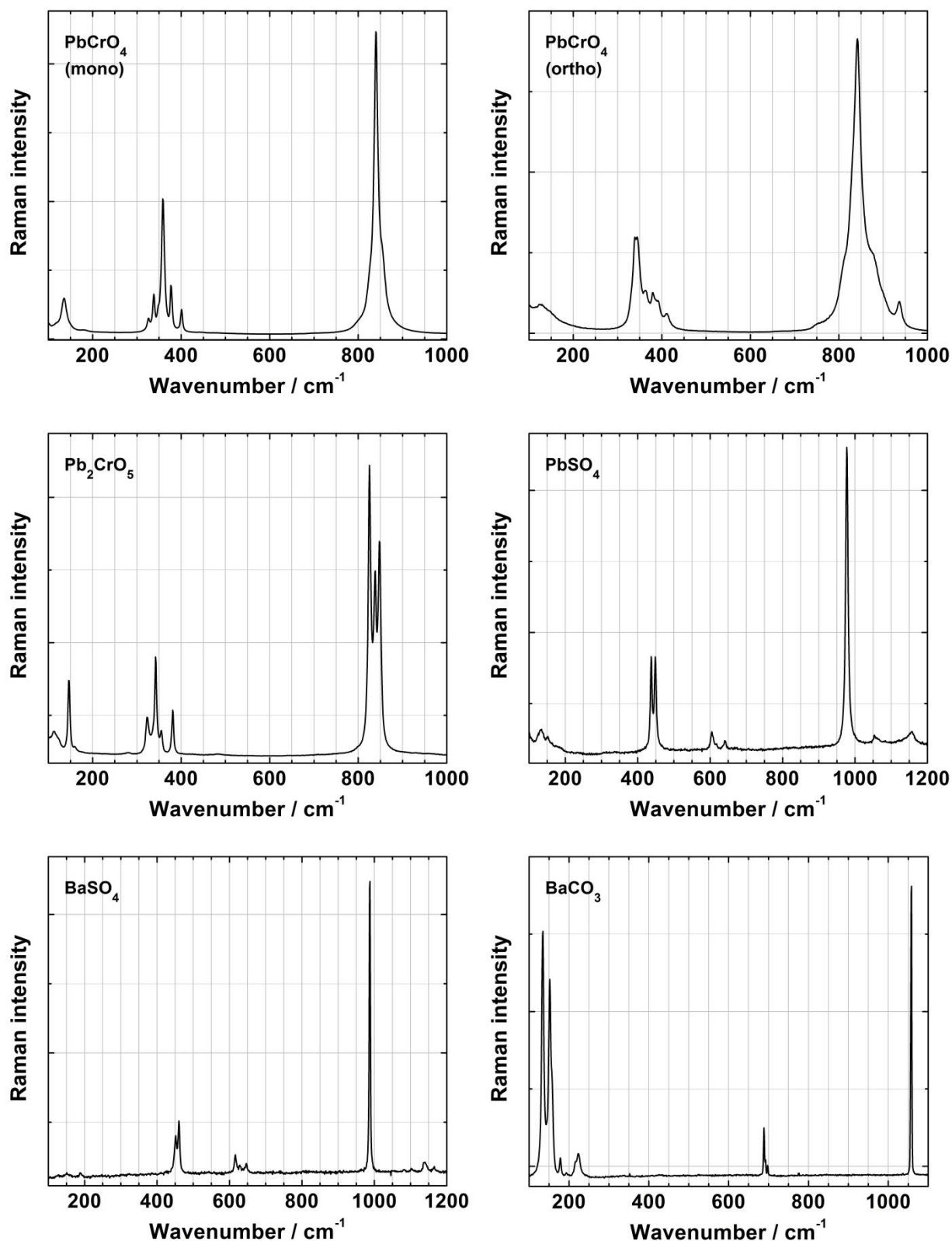


Figure VI.3.1. Raman spectra of lead chromate (PbCrO_4 , monoclinic crystal structure); lead chromate (PbCrO_4 , orthorhombic crystal structure); basic lead chromate (Pb_2CrO_5); lead sulfate (PbSO_4); barium sulfate (BaSO_4) and barium carbonate (BaCO_3).

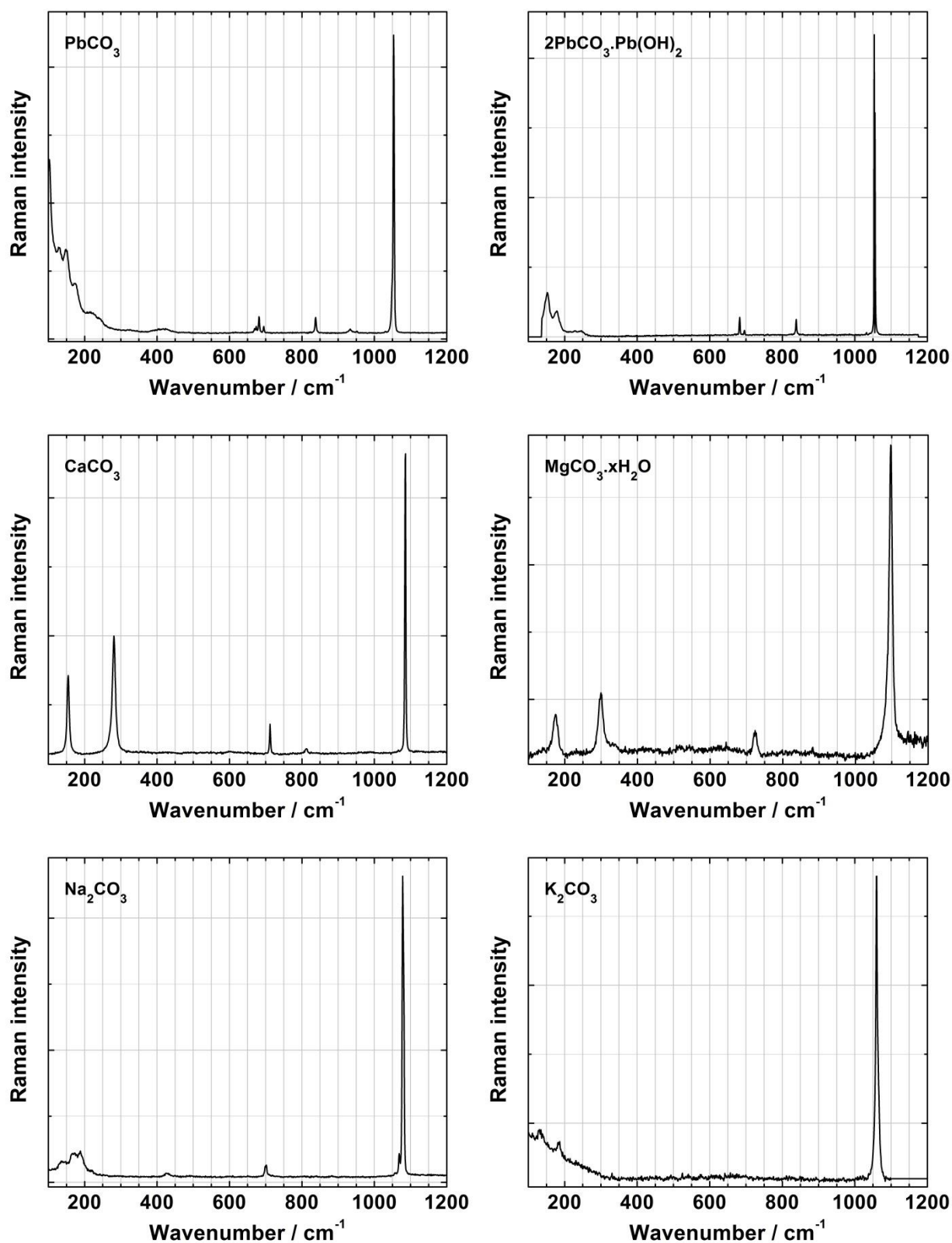


Figure VI.3.2. Raman spectra of lead carbonate (PbCO_3); lead white ($2\text{PbCO}_3 \cdot \text{Pb(OH)}_2$)¹⁶⁴, calcium carbonate (CaCO_3); magnesium carbonate ($\text{MgCO}_3 \cdot x\text{H}_2\text{O}$); sodium carbonate (Na_2CO_3) and potassium carbonate (K_2CO_3).

¹⁶⁴ Spectrum from Spectra ID v3.02, ThermoGalactic (database available at the DCR FCT NOVA).

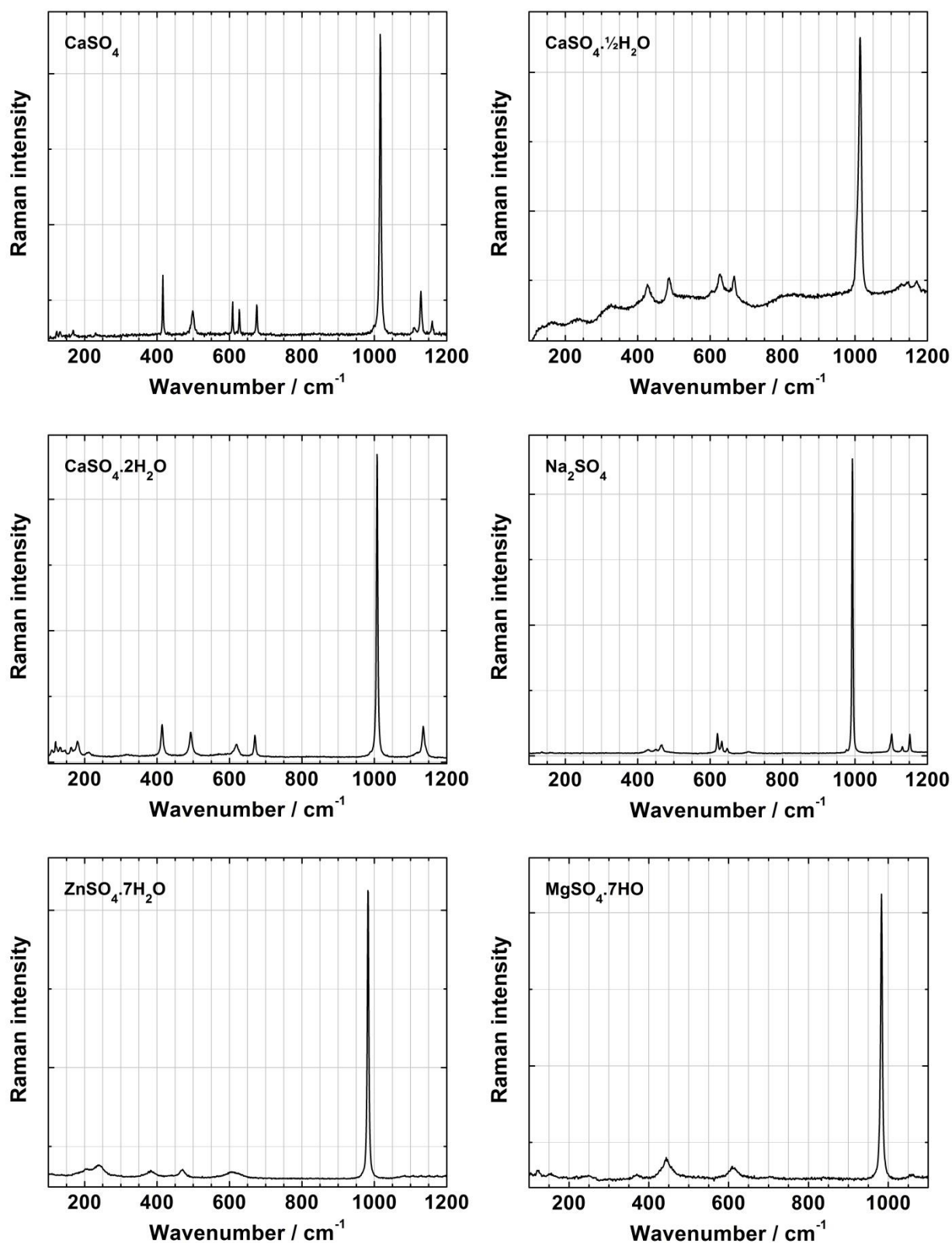


Figure VI.3.3. Raman spectra of calcium sulfate anhydrous (CaSO₄); calcium sulfate hemihydrate (CaSO₄·½H₂O); calcium sulfate dihydrate (CaSO₄·2H₂O); sodium sulfate (Na₂SO₄); zinc sulfate heptahydrate (ZnSO₄·7H₂O) and magnesium sulfate heptahydrate (MgSO₄·7H₂O).

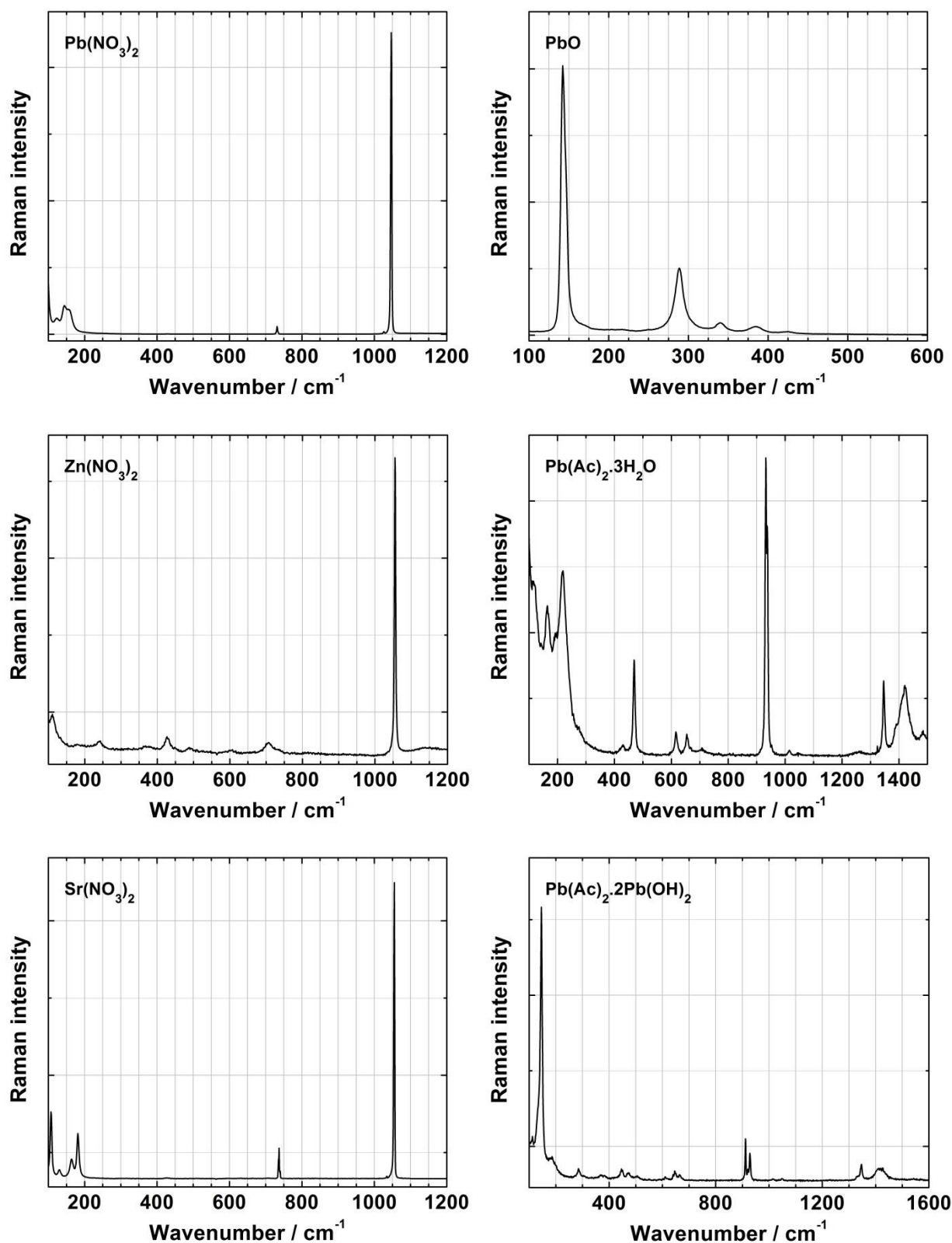


Figure VI.3.4. Raman spectra of lead nitrate (Pb(NO₃)₂); lead oxide (PbO); zinc nitrate (Zn(NO₃)₂); lead acetate trihydrate (Pb(CH₃CO₂)₂·3H₂O); strontium nitrate (Sr(NO₃)₂) and lead subacetate (Pb(Ac)₂·2Pb(OH)₂).

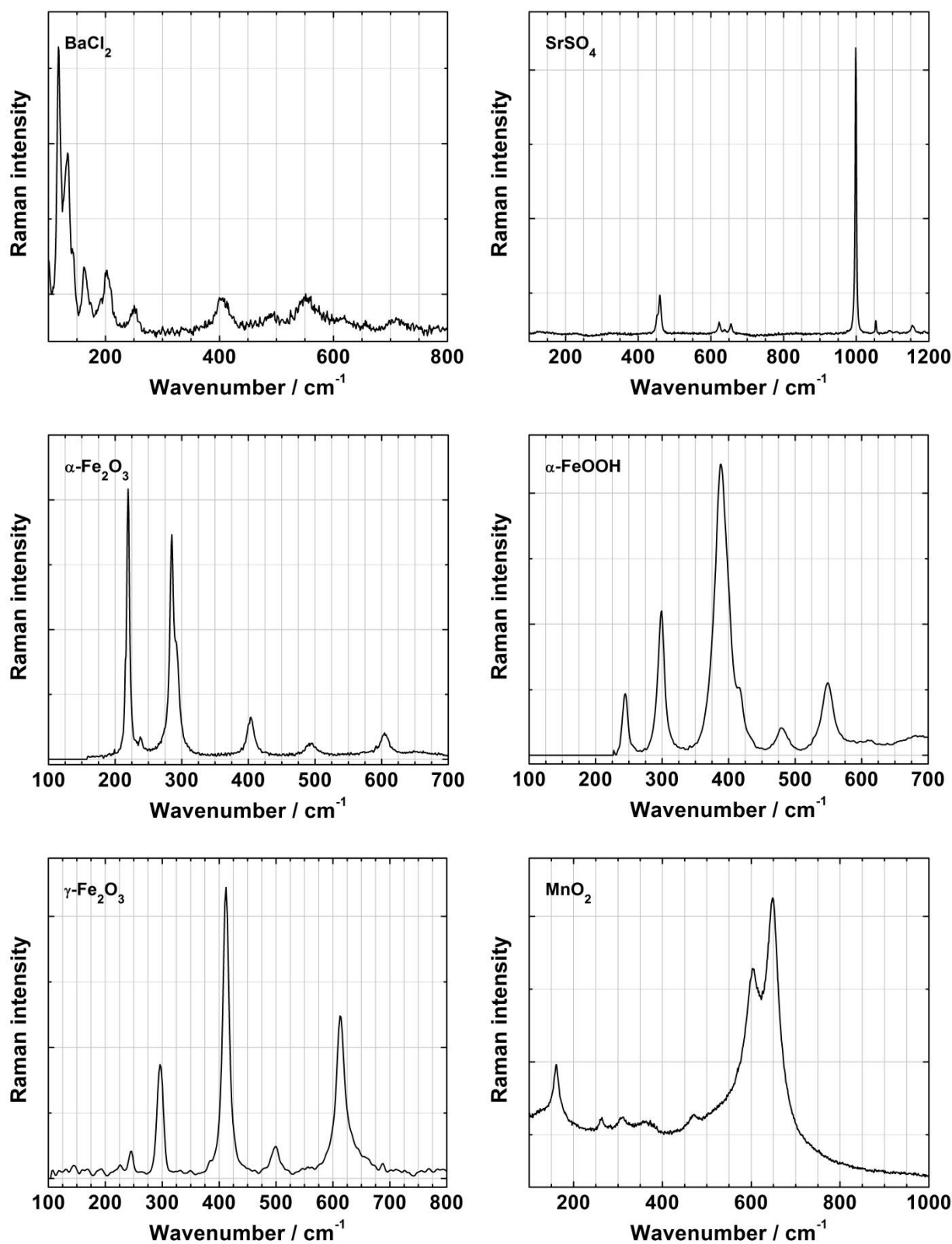


Figure VI.3.5. Raman spectra of barium chloride (BaCl_2); strontium sulfate (SrSO_4)¹⁶⁵; hematite ($\alpha\text{-Fe}_2\text{O}_3$)¹⁶⁶; goethite ($\alpha\text{-FeOOH}$)¹⁶⁶; maghemite ($\gamma\text{-Fe}_2\text{O}_3$)¹⁶⁶ and manganese oxide (MnO_2).

¹⁶⁵ Spectrum obtained by Cristina Montagner (DCR FCT NOVA).

¹⁶⁶ Spectrum from Spectra ID v3.02, ThermoGalactic (database available at the DCR FCT NOVA).

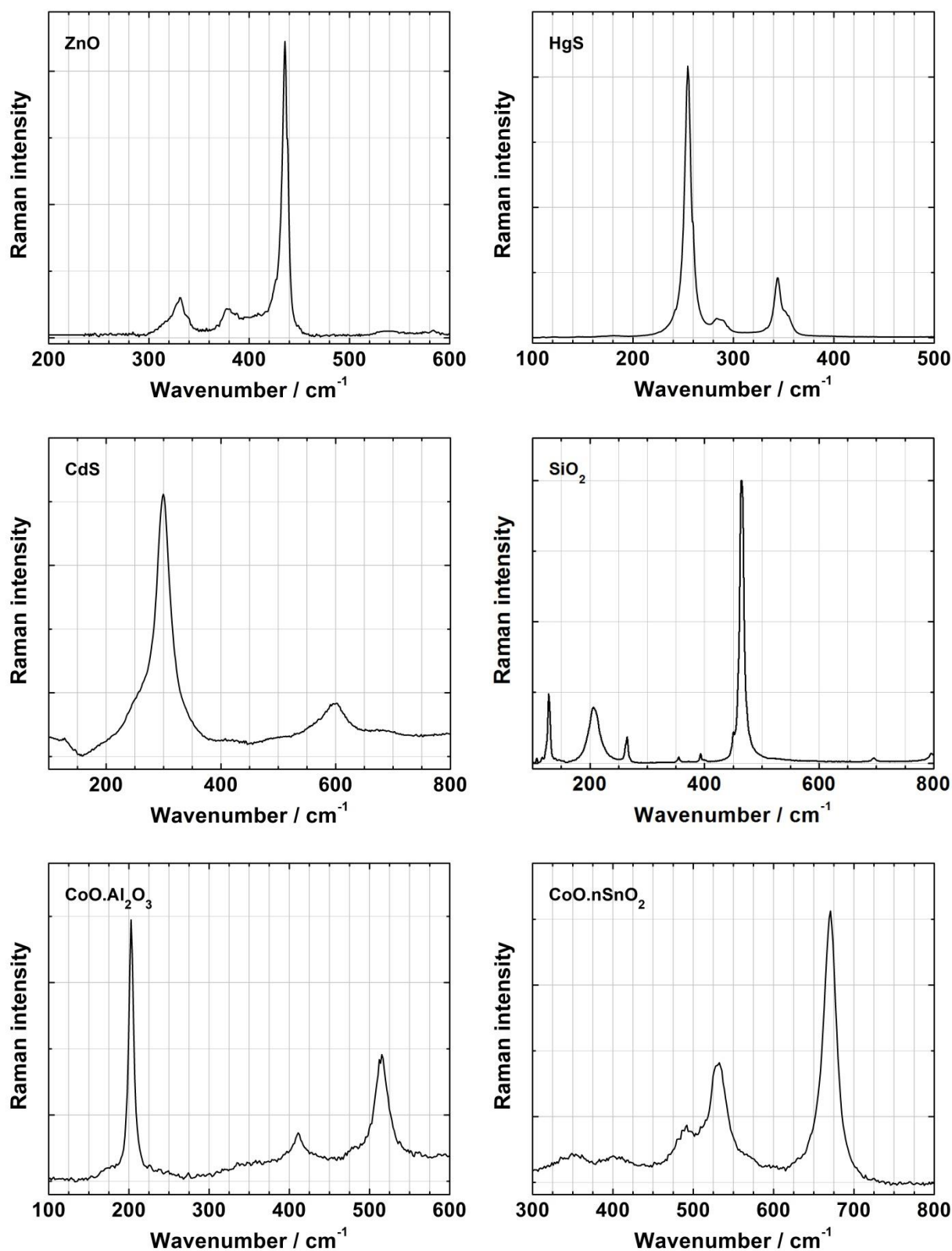


Figure VI.3.6. Raman spectra of zinc white (ZnO)¹⁶⁷, vermilion (HgS); cadmium yellow (CdS); quartz (SiO₂)¹⁶⁷; cobalt blue (CoO.Al₂O₃) and cerulean blue (CoO.nSnO₂).

¹⁶⁷ Spectrum from Spectra ID v3.02, ThermoGalactic (database available at the DCR FCT NOVA).

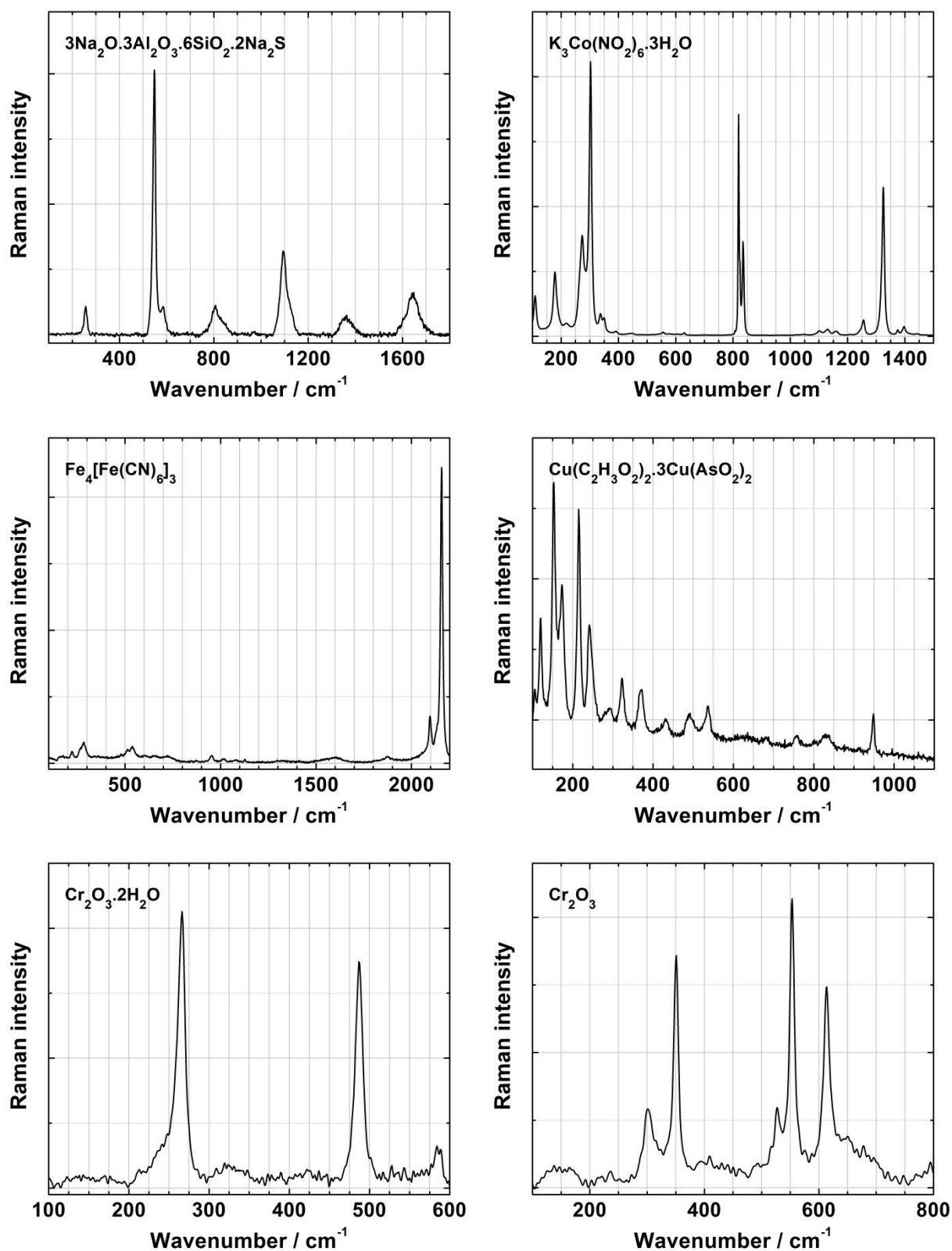


Figure VI.3.7. Raman spectra of ultramarine blue ($3\text{Na}_2\text{O}\cdot 3\text{Al}_2\text{O}_3\cdot 6\text{SiO}_2\cdot 2\text{Na}_2\text{S}$); cobalt yellow ($\text{K}_3\text{Co}(\text{NO}_2)_6\cdot 3\text{H}_2\text{O}$); Prussian blue ($\text{Fe}_4[\text{Fe}(\text{CN})_6]_3$); emerald green ($\text{Cu}(\text{C}_2\text{H}_3\text{O}_2)_2\cdot 3\text{Cu}(\text{AsO}_2)_2$); viridian ($\text{Cr}_2\text{O}_3\cdot 2\text{H}_2\text{O}$); chromium (III) oxide (Cr_2O_3).

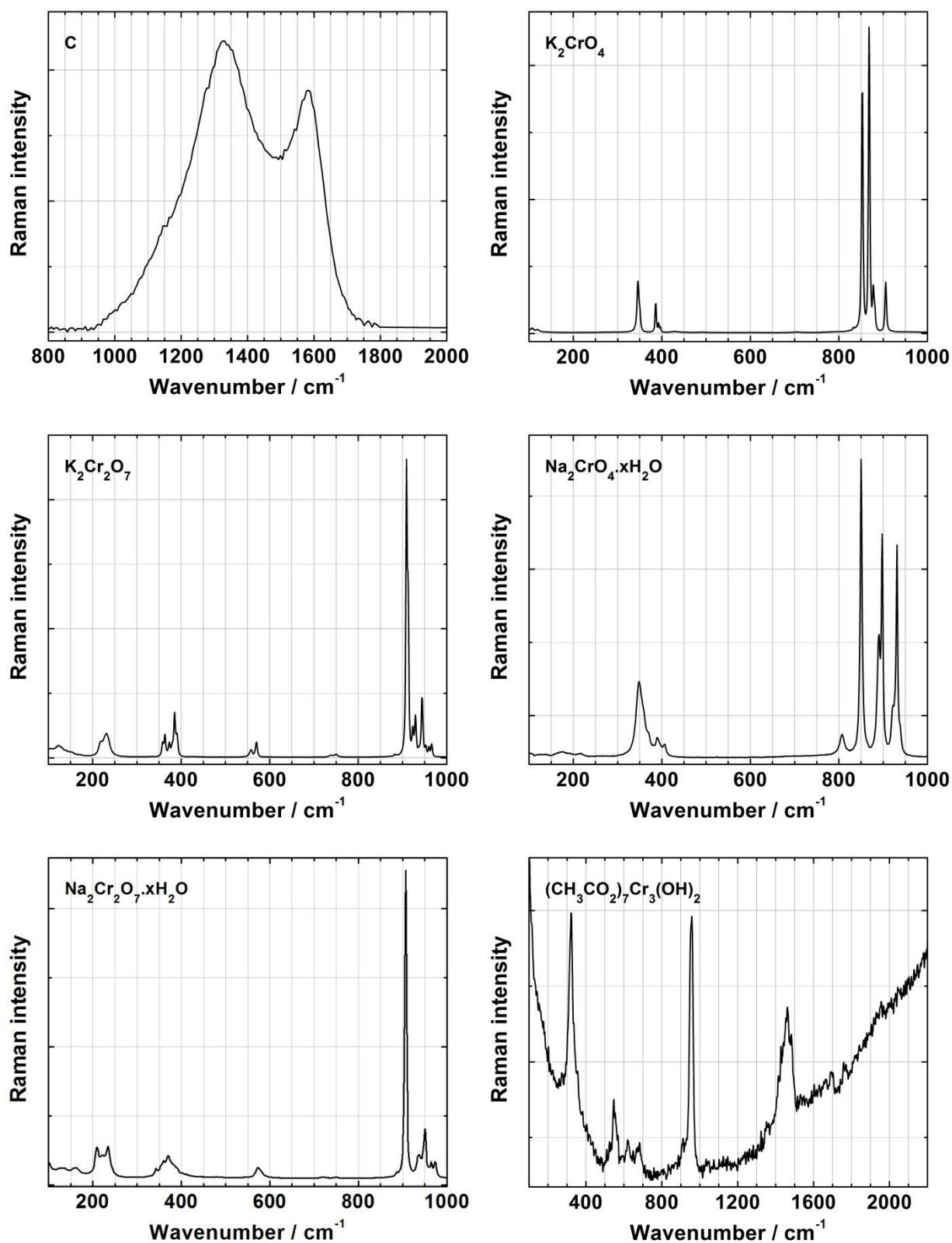


Figure VI.3.8. Raman spectra of carbon black (C); potassium chromate (K_2CrO_4); potassium dichromate ($K_2Cr_2O_7$); sodium chromate ($Na_2CrO_4 \cdot xH_2O$); sodium dichromate ($Na_2Cr_2O_7 \cdot xH_2O$); chromium acetate hydroxide ($(CH_3CO_2)_7Cr_3(OH)_2$).

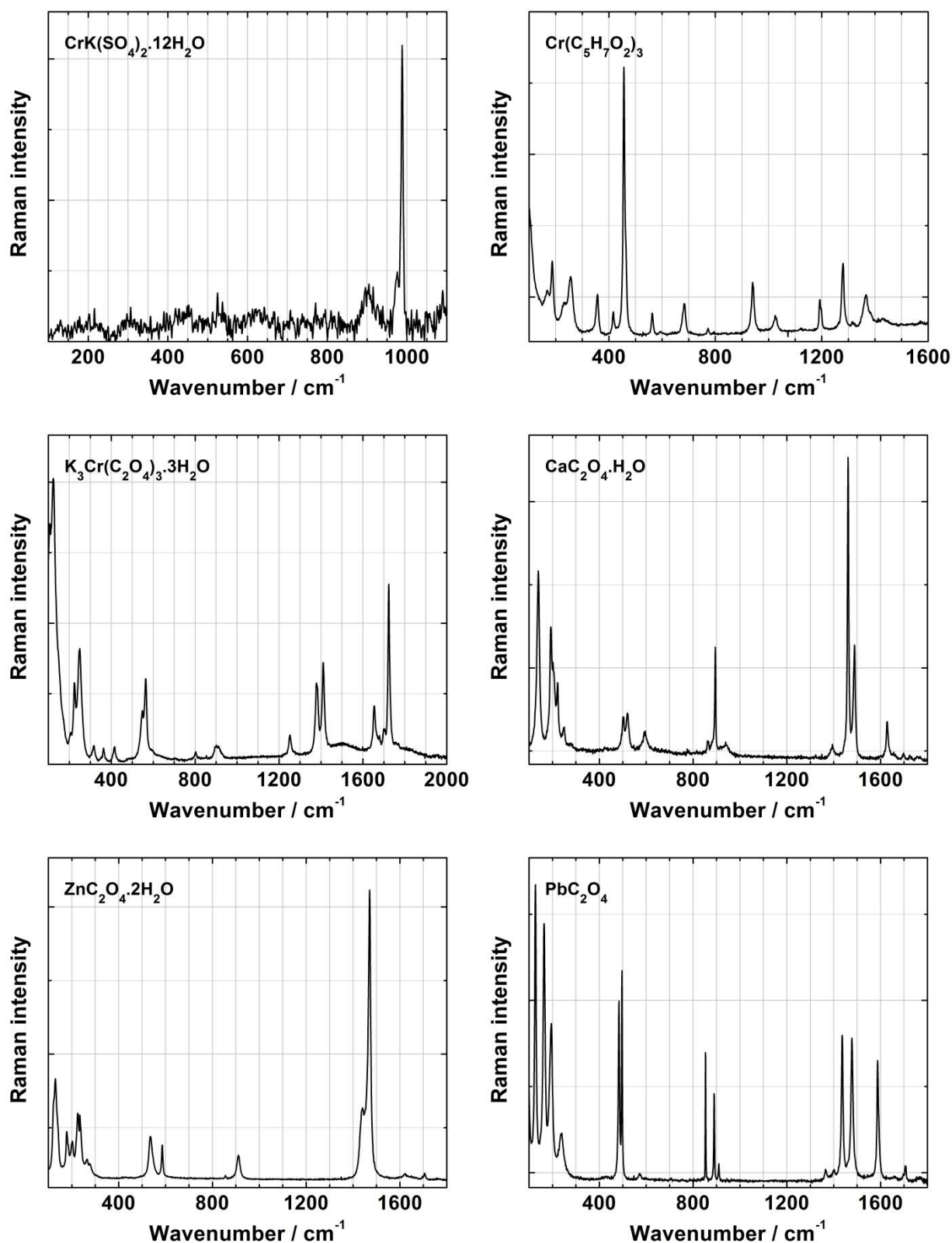


Figure VI.3.9. Raman spectra of chromium potassium sulfate dodecahydrate ($\text{CrK}(\text{SO}_4)_2 \cdot 12\text{H}_2\text{O}$); chromium acetylacetonate ($\text{Cr}(\text{C}_5\text{H}_7\text{O}_2)_3$); potassium chromium oxalate trihydrate ($\text{K}_3\text{Cr}(\text{C}_2\text{O}_4)_3 \cdot 3\text{H}_2\text{O}$); calcium oxalate monohydrate ($\text{CaC}_2\text{O}_4 \cdot \text{H}_2\text{O}$); zinc oxalate dihydrate ($\text{ZnC}_2\text{O}_4 \cdot 2\text{H}_2\text{O}$) and lead oxalate (PbC_2O_4).

Table VI.3.1. Main characteristic Raman bands of the reference compounds (see Figures VI.3.1 to VI.3.9) (Hummel, 2002; Mayo *et al.*, 2004; Nakamoto, 2009)*.

Compound	Bands (cm ⁻¹)	Assignment	Compound	Bands (cm ⁻¹)	Assignment
Lead chromate PbCrO ₄ (monoclinic)	135	<i>lattice mode</i>	Sodium sulfate Na ₂ SO ₄	464,	δ(SO ₄ ²⁻)
	325, 337, 357,	δ(CrO ₄ ²⁻)		620, 632, 647	
	375, 399			993	v _s (SO ₄ ²⁻)
	839	v _s (CrO ₄ ²⁻)	Zinc sulfate	384, 470,	δ(SO ₄ ²⁻)
Lead chromate PbCrO ₄ (orthorhombic)	341, 362, 380,	δ(CrO ₄ ²⁻)	heptahydrate	606	
	391, 410		ZnSO ₄ ·7H ₂ O	982	v _s (SO ₄ ²⁻)
	841	v _s (CrO ₄ ²⁻)	Magnesium sulfate heptahydrate MgSO ₄ ·7H ₂ O	445, 609	δ(SO ₄ ²⁻)
	936	v _{as} (CrO ₄ ²⁻)		983	v _s (SO ₄ ²⁻)
Basic lead chromate Pb ₂ CrO ₅	144	<i>lattice mode</i>	Lead nitrate Pb(NO ₃) ₂	731	δ(NO ₃ ⁻)
	322, 341, 355,	δ(CrO ₄ ²⁻)		1046	v _s (NO ₃)
	380		Lead oxide PbO	142	v(PbO)
	825, 837, 846	v _s (CrO ₄ ²⁻)		288	
Lead sulfate PbSO ₄	438, 449,	δ(SO ₄ ²⁻)	Zinc nitrate	427, 706	δ(NO ₃ ⁻)
	605, 641		Zn(NO ₃) ₂	1056	v _s (NO ₃)
	978	v _s (SO ₄ ²⁻)	Lead acetate trihydrate Pb(CH ₃ CO ₂) ₂ ·3H ₂ O	163, 217	<i>lattice mode</i>
Barium sulfate BaSO ₄	451, 460,	δ(SO ₄ ²⁻)		469, 616, 657	δ(COO ⁻)
	616, 646			932, 937	ρ(CH)
	986	v _s (SO ₄ ²⁻)		1346, 1420	δ(CH)
Barium carbonate BaCO ₃	135, 152	<i>lattice mode</i>	Strontium nitrate Sr(NO ₃) ₂	736	δ(NO ₃ ⁻)
	688	δ(CO ₃ ²⁻)		1055	v _s (NO ₃)
	1058	v _s (CO ₃ ²⁻)	Lead subacetate Pb(Ac) ₂ ·2Pb(OH) ₂	146, 285	v(PbO)
Lead carbonate PbCO ₃	683, 838	δ(CO ₃ ²⁻)		448, 471, 647	δ(COO ⁻)
	1054	v _s (CO ₃ ²⁻)		912, 928	ρ(CH)
Lead white 2PbCO ₃ ·Pb(OH) ₂	683, 838	δ(CO ₃ ²⁻)	1346, 1420	δ(CH)	
	1054, 1056	v _s (CO ₃ ²⁻)	Barium chloride BaCl ₂	117, 133	<i>lattice mode</i>
Calcium carbonate CaCO ₃	281	<i>lattice mode</i>		163, 203	δ(BaCl)
	711	δ(CO ₃ ²⁻)		403, 550	v(BaCl)
	1085	v _s (CO ₃ ²⁻)	Strontium sulfate SrSO ₄	460,	δ(SO ₄ ²⁻)
Magnesium carbonate MgCO ₃ ·xH ₂ O	175, 300	<i>lattice mode</i>		623, 656	
	724	δ(CO ₃ ²⁻)		998	v _s (SO ₄ ²⁻)
Sodium carbonate Na ₂ CO ₃	1097	v _s (CO ₃ ²⁻)	Hematite α-Fe ₂ O ₃	220, 285, 405	δ(FeO)
	698	δ(CO ₃ ²⁻)		605	v(FeO)
Potassium carbonate K ₂ CO ₃	182	<i>lattice mode</i>	Goethite α-FeOOH	245, 299	δ(FeO)
	1060	v _s (CO ₃ ²⁻)		389, 550	v(FeO)
Calcium sulfate anhydrous CaSO ₄	416, 499,	δ(SO ₄ ²⁻)	Maghemite γ-Fe ₂ O ₃	296, 412	δ(FeO)
	608, 627, 675			613	v(FeO)
	1016	v _s (SO ₄ ²⁻)	Manganese oxide MnO ₂	603, 650	v(MnO)
Calcium sulfate hemihydrate CaSO ₄ ·½H ₂ O	428, 486,	δ(SO ₄ ²⁻)		Zinc oxide ZnO	331, 436
	628, 666				
1013	v _s (SO ₄ ²⁻)	Vermilion HgS	254, 285	δ(S-Hg-S)	
Calcium sulfate dihydrate CaSO ₄ ·2H ₂ O	414, 493,		δ(SO ₄ ²⁻)	344	v(HgS)
	618, 669				
1007	v _s (SO ₄ ²⁻)				

Table VI.3.1. (continued).

Compound	Bands (cm ⁻¹)	Assignment	Compound	Bands (cm ⁻¹)	Assignment
Cadmium yellow CdS	300 609	$\nu(\text{CdS})$	Potassium dichromate K ₂ Cr ₂ O ₇	363, 373, 385 909 923, 929, 944	$\delta(\text{CrO}_3)$ $\nu_s(\text{CrO}_3)$ $\nu_{as}(\text{CrO}_3)$
Quartz SiO ₂	129 207, 265 465	<i>lattice mode</i> $\delta(\text{SiO})$ $\delta(\text{Si-O-Si})$	Sodium chromate Na ₂ CrO ₄ .xH ₂ O	350, 390, 406 850 890, 898, 931	$\delta(\text{CrO}_4^{2-})$ $\nu_s(\text{CrO}_4^{2-})$ $\nu_{as}(\text{CrO}_4^{2-})$
Cobalt blue CoO.Al ₂ O ₃	202 520	$\nu(\text{CoO})$	Sodium dichromate Na ₂ Cr ₂ O ₇ .xH ₂ O	369 907 935, 950, 964	$\delta(\text{CrO}_3)$ $\nu_s(\text{CrO}_3)$ $\nu_{as}(\text{CrO}_3)$
Cerulean blue CoO.nSnO ₂	532 670	$\nu(\text{CoO})$ $\nu(\text{SnO})$	Chromium acetate hydroxide (CH ₃ CO ₂) ₇ Cr ₃ (OH) ₂	321 546 956 1460	$\delta(\text{CrO})$ $\delta(\text{COO}^-)$ $\rho(\text{CH}_3)$ $\delta(\text{CH}_3)$
Ultramarine blue 3Na ₂ O.3Al ₂ O ₃ .6SiO ₂ .2Na ₂ S	258 548 1096	$\delta(\text{S}_3^-)$ $\nu_s(\text{S}_3^-)$ overtone	Chromium potassium sulfate dodecahydrate CrK(SO ₄) ₂ .12H ₂ O	976, 988	$\nu_s(\text{SO}_4^{2-})$
Cobalt yellow K ₃ Co(NO ₂) ₆ .3H ₂ O	178 302 820, 835 1325	<i>lattice mode</i> $\nu(\text{CoN})$ $\delta(\text{NO})$ $\nu_{as}(\text{NO})$	Chromium acetylacetonate Cr(C ₅ H ₇ O ₂) ₃	456, 682 940 1026 1193, 1280, 1365	$\delta(\text{CC})/\nu(\text{CrO})$ $\nu(\text{CC})/\nu(\text{CO})$ $\rho(\text{CH}_3)$ $\delta(\text{CH}_3)$
Prussian blue Fe ₄ [Fe(CN) ₆] ₃	276 535 2096, 2158	$\delta(\text{C-Fe-C})$ $\delta(\text{Fe-C}\equiv\text{N})$ $\nu(\text{C}\equiv\text{N})$	Potassium chromium oxalate trihydrate K ₃ Cr(C ₂ O ₄) ₃ .3H ₂ O	224, 248 548, 565 1380, 1410 1654, 1722	<i>lattice mode</i> $\nu(\text{CC})/\nu(\text{CrO})$ $\nu_s(\text{CO})$ $\nu(\text{C=O})$
Emerald green Cu(C ₂ H ₃ O ₂) ₂ .3Cu(AsO ₂) ₂	155, 175, 217, 243 372 490, 539 686 761, 835 950 2926	$\delta(\text{O-Cu-O})$ $\delta(\text{As-O})$ $\nu(\text{Cu-O})$ $\delta_s(\text{COO}^-)$ $\nu(\text{As-O})$ $\nu(\text{C-C})$ $\nu_s(\text{CH}_3)$	Calcium oxalate monohydrate CaC ₂ O ₄ .H ₂ O	139, 193 501, 520 895 1461, 1490 1628	<i>lattice mode</i> $\nu(\text{CC})$ $\delta(\text{OCO})$ $\nu_s(\text{CO})$ $\nu_{as}(\text{C=O})$
Viridian Cr ₂ O ₃ .2H ₂ O	266, 490 552	$\delta(\text{O-Cr-O})$ $\nu_{as}(\text{O-Cr-O})$	Zinc oxalate dihydrate ZnC ₂ O ₄ .2H ₂ O	130, 225, 235 535, 585 910 1440, 1470	<i>lattice mode</i> $\nu(\text{CC})/\nu(\text{ZnO})$ $\delta(\text{OCO})$ $\nu_s(\text{CO})$
Chromium (III) oxide Cr ₂ O ₃	302, 350 550 612	$\delta(\text{O-Cr-O})$ $\nu_{as}(\text{O-Cr-O})$ $\nu_{as}(\text{O-Cr-O})$	Lead oxalate PbC ₂ O ₄	127, 163, 195 484, 497 890 1436, 1478 1587	<i>lattice mode</i> $\nu(\text{CC})/\nu(\text{PbO})$ $\delta(\text{OCO})$ $\nu_s(\text{CO})$ $\nu_{as}(\text{C=O})$
Carbon black C	1340 1595	$sp^3(\text{CC})$ $sp^2(\text{CC})$			
Potassium chromate K ₂ CrO ₄	346, 385 853, 868, 878 906	$\delta(\text{CrO}_4^{2-})$ $\nu_s(\text{CrO}_4^{2-})$ $\nu_{as}(\text{CrO}_4^{2-})$			

* ν = stretching, δ = bending, as = asymmetric, s = symmetric, sh (shoulder).

VI.4. Infrared spectra

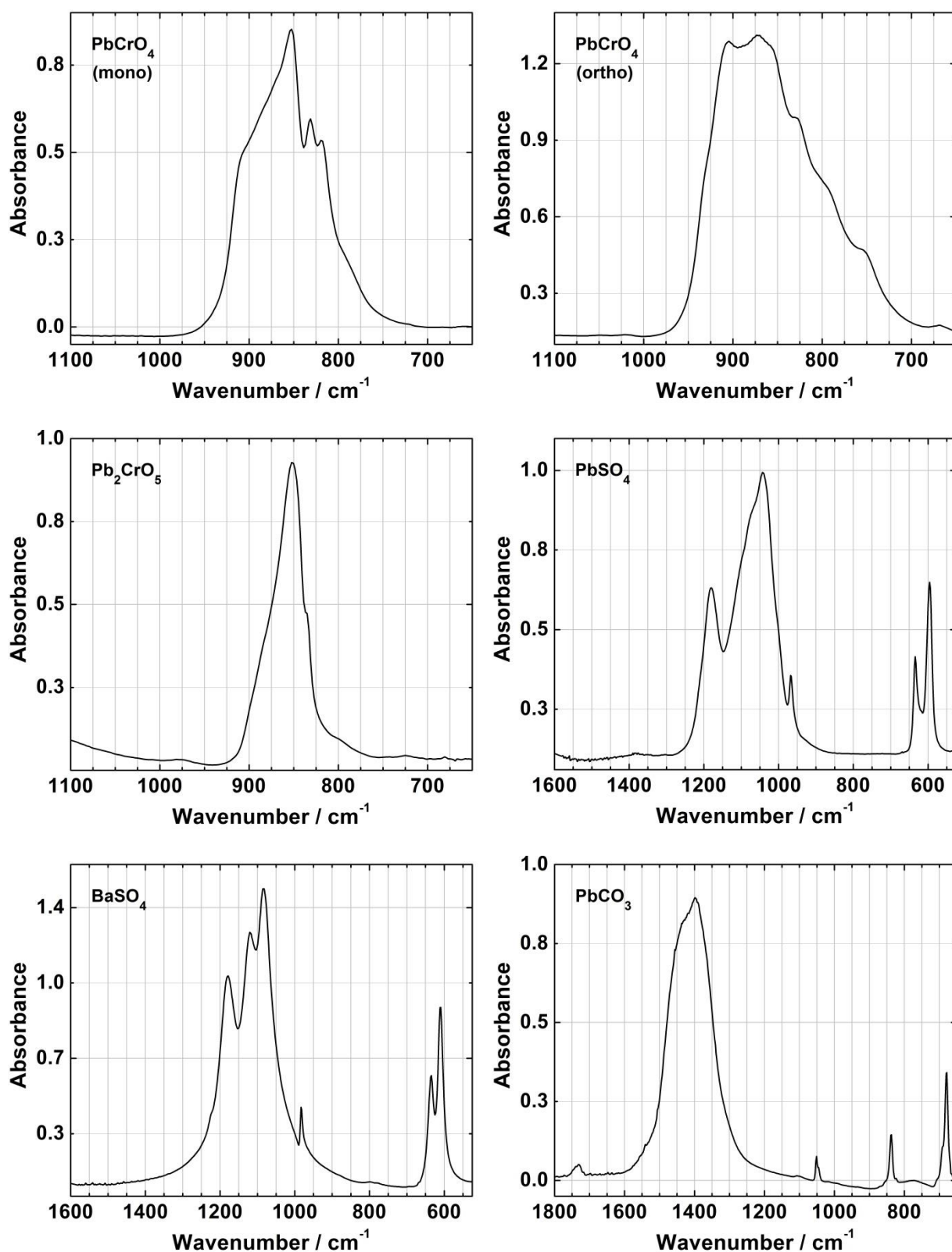


Figure VI.4.1. Infrared spectra of lead chromate (PbCrO₄, monoclinic crystal structure); lead chromate (PbCrO₄, orthorhombic crystal structure); basic lead chromate (Pb₂CrO₅); lead sulfate (PbSO₄); barium sulfate (BaSO₄) and lead carbonate (PbCO₃).

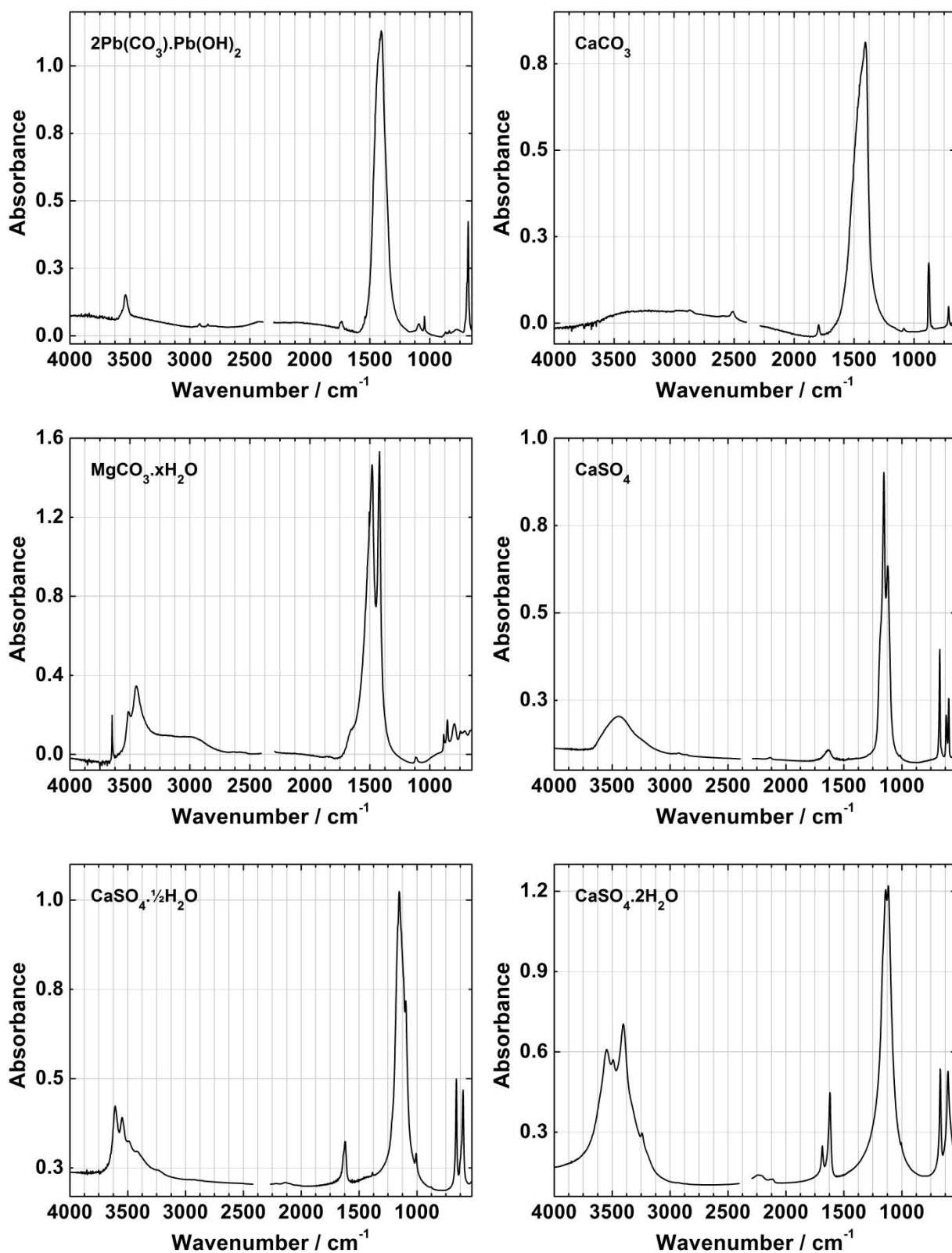


Figure VI.4.2. Infrared spectra of lead white ($2\text{PbCO}_3 \cdot \text{Pb}(\text{OH})_2$); calcium carbonate (CaCO_3); magnesium carbonate ($\text{MgCO}_3 \cdot x\text{H}_2\text{O}$); calcium sulfate anhydrous (CaSO_4); calcium sulfate hemihydrate ($\text{CaSO}_4 \cdot \frac{1}{2}\text{H}_2\text{O}$) and calcium sulfate dihydrate ($\text{CaSO}_4 \cdot 2\text{H}_2\text{O}$).

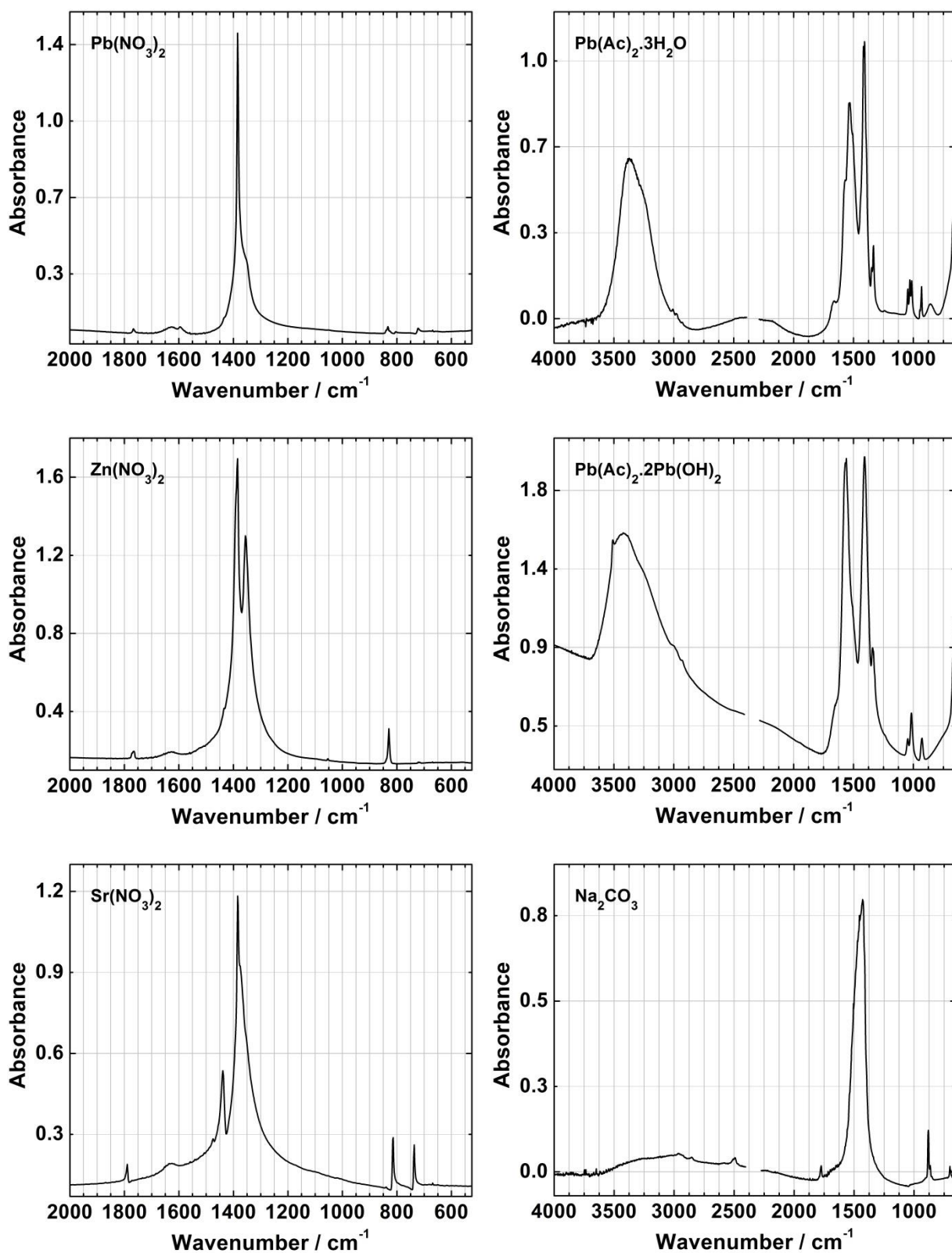


Figure VI.4.3. Infrared spectra of lead nitrate (Pb(NO₃)₂); lead acetate trihydrate (Pb(CH₃CO₂)₂·3H₂O); zinc nitrate (Zn(NO₃)₂); lead subacetate (Pb(Ac)₂·2Pb(OH)₂); strontium nitrate (Sr(NO₃)₂) and sodium carbonate (Na₂CO₃).

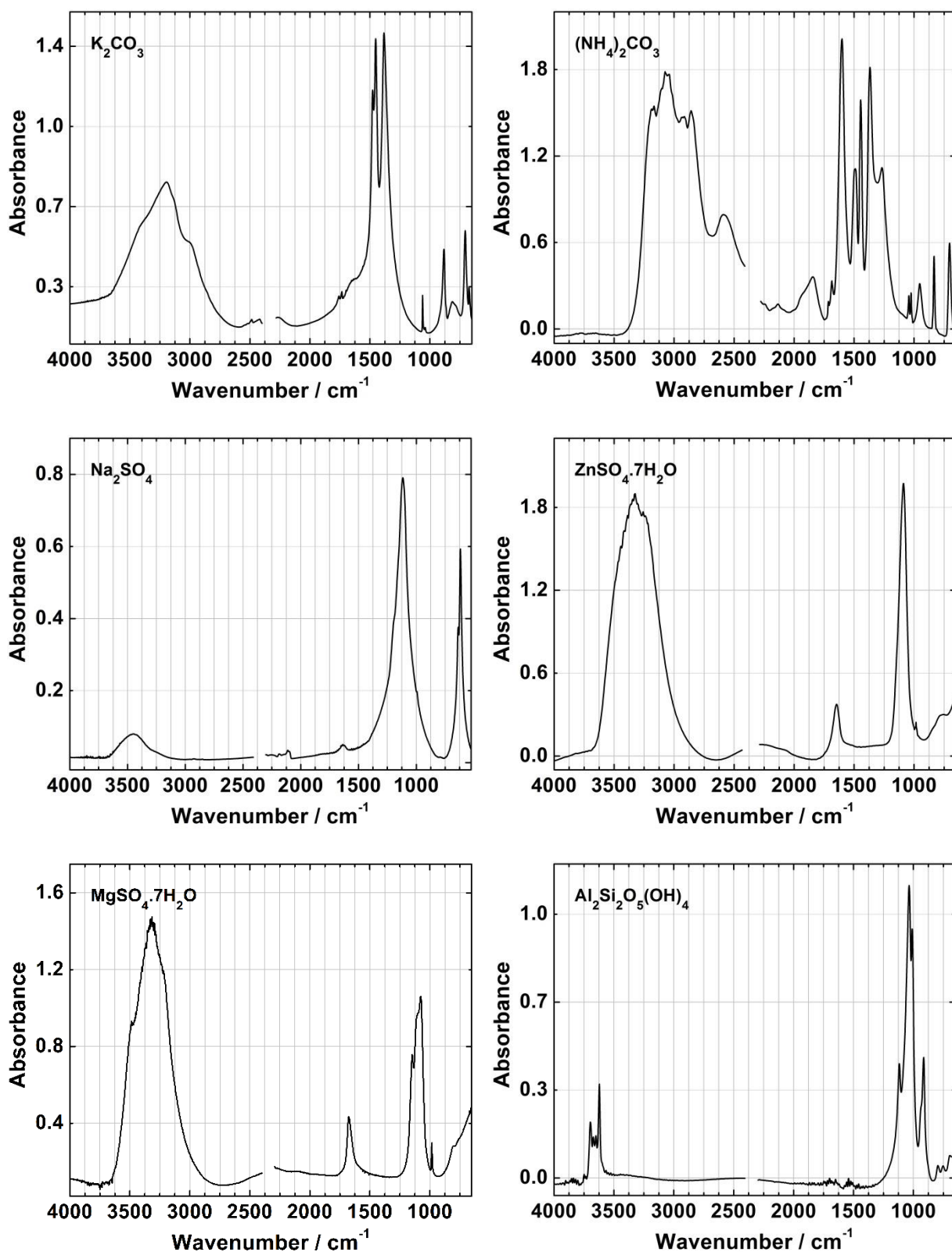


Figure VI.4.4. Infrared spectra of potassium carbonate (K₂CO₃); ammonium carbonate ((NH₄)₂CO₃); sodium sulfate (Na₂SO₄); zinc sulfate heptahydrate (ZnSO₄·7H₂O); magnesium sulfate heptahydrate (MgSO₄·7H₂O) and kaolin (Al₂Si₂O₅(OH)₄).

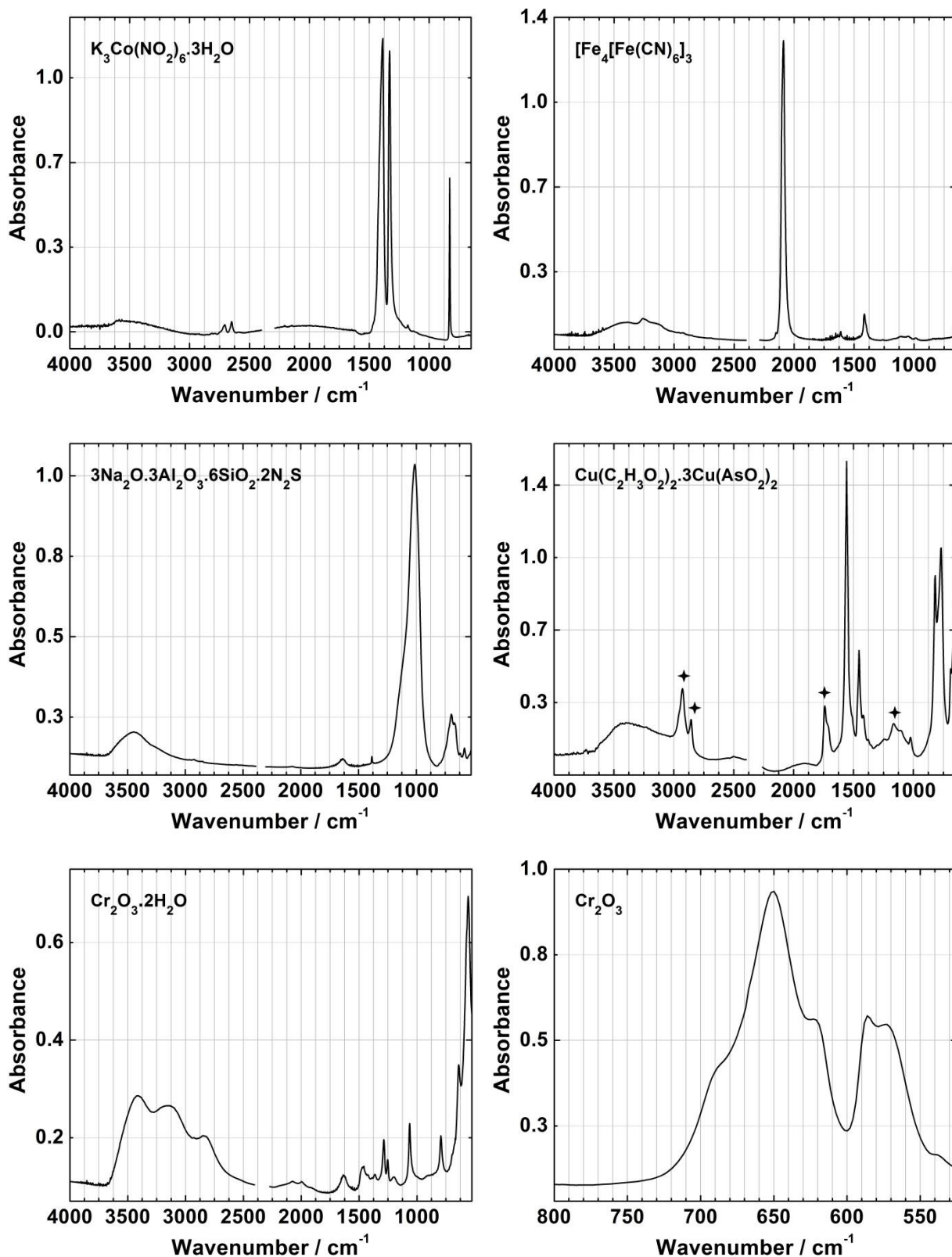


Figure VI.4.5. Infrared spectra of cobalt yellow ($\text{K}_3\text{Co}(\text{NO}_2)_6 \cdot 3\text{H}_2\text{O}$); Prussian blue ($[\text{Fe}_4[\text{Fe}(\text{CN})_6]_3]$); ultramarine blue ($3\text{Na}_2\text{O} \cdot 3\text{Al}_2\text{O}_3 \cdot 6\text{SiO}_2 \cdot 2\text{N}_2\text{S}$); emerald green ($\text{Cu}(\text{C}_2\text{H}_3\text{O}_2)_2 \cdot 3\text{Cu}(\text{AsO}_2)_2$, the only reference available is from an historic oil paint (+)¹⁶⁸); viridian ($\text{Cr}_2\text{O}_3 \cdot 2\text{H}_2\text{O}$) and chromium (III) oxide (Cr_2O_3).

¹⁶⁸ Spectrum obtained by Marta Félix Campos (DCR FCT NOVA).

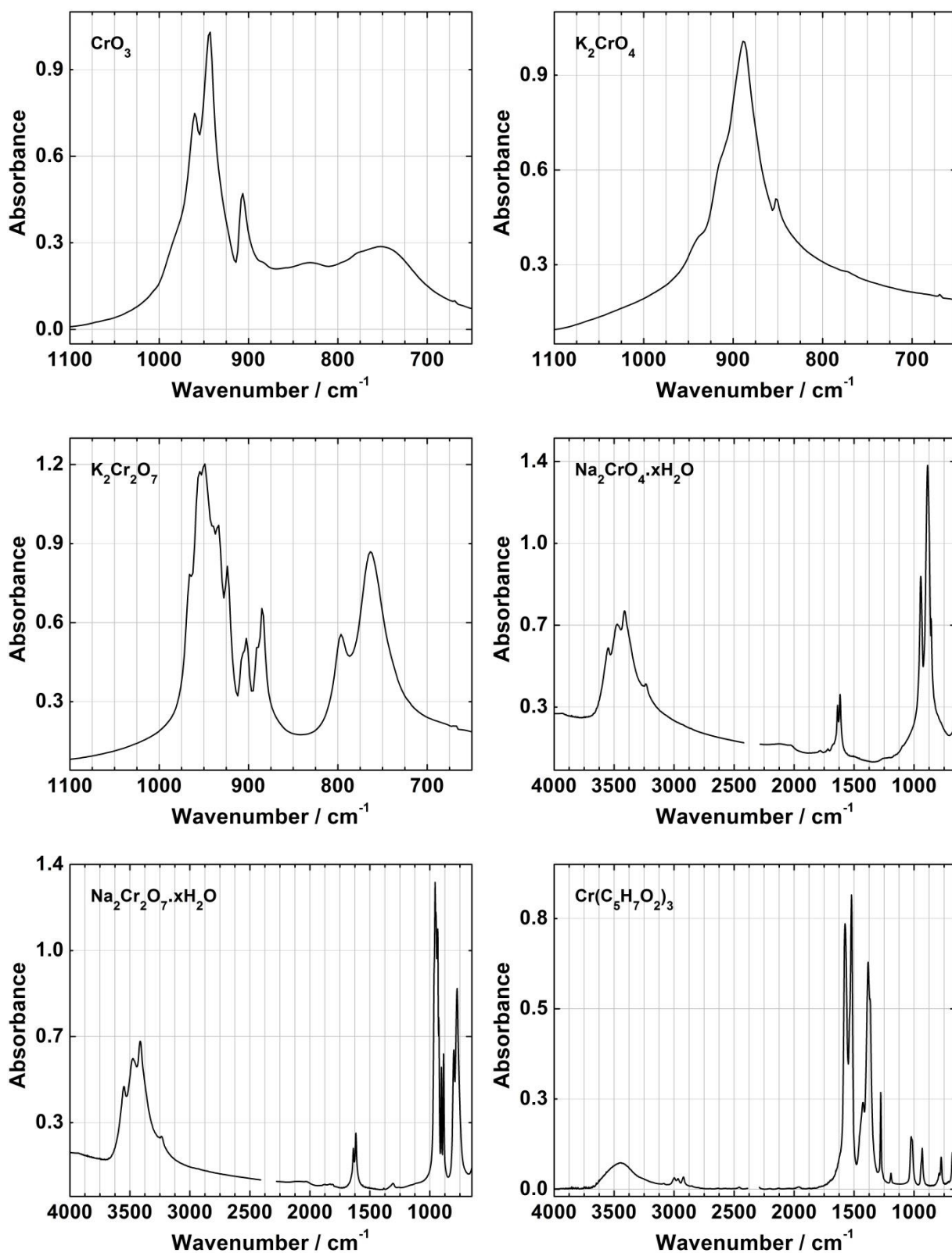


Figure VI.4.6. Infrared spectra of and chromium (VI) oxide (CrO_3); potassium chromate (K_2CrO_4); potassium dichromate ($\text{K}_2\text{Cr}_2\text{O}_7$); sodium chromate ($\text{Na}_2\text{CrO}_4 \cdot x\text{H}_2\text{O}$); sodium dichromate ($\text{Na}_2\text{Cr}_2\text{O}_7 \cdot x\text{H}_2\text{O}$) and chromium acetylacetonate ($\text{Cr}(\text{C}_5\text{H}_7\text{O}_2)_3$).

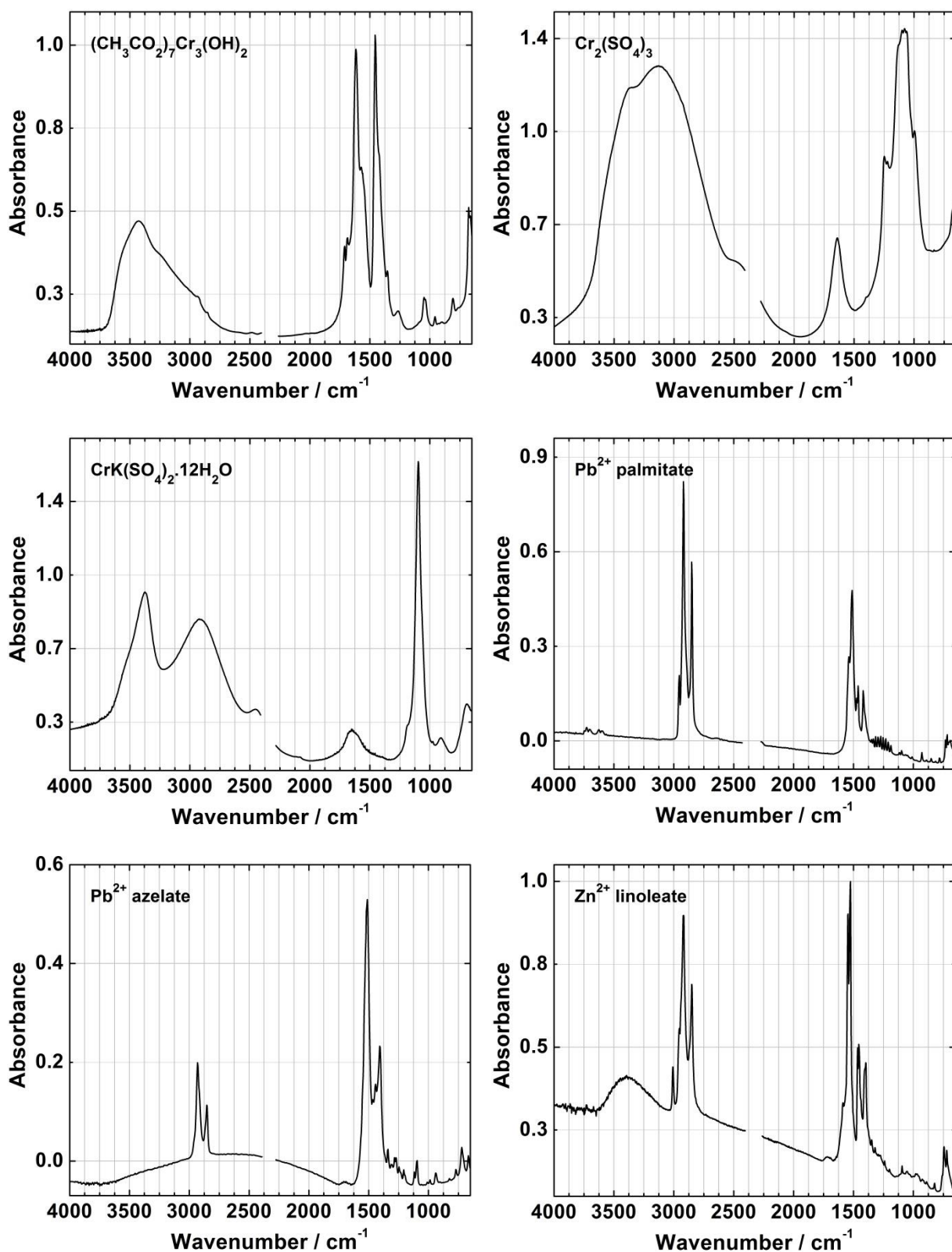


Figure VI.4.7. Infrared spectra of and chromium acetate hydroxide ($(\text{CH}_3\text{CO}_2)_7\text{Cr}_3(\text{OH})_2$); chromium sulfate ($\text{Cr}_2(\text{SO}_4)_3$); chromium potassium sulfate dodecahydrate ($\text{CrK}(\text{SO}_4)_2 \cdot 12\text{H}_2\text{O}$); lead palmitate; lead azelate and zinc linoleate.

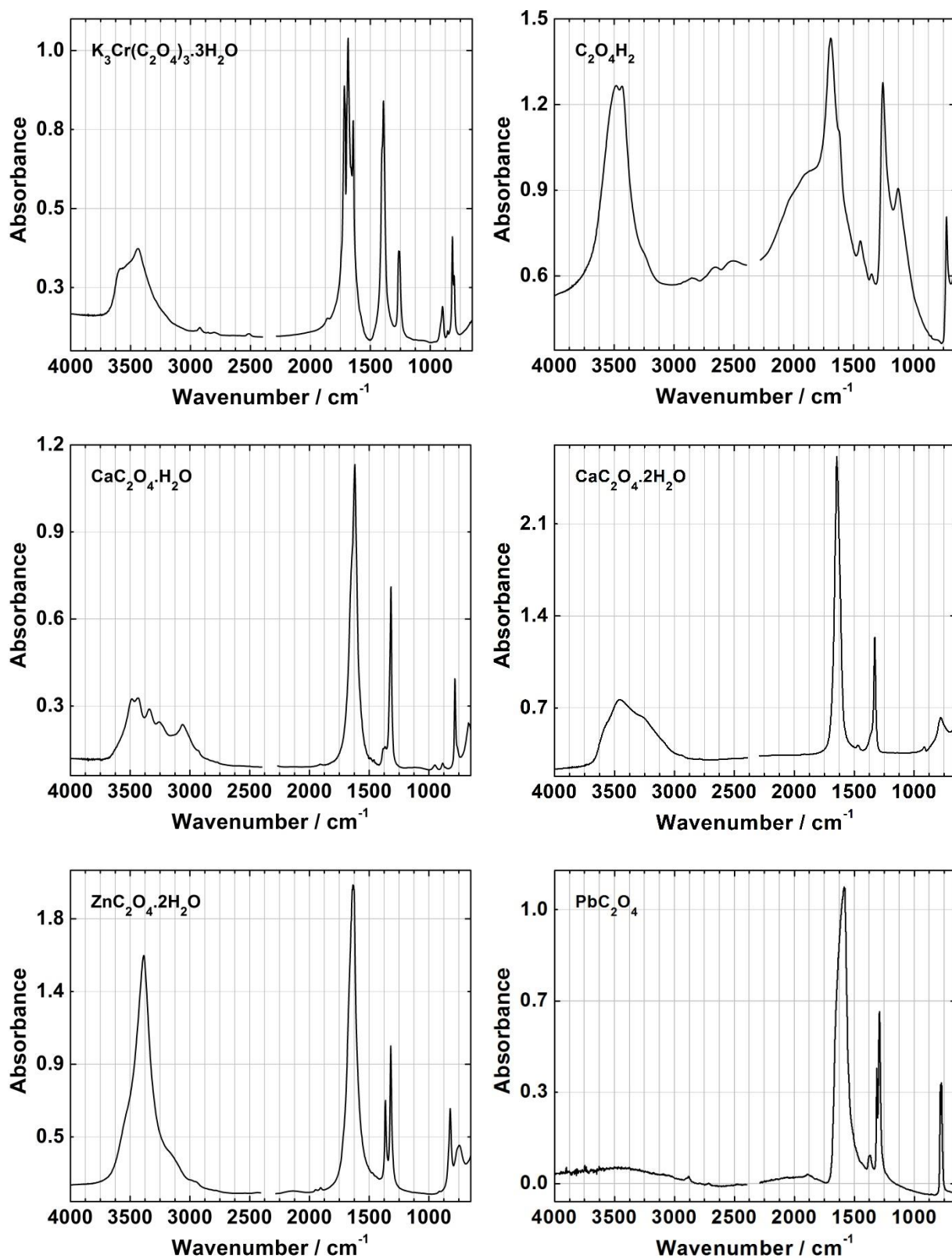


Figure VI.4.8. Infrared spectra of potassium chromium oxalate trihydrate ($\text{K}_3\text{Cr}(\text{C}_2\text{O}_4)_3 \cdot 3\text{H}_2\text{O}$); oxalic acid ($\text{C}_2\text{O}_4\text{H}_2$); calcium oxalate monohydrate ($\text{CaC}_2\text{O}_4 \cdot \text{H}_2\text{O}$); calcium oxalate dihydrate ($\text{CaC}_2\text{O}_4 \cdot 2\text{H}_2\text{O}$)¹⁶⁹; zinc oxalate dihydrate ($\text{ZnC}_2\text{O}_4 \cdot 2\text{H}_2\text{O}$), lead oxalate (PbC_2O_4).

¹⁶⁹ Spectrum kindly provided by Letizia Monico and Costanza Miliani (Monico *et al.*, 2013c).

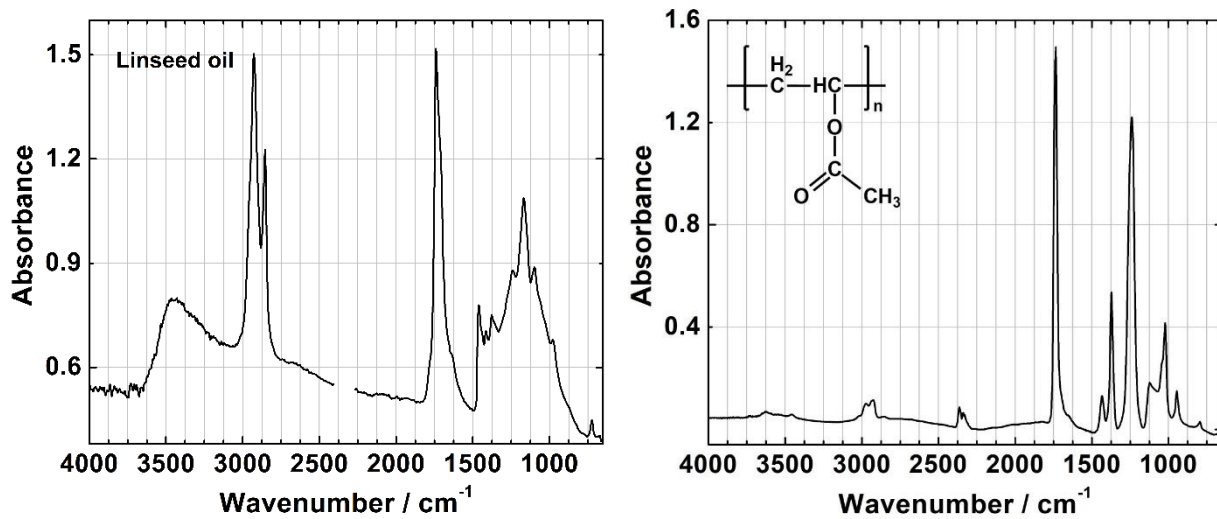


Figure VI.4.9. Infrared spectra of linseed oil and poly(vinyl) acetate $\left[\text{CH}_2\text{CH}(\text{O}_2\text{CCH}_3) \right]_n$ ¹⁷⁰.

¹⁷⁰ Spectrum obtained by Joana Lia Ferreira (DCR FCT NOVA).

Table VI.4.1. Main characteristic infrared bands of the reference compounds (see Figures VI.4.1 to VI.4.9) (Hummel, 2002; Mayo *et al.*, 2004; Nakamoto, 2009)*.

Compound	Bands (cm ⁻¹)	Assignment	Compound	Bands (cm ⁻¹)	Assignment
Lead chromate PbCrO ₄ (monoclinic)	853/831/820	$\nu_{as}(\text{CrO}_4^{2-})$	Zinc nitrate Zn(NO ₃) ₂	1385, 1355 829	$\nu_{as}(\text{NO}_3^-)$ $\delta_{as}(\text{NO}_3^-)$
Lead chromate PbCrO ₄ (orthorhombic)	905/873/827/753	$\nu_{as}(\text{CrO}_4^{2-})$	Lead subacetate Pb(Ac) ₂ ·2Pb(OH) ₂	3508,3423	$\nu(\text{OH})$
Basic lead chromate Pb ₂ CrO ₅	852	$\nu_{as}(\text{CrO}_4^{2-})$		1564	$\nu_{as}(\text{COO}^-)$
Lead sulfate PbSO ₄	1163, 1059	$\nu_{as}(\text{SO}_4^{2-})$		1409	$\delta(\text{CH}_2)$
	965	$\nu_s(\text{SO}_4^{2-})$		1340	$\nu_s(\text{COO}^-)$
Barium sulfate BaSO ₄	626, 599	$\delta_{as}(\text{SO}_4^{2-})$	1016	$\delta(\text{CH}_2)$	
	1186, 1120, 1085	$\nu_{as}(\text{SO}_4^{2-})$	929	$\delta(\text{CH}_3)$	
	984	$\nu_s(\text{SO}_4^{2-})$	Strontium nitrate Sr(NO ₃) ₂	1438, 1384	$\nu_{as}(\text{NO}_3^-)$
637, 611	$\delta_{as}(\text{SO}_4^{2-})$	815, 737		$\delta_{as}(\text{NO}_3^-)$	
Lead carbonate PbCO ₃	1405	$\nu_{as}(\text{CO}_3^{2-})$	Sodium carbonate Na ₂ CO ₃	1430	$\nu_{as}(\text{CO}_3^{2-})$
	1051	$\nu_s(\text{CO}_3^{2-})$	882, 702	$\delta_{as}(\text{CO}_3^{2-})$	
	837, 679	$\delta_{as}(\text{CO}_3^{2-})$	Potassium carbonate K ₂ CO ₃	1456, 1375	$\nu_{as}(\text{CO}_3^{2-})$
Lead white 2PbCO ₃ ·Pb(OH) ₂	3535	$\nu(\text{OH})$	Ammonium carbonate (NH ₄) ₂ CO ₃	1060	$\nu_s(\text{CO}_3^{2-})$
	1405	$\nu_{as}(\text{CO}_3^{2-})$		883, 706	$\delta_{as}(\text{CO}_3^{2-})$
	1045	$\nu_s(\text{CO}_3^{2-})$		3187-2857	$\nu(\text{NH})$
	681	$\delta_{as}(\text{CO}_3^{2-})$		1600	$\delta(\text{NH})$
Calcium carbonate CaCO ₃	1422	$\nu_{as}(\text{CO}_3^{2-})$	1490, 1444, 1368	$\nu_{as}(\text{CO}_3^{2-})$	
	875, 712	$\delta_{as}(\text{CO}_3^{2-})$	1267	$\delta_{as}(\text{CO}_3^{2-})$	
Magnesium carbonate MgCO ₃ ·xH ₂ O	3648, 3511, 3447	$\nu(\text{OH})$	Sodium sulfate Na ₂ SO ₄	1116	$\nu_{as}(\text{SO}_4^{2-})$
	1483, 1420	$\nu_{as}(\text{CO}_3^{2-})$		617	$\delta_{as}(\text{SO}_4^{2-})$
Calcium sulfate anhydrous (CaSO ₄)	854, 797	$\delta_{as}(\text{CO}_3^{2-})$	Zinc sulfate heptahydrate	3320	$\nu(\text{OH})$
	1155, 1121	$\nu_{as}(\text{SO}_4^{2-})$	1647	$\delta(\text{H}_2\text{O})$	
Calcium sulfate hemihydrate CaSO ₄ ·½H ₂ O	673, 616, 595	$\delta_{as}(\text{SO}_4^{2-})$	ZnSO ₄ ·7H ₂ O	1090	$\nu_{as}(\text{SO}_4^{2-})$
	3606, 3545, 3490	$\nu(\text{OH})$	Magnesium sulfate heptahydrate MgSO ₄ ·7H ₂ O	3316	$\nu(\text{OH})$
1624	$\delta(\text{H}_2\text{O})$	1675		$\delta(\text{H}_2\text{O})$	
Calcium sulfate dihydrate CaSO ₄ ·2H ₂ O	1150, 1096 sh	$\nu_{as}(\text{SO}_4^{2-})$	1147, 1076	$\nu_{as}(\text{SO}_4^{2-})$	
	659, 601	$\delta_{as}(\text{SO}_4^{2-})$	984	$\delta_{as}(\text{SO}_4^{2-})$	
Lead nitrate Pb(NO ₃) ₂	3545, 3405	$\nu(\text{OH})$	Kaolin Al ₂ Si ₂ O ₅ (OH) ₄	3695, 3622	$\nu(\text{OH})$
	1684, 1621	$\delta(\text{H}_2\text{O})$		1117, 1036, 1010	$\nu_{as}(\text{Si-O-Si})$
	1140, 1122	$\nu_{as}(\text{SO}_4^{2-})$	Cobalt yellow K ₃ Co(NO ₂) ₆ ·3H ₂ O	914	$\nu(\text{Al-O-H})$
669, 604	$\delta_{as}(\text{SO}_4^{2-})$	2705, 2649		$\nu_{as}(\text{NO}_2)$	
Lead acetate trihydrate Pb(CH ₃ CO ₂) ₂ ·3H ₂ O	1384	$\nu_{as}(\text{NO}_3^-)$		1390	$\nu_{as}(\text{NO}_2)$
	833, 722	$\delta_{as}(\text{NO}_3^-)$	1330	$\nu_s(\text{NO}_2)$	
Lead acetate trihydrate Pb(CH ₃ CO ₂) ₂ ·3H ₂ O	3367	$\nu(\text{OH})$	829	$\delta(\text{ONO})$	
	1532	$\nu_{as}(\text{COO}^-)$	Prussian blue Fe ₄ [Fe(CN) ₆] ₃	2088	$\nu(\text{CN})$
	1416, 1407	$\delta(\text{CH}_2)$		Ultramarine blue 3Na ₂ O·3Al ₂ O ₃ ·6SiO ₂ ·2Na ₂ S	1013
	1348, 1333	$\nu_s(\text{COO}^-)$	696		$\delta(\text{Si-O})$
	1047, 1029, 1014	$\delta(\text{CH}_2)$	Emerald green Cu(C ₂ H ₃ O ₂) ₂ ·3Cu(AsO ₂) ₂		1558
932	$\delta(\text{CH}_3)$	1453		$\delta(\text{CH}_2)$	
			819, 769	$\nu(\text{As-O})$	

Table VI.4.1. (continued).

Compound	Bands (cm ⁻¹)	Assignment	Compound	Bands (cm ⁻¹)	Assignment
Viridian ¹⁷¹ Cr ₂ O ₃ ·2H ₂ O	3406, 3130, 2835 1063 793	v(OH)	Lead azelate	2930, 2853 1513 1443 1406	v(CH) v _{as} (COO ⁻) δ(CH ₂) v _s (COO ⁻)
Chromium (III) oxide Cr ₂ O ₃	650	v(CrO)			
Chromium (VI) oxide CrO ₃	960/944/907	v _{as} (CrO ₃)	Zinc linoleate	3007 2954, 2920, 2850 1547, 1527 1465, 1455 1404	v(C=C-H) v(CH) v _{as} (COO ⁻) δ(CH ₂) v _s (COO ⁻)
Potassium chromate K ₂ CrO ₄	888/852	v _{as} (CrO ₄ ²⁻)			
Potassium dichromate K ₂ Cr ₂ O ₇	950/924 902/885	v _{as} (CrO ₃) v _s (CrO ₃)	Potassium chromium oxalate trihydrate K ₃ Cr(C ₂ O ₄) ₃ ·3H ₂ O	3438 1717, 1686, 1644 1391, 1263 898, 815	v(OH) v _{as} (COO ⁻) v _s (COO ⁻) δ(COO ⁻)
Sodium chromate Na ₂ CrO ₄ ·xH ₂ O	796/763 3550, 3474, 3412	v _{as} (CrOCr) v(OH)	Oxalic acid C ₂ O ₄ H ₂	1690 1257 1127 724	v(C=O) δ(COH) v(CO) δ(COO)
Sodium dichromate Na ₂ Cr ₂ O ₇ ·xH ₂ O	1637, 1617 944/888/858 3549, 3474, 3414	δ(H ₂ O) v _{as} (CrO ₄ ²⁻) v(OH)			
Chromium acetylacetonate Cr(C ₅ H ₇ O ₂) ₃	1637, 1617 957/936 904/886	δ(H ₂ O) v _{as} (CrO ₃) v _s (CrO ₃)	Calcium oxalate monohydrate CaC ₂ O ₄ ·H ₂ O	3484-3061 1620 1318 782	v(OH) v _{as} (COO ⁻) v _s (COO ⁻) δ(COO ⁻)
			801/774 1575 1521 1383 1278	v _{as} (CrOCr) v _s (CO) _{ring} v _{as} (CC) _{ring} δ(CH ₃) v _s (CC) _{ring}	Calcium oxalate dihydrate CaC ₂ O ₄ ·2H ₂ O
Chromium acetate hydroxide (CH ₃ CO ₂) ₇ Cr ₃ (OH) ₂	3423 1616 1455 1354	v(OH) v _{as} (COO ⁻) δ(CH ₂) v _s (COO ⁻)	Zinc oxalate dihydrate ZnC ₂ O ₄ ·2H ₂ O	3385 1634 1364, 1320 822	v(OH) v _{as} (COO ⁻) v _s (COO ⁻) δ(COO ⁻)
Chromium sulfate Cr ₂ (SO ₄) ₃	1049 676 1248 sh, 1080 995	δ(CH ₂) δ(COO ⁻) v _{as} (SO ₄ ²⁻) v _s (SO ₄ ²⁻)	Lead oxalate PbC ₂ O ₄	1588 1312, 1290 782, 773	v _{as} (COO ⁻) v _s (COO ⁻) δ(COO ⁻)
			3374, 2922 1097	v(OH) v _{as} (SO ₄ ²⁻)	Linseed oil
Chromium potassium sulfate dodecahydrate CrK(SO ₄) ₂ ·12H ₂ O	692, 615	δ _{as} (SO ₄ ²⁻)	Poly(vinyl) acetate [CH ₂ CH(O ₂ CCH ₃)] _n	2974 2927 1738 1373 1242	v(CH ₃) v(CH ₂) v(C=O) δ(CH ₃) v(C=O-O-C)
Lead palmitate	2955, 2919, 2850 1538 sh, 1513 1461 1418	v(CH) v _{as} (COO ⁻) δ(CH ₂) v _s (COO ⁻)			

* v = stretching, δ = bending, as = asymmetric, s = symmetric, sh (shoulder).

¹⁷¹ Zumbuehl *et al.* (2009) suggest that the infrared bands at 1252 and 1286 cm⁻¹ are due to the presence of a chromium borate (Cr₃BO₆), which forms during the viridian manufacture by calcination.

VI.5. μ -XANES spectra

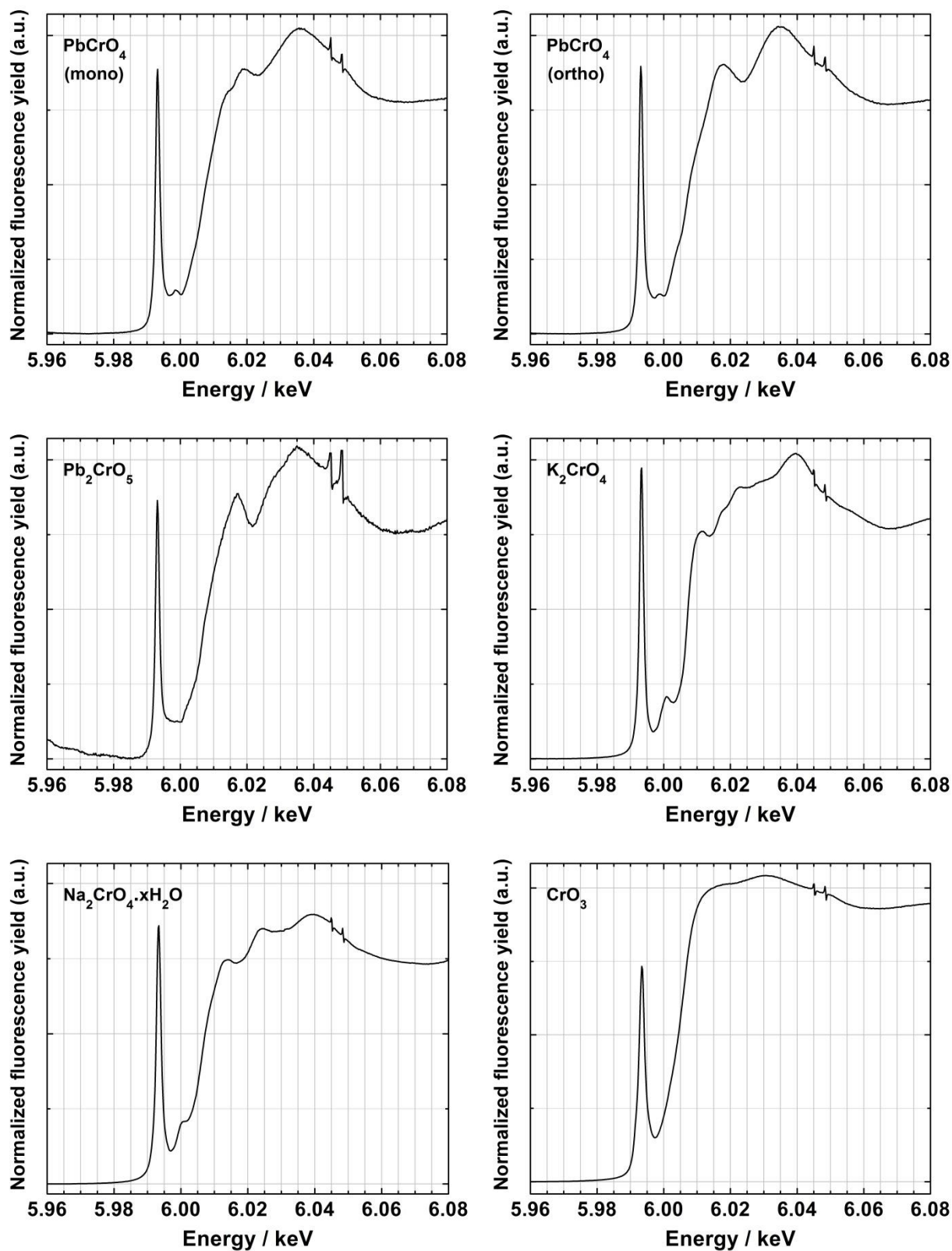


Figure VI.5.1. Cr K-edge μ -XANES spectra of Cr^{6+} reference compounds: lead chromate (PbCrO_4 , monoclinic crystal structure); lead chromate (PbCrO_4 , orthorhombic crystal structure); basic lead chromate (Pb_2CrO_5), potassium chromate (K_2CrO_4); sodium chromate ($\text{Na}_2\text{CrO}_4 \cdot x\text{H}_2\text{O}$) and chromium (VI) oxide (CrO_3).

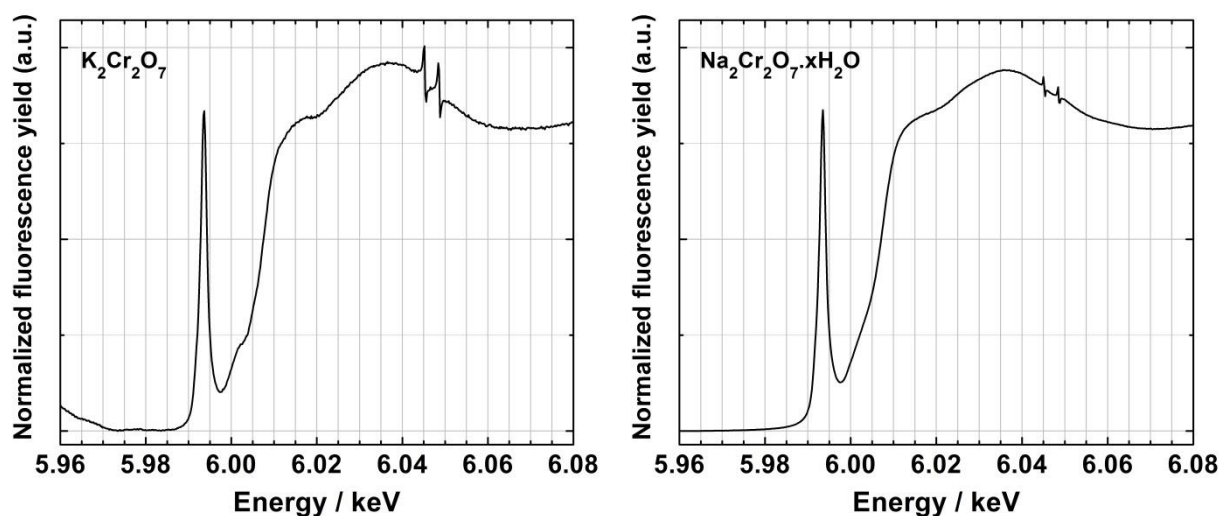


Figure VI.5.2. Cr K-edge μ -XANES spectra of Cr^{6+} reference compounds: potassium dichromate ($\text{K}_2\text{Cr}_2\text{O}_7$) and sodium dichromate ($\text{Na}_2\text{Cr}_2\text{O}_7 \cdot x\text{H}_2\text{O}$).

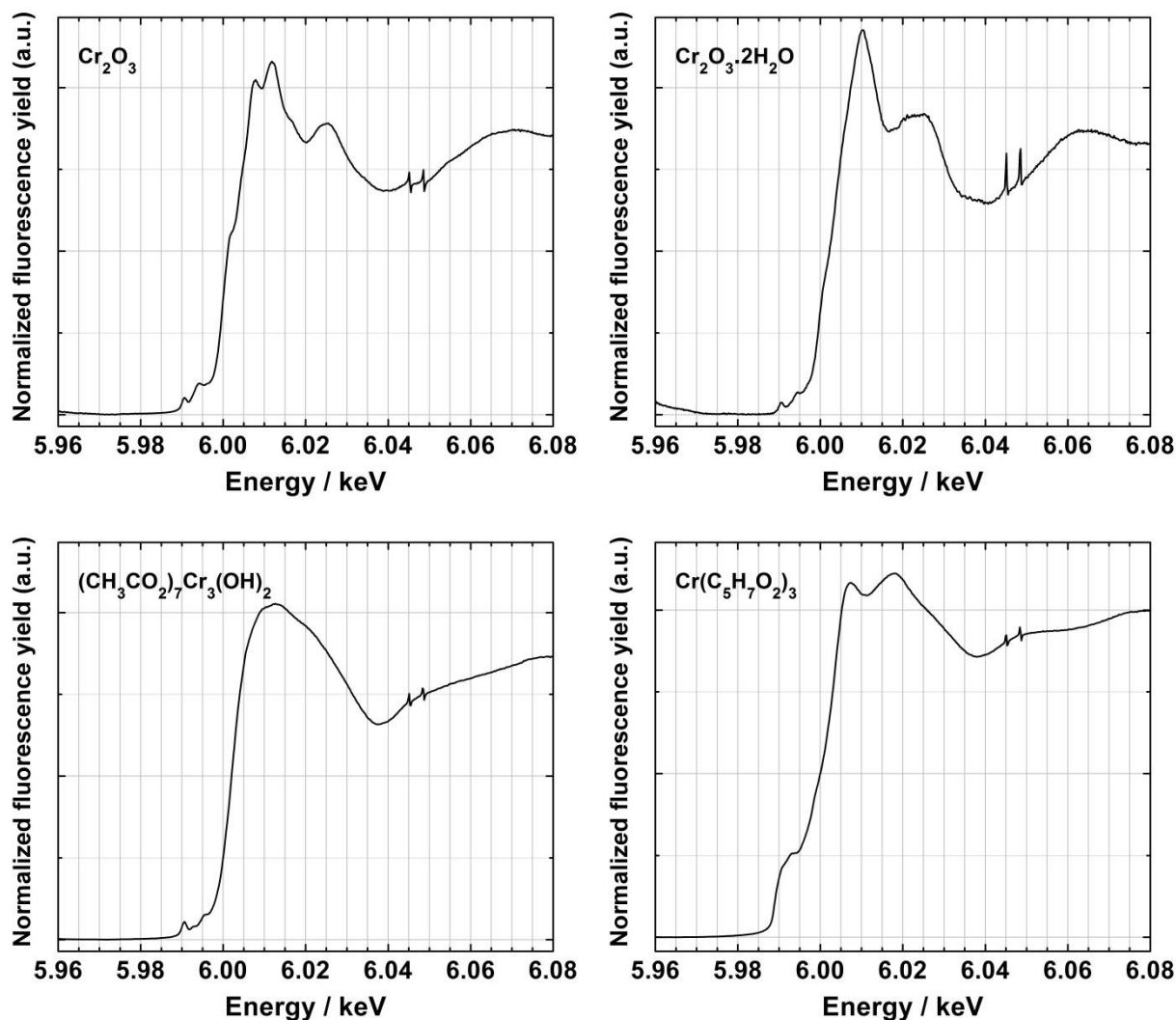


Figure VI.5.3. Cr K-edge μ -XANES spectra of Cr^{3+} reference compounds: chromium (III) oxide (Cr_2O_3); viridian ($\text{Cr}_2\text{O}_3 \cdot 2\text{H}_2\text{O}$); chromium acetate hydroxide ($(\text{CH}_3\text{CO}_2)_7\text{Cr}_3(\text{OH})_2$) and chromium acetylacetonate ($\text{Cr}(\text{C}_5\text{H}_7\text{O}_2)_3$).

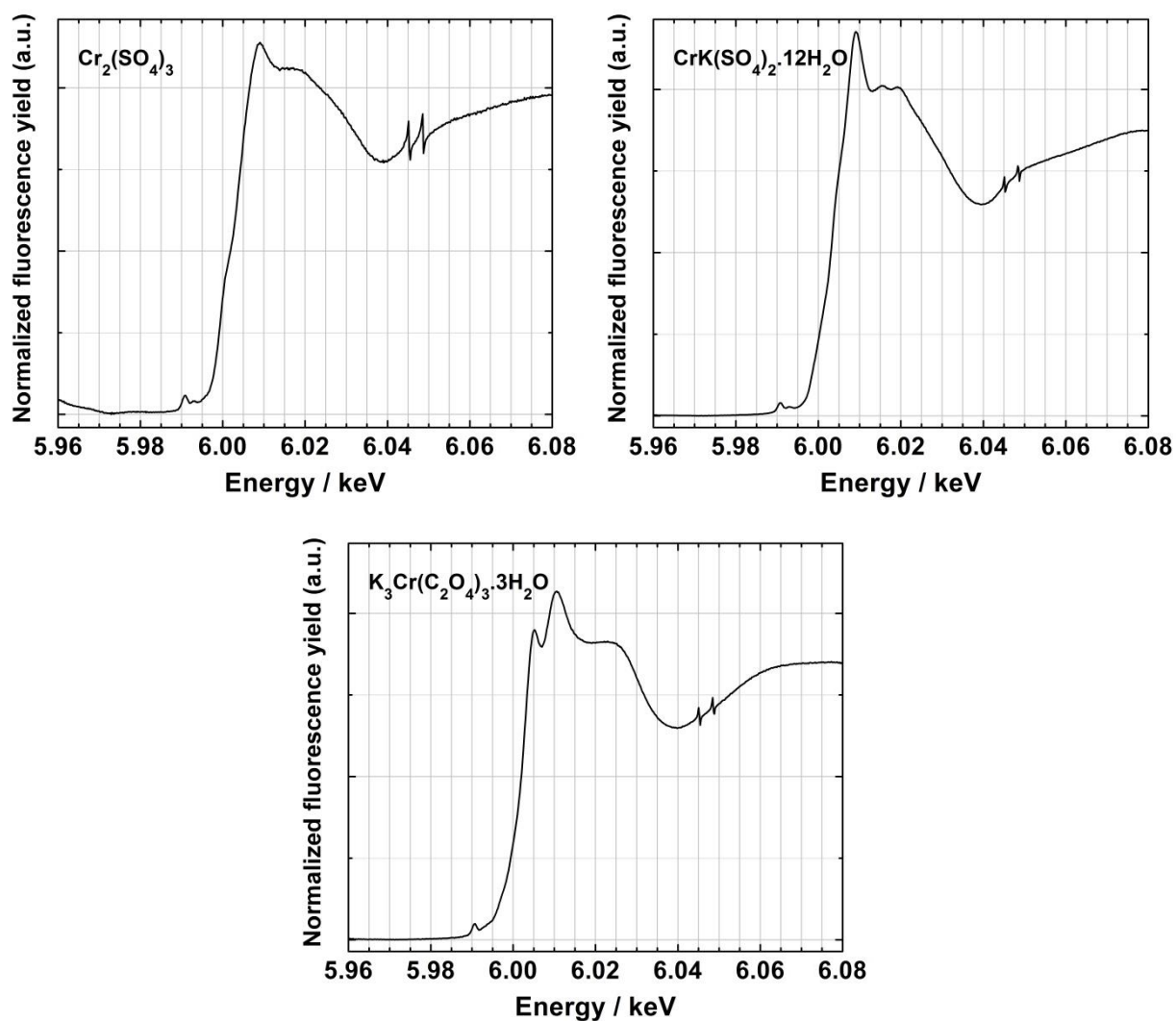


Figure VI.5.4. Cr K-edge μ -XANES spectra of Cr^{3+} reference compounds: chromium sulfate ($\text{Cr}_2(\text{SO}_4)_3$); chromium potassium sulfate dodecahydrate ($\text{CrK}(\text{SO}_4)_2 \cdot 12\text{H}_2\text{O}$) and potassium chromium oxalate trihydrate ($\text{K}_3\text{Cr}(\text{C}_2\text{O}_4)_3 \cdot 3\text{H}_2\text{O}$).

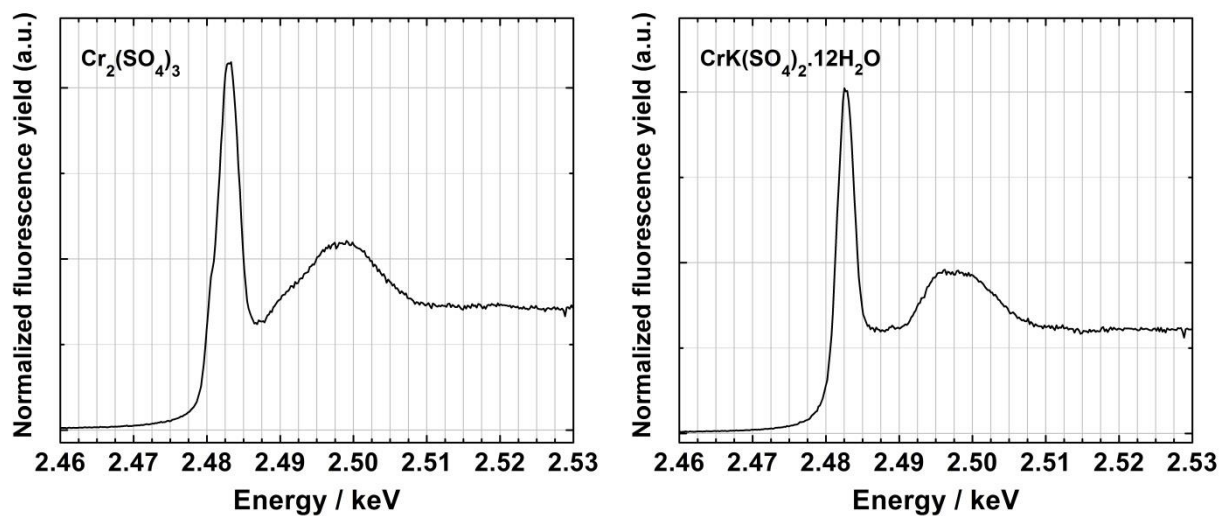


Figure VI.5.5. S K-edge μ -XANES spectra of chromium sulfate ($\text{Cr}_2(\text{SO}_4)_3$) and chromium potassium sulfate dodecahydrate ($\text{CrK}(\text{SO}_4)_2 \cdot 12\text{H}_2\text{O}$).

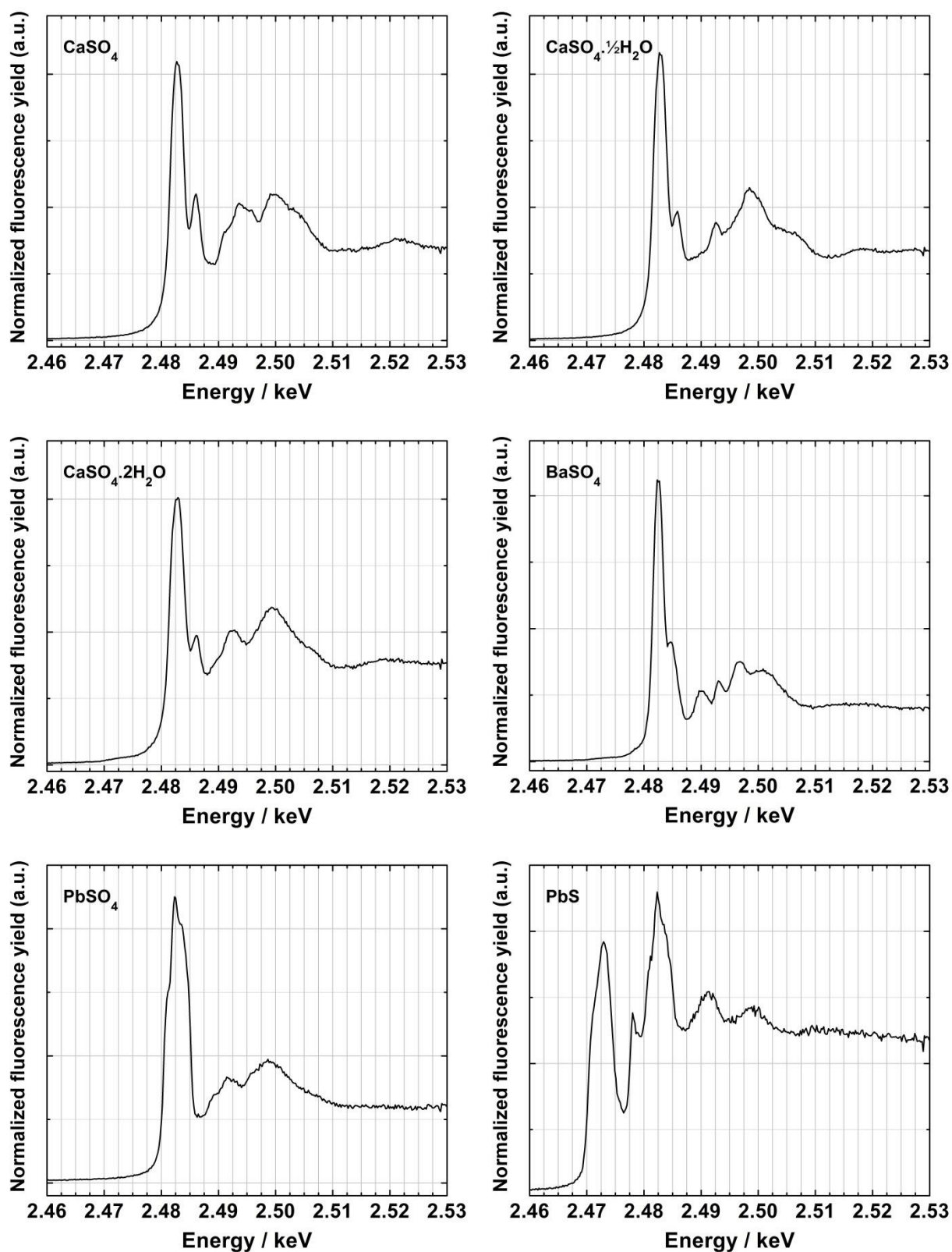


Figure VI.5.6. S K-edge μ -XANES spectra of calcium sulfate (CaSO_4); calcium sulfate hemihydrate ($\text{CaSO}_4 \cdot \frac{1}{2}\text{H}_2\text{O}$); calcium sulfate dihydrate ($\text{CaSO}_4 \cdot 2\text{H}_2\text{O}$); barium sulfate (BaSO_4); lead sulfate (PbSO_4) and lead sulfide (PbS).

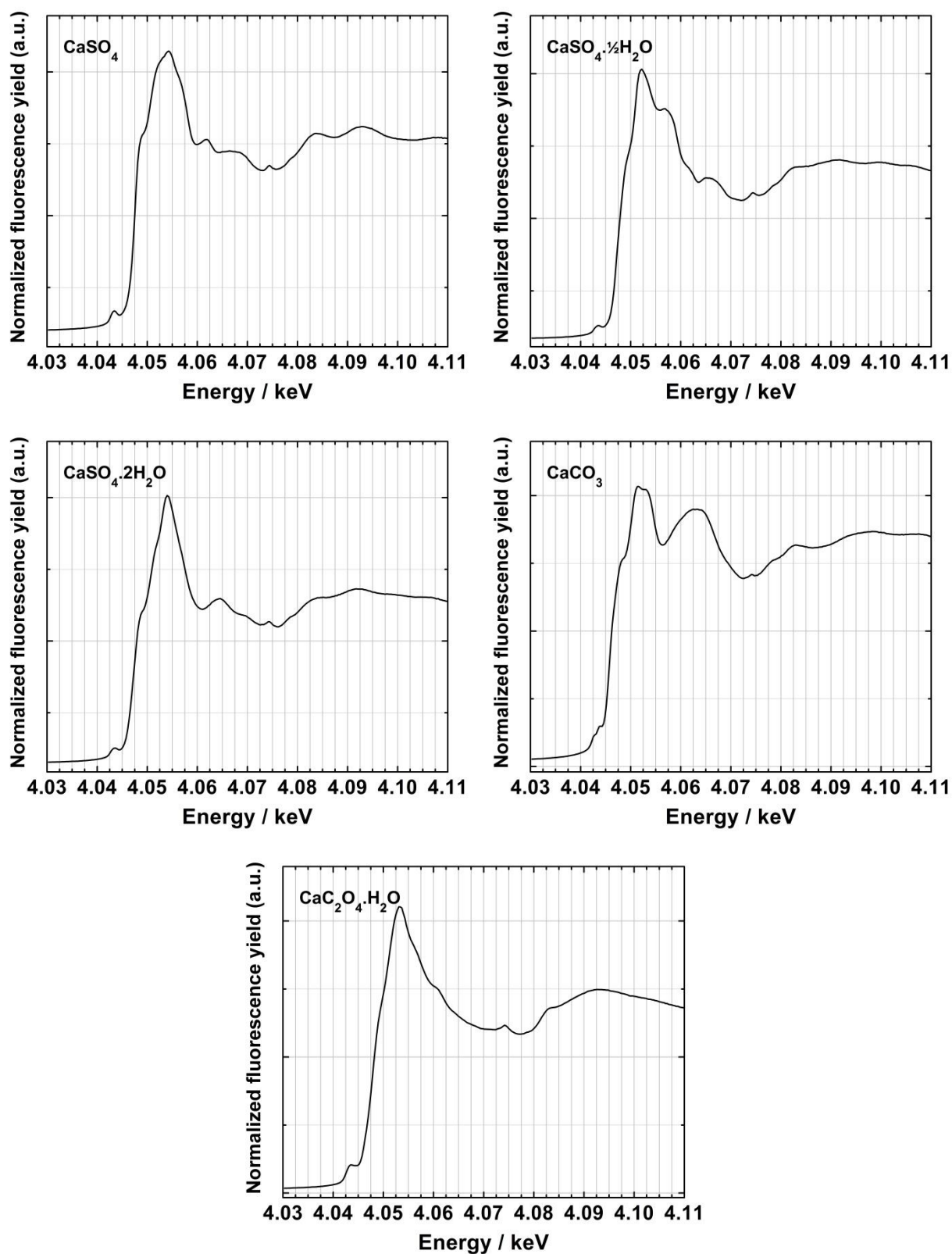


Figure VI.5.7. Ca K-edge μ -XANES spectra of calcium sulfate (CaSO₄); calcium sulfate hemihydrate (CaSO₄·½H₂O); calcium sulfate dihydrate (CaSO₄·2H₂O); calcium carbonate (CaCO₃) and calcium oxalate monohydrate (CaC₂O₄·H₂O).

Appendix VII. Characterisation of the synthesised lead nitrate and subacetate

The lead sources used in the production of lead chromate pigments, namely lead nitrate ($\text{Pb}(\text{NO}_3)_2$) and lead subacetate ($\text{Pb}(\text{Ac})_2 \cdot 2\text{Pb}(\text{OH})_2$) were synthesised in accordance to W&N 19th century manufacturing processes (see transcriptions in Appendix II.3.1 (p. 187) and synthesis methods in Appendix V.2.1.1 (p. 233). Their characterisation was carried out in order to verify their composition. As may be seen in Figure VII.1A, the infrared spectrum of the synthesised lead nitrate matches the one of the reference, with an additional band at 3500 cm^{-1} , probably due to some hydration. Lead subacetate had to be characterised by μ -FTIR and XRD since its correct synthesis was not straightforward, influencing the composition of the final lead chromate product, occasionally leading to the formation of the less stable orthorhombic lead chromate. The infrared spectra of the 'correct' and 'wrong' lead subacetate are very similar (Figure VII.1B), matching with its reference (Figure VI.3.3), however their crystallinity is different as shown by their diffraction patterns in Figure VII.1C and D. For a correct synthesis of the lead subacetate and thus of the monoclinic lead chromate pigments, it is necessary that it does not fully crystallise, being in solution in adequate quantities.

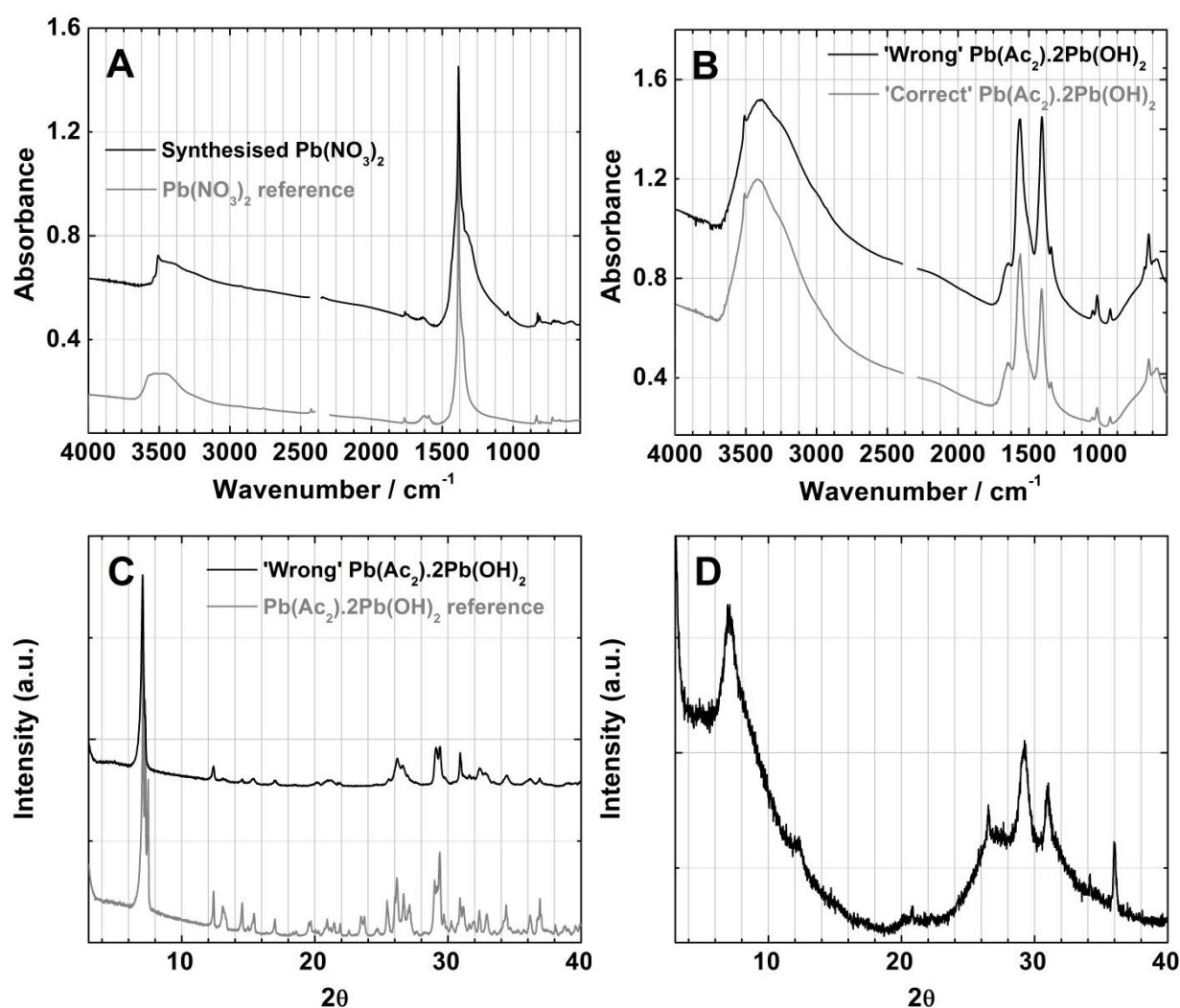


Figure VII.1. Infrared spectra of **A)** lead nitrate (synthesised and reference) and **B)** lead subacetate ('correct' and 'wrong'). Diffraction patterns of the lead subacetate **C)** 'wrong' and reference, and **D)** 'correct'.

Appendix VIII. Characterisation of references for $\text{PbCr}_{1-x}\text{S}_x\text{O}_4$

To fingerprint the effect of sulfate ions on the vibrational spectra and crystal structure of $\text{PbCr}_{1-x}\text{S}_x\text{O}_4$ mixed crystals and mixed-phase crystals, a set of references with increasing x values (x = molar fraction) was prepared following the essential steps and starting materials of W&N 19th century lead chromate manufacturing process. An aqueous solution of lead nitrate (0.4 M) was added to an aqueous solution containing the chromate and sulfate compounds, always under agitation. The latter compounds were added in the quantities shown in Table VIII.1, dissolved in 25 ml of water and then added to 50 ml of water. Pigment precipitation always occurred under acidic conditions (Table VIII.2). All pigments were thoroughly washed, dried and then ground to a powder.

Table VIII.1. Reference codes and quantities of the starting materials for the synthesis of $\text{PbCr}_{1-x}\text{S}_x\text{O}_4$ crystals with variable sulfate to chromate ratio.

Reference Code	$\text{K}_2\text{Cr}_2\text{O}_7$		Na_2SO_4		$\text{Pb}(\text{NO}_3)_2$	
	by mol	by wt.(g)	by mol	by wt.(g)	by mol	by wt.(g)
CY1	0.005	1.471	-	-		
CY2	0.0045	1.324	0.0005	0.071		
CY3	0.004	1.177	0.001	0.142		
CY4	0.0035	1.030	0.0015	0.213		
CY5	0.003	0.883	0.002	0.284		
CY6	0.0025	0.735	0.0025	0.355	0.01	3.312
CY7	0.002	0.588	0.003	0.426		
CY8	0.0015	0.441	0.0035	0.497		
CY9	0.001	0.294	0.004	0.568		
CY10	0.0005	0.147	0.0045	0.639		
CY11	-	-	0.005	0.710		

As the SO_4^{2-} molar fraction increased, pigments with lighter shades of yellow were obtained, as shown by their colourimetric values in Table VIII.2. It is possible to observe an increase in the L^* coordinate and a decrease of the a^* coordinate resulting in less red colour.

All pigments were also characterised by μ -FTIR, μ -Raman and XRD. Infrared and Raman spectra are presented in Figures VIII.2 to VIII.5 and the characteristic band assignments may be consulted in Table VIII.3. The diffraction patterns are shown in Figure VIII.6 to VIII.9. All techniques clearly detect the presence of $\text{PbCr}_{1-x}\text{S}_x\text{O}_4$. The semi-quantitative composition obtained is shown in Table VIII.2.

With XRD, as demonstrated by Crane *et al.*, it is observed that as the content of sulfate ions is higher, there is a progressive shift of the monoclinic lead chromate diffraction peaks to higher values, which saturates when the SO_4^{2-} molar fraction is 0.4. The detection of the diffraction peaks of the orthorhombic lead sulfate, shifted to lower values, occurs when the SO_4^{2-} molar fraction is around 0.5. Between SO_4^{2-} molar fractions of 0.5 to 0.8, the diffraction patterns present both phases (mixed-phase crystals) and as the content of sulfate ions is higher, the diffraction peaks of the monoclinic lead chromate disappear and those of the orthorhombic lead sulfate become stronger and less shifted.

When the SO_4^{2-} molar fraction is higher than 0.9, only the diffraction peaks of the orthorhombic lead sulfate are detected (Crane *et al.*, 2001; Monico *et al.*, 2013a).

By μ -Raman, the main differences appear in the $\delta(\text{CrO}_4^{2-})$ peaks profile, which significantly changes when the SO_4^{2-} molar fraction is higher than 0.6. Also, at this point, the $\delta(\text{SO}_4^{2-})$ peaks start to appear. Furthermore, as the content of sulfate anions increases, the $\nu_{\text{as}}(\text{CrO}_4^{2-})$ peak presents a slight shift from 839 to 843 cm^{-1} and the $\nu_{\text{as}}(\text{SO}_4^{2-})$ peak presents a gradual shift from 968 to 976 cm^{-1} (see also Monico *et al.*, 2014a).

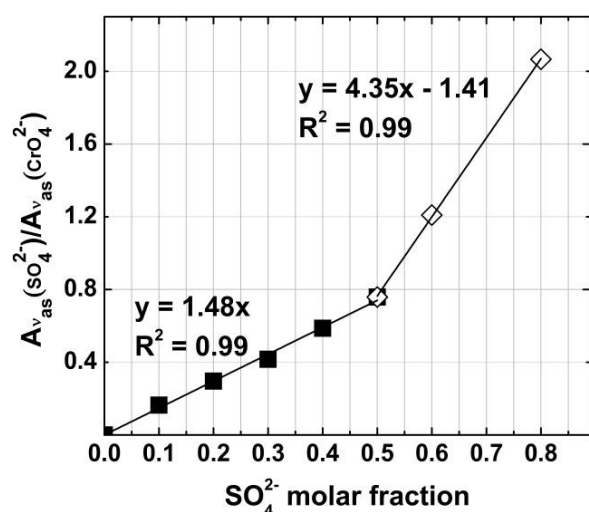


Figure VIII.1. Variation of the $A_{\nu_{\text{as}}(\text{SO}_4^{2-})}/A_{\nu_{\text{as}}(\text{CrO}_4^{2-})}$ as a function of the SO_4^{2-} molar fraction. The ratio was calculated using the absorbance of $\nu_{\text{as}}(\text{SO}_4^{2-})$ at 1100 cm^{-1} normalized to the $\nu_{\text{as}}(\text{CrO}_4^{2-})$ at 853 cm^{-1} after baseline correction.

By μ -FTIR, identifying the higher content of sulfate ions is straightforward due to a shift and change of the $\nu_{\text{as}}(\text{CrO}_4^{2-})$ of the pure lead chromate and $\nu_{\text{as}}(\text{SO}_4^{2-})$ of the pure lead sulfate peaks profile. It was possible to construct μ -FTIR calibration curves of the sulfate ions content in the $\text{PbCr}_{1-x}\text{S}_x\text{O}_4$ crystals by plotting the ratio $A_{\nu_{\text{as}}(\text{SO}_4^{2-})}/A_{\nu_{\text{as}}(\text{CrO}_4^{2-})}$ against the SO_4^{2-} molar fraction, Table VIII.3 and Figure VIII.1. There is a calibration curve for pigments with SO_4^{2-} molar fraction ≤ 0.5 (with a ratio $A_{\nu_{\text{as}}(\text{SO}_4^{2-})}/A_{\nu_{\text{as}}(\text{CrO}_4^{2-})} < 1$) and another one for those with a higher content of SO_4^{2-} . This enabled the semi-quantification of the reconstructed pigments composed of $\text{PbCr}_{1-x}\text{S}_x\text{O}_4$ crystals.

Table VIII.2. Semi-quantitative composition (determined by complementary analysis of XRD and μ -FTIR data), final pH and $L^*a^*b^*$ coordinates of the synthesised $\text{PbCr}_{1-x}\text{S}_x\text{O}_4$ crystals.

Code	General composition	Final pH	L^*	a^*	b^*
CY1	PbCrO_4	1.18	77.83 ± 0.05	21.20 ± 0.02	82.70 ± 0.18
CY2	$\text{PbCr}_{x>0.9}\text{S}_{x<0.1}\text{O}_4$	1.37	79.24 ± 0.63	17.94 ± 0.05	84.30 ± 0.30
CY3	$\text{PbCr}_{0.9}\text{S}_{0.1}\text{O}_4$	1.42	81.67 ± 0.03	14.69 ± 0.05	85.75 ± 0.16
CY4	$\text{PbCr}_{0.8}\text{S}_{0.2}\text{O}_4$	1.48	82.54 ± 0.03	10.80 ± 0.02	86.48 ± 0.31
CY5	$\text{PbCr}_{0.7}\text{S}_{0.3}\text{O}_4$	1.43	84.31 ± 0.08	7.78 ± 0.02	86.90 ± 0.25
CY6	$\text{PbCr}_{0.6}\text{S}_{0.4}\text{O}_4$	1.51	86.40 ± 0.02	6.58 ± 0.03	92.41 ± 0.08
CY7	$\text{PbCr}_{0.5}\text{S}_{0.5}\text{O}_4$	1.59	88.51 ± 0.03	5.34 ± 0.03	93.46 ± 0.13
CY8	$\text{PbCr}_{0.4}\text{S}_{0.6}\text{O}_4$	1.72	88.46 ± 0.11	5.38 ± 0.06	95.44 ± 0.07
CY9	$\text{PbCr}_{0.2}\text{S}_{0.8}\text{O}_4$	2.02	90.78 ± 0.05	-2.16 ± 0.04	81.42 ± 0.18
CY10	$\text{PbCr}_{0.1}\text{S}_{0.9}\text{O}_4$	2.18	93.04 ± 0.03	-5.70 ± 0.01	63.67 ± 0.06
CY11	PbSO_4	3.54	98.09 ± 0.06	-0.11 ± 0.01	0.60 ± 0.05

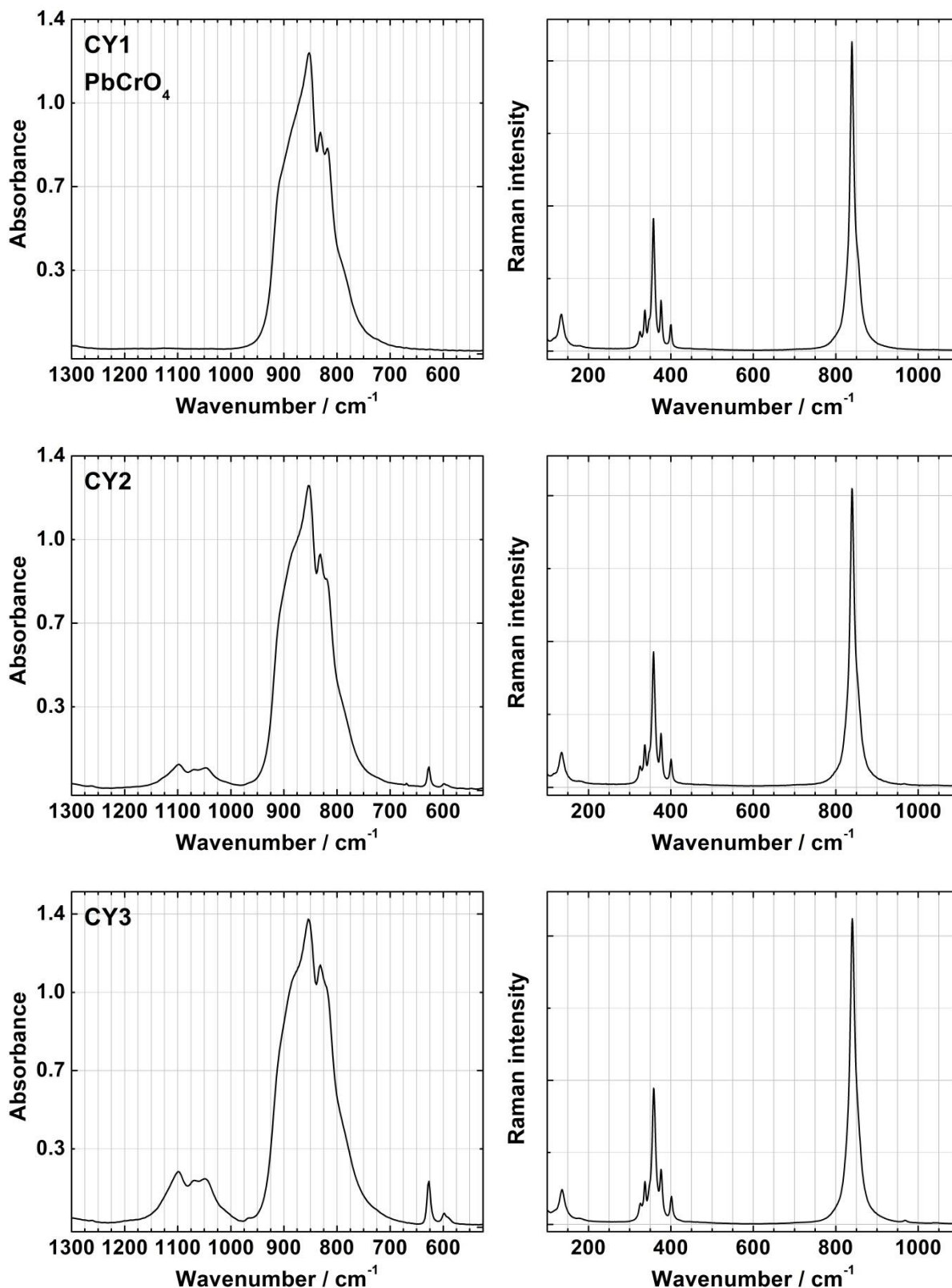


Figure VIII.2. Infrared (left) and Raman (right) spectra of CY1 (PbCrO₄), CY2 and CY3 pigment references.

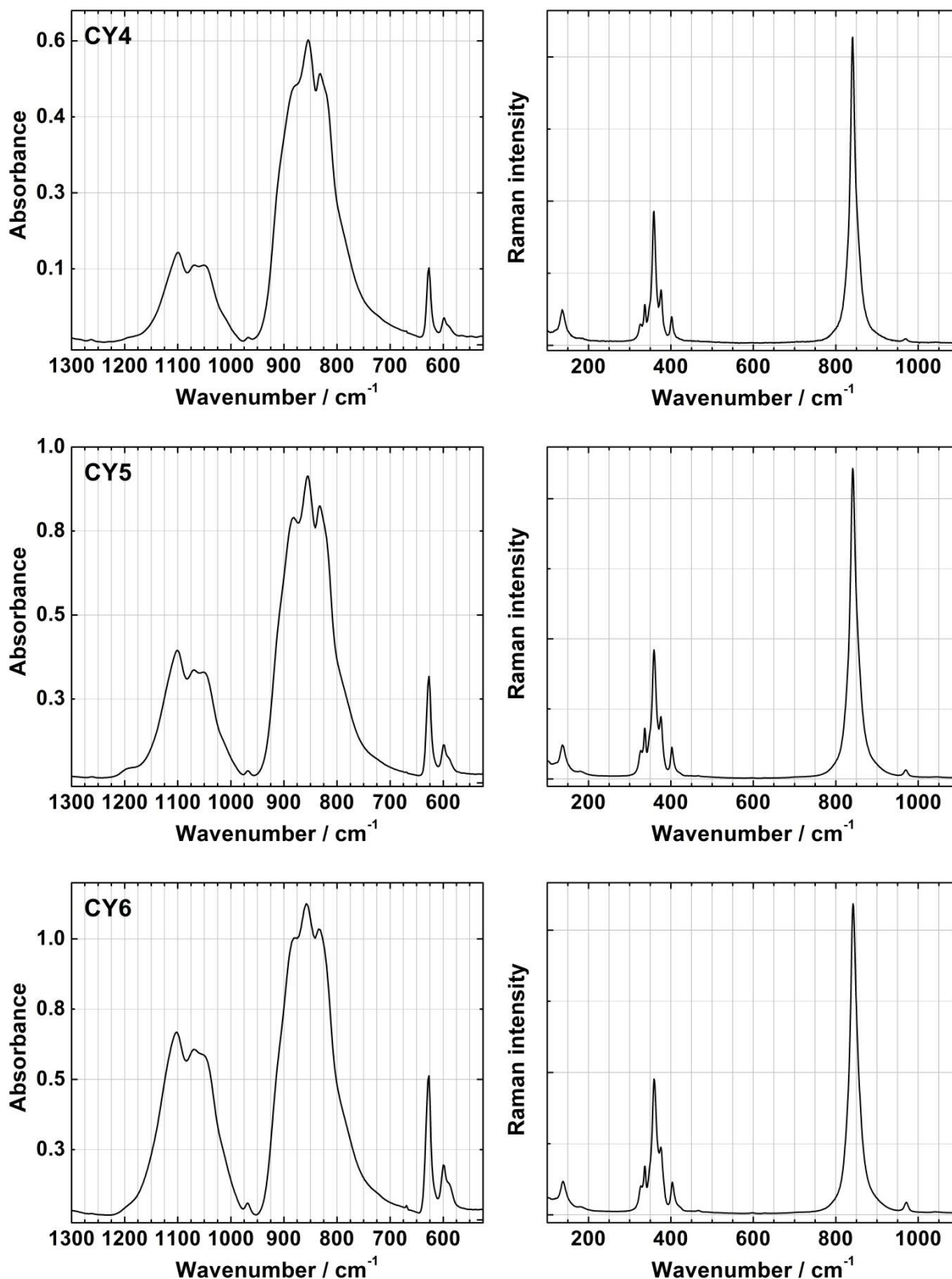


Figure VIII.3. Infrared (left) and Raman (right) spectra of CY4, CY5 and CY6 pigment references.

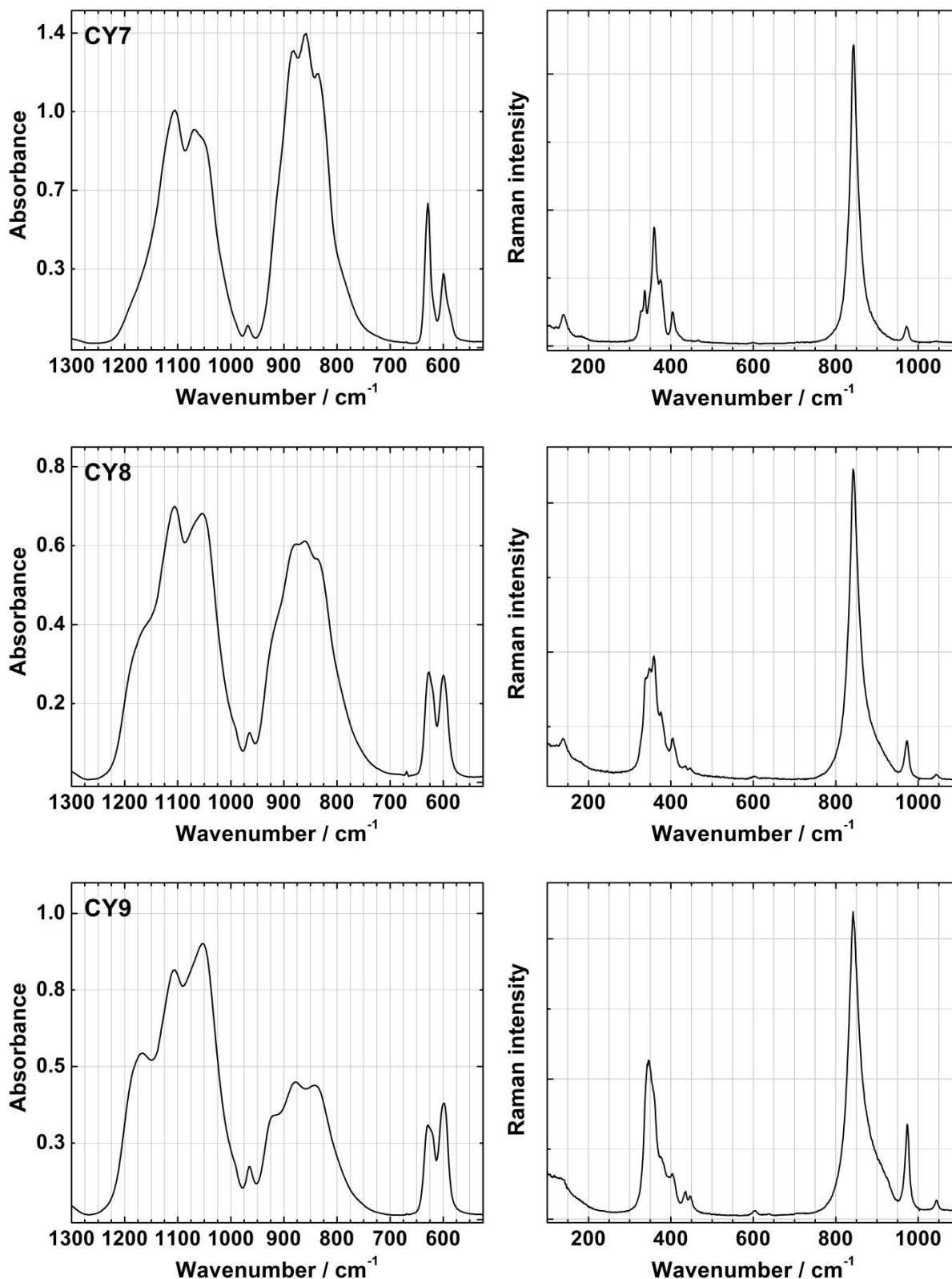


Figure VIII.4. Infrared (left) and Raman (right) spectra of CY7, CY8 and CY9 pigment references.

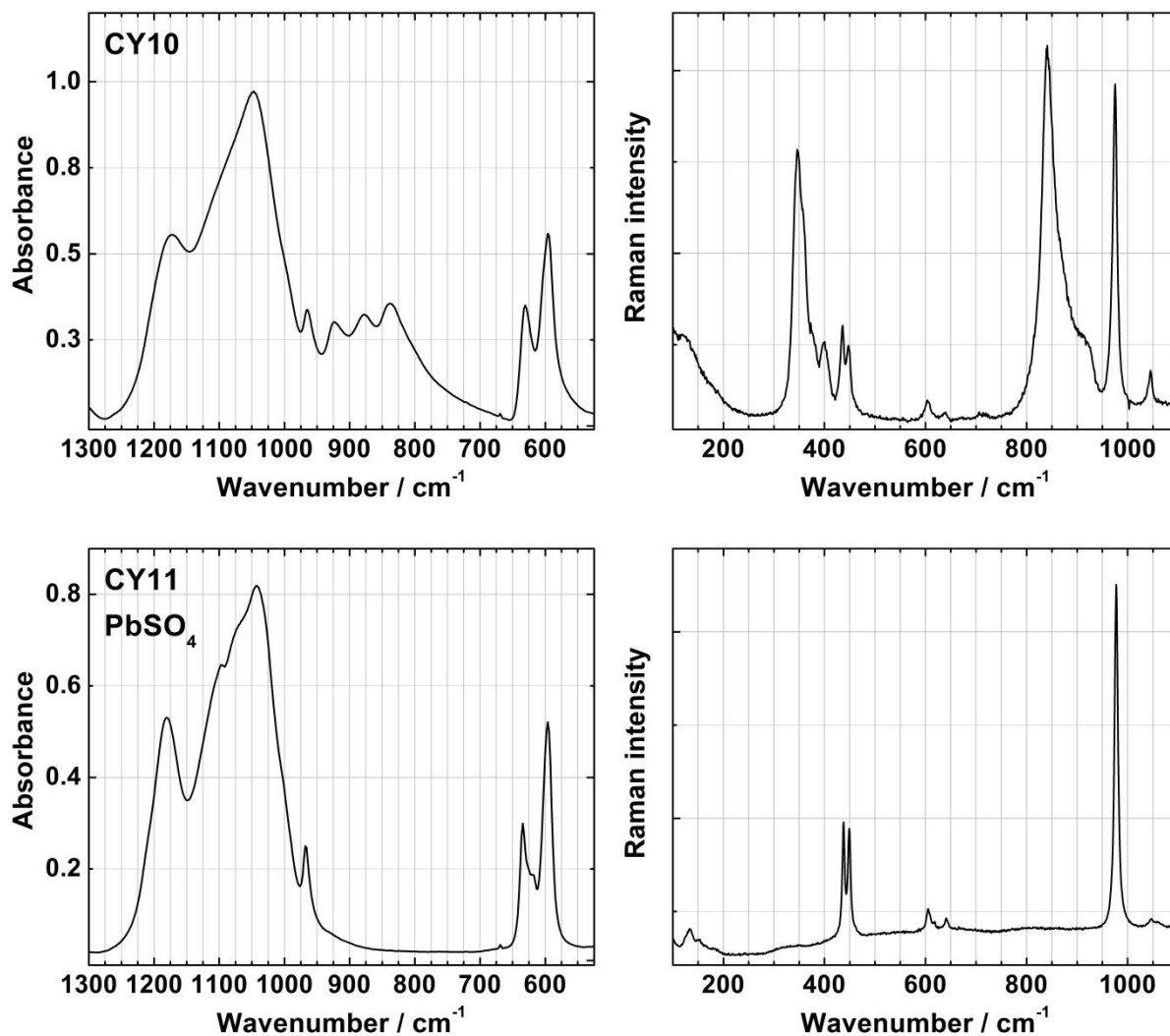


Figure VIII.5. Infrared (left) and Raman (right) spectra of CY10 and CY11 (PbSO₄) pigment references.

Table VIII.3. Characteristic infrared and Raman bands of the synthesised references of $\text{PbCr}_{1-x}\text{S}_x\text{O}_4$ crystals (see Figures VIII.2 to VIII.5).

	CY1:PbCrO ₄	CY2	CY3	CY4	CY5	CY6	CY7	CY8	CY9	CY10	CY11:PbSO ₄	
Infrared	$\nu_{\text{as}}(\text{SO}_4^{2-})$ -	1098, 1048	1099, 1049	1100, 1050	1100, 1050	1101, 1069	1105, 1067	1105, 1052	1167, 1105, 1052	1171, 1047	1181, 1043	
	$\nu_{\text{s}}(\text{SO}_4^{2-})$ -	-	-	966	967	968	968	965	965	965	967	
	$\nu_{\text{as}}(\text{CrO}_4^{2-})$ 853/831/818	853/831/819	853/831/820	882/854/832	882/855/833	882/857/834	882/858/834	881/858/836	920/878/838	923/877/838	-	
	[1/0.75/0.71]	[1/0.79/0.72]	[1/0.86/0.80]	[0.86/1/0.80]	[0.88/1/0.89]	[0.9/1/0.92]	[0.94/1/0.93]	[0.99/1/0.95]	[0.8/1/0.98]	[0.88/0.93/1]	-	
	$\delta_{\text{as}}(\text{SO}_4^{2-})$ -	627, 598	627, 598	627, 598	627, 598	627, 598	627, 598	627, 598	627, 598	628, 598	630, 595	634, 596
$A_{\nu_{\text{as}}(\text{SO}_4^{2-})}/A_{\nu_{\text{as}}(\text{CrO}_4^{2-})}^*$ 0	0.073	0.164	0.296	0.416	0.587	0.758	1.209	2.066	-	-	-	
Raman	lattice mode -	-	-	-	-	80 (vw)	80 (vw)	81 (vw)	82 (w)	86 (w)	97 (vw)	
	-	-	-	-	-	-	-	-	-	-	134 (vw)	
	134 (w)	135 (w)	136 (w)	136 (w)	137 (w)	138 (w)	139 (w)	139 (vw)	-	-	-	
	$\delta(\text{CrO}_4^{2-})$ 325 (vw)	325 (vw)	326 (vw)	326 (vw)	327 (vw)	327 (vw)	327 (vw)	327 (vw)	-	-	-	
	337 (w)	336 (w)	337 (w)	337 (w)	337 (w)	337 (w)	337 (w)	337 (w)	338 (m-w)	-	-	
	347 (sh)	347 (sh)	-	-	-	-	-	-	348 (m)	348 (m, br)	348 (m, br)	
	357 (m)	358 (m)	358 (m)	358 (m)	359 (m)	359 (m)	359 (m)	359 (m)	359 (m-s)	-	-	
	376 (w)	376 (w)	376 (w)	376 (w)	376 (w)	376 (w)	376 (sh)	375 (sh)	375 (w)	375 (sh)	375 (sh)	
	400 (vw)	400 (vw)	401 (vw)	401 (vw)	402 (vw)	403 (vw)	404 (vw)	404 (vw)	404 (w)	404 (w)	400 (w)	
	$\delta(\text{SO}_4^{2-})$ -	-	-	-	-	-	-	-	435 (vw)	435 (w)	436 (w)	438 (m-s)
	-	-	-	-	-	-	-	-	447 (vw)	447 (w)	448 (w)	449 (m)
	-	-	-	-	-	-	-	-	-	604 (vw)	605 (vw)	605 (w)
	-	-	-	-	-	-	-	-	-	-	638 (vw)	641 (w)
	$\nu_{\text{s}}(\text{CrO}_4^{2-})$ 839 (vs)	839 (vs)	840 (vs)	841 (vs)	841 (vs)	841 (vs)	842 (vs)	843 (vs)	843 (vs)	843 (vs)	843 (vs)	-
	$\nu_{\text{s}}(\text{SO}_4^{2-})$ -	-	968 (vw)	969 (vw)	970 (vw)	971 (vw)	971 (vw)	971 (vw)	973 (w)	973 (m-w)	976 (m-s)	978 (vs)
$\nu_{\text{as}}(\text{SO}_4^{2-})$ -	-	-	-	-	-	-	-	1044 (vw)	1045 (vw)	1046 (w)	1047 (vw)	
-	-	-	-	-	-	-	-	-	-	1153 (vw)	1155 (vw)	

* The ratio was calculated using the absorbance of $\nu_{\text{as}}(\text{SO}_4^{2-})$ at 1100 cm^{-1} normalized to the $\nu_{\text{as}}(\text{CrO}_4^{2-})$ at 853 cm^{-1} after baseline correction.

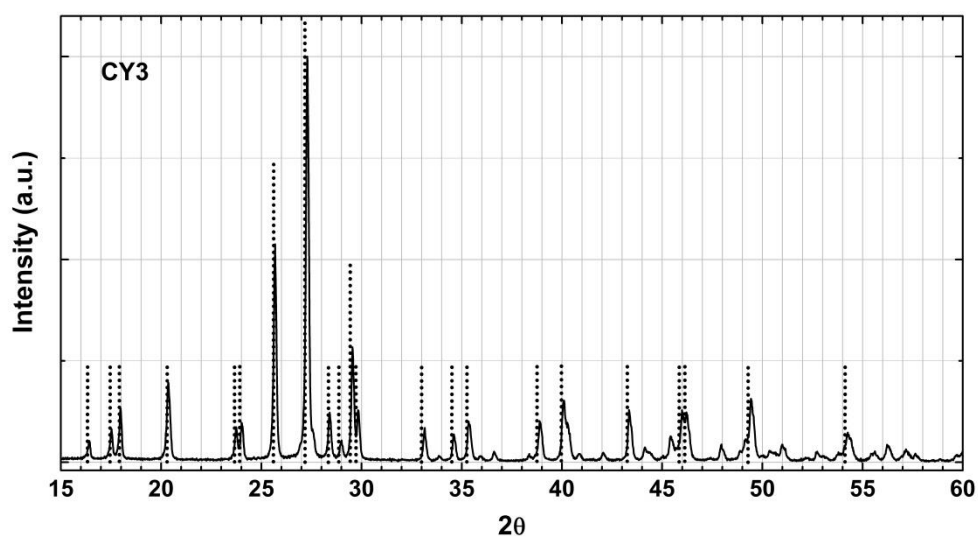
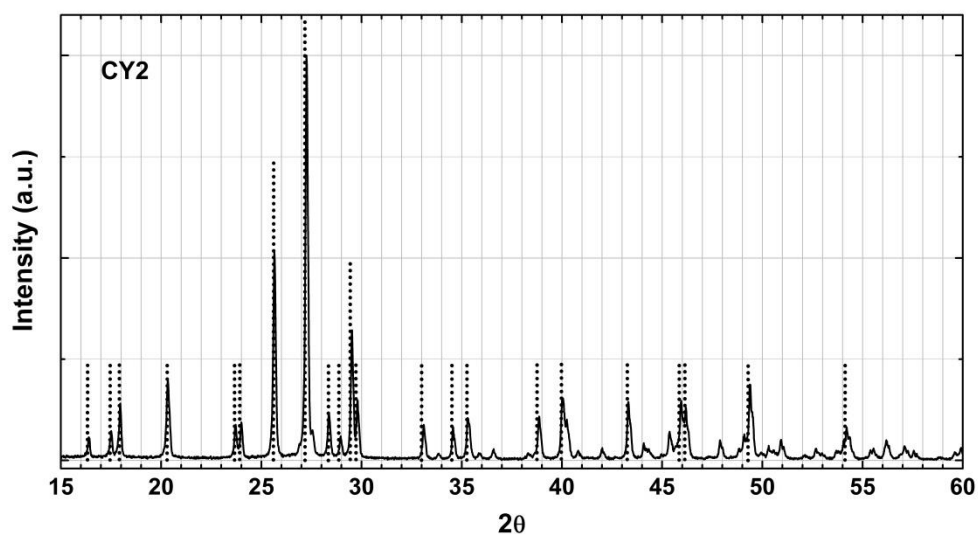
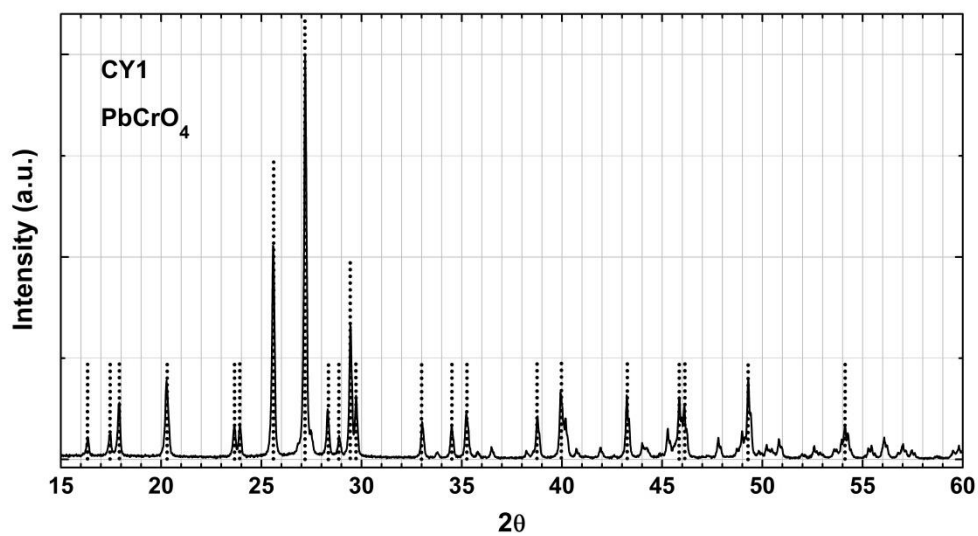


Figure VIII.6. Diffraction pattern of CY1 (PbCrO_4), CY2 and CY3 pigment references. The main diffraction peaks of lead chromate monoclinic crystal structure are marked in black dotted lines.

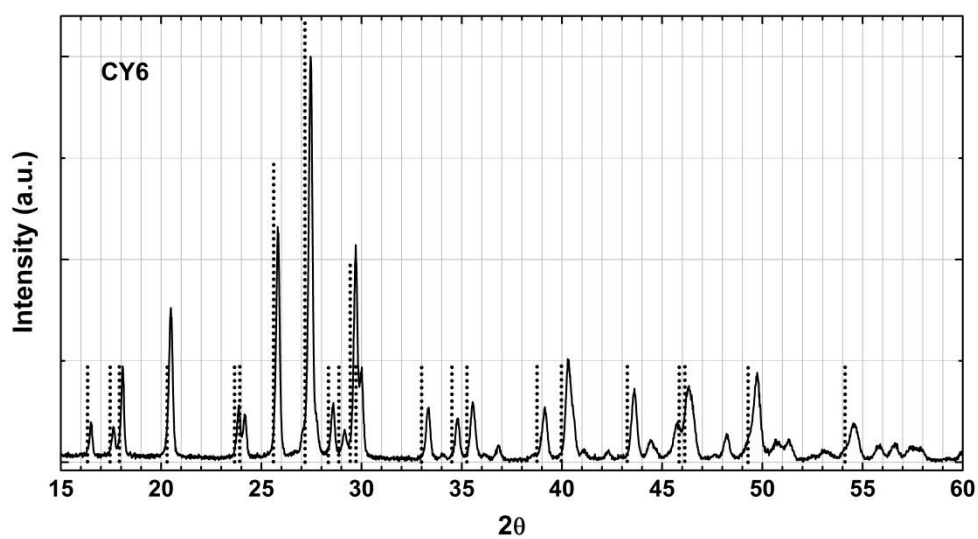
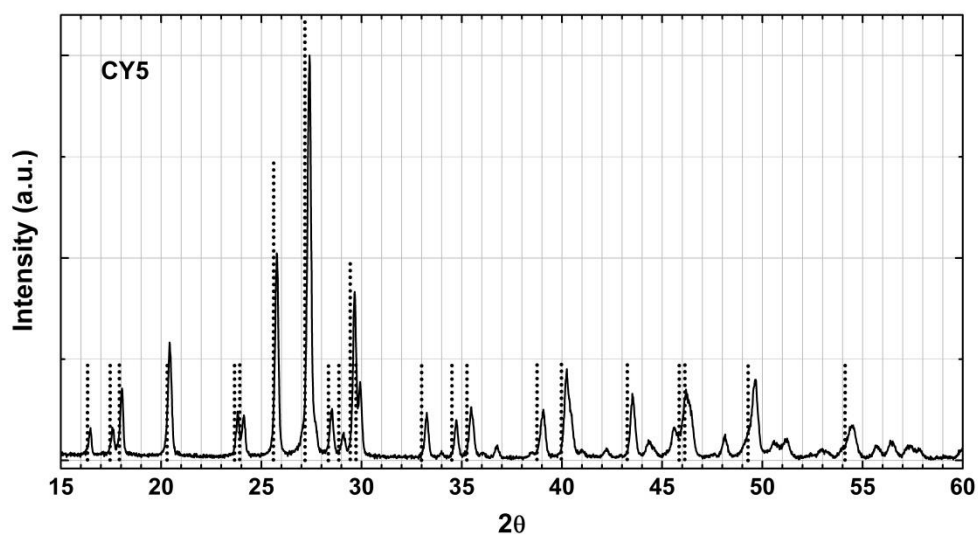
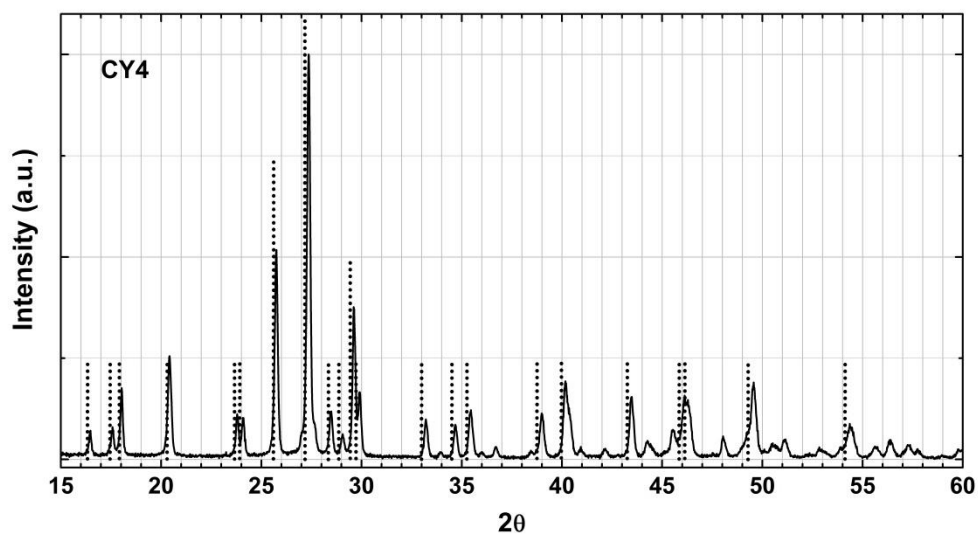


Figure VIII.7. Diffraction pattern of CY4, CY5 and CY6 pigment references. The main diffraction peaks of lead chromate monoclinic crystal structure are marked in black dotted lines.

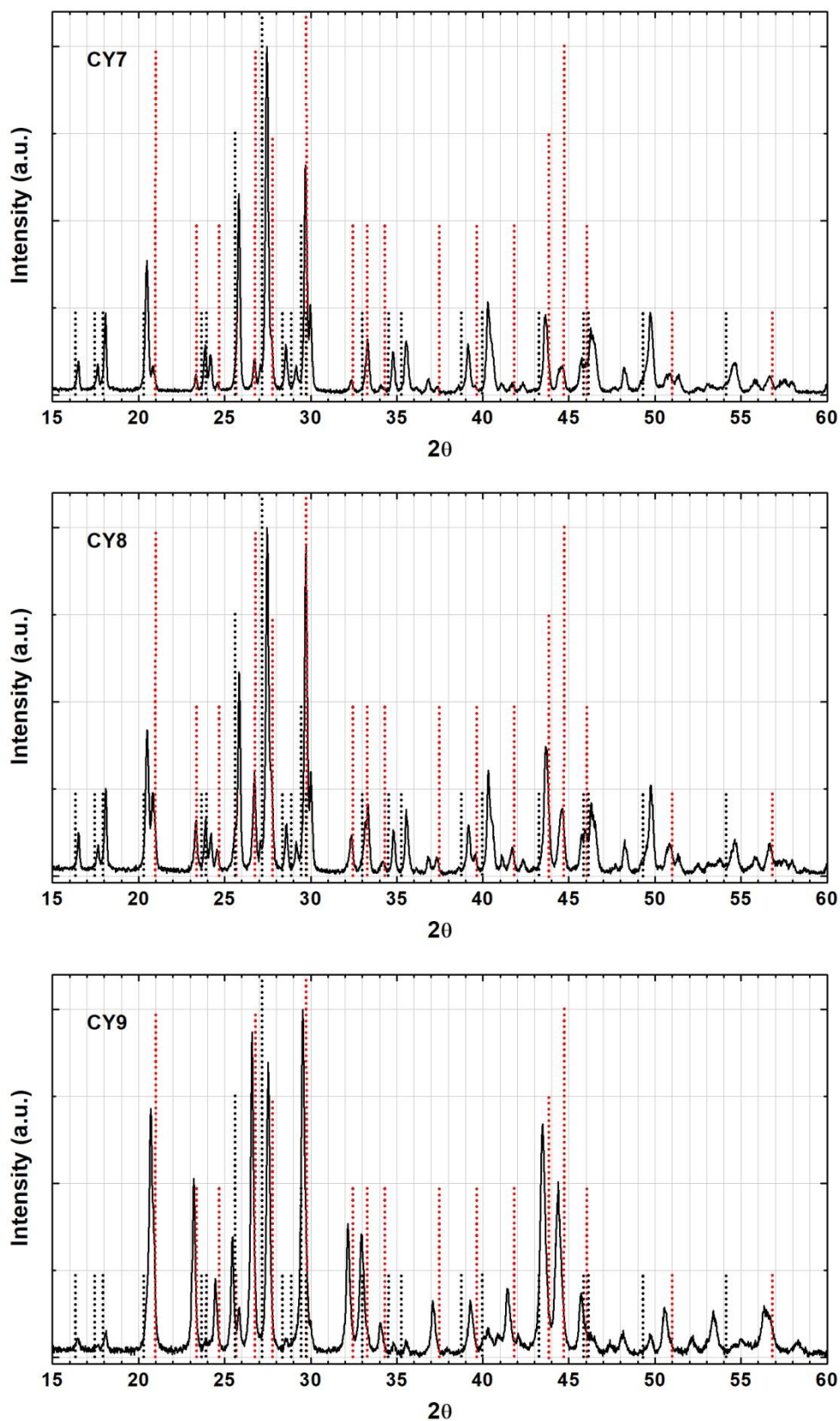


Figure VIII.8. Diffraction pattern of CY7, CY8 and CY9 pigment references. The main diffraction peaks of lead chromate monoclinic and lead sulfate orthorhombic crystal structure are marked in black and red dotted lines, respectively.

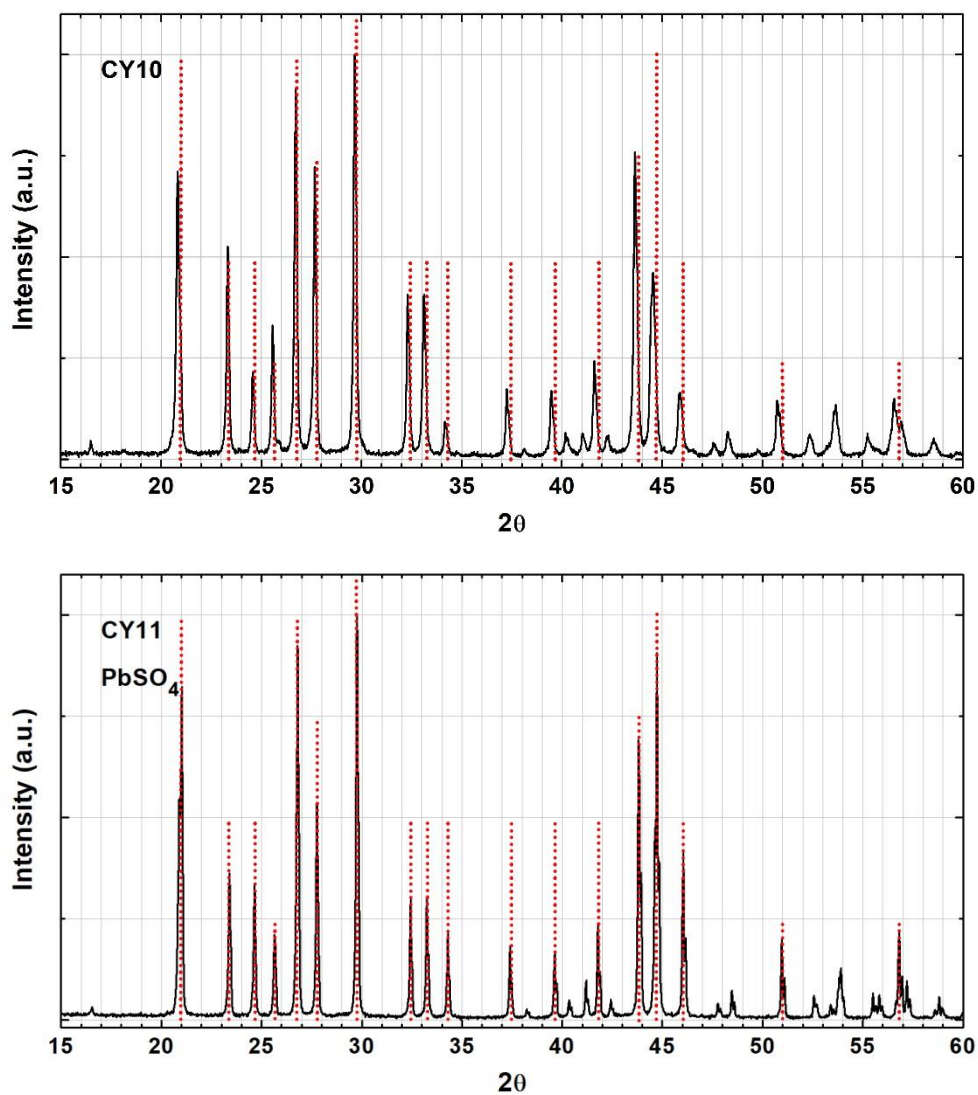


Figure VIII.9. Diffraction pattern of CY10 and CY11 (PbSO₄) pigment references. The main diffraction peaks of lead sulfate orthorhombic crystal structure are marked in red dotted lines.

Appendix IX. pH measurements

IX.1. Lead chromate pigments

Table IX.1.1. pH measurements throughout **PR1a** pigment syntheses. The pH of the solution is presented from top to bottom of the column, after each ingredient addition. pH range of the lead solution is shown in the end of the table. Final pH was obtained after the addition of all ingredients, before filtration.

Ingredients	PR1a_1	PR1a_2
K ₂ Cr ₂ O ₇ (aq)	3.74	3.76
Na ₂ CO ₃ (aq)	9.02	9.04
H ₂ SO ₄ (aq)	1.89	1.29
*Pb(Ac) ₂ .2Pb(OH) (aq)	3.62	3.90
Final pH	3.45	3.90

* 8 ≤ pH ≤ 9

Table IX.1.2. pH measurements throughout **PR1b** pigment syntheses. The pH of the solution is presented from top to bottom of the column, after each ingredient addition. pH range of the lead solution is also shown in the end of the table. Final pH was obtained after the addition of all ingredients, before filtration.

Ingredients	PR1b	PR1b_1	PR1b_2	PR1b*
K ₂ Cr ₂ O ₇ (aq)	3.91	3.81	3.80	3.90
Na ₂ CO ₃ (aq)	8.89	9.07	9.07	9.04
H ₂ SO ₄ (aq)	1.40	5.90	2.40	-
*Pb(NO ₃) ₂ (aq)	1.00	1.37	1.03	1.42
Final pH	1.11	1.37	1.17	1.48

* pH ≈ 4

Table IX.1.3. pH measurements throughout **L1** pigment syntheses. The pH of the solution is presented from top to bottom of the column, after each ingredient addition. pH range of the lead solution is also shown in the end of the table. Final pH was obtained after the addition of all ingredients, before filtration.

Ingredients	L1_1	L1_2	L1_3
K ₂ Cr ₂ O ₇ + Na ₂ CO ₃ (aq)	10.16	10.32	10.58
Na ₂ SO ₄ (aq)	10.10	10.27	10.49
PbSO ₄	9.46	9.79	9.72
*Pb(NO ₃) ₂ (aq)	6.36	6.56	-
Final pH	6.16	6.45	6.20

* pH ≈ 4

Table IX.1.4. pH measurements throughout **L2a** pigment syntheses. The pH of the solution is presented from top to bottom of the column, after each ingredient addition. pH range of the lead solution is also shown in the end of the table. Final pH was obtained after the addition of all ingredients, before filtration.

Ingredients	L2a_1	L2a_2	L2a_3
Na ₂ SO ₄ (aq)	5.66	5.41	5.75
K ₂ Cr ₂ O ₇ + Na ₂ CO ₃ (aq)	10.53	10.78	10.58
BaSO ₄	10.53	10.78	10.58
*Pb(NO ₃) ₂ (aq)	10.4	-	-
H ₂ SO ₄	1.11	-	-
Final pH	1.24	1.10	1.19

* pH ≈ 4

Table IX.1.5. pH measurements throughout **L2b** pigment syntheses. The pH of the solution is presented from top to bottom of the column, after each ingredient addition. pH range of the lead solution is also shown in the end of the table. Final pH was obtained after the addition of all ingredients, before filtration.

Ingredients	L2b_1	L2b_2
Na ₂ SO ₄ (aq)	6.01	6.16
K ₂ Cr ₂ O ₇ + Na ₂ CO ₃ (aq)	10.74	10.40
Pb(NO ₃) ₂ (aq)	10.03	9.90
H ₂ SO ₄	2.03	1.90
Final pH	2.21	1.85

* pH ≈ 4

Table IX.1.6. pH measurements throughout **L3a** pigment syntheses. The pH of the solution is presented from top to bottom of the column, after each ingredient addition. pH range of the lead solution is also shown in the end of the table. Final pH was obtained after the addition of all ingredients, before filtration.

Ingredients	L3a*_1	L3a*_2	L3a
K ₂ Cr ₂ O ₇ (aq)	3.71	3.95	3.82
Na ₂ CO ₃ (aq)	9.50	9.64	9.56
Na ₂ SO ₄ (aq)	9.45	9.59	9.50
*Pb(NO ₃) ₂ (aq)	9.46	9.60	6.02
CaSO ₄ .2H ₂ O	7.44	7.45	6.09
Final pH	7.44	7.45	6.09

* pH ≈ 4

Table IX.1.7. pH measurements throughout **L3b** pigment synthesis. The pH of the solution is presented from top to bottom of the column, after each ingredient addition. pH range of the lead solution is also shown in the end of the table. Final pH was obtained after the addition of all ingredients, before filtration.

Ingredients	L3b
K ₂ Cr ₂ O ₇ (aq)	3.83
Na ₂ CO ₃ (aq)	9.51
Na ₂ SO ₄ (aq)	9.47
*Pb(NO ₃) ₂ (aq)	7.1
Final pH	5.97

* pH ≈ 4

Table IX.1.8. pH measurements throughout **M1a** pigment syntheses. The pH of the solution is presented from top to bottom of the column, after each ingredient addition. pH range of the lead solution is also shown in the end of the table. Final pH was obtained after the addition of all ingredients, before filtration.

Ingredients	M1a_1	M1a_2	M1a_3
K ₂ Cr ₂ O ₇ (aq)	3.90	3.84	4.11
Na ₂ CO ₃ (aq)	7.19	7.18	7.73
CaCO ₃	7.30	7.45	7.93
*Pb(NO ₃) ₂ (aq)	6.01	6.70	6.63
Final pH	6.01	6.70	6.63

* pH ≈ 4

Table IX.1.9. pH measurements throughout **M1b** pigment synthesis. The pH of the solution is presented from top to bottom of the column, after each ingredient addition. pH range of the lead solution is also shown in the end of the table. Final pH was obtained after the addition of all ingredients, before filtration.

Ingredients	M1b
K ₂ Cr ₂ O ₇ (aq)	4.32
Na ₂ CO ₃ (aq)	7.27
*Pb(NO ₃) ₂ (aq)	3.64
Final pH	3.64

* pH ≈ 4

Table IX.1.10. pH measurements throughout **M2a** pigment syntheses. The pH of the solution is presented from top to bottom of the column, after each ingredient addition. pH range of the lead solution is also shown in the end of the table. Final pH was obtained after the addition of all ingredients, before filtration.

Ingredients	M2a_1	M2a_2	M2a_3
K ₂ Cr ₂ O ₇ (aq)	4.05	4.02	3.68
Na ₂ CO ₃ (aq)	7.22	7.24	7.18
H ₂ SO ₄	5.49	5.32	6.11
*Pb(Ac) ₂ .2Pb(OH) (aq)	5.70	5.40	6.11
BaSO ₄	6.62	6.46	6.20
Final pH	6.62	6.46	6.20

* 8 ≤ pH ≤ 9

Table IX.1.11. pH measurements throughout **D1a** pigment synthesis. The pH of the solution is presented from top to bottom of the column, after each ingredient addition. pH range of the lead solution is also shown in the end of the table. Final pH was obtained after the addition of all ingredients, before filtration.

Ingredients	D1a
K ₂ Cr ₂ O ₇ (aq)	3.95
Na ₂ CO ₃ (aq)	6.91
H ₂ SO ₄	6.60
BaSO ₄	6.56
CaSO ₄ .2H ₂ O	6.43
*Pb(Ac) ₂ .2Pb(OH) (aq)	7
H ₂ SO ₄	6.0
Final pH	6.92

* 8 ≤ pH ≤ 9

Table IX.1.12. pH measurements throughout **D1b** pigment syntheses. The pH of the solution is presented from top to bottom of the column, after each ingredient addition. pH range of the lead solution is also shown in the end of the table. Final pH was obtained after the addition of all ingredients, before filtration.

Ingredients	D1b_1	D1b_2	D1b_3
K ₂ Cr ₂ O ₇ (aq)	3.78	3.77	3.68
Na ₂ CO ₃ (aq)	7.83	7.98	7.22
BaSO ₄	7.84	8.18	7.24
*Pb(Ac) ₂ .2Pb(OH) (aq)	-	-	-
H ₂ SO ₄	-	-	-
Final pH	6.53	6.74	6.67

* 8 ≤ pH ≤ 9

Table IX.1.13. pH measurements throughout **D2a** pigment syntheses. The pH of the solution is presented from top to bottom of the column, after each ingredient addition. pH range of the lead solution is also shown in the end of the table. Final pH was obtained after the addition of all ingredients, before filtration.

Ingredients	D2a_1	D2a_2	D2a_3
K ₂ Cr ₂ O ₇ (aq)	3.76	3.70	3.79
Na ₂ CO ₃ (aq)	6.60	6.62	7.14
*Pb(Ac) ₂ .2Pb(OH) (aq)	6.70	6.70	6.90
BaSO ₄ + CaSO ₄ .2H ₂ O	7.16	-	
H ₂ SO ₄	6.90	-	
Final pH	6.90	6.85	6.74

* 8 ≤ pH ≤ 9

IX.2. Other yellow chromate pigments

Table IX.2.1. pH measurements throughout **LY1a** pigment syntheses. The pH of the solution is presented from top to bottom of the column, after each ingredient addition. pH range of the barium chloride is also shown in the end of the table. Final pH was obtained after the addition of all ingredients, before filtration.

Ingredients	LY1a_1	LY1a_2	LY1a_3
K ₂ Cr ₂ O ₇ (aq)	3.74	3.80	3.70
‡BaCl ₂ (aq)	-	-	-
Final pH	< 1	< 1	< 1

‡ pH ≈ 5

Table IX.2.2. pH measurements throughout **CY1a** pigment syntheses. The pH of the solution is presented from top to bottom of the column, after each ingredient addition. pH range of the zinc nitrate is also shown in the end of the table. Final pH was obtained after the addition of all ingredients, before filtration.

Ingredients	CY1a_1	CY1a_2	CY1a_3
K ₂ Cr ₂ O ₇ (aq)	3.57	3.53	3.52
K ₂ CO ₃	6.21	6.28	6.31
‡Zn(NO ₃) ₂ (aq)	~ 5	~ 5	~ 5
K ₂ CO ₃	-	-	-
Final pH	5.21	5.32	5.23

‡ pH ≈ 4

Table IX.2.3. pH measurements throughout **SY1a** pigment syntheses. The pH of the solution is presented from top to bottom of the column, after each ingredient addition. pH range of strontium nitrate is also shown in the end of the table. Final pH was obtained after the addition of all ingredients, before filtration.

Ingredients	SY1a_1	SY1a_2
$\text{K}_2\text{Cr}_2\text{O}_7 + \text{Na}_2\text{CO}_3$ (aq)	9.67	9.88
$\ddagger\text{Sr}(\text{NO}_3)_2$ (aq)	8.85	8.71
Final pH	8.56	8.65

\ddagger pH \approx 5

Appendix X. Characterisation of lead chromate pigment reconstructions

X.1. Primrose Chrome

μ -EDXRF: Pb, Cr

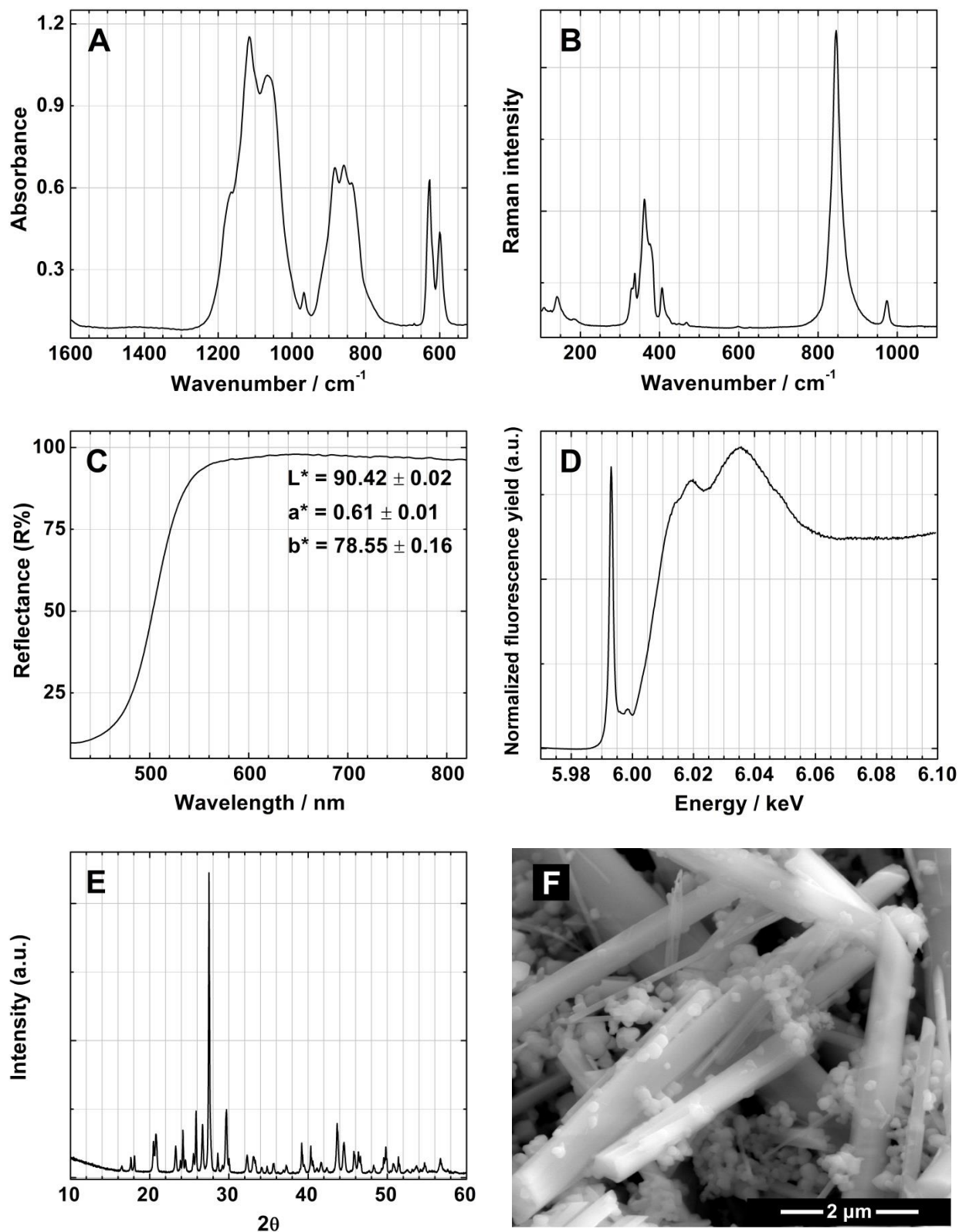


Figure X.1.1. PR1a pigment reconstruction: elements detected by μ -EDXRF, representative **A**) infrared, **B**) μ -Raman, **C**) FORS, **D**) Cr K-edge μ -XANES spectra, **E**) diffraction pattern and **F**) SEM image.

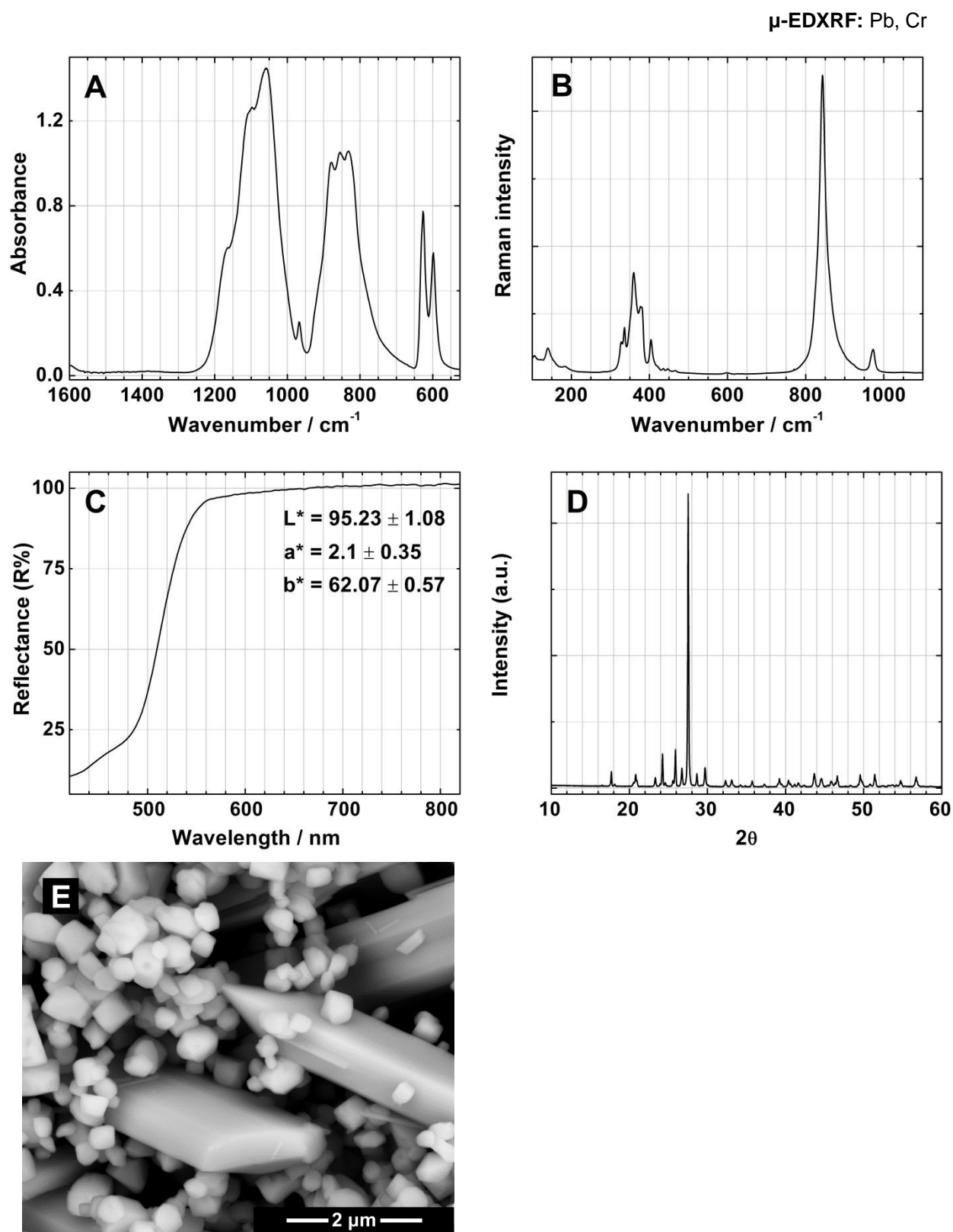


Figure X.1.2. PR1b pigment reconstruction: elements detected by μ -EDXRF, **A**) infrared, **B**) μ -Raman, **C**) FORS spectra, **D**) diffraction pattern and **E**) SEM image.

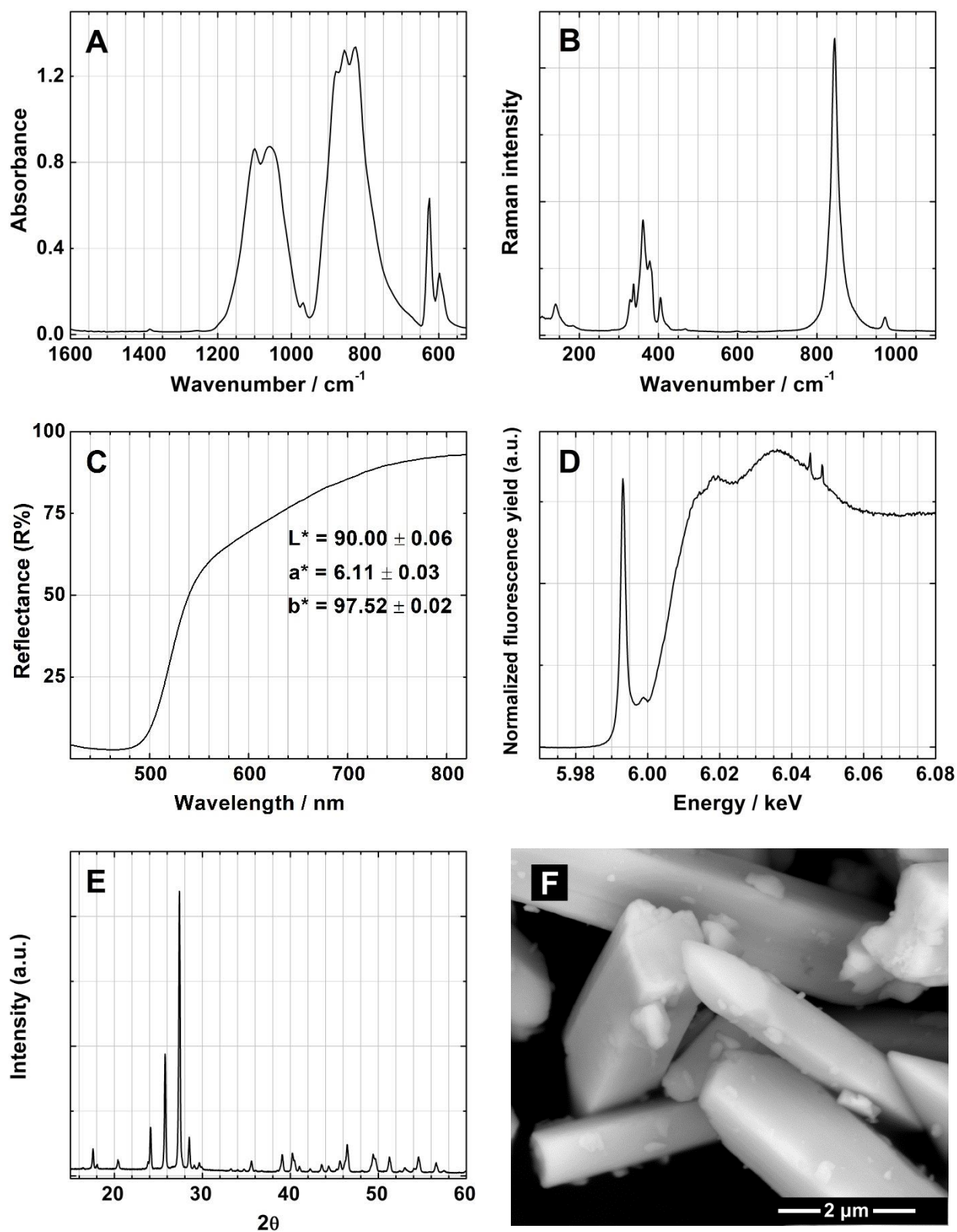


Figure X.1.3. PR1*b** pigment reconstruction: elements detected by μ -EDXRF, **A**) infrared, **B**) μ -Raman, **C**) FORS, **D**) Cr K-edge μ -XANES spectra, **E**) diffraction pattern and **F**) SEM image.

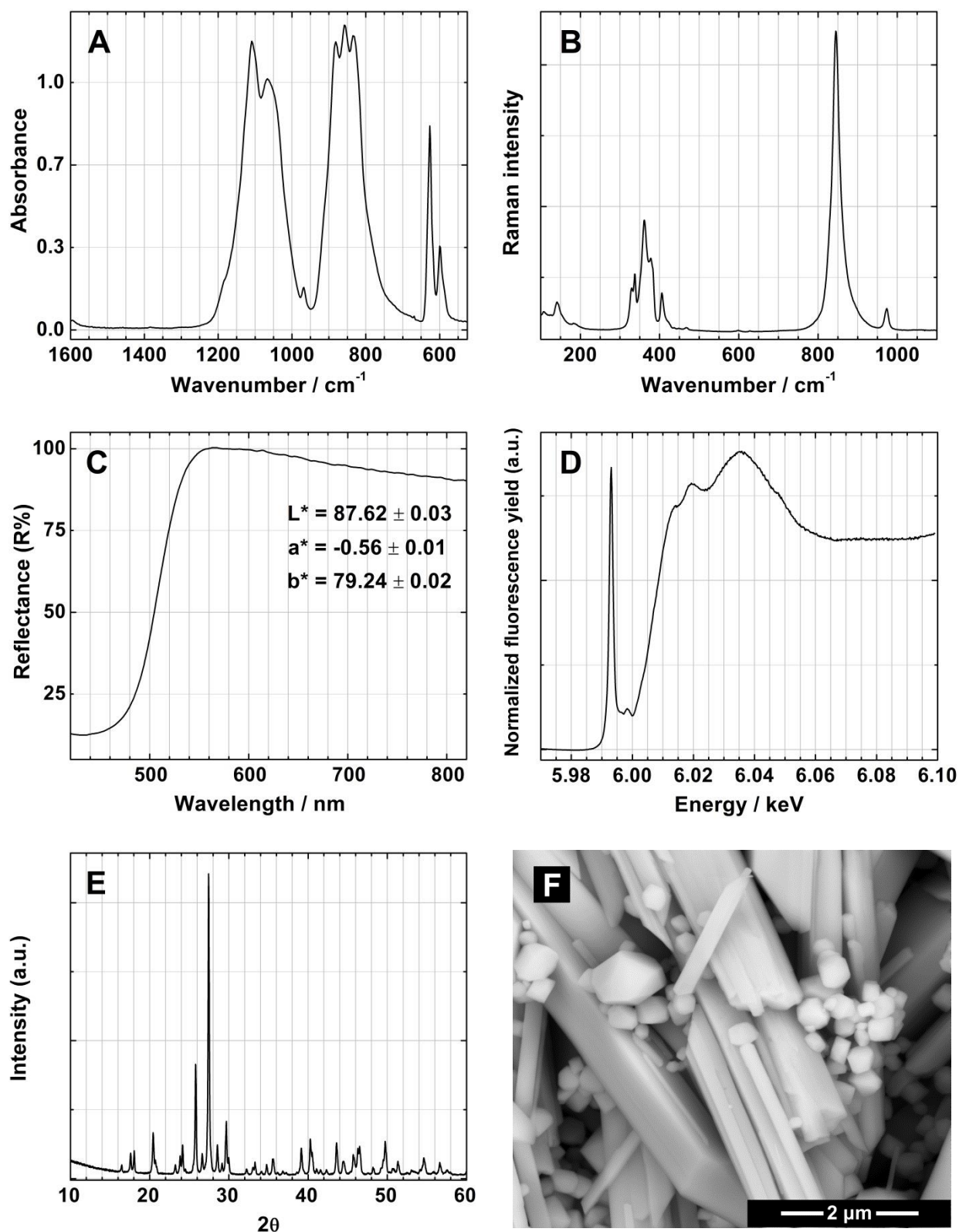


Figure X.1.4. PR1b_1 pigment reconstruction: elements detected by μ -EDXRF, **A**) infrared, **B**) μ -Raman, **C**) FORS, **D**) Cr K-edge μ -XANES spectra, **E**) diffraction pattern and **F**) SEM image.

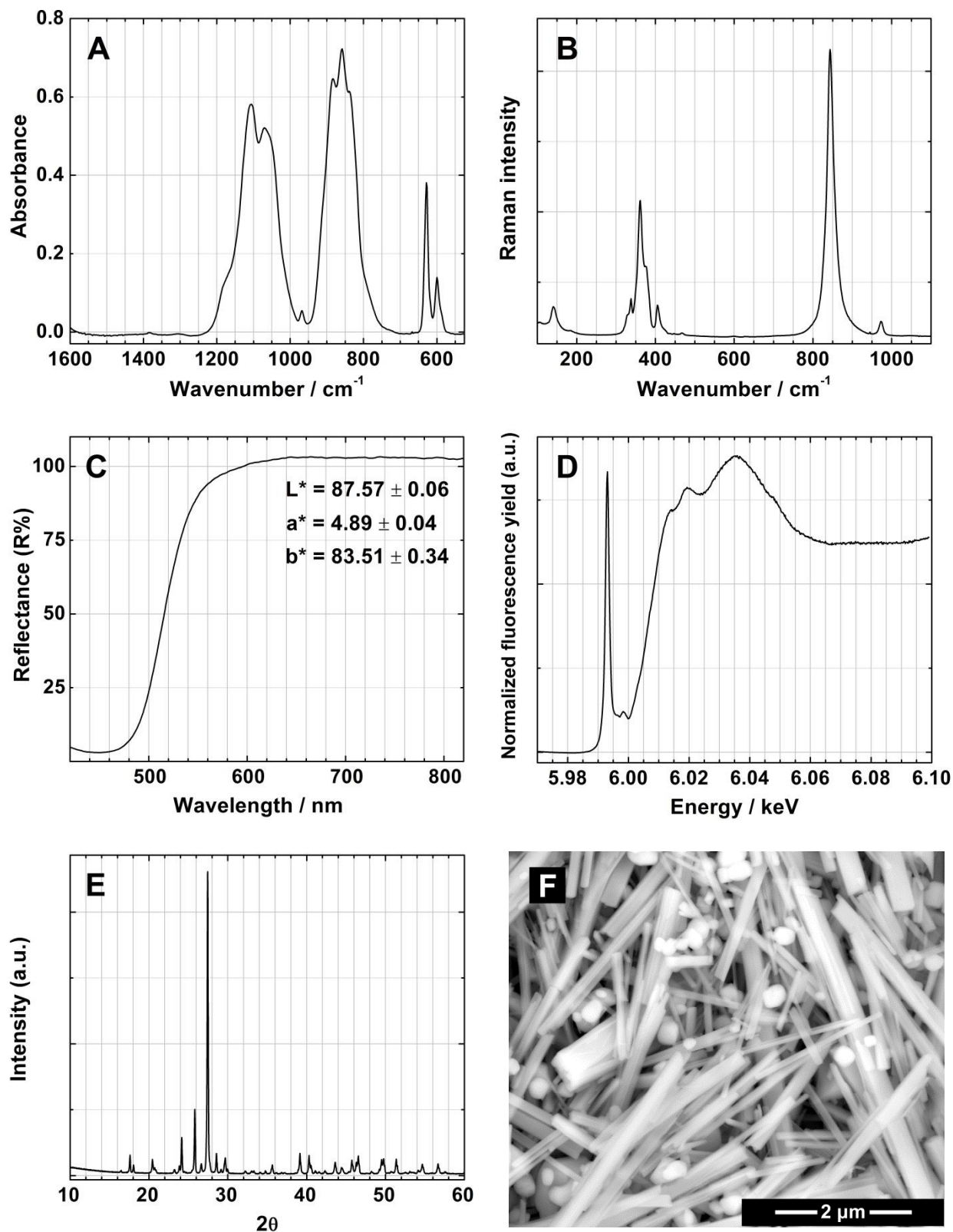


Figure X.1.5. PR1b_2 pigment reconstruction: elements detected by μ -EDXRF, **A)** infrared, **B)** μ -Raman, **C)** FORS, **D)** Cr K-edge μ -XANES spectra, **E)** diffraction pattern and **F)** SEM image.

X.2. Lemon/Pale Chrome

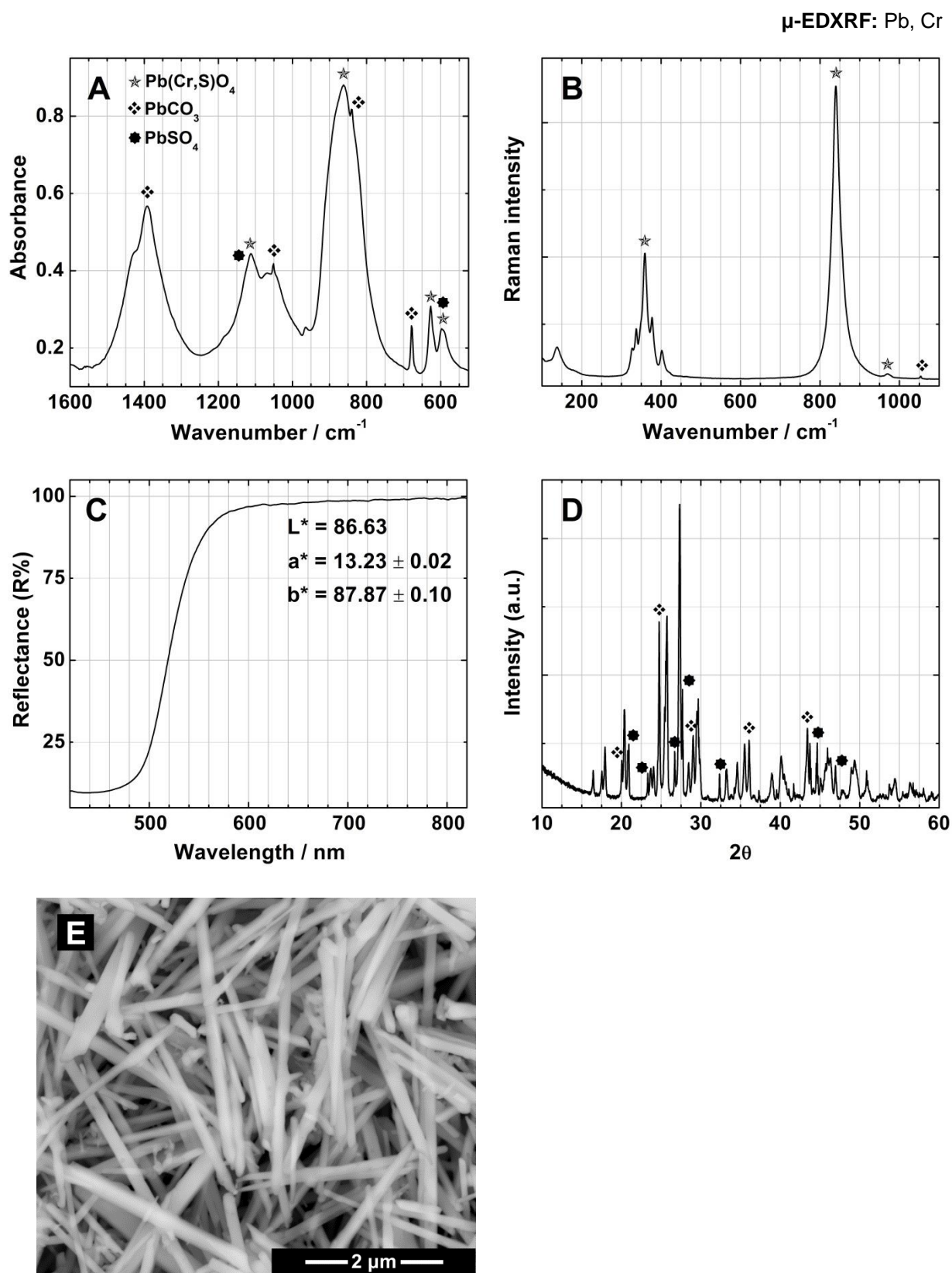


Figure X.2.1. L1 pigment reconstruction: elements detected by μ -EDXRF, representative **A**) infrared, **B**) μ -Raman, **C**) FORS spectra, **D**) diffraction pattern and **E**) SEM image; (\star) $\text{PbCr}_{0.8}\text{S}_{0.2}\text{O}_4$, (\diamond) PbCO_3 and (\bullet) PbSO_4 .

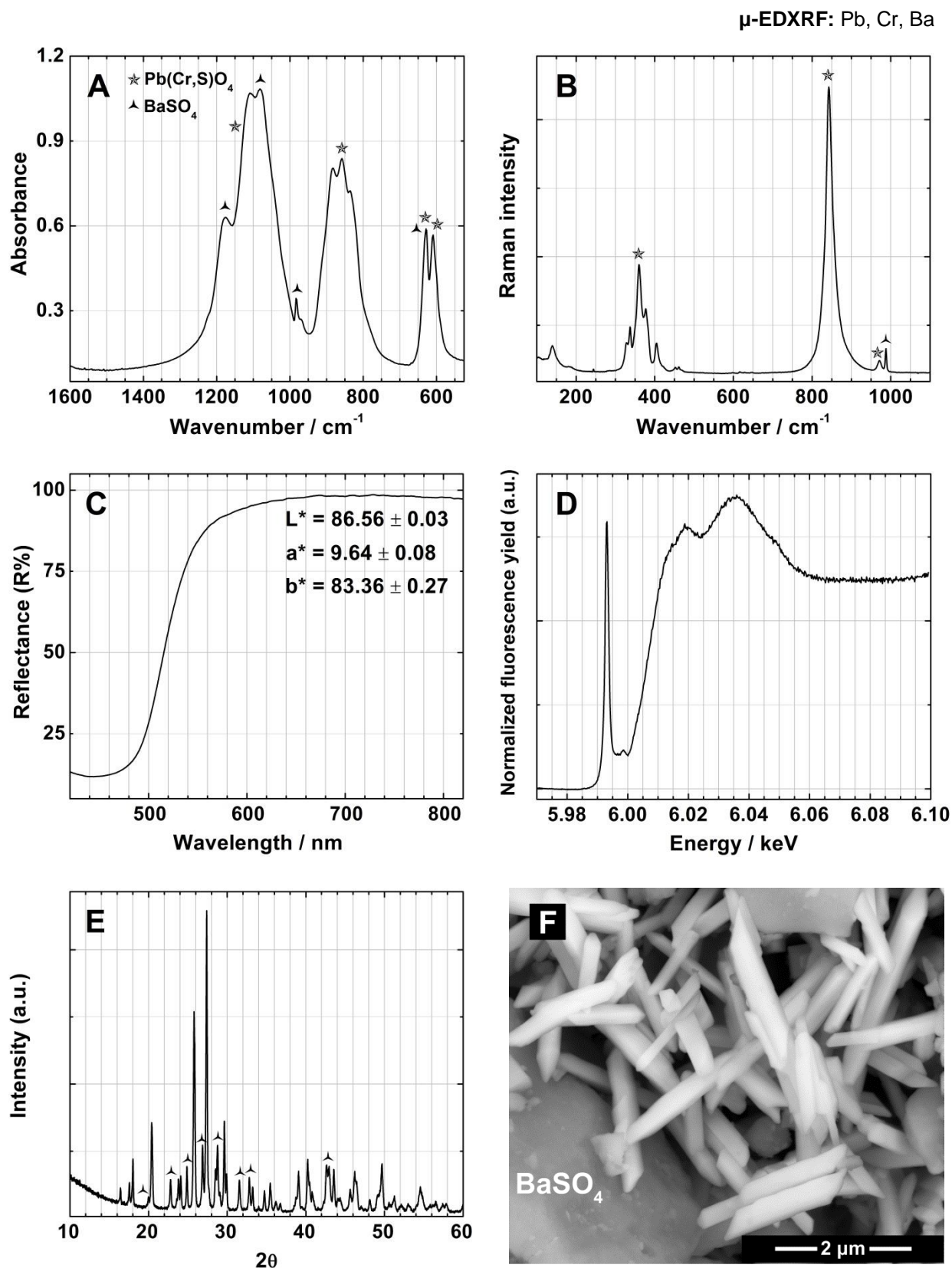


Figure X.2.2. L2a pigment reconstruction: elements detected by μ -EDXRF, representative **A**) infrared, **B**) μ -Raman, **C**) FORS, **D**) Cr K-edge μ -XANES spectra, **D**) diffraction pattern and **E**) SEM image; (\star) $\text{PbCr}_{0.6}\text{S}_{0.4}\text{O}_4$, (\blacktriangle) BaSO_4 .

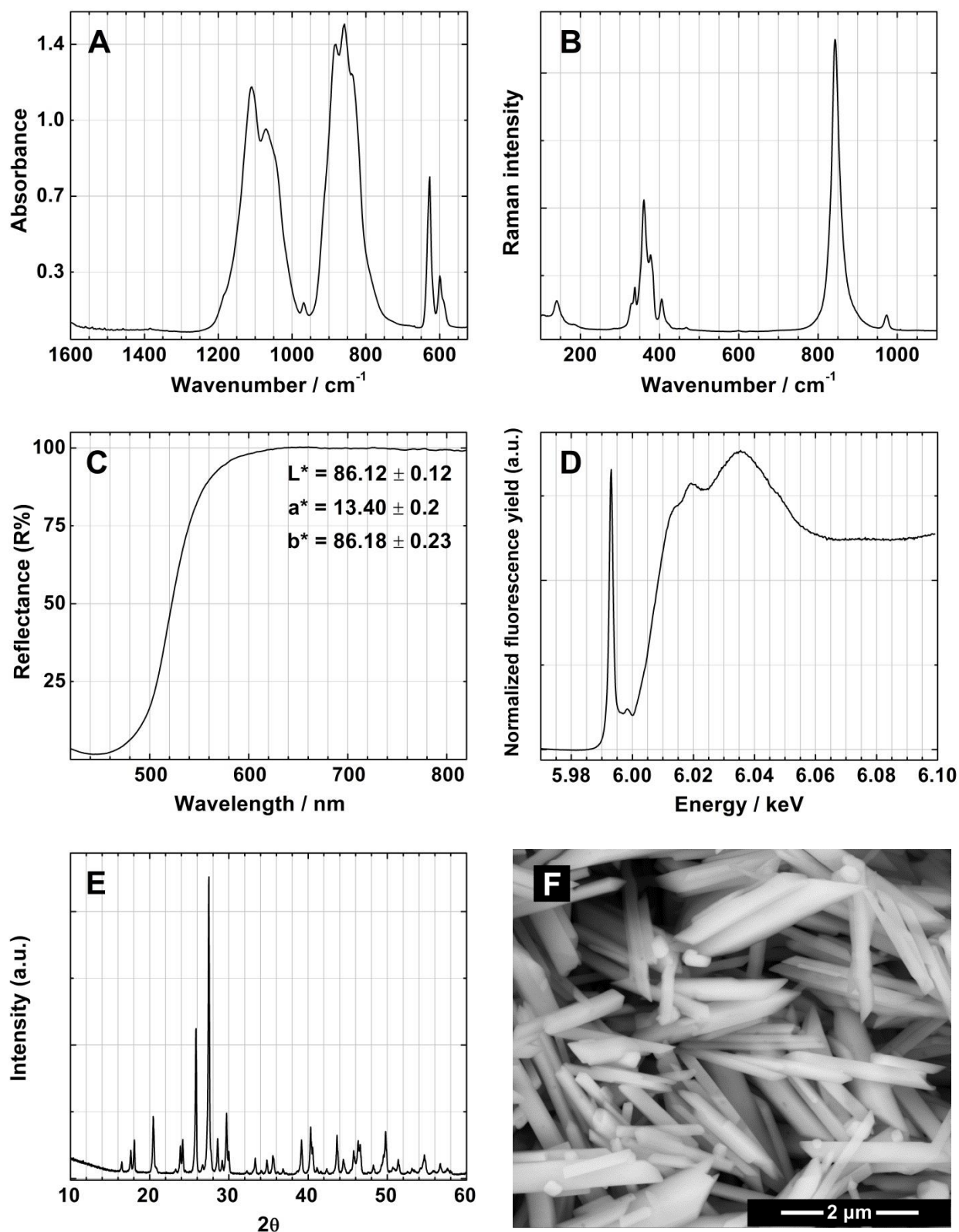


Figure X.2.3. L2b pigment reconstruction: elements detected by μ -EDXRF, representative **A**) infrared, **B**) μ -Raman, **C**) FORS, **D**) Cr K-edge μ -XANES spectra, **E**) diffraction pattern and **F**) SEM image.

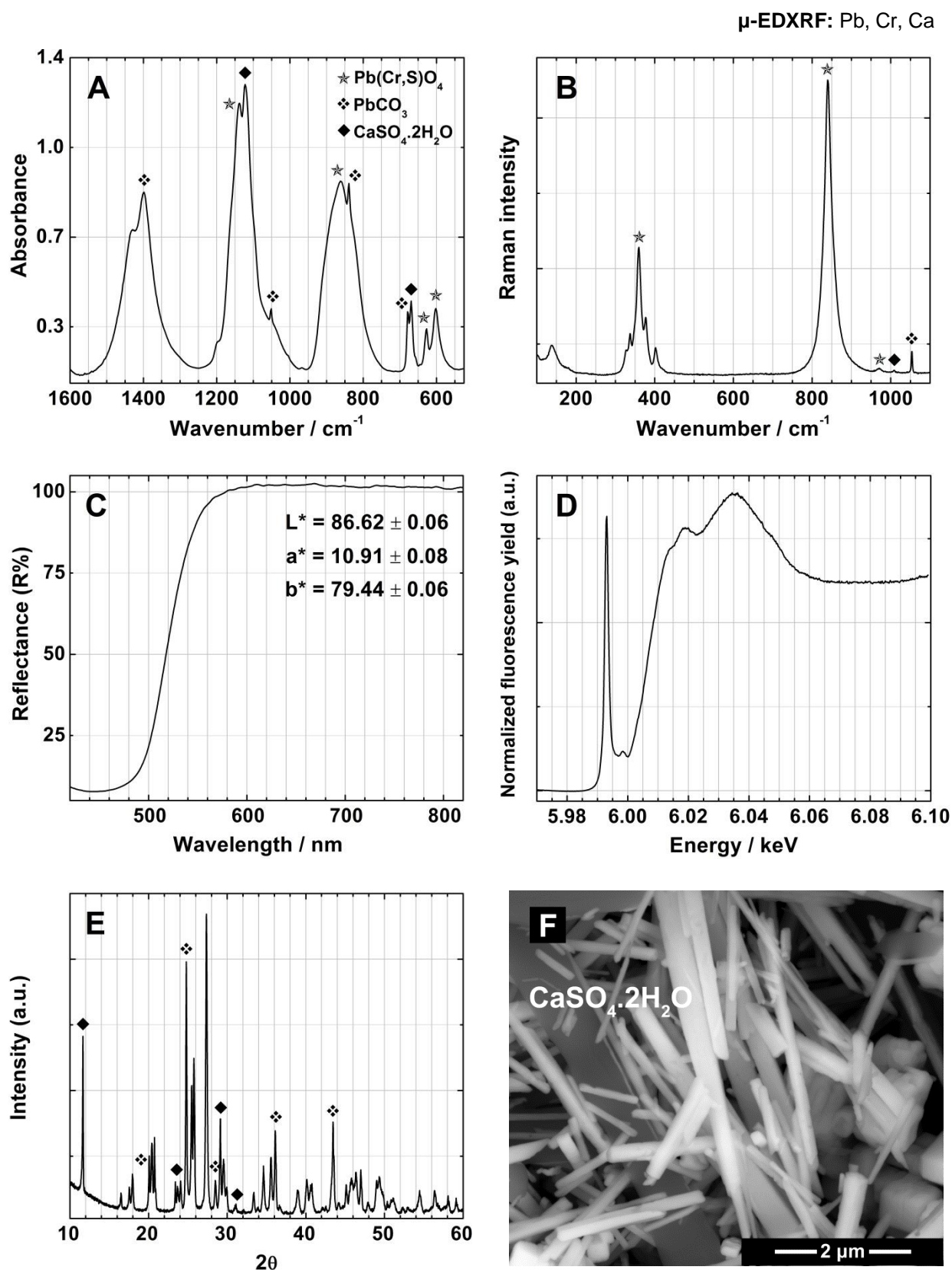


Figure X.2.4. L3a pigment reconstruction: elements detected by μ -EDXRF, representative **A**) infrared, **B**) μ -Raman, **C**) FORS, **D**) Cr K-edge μ -XANES spectra, **E**) diffraction pattern and **F**) SEM image; (☆) $\text{PbCr}_{0.8}\text{S}_{0.2}\text{O}_4$, (❖) PbCO_3 and (◆) $\text{CaSO}_4 \cdot 2\text{H}_2\text{O}$.

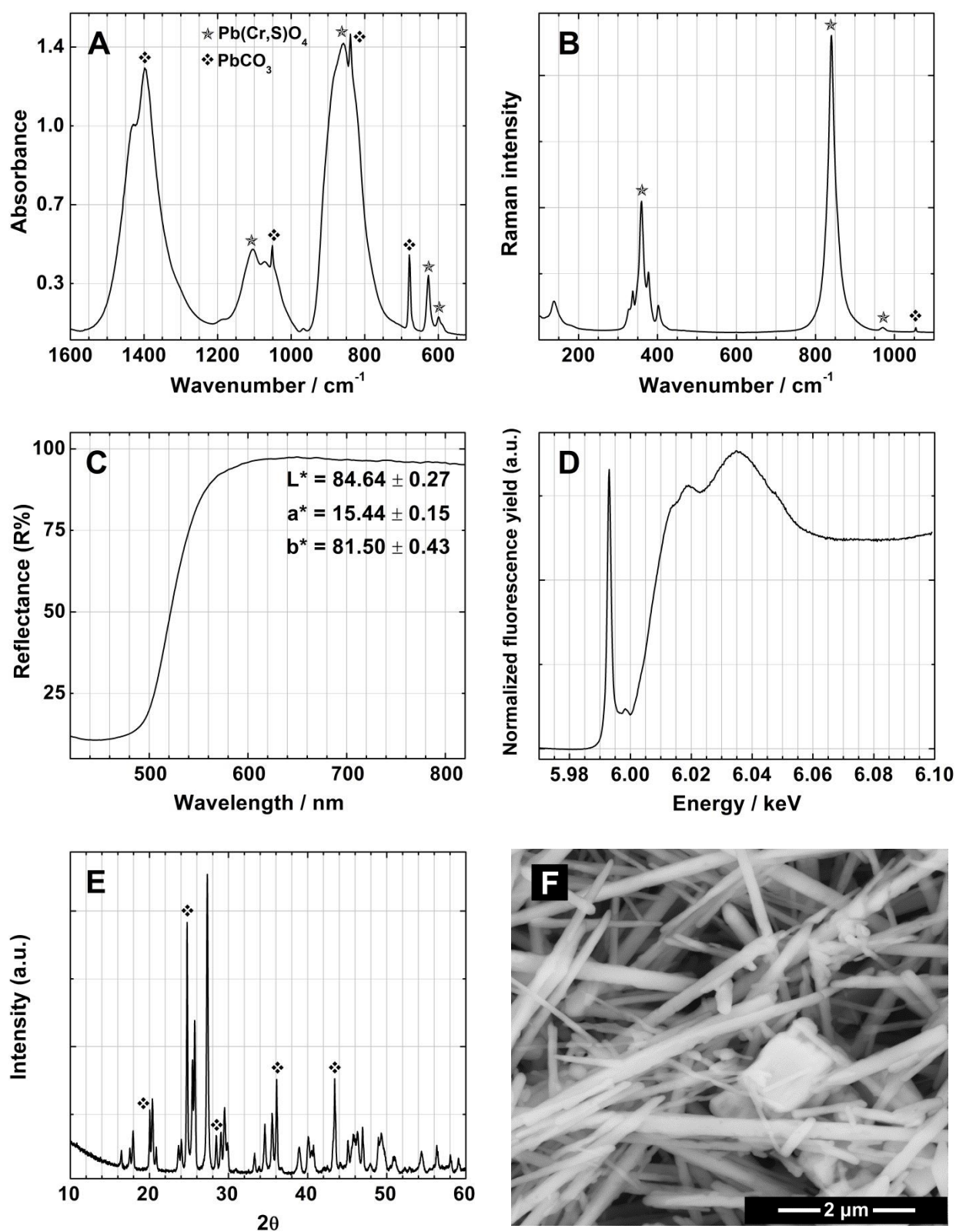


Figure X.2.5. L3b pigment reconstruction: elements detected by μ -EDXRF, representative **A**) infrared, **B**) μ -Raman, **C**) FORS, **D**) Cr K-edge μ -XANES spectra, **E**) diffraction pattern and **F**) SEM image; (\star) $\text{PbCr}_{0.8}\text{S}_{0.2}\text{O}_4$, (\diamond) PbCO_3 .

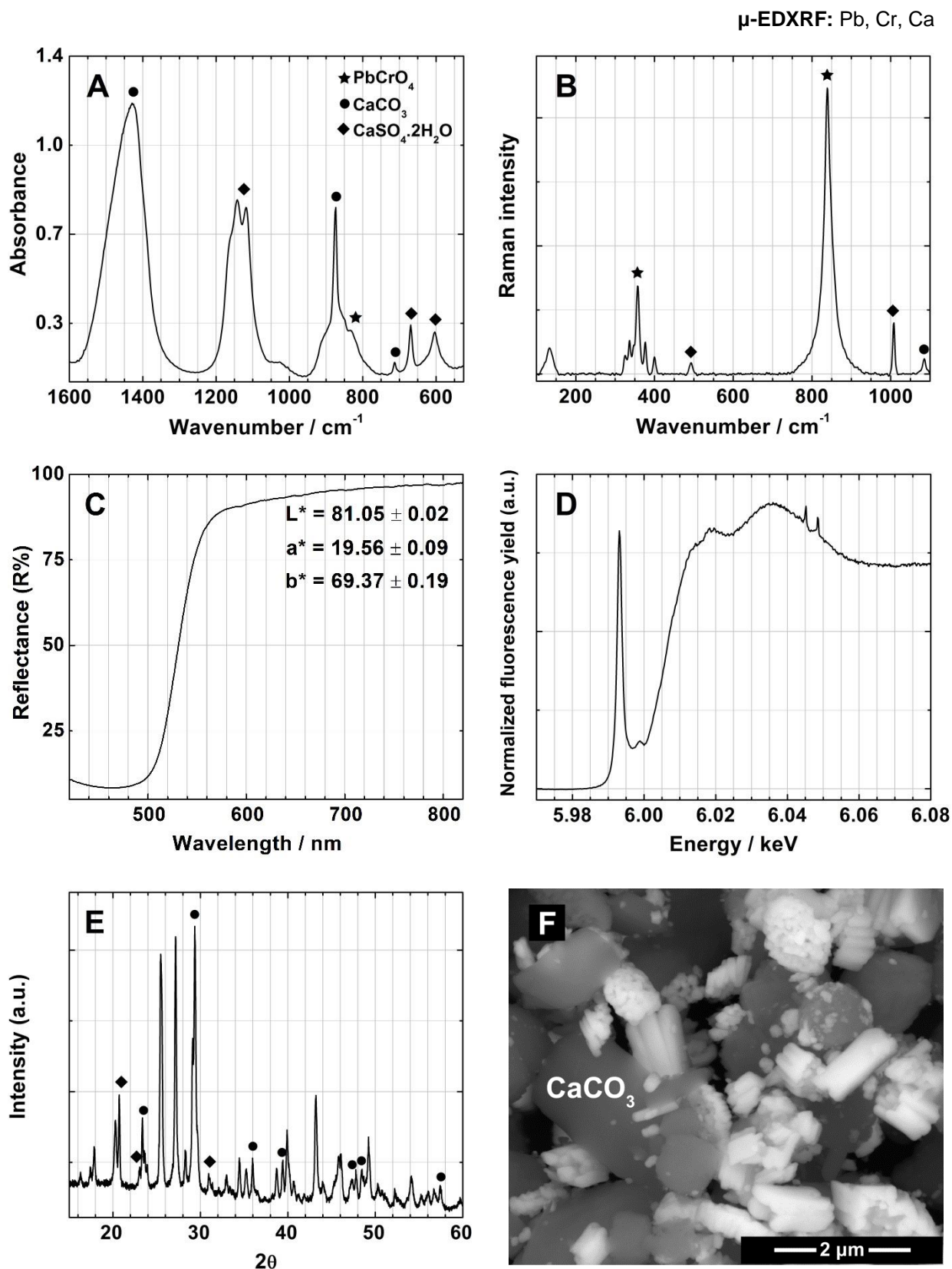


Figure X.2.6. L3a*_1 pigment reconstruction: elements detected by μ -EDXRF, **A**) infrared, **B**) μ -Raman, **C**) FORS, **D**) Cr K-edge μ -XANES spectra, **E**) diffraction pattern and **F**) SEM image; (★) PbCrO_4 , (●) CaCO_3 and (◆) $\text{CaSO}_4 \cdot 2\text{H}_2\text{O}$.

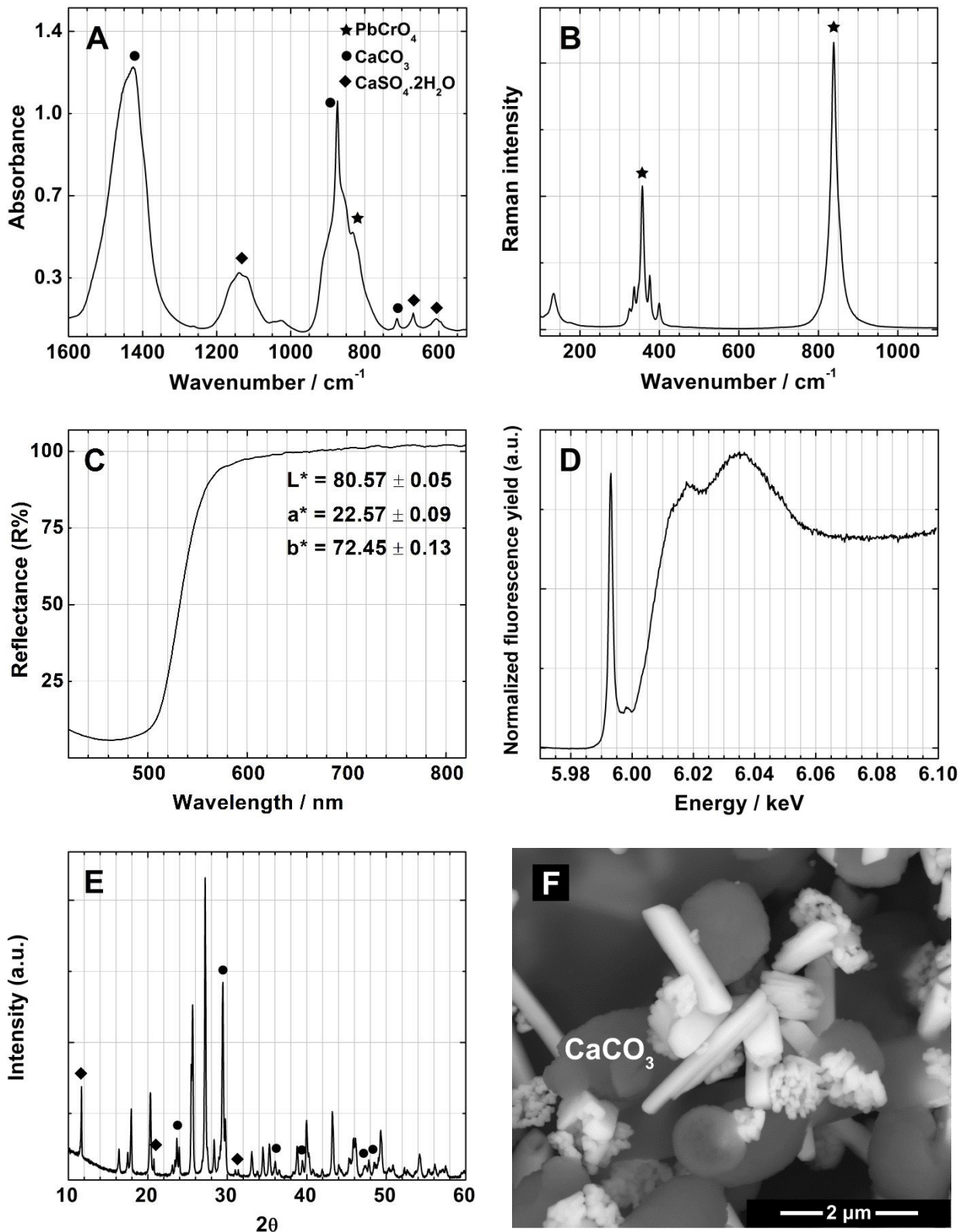


Figure X.2.7. L3a* 2 pigment reconstruction: elements detected by μ -EDXRF, **A**) infrared, **B**) μ -Raman, **C**) FORS, **D**) Cr K-edge μ -XANES spectra, **E**) diffraction pattern and **F**) SEM image; (\star) PbCrO_4 , (\bullet) CaCO_3 and (\blacklozenge) $\text{CaSO}_4 \cdot 2\text{H}_2\text{O}$.

X.3. Middle & Deep Chrome

μ -EDXRF: Pb, Cr, Ca

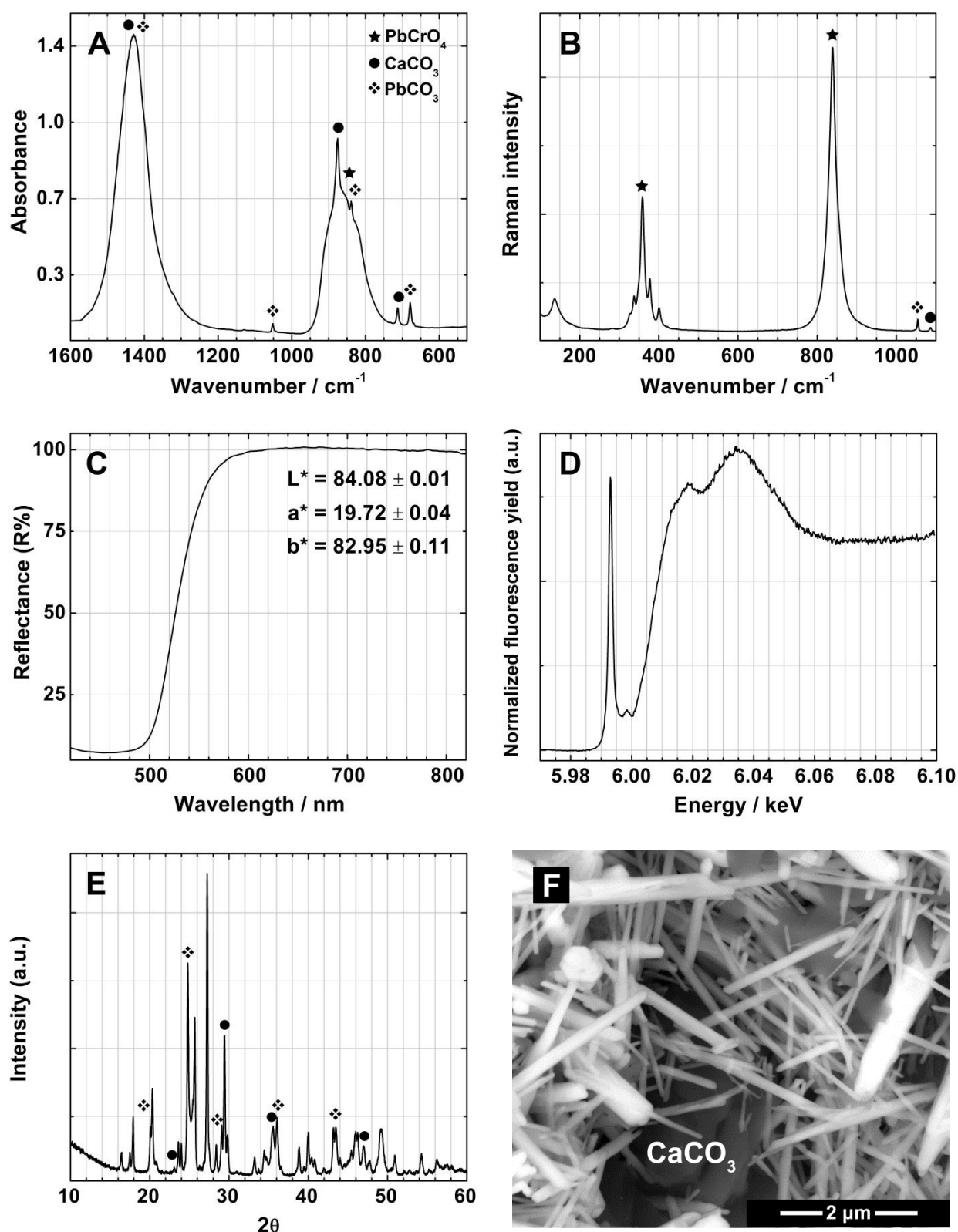


Figure X.3.1. M1a pigment reconstruction: elements detected by μ -EDXRF, representative **A)** infrared, **B)** μ -Raman, **C)** FORS, **D)** Cr K-edge μ -XANES spectra, **E)** diffraction pattern and **F)** SEM image; (\star) PbCrO_4 , (\diamond) PbCO_3 and (\bullet) CaCO_3 .

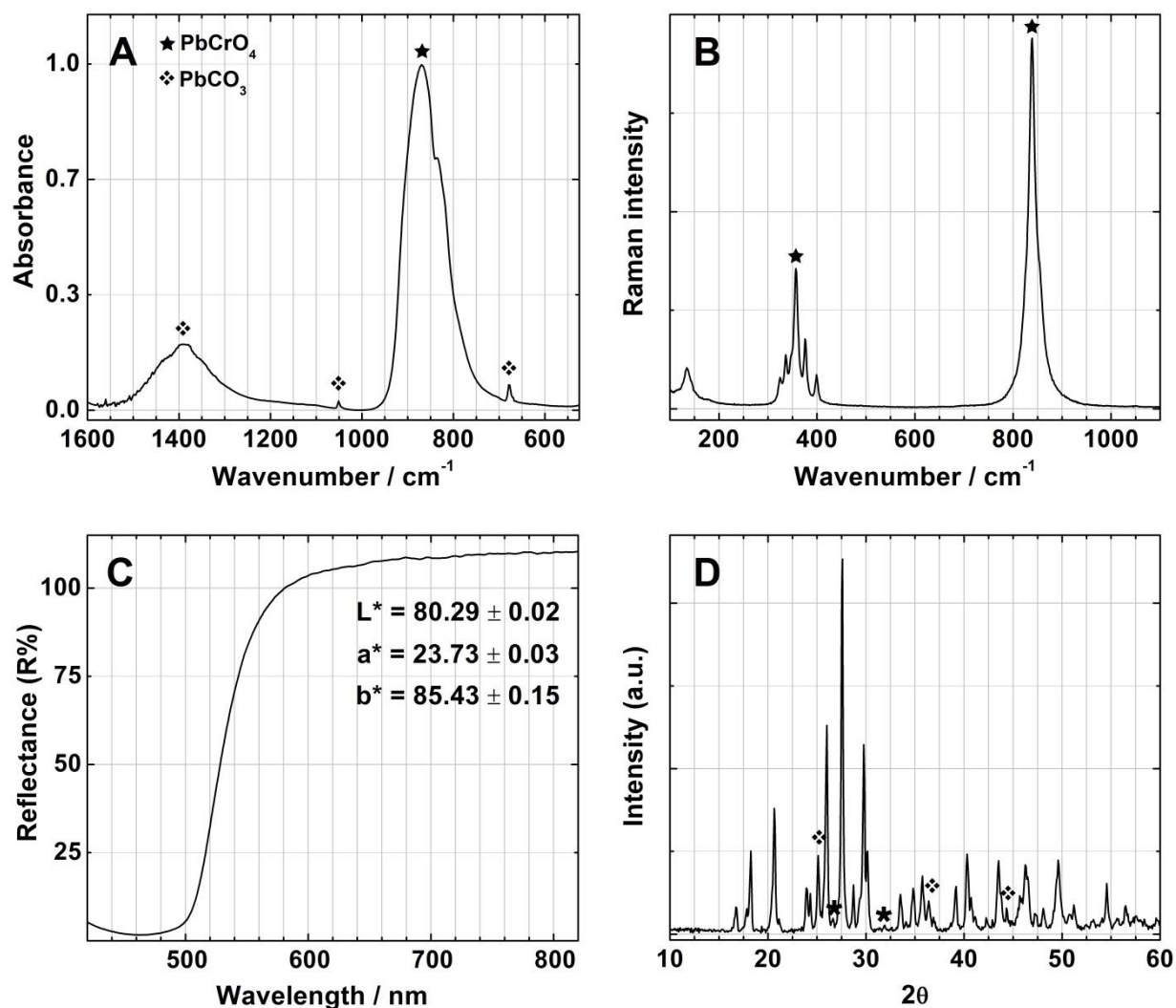


Figure X.3.2. M1b pigment reconstruction: elements detected by μ -EDXRF, **A**) infrared, **B**) μ -Raman, **C**) FORS spectra, and **D**) diffraction pattern; (\star) PbCrO_4 , (\diamond) PbCO_3 and (\star) Pb_2CrO_5 .

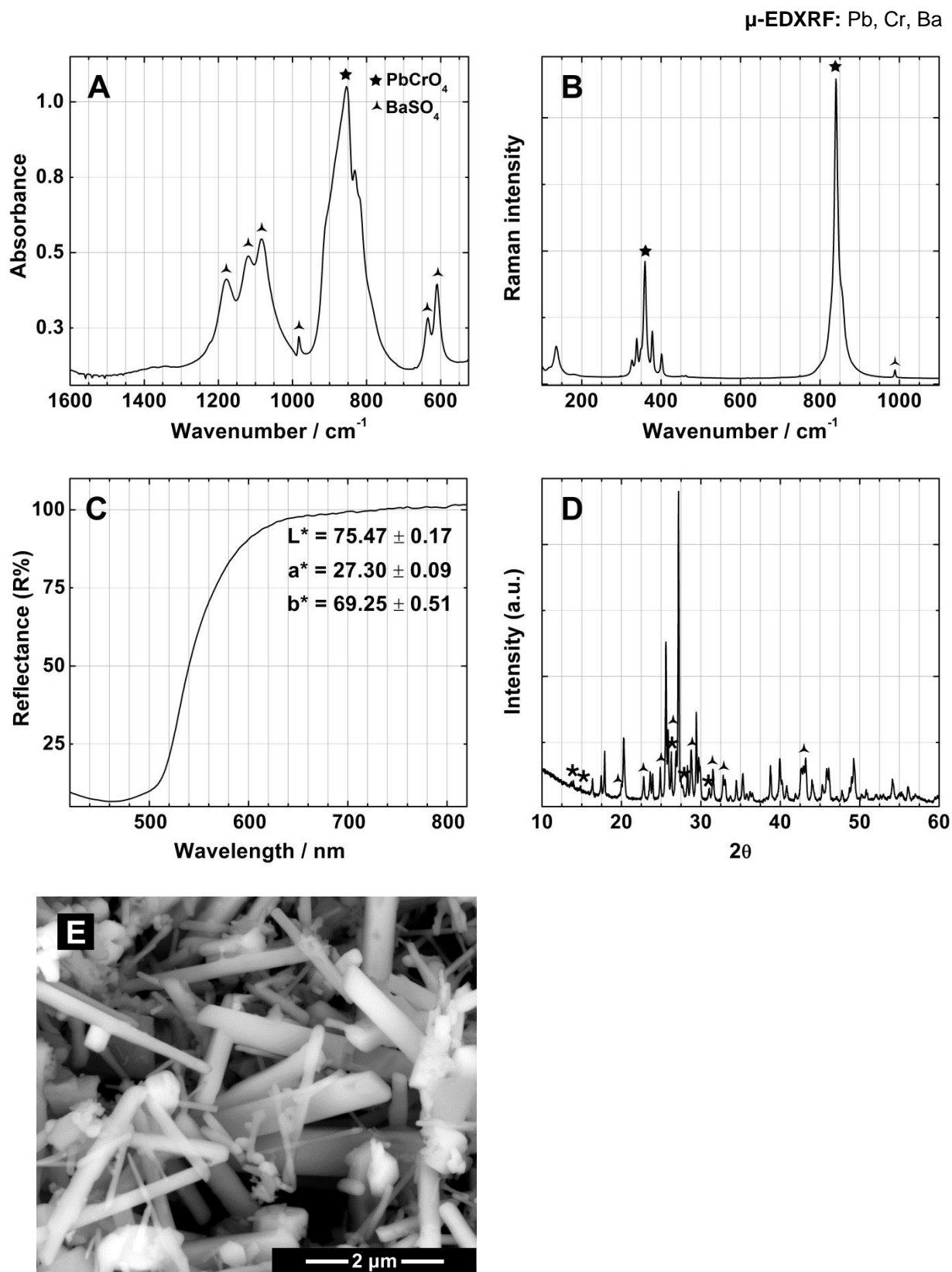


Figure X.3.3. M2a pigment reconstruction: elements detected by μ -EDXRF, representative **A**) infrared, **B**) μ -Raman, **C**) FORS spectra, **D**) diffraction pattern and **E**) SEM image; (\star) PbCrO_4 , (\blacktriangle) BaSO_4 and (\star) Pb_2CrO_5 .

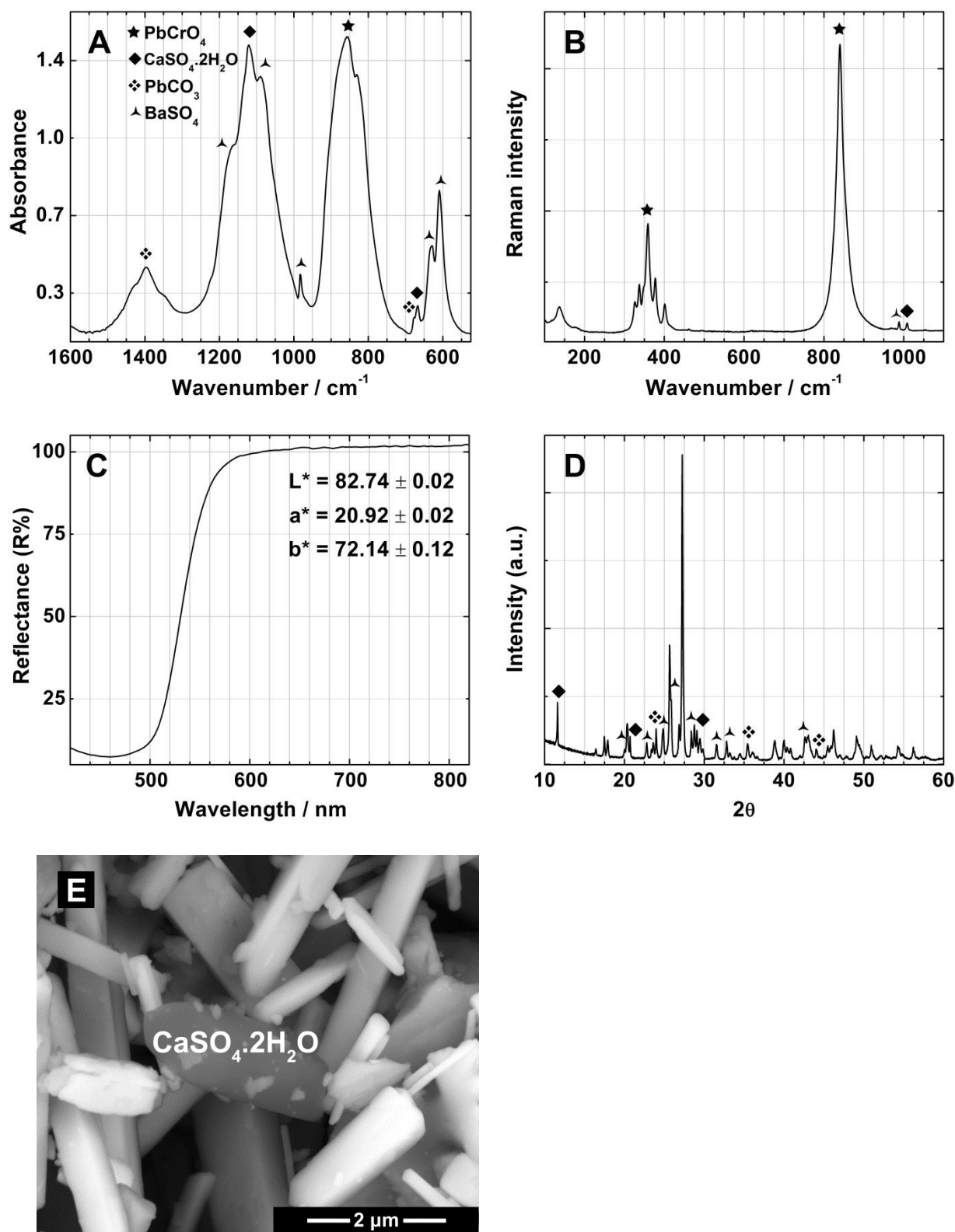


Figure X.3.4. D1a pigment reconstruction: elements detected by μ -EDXRF, representative **A**) infrared, **B**) μ -Raman, **C**) FORS spectra, **D**) diffraction pattern and **E**) SEM image; (\star) PbCrO₄, (\blacklozenge) CaSO₄·2H₂O, (\blacktriangle) BaSO₄ and (\blacklozenge) PbCO₃.

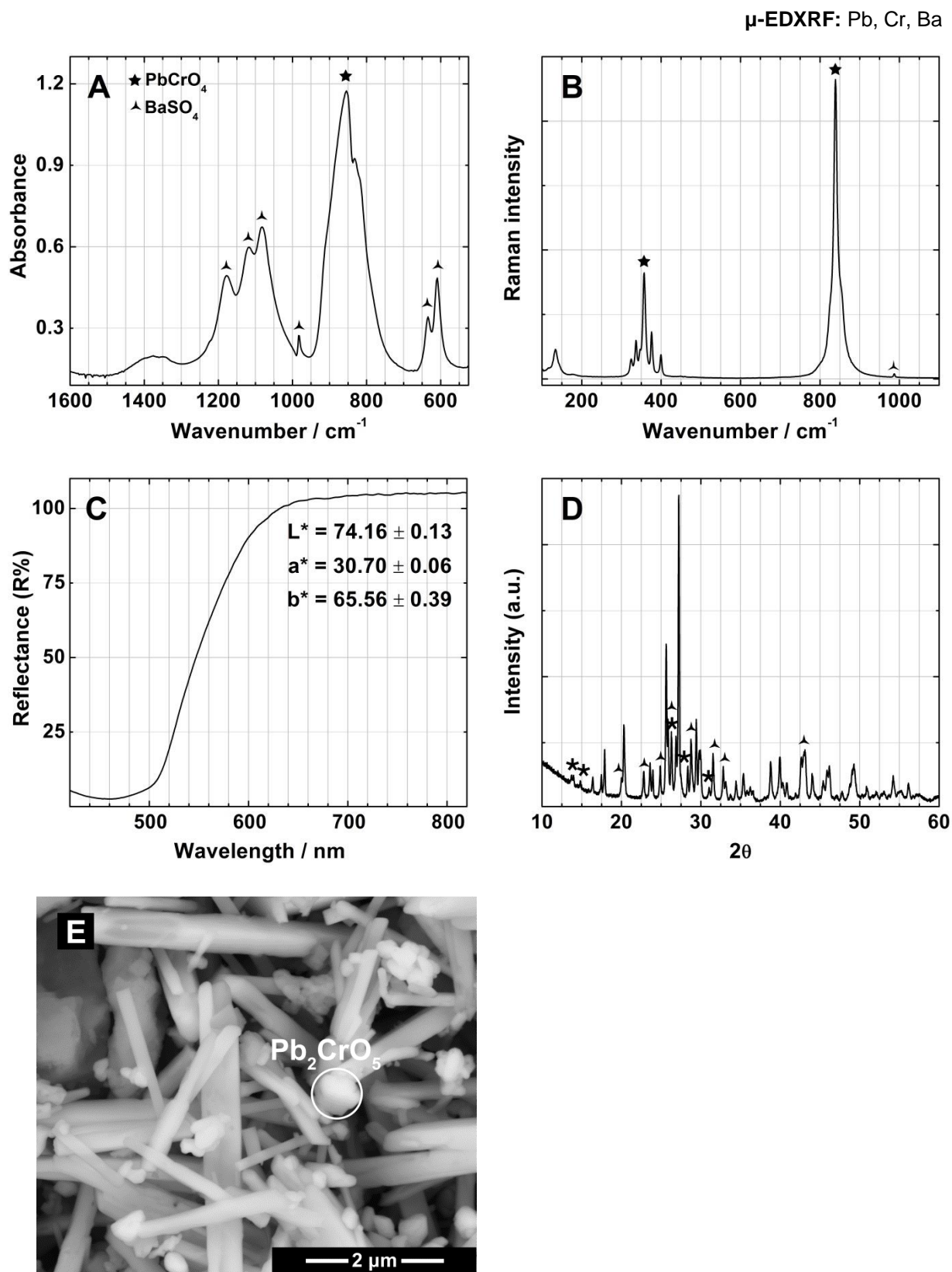


Figure X.3.5. D1b pigment reconstruction. elements detected by μ -EDXRF, representative **A**) infrared, **B**) μ -Raman, **C**) FORS spectra, **D**) diffraction pattern and **E**) SEM image; (\star) PbCrO_4 , (\blacktriangle) BaSO_4 and (\star) Pb_2CrO_5 .

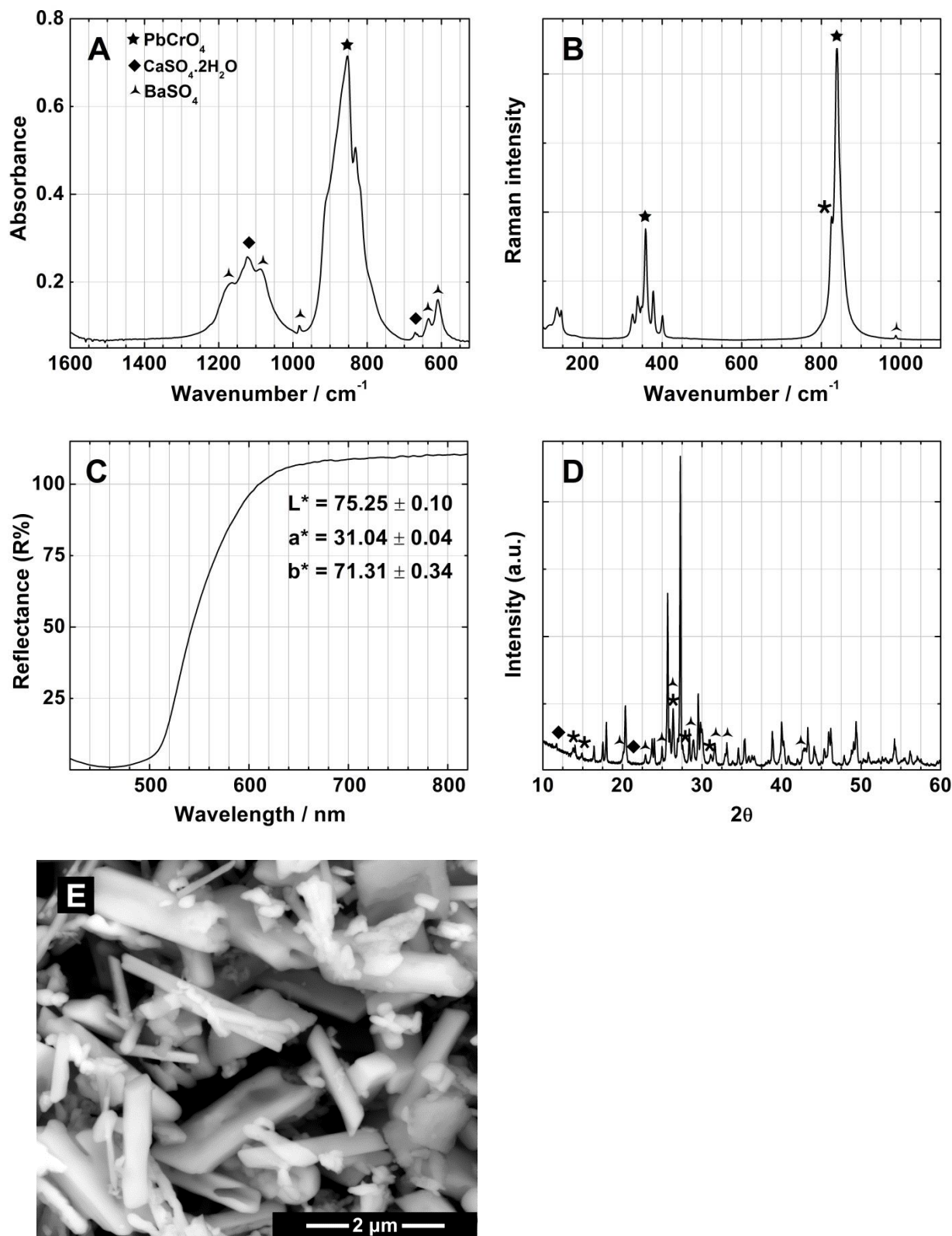


Figure X.3.6. D2a pigment reconstruction: elements detected by μ -EDXRF, representative **A**) infrared, **B**) μ -Raman, **C**) FORS spectra, **D**) diffraction pattern and **E**) SEM image; (\star) PbCrO_4 , (\blacklozenge) $\text{CaSO}_4 \cdot 2\text{H}_2\text{O}$, (\blacktriangle) BaSO_4 and (\star) Pb_2CrO_5 .

Appendix XI. Additional characterisation of the historic lead chromate paint tubes

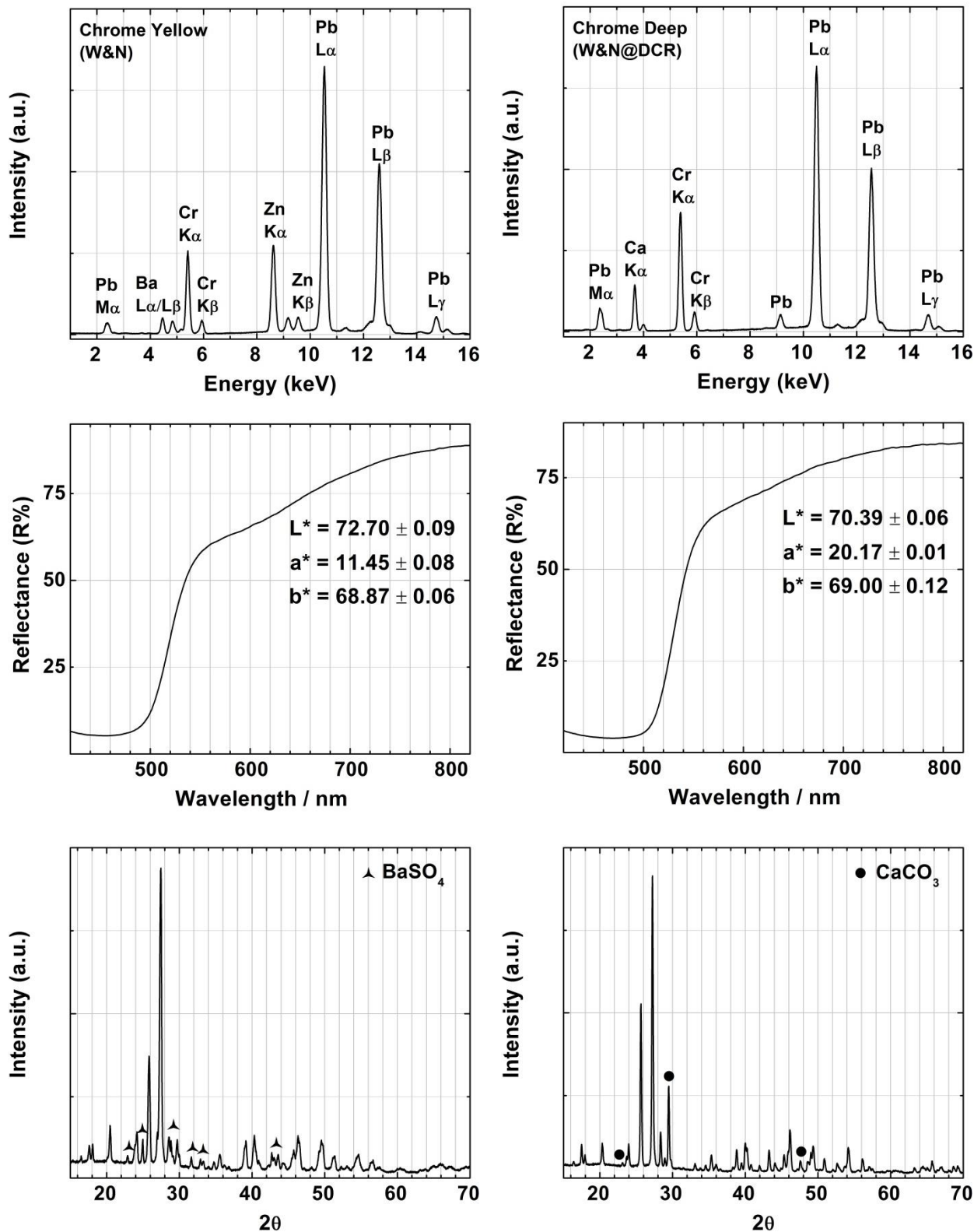


Figure XI.1. μ -EDXRF spectra, FORS spectra (acquired in paints applied on filter paper) and diffraction patterns of the W&N *Chrome Yellow* (left) and *Chrome Deep* (right) oil paint tubes (see Table 3.5, p. 55); (\blacktriangle) BaSO₄ and (\bullet) CaCO₃. μ -EDXRF and FORS spectra of the W&N *Chrome Deep* oil paint tube belonging to Columbano are similar to the one presented; no diffraction pattern was acquired due to the lack of quantity.

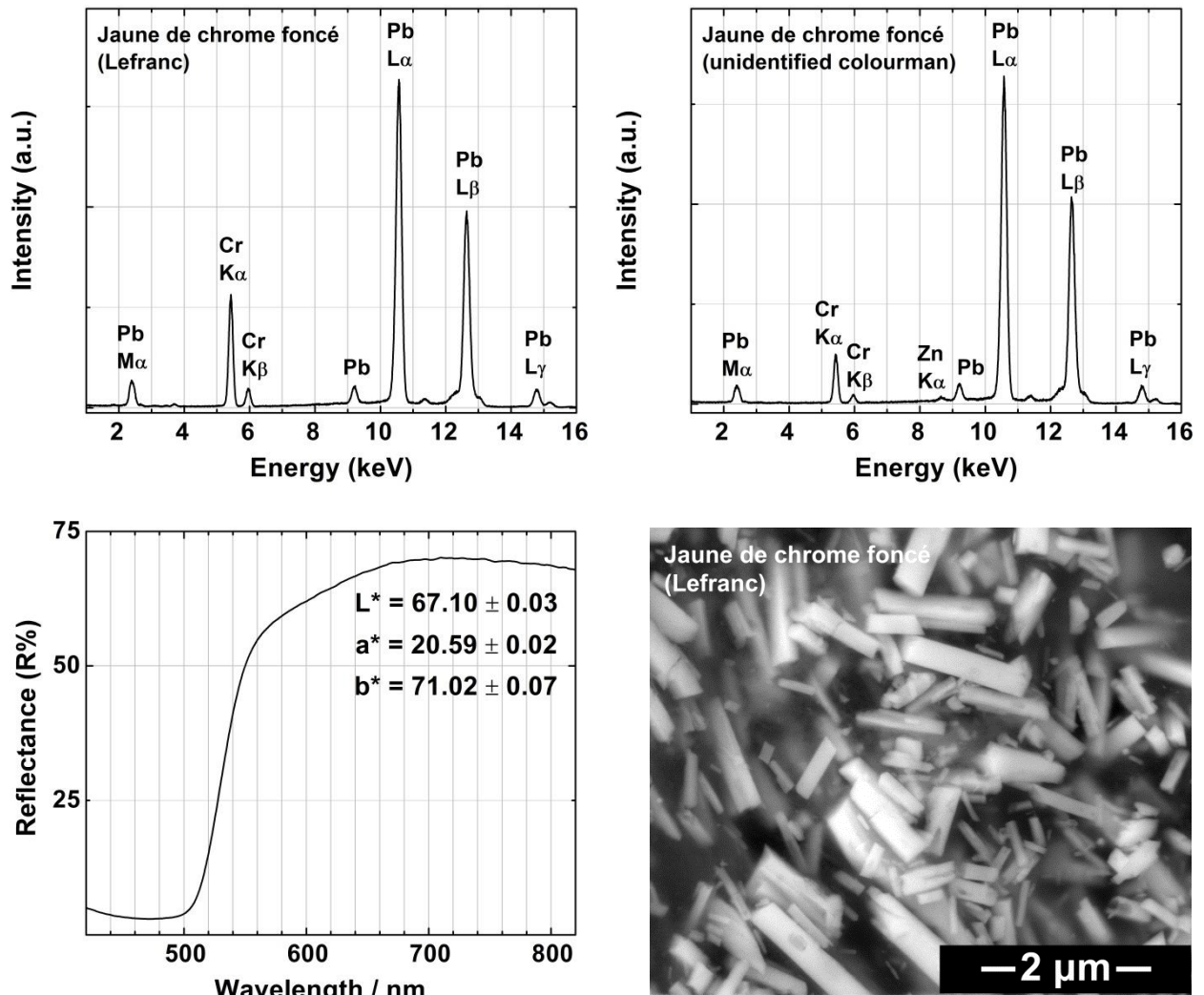

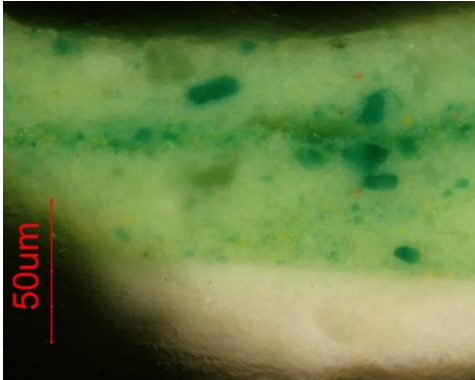
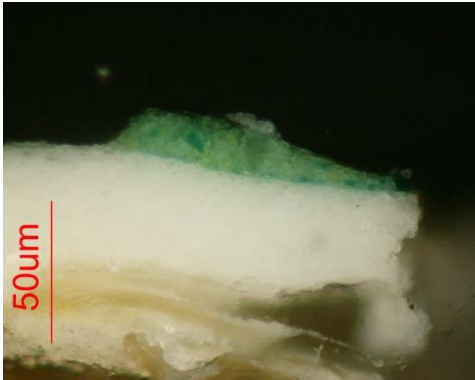


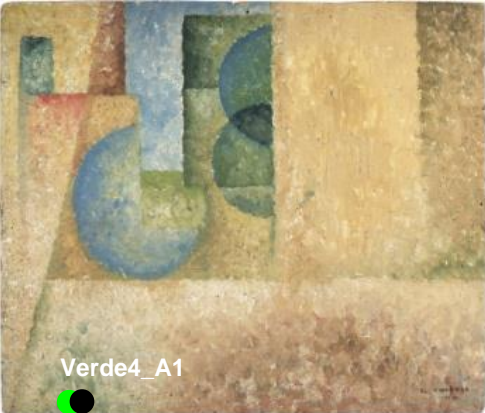
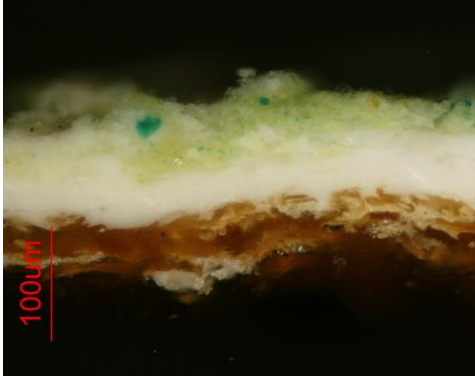

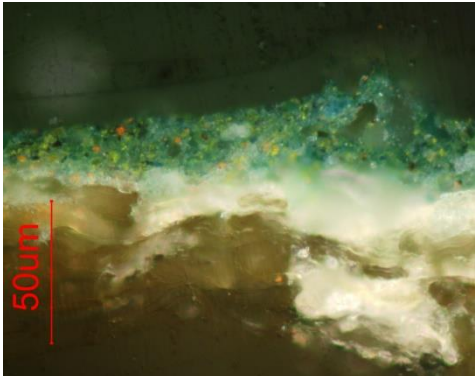
Figure XI.2. Top: μ -EDXRF spectra of Lefranc's *Jaune de Chrome foncé* and *Jaune de Chrome foncé - tempera farge* (unidentified colourman) paint tubes (Melo *et al.*, 2009). Bottom: FORS and SEM image of the Lefranc's *Jaune de Chrome foncé* oil paint tube (bottom) (see Table 3.5, p. 55). No diffraction pattern was acquired due to the lack of quantity.

Appendix XII. μ -Raman characterisation of cross-sections from selected paintings by Amadeo

The identification of the compounds was performed in accordance with the spectra and band assignments shown in Appendix VI.3 (p. 245).

Painting	Cross-sections (●)	<i>In situ</i> μ -EDXRF (●)	Compounds identified by μ -Raman (<i>on cross-section</i>)
 <p>VF_A3</p> <p>V4_A2</p> <p><i>Untitled</i>, c. 1914, 18 x 33 cm (Inv. 91P221, cat. n° P85) © FCG</p>	 <p>50um</p> <p>VF_A3</p>	<p>Pb, Ba, Cr, Fe, (Sr)</p>	<p>Green layer: Viridian ($\text{Cr}_2\text{O}_3 \cdot 2\text{H}_2\text{O}$) Chrome Yellow ($\text{PbCrO}_4$) Vermilion ($\text{HgS}$) Barytes ($\text{BaSO}_4$) Lead white ($2\text{PbCO}_3 \cdot \text{Pb}(\text{OH})_2$)</p> <p>Ground layer: $2\text{PbCO}_3 \cdot \text{Pb}(\text{OH})_2$</p>
	 <p>50um</p> <p>V4_A2</p>	<p>Pb, Cr, Fe, Ba, Cd*</p>	<p>Green layer: $\text{Cr}_2\text{O}_3 \cdot 2\text{H}_2\text{O}$ PbCrO_4 Goethite ($\alpha\text{-FeOOH}$) HgS BaSO_4</p> <p>Ground layer: $2\text{PbCO}_3 \cdot \text{Pb}(\text{OH})_2$</p>

* The detection of the element cadmium (Cd) by μ -EDXRF suggests the presence of the cadmium yellow (CdS) pigment, however its clear identification by μ -Raman was not possible.


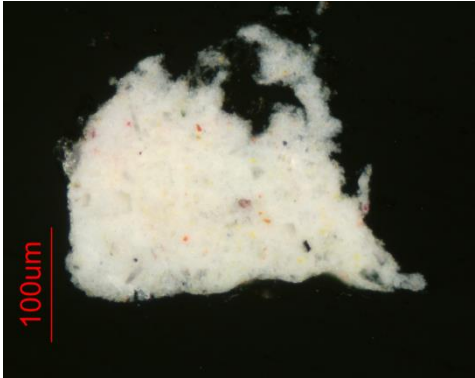
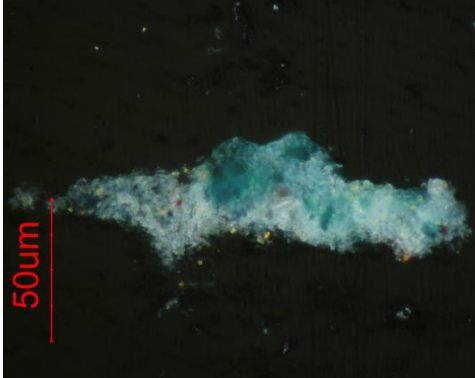
Painting	Cross-sections (●)	In situ μ-EDXRF (●)	Compounds identified by μ-Raman (<i>on cross-section</i>)
 <p>Verde4_A1</p>	 <p>Verde4_A1</p>	<p>Pb, Zn, Cr, Fe, Ba, Co, Cd*, (Sr)</p>	<p>Green layer: $\text{Cr}_2\text{O}_3 \cdot 2\text{H}_2\text{O}$ PbCrO_4 Cobalt yellow ($\text{K}_3[\text{Co}(\text{NO}_2)_6] \cdot 3\text{H}_2\text{O}$) Zinc white ($\text{ZnO}$) Strontium sulfate ($\text{SrSO}_4$) BaSO_4 $2\text{PbCO}_3 \cdot \text{Pb}(\text{OH})_2$</p> <p>Ground layer: $2\text{PbCO}_3 \cdot \text{Pb}(\text{OH})_2$</p>
 <p>Verde_Esc.A1</p>	 <p>Verde_Esc.A1</p>	<p>Pb, Fe, Cr, Ba, Ca*, Hg, Cd*</p>	<p>Green layer: Prussian blue ($\text{Fe}_4[\text{Fe}(\text{CN})_6]_3$) PbCrO_4 $\text{Cr}_2\text{O}_3 \cdot 2\text{H}_2\text{O}$ Ultramarine blue ($3\text{Na}_2\text{O} \cdot 3\text{Al}_2\text{O}_3 \cdot 6\text{SiO}_2 \cdot 2\text{Na}_2\text{S}$) HgS Carbon black (C) $\text{BaSO}_4 + \text{SrSO}_4$ $2\text{PbCO}_3 \cdot \text{Pb}(\text{OH})_2$</p>

Untitled, 1914, 26.8 x 32.9 cm (Inv. 91P224, cat. n° P88) © FCG

Untitled, c. 1914, 18.7 x 12.5 cm (Inv. 91P220, cat. n° P140) © FCG

* The detection of the element cadmium (Cd) by μ-EDXRF suggests the presence of the cadmium yellow (CdS) pigment, however its clear identification by μ-Raman was not possible.


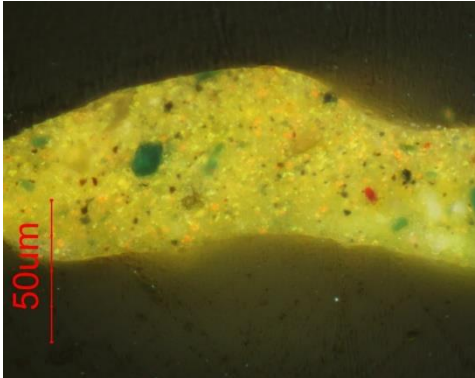
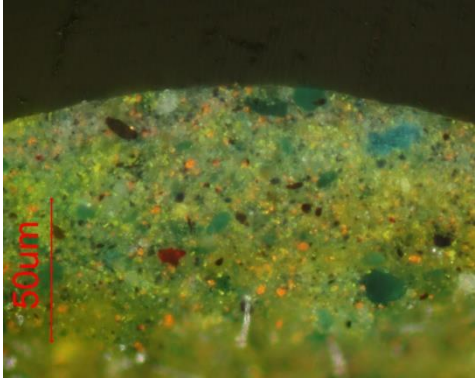
‡ The detection of the element calcium (Ca) by μ-EDXRF is likely due to the cardboard composition.

Painting	Cross-sections (●)	In situ μ-EDXRF (●)	Compounds identified by μ-Raman (on cross-section)
		Pb, Ba, Sr, Fe, Ca [‡] , (Co)	White layer: $2\text{PbCO}_3 \cdot \text{Pb}(\text{OH})_2$ BaSO_4 Chromium oxide (Cr_2O_3) PbCrO_4 HgS
		Pb, Ba, Cr, Sr, Fe, Ca [‡] , Co [#] , (Zn)	Blue layer: $3\text{Na}_2\text{O} \cdot 3\text{Al}_2\text{O}_3 \cdot 6\text{SiO}_2 \cdot 2\text{Na}_2\text{S}$ $\text{Cr}_2\text{O}_3 \cdot 2\text{H}_2\text{O}$ PbCrO_4 BaSO_4 $2\text{PbCO}_3 \cdot \text{Pb}(\text{OH})_2$

Untitled, c. 1914, 18.7 x 12.8 cm (Inv. CP0143, cat. n° P122) © FCG

[‡] The detection of the element calcium (Ca) by μ-EDXRF is likely due to the cardboard composition.

[#] The detection of the element cobalt (Co) by μ-EDXRF suggests the presence of a cobalt-based pigment, however its clear identification by μ-Raman was not possible.


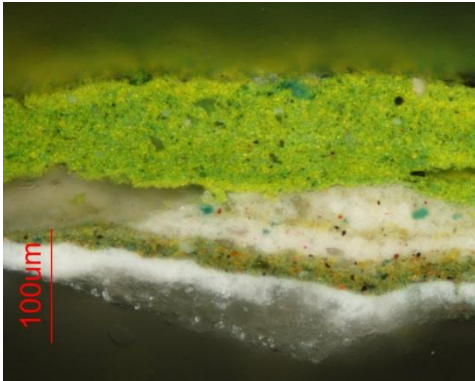
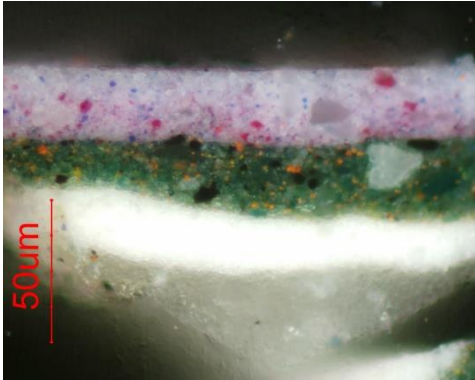
Painting	Cross-sections (●)	In situ μ-EDXRF (●)	Compounds identified by μ-Raman (on cross-section)
		Pb, Fe, Cr, Ba, Hg, Co [#] , Zn, Cd [*]	Green layer: $\text{Cr}_2\text{O}_3 \cdot 2\text{H}_2\text{O}$ PbCrO₄ $3\text{Na}_2\text{O} \cdot 3\text{Al}_2\text{O}_3 \cdot 6\text{SiO}_2 \cdot 2\text{Na}_2\text{S}$ HgS C Chalk (CaCO_3) BaSO_4 $2\text{PbCO}_3 \cdot \text{Pb}(\text{OH})_2$
	Verde_claro1_A1		Cr, Pb, Fe, Hg, Ba, Cd [*] , Zn, Co [#]
Verde_Esc.A1			

Untitled, c. 1914, 17.4 x 13.3 cm (Inv. 87P158, cat. n° P138) © FCG

[#] The detection of the element cobalt (Co) by μ-EDXRF suggests the presence of a cobalt-based pigment, however its clear identification by μ-Raman was not possible.

^{*} The detection of the element cadmium (Cd) by μ-EDXRF suggests the presence of the cadmium yellow (CdS) pigment, however its clear identification by μ-Raman was not possible.

Painting	Cross-sections (●)	In situ μ-EDXRF (●)	Compounds identified by μ-Raman (<i>on cross-section</i>)
 <p data-bbox="360 1082 887 1137"><i>Janelas do Pescador</i>, c. 1915-16, 27.4 x 34.8 cm (Inv. 77P16, cat. n° P168) © FCG</p>	 <p data-bbox="974 730 1010 751">Az1</p>	Pb, Zn, Fe, Cr, Ba, Co, Cd, (Hg)	<p data-bbox="1700 288 1827 309">Blue layer:</p> <p data-bbox="1700 328 1995 352">$3\text{Na}_2\text{O}\cdot 3\text{Al}_2\text{O}_3\cdot 6\text{SiO}_2\cdot 2\text{Na}_2\text{S}$</p> <p data-bbox="1700 371 1850 395">$\text{Fe}_4[\text{Fe}(\text{CN})_6]_3$</p> <p data-bbox="1700 424 1843 445">Green layer:</p> <p data-bbox="1700 464 1850 488">$\text{Fe}_4[\text{Fe}(\text{CN})_6]_3$</p> <p data-bbox="1700 507 1827 531">$\text{Cr}_2\text{O}_3\cdot 2\text{H}_2\text{O}$</p> <p data-bbox="1700 550 1805 571">$\alpha\text{-FeOOH}$</p> <p data-bbox="1700 590 1861 614">$\text{HgS} + \text{PbCrO}_4$</p> <p data-bbox="1700 633 1778 654">BaSO_4</p> <p data-bbox="1700 673 1888 697">$2\text{PbCO}_3\cdot \text{Pb}(\text{OH})_2$</p> <p data-bbox="1700 726 1861 746">Ground layer:</p> <p data-bbox="1700 766 1778 786">BaSO_4</p>
	 <p data-bbox="974 1289 1010 1310">B1</p>		Pb, Ba, Sr, Zn

Painting	Cross-sections (●)	In situ μ-EDXRF (●)	Compounds identified by μ-Raman (<i>on cross-section</i>)
		Pb, Cr, Ba, Fe, Co, Sr, Ca, Zn, Hg	<p>Green layer: $3\text{Na}_2\text{O} \cdot 3\text{Al}_2\text{O}_3 \cdot 6\text{SiO}_2 \cdot 2\text{Na}_2\text{S}$ $\text{Fe}_4[\text{Fe}(\text{CN})_6]_3$ PbCrO₄ + BaSO₄ + SrSO₄</p> <p>White layer: $2\text{PbCO}_3 \cdot \text{Pb}(\text{OH})_2 + \text{Cr}_2\text{O}_3 \cdot 2\text{H}_2\text{O}$ Hematite ($\alpha\text{-Fe}_2\text{O}_3$) Maghemite ($\gamma\text{-Fe}_2\text{O}_3$) PbCrO₄ + $\text{Fe}_4[\text{Fe}(\text{CN})_6]_3$</p> <p>Green layer: $3\text{Na}_2\text{O} \cdot 3\text{Al}_2\text{O}_3 \cdot 6\text{SiO}_2 \cdot 2\text{Na}_2\text{S}$ $\text{Fe}_4[\text{Fe}(\text{CN})_6]_3 + \text{Cr}_2\text{O}_3 \cdot 2\text{H}_2\text{O}$ HgS + PbCrO₄ + BaSO₄ $2\text{PbCO}_3 \cdot \text{Pb}(\text{OH})_2$</p> <p>Ground layer: BaSO₄</p>
			Pb, Zn, Ba, Fe, Hg, Cr, Co

Janelas do Pescador, c. 1915-16, 27.4 x 34.8 cm
(Inv. 77P16, cat. n° P168) © FCG

Appendix XIII. Characterisation of yellow and green samples from selected paintings by Amadeo

The characterisation of all samples was based on the data shown in Appendix VI (p. 243).

XIII.1. Quadro G (cat. n° P41)



Figure XIII.1.1. Amadeo de Sousa-Cardoso painting: *Gemälde G / Quadro G*, c.1912, 51 x 29.5 cm (Inv. 77P2, cat. n° P41, Freitas, 2008, p. 182) © FCG. Analysis areas: μ-EDXRF (●), μ-sampling (●) and cross-sections (●).

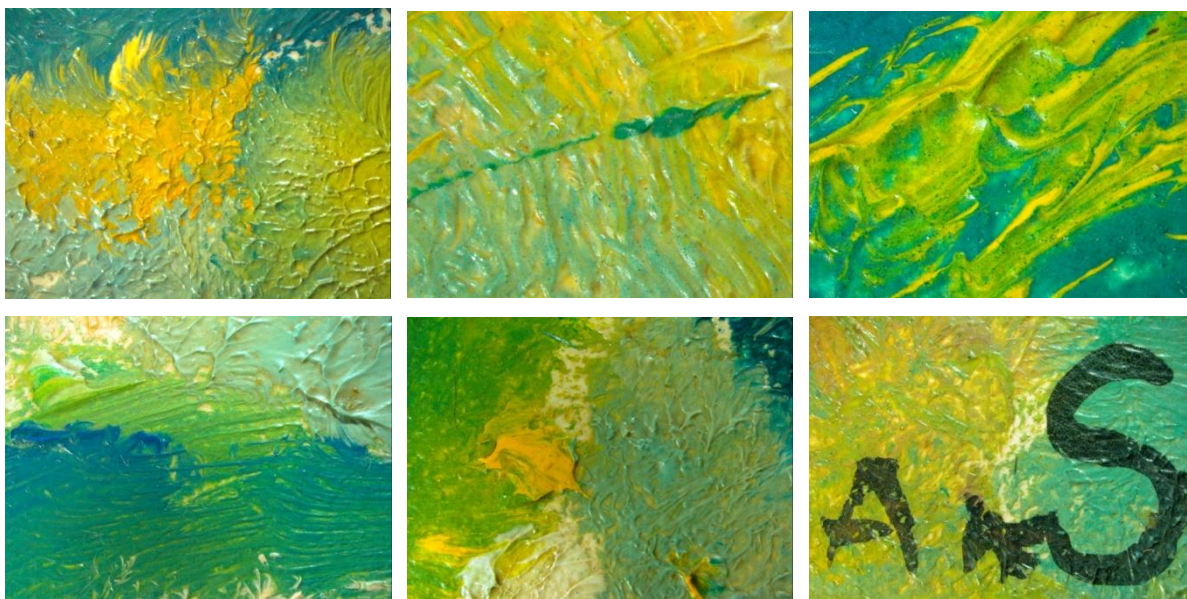


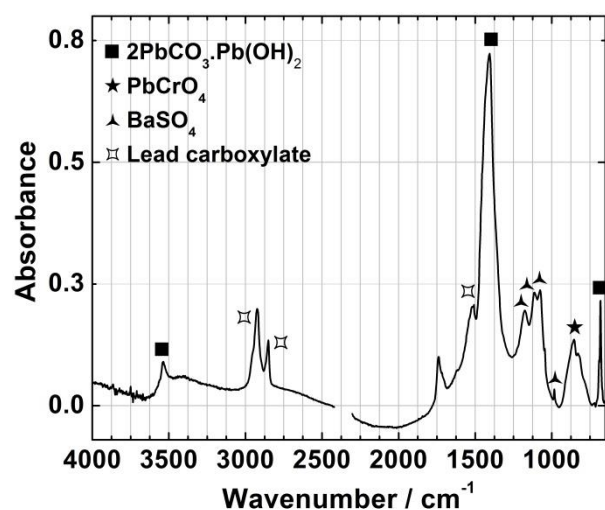
Figure XIII.1.2. Photomicrographs (7x to 25x) of Amadeo de Sousa-Cardoso painting: *Gemälde G / Quadro G*, c.1912 (Inv. 77P2, cat. n° P41).

● **Multi-analytical characterisation of yellow micro-sample μ 5**

μ -EDXRF: Pb, Cu, Ba, Cr, Sr, Fe, Co, As, Ca, Zn

μ -FTIR

Compounds identified by μ -Raman



Compounds identified by μ -Raman:

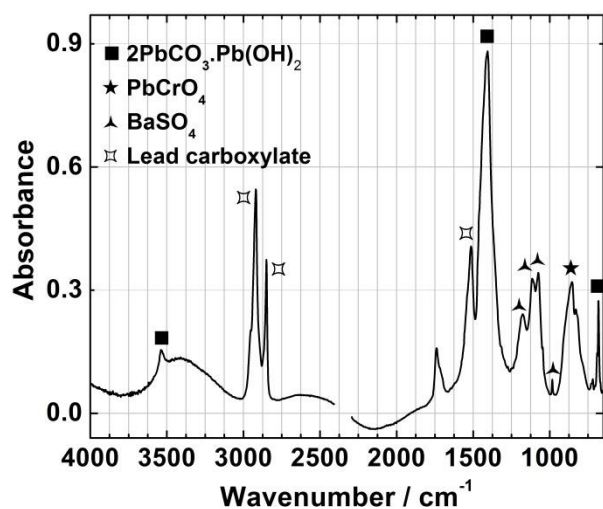
- PbCrO_4
- BaSO_4
- $2\text{PbCO}_3 \cdot \text{Pb(OH)}_2$

● Multi-analytical characterisation of yellow micro-sample $\mu 1$ and cross-section O1

μ -EDXRF: Pb, Cr, Ba, Zn, Cu, Ca, Fe, Sr, (Co)

μ -FTIR

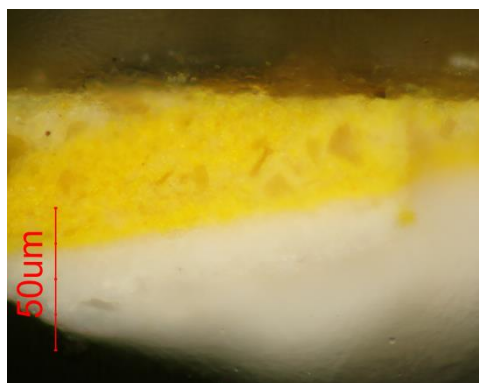
Compounds identified by μ -Raman



PbCrO₄
BaSO₄
2PbCO₃·Pb(OH)₂
HgS

MO of cross-section O1

Compounds identified by μ -Raman



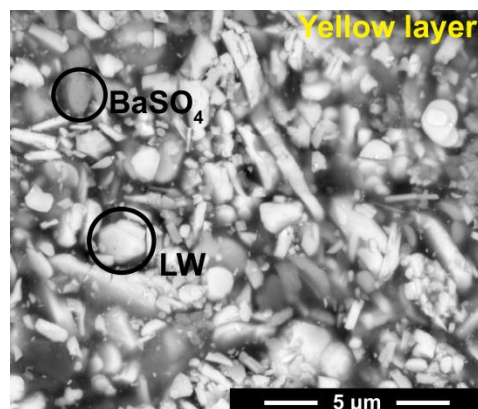
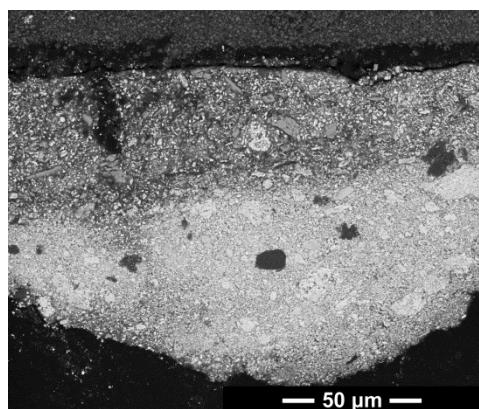
Yellow layer:

PbCrO₄
BaSO₄
2PbCO₃·Pb(OH)₂

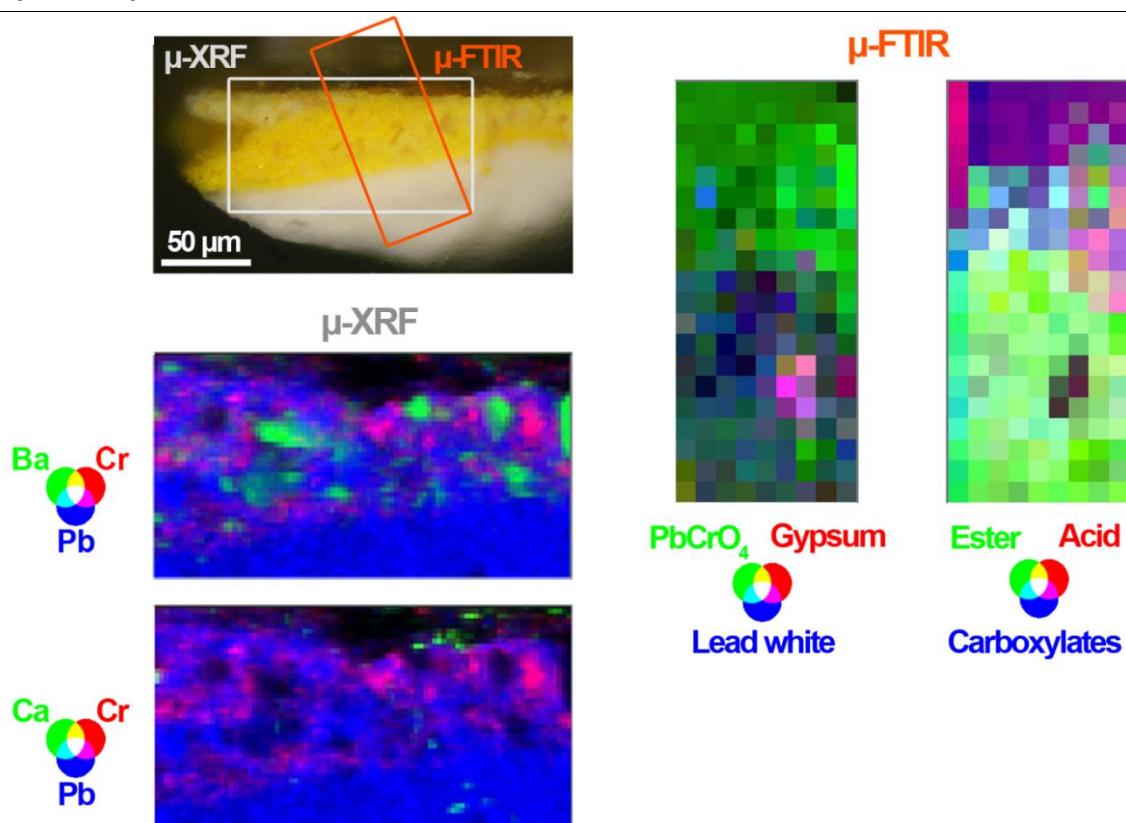
Ground layer:

2PbCO₃·Pb(OH)₂

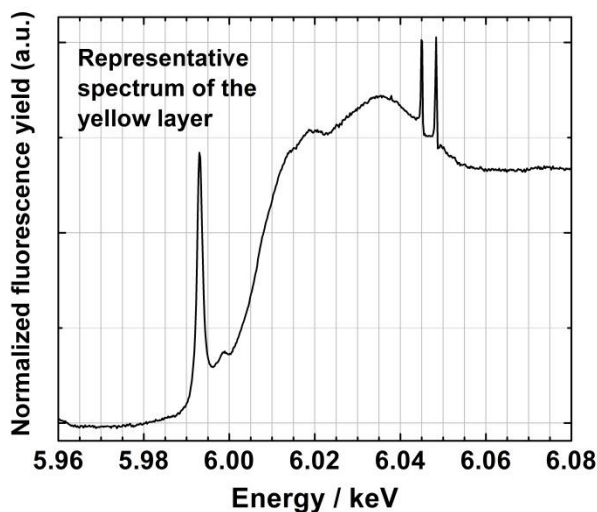
SEM-EDS



SR μ -XRF & μ -FTIR



SR Cr K-edge μ -XANES



In the top yellow layer, SEM-EDS, SR μ -XRF and μ -FTIR complementary analysis show a high content of lead white (most probably obtained by the stack process) and barytes with a small content of lead chromate and chalk particles. SR μ -FTIR mapping also shows a higher content of acid and metal carboxylates, most probably lead based, at the surface of the cross-section. However, SR μ -XRF mapping at different energies (5.993 and 6.1 keV) determined that no degradation via Cr^{6+} reduction to Cr^{3+} has occurred in this sample.

SEM-EDS analysis identified lead chromate rod-like particles with different dimensions, between 0.4 and 2.5 μ m in length and approximately 0.3 μ m in width.

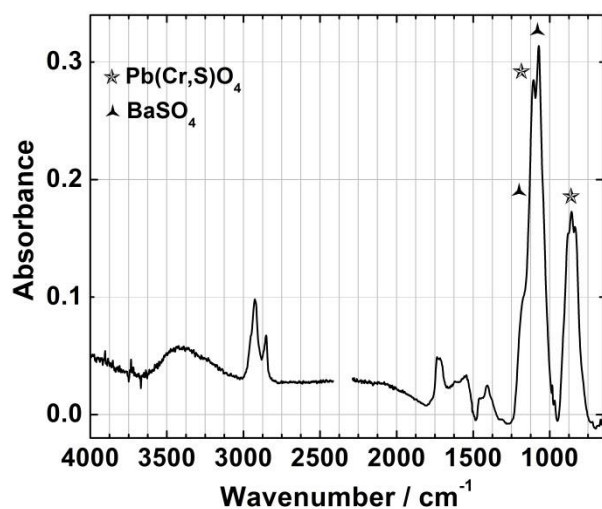
The white ground layer is composed by a high content of lead white (probably obtained by the stack process) together with a small content of chalk and gypsum particles.

● Multi-analytical characterisation of yellow micro-sample $\mu 2$

μ -EDXRF: Pb, Cr, Ba, Zn, Cu, Ca, Fe, Sr, (Co)

μ -FTIR

Compounds identified by μ -Raman



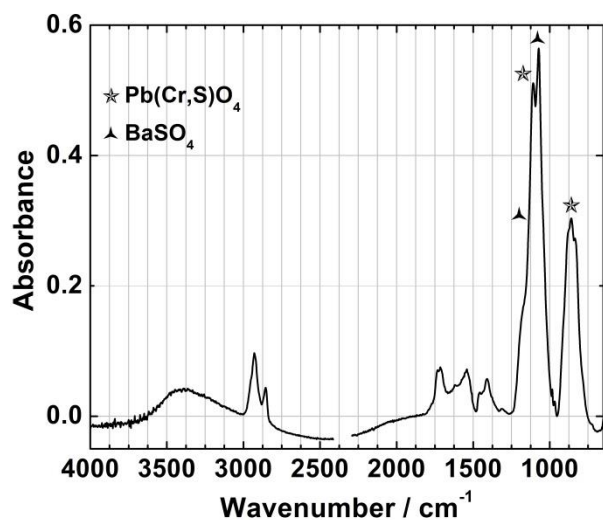
$\text{PbCr}_{1-x}\text{S}_x\text{O}_4$
 BaSO_4

● Multi-analytical characterisation of yellow micro-sample $\mu 3$

μ -EDXRF: Pb, Cr, Ba, Fe, Co, Ca, Zn

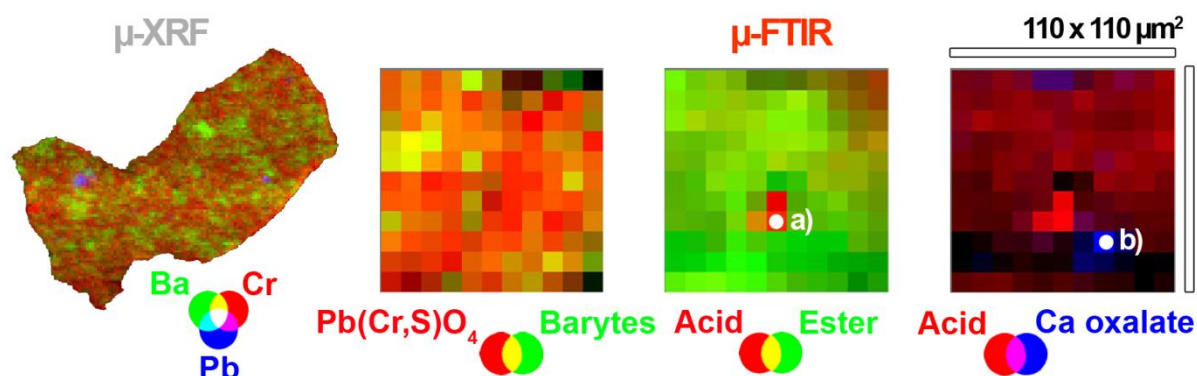
μ -FTIR

Compounds identified by μ -Raman

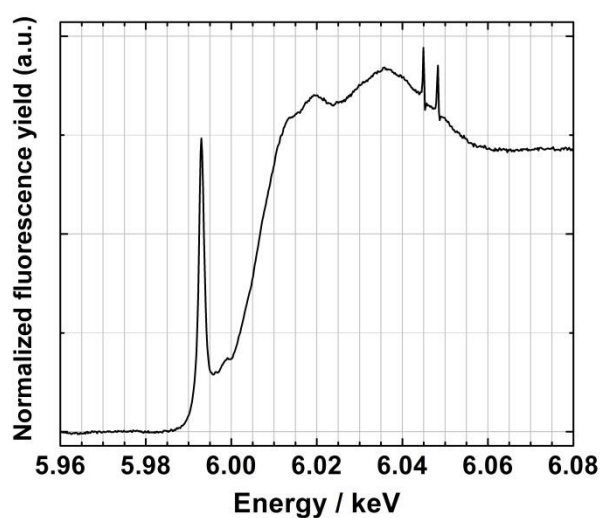


$\text{PbCr}_{1-x}\text{S}_x\text{O}_4$
 BaSO_4

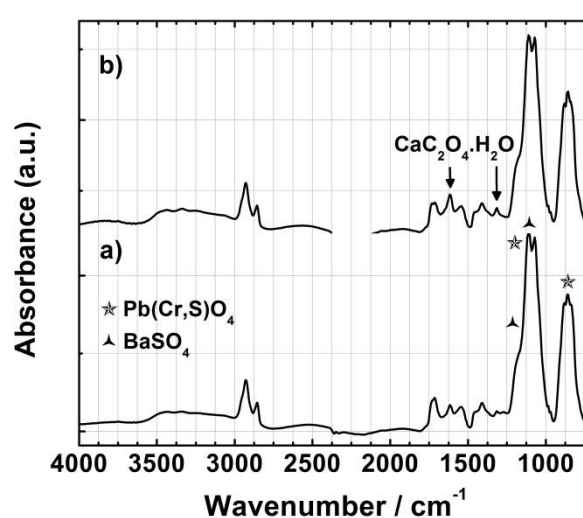
SR μ -XRF & μ -FTIR



SR Cr K-edge μ -XANES



SR μ -FTIR



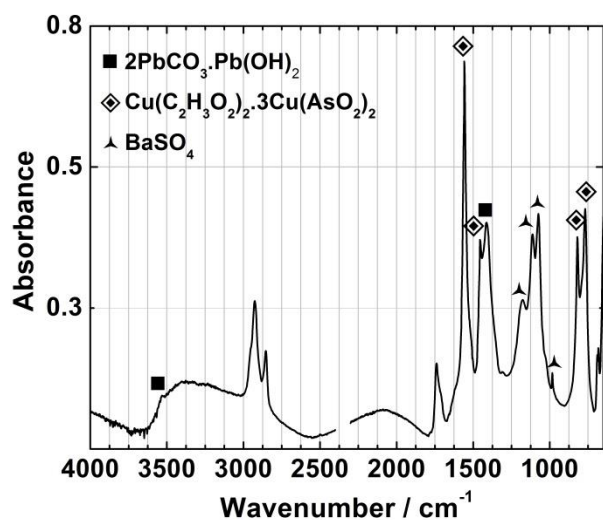
SR μ -XRF and SR μ -XANES analysis was performed in a fragment of the yellow μ -sample analysed by μ -FTIR. A mixture of mixed crystals of lead chromate and lead sulfate together with barytes was detected. SR μ -FTIR mapping also shows a small area (a) where a higher content of acid is detected and near it the presence of calcium oxalate monohydrate, CaC₂O₄·H₂O (b). However, SR μ -XRF mapping at different energies (5.993 and 6.1 keV) determined that no degradation via Cr⁶⁺ reduction to Cr³⁺ has occurred in this sample.

● Multi-analytical characterisation of green micro-sample $\mu 6$ and cross-section V5

μ -EDXRF: Pb, Cu, As, Ba, Cr, Sr, Fe, Ca

μ -FTIR

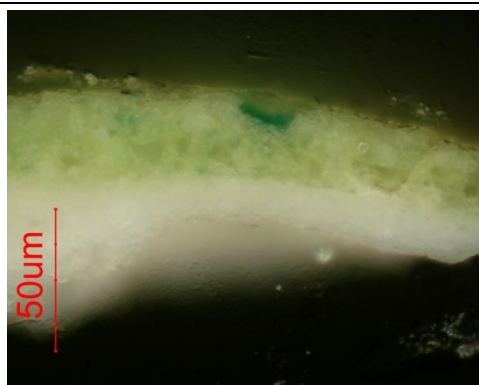
Compounds identified by μ -Raman



Emerald green ($\text{Cu}(\text{C}_2\text{H}_3\text{O}_2)_2 \cdot 3\text{Cu}(\text{AsO}_2)_2$)
 PbCrO_4
 BaSO_4
 $2\text{PbCO}_3 \cdot \text{Pb}(\text{OH})_2$

MO of cross-section V5

Compounds identified by μ -Raman



Green layer:
 $\text{Cu}(\text{C}_2\text{H}_3\text{O}_2)_2 \cdot 3\text{Cu}(\text{AsO}_2)_2$
 $\text{PbCr}_{1-x}\text{S}_x\text{O}_4$
 BaSO_4
 $2\text{PbCO}_3 \cdot \text{Pb}(\text{OH})_2$

Ground layer:
 $2\text{PbCO}_3 \cdot \text{Pb}(\text{OH})_2$

XIII.2. Untitled (*O Jockey*, cat. n° P58)

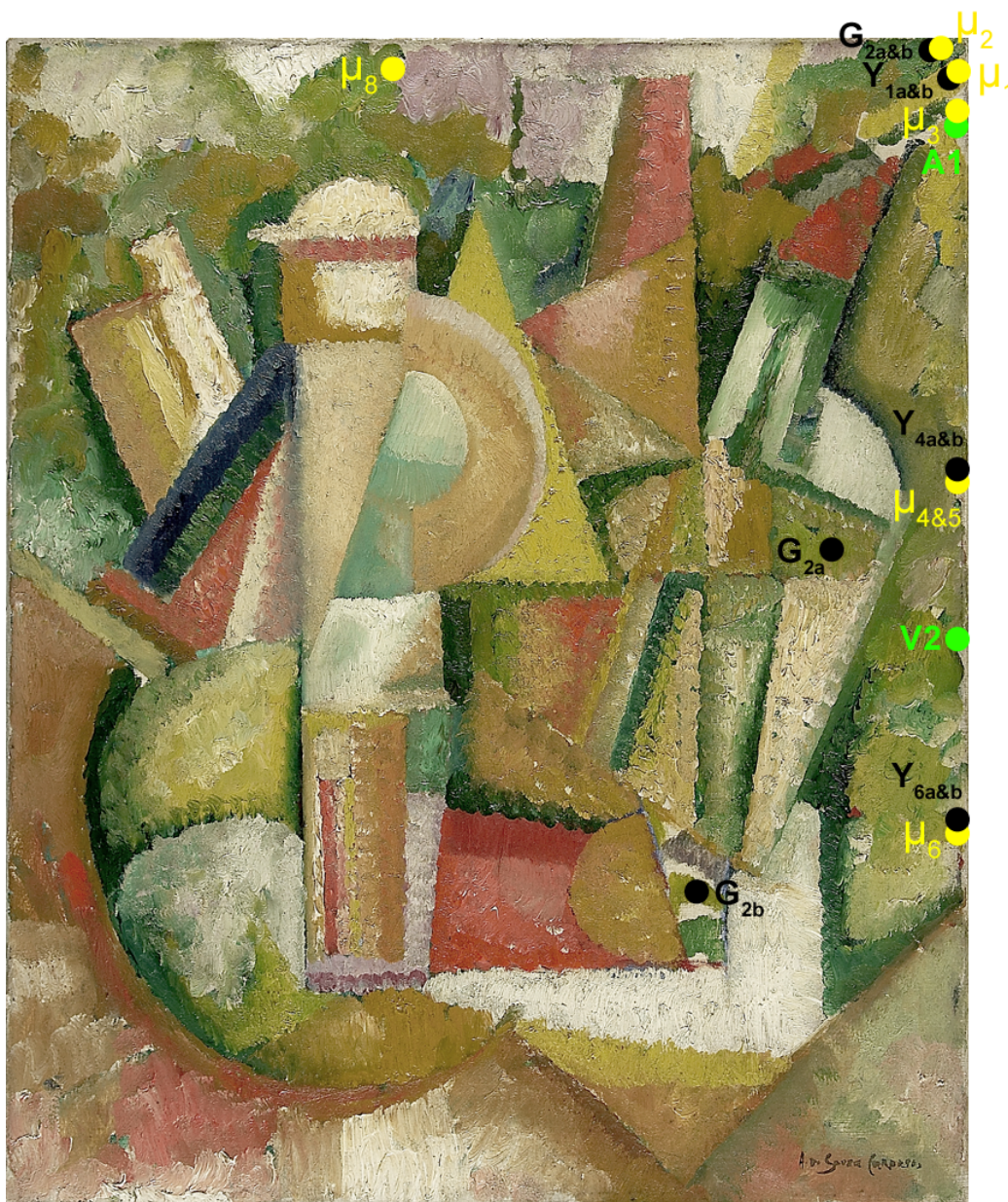


Figure XIII.2.1. Amadeo de Sousa-Cardoso painting: *Untitled, O Jockey*, c.1913, 61 x 50 cm (Inv. 77P5, cat. n° P58, Freitas, 2008, p. 209) © FCG. Analysis areas: μ-EDXRF (●), μ-sampling (●) and cross-sections (●).

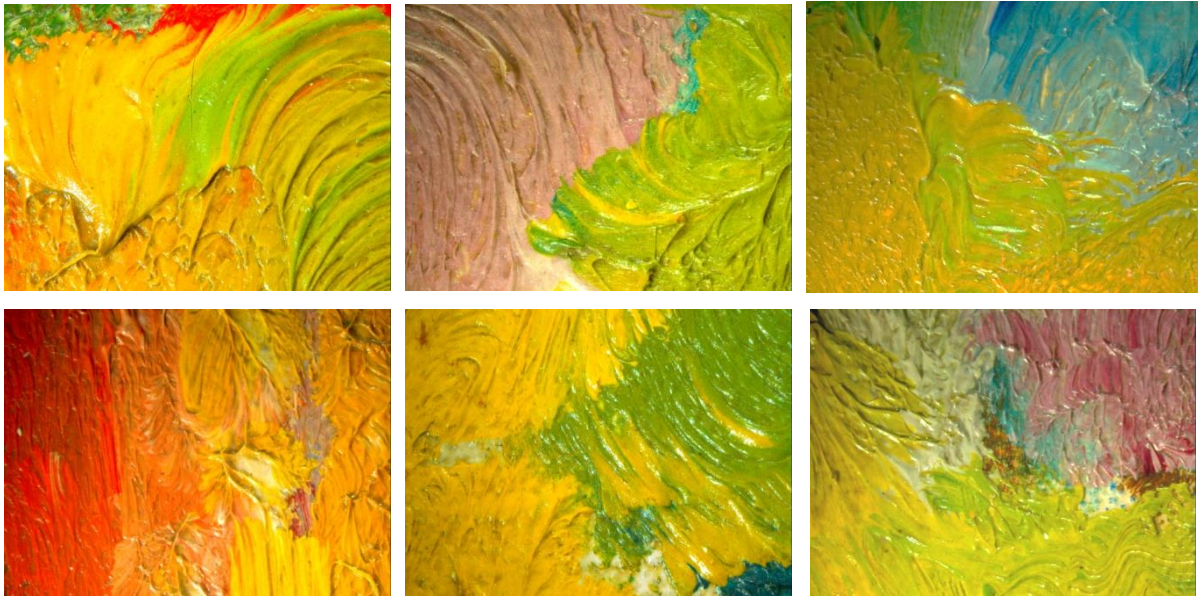


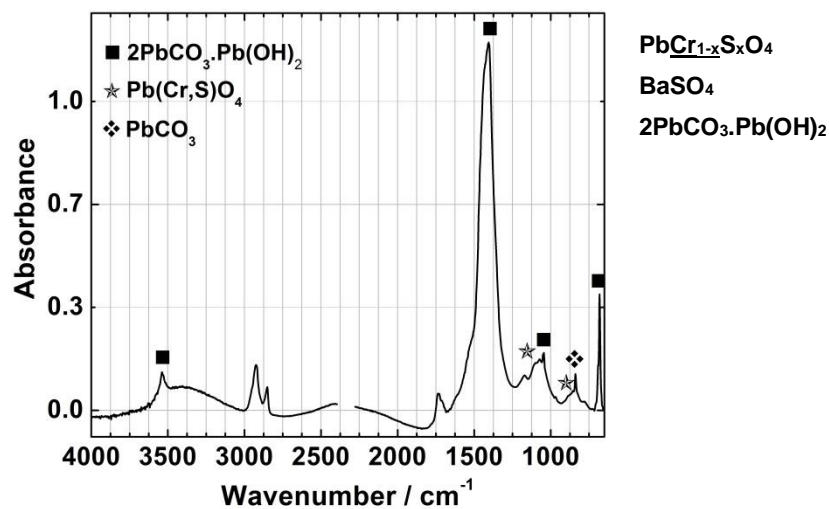
Figure XIII.2.2. Photomicrographs (10x) of Amadeo de Sousa-Cardoso painting: *Untitled, O Jockey*, c.1913 (Inv. 77P5, cat. n° P58).

● **Multi-analytical characterisation of yellow micro-sample μ 1**

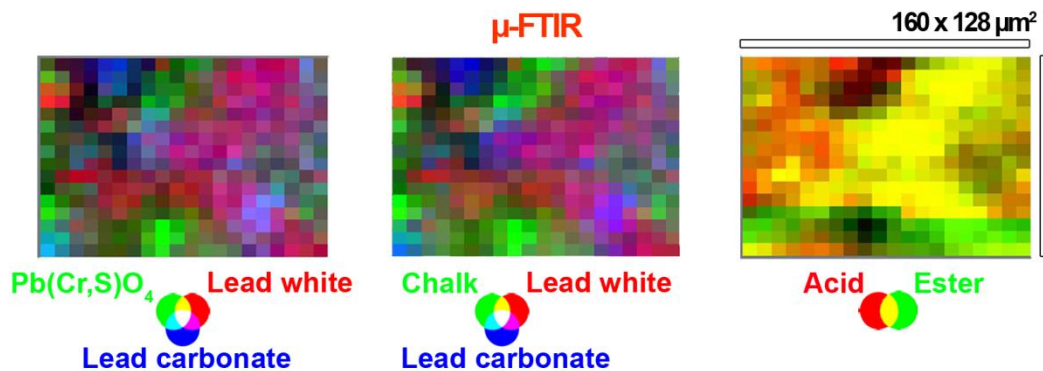
μ -EDXRF: Pb, Cr, Ba, Zn, Ca, Fe

μ -FTIR

Compounds identified by μ -Raman



SR μ -FTIR

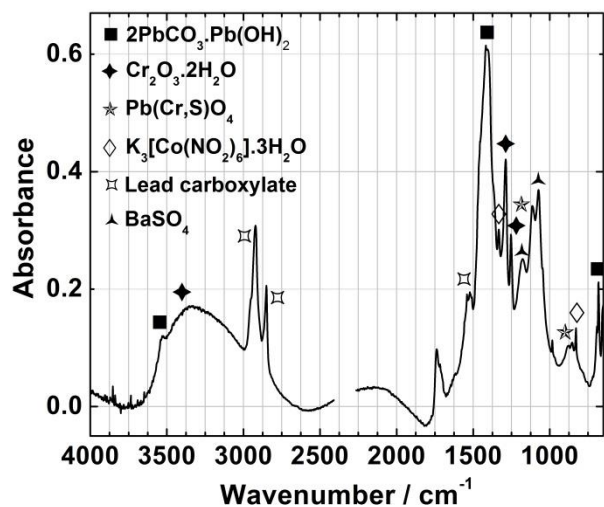


● Multi-analytical characterisation of green micro-sample $\mu 2$

μ -EDXRF: Pb, Cr, Ba, Co, Fe, Ca, Zn, Cu

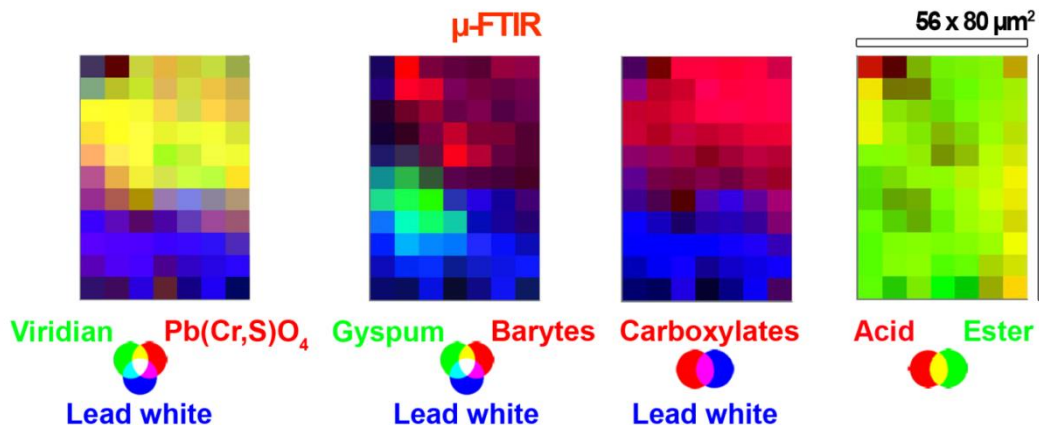
μ -FTIR

Compounds identified by μ -Raman



- Compounds identified by μ -Raman:
- $\text{Cr}_2\text{O}_3 \cdot 2\text{H}_2\text{O}$
 - $\text{PbCr}_{1-x}\text{S}_x\text{O}_4$
 - BaSO_4
 - $2\text{PbCO}_3 \cdot \text{Pb(OH)}_2$
 - $\text{K}_3[\text{Co(NO}_2)_6] \cdot 3\text{H}_2\text{O}$

SR μ -FTIR

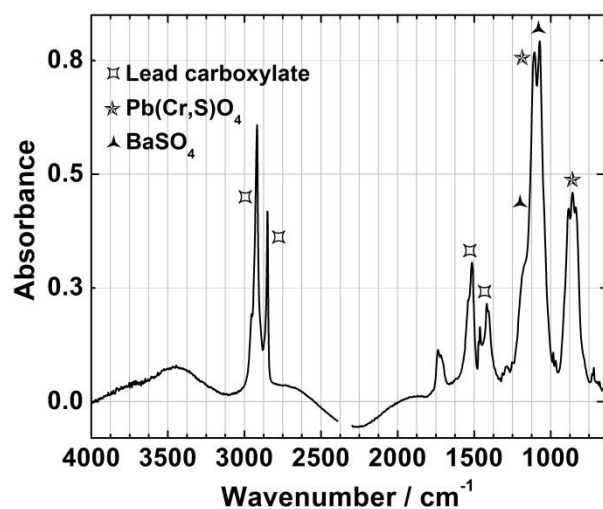


● Multi-analytical characterisation of yellow micro-sample $\mu 3$ and cross-section A1

μ -EDXRF: Pb, Cr, Ba, Zn, Ca, Fe

μ -FTIR

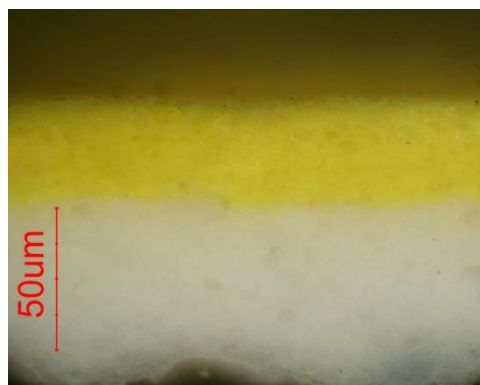
Compounds identified by μ -Raman



$\text{PbCr}_{1-x}\text{S}_x\text{O}_4$
 BaSO_4
 $2\text{PbCO}_3 \cdot \text{Pb}(\text{OH})_2$
 PbCO_3

MO of cross-section A1

Compounds identified by μ -Raman



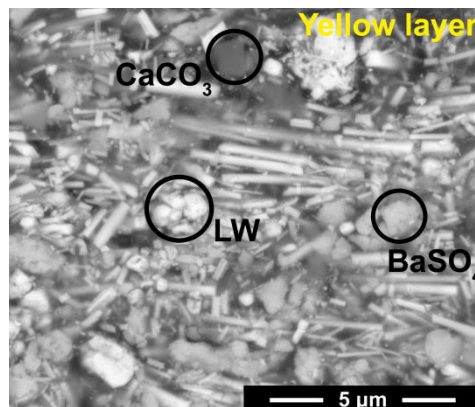
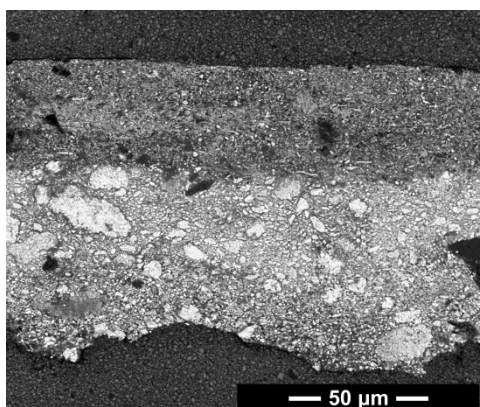
Yellow layer:

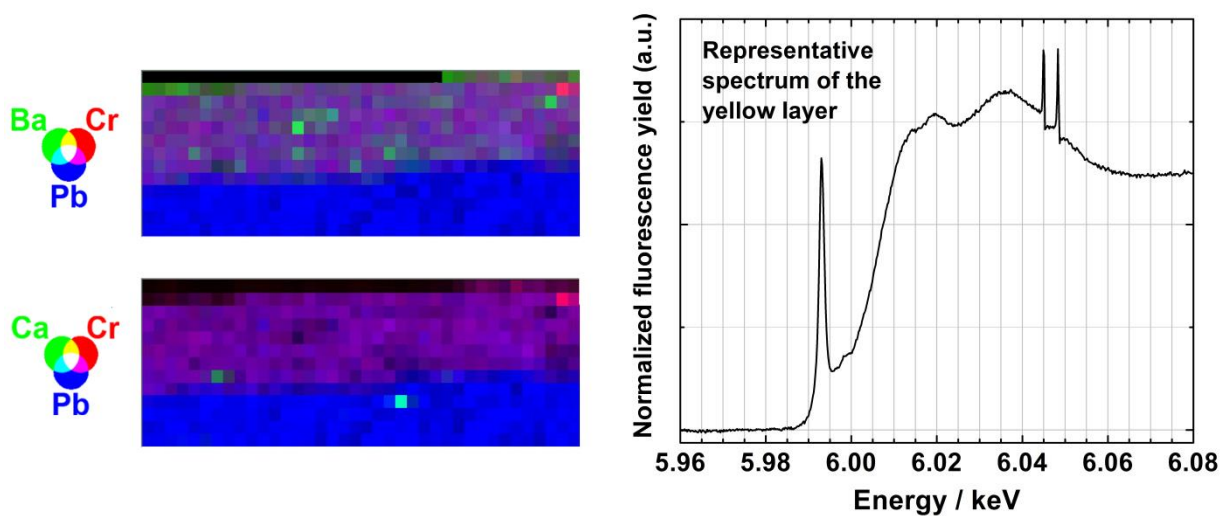
$\text{PbCr}_{1-x}\text{S}_x\text{O}_4$
 BaSO_4

Ground layer:

$2\text{PbCO}_3 \cdot \text{Pb}(\text{OH})_2$

SEM-EDS





In the top yellow layer, SEM-EDS and SR μ -XRF complementary analysis revealed the presence of lead chromate, lead white (most probably obtained by the stack process), chalk and barytes. SR μ -XRF mapping at different energies (5.993 and 6.1 keV) determined that no degradation via Cr^{6+} reduction to Cr^{3+} has occurred in this sample.

SEM-EDS identified lead chromate rod-like particles with different dimensions, between 0.3 and 3 μm in length and 0.07 and 0.8 in width.

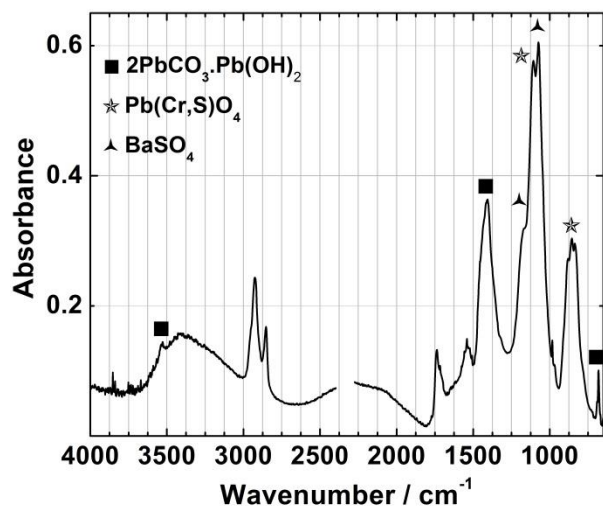
The white ground layer is composed by lead white particles, most probably obtained by the stack process.

● Multi-analytical characterisation of yellow micro-sample $\mu 4$

μ -EDXRF: Pb, Cr, Ba, Cu, As, Fe, Co, Sr, Ca, Zn, Hg, Ni

μ -FTIR

Compounds identified by μ -Raman



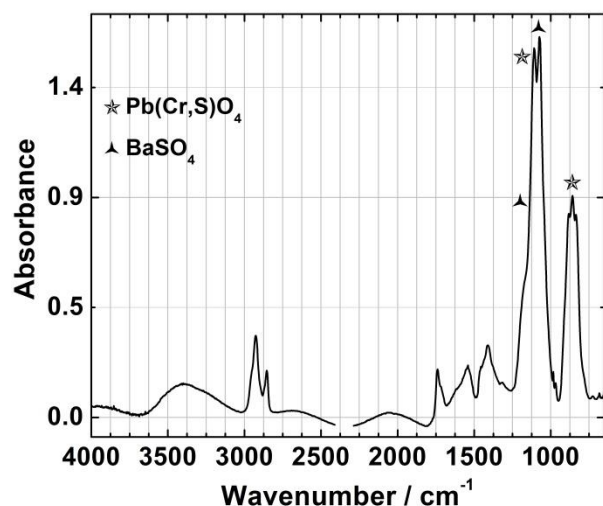
$\text{PbCr}_{1-x}\text{S}_x\text{O}_4$
 BaSO_4
 $2\text{PbCO}_3.\text{Pb(OH)}_2$

● Multi-analytical characterisation of yellow micro-sample $\mu 5^*$

μ -EDXRF: Pb, Cr, Ba, Fe, Zn, Ca, Co, Cu

μ -FTIR

Compounds identified by μ -Raman



$\text{PbCr}_{1-x}\text{S}_x\text{O}_4$
 BaSO_4
 $2\text{PbCO}_3.\text{Pb(OH)}_2$
 HgS

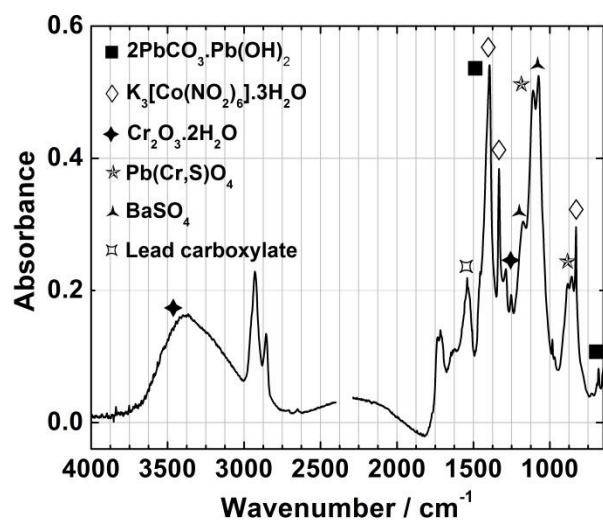
* The infrared spectrum of yellow micro-sample $\mu 6$ is identical to that of $\mu 5$.

● Multi-analytical characterisation of green micro-sample $\mu 8$

μ -EDXRF: Pb, Cr, Ba, Zn, Co, Fe, Ca, Cu

μ -FTIR

Compounds identified by μ -Raman



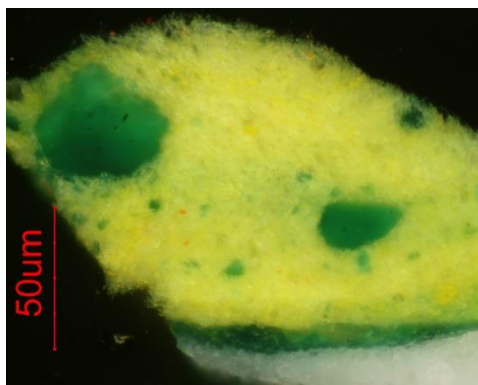
- $\text{Cr}_2\text{O}_3 \cdot 2\text{H}_2\text{O}$
- $\text{PbCr}_{1-x}\text{S}_x\text{O}_4$
- BaSO_4
- $2\text{PbCO}_3 \cdot \text{Pb(OH)}_2$
- $\text{K}_3[\text{Co}(\text{NO}_2)_6] \cdot 3\text{H}_2\text{O}$
- HgS

● Multi-analytical characterisation of green cross-section V2

μ -EDXRF: Pb, Cr, Co, Fe, Ba, K, Zn, Hg, Ca

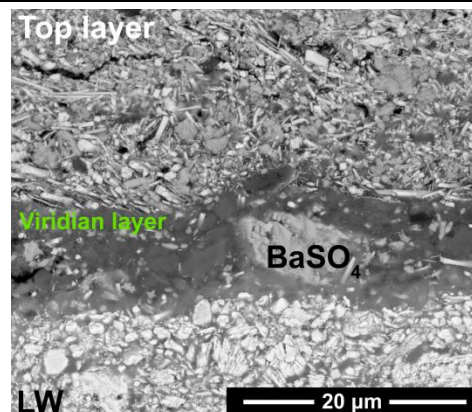
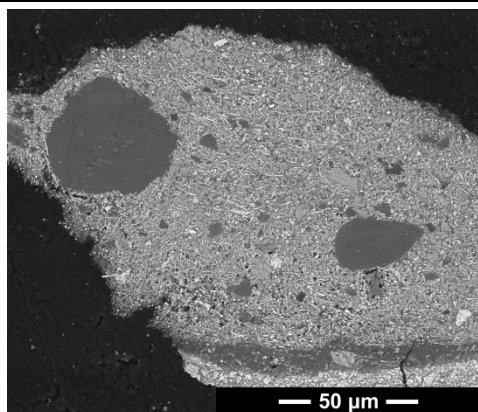
MO

Compounds identified by μ -Raman

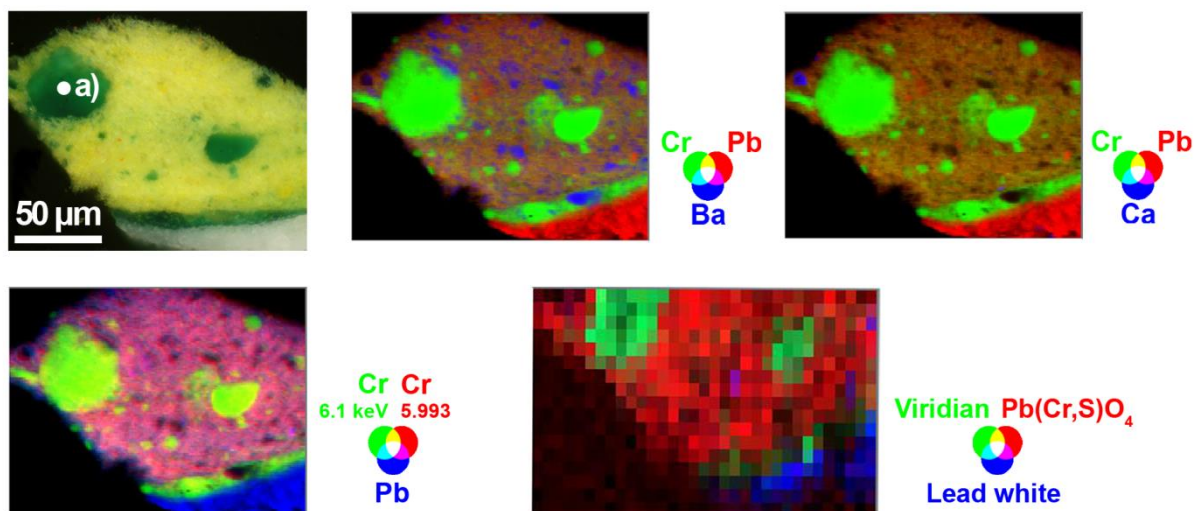


- 1st Green layer:**
 - $\text{PbCr}_{1-x}\text{S}_x\text{O}_4$
 - BaSO_4
 - $\text{Cr}_2\text{O}_3 \cdot 2\text{H}_2\text{O}$
 - HgS
- 2nd Green layer:**
 - $\text{Cr}_2\text{O}_3 \cdot 2\text{H}_2\text{O}$
- Ground layer:**
 - $2\text{PbCO}_3 \cdot \text{Pb(OH)}_2$

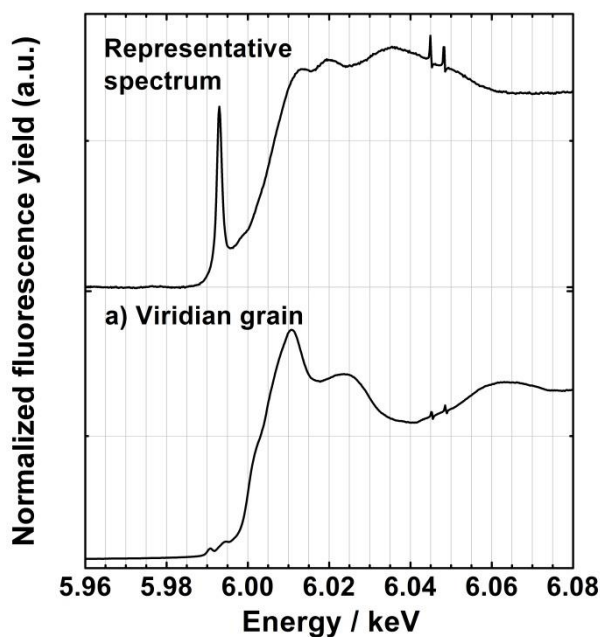
SEM-EDS



SR μ -XRF & μ -FTIR



SR Cr K-edge μ -XANES



In the top light green layer, SEM-EDS, SR μ -XRF and μ -FTIR complementary analysis identified mixed crystals of lead chromate and lead sulfate, viridian, lead white (most probably obtained by the stack process) and barytes. It was also possible to identify vermilion sub-rounded particles aggregated. SEM-EDS analysis revealed the presence of lead chromate rod-like particles with different dimensions, between 0.2 and 4.7 μ m in length and 0.07 and 0.4 in width. SR μ -XRF mapping at different energies (5.993 and 6.1 keV) in a yellow colour area determined that no degradation via Cr^{6+} reduction to Cr^{3+} has occurred in this sample.

The middle green layer is composed of viridian and barytes particles. By EDS, it was also possible to detect the presence of the element Al, probably related to the oil paint manufacture.

The white ground layer is composed by lead white (most probably obtained by the stack process) particles.

XIII.3. Untitled (cat. nº P75)



Figure XIII.3.1. Amadeo de Sousa-Cardoso painting: *Untitled*, c.1913, 34.4 x 28.2 cm (Inv. 92P209, cat. nº P75, Freitas, 2008, p. 229) © FCG. Analysis areas: μ -EDXRF (●), μ -sampling (●) and cross-sections (●).



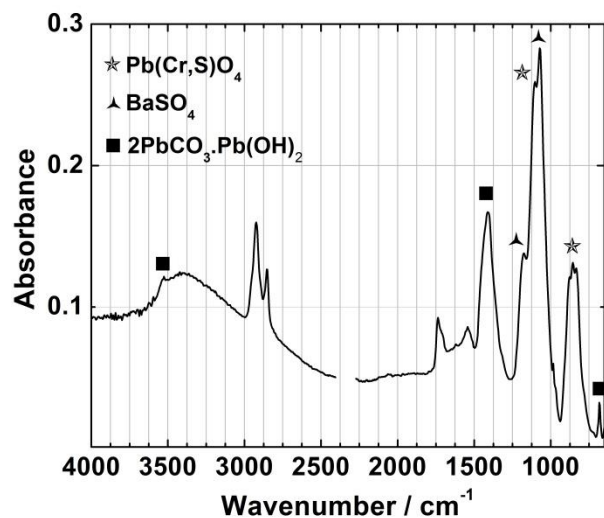
Figure XIII.3.2. Photomicrographs (7x to 10x) of Amadeo de Sousa-Cardoso painting: *Untitled*, c.1913 (Inv. 92P209, cat. nº P75).

● Multi-analytical characterisation of yellow micro-sample μ 1 and cross-section A1

μ -EDXRF: Pb, Ba, Cr, Fe, Sr, Zn, Ca

μ -FTIR

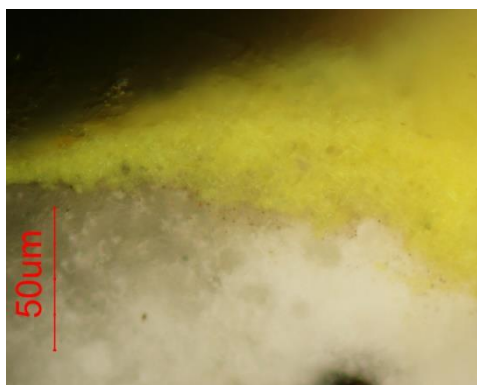
Compounds identified by μ -Raman



$\text{PbCr}_{1-x}\text{S}_x\text{O}_4$
 BaSO_4
 $2\text{PbCO}_3 \cdot \text{Pb}(\text{OH})_2$
 HgS

MO of cross-section A1

Compounds identified by μ -Raman



Yellow layer:
 $\text{PbCr}_{1-x}\text{S}_x\text{O}_4$
 BaSO_4

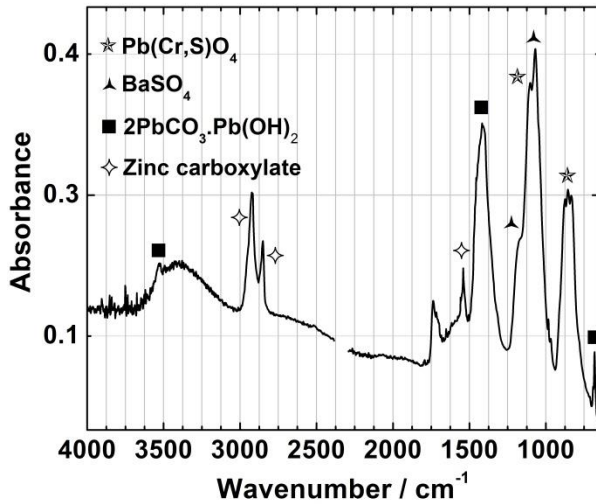
Ground layer:
 CaCO_3

● Multi-analytical characterisation of yellow micro-sample $\mu 2$

μ -EDXRF: Pb, Cr, Ba, Ca, Zn, Fe, Sr

μ -FTIR

Compounds identified by μ -Raman



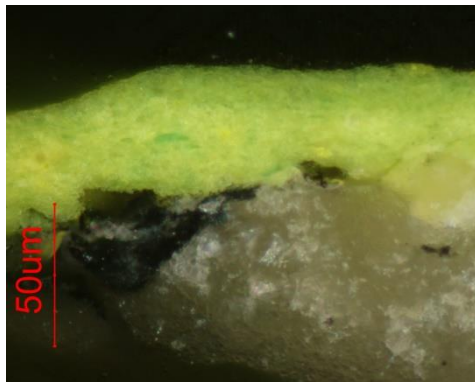
$PbCr_{1-x}S_xO_4$
 $BaSO_4$
 $2PbCO_3.Pb(OH)_2$
 $CaCO_3$

● Multi-analytical characterisation of green cross-section V1

μ -EDXRF: Pb, As, Cu, Cr, Ba, Ca, Zn, Sr, Fe

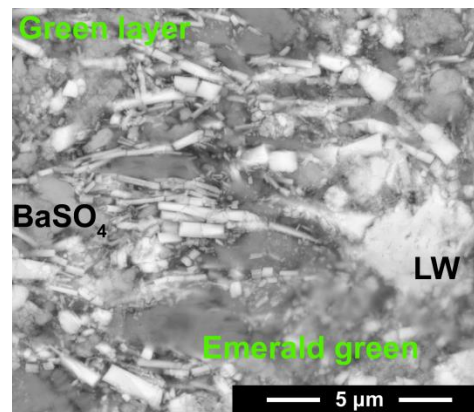
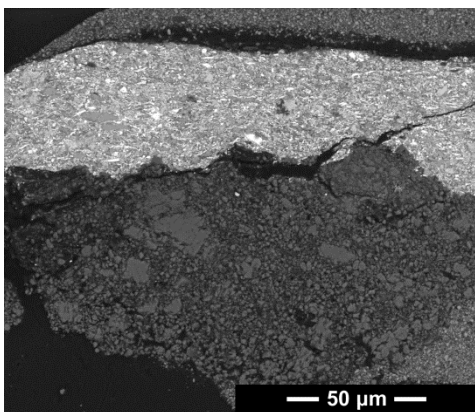
MO

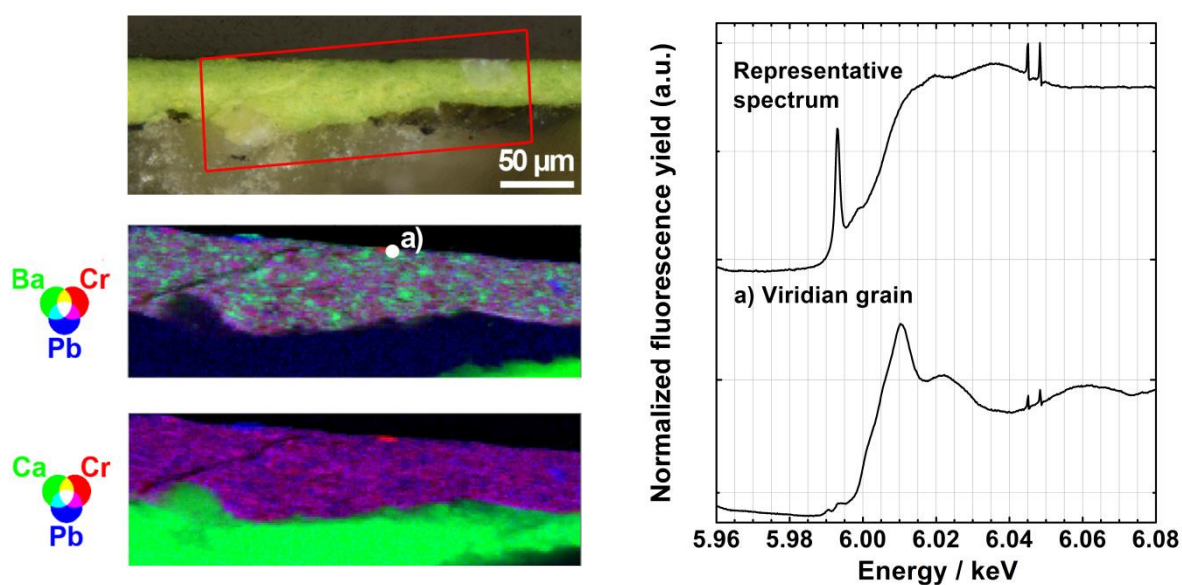
Compounds identified by μ -Raman



Green layer:
 $PbCr_{1-x}S_xO_4$
 $BaSO_4$
 $Cu(C_2H_3O_2).3Cu(AsO_2)_2$

SEM-EDS





In the top green layer, SEM-EDS and SR μ -XRF complementary analysis show a mixture of lead chromate with emerald green, lead white (most probably obtained by the stack process) and barytes. A viridian grain was detected by SR μ -XRF and μ -XANES (a), however, this grain is most probably part of the green paint composition since SR μ -XRF mapping at different energies (5.993 and 6.1 keV) determined that no degradation via Cr^{6+} reduction to Cr^{3+} has occurred in this sample.

SEM-EDS analysis revealed the presence of lead chromate rod-like particles with different dimensions, between 0.2 and 2 μm in length and 0.07 and 0.5 in width.

The white ground layer is composed of chalk particles.

XIII.4. *Mucha* (cat. nº P172)

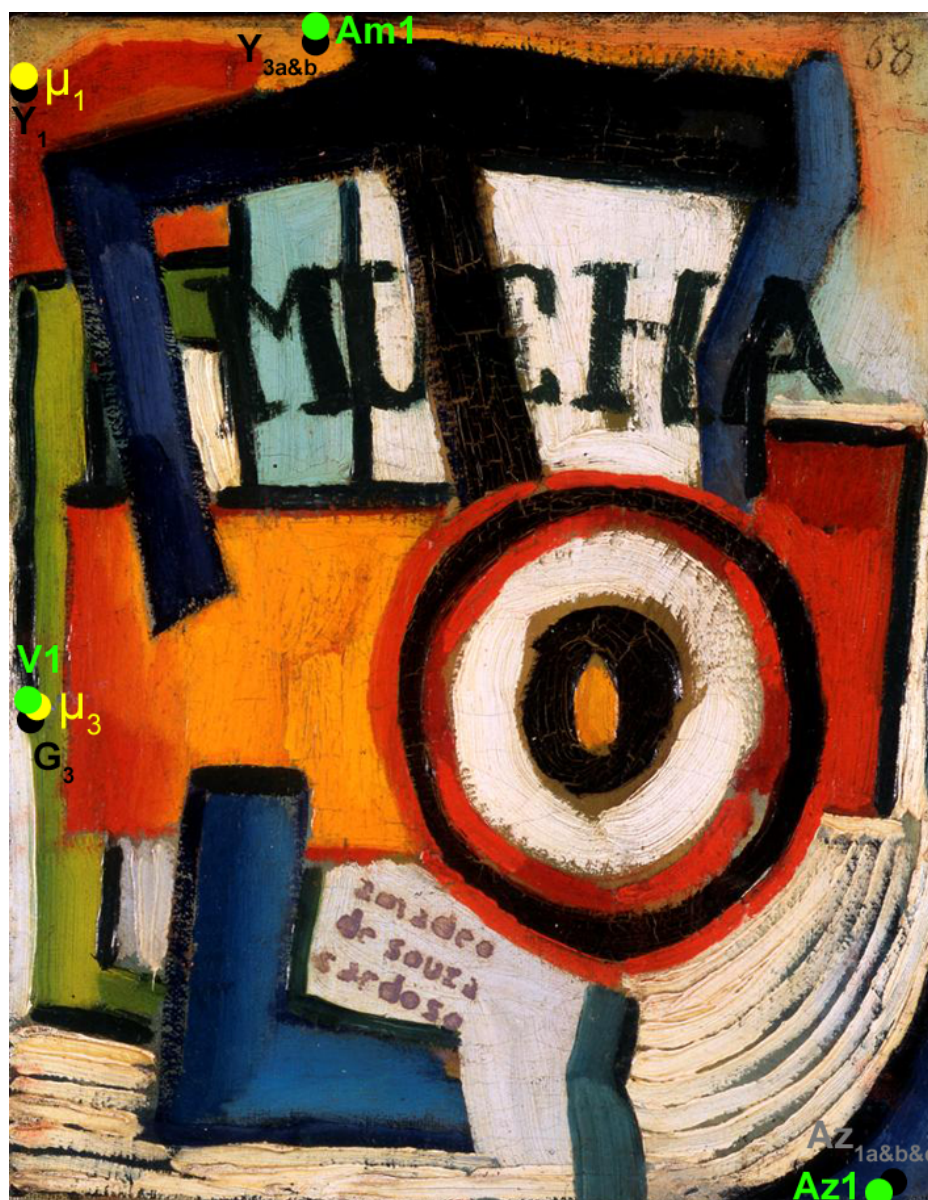


Figure XIII.4.1. Amadeo de Sousa-Cardoso painting: *Mucha*, c.1915-16, 27.3 x 21.4 cm (Inv. 86P21, cat. nº P172, Freitas, 2008, p. 322) © FCG. Analysis areas: μ -EDXRF (●), μ -sampling (●) and cross-sections (●).



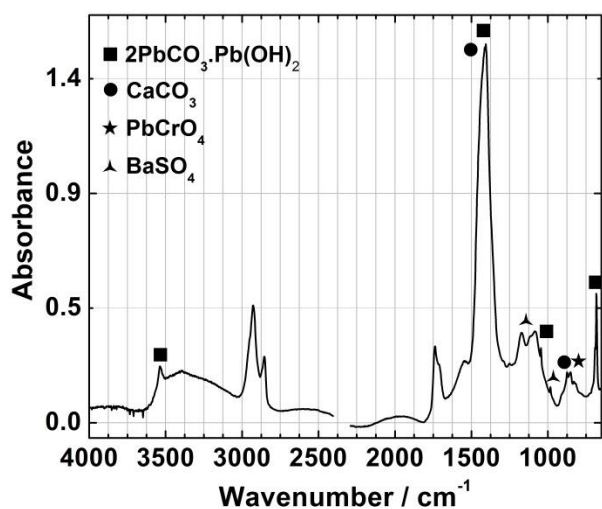
Figure XIII.4.2. Photomicrographs (7x to 32x) of Amadeo de Sousa-Cardoso painting: *Mucha*, c.1915-16 (Inv. 86P21, cat. nº P172), from Melo *et al.*, 2009.

● Multi-analytical characterisation of yellow micro-sample μ 1 and cross-section Am1

μ -EDXRF: Zn, Pb, Ba, Ca, Cr, Fe, Hg, Sr, K, Co

μ -FTIR

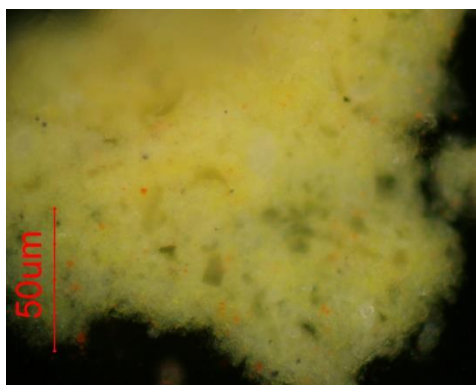
Compounds identified by μ -Raman



PbCrO₄
BaSO₄
CaCO₃
2PbCO₃.Pb(OH)₂
HgS

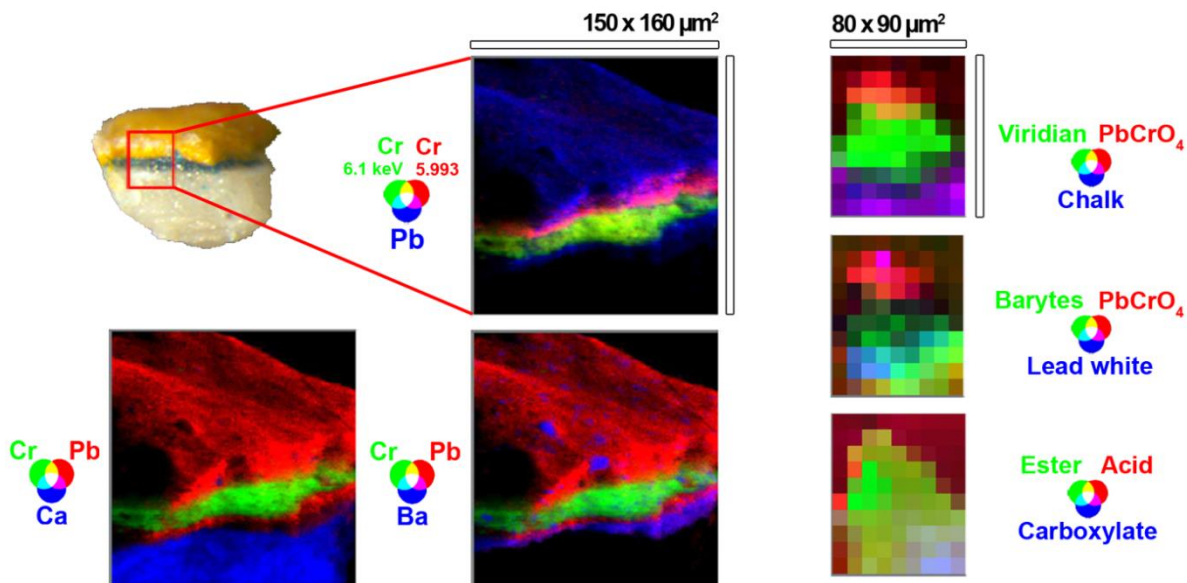
MO of cross-section Am1

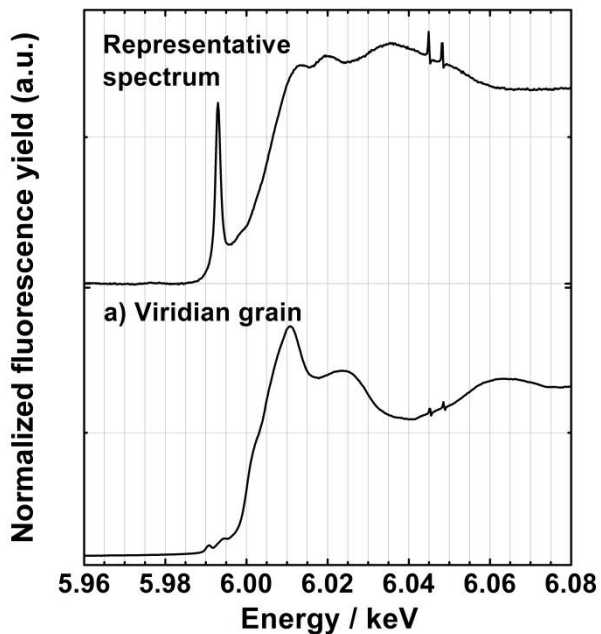
Compounds identified by μ -Raman



Yellow layer:
PbCrO₄
HgS
BaSO₄
CaCO₃
2PbCO₃.Pb(OH)₂

SR μ -XRF & μ -FTIR of a multilayer cross-section taken from the same area as yellow micro-sample μ 1

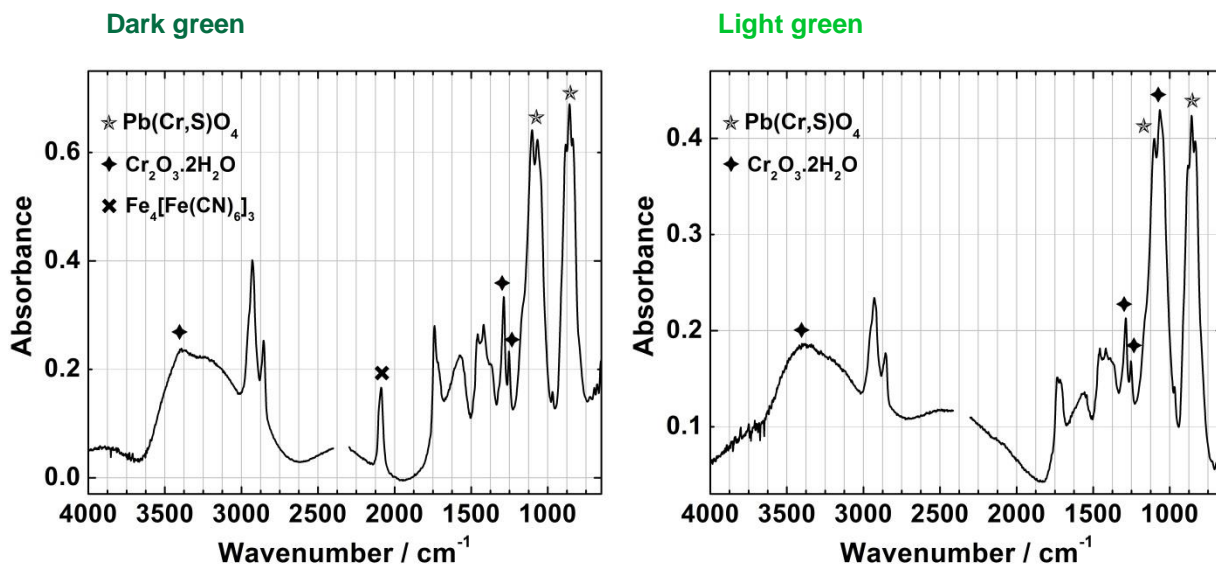




● Multi-analytical characterisation of green micro-sample μ 3 and cross-section V1

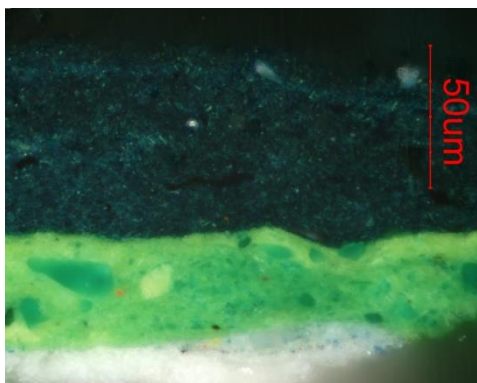
μ -EDXRF: Pb, Cr, Zn, Ca, Ba, Fe, Sr

μ -FTIR

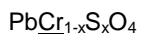
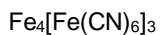


MO of cross-section V1

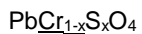
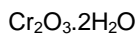
Compounds identified by μ -Raman



1st Green layer:



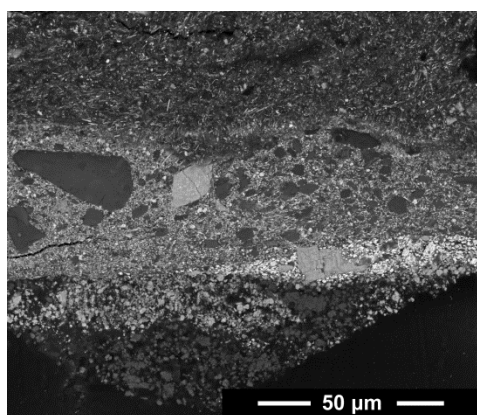
2nd Green layer:



Ground layer:

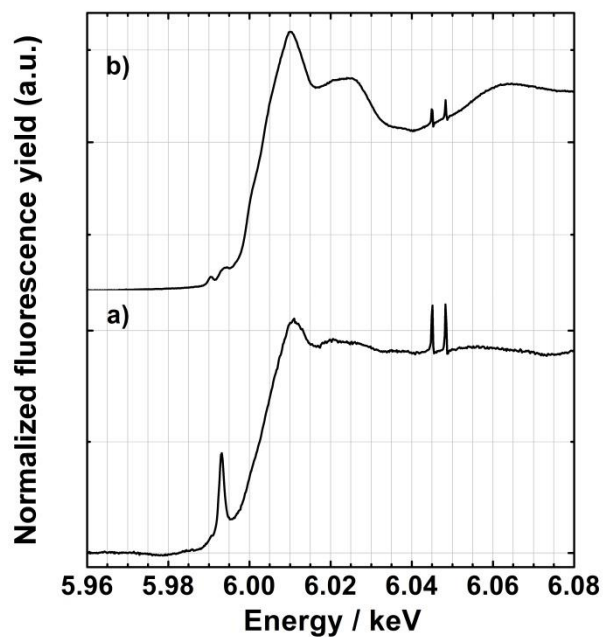
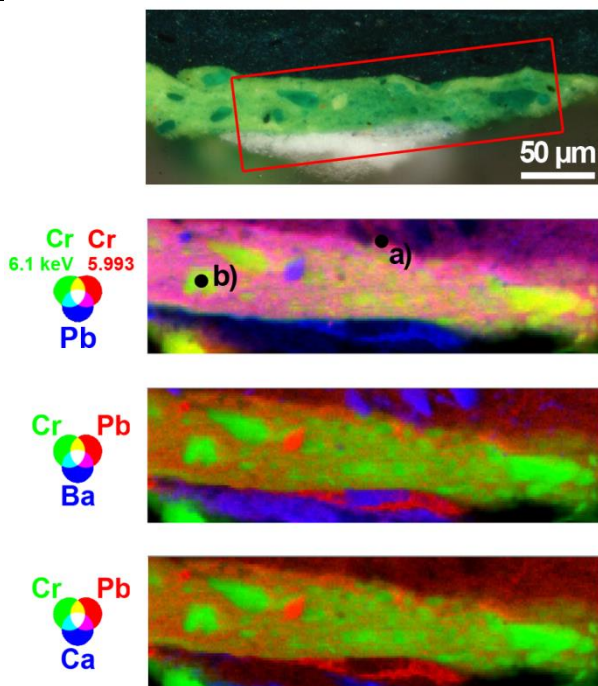


SEM-EDS



SR μ -XRF

SR Cr K-edge μ -XANES



In the top dark green layer, SEM-EDS revealed a high content of oil with several particles dispersed. SEM-EDS and SR μ -XRF complementary analysis show a mixture of lead chromate, barytes, lead white (most probably obtained by the stack process) and chalk. SEM-EDS analysis identified lead chromate rod-like particles with different dimensions, between 0.3 and 3 μm in length and approximately 0.3 μm in width. EDS analysis also revealed the presence of the element Fe probably due to Prussian blue and, Na, Mg, Al and K probably related to the oil paint formulation.

In the light green layer, SEM-EDS and SR μ -XRF complementary analysis show a mixture of lead chromate, viridian and lead white (most probably obtained by the stack process). SR μ -XRF mapping at different energies (5.993 and 6.1 keV) determined that no degradation via Cr^{6+} reduction to Cr^{3+} has occurred in this layer. SEM-EDS analysis shows lead chromate rod-like particles with different dimensions, between 0.2 and 2 μm in length and approximately 0.2 μm in width. The elements Na and Mg were also detected by EDS, most probably related to the oil paint formulation.

In the bluish layer, SEM-EDS and SR μ -XRF complementary analysis show mainly lead white (most probably obtained by the stack process) and a big barytes particle.

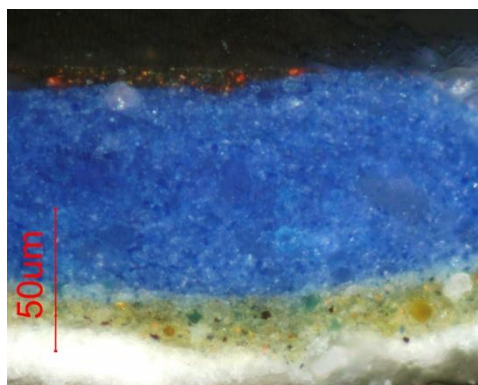
The white ground layer is composed of two layers, one of barytes with lead white and another of chalk.

● Multi-analytical characterisation of yellow cross-section Az1

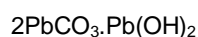
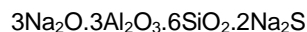
μ -EDXRF: Pb, Co, Zn, Ba, Ca, Sn, Fe, Cr, Sr, Ni

MO

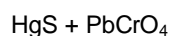
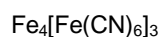
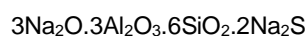
Compounds identified by μ -Raman



Blue layer:



Intermediate layer:



Ground layer:



Appendix XIV. Characterisation of other yellow chromate pigment reconstructions

XIV.1. Lemon Yellow (barium chromate)

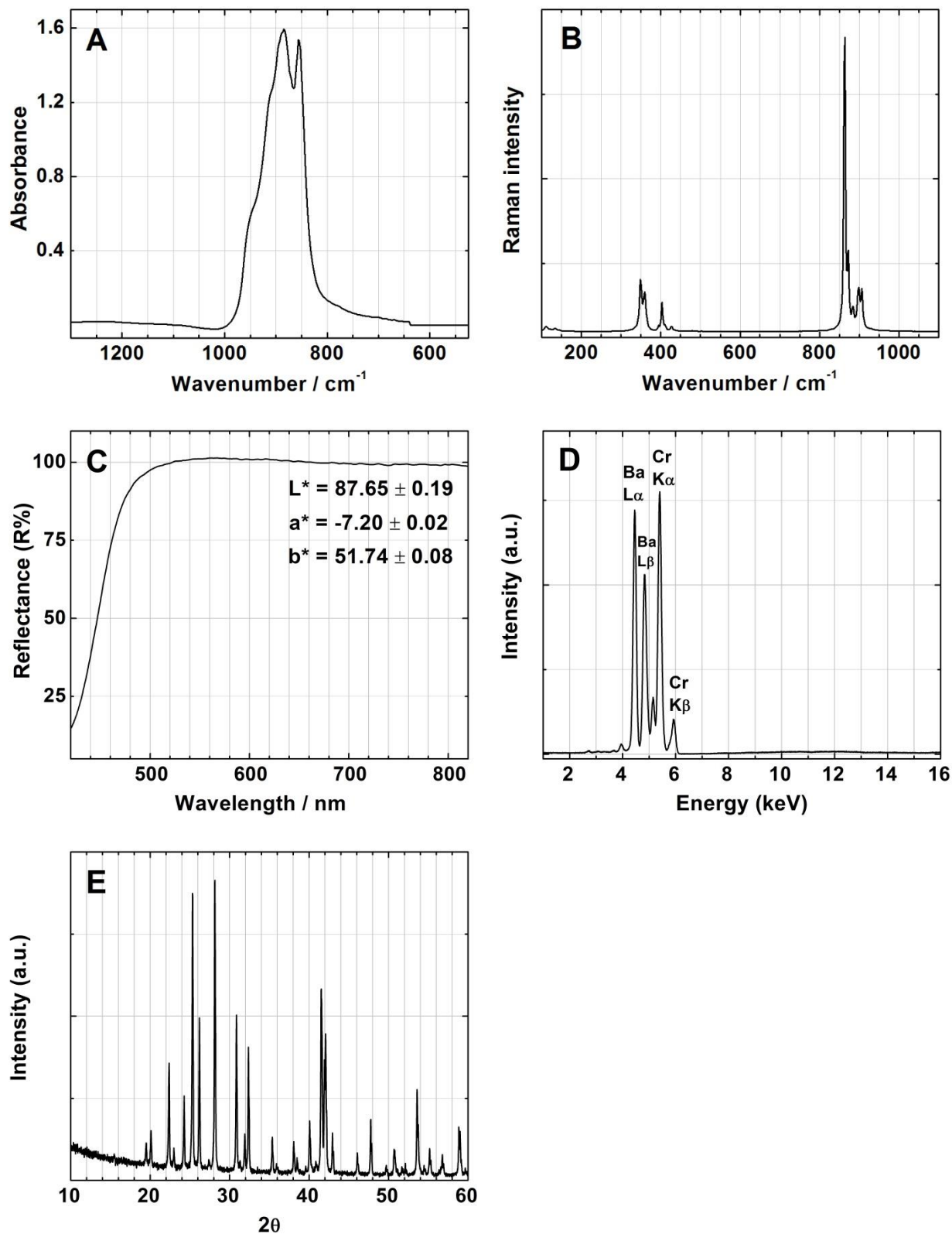


Figure XIV.1.1. Representative A) infrared, B) μ -Raman, C) FORS, D) μ -EDXRF spectra and E) diffraction pattern of LY1a pigment reconstruction.

XIV.2. Citron Yellow (zinc potassium chromate)

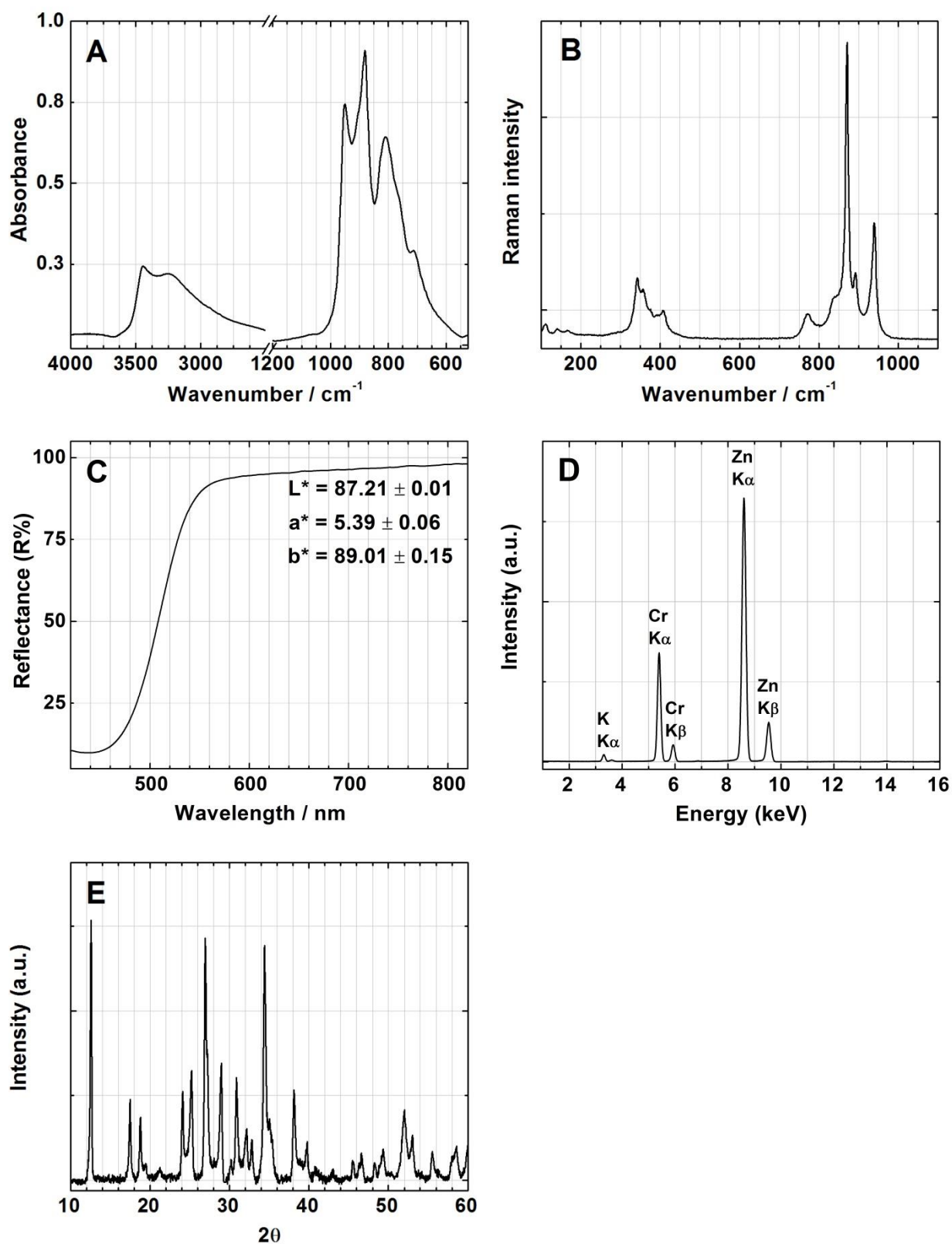


Figure XIV.2.1. Representative **A**) infrared, **B**) μ -Raman, **C**) FORS, **D**) μ -EDXRF spectra and **E**) diffraction pattern of **CY1a** pigment reconstruction.

XIV.3. Strontia Yellow (strontium chromate)

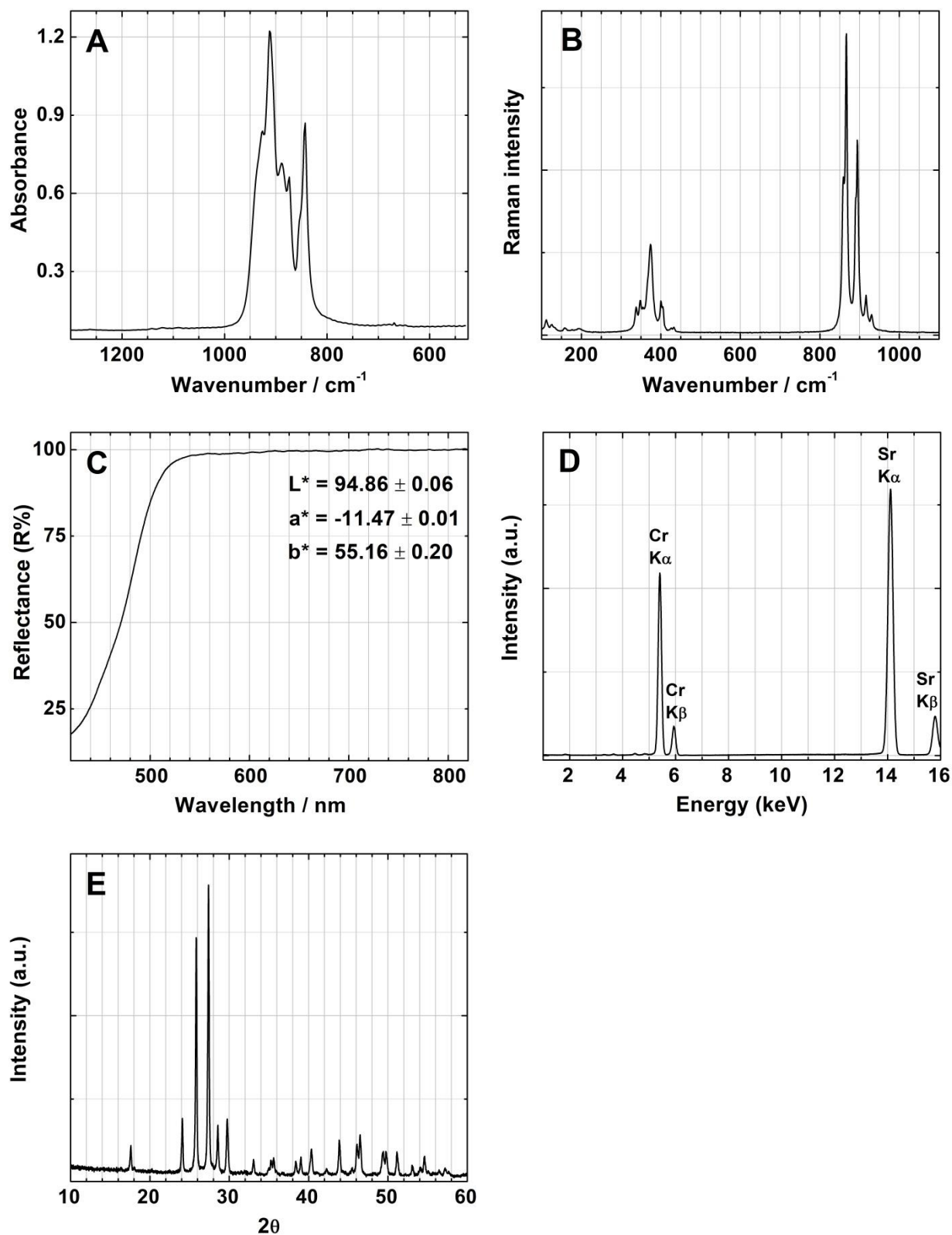


Figure XIV.3.1. Representative **A)** infrared, **B)** μ -Raman, **C)** FORS, **D)** μ -EDXRF spectra and **E)** diffraction pattern of **SY1a** pigment reconstruction.

Appendix XV. Additional characterisation of the historic W&N *Lemon Yellow* oil paint tube

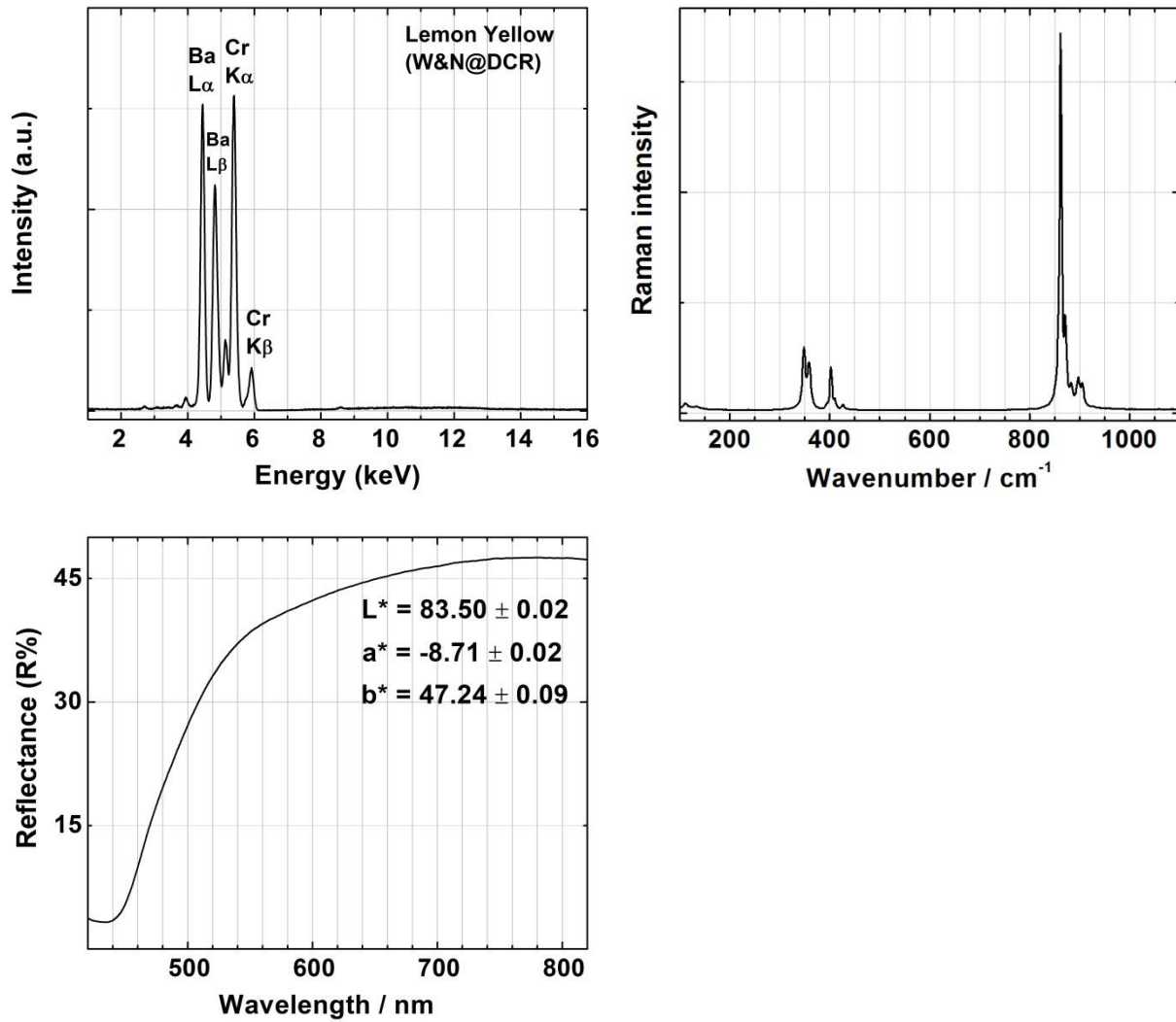


Figure XV.1. μ -EDXRF, Raman and FORS spectra of the W&N *Lemon Yellow* oil paint tube¹⁷².

¹⁷² The μ -EDXRF, Raman and FORS spectra were obtained by Marta Félix Campos (DCR FCT NOVA).

Appendix XVI. Colourimetric values and $I_{Cr\ K\ pre-edge}$ before and after irradiation

Table XVI.1. Oil paints before and after irradiation with a Xenon lamp ($\lambda_{irr} > 300\text{ nm}$): pigment composition, $L^*a^*b^*$ coordinates, ΔE^* , and intensity of the Cr K pre-edge peak at 5.993 keV.

Pigment Composition [§]	t_{irr} / h	L^*	a^*	b^*	ΔE^*	$I_{E=5.993\text{ keV}}^{Cr}$
PbCrO₄	0	63.9 ± 0.4	18.2 ± 0.1	67.6 ± 0.6		1.117 ± 0.004
	1500	60.2 ± 0.2	17.9 ± 0.1	59.5 ± 0.2	8.9	1.083 ± 0.004
W&N oil paint	0	70.7 ± 0.04	22.3 ± 0.1	78.1 ± 0.03		1.296 ± 0.022
Chrome Deep	1500	65.2 ± 0.1	18.9 ± 0.02	67.03 ± 0.1	12.8	1.261 ± 0.012
PbCrO ₄ (50%)	3000	64.2 ± 0.1	18.4 ± 0.02	63.9 ± 0.1	16.1	1.204 ± 0.007
CaCO ₃ (50%)	4500	63.6 ± 0.1	17.6 ± 0.03	63.4 ± 0.1	16.9	-
MgCO ₃ .xH ₂ O	8500	62.9 ± 0.1	17.6 ± 0.03	62.9 ± 0.04	17.7	-
	10000	63.1 ± 0.2	17.7 ± 0.1	62.0 ± 0.2	17.6	1.099 ± 0.016
W&N oil paint	0	77.2 ± 0.04	13.4 ± 0.2	78.5 ± 0.1		1.284 ± 0.011
Chrome Yellow	1500	66.5 ± 0.1	7.7 ± 0.03	57.3 ± 0.03	24.4	1.171 ± 0.038
PbCr _{0.6} S _{0.4} O ₄ (80%)	3000	65.6 ± 0.3	6.7 ± 0.04	56.3 ± 0.6	25.9	1.127 ± 0.018
BaSO ₄ (20%)	4500	65.8 ± 0.2	6 ± 0.05	55.6 ± 0.3	26.6	-
MgCO ₃ .xH ₂ O	6000	66.1 ± 0.2	6.1 ± 0.05	56.9 ± 0.2	25.4	-
	8500	64.7 ± 0.1	4.4 ± 0.05	56.9 ± 0.04	26.6	1.061 ± 0.006
PR1b*	0	70.1 ± 0.04	17.7 ± 0.07	82.5 ± 0.07		1.172 ± 0.023
PbCr _{0.6} S _{0.4} O ₄	1000	-	-	-	-	1.121 ± 0.018
	1500	59.9 ± 0.2	7.2 ± 0.2	56.9 ± 0.4	29.5	1.070 ± 0.022
	3000	57.9 ± 0.2	5.8 ± 0.3	54.9 ± 0.9	32.4	1.024 ± 0.026
	4000	56.3 ± 0.4	5.8 ± 0.04	51.1 ± 0.1	36.3	-
	5500	55.1 ± 0.03	3.9 ± 0.03	48.2 ± 0.2	39.8	-
	7750	54.9 ± 0.04	3.9 ± 0.02	47.2 ± 0.4	40.8	0.913 ± 0.007
	9000	53.7 ± 0.5	3.5 ± 0.1	47.5 ± 0.2	41.1	-
	11000	54.3 ± 0.1	2.8 ± 0.02	46.4 ± 0.1	42.1	0.929 ± 0.018
L3a*_1	0	64.8 ± 0.1	24.9 ± 0.05	73.4 ± 0.2		1.159 ± 0.020
PbCrO ₄ (15%)	1000	-	-	-	-	1.067 ± 0.019
CaCO ₃ (54%)	1500	48.1 ± 0.1	14.3 ± 0.1	39.9 ± 0.2	38.9	1.031 ± 0.019
CaSO ₄ .2H ₂ O (31%)	3000	46.6 ± 0.2	13.8 ± 0.1	38.2 ± 0.4	41.1	0.961 ± 0.028
	4000	46.3 ± 0.2	12.7 ± 0.1	35.3 ± 0.1	44.0	-
	5500	45.1 ± 0.1	11.9 ± 0.1	33.5 ± 0.3	46.4	-
	7750	44.7 ± 0.1	11.1 ± 0.05	31.7 ± 0.2	48.2	0.905 ± 0.015
	9000	43.8 ± 0.04	11.7 ± 0.1	34.2 ± 0.6	46.4	-
	11000	43.2 ± 0.2	11.7 ± 0.04	34.6 ± 0.04	46.3	0.929 ± 0.012

[§] Characterisation of the reconstructed pigments following original W&N recipes and of the historic oil paint tubes may be consulted in Appendix X (p. 293) and XI (p. 311), respectively. The molar fractions of the PbCr_{1-x}S_xO₄ are approximate values resulting from a comparison of the infrared spectrum and diffraction pattern of the pigments with the reference set of PbCr_{1-x}S_xO₄ synthesised in the laboratory (see Appendix VIII, p. 275). The semi-quantification of the compounds was obtained by XRD (MgCO₃.xH₂O was not accounted for because it was not detected by XRD).

Table XVI.2. PVAc paints before and after irradiation with a Xenon lamp ($\lambda_{\text{irr}} > 300 \text{ nm}$): pigment composition, $L^*a^*b^*$ coordinates, ΔE^* , and intensity of the Cr K pre-edge peak at 5.993 keV.

Pigment Composition [§]	$t_{\text{irr}} / \text{h}$	L^*	a^*	b^*	ΔE^*	$I_{E=5.993 \text{ keV}}^{\text{Cr}}$
PR1b_2 PbCr _{0.5} S _{0.5} O ₄	0	80.5 ± 0.02	2.4 ± 0.1	83.8 ± 0.2		1.318 ± 0.013
	1500	76.3 ± 0.02	4 ± 0.05	71.8 ± 0.1	12.8	-
	3000	76.1 ± 0.02	3.6 ± 0.05	71.8 ± 0.1	12.9	1.299 ± 0.011
	4500	75.5 ± 0.01	3.5 ± 0.02	70.7 ± 0.01	14.1	-
	6000	75.2 ± 0.1	3.7 ± 0.01	72.4 ± 0.2	12.6	1.265 ± 0.028
	8500	73.9 ± 0.05	2.7 ± 0.05	71.1 ± 0.1	14.4	1.239 ± 0.016
M1a PbCrO ₄ (30%) CaCO ₃ (40%) PbCO ₃ (30%)	0	79.2 ± 0.03	20.2 ± 0.1	88.3 ± 0.04		1.323 ± 0.018
	1500	71.3 ± 0.1	19.2 ± 0.04	74.8 ± 0.2	15.8	-
	3000	71.5 ± 0.1	18.5 ± 0.03	74.8 ± 0.2	15.7	1.288 ± 0.019
	4500	71 ± 0.1	18.6 ± 0.1	74.1 ± 0.2	16.5	-
	6000	71.2 ± 0.04	18.2 ± 0.1	75.8 ± 0.04	15.0	1.260 ± 0.008
	8500	70.6 ± 0.06	17.7 ± 0.05	74.4 ± 0.03	16.6	1.235 ± 0.037
L3a PbCr _{0.8} S _{0.2} O ₄ (20%) CaSO ₄ ·2H ₂ O (45%) PbCO ₃ (35%)	0	80.3 ± 0.1	14.5 ± 0.1	88.1 ± 0.1		1.315 ± 0.009
	1500	73.2 ± 0.01	13.9 ± 0.1	74.8 ± 0.04	15.1	-
	3000	72.8 ± 0.02	13.4 ± 0.03	73.5 ± 0.05	16.4	1.281 ± 0.015
	4500	72 ± 0.03	13.5 ± 0.05	72.2 ± 0.1	17.9	-
	6000	71.8 ± 0.1	13.2 ± 0.05	72.1 ± 0.2	18.1	1.246 ± 0.004
	8500	70.6 ± 0.01	12.7 ± 0.03	70.5 ± 0.02	20.2	1.214 ± 0.004
L3b PbCr _{0.8} S _{0.2} O ₄ (40%) PbCO ₃ (60%)	0	79.8 ± 0.4	15.2 ± 0.6	88 ± 0.1		1.326 ± 0.010
	1500	71.6 ± 0.2	14.4 ± 0.01	72.2 ± 0.2	17.8	-
	3000	71.8 ± 0.03	13.8 ± 0.05	72.1 ± 0.1	17.8	1.290 ± 0.019
	4500	71.2 ± 0.03	13.9 ± 0.01	71.8 ± 0.1	18.4	-
	6000	70.8 ± 0.01	13.6 ± 0.03	71 ± 0.02	19.3	1.248 ± 0.007
	8500	69.6 ± 0.2	13 ± 0.03	69.6 ± 0.05	21.1	1.223 ± 0.017

[§] Characterisation of the reconstructed pigments following original W&N recipes may be consulted in Appendix X (p. 293). As mentioned, the molar fractions of the PbCr_{1-x}S_xO₄ are approximate values resulting from a comparison of the infrared spectrum and diffraction pattern of the pigments with the reference set of PbCr_{1-x}S_xO₄ synthesised in the laboratory (see Appendix VIII, p. 275). The semi-quantification of the compounds was obtained by XRD.

Table XVI.2. (continued).

Pigment Composition [§]	t_{irr} / h	L^*	a^*	b^*	ΔE^*	$I_{E=5.993\text{ keV}}^{Cr}$
PR1b_1 PbCr _{0.5} S _{0.5} O ₄	0	83 ± 0.1	6.4 ± 0.03	91.2 ± 0.1		1.337 ± 0.015
	1500	75 ± 0.03	6.7 ± 0.1	76.5 ± 0.1	16.8	-
	3000	73.7 ± 0.1	5.7 ± 0.1	73.6 ± 0.1	19.9	1.278 ± 0.006
	4500	72.9 ± 0.1	5.5 ± 0.03	72.1 ± 0.1	21.6	-
	6000	72.9 ± 0.04	4.9 ± 0.04	71.8 ± 0.1	21.8	1.204 ± 0.02
	8500	71.5 ± 0.04	4 ± 0.1	70.2 ± 0.2	24.0	-
PR1a PbCr _{0.3} S _{0.7} O ₄	0	84.5 ± 0.05	0.3 ± 0.01	84.6 ± 0.1		1.329 ± 0.011
	1500	75 ± 0.02	1 ± 0.02	67.2 ± 0.03	19.8	-
	3000	74 ± 0.1	1 ± 0.01	65.5 ± 0.1	21.7	1.239 ± 0.019
	4500	73.3 ± 0.04	-0.4 ± 0.03	64.5 ± 0.1	22.9	-
	6000	72.9 ± 0.03	-1.7 ± 0.03	63.1 ± 0.05	24.5	1.188 ± 0.019
	8500	72.2 ± 0.01	-2.5 ± 0.1	61.5 ± 0.2	26.2	-
L2b PbCr _{0.5} S _{0.5} O ₄	0	81.6 ± 0.04	13 ± 0.1	89.6 ± 0.1		1.334 ± 0.008
	1500	72.7 ± 0.1	12.4 ± 0.03	71.8 ± 0.1	19.9	-
	3000	71.8 ± 0.1	11.5 ± 0.03	68.1 ± 0.01	23.6	1.273 ± 0.011
	4500	70.7 ± 0.1	11.2 ± 0.1	65.7 ± 0.03	26.3	-
	6000	70. ± 0.1	10.6 ± 0.03	66.5 ± 0.1	25.8	1.172 ± 0.018
	8500	68.3 ± 0.03	9.6 ± 0.04	63.4 ± 0.02	29.5	-
L2a PbCr _{0.6} S _{0.4} O ₄ (50%) BaSO ₄ (50%)	0	80.8 ± 0.05	9.2 ± 0.02	89.6 ± 0.1		1.290 ± 0.02
	1500	69.9 ± 0.04	9.1 ± 0.04	69.9 ± 0.1	22.6	-
	3000	69.3 ± 0.1	8.8 ± 0.03	68.7 ± 0.5	23.9	1.226 ± 0.003
	4500	68.2 ± 0.1	8.4 ± 0.03	66.7 ± 0.4	26.2	-
	6000	67.9 ± 0.04	7.8 ± 0.02	66.6 ± 0.1	26.5	1.137 ± 0.014
	8500	66.4 ± 0.05	7 ± 0.04	65.3 ± 0.1	28.4	-
L3a*_2 PbCrO ₄ (34%) CaCO ₃ (54%) CaSO ₄ ·2H ₂ O (12%)	0	74.4 ± 0.04	25.6 ± 0.1	82.1 ± 0.04		1.293 ± 0.001
	1500	59.5 ± 0.01	21.2 ± 0.05	55.1 ± 0.1	31	-
	3000	56.4 ± 0.02	19.4 ± 0.1	49.5 ± 0.1	37.7	1.225 ± 0.009
	4500	54.5 ± 0.02	18.4 ± 0.05	46.4 ± 0.1	41.4	-
	6000	54.2 ± 0.1	18.1 ± 0.04	45.9 ± 0.2	42.1	1.132 ± 0.002
	8500	52.1 ± 0.1	16.6 ± 0.02	43.1 ± 0.03	45.8	-

[§] Characterisation of the reconstructed pigments following original W&N recipes may be consulted in Appendix X (p. 293). As mentioned, the molar fractions of the PbCr_{1-x}S_xO₄ are approximate values resulting from a comparison of the infrared spectrum and diffraction pattern of the pigments with the reference set of PbCr_{1-x}S_xO₄ synthesised in the laboratory (see Appendix VIII, p. 275). The semi-quantification of the compounds was obtained by XRD.

Appendix XVII. FORS, μ -FTIR and Cr K-edge μ -XANES spectra of the PVAc paints before and after irradiation

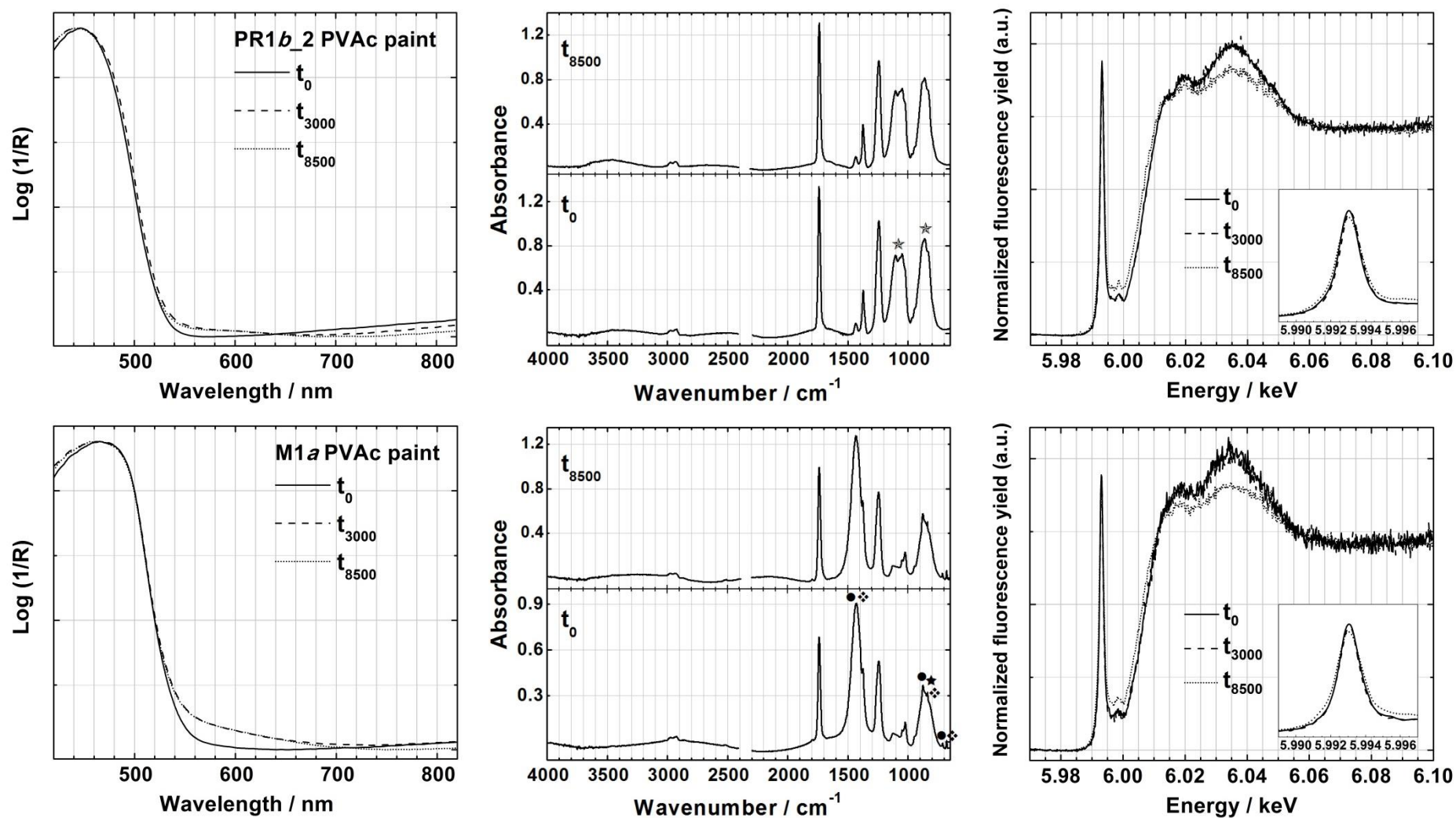


Figure XVII.1. Normalized FORS, μ -FTIR spectra: (\star) $\text{PbCr}_{1-x}\text{S}_x\text{O}_4$, (\star) PbCrO_4 , (\diamond) PbCO_3 and (\bullet) CaCO_3 , the remaining bands correspond to the PVAc binder; and normalized Cr K-edge XANES spectra of PR1b_2 and M1a PVAc paints before and after irradiation.

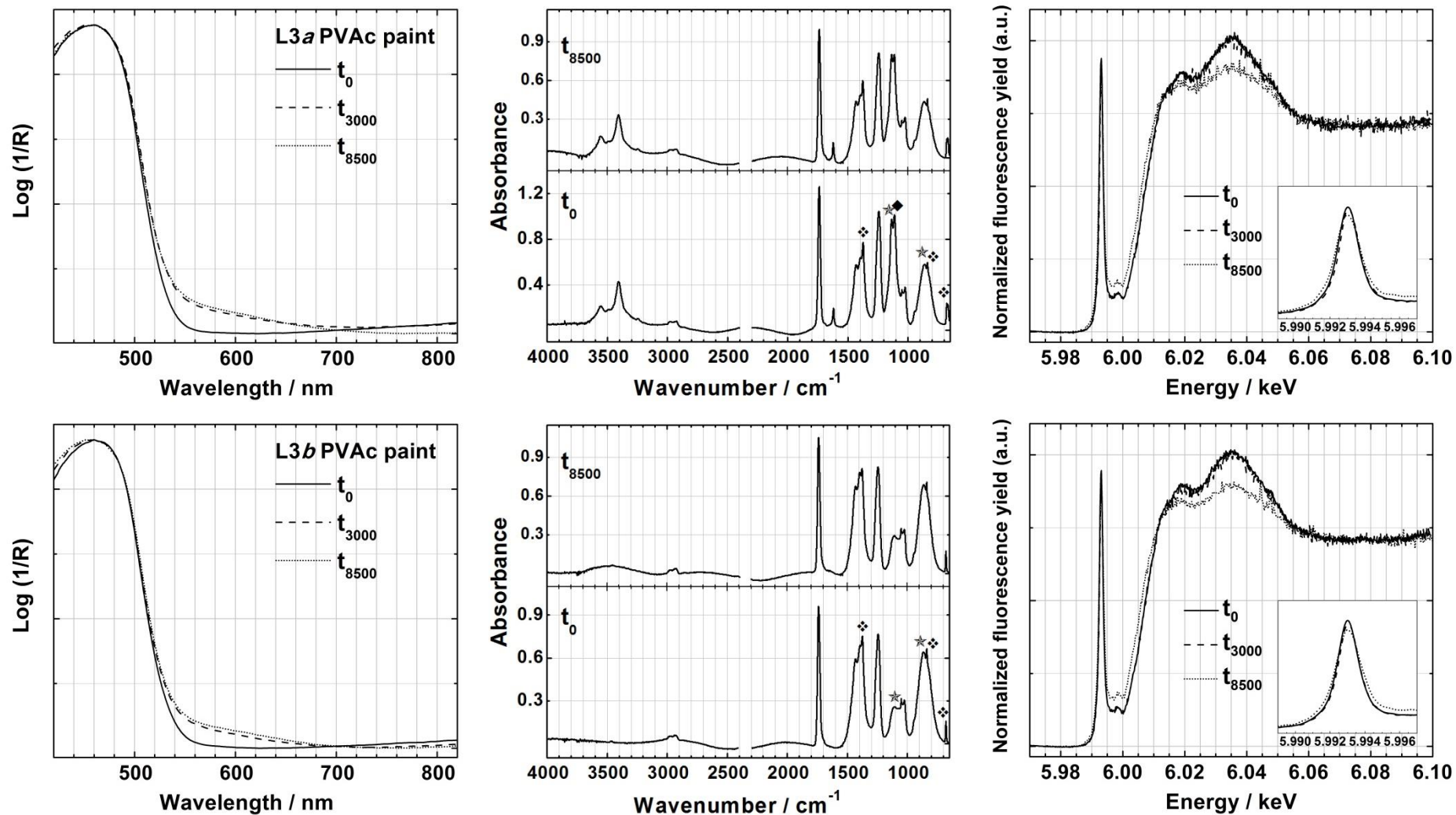


Figure XVII.2. Normalized FORS, μ -FTIR spectra: (\star) $\text{PbCr}_{1-x}\text{S}_x\text{O}_4$, (\diamond) PbCO_3 and (\blacklozenge) $\text{CaSO}_4 \cdot 2\text{H}_2\text{O}$, the remaining bands correspond to the PVAc binder; and normalized Cr K-edge XANES spectra of L3a and L3b PVAc paints before and after irradiation.

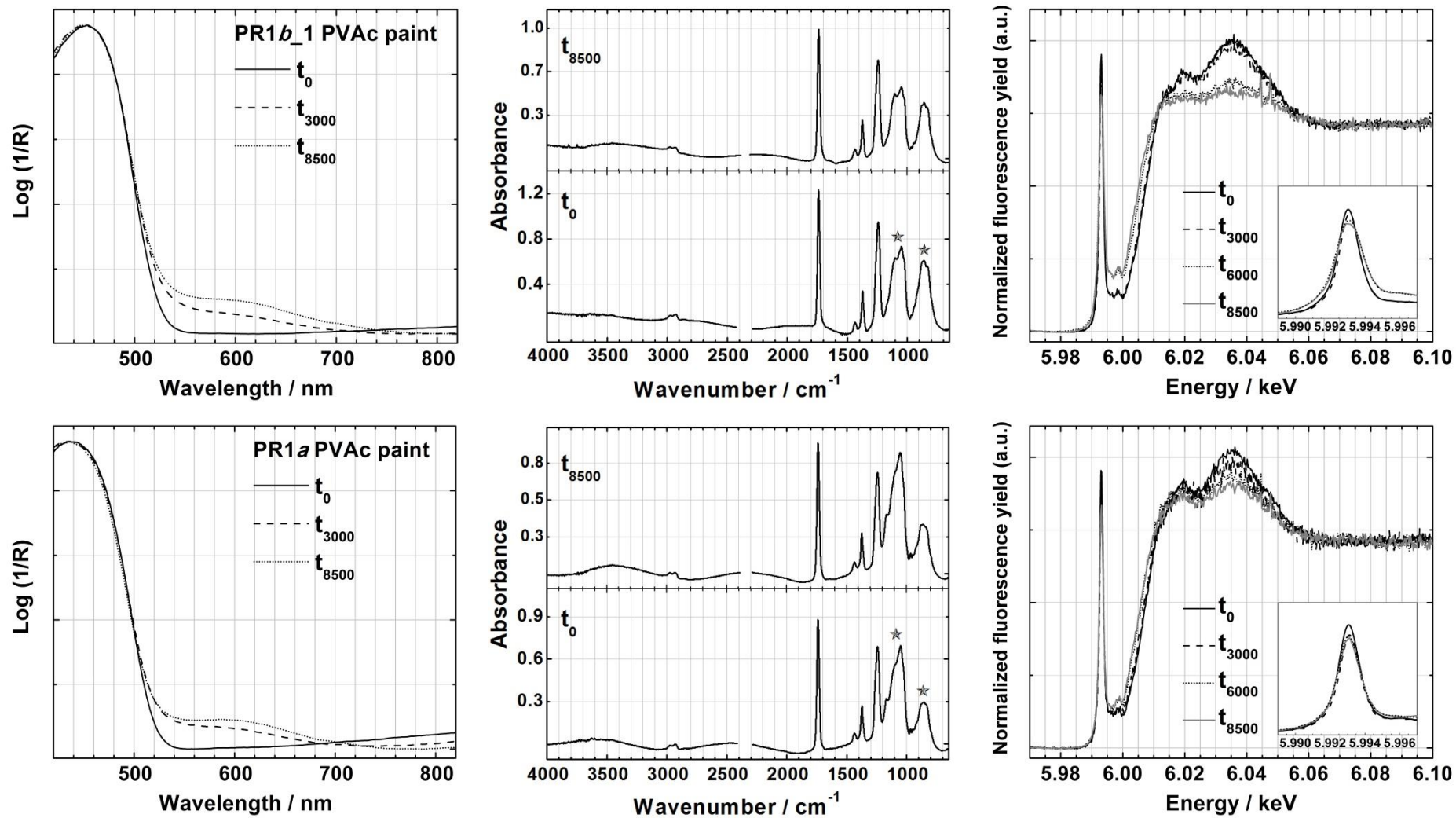


Figure XVII.3. Normalized FORS, μ -FTIR spectra: (\star) $\text{PbCr}_{1-x}\text{S}_x\text{O}_4$, the remaining bands correspond to the PVAc binder; and normalized Cr K-edge XANES spectra of PR1b_1 and PR1a PVAc paints before and after irradiation.

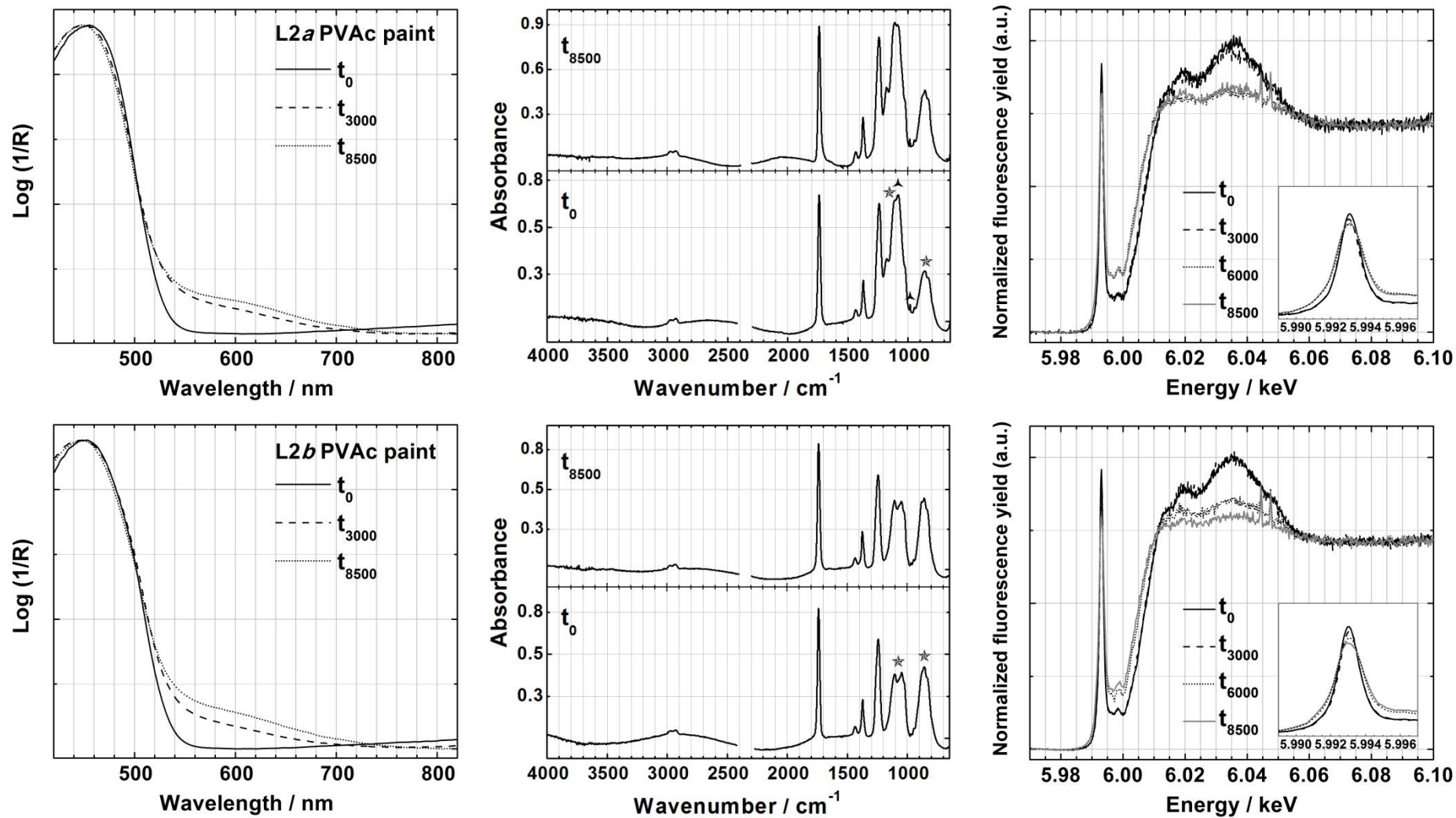


Figure XVII.4. Normalized FORS, μ -FTIR spectra: (\star) $\text{PbCr}_{1-x}\text{S}_x\text{O}_4$, (\blacktriangle) BaSO_4 , the remaining bands correspond to the PVAc binder; and normalized Cr K-edge XANES spectra of L2a and L2b PVAc paints before and after irradiation.

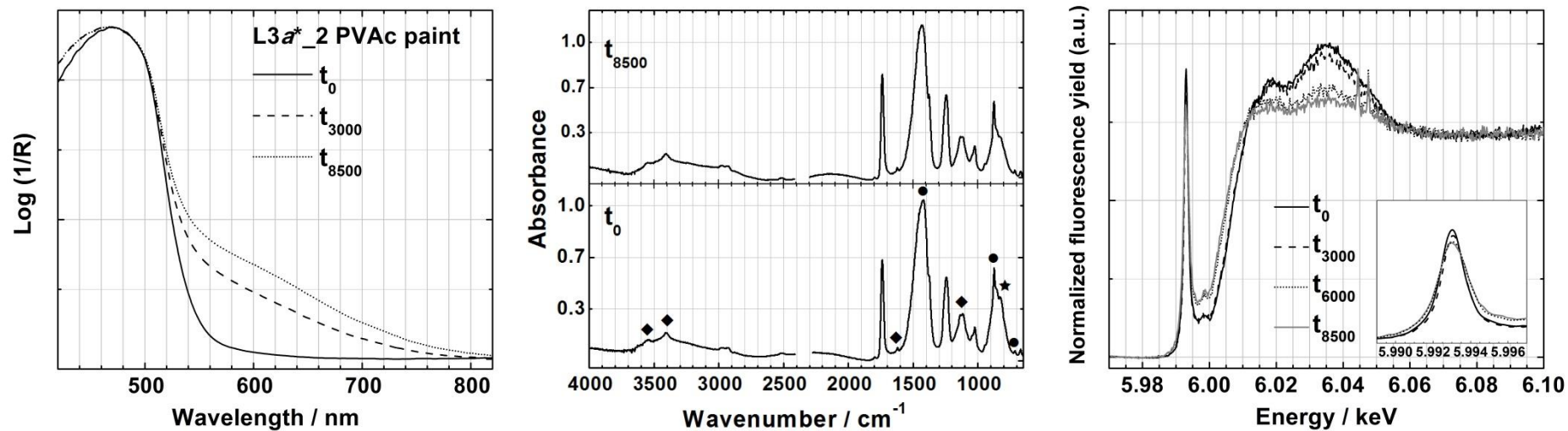


Figure XVII.5. Normalized FORS, μ -FTIR spectra: (★) PbCrO₄, (●) CaCO₃, (◆) CaSO₄·2H₂O, the remaining bands correspond to the PVAc binder; and normalized Cr K-edge XANES spectra of L3a*_2 PVAc paint before and after irradiation.

Appendix XVIII. Additional characterisation of the PVAc paints before and after irradiation

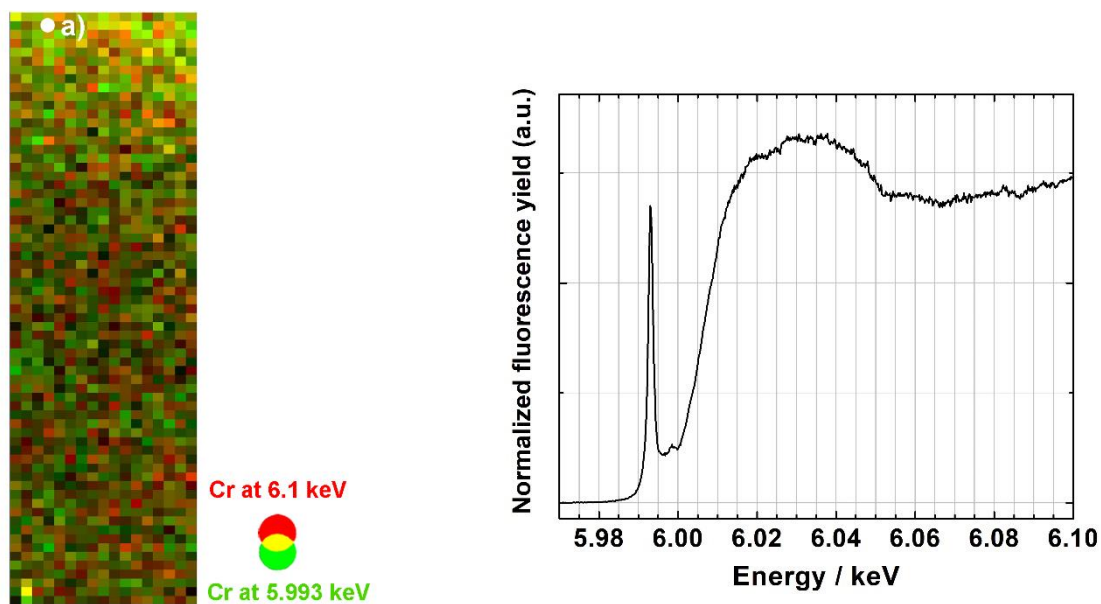


Figure XVIII.1. SR μ -XRF elemental maps (left) obtained at Cr K-edge (5.993 and 6.1 keV) of an embedding-free thick cross-section of the PR1a PVAc paint after 5250h of irradiation time (map size: $26 \times 100 \mu\text{m}^2$, with $1.5 \times 1.5 \mu\text{m}^2$ pixel size), and the normalized Cr K-edge XANES spectrum (right) acquired at point a).

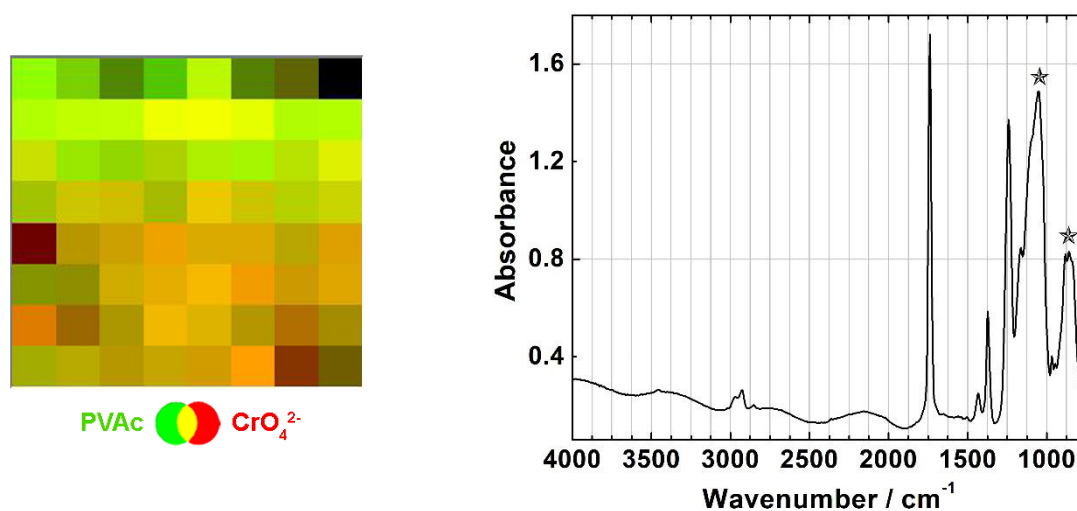


Figure XVIII.2. SR μ -FTIR chemical maps (left) of an embedding-free thin cross-section of the PR1a PVAc paint after 5250h of irradiation time (map size: $80 \times 80 \mu\text{m}^2$, with $10 \times 10 \mu\text{m}^2$ pixel size), and the respective infrared map average spectrum (right); ROI: polyvinyl acetate (1710-1770 cm^{-1}) and chromate (800-920 cm^{-1}); (\star) $\text{PbCr}_{1-x}\text{S}_x\text{O}_4$.

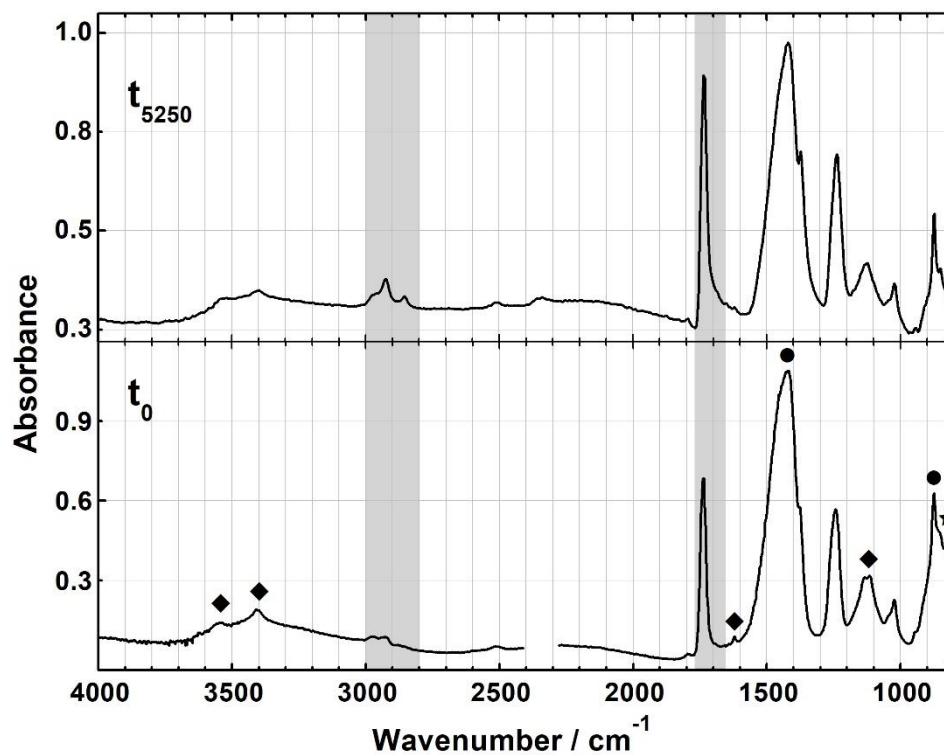


Figure XVIII.3. Infrared spectra of the L3a*_2 PVAc paint before and after 5250h of irradiation time, obtained using the SR μ -FTIR; (★) PbCrO_4 , (●) CaCO_3 , (◆) $\text{CaSO}_4 \cdot 2\text{H}_2\text{O}$, the remaining bands correspond to the PVAc binder. The $\nu(\text{CH})$ and $\nu(\text{C}=\text{O})$ regions are highlighted to show the differences resulting from the presence of degradation products.

Appendix XIX. Additional characterisation of the oil paints before and after irradiation

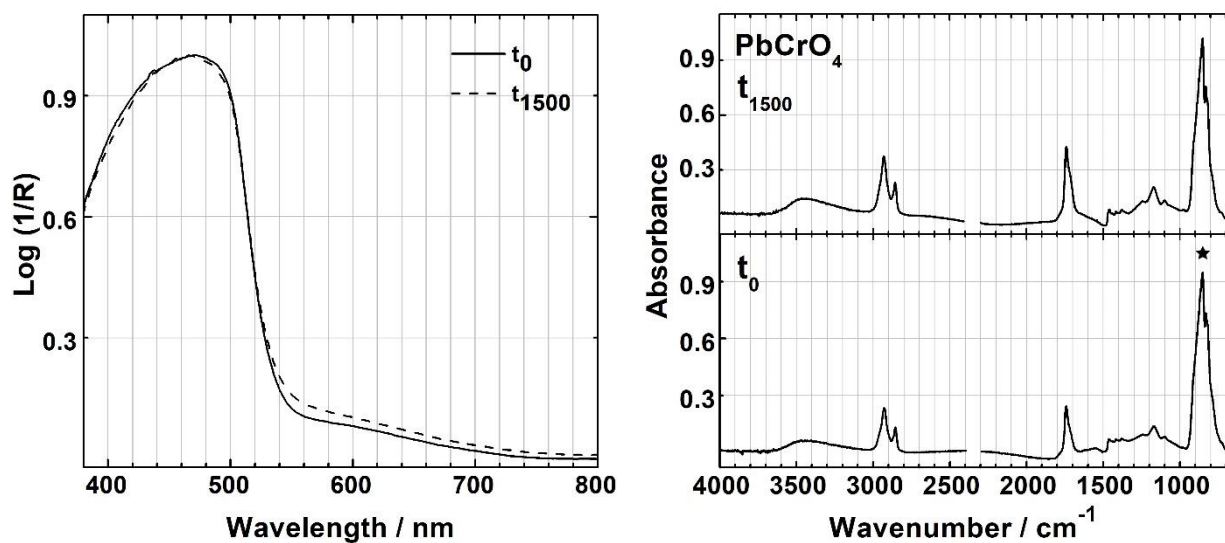


Figure XIX.1. FORS (left) and infrared (right) spectra of the lead chromate oil paint reference before and after irradiation with a Xenon lamp; (*) PbCrO_4 .

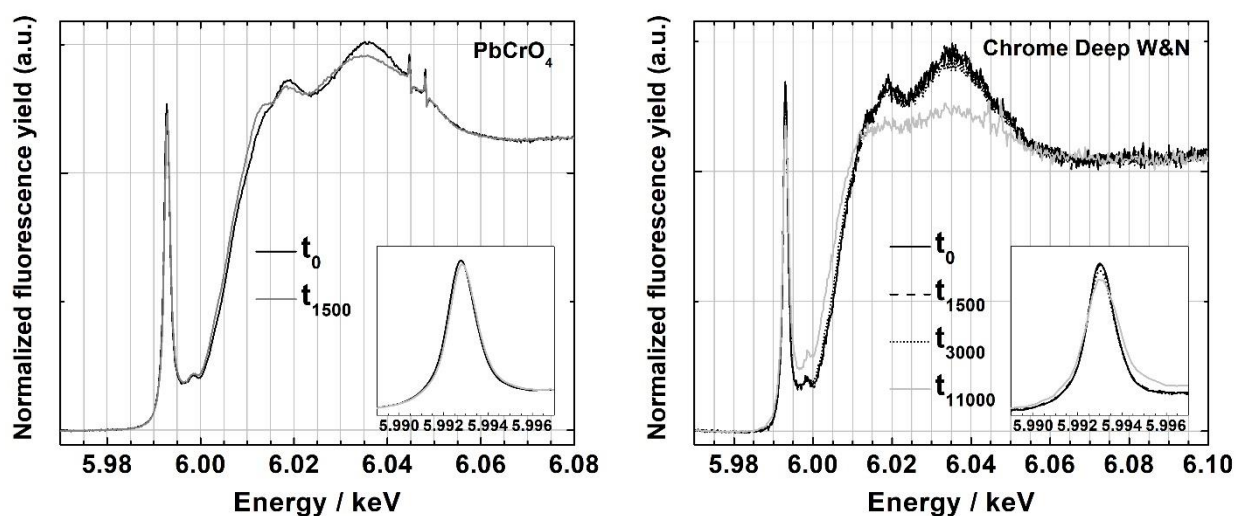


Figure XIX.2. Normalized Cr K-edge μ -XANES spectra of the lead chromate reference and the W&N *Chrome Deep* oil paints before and after irradiation with a Xenon lamp ($\lambda_{\text{irr}} > 300$ nm).

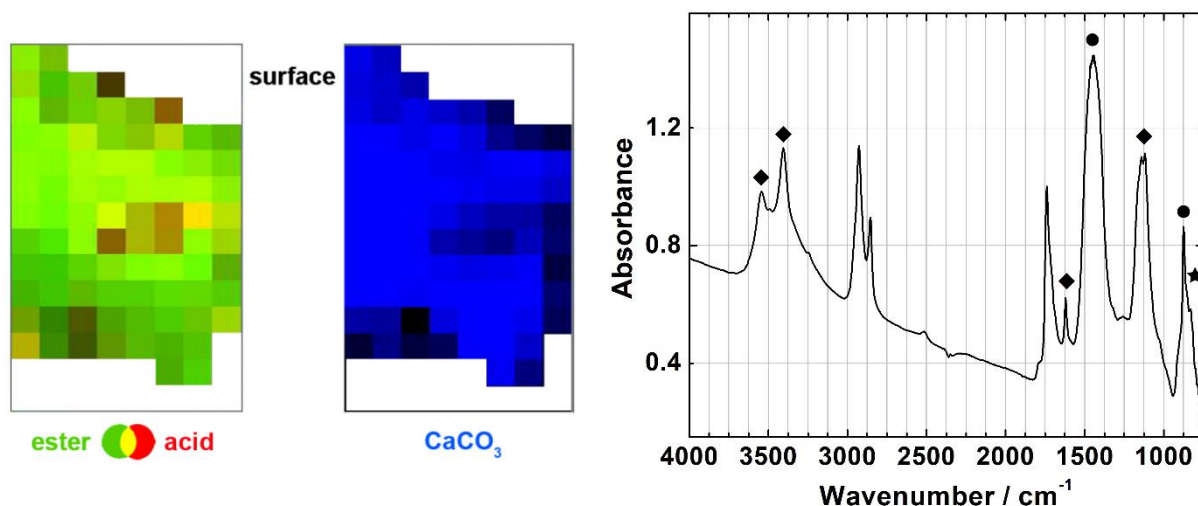


Figure XIX.3. SR μ -FTIR chemical maps (left) of an embedding-free thin cross-section of the Middle oil paint reconstruction, naturally aged for 2 and a half years (map size: $80 \times 140 \mu\text{m}^2$, with $10 \times 10 \mu\text{m}^2$ pixel size), and the respective infrared map average spectrum (right); ROI: ester ($1755\text{-}1720 \text{ cm}^{-1}$), acid ($1718\text{-}1700 \text{ cm}^{-1}$) and CaCO_3 ($1550\text{-}1520 \text{ cm}^{-1}$); (★) PbCrO_4 , (●) CaCO_3 , (◆) $\text{CaSO}_4 \cdot 2\text{H}_2\text{O}$.

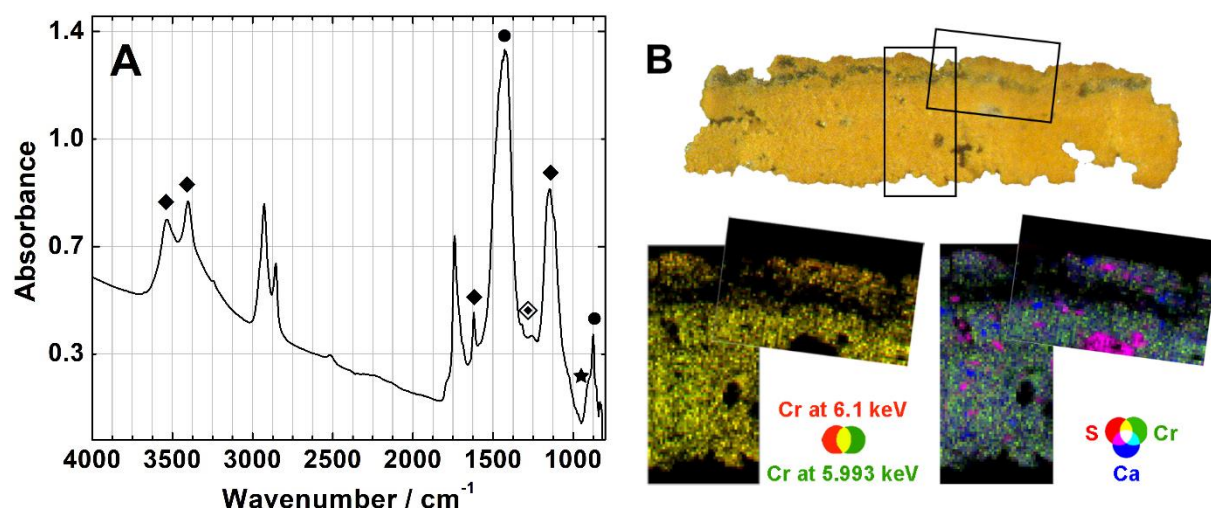


Figure XIX.4. A) Infrared map average spectrum for SR μ -FTIR maps shown in Figure 4.10 (p. 107); **B)** optical microscope image of an embedding-free thin cross-section of the Middle oil paint after 7750h of irradiation, where the black area highlighted corresponds to the SR μ -XRF maps at Cr 5.993 and 6.1 keV (left), and at 5.993 keV of Cr, S and Ca (right) (vertical map size: $92 \times 192 \mu\text{m}^2$ and diagonal map size: $152 \times 100 \mu\text{m}^2$, with $2 \times 2 \mu\text{m}^2$ pixel size); (★) PbCrO_4 , (●) CaCO_3 , (◆) $\text{CaSO}_4 \cdot 2\text{H}_2\text{O}$ and (◇) $\text{CaC}_2\text{O}_4 \cdot x\text{H}_2\text{O}$.

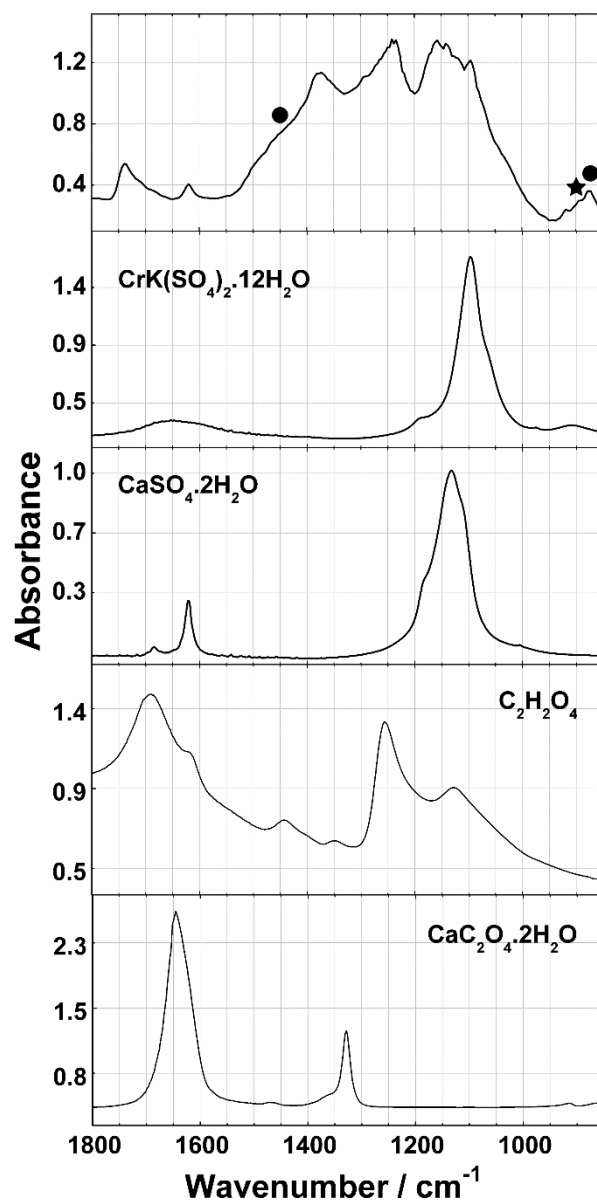


Figure XIX.5. SR infrared spectrum obtained on the surface of an embedding-free thin cross-section of the Middle oil paint CR7 after 7750h of irradiation and four reference compounds between 1800 and 850 cm⁻¹: chromium potassium sulfate CrK(SO₄)₂·12H₂O, gypsum (CaSO₄·2H₂O), oxalic acid (C₂H₂O₄), calcium oxalate dihydrate (CaC₂O₄·2H₂O, weddellite); (●) CaCO₃ and (★) PbCrO₄.

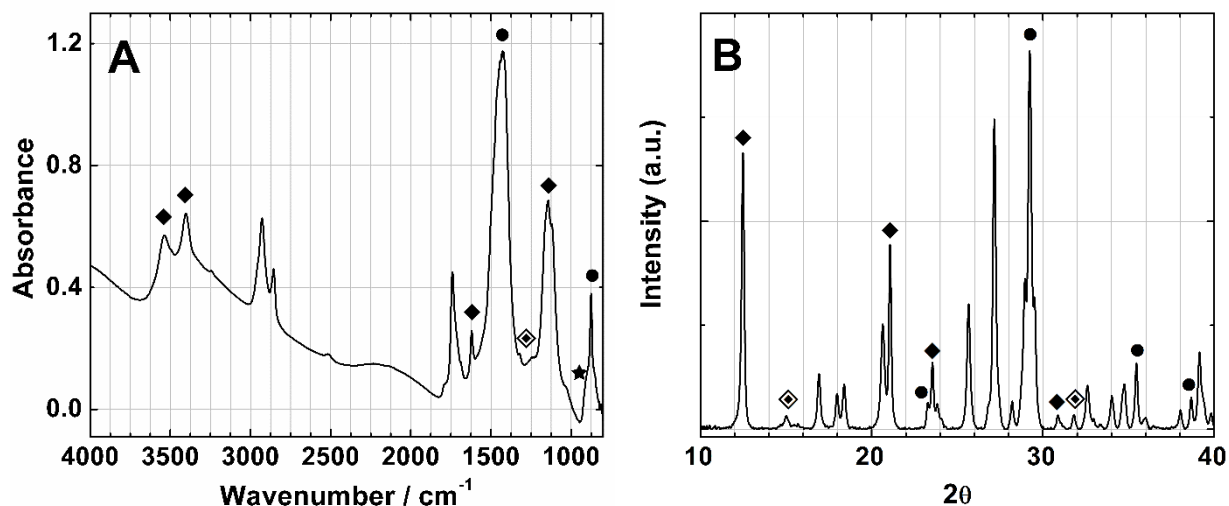


Figure XIX.6. A) Infrared map average spectrum for SR μ -FTIR map and B) diffraction pattern obtained at the surface of the analysed cross-sections from the Middle oil paint after 11000h of irradiation, shown in Figure 4.13 (p. 109); (★) PbCrO_4 , (●) CaCO_3 , (◆) $\text{CaSO}_4 \cdot 2\text{H}_2\text{O}$ and (◇) $\text{CaC}_2\text{O}_4 \cdot 2\text{H}_2\text{O}$.

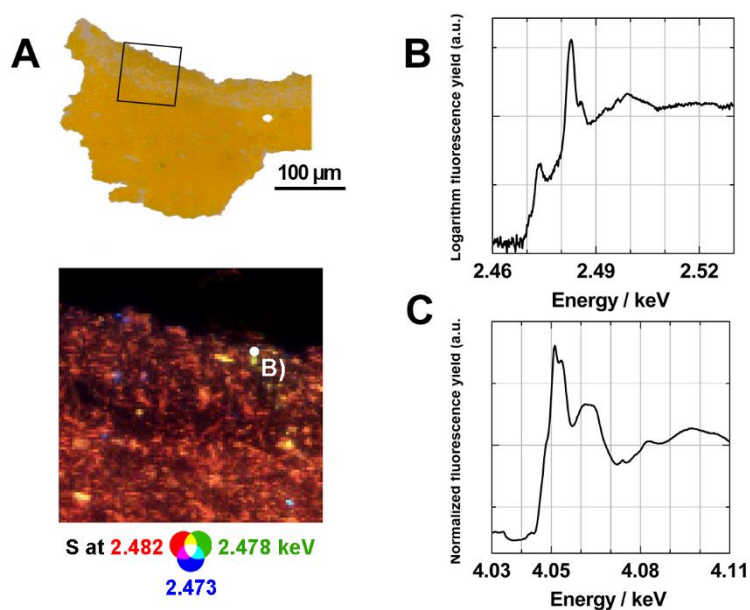


Figure XIX.7. A) Optical microscope image of an embedding-free thin cross-section of the Middle oil paint after 11000h of irradiation, where the black area highlighted corresponds to the SR μ -XRF map around S K-edge at 2.473, 2.478 and 2.842 keV (size: $100 \times 100 \mu\text{m}^2$, with $1 \times 1 \mu\text{m}^2$ step size); B) S K-edge μ -XANES spectra of the point in the map; and C) Ca K-edge μ -XANES spectra obtained at the lower part of the SR μ -XRF map around Ca K-edge shown in Figure 4.13 (p. 109).

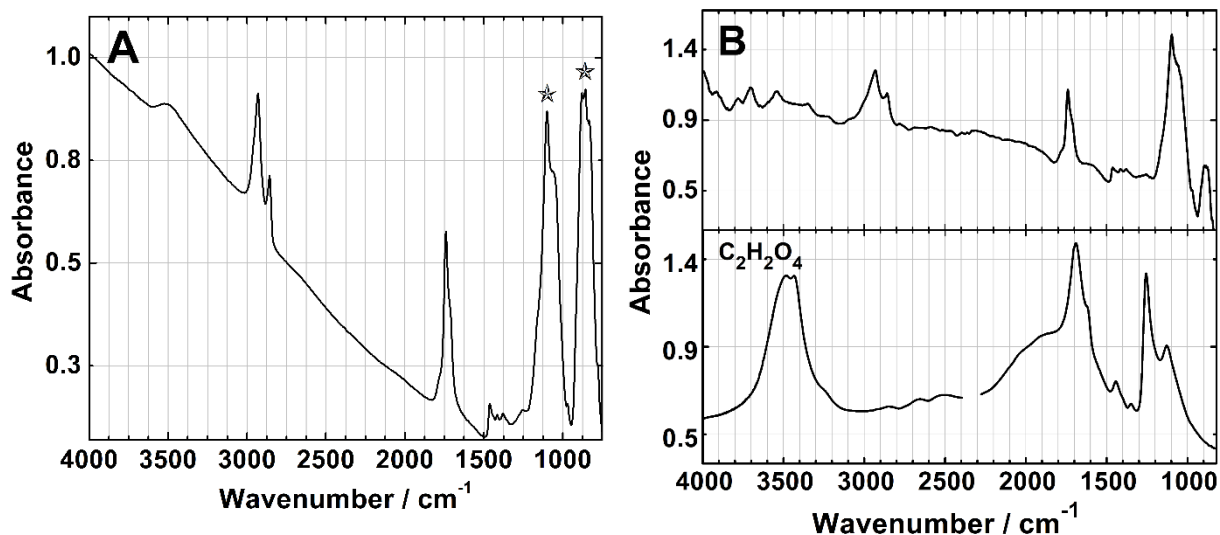


Figure XIX.8. A) Infrared map average spectrum for SR μ -FTIR maps ($t_{ir} = 7750\text{h}$) shown in Figure 4.16 (p. 113) and B) SR infrared spectrum obtained on the surface of an embedding-free thin cross-section of the Lemon oil paint after 11000h of irradiation and of the reference compound oxalic acid $\text{C}_2\text{H}_2\text{O}_4$: (*) $\text{PbCr}_{0.6}\text{S}_{0.4}\text{O}_4$.

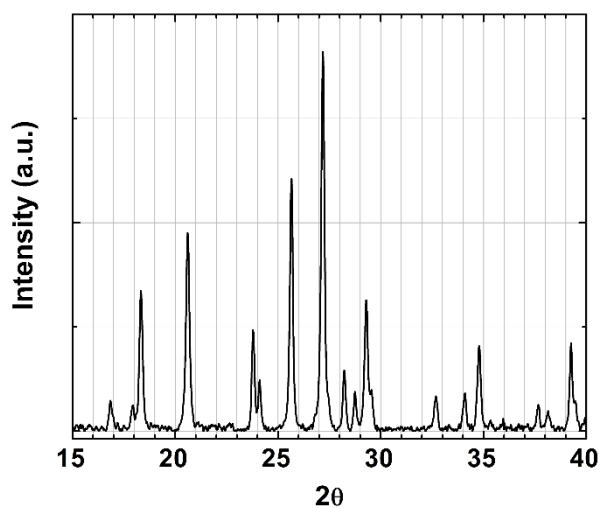


Figure XIX.9. Diffraction pattern obtained at the surface of a cross-section from the Lemon oil paint after 11000h of irradiation, which corresponds solely to monoclinic lead chromate (Figure 3.6, p. 57).

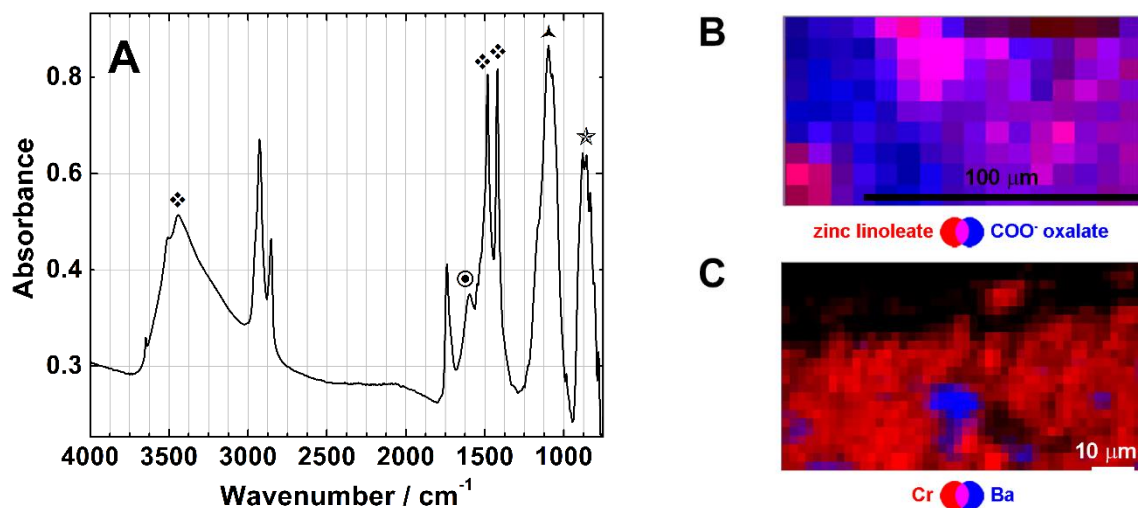


Figure XIX.10. **A)** Infrared map average spectrum for SR μ -FTIR maps shown in Figure 4.19 (p. 117) and in B; **B)** SR μ -FTIR map (size: $136 \times 72 \mu\text{m}^2$, with $8 \times 8 \mu\text{m}^2$ step size) of zinc linoleate ($1560\text{-}1525 \text{ cm}^{-1}$) and oxalate compound ($1620\text{-}1570 \text{ cm}^{-1}$); **C)** SR μ -XRF map at 5.993 keV of Cr and Ba (map size: $92 \times 46 \mu\text{m}^2$, with $2 \times 2 \mu\text{m}^2$ step size), of cross-sections from the W&N *Chrome Yellow* oil paint after 5250h (for μ -FTIR maps) and 8500h of irradiation; (☆) $\text{PbCr}_{0.6}\text{S}_{0.4}\text{O}_4$, (▲) BaSO_4 , (♠) $\text{MgCO}_3 \cdot x\text{H}_2\text{O}$ and (⊙) oxalate compound.

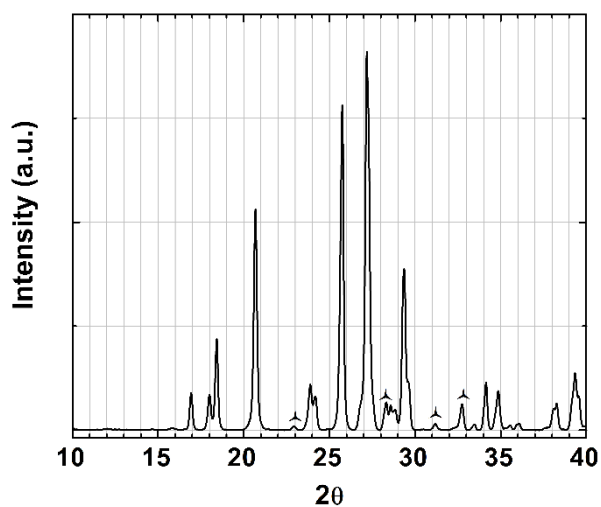


Figure XIX.11. Diffraction pattern obtained at the surface of a cross-section from the W&N *Chrome Yellow* oil paint after 8500h of irradiation; (▲) BaSO_4 .

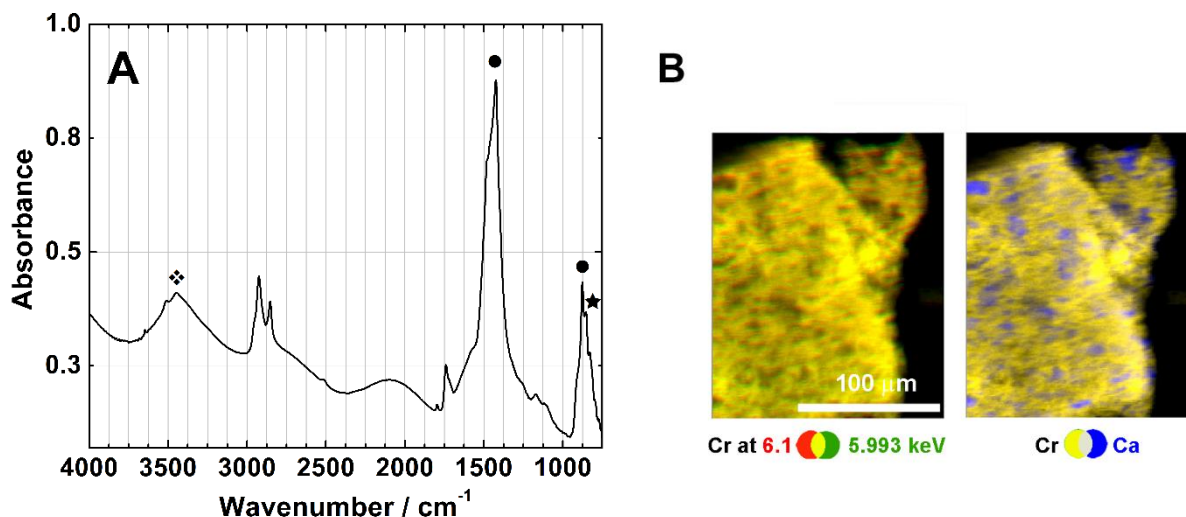


Figure XIX.12. **A)** Infrared map average spectrum for SR μ -FTIR map shown in Figure 4.21 (p. 119); **B)** SR μ -XRF maps at Cr 5.993 and 6.1 keV (left), and at 5.993 keV of Cr and Ca (right) (map size: $140 \times 200 \mu\text{m}^2$, with $1 \times 1 \mu\text{m}^2$ step size) acquired on a cross-section of the W&N *Chrome Deep* oil paint after 10000h of irradiation; (★) PbCrO_4 , (●) CaCO_3 , (◆) $\text{MgCO}_3 \cdot x\text{H}_2\text{O}$.

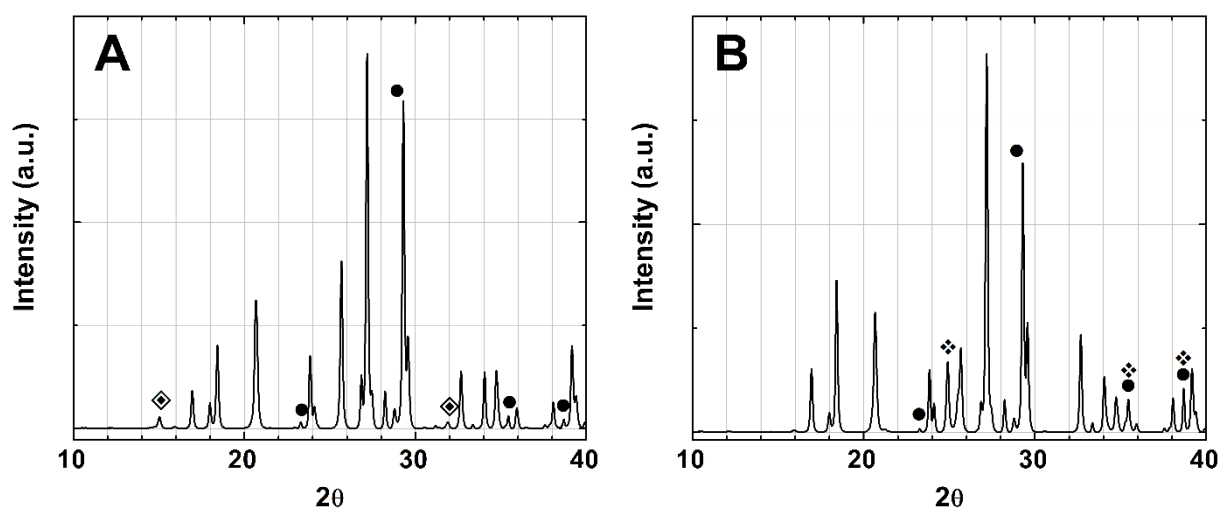


Figure XIX.13. Diffraction patterns from the SR μ -XRD map shown in Figure 4.21 (p. 119) acquired on a cross-section of the W&N *Chrome Deep* oil paint after 10000h of irradiation, representative of the presence of **A)** calcium oxalate dihydrate and **B)** cerussite; (●) CaCO_3 , (◆) $\text{CaC}_2\text{O}_4 \cdot 2\text{H}_2\text{O}$ and (★) PbCO_3 .

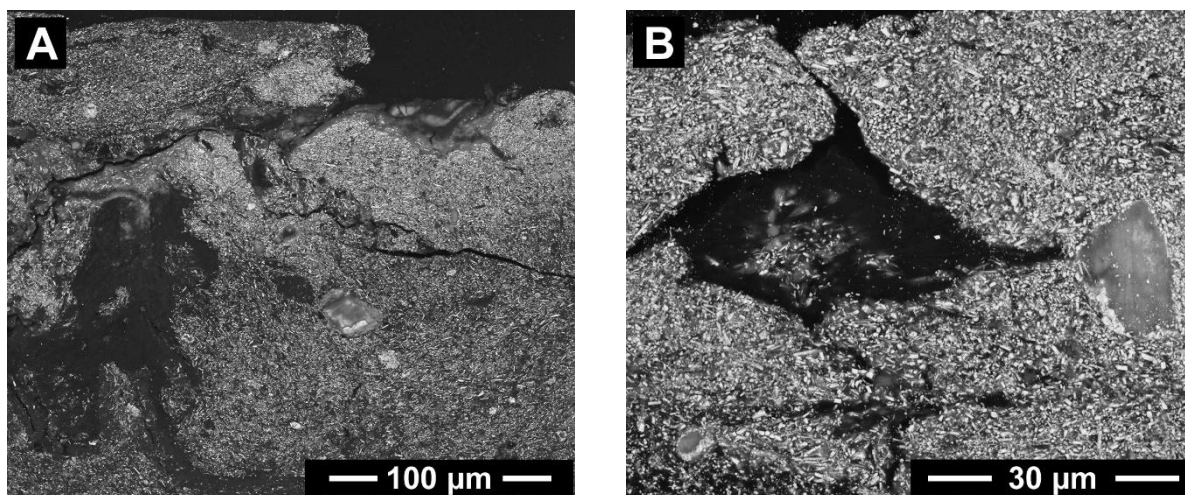


Figure XIX.14. A) SEM images of cross-sections from the *Lefranc Jaune de Chrome* oil paint A) before and B) after 5250h of irradiation with a Xenon lamp ($\lambda_{irr} > 300$ nm).

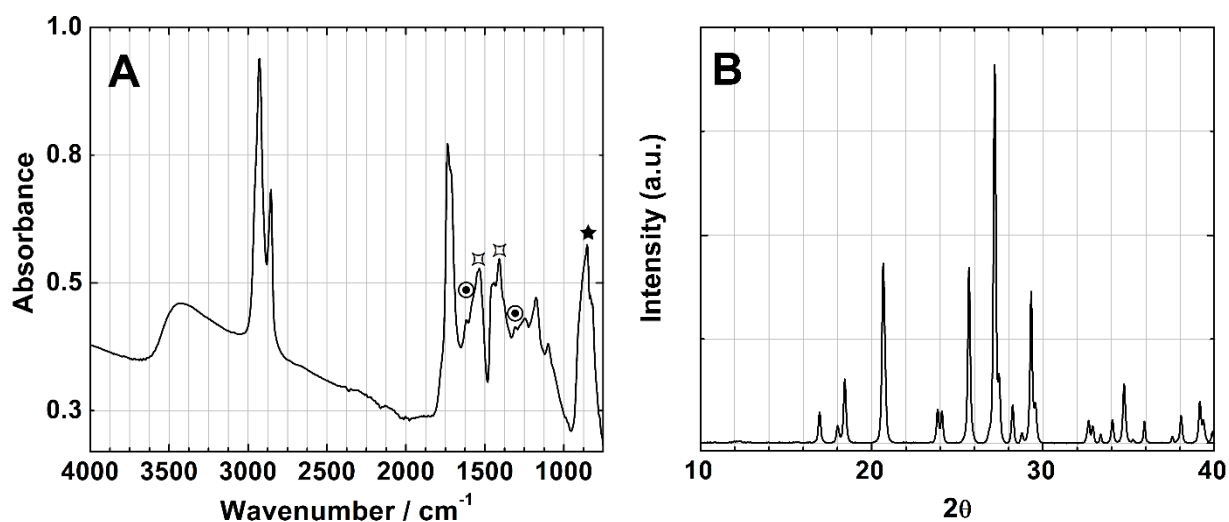


Figure XIX.15. A) Infrared map average spectrum for SR μ -FTIR map shown in Figure 4.23 (p. 121); and B) diffraction pattern obtained at the surface of a cross-section from the *Lefranc Jaune de Chrome* oil paint after 8500h of irradiation; (★) PbCrO_4 .

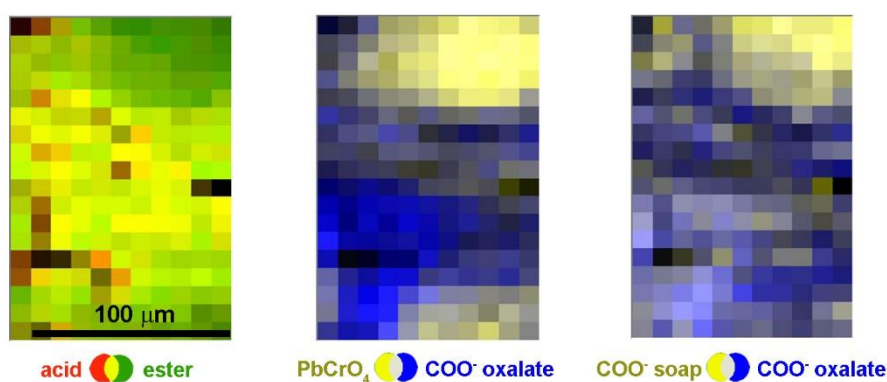


Figure XIX.16. SR μ -FTIR maps (size: $180 \times 110 \mu\text{m}^2$, with $10 \times 10 \mu\text{m}^2$ step size) of an embedding-free cross-section from the *Lefranc Jaune de Chrome* oil paint after 5250h of irradiation, ROI: acids (1718-1700 cm^{-1}), esters (1755-1720 cm^{-1}), carboxylate compounds (1555-1510 cm^{-1}), oxalate compounds (1615-1555 cm^{-1}), lead chromate (920-800 cm^{-1}).

Appendix XX. Reduction reactions, standard reduction potentials (E^0) and dissociation constants (pK_a at 25°C)

Table XX.1. Reduction reactions and standard reduction potentials (E^0 at 25°C) (Bard *et al.*, 1985; Lide, 2006).

Reactions	E^0/V
$S^0 + 2e \rightleftharpoons S^{II-}$	-0.476
$2C^{IV}O_2 + 2H^+ + 2e \rightleftharpoons H_2C^{III}_2O_4$	-0.475
$2H_2C^{IV}O_3 + 2H^+ + 2e \rightleftharpoons H_2C^{III}_2O_4 + 2H_2O$	-0.391
$S^0 + 2H^+ + 2e \rightleftharpoons H_2S^{II-}$	0.142
$S^{VI}O_4^{2-} + 4H^+ + 2e \rightleftharpoons H_2S^{IV}O_3 + H_2O$	0.172
$H_2S^{IV}O_3 + 4H^+ + 4e \rightleftharpoons S^0 + 3H_2O$	0.449
$2C^{IV}O_3^{2-} + 4H^+ + 2e \rightleftharpoons C^{III}_2O_4^{2-} + 2H_2O$	0.478
$Cr^{VI}_2O_7^{2-} + 14H^+ + 6e \rightleftharpoons 2Cr^{3+} + 7H_2O$	1.232
$HCr^{VI}O_4^{2-} + 7H^+ + 3e \rightleftharpoons Cr^{3+} + 4H_2O$	1.350

Table XX.2. Dissociation constants (pK_a at 25°C) (Cotton *et al.*, 1999; Lide, 2006).

Reaction	pK_a
$H_2SO_4 \rightleftharpoons H^+ + HSO_4^-$	
$HSO_4^- \rightleftharpoons H^+ + SO_4^{2-}$	1.99
$H_2SO_3 \rightleftharpoons H^+ + HSO_3^-$	1.85
$HSO_3^- \rightleftharpoons H^+ + SO_3^{2-}$	7.2
$H_2S \rightleftharpoons H^+ + HS^-$	7.05
$HS^- \rightleftharpoons H^+ + S^{2-}$	19
$Cr_2O_7^{2-} + H_2O \rightleftharpoons 2HCrO_4^-$	2.2
$H_2CrO_4 \rightleftharpoons H^+ + HCrO_4^-$	0.74
$HCrO_4^{2-} \rightleftharpoons H^+ + CrO_4^{2-}$	6.49
$C_2H_2O_4 \rightleftharpoons H^+ + C_2HO_4^-$	1.25
$C_2HO_4^- \rightleftharpoons H^+ + C_2O_4^{2-}$	3.81